THE MODULAR SYNTHESIS AND FUNCTIONALIZATION OF CYCLIC COMPOUNDS USING MODERN METHODS

Thesis by

Caitlin Rebecca Lacker

In Partial Fulfillment of the Requirements

for the Degree of

Doctor of Philosophy

CALIFORNIA INSTITUTE OF TECHNOLOGY

Pasadena, California

2022

(Defended August 16, 2021)

Caitlin Rebecca Lacker

ORCID: 0000-0003-2531-2636

To my family and friends, thank you for everything

ACKNOWLEDGEMENTS

I am very grateful for my time at the California Institute of Technology. The Caltech chemistry department is uniquely collaborative and welcoming. I feel very fortunate to have developed as a scientist here and to have had the opportunity to work with so many talented, incredibly intelligent and generous people. In that vein, I have a lot of people to thank.

First and foremost, I would like to thank my research advisor, Professor Sarah Reisman, for giving me this opportunity. Sarah is incredibly smart and a talented chemist. Her eye for synthesis is unique, and she is persistent and extremely hard-working. I want to thank her for her support and encouragement over the years. When I've needed help or a pep talk, or even to vent about something, she's always made time for me. I know it's not easy to do what she does, and I really appreciate how hard she works for her students.

I would like to thank the members of my committee, Professors Greg Fu, Brian Stotlz, and Linda Hsieh-Wilson. Greg has been a supportive committee chair from the beginning, always offering insightful advice and checking in to see how my postdoc search was going. Sharing the third floor of Schlinger with Brian and the rest of the Stoltz lab is one of the best parts about working there. Having Brian's perspective and supportive presence at joint group meetings has been incredibly helpful over the years, and he is always fun to run into in the hallway to chat with. I am also very grateful to Linda for her chemical biology perspective at my yearly meetings, especially in the context of proposal writing.

I incredibly grateful to all of the wonderful the people working at Caltech, without whom all the work we do would not be possible. Dr. Scott Virgil does a fantastic job

running the catalysis center. He is always willing to drop what he is doing to help a student with an instrument or work through a problem. Scott's advice and insight has been key to several research problems I was struggling with during my time here. I would also like to thank Dr. David VanderVelde for all he does in the NMR lab, and Dr. Mona Shahgholi and Naseem Torian for their mass spectrometry assistance. I would like to thank Alison Ross for her hard work as the graduate program manager for CCE. She has always answered my questions and is so helpful. I am also very grateful to Lynne Martinez, Veronica Triay, and Beth Marshall for all they have done for us with everything from writing grants to scheduling meetings and ordering textbooks.

During my time in the Reisman lab, I have been fortunate to work with many wonderful labmates. I'm incredibly grateful to have been part of a lab culture that encourages you to ask questions and never shames you for not knowing something. Over the years, whenever I have asked people for help, they have always said yes. I hope that I have been able to help younger students the way I was helped my first few years.

First of all, I would like to thank my mentors and my very first project partners, Dr. Jorden Beck and Dr. Lauren Chapmen. I couldn't have had more wonderful people to work with. Not only are they both incredibly smart and competent chemists, but they were patient and encouraging teachers as well. Lauren was a 5th year when I first started, and she was so kind and generous with her time towards a 1st year. Working next to her in lab made my first year really special. She is who I seek to emulate when mentoring younger students. Jordan was so fun to work with. His energy and intelligence and ability to problem solve helped me stay motivated and encouraged when we ran into problems with chemistry. Jordan taught me so much about how to be a chemist, from setting up a reaction to

processing 2D NMR data. I'm a proud graduate of the Jordan Casey Beck School of Chromatography. Without him, I wouldn't be the researcher that I am today.

I'm grateful to all of my wonderful project partners I've worked with over the years. Everyone that I've gotten to work with on Team Nickel has been such an inspiration to me. Their thoughtfulness, intelligence, and creativity have taught me so much. I have thoroughly enjoyed all of our conversations over the years. We all knew each other's projects almost as well as we knew our own, and it was always fun to bounce ideas off each other and think about how our work fit together in the larger picture of nickel catalysis. I was also privileged to mentor two undergraduate students, Dana Gephart and Robin McDonald.

Travis DeLano in particular has been my project partner on and off for the past four years or so. I always know Travis has my back, and that I can trust him with our work. We have a similar approach towards chemistry that makes working together easy. He is so smart and talented; I learned so much from him and I know he will be successful wherever he goes. I'd also like to thank Sara Dibrell. While we were only project partners for a few months, Sara is incredible to work with. She is competent and generous, and someone you are lucky to have on your side.

I got to work with Mike Maser for about 6 months or so on our HTE/machine learning collaboration, and it was an extremely rewarding experience. As we were trying to figure out how we were going to carry out this project, it always made my day when I would make a suggestion and Mike would get excited about it. Mike is smart and talented, but also humble and encouraging of other people and their ideas.

Finally, I would like to thank my newest project partner, Emily Chen. I wish that I got to spend more time with her in the lab, but COVID restrictions and grant-writing cut that time short. Emily is hilarious, kind, and very smart. It has been such a joy working with her, even if it was only for a short time. I know that she is ready for whatever comes her way.

The problem with working with so many great people over the years is it makes it for a long list of acknowledgements. As I won't have time to do them all in person at my defense, I hope that they can look at this document and get a glimpse of how much they meant to me.

Thank you to Jordan for being a great mentor and so much fun to work with. Thank you to Dr. Julie Hofstra for her friendship, love, support, and frequent outings to get crepes. Julie was such a wonderful friend to me during my time at Caltech. Thank you to Alice Wong for Gardettos, the Moana soundtrack, and making the office fun. Thank you to Dr. Kelsey Poremba for her kindness and patience.

Thank you to Karli Holman for her friendship. Our long talks about life in the bay, playing Pokemon, and watching Avatar the Last Airbender are memories I'll treasure. Also, I couldn't have asked for a better co-party planner. Thank you to Travis for being a great project partner over the years and for his enthusiasm and energy. And, perhaps most of all, thanks for the most nicknames I have ever had in my life. And of course, Wednesday Lunch Bunch with the two of them was always a treat. Thank you to Mike for being great to talk to and work with. The quiet days when it was just the two of us in the bay working where we ended up having some really good conversations were some of my favorites.

Thank you to Alex Shimozono for all of the great discussions about chemistry and for always persevering. And thanks to all four for being great bay mates.

Thank you to Ray Turro for just generally being everyone's favorite person in lab. Ray is incredibly kind, patient, and generous, as well as ridiculously smart. He always has time for me to pester him about chemistry or talk about whatever is going on in life. Thanks to Jeff Kerkovius for being a great person to talk to and be around. Jeff is fun and smart, and makes some really great puns. He is also a ridiculously talented chemist, and I can't wait to see what he comes up with next. Also, special thanks to his wife Miranda for all of the great talks we have had over the years at various holiday parties, socials, and camping trips about everything from books and videogames to what it means to be a woman in our current culture. Thanks to my fellow Texan Sara Dibrell for somehow being smart, hardworking, organized, and also incredibly kind and friendly. The lab would not function without her. If you need to get something done, Sara can do it. And thank you to Yujia Tao for being so hilarious and sweet. She keeps the lab interesting and fun. Her energy, enthusiasm, and brutal yet hilarious honesty make her a joy to be around.

Thanks to Andrea Stegner for her kindness and friendship. Running into her on walks during quarantine always brightened my day. Thanks to Lexie Beard for her kindness. I only recently got the opportunity to know her better, and I wish we'd gotten to spend more time together. Thanks to Ally Stanko for her generosity and positivity. It was fun being bay mates with her for the last few months at Caltech, and I loved to opportunity to get to know her more.

Thank you to all of the first years Jordan Thompson, Cedric Lozano, Daniel Cheng, and Emily Chen. I'm excited for what you will do next! Thank you especially to Emily for

being such a wonderful mentee. I wish you all of the best! Thanks also to my friends outside of the lab Dylan Freas, Wendy Zhang, and the whole of the Stoltz lab.

I'd also like to thank all of the wonderful postdocs I've had the privilege to work with over the years. Their kindness and support have made all of the difference. In particular, I'd like to thank Dr. Suzie Stevenson, Dr. Elliot Farney, Dr. Justin Su, Dr. Mike Rombola, Dr. Marco Brandstaetter, and Dr. Connor Farley for all of their friendship and mentorship over the years.

Most importantly, I have to thank my two classmates, Nick Fastuca and Skyler Mendoza. It's hard for me to express just how much these two wonderful friends mean to me. They have always been supportive, kind, and generous. They made the Yosemite camping trip one of the most fun experiences of my life. Nick is an incredibly generous friend. One time when I was having a bad week, he baked an entire chocolate cake for me. He is also silly, hilarious, and incredibly cool, and he's one of those people who can pick up almost any hobby. He can always put a smile on my face. Skyler is one of those people who will drop everything to help you or spend time with you. He is an attentive listener and thoughtful friend. My favorite part of any day was when Skyler would wander over from the other side of the lab to talk to me. He has always been there for me, and I hope I have been able to be even half the friend to him that he's been to me. These two people made such an impact on my life, and my experience at Caltech would have been drastically different and a lot less fun without them.

In addition to my labmates and coworkers, I have a lot of people outside of my lab to thank. I would like to thank my church family at Grace Pasadena for the love, support, and community over the years. I'd especially like to thank Nathan for his friendship these

past five years. His blatant, unrepentant honesty is only matched by his thoughtfulness and generosity. Thanks to him, Sofia, and Kendall for the Thursday night zoom calls during quarantine that helped to keep me sane. Thank you to my friends from various city groups over the years Erisa, Chris, Caroline, Carolyn, Donna, and Marcia for all of the love, support and encouragement in all stages of life.

I'd like to thank Julia, Rachel, and Kimi for their enduring friendship since high school. I'm so appreciative for their continued friendship despite the distance that keeps us apart at times. I'd also like to thank Emily Covert, one of my closest friends, for always being there for me and accepting me just as I am. Finally, I'd like to thank Stephanie Breunig, who was my roommate for the past four years. Stephanie is and incredibly kind and thoughtful person. Her selflessness and generosity are inspiring. We have shared so many adventures and life events. I could not have found anyone better to go through graduate school with, with research setbacks, sorrows, quarantines, and holidays away from family. She has been there for me during both the hard times and joyful times, and I'm so incredibly thankful for her.

Most of all, I'd like to thank my family for all of their support over the years, especially my parents, Ann and Steve Lacker. They have always shown me unconditional love and support. I can't fully express all that they have meant to me my whole life. They have encouraged my interests, allowed me to explore the world around me, taught me, loved me, and done their best to answer my many, many questions. They have always been there for me with both love and wisdom. I am so blessed to have them as parents.

ABSTRACT

Accessing libraries of similar compounds quickly is important in the pharmaceutical industry, as it allows for the expedient investigation of a wide variety of parameters. An efficient strategy to access compounds of interest is to start from a single intermediate containing an interesting or pharmaceutically active structure and decorating it with varying functionality to generate a library of related compounds. Cross-coupling is a powerful tool for this type of divergent, modular approach.

Herein, we discuss several strategies geared towards the synthesis of small libraries of compounds of interest. First, a modular approach towards a library of enantioenriched *trans* cyclobutanes is discussed. This strategy allows for the synthesis of diverse substrates from a single enantioenriched intermediate, and this approach was applied to the synthesis of the small molecule (+)-rumphellaone A. Finally, the development of an enantioselective nickel-catalyzed photoredox cross-coupling to form *N*-(hetero)benzylic azoles in collaboration with researchers at Merck is discussed.

PUBLISHED CONTENT AND CONTRIBUTIONS

Portions of the work described herein were disclosed in the following communications:

1. Chapman, L. M.; Beck, J. C.; Lacker, C. R.; Reisman, S. E. *J. Org. Chem.* **2018**, *83*, 6066–6085. DOI: 10.1021/acs.joc.8b00728. Copyright © 2018 American Chemical Society

   C.R.L. contributed to the reaction development, conducted experiments, and participated in preparation of the supporting data and writing of the manuscript.

2. Beck, J. C.[‡]; Lacker, C. R.[‡]; Chapman, L. M.; Reisman, S. E. *Chem. Sci*, **2019**, *10*, 2315–2319. DOI: 10.1039/C8SC05444D. Copyright © 2019 The Royal Society of Chemistry

   C.R.L. contributed to the reaction development, conducted experiments, and participated in preparation of the supporting data and writing of the manuscript.

TABLE OF CONTENTS

LIST OF ABBREVIATIONS

$[\alpha]_D$	angle of optical rotation of plane-polarized light
Å	angstrom(s)
Ac	acetyl
acac	acetylacetonate
alk	alkyl
^{t}Am	*tert*-amyl
APCI	atmospheric pressure chemical ionization
app	apparent
aq	aqueous
Ar	aryl
atm	atmosphere(s)
bathophen	bathophenanthroline
BBN	borabicyclo[3.3.1]nonane
BHT	2,6-di-*tert*-butyl-4-methylphenol ("butylated hydroxytoluene")
BiOX	bi(oxazoline)
BINAP	2,2'-bis(diphenylphosphino)-1,1'-binaphthyl
BINOL	1,1'-bi(2-naphthol)
Bn	benzyl
Boc	*tert*-butoxycarbonyl
BOX	bis(oxazoline)
bp	boiling point
br	broad

Bu	butyl
^{i}Bu	*iso*-butyl
^{n}Bu	butyl or *norm*-butyl
^{s}Bu	*sec*-butyl
^{t}Bu	*tert*-butyl
Bz	benzoyl
c	concentration of sample for measurement of optical rotation
^{13}C	carbon-13 isotope
/C	supported on activated carbon charcoal
°C	degrees Celsius
calc'd	calculated
CAM	cerium ammonium molybdate
cat.	catalyst
Cbz	benzyloxycarbonyl
cf.	consult or compare to (Latin: *confer*)
cis	on the same side
cm^{-1}	wavenumber(s)
cod	1,5-cyclooctadiene
conc.	concentrated
conv.	conversion
Cp	cyclopentadienyl
Cy	cyclohexyl
Cyp	cyclopentyl

Δ	heat or difference
δ	chemical shift in ppm
d	doublet
d	deutero or dextrorotatory
D	deuterium
dba	dibenzylideneacetone
DBU	1,8-diazabicyclo[5.4.0]undec-7-ene
DCE	1,2-dichloroethane
DIPEA	*N*,*N*-diisopropylethylamine
DIBAL	diisobutylaluminum hydride
DFT	density functional theory
DKR	dynamic kinetic resolution
DMA	*N*,*N*-dimethylacetamide
DMAP	4-(dimethylamino)pyridine
DMBA	2,6-dimethylbenzoic acid
DME	1,2-dimethoxyethane
DMF	*N*,*N*-dimethylformamide
DMI	1,3-dimethyl-2-imidazolidinone
DMPU	*N*,*N*'-dimethylpropylene urea
DMSO	dimethylsulfoxide
dppb	1,4-bis(diphenylphosphino)butane
dppbz	1,2-bis(diphenylphosphino)benzene
dppf	1,1'-bis(diphenylphosphino)ferrocene

dppe	1,2-bis(diphenylphosphino)ethane
dr	diastereomeric ratio
dtbpy	4,4'-di-*tert*-butyl-2,2'-bipyridine
DYKAT	dynamic kinetic asymmetric transformation
E	methyl carboxylate (CO_2CH_3)
E^+	electrophile
E	trans (entgegen) olefin geometry
EDCI	*N*-(3-dimethylaminopropyl)-*N*'-ethylcarbodiimide hydrochloride
ee	enantiomeric excess
e.g.	for example (Latin: *exempli gratia*)
EI	electron impact
epi	epimeric
equiv	equivalent(s)
ESI	electrospray ionization
Et	ethyl
et al.	and others (Latin: *et alii*)
FAB	fast atom bombardment
g	gram(s)
GC	gas chromatography
h	hour(s)
^1H	proton
[H]	reduction
HC	homocoupling

hex	hexyl
HMDS	hexamethyldisilazane
HMPA	hexamethylphosphoramide
$h\nu$	light
HPLC	high performance liquid chromatography
HRMS	high resolution mass spectrometry
Hz	hertz
IC_{50}	half maximal inhibitory concentration (50%)
i.e.	that is (Latin: *id est*)
in situ	in the reaction mixture
IPA	isopropanol
IR	infrared spectroscopy
J	coupling constant
k	rate constant
kcal	kilocalorie(s)
kg	kilogram(s)
L	liter or neutral ligand
l	levorotatory
LA	Lewis acid
LC/MS	liquid chromatography–mass spectrometry
LDA	lithium diisopropylamide
LED	light-emitting diode
m	multiplet or meter(s)

M	molar or molecular ion
m	meta
μ	micro
m-CPBA	*meta*-chloroperbenzoic acid
Me	methyl
mg	milligram(s)
MHz	megahertz
min	minute(s)
mL	milliliter(s)
MM	mixed method
mol	mole(s)
MOM	methoxymethyl
mp	melting point
Ms	methanesulfonyl (mesyl)
MS	molecular sieves or mass spectrometry
m/*z*	mass-to-charge ratio
naph	naphthyl
nbd	norbornadiene
NBS	*N*-bromosuccinimide
ND	not determined
NHC	*N*-heterocyclic carbene
NHP	*N*-hydroxyphthalimide
nm	nanometer(s)

NMP	*N*-methyl-2-pyrrolidone
NMR	nuclear magnetic resonance
o	ortho
[O]	oxidation
p	para
Pc	phthalocyanine
Ph	phenyl
pH	hydrogen ion concentration in aqueous solution
phen	1,10-phenanthroline
PHOX	phosphinooxazoline
pin	pinacol
Piv	pivaloyl
pK_a	acid dissociation constant
Pr	propyl
^{i}Pr	isopropyl
^{n}Pr	propyl or *norm*-propyl
py	pyridine
PyBOX	pyridine-bis(oxazoline)
PyOx	pyridine-oxazoline
pyphos	(2-diphenylphosphino)ethylpyridine
q	quartet
quant.	quantitative
QuinOx	quinoline-oxazoline

R	alkyl group
R_L	large group
R	rectus
RCM	ring-closing metathesis
recry.	recrystallization
ref	reference
R_f	retention factor
rt	room temperature
s	singlet or seconds
S	sinister
sat.	saturated
SET	single-electron transfer
SFC	supercritical fluid chromatography
SM	starting material
t	triplet
TBAB	tetra-*n*-butylammonium bromide
TBAF	tetra-*n*-butylammonium fluoride
TBAI	tetra-*n*-butylammonium iodide
TBAT	tetra-*n*-butylammonium difluorotriphenylsilicate
TBS	*tert*-butyldimethylsilyl
TDAE	tetrakis(dimethylamino)ethylene
Tf	trifluoromethanesulfonyl
TFA	trifluoroacetic acid

temp	temperature
terpy	2,2′:6′,2″-terpyridine
THF	tetrahydrofuran
TIPS	triisopropylsilyl
TLC	thin layer chromatography
TMEDA	*N*,*N*,*N*’,*N*’-tetramethylethylenediamine
TMS	trimethylsilyl
TOF	time-of-flight
tol	toluene
trans	on the opposite side
Ts	*para*-toluenesulfonyl (tosyl)
UV	ultraviolet
vide infra	see below
v/v	volume per volume
w/v	weight per volume
X	anionic ligand or halide
xs	excess
Y	anionic ligand or halide
Z	cis (zusammen) olefin geometry

Chapter 1

Enantioselective Ketene Trapping and Diastereoselective C–H Activation: Methods Developed from the Total Synthesis of (+)-Psiguadial B[1]

1.1 INTRODUCTION

Figure 1.1 *Cyclobutane-containing natural products, and a strategy towards (+)-psiguadial B*

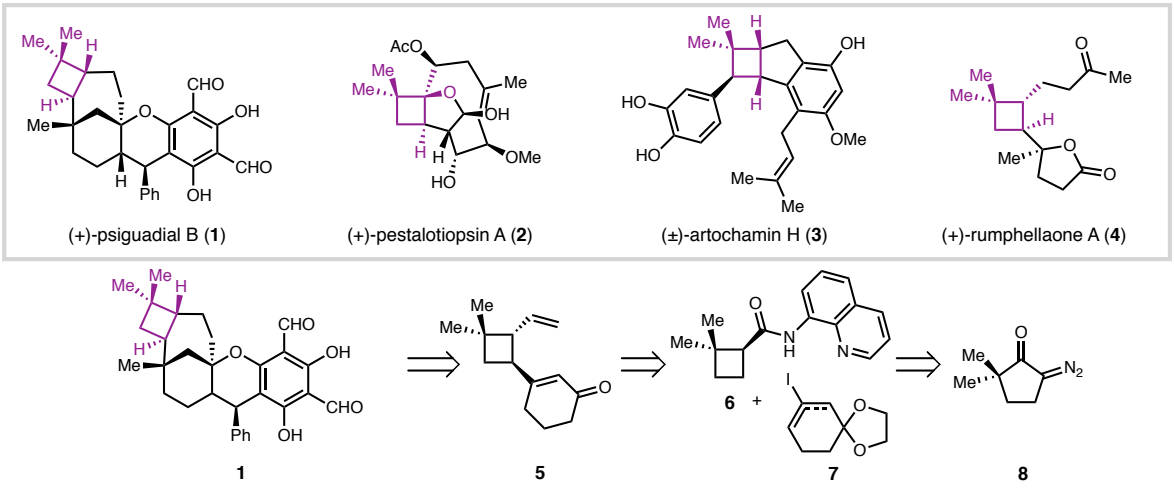

Cyclobutanes are found in a wide variety of natural products. Despite their prominence, cyclobutanes can be challenging to form synthetically, particularly *trans*-cyclobutanes, such as those found in **1**, **2**, and **4** (**Figure 1.1**).[1–6] One common method for

[1] Portions of this chapter were adapted from the following communications: Chapman, L. M.; Beck, J. C.; Lacker, C. R.; Wu, L.; Reisman, S. E. *J. Org. Chem.* **2018**, *83*, 6066.; DOI: 10.1021/acs.joc.8b00728, copyright 2018 American Chemical Society; Beck, J. C.; Lacker, C. R.; Chapman, L. M.; Reisman, S. E. *Chem. Sci.* **2019**, *10*, 2315., DOI: 10.1039/C8SC05444D, copyright 2019 Royal Society of Chemistry. The research discussed in this chapter was completed in collaboration with Dr. Jordan C. Beck as well as Dr. Lauren M. Chapman, former graduate students in the Reisman Lab.

the synthesis of cyclobutanes is the [2+2] cycloaddition. However, regio- and stereoselectivity can be challenging to control using this methodology. In addition, *trans* cyclobutanes in particular are difficult to synthesize.[7] In light of these challenges, a novel method for the synthesis of cyclobutanes was developed by our lab for the 2016 total synthesis of (+)-psiguadial B (**1**), a meroterpenoid isolated from the *Psidium guajava* in 2010, which contains a fused *trans*-cyclobutane.[1,8,9] The cyclobutane was introduced enantioselectively using a photoinduced Wolff rearrangement with asymmetric trapping of the *in situ* generated ketene. This tandem Wolff rearrangement/asymmetric ketene addition method utilizes a ring contraction approach, obviating some of the selectivity challenges inherent to a [2+2] approach. Intermediate **6** was then elaborated by a directed C–H activation followed by a selective epimerization to afford the desired *trans* cyclobutane (**5**).

1.1.1 Asymmetric Ketene Trapping

Scheme 1.1 *Synthesis of* ***6*** *racemically and via a chiral resolution*

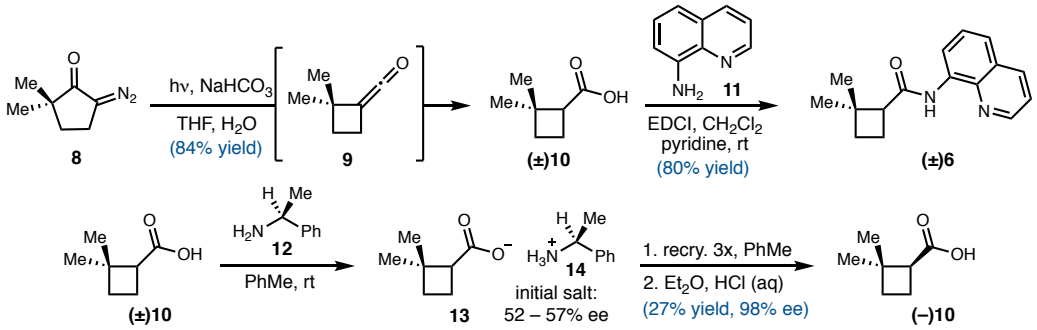

Cyclobutamide **6** was chosen as the target compound. It was thought that the quinolinamide could be used as a directing group for C–H activation to build up the framework of (+)-psiguadial B. This compound was first synthesized racemically in two steps (**Scheme 1.1**). First, a photoinduced Wolff rearrangement was used to generate carboxylic acid ±**10** from diazoketone **8**.[10,11] (±)**10** was then coupled with 8-

aminoquinoline (**11**) to generate racemic cyclobutamide (±)**6**. Prior to coupling, carboxylic acid (±)**10** could be resolved through recrystallization with chiral amine **12**. However, this method required multiple recrystallizations and afforded the enantioenriched acid in low yield. To circumvent this issue, it was proposed that ketene **9** could be trapped *in situ* with 8-aminoquinoline in an enantioselective fashion using a chiral catalyst.

Scheme 1.2 *Previous asymmetric and stereospecific nucleophilic ketene trapping*

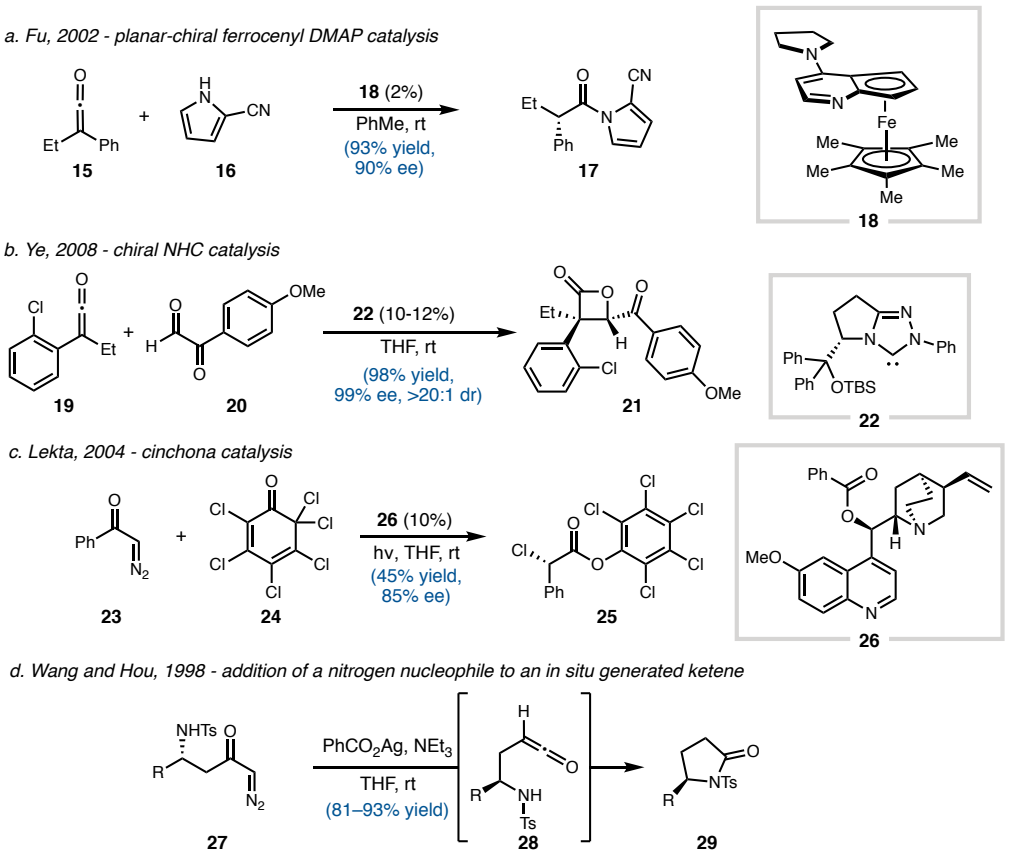

There are relatively few examples of enantioselective engagement of ketenes in the literature. The Fu lab has been able to access enantioenriched amides (as well as other enantioenriched products) from isolable ketenes through the use of planar-chiral ferrocenyl DMAP catalysts such as **18** (**Scheme 1.2a**).[12–16] Chiral NHC catalysts (**22**) have been used by Ye and coworkers for a variety of enantioselective reactions with isolable ketenes,

including the preparation of chiral β lactones (**21**) (**Scheme 1.2b**).[17] Though powerful and effective transformations, these reactions have only been reported with isolable ketene substrates, and to the best of our knowledge, have not been effective with ketene substrates generated *in situ*. At the outset of this project, we were aware of only one literature example of *in situ* ketene generation with subsequent asymmetric *intermolecular* nucleophilic addition to afford enantioenriched products. In 2004, the Leckta group disclosed a method to trap an *in situ* generated ketene from the corresponding diazoketone **23** to access enantioenriched ester **25** using cinchona alkaloid catalysis (**Scheme 1.2c**).[18] Though they were able to access the desired products, the yields and enantioselectivities were still inferior to the systems reported by Fu and Ye, indicating the inherent difficulty of asymmetric trapping of *in situ* generated ketenes. In 1998, Wang and Hou disclosed an example of an *intramolecular* addition of a nitrogen nucleophile to an *in situ* generated ketene to afford cyclic lactams **29** in good yield.[19] This example was promising, indicating that an *in situ* generated ketene could indeed be trapped by a nitrogen nucleophile.

With these reactions in mind, these three catalyst types were evaluated for their ability to effect enantioselective trapping of ketene **9**.[8,9,20] It was anticipated that this transformation would be difficult owing to the large amount of background reactivity observed in the absence of catalyst (**Figure 1.2**). Gratifyingly, promising reactivity was observed with planar-chiral DMAP-type catalysts such as catalyst ***ent*-18**, which afforded the desired enantioenriched cyclobutamide (–)-**6** in 46% ee, but with poor yields. Similarly, NHC catalyst **32** afforded (–)-**6** with good enantioselectivity, but with poor yields and reproducibility issues. This could be attributed to potential decomposition of the NHC catalysts under the photolytic conditions required to generate the ketene. Despite the low

Figure 1.2 *Summary of catalyst reactivity*

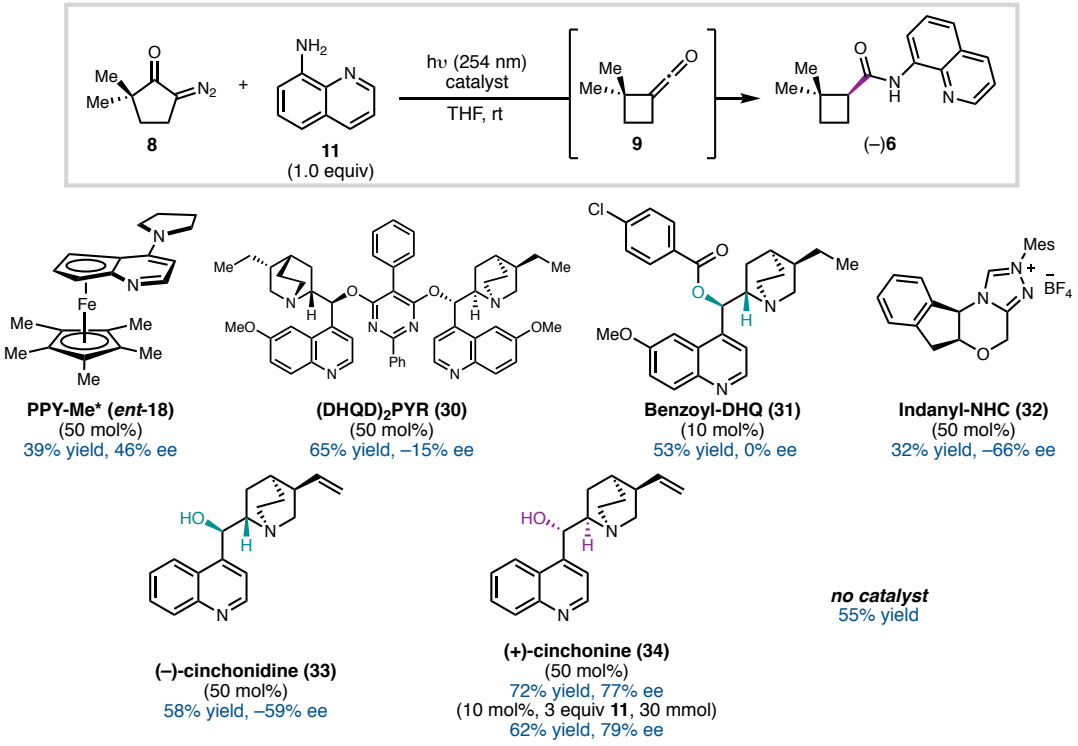

yields, these reactions provided proof of principle for the enantioselective trapping of ketene **9**. After further investigation, cinchonine (**34**), a naturally occurring cinchona alkaloid, was determined to be the optimal catalyst for this reaction, affording the desired product in 72% yield and 77% ee. The *pseudo*-enantiomer of cinchonine, cinchonidine (**33**) afforded the opposite enantiomer of product, albeit in lower yield and only –57% ee, which was intractable for synthesis. Investigation of various solvents revealed that THF provided the highest levels of enantioselectivity. More concentrated reaction mixtures led to lower yields, presumably due to poor light penetration as a result of the sparing solubility of **34** in THF. When scaling the reaction to quantities relevant for total synthesis (30 mmol), the catalyst loading of **34** could be reduced to 10 mol %, which provided (–)-**6** in 62% yield and 79% ee. Multiple grams of enantiopure material could be obtained through a single

recrystallization. Development of these scalable, robust conditions allowed for the completion of the total synthesis of (+)-psiguadial B (**1**). Interestingly, dimeric cinchona catalyst **30** and modified quinine-based catalyst **31,** which both lack a free hydroxyl group, gave the desired product with little to no enantioselectivity. Interested in potential applications of this reaction to the preparation of other enantioenriched amides, the possible mechanisms for this reaction were considered.

Figure 1.3 *Potential reaction mechanisms for enantioselective ketene trapping*

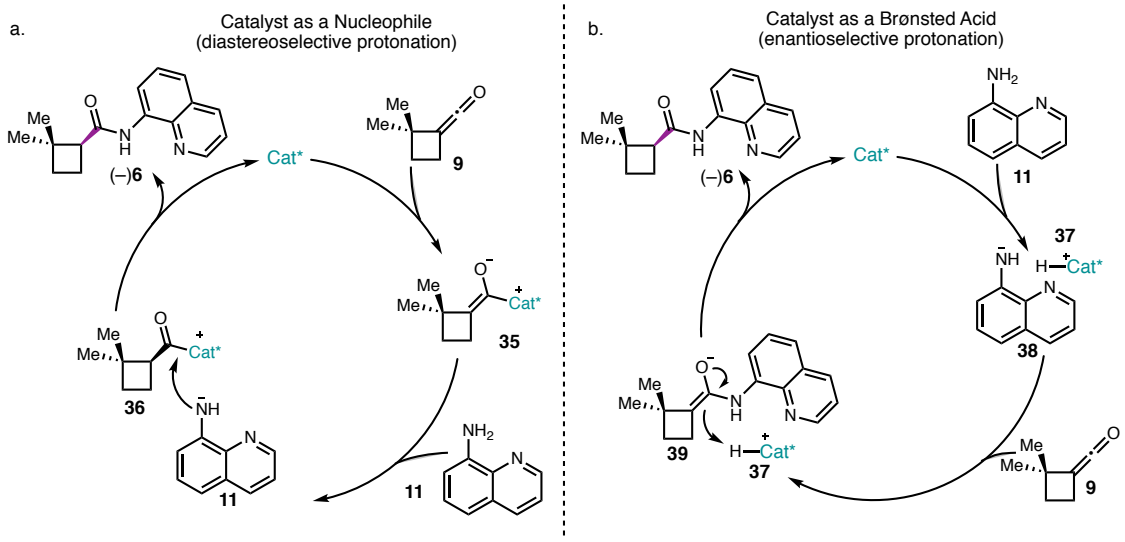

Two potential mechanisms for enantioselective trapping of ketenes were considered: 1) diastereoselective protonation and 2) enantioselective protonation (**Figure 1.3**). The diastereoselective protonation mechanism postulates that enantioselectivity is imparted through a diastereoselective protonation of chiral, zwitterionic enolate intermediate **35**.[21–26] This intermediate would be formed by nucleophilic trapping of ketene **9** by the chiral catalyst (**Figure 1.3a**). Due to the high nucleophilicity of the quinuclidine core of cinchona-type catalysts, this is thought to be the mechanism of most cinchona alkaloid-mediated asymmetric reactions with ketenes. It has also been shown

computationally that stabilizing hydrogen bonds can form between the enolate and the quinuclidine core of cinchona catalysts, the rigidity of which could help afford enantioselectivity.[25,26]

Another potential mechanism was proposed by the Fu group based on their work with planar-chiral ferrocenyl DMAP catalysts.[13] Instead of acting as a nucleophile (Lewis base), the catalyst could act as a Brønsted base and deprotonate the amine nucleophile (here, 8-aminoquinoline **11**). This nucleophile could engage the ketene to form enolate **39**, which could then undergo enantioselective protonation by the protonated chiral catalyst (**37**) (**Figure 5b**). A particularly compelling piece of evidence for this mechanism disclosed by the authors for their system is the observation that the resting state of the catalyst is not the neutral catalyst, but the ion pair formed by deprotonation of the amine by the catalyst (such as **37** and **38**).

Scheme 1.3 *Preliminary mechanistic studies*

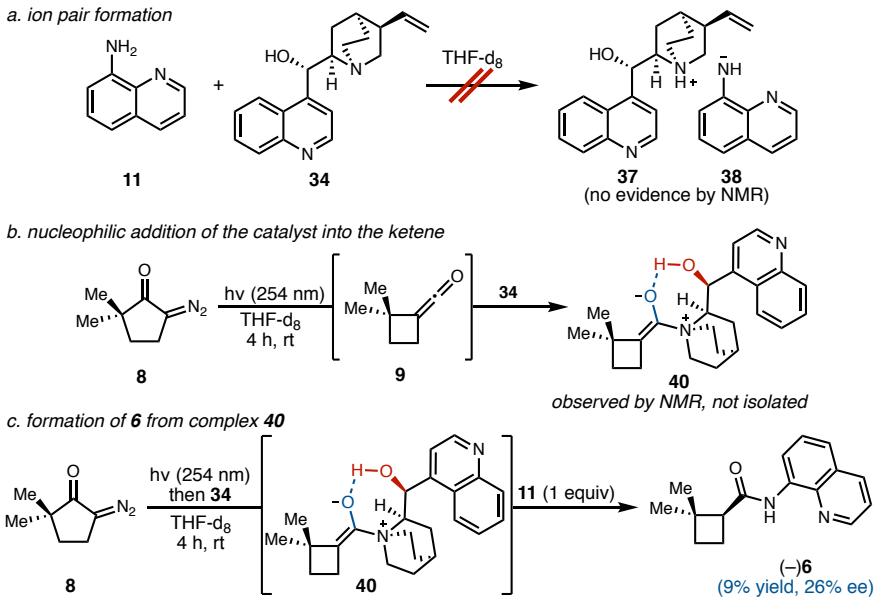

A number of experiments were performed in hopes of gaining a better understanding of the mechanism responsible for providing the observed product.[20] When

8-aminoquinoline (**11**) and cinchonine (**34**) were combined in THF-d_8, no formation of the ion pair **37** and **38** was observed by NMR, as would be expected for the enantioselective protonation mechanism (**Scheme 1.3a**). However, this does not preclude formation of a small amount of this species in the reaction mixture. In addition, when a solution of **8** and **38** was irradiated in THF-d_8 for four hours, NMR shifts indicative of the formation of complex **40** were observed, which would support the diastereoselective protonation mechanism (**Scheme 1.3b**). However, when this complex was then treated with **11**, formation of the desired product was observed in only 9% yield and 26 % ee, indicating that complex **40** might not be a viable intermediate in the active mechanism (**Scheme 1.3c**). Therefore, at this time, the predominant reaction mechanism for the formation of cyclobutamide **6** remains unclear.

Figure 1.4 *Model for diastereoselective protonation*

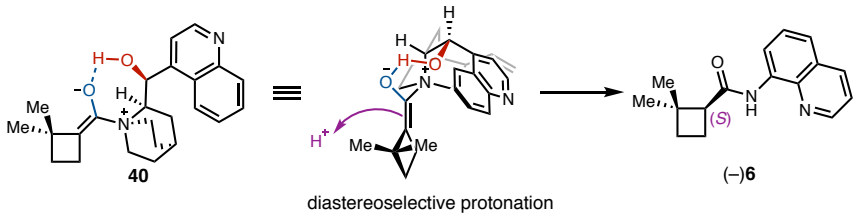

One interesting aspect of this system is the loss of enantioselectivity when the hydroxyl group of the cinchona catalyst is masked. This contrasts examples from Lekta and Calter, where cinchona catalysts containing a masked hydroxyl group afford the desired product in good enantioselectivity.[18,24–26] Based on these results and simple molecular models, formation of a hydrogen bond between this free hydroxyl and the enolate oxygen in complex **40** could be a significant interaction that imparts rigidity to the system and helps to enforce the observed enantioselectivity in this system (**Figure 1.4**). With the hydrogen bond in place, the conformation of the quinoline over the *re* face in **40**

could promote protonation from the *si* face to afford the observed enantiomer (–)**6**. However, the low enantioselectivity observed upon treatment of **40** with 8-aminoquinoline to form (–)**6** renders this hypothesis somewhat tenuous.

1.1.2 C–H Alkenylation

Scheme 1.4 *C–H functionalizations of cyclobutanes*

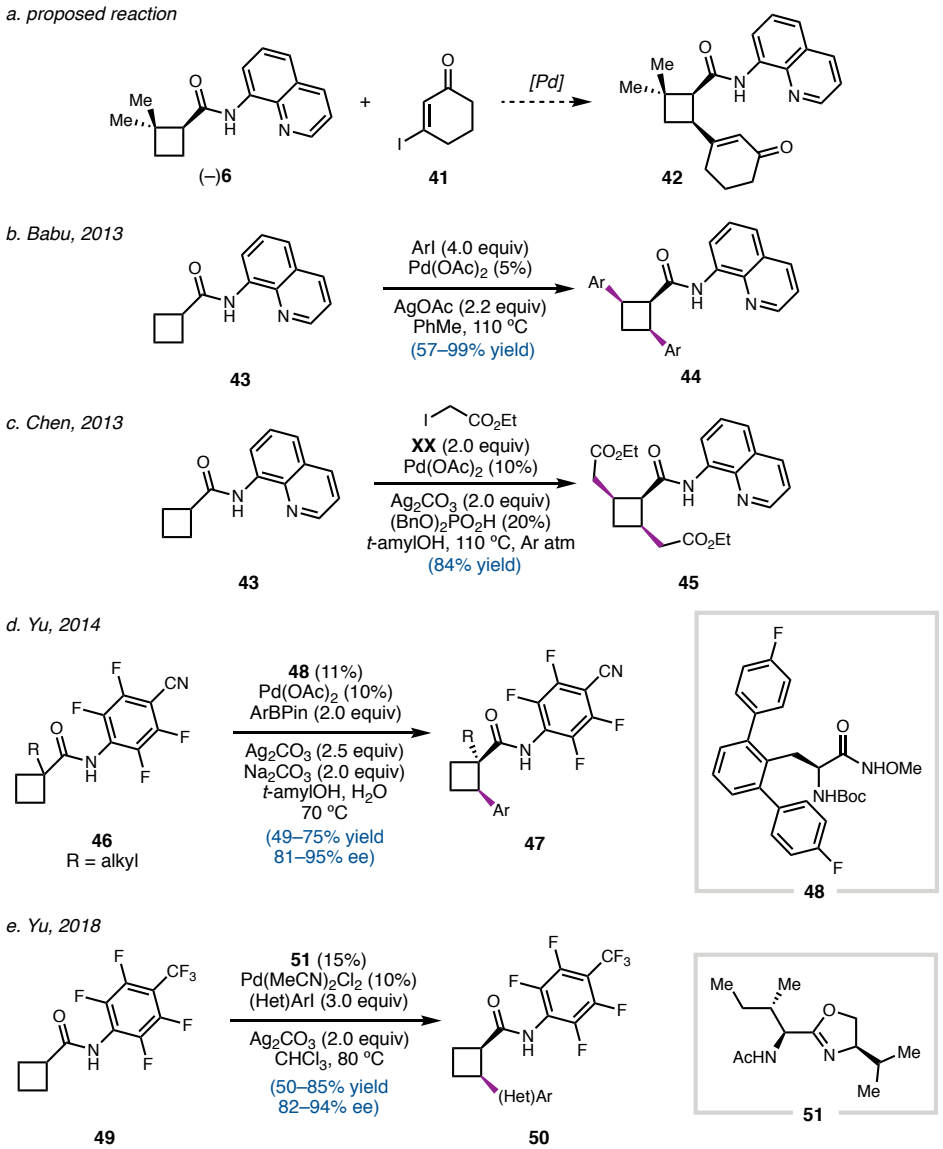

With enantioenriched cyclobutamide (–)**6** in hand, the next step was to install functionality at the β position to help build up the structure of (+)-psiguadial B. 8-

aminoquinoline is a well-known directing group for C–H activation of alkyl C–H bonds (**Scheme 1.4a,b**).[27,28] Both Babu and Chen demonstrated that 8-aminoquinoline was a good directing group for palladium-catalyzed diastereoselective arylation and alkylation of cyclobutamide **43** respectively (**Scheme 1.4b,c**).[29,30] Both observed bis-functionalization of the cyclobutane. Yu and coworkers have demonstrated elegant enantioselective C–H

Scheme 1.5 *C–H functionalization in total synthesis*

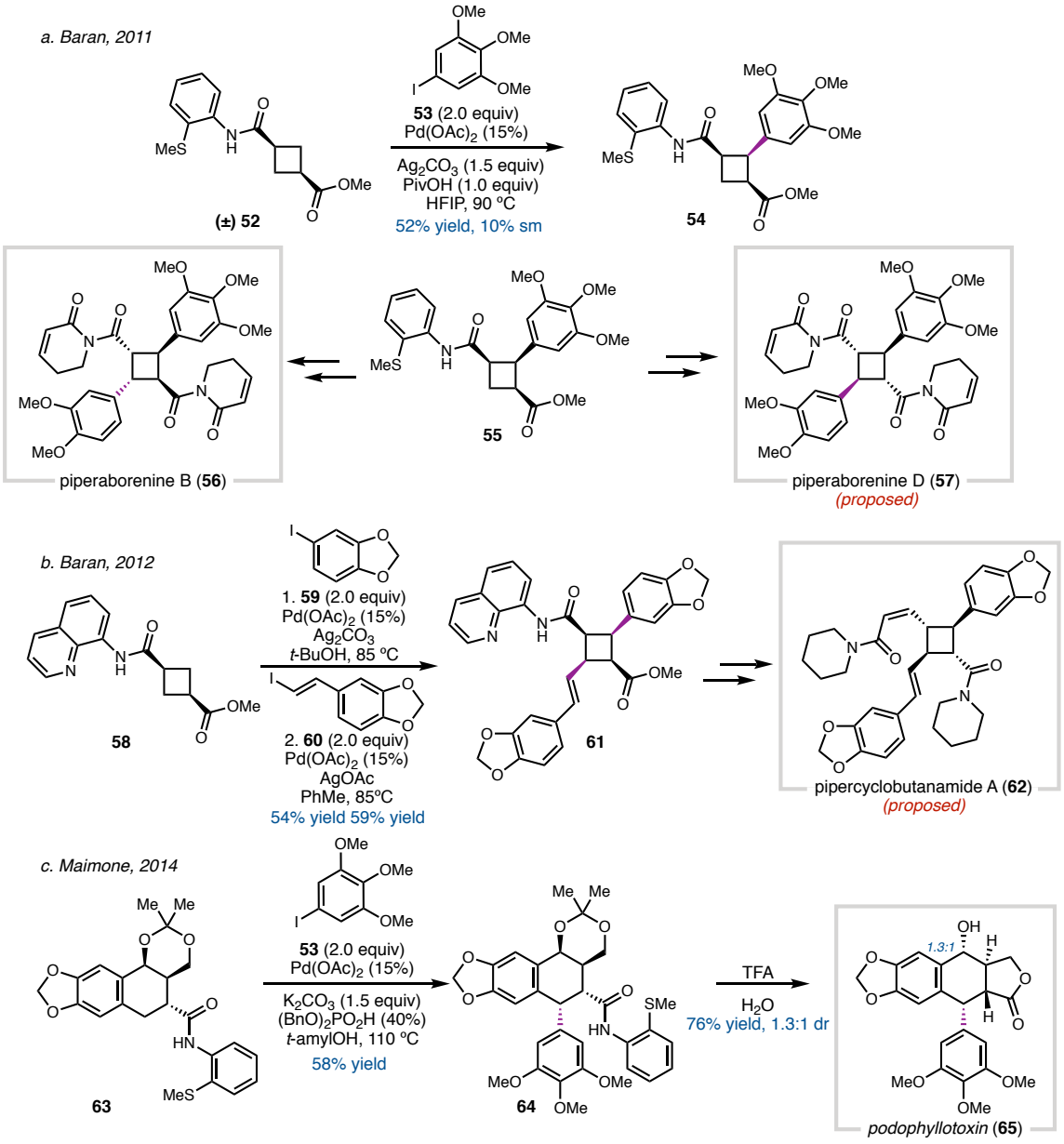

arylation methods of tertiary and secondary cyclobutamides **46** and **49** using chiral ligands to afford the mono-arylated products in good yield and ee.[31,32]

In addition to C–H activation methodologies for the functionalization of cyclobutanes, diastereoselective C–H activation of more complex substrates in total synthesis has also been shown.[33–36] In 2011, Baran and coworkers utilized multiple diastereoselective C–H arylations of cyclobutane intermediates in their racemic syntheses of piperaborenine B (**56**) and the proposed structure of piperaborenine D (**57**) (**Scheme 1.5a**).[33] Similarly, in 2012, they utilized a C–H activation strategy in their synthetic efforts towards the proposed structure of pipercyclobutanamide A (**62**) (**Scheme 1.5b**).[34] Together, these strategies demonstrated that C–H functionalization of cyclobutamides is an effective tool for total synthesis. In 2014, Maimone showed that diastereoselective C–H arylation was also effective in total synthesis for the functionalization of six-membered substrate **53** for their total synthesis of podophyllotoxin (**65**) (**Scheme 1.5c**).[36]

Figure 1.5 *Synthesis of both enantiomers of* ***5*** *from a single intermediate*

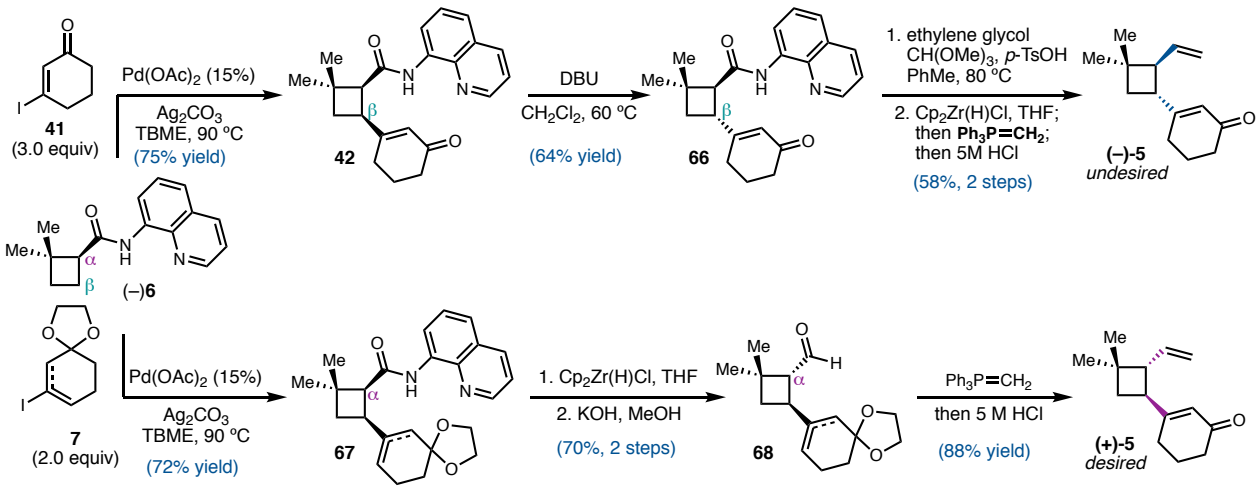

We were pleased to find that treatment of (–)**6** with $Pd(OAc)_2$ (15 mol %), Ag_2CO_3, and alkenyl iodide **41** in TBME at 90 °C without the use of a ligand smoothly effected the

desired C(sp^3)–H alkenylation reaction to give *cis* cyclobutane **42** in 75% yield (**Figure 1.5**).[8] Following epimerization of the β-position, *trans* cyclobutane **66** could be elaborated to (–)-**5**. However, it was soon found that this was the undesired enantiomeric series for the synthesis of (+)-psiguadial B. As (+)-**5** could not be synthesized in synthetically tenable yield or ee due to the poor catalytic behavior of cinchonidine (**33**) compared to cinchonine (**34**) for the asymmetric Wolff rearrangement, another approach was required. Fortunately, simply switching to alkenyl iodide **7** allowed for epimerization at the α position to afford *trans* cyclobutane **38**, which could then be elaborated to (+)-**5** in the same number of steps and a higher overall yield. It is notable that this strategy allowed for the efficient synthesis of both enantiomers of **5** from an intermediate synthesized using one enantiomer of organocatalyst.

Figure 1.6 *Reactions developed for the synthesis of (+)-psiguadial B*

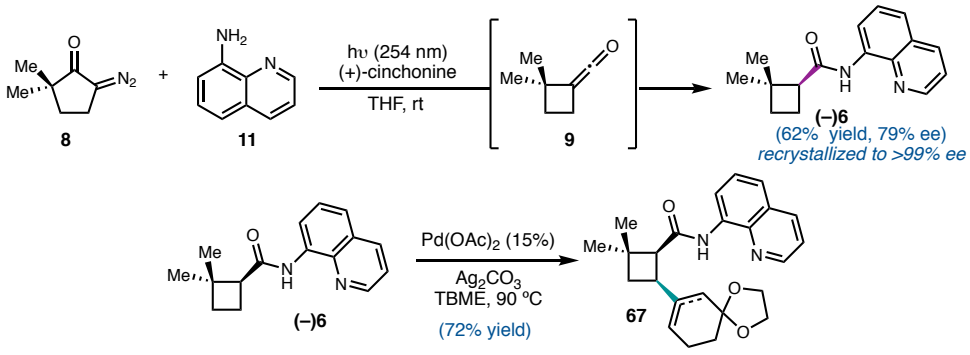

Development of these two reactions was key for the completion of the total synthesis of (+)-psiguadial B.[8] Both of these reactions were highly scalable and robust, allowing for synthesis of *cis* cyclobutane products on multigram scale (**Figure 1.6**). Due to the scalability and utility of these reactions, we sought to investigate them individually to broaden their scope and applicability.

1.2 WOLFF REARRANGEMENT AND ASYMMETRIC KETENE TRAPPING

Figure 1.7 *General approach for the synthesis of enantioenriched products* ***6, 73–76***

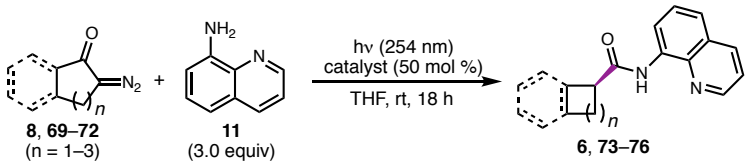

First, the tandem Wolff rearrangement/asymmetric ketene addition sequence was investigated. It was hoped that this reaction could be used to access enantioenriched products of various ring sizes (**Figure 1.7**). To this end, a variety of cyclic α-diazoketones were synthesized using known methods.[10,11] In addition, a variety of cinchona alkaloid-type catalysts were investigated.

Figure 1.8 *Cinchona-type catalysts and dimers*

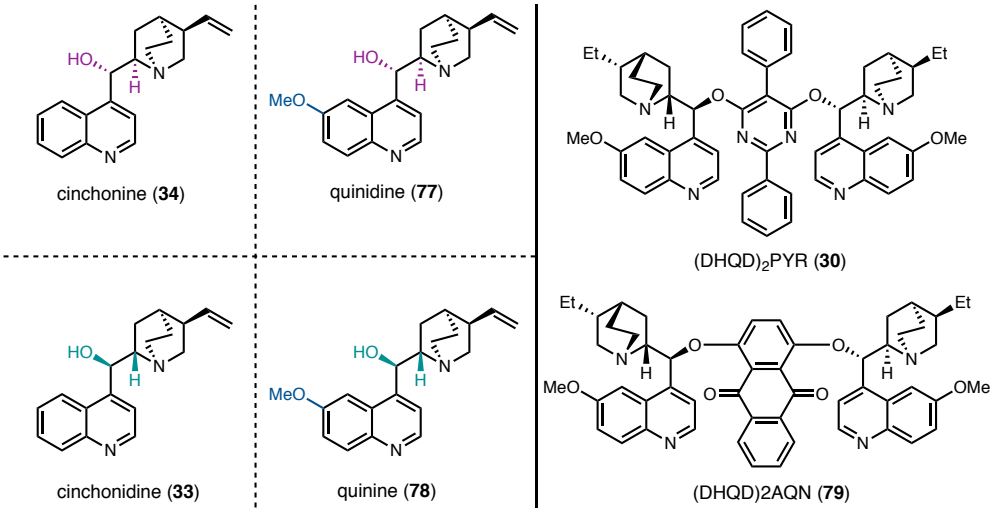

The four naturally occurring cinchona catalysts are cinchonine (**34**), cinchonidine (**33**), quinidine (**77**), and quinine (**79**) (**Figure 1.8**). The differences among these four catalysts can be grouped into two categories: 1) structural differences at the quinuclidine

and hydroxy core, and 2) the electronic differences on the quinoline ring. For example, cinchonine (**34**) and cinchonidine (**33**) have different quinuclidine methine and hydroxyl stereochemistry, yet both have unsubstituted quinoline rings. They are therefore thought of as *pseudo*-enantiomers, as are quinidine and quinine. Preservation of the quinuclidine stereochemistry at the bridgehead carbon as well as the pendent alkene across all four alkaloids means there are no true enantiomeric pairs. On the other hand, cinchonine (**34**) and quinidine (**77**) have identical hydroxyl and quinuclidine methine stereochemistry (highlighted in purple), but only quinidine contains a methoxy group on the quinoline, resulting in different electronic properties on the quinoline. Cinchonidine (**33**) and quinine (**79**) have the same relationship. As these are naturally occurring compounds, the opposite enantiomers are not easily accessible. In addition to the natural occurring catalysts, hydrogenated and C9-epimerized versions of each of the parent catalysts were synthesized using known methods (**Table 1.1**, section 1.5.2).[37,38] Two commercially available dimers of dihydroquinidine (DHQD) (**81**), $(DHQD)_2PYR$ (**30**) and $(DHQD)_2AQN$ (**79**), were also screened to examine whether cinchona catalysts containing masked hydroxyl groups would continue to afford lower enantioselectivities than cinchona catalysts with free hydroxyl groups, as observed previously.

Each reaction was run with 50% catalyst on a 0.05 mmol scale in a quartz test tube using conditions previously developed for the synthesis of cyclobutamide **6**. The results are shown in **Table 1.1**. Unfortunately, no one catalyst performed the best overall. While cinchonine was again shown to be the optimal catalyst for cyclopentanone **8**, it only afforded the other products with a maximum of 64% ee (entry 1). Interestingly, *epi*-quinidine (**85**) and quinidine (**77**) proved to be the optimal catalysts for cyclohexanone and

Table 1.1 *Wolff rearrangement catalyst and substrate screens*

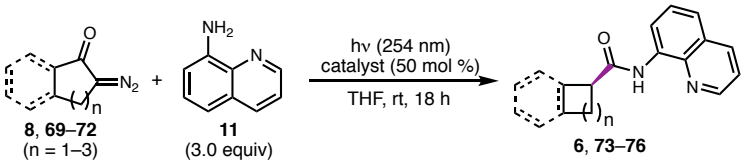

8, **69**–**72** (n = 1–3) + **11** (3.0 equiv) → **6**, **73**–**76**

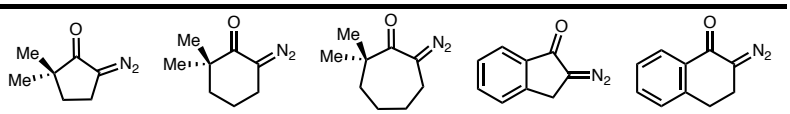

8 **69** **70** **71** **72**

entry	catalyst	% yield[a]	% ee[b]	% yield[a]	% ee[b]	% yield[a]	% ee[b]	% yield[a]	% ee[b]	% yield[a]	% ee[b]
1	cinchonine (**34**)	61[c]	79	64	58	49	64	48	9	54	35
2	DHCN (**80**)	56	65	68	48	51	61	-	-	47	34
3	*epi*-CN (**84**)	50	24	52	64	60	7	43	7	65	42
4	cinchonidine (**33**)	64	–57	62	–22	56	–51	48	–3	38	–20
5	DHCD (**82**)	58	–47	61	–3	52	–35	-	-	57	–10
6	*epi*-CD (**86**)	51	4	66	25	55	–12	-	-	57	18
7	quinidine (**77**)	67	64	69	50	59[c]	71	48	25	42	23
8	DHQD (**81**)	36	56	70	40	47	64	-	-	43	25
9	*epi*-QD (**85**)	58	48	77[c]	71	55	7	40	7	61	41
10	quinine (**78**)	66	–54	66	0	54	–34	48	–26	42	–23
11	DHQN (**83**)	19	–18	62	31	47	–14	-	-	52	–10
12	*epi*-QN (**87**)	58	–9	67	18	57	–12	-	-	51	11
13	$(DHQD)_2PYR$ (**30**)	90	–16	60	–59	65	–7	47	–5	42[c]	–75
14	$(DHQD)_2AQN$ (**79**)	50	53	49	–23	50	37	31[c]	34	35	–1

[a] Reactions performed on 0.05 mmol scale and irradiated for 18 hours. Yield determined by 1H NMR analysis versus an added internal standard. [b] Determined by SFC using a chiral stationary phase. [c] 0.200 mmol scale, irradiated for 48 hours, isolated yield.

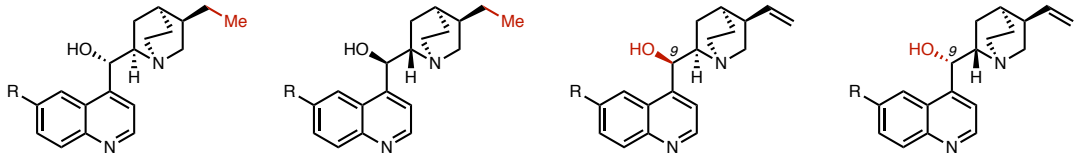

R = H, dihydrocinchonine (DHCN, **80**)
R = OMe, dihydroquinidine (DHQD, **81**)

R = H, dihydrocinchonidine (DHCD, **82**)
R = OMe, dihydroquinine (DHQN, **83**)

R = H, *epi*-C9 cinchonine (*epi*-CN, **84**)
R = OMe, *epi*-C9 quinidine (*epi*-QD, **85**)

R = H, *epi*-C9 cinchonidine (*epi*-CD, **86**)
R = OMe, *epi*-C9 quinine (*epi*-QN, **87**)

cycloheptanone substrates **69** and **70**, respectively, affording the desired products in 71% ee (entries 7, 9). It is notable that cinchonine (**34**) and quinidine (**77**) both have the same quinuclidine stereochemistry. Surprisingly, dimeric catalysts **30** and **79** performed the best for substrates **72** and **71**, respectively, though 5-membered substrate **71** performed poorly overall and was only isolated at a maximum of 34% ee (entries 13, 14). However, $(DHQD)_2AQN$ (**79**) performed poorly overall, affording the desired products in poor ee and low yield. This low reactivity and selectivity could be attributed to the fact that dissolution of **79** in THF results in a dark brown mixture, leading to poor light penetration

in the reaction. The moderate yield and good enantioselectivity afforded by $(DHQD)_2PYR$ (**30**) for substrate **72** contrasts the low ee's observed when using catalysts with masked hydroxyl groups for α-diazoketone **8** (entry 13, **Figure 1.2**), indicating that another mechanism could be active for these substrates. Overall, hydrogenated catalysts **80**–**83** afforded the products in lower ee than their parent catalysts (entries 2, 5, 8, 11), and the *epi*-catalysts (**84**–**87**) only improved the ee for 6-membered substrates **69** and **72** over the parent catalyst (entries 3, 6, 9, 12). To test scalability, each substrate was submitted to the reaction conditions on 0.200 mmol scale with its optimal catalyst. After 48 h, each product was isolated with comparable yield and ee to the small-scale reaction (entries 1, 7, 9, 13, 14).

Table 1.2 *Catalyst loading and reaction scale screening*

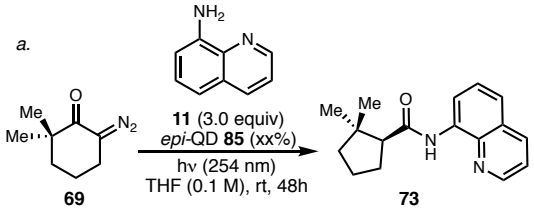

entry	cat loading (mol %)	% yield	%ee
1	50	73	71
2	30	81	69
3	20	76	67
4	10	81	63
5[a]	20	80	67
6[b]	20	81	68

[a]1.00 mmol scale, irradiated for 48h,
[b]5.00 mmol scale, irradiated for 5 days

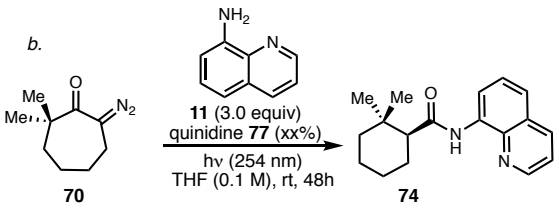

entry	cat loading (mol %)	% yield	%ee
1	50	66	73
2	30	71	66
3	20	61	62
4	10	61	55
5[a]	20	67	65

[a]1.00 mmol scale, irradiated for 48h

Next, catalyst loading was investigated. Substrates **69** and **70** were submitted to reaction conditions with lower catalyst loading (**Table 1.2**). While 7-membered substrate **70** showed about a 10% decrease in ee upon lowering the catalyst loading to 20% (**Table 1.2**b, entry 3), 6-membered substrate **69** showed only a minimal decrease in ee (**Table 1.2**a,

entry 3), though both suffered at 10% catalyst loading. Both reactions were scaled up to 1.00 mmol at 20% catalyst loading with comparable yields and ee's (**Table 1.2**a, entry 5, **Table 1.2**b, entry 5). **69** was scaled up to 5.00 mmol and afforded the product in 81% yield, 68% ee after 5 days (**Table 1.2**a, entry 6).

Figure 1.9 *Wolff rearrangement summary*

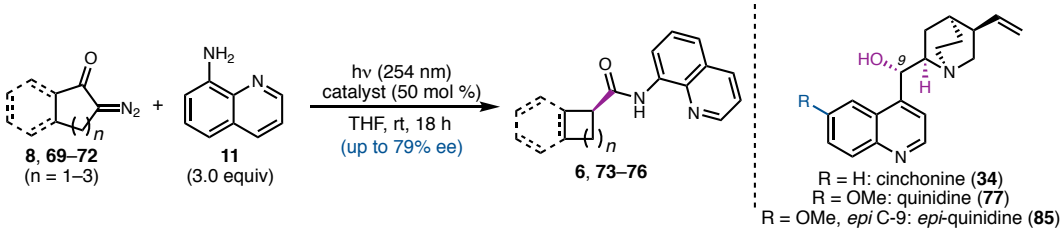

Though we were unable to identify a unified catalyst system for all substrates, decent yields as well as enantioselectivities greater than 70% were obtained for all but one substrate (**71**) after some catalyst optimization (**Figure 1.9**). In addition, several interesting trends were observed. In particular, the best-performing catalysts were related to quinidine. Cinchonine (**34**) is nearly structurally identical to quinidine, as is *epi*-QD (**85**). $(DHQD)_2PYR$ (**30**) and $(DHQD)_2AQN$ (**79**) are both dimers of dihydroquinidine (DHQD, **81**). However, the extreme variation in yields and enantioselectivities between substrates for a single catalyst is indicative of a more complex process. Indeed, the stark differences in results between gem-dimethyl substrates **8**, **69**, and **70** and fused substrates **71**–**72** indicate that substrate structure has a profound effect on the ability of the catalyst to impart enantioselectivity. The success of $(DHQD)_2PYR$ and the epimerized catalysts on cyclohexanone substrates alone (**69** and **72**) also suggests the potential influence of ring size on enantioselectivity.

1.3 C–H ARYLATION OF CYCLOBUTAMIDE 6

Table 1.3 *C–H arylation substrate scope*

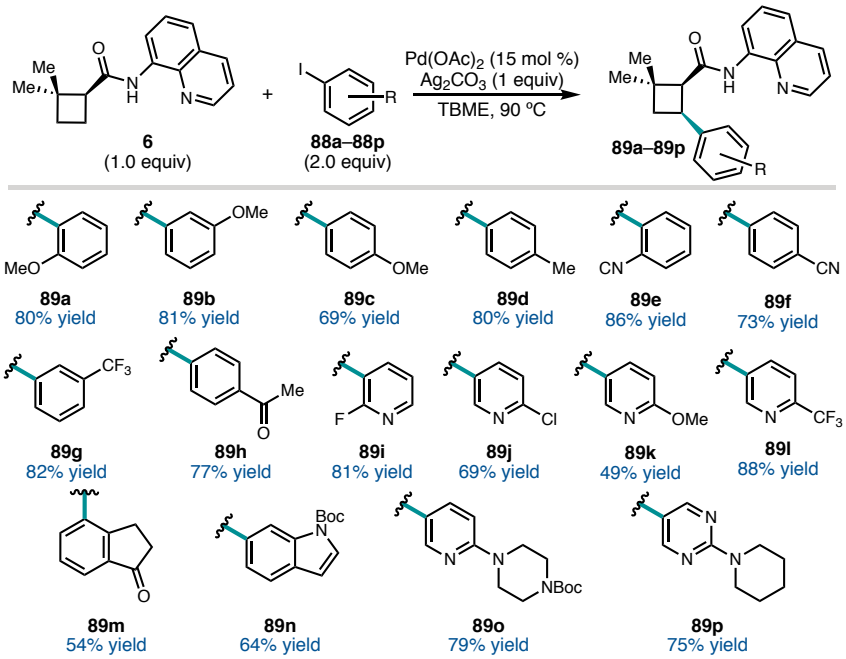

Having developed optimized conditions for the C(Csp^3)–H alkenylation of cyclobutamide **6**, we sought to investigate the breadth of coupling partners that could be utilized in this reaction. In particular, we were interested in the heteroarylation of C(Csp^3)–H bonds using these conditions. We were pleased to find that the conditions developed for the synthesis of (+)-psiguadial B (**1**) (namely, $Pd(OAc)_2$ (15%), $AgCO_3$ (1.0 equiv), and ArI (2.0 equiv) in TBME at 90 ºC) could afford a variety of cross-coupled products in good yields as a single diastereomer (**Table 1.3**). Substitution is tolerated at the *ortho*, *meta*, and *para* positions (**89a–89c**), and both electron donating and electron withdrawing groups were tolerated. A variety of nitrogen-containing heterocycles were found to be successful substrates as well. Pyridines with varying functionalities and substitution patterns are well tolerated (**89i–89l**, **89o**). Bicycle **89m** and indole **89n** both performed moderately well

under the reaction conditions. In particular, we were pleased to find that highly polar heterocycles **89o** and **89p** were well-tolerated, yielding products containing five nitrogen atoms each.

Table 1.4 *Low-yielding C–H arylation substrates*

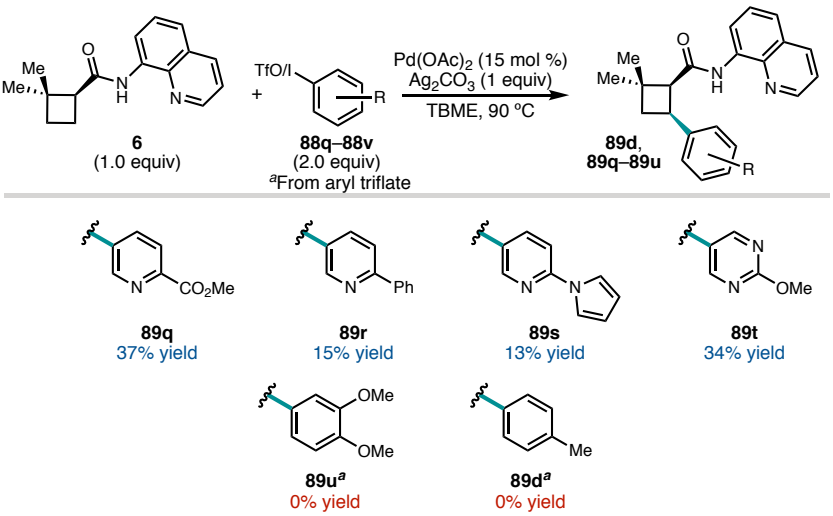

There were several limitations to this reaction (**Table 1.4**). Attempting to lower the catalyst loading to 7.5% or lowering the equivalents of aryl iodide to one equivalent both resulted in significant decreases in yield across the board. Some substrates could tolerate lower temperatures, though 90 ºC was required by most. In addition, certain pyridine substrates performed poorly. Pyridines with esters or aryl groups at 2-position all cross-coupled in low yields (**89q**, **89r**), as did 2-pyrrole substrate **89s**. Methoxy pyrimidine **89t** also performed very poorly, about 15% lower yield than the corresponding pyridine substrate (**89k**). Aryl triflates were not successful under these reaction conditions, though no further optimization was attempted; it is possible that modifications could be made that would accommodate these substrates.

1.4 CONCLUSION

Figure 1.10 *Summary of reaction development*

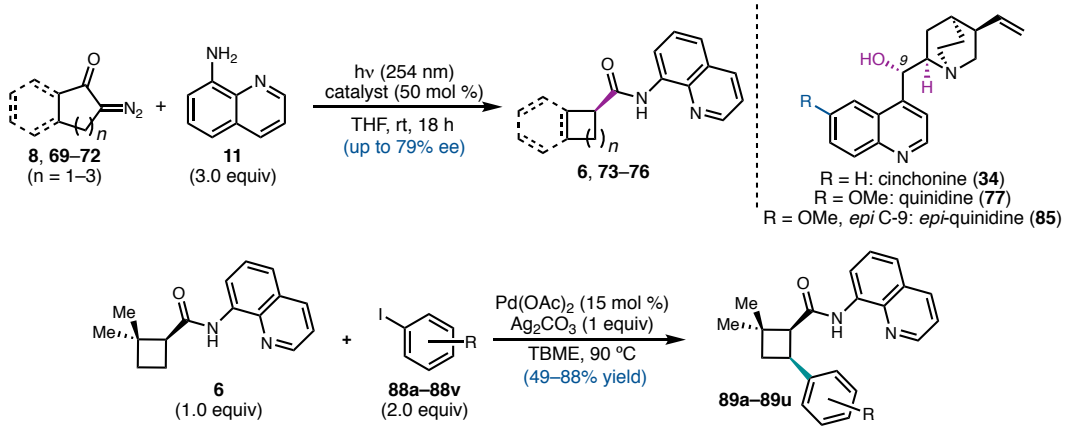

In conclusion, two reactions developed for the total synthesis of (+)-psiguadial B were developed into broader methods. The tandem Wolff rearrangement/asymmetric ketene addition suffered from lack of generality with regard to catalyst, but optimal catalysts were found for most substrates to afford products in synthetically useful yields and ee's. Cyclobutamide **6** was subjected to palladium-catalyzed C–H activation conditions with a variety of aryl and heteroaryl iodides to afford *cis* arylated products in good yields. These results were disclosed in separate publications in 2018 and early 2019, respectively.[9,39] Having developed a robust and scalable method to synthesize enantioenriched cyclobutamide **6** as well as a method to readily diversify **6** to a variety of arylated products, we then hoped to apply these methods to a broader, modular approach towards enantioenriched cyclobutanes as well as towards the synthesis of other *trans*-cyclobutane containing natural products (see Chapter 2).

1.5 EXPERIMENTAL SECTION

1.5.1 Materials and Methods

Unless otherwise stated, reactions were performed under a nitrogen atmosphere using freshly dried solvents. Methylene chloride (CH_2Cl_2), diethyl ether (Et_2O), tetrahydrofuran (THF), 1,4-dioxane, *tert*-butyl methyl ether (TBME), and toluene (PhMe) were dried by passing through activated alumina columns. Methanol (MeOH) was distilled over calcium hydride. Acetonitrile (MeCN), *tert*-butanol (*t*-BuOH), anhydrous *N,N*-dimethylformamide (DMF), anhydrous *N,N*-dimethylacetamide (DMA), chloroform ($CHCl_3$), and absolute ethanol (EtOH) were used as received from Fisher Scientific. Aryl iodides were purchased from Sigma-Aldrich or Combi-Blocks or prepared according to literature procedures. $Pd(OAc)_2$ was purchased from Strem and stored in a dessicator. All other commercially obtained reagents were purchased from Sigma-Aldrich and used as received unless specifically indicated. All reactions were monitored by thin-layer chromatography using EMD/Merck silica gel 60 F254 pre-coated plates (0.25 mm). Silica gel and basic alumina column chromatography was performed as described by Still et al. (W. C. Still, M. Kahn, A. Mitra, *J. Org. Chem*. **1978**, *43*, 2923.) using silica gel (particle size 0.032–0.063) purchased from Silicycle and aluminum oxide (activated, basic, Brockmann I, 58 Å pore size, powder) purchased from Sigma-Aldrich. ^{1}H and ^{13}C NMR were recorded on a Varian Inova 500 (at 500 MHz and 125 MHz, respectively) or a Bruker Avance III HD with Prodigy cyroprobe (at 400 MHz and 101 MHz, respectively). ^{19}F NMR spectra were recorded on a Varian Inova 400 (at 376 MHz). NMR data is reported relative to internal chloroform (^{1}H, $\delta = 7.26$, ^{13}C, $\delta = 77.2$) or to internal methanol (^{1}H, $\delta = 3.31$, ^{13}C, $\delta = 49.0$) and $PhCF_3$ (^{19}F, $\delta = -63.7$). Data for ^{1}H NMR spectra are reported as follows: chemical

shift (δ ppm) (multiplicity, coupling constant (Hz), integration). Multiplicity and qualifier abbreviations are as follows: s = singlet, d = doublet, t = triplet, q = quartet, m = multiplet. IR spectra were recorded on a Perkin Elmer Paragon 1000 spectrometer and are reported in frequency of absorption (cm^{-1}). HRMS were acquired using either an Agilent 6200 Series TOF with an Agilent G1978A Multimode source in electrospray ionization (ESI), atmospheric pressure chemical ionization (APCI), or mixed (MM) ionization mode. Specific optical rotations were recorded on a Jasco P-2000 polarimeter using a 100 mm cell.

Abbreviations used: Et_2O – diethyl ether; CH_2Cl_2 – methylene chloride; PhMe – toluene; EtOAc – ethyl acetate; THF – tetrahydrofuran; *t*-BuOH – *tert*-butanol; $CHCl_3$ – chloroform; MeCN – acetonitrile; DMF – *N,N*-dimethylformamide; DMA – *N,N*-dimethylacetamide; dtbbpy – 4,4'-di*tert*butylbipyridine; dme – 1,2-dimethoxyethane; TBME – *tert*-butyl methyl ether.

1.5.2 Synthesis of Hydrogenated and epi-Cinchona Alkaloids

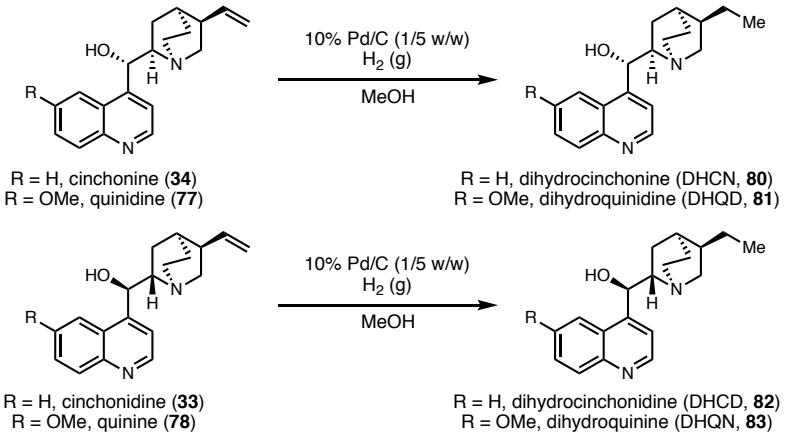

General Procedure 1: Synthesis of hydrogenated catalysts **80–83**[37]

To a flame-dried round bottom flask was added cinchona alkaloid (**33**, **34**, **77**, **78**) (1.0 equiv) and 10% Pd/C (1/5 w/w). Flask was evacuated and backfilled with nitrogen x 3. Dry

methanol (distilled over CaH_2) (0.13M) was then added. The reaction mixture was sparged with H_2 for 5 minutes, then allowed to stir under a H_2 atmosphere at room temperature overnight. The next day the reaction was sparged with nitrogen. The reaction mixture was diluted with formic acid to dissolve the resultant precipitate, and Pd/C was removed by filtration over celite, washing with methanol. The reaction mixture was concentrated *in vacuo*, then diluted with ~ 5 mL H_2O. The solution was stirred and aq conc NH_3 was added until a precipitate formed. The precipitate was collected by filtration, washed with water, and dried at 45 ºC under high vac for ~ 6 hours. **80**–**83** were isolated cleanly without any further purification in 72–85% yield. NMR spectra matched lit report.

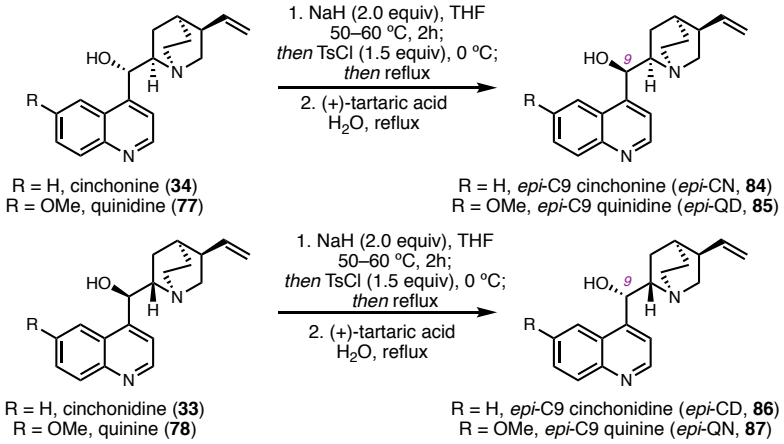

General Procedure 2: Synthesis of *epi*-C9-cinchona catalysts (**84–87**)[38]

To a 3-neck flame-dried flask was added cinchona alkaloid (**33**, **34**, **77**, **78**) (1.0 equiv). The flask was evacuated and backfilled with nitrogen x 3. THF (0.93 M) was added followed by NaH (2.0 equiv, 60% dispersion in oil). The reaction was heated to 50–60 ºC and stirred for 2 h. Turned banana yellow. After 2 hours, removed from heat and cooled in an ice bath to 0 ºC. Tosyl chloride (TsCl) (1.5 equiv) was dissolved in THF (0.56 M wrt TsCl) and cooled to 0 ºC. The chilled solution was added to the reaction mixture (reaction turned more white). Once the addition was complete, the reaction mixture was heated to

reflux and stirred overnight. Once the reaction was complete, it was allowed to cool. 1 M HCl (~ 20 equiv HCl) was added and the reaction mixture turned orange. Washed with Et_2O x 2, discarded organic layers. Na_2CO_3 (26 equiv, until pH 11) was added to the aqueous layer. Extracted with Et_2O x 4. Combined organic layers, washed with sat. aq. NaCl, and dried over $MgSO_4$, filter, and concentrated *in vacuo*. Crude material purified by silica gel chromatography (40:1 $CHCl_3$/MeOH).

To a flask containing *O*-tosyl cinchona alkaloid was added (+)-tartaric acid (1.04 equiv) and H_2O (0.09 M). The reaction mixture was heated to reflux. As it was heated, the solids began to dissolve. After 1 hour, the reaction mixture was allowed to cool. Na_2CO_3 was added slowly until the reaction mixture stopped bubbling and turned opaque (~pH 10–11). Extracted with Et_2O x 6, washed combined organic layers with sat aq. $NaHCO_3$, dried the organic layer over $MgSO_4$, filtered, and concentrated *in vacuo*. Purified by silica gel chromatography, 20:20:1:1 hexanes/$CHCl_3$/MeOH/NEt_3. NMR spectra of isolated products **84–87** matched lit report.

1.5.3 Synthesis of Diazoketones 8, 69–72

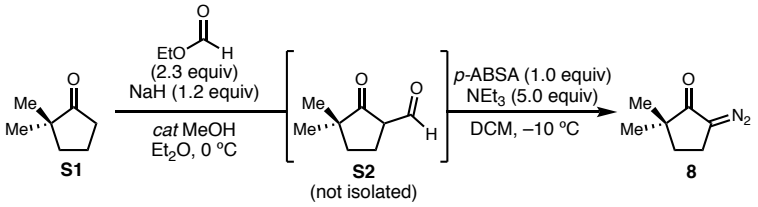

Preparation of diazoketone 8:[10,11] To each of two flame-dried 1 L round-bottom flasks was added NaH (60% dispersion in mineral oil, 3.17 g, 79.2 mmol, 1.20 equiv) and the atmosphere was exchanged for N_2 one time. Dry Et_2O (30.0 mL) was then added via syringe, and the suspension was cooled to 0 °C. Ethyl formate (12.4 mL, 152 mmol, 2.30 equiv) was then added, followed by 2,2-dimethylcyclopentanone (7.40 g, 66.0 mmol) either

neat, or as a 3.0 M solution in Et_2O. A catalytic amount of wet methanol (~100 μL) was then added and the reaction left to stir at 0 °C. Upon completion, the reaction solidified to a chunky, white solid that dissolved readily upon the addition of DI H_2O. At this point, both reaction mixtures were combined for workup: after dilution with Et_2O, the layers were separated, and the aqueous layer was washed with Et_2O x 3 to remove organic impurities and a small amount of unreacted starting material. The aqueous layer was then cooled to 0 °C and acidified to pH = 3 using 5 M HCl. Et_2O was then added, and the acidified aqueous layer was extracted x 6. The combined organics were then dried over Mg_2SO_4, filtered, and concentrated *in vacuo* into a 500 mL round-bottom flask.

The crude α-formyl ketone (**S2**) was taken up in CH_2Cl_2 (132 mL) and the solution cooled to –10 °C. Triethylamine (55.2 mL, 396 mmol, 5.00 equiv) was added, followed by solid *p*-ABSA (31.8 g, 132 mmol, 1.00 equiv) in three portions. The reaction was stirred for 3 hours and allowed to gradually reach 10 °C, at which point an aqueous solution of KOH (55.0 mL, 4 M) was added. Additional CH_2Cl_2 and H2O were added, the layers were separated and the aqueous layer extracted with CH_2Cl_2 until no product remained by TLC. The combined organics were dried over Mg_2SO_4, filtered, and concentrated *in vacuo*. The crude residue was purified by silica gel flash chromatography (20–30% Et_2O/pentane) to afford **8** (17.4 g, 95% yield) as a bright yellow oil.

^{1}H NMR (400 MHz, $CDCl_3$) δ 2.88 (t, *J* = 7.0 Hz, 2H), 1.77 (t, *J* = 7.2 Hz, 2H), 1.04 (d, *J* = 1.0 Hz, 6H).

^{1}H NMR (400 MHz, d_8-THF) δ 2.94 (t, *J* = 7.0 Hz, 2H), 1.79 (t, *J* = 7.2 Hz, 2H), 1.04 (s, 6H).

^{13}C NMR (101 MHz, $CDCl_3$) δ 204.8, 56.6, 46.3, 35.7, 24.1, 21.2.

^{13}C NMR (101 MHz, d_8-THF) δ 203.6, 56.1, 46.9, 36.6, 24.5, 21.9.

FTIR (NaCl, thin film) 3754, 3414, 3332, 2962, 2934, 2892, 2869, 2672, 2642, 2578, 2510, 2080, 1981, 1673, 1581, 1471, 1460, 1382, 1362, 1339, 1309, 1267, 1245, 1204, 1133, 1110, 1058, 1030, 994, 977, 948, 919, 893, 780, 726, 697 cm.$^{-1}$

Diazoketones **69**–**72** were prepared according to the procedure developed for **8**. Spectroscopic data for **71** and **72** are consistent with that reported in the literature.[40–44]

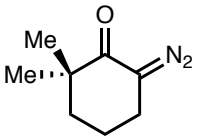

69

(69): Yellow Oil, (1.76 g, 36% yield over 2 steps).

^{1}H NMR (400 MHz, $CDCl_3$) δ 2.71 (t, J = 6.5 Hz, 2H), 1.82 – 1.73 (m, 2H), 1.68 –1.61 (m, 2H), 1.15 (s, 6H).

^{13}C NMR (101 MHz, $CDCl_3$) δ 200.1, 62.6, 42.0, 37.5, 26.7, 22.9, 18.5.

FTIR (NaCl, thin film) 2943, 2864, 2082, 1626, 1472, 1449, 1381, 1342, 1317, 1275, 1261, 1220, 1201, 1162, 1122, 1044, 1011, 910, 853, 738, 658 cm.$^{-1}$

HRMS (EI) calc'd for $C_8H_{12}N_2O$ $[M]^+$ 152.0950, found 152.0956.

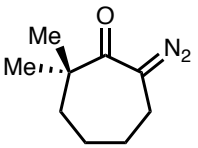

70

(70): Yellow Oil, (400.0 mg, 26% yield over 2 steps)

^{1}H NMR (400 MHz, $CDCl_3$) δ 2.55 (ddt, J = 7.0, 4.8, 2.3 Hz, 2H), 1.75 (dt, J = 4.4, 2.8 Hz, 4H), 1.57 (ddt, J = 6.3, 3.4, 1.7 Hz, 2H), 1.17 (s, 6H).

^{13}C NMR (101 MHz, $CDCl_3$) δ 202.2, 68.3, 47.0, 37.9, 29.5, 25.8, 25.7, 25.6.

FTIR (NaCl, thin film) 2981, 2966, 2927, 2858, 2083, 1704, 1617, 1474. 1448, 1387. 1364, 1350, 1324, 1272, 1251, 1231, 1203, 1147, 1113, 1057, 1020, 980, 953, 871, 845, 736, 656 cm.$^{-1}$

HRMS (EI) calc'd for $C_9H_{14}N_2O$ $[M]^+$ 166.1106, found 166.1095.

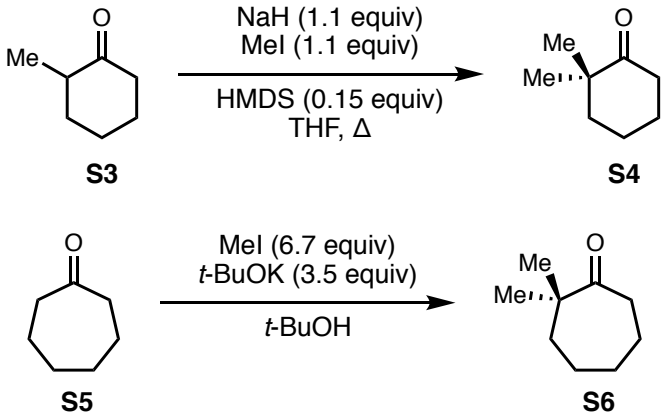

Gem-dimethyl ketones **S4** and **S6** were synthesized according to known methods.[41,45]

1.5.4 Small-scale screening protocol for enantioenriched amides 6, 73–76:

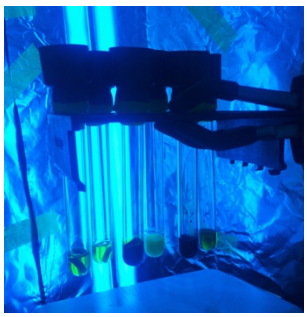

Oven-dried quartz tubes were each charged with aminoquinoline (21.6 mg, 0.150 mmol, 3.00 equiv) and catalyst (50 mol %). Inside a N_2-filled glovebox, diazoketones **8**, **69–72** (0.05 mmol) were then added to each as a solution in 0.500 mL THF (excluding diazoketone **72**, which was added as a solid outside of the glovebox). The reactions were then sealed with a 19/38 rubber septum around the outside of each tube and sealed with electrical tape. The reactions were then brought out of the glovebox and placed in a bottomless test tube rack in front of a Honeywell 254 nm lamp. The reactions were irradiated with stirring at room temperature for 18 hours. The reactions were then concentrated *in vacuo,* and the crude reaction mixtures were analyzed by ^{1}H NMR with an added internal standard to determine % yield. The crude residues were purified by silica gel preparative TLC (2% Et_2O/CH_2Cl_2) to provide 18, 42–45 in varying yields and enantiopurities.

1.5.5 Large-scale protocol for enantioenriched amide 6

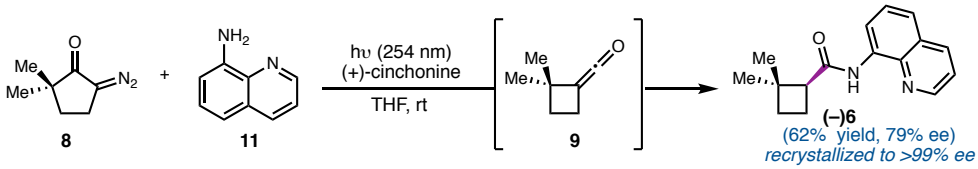

To a flame-dried, 1 L quartz flask was added 8-aminoquinoline (**11**) (12.9 g, 89.5 mmol, 3.00 equiv) and (+)-cinchonine (**34**) (879 mg, 2.99 mmol, 0.100 equiv). The flask was evacuated and backfilled with N_2 three times, and dry THF (600 mL) was then added via cannula. Diazoketone **8** (4.12 g, 29.8 mmol, 1.00 equiv) was added last via syringe and the reaction was irradiated with stirring using a Honeywell 254 nm lamp at room temperature. Reaction progress was monitored by TLC (72-168 hours are typically required for complete conversion on this scale, and rotation of the flask every day provided faster conversion). Upon completion, the reaction mixture was concentrated *in vacuo*, the solids were taken up in CH_2Cl_2, and the suspension filtered. The filter cake was washed with CH_2Cl_2 three times and the filtrate was concentrated *in vacuo* to give a crude residue that was purified by silica gel flash chromatography (isocratic: 6% EtOAc/hexane) to provide **6** (4.69 g, 62%) as a pale-yellow solid. The enantiomeric excess was determined to be 79% by chiral SFC analysis (AD-H, 2.5 mL/min, 20% IPA in CO_2, λ = 254 nm): t_R (major) = 4.23 min, t_R (minor) = 5.64 min. $[\alpha]_D^{25.0}$ = –66.0° (c = 0.560, $CHCl_3$). Enantioenriched cyclobutane **6** was dissolved in a minimal amount of CH_2Cl_2 in a 100 mL round-bottom flask. An equal amount of hexanes was carefully layered on top of the CH_2Cl_2 to form a biphasic mixture. The layers were allowed to diffuse overnight to provide **6** as white, crystalline needles (mp: 66–68 °C). The supernatant was concentrated under reduced

pressure and this process was repeated again to provide additional **6** (3.50 g total, 83% recovery of theoretical total of the desired enantiomer, 46% overall from **8**).

$[\alpha]_D^{25.0}$ = –109° (c = 0.720, $CHCl_3$).

^{1}H NMR (400 MHz, $CDCl_3$) δ 9.68 (s, 1H), 8.80 (t, *J* = 1.8 Hz, 1H), 8.79 (dd, *J* = 13.6, 1.6 Hz, 1H), 8.15 (dd, *J* = 8.3, 1.7 Hz, 1H), 7.52 (q, *J* = 8.2, 7.5 Hz, 1H), 7.48 (dd, *J* = 8.3, 1.6 Hz, 1H), 7.45 (dd, *J* = 8.3, 4.2 Hz, 1H), 3.07 (ddd, *J* = 9.1, 8.2, 0.9 Hz, 1H), 2.48 (dq, *J* = 11.4, 9.4 Hz, 1H), 2.06 (dtd, *J* = 11.6, 8.6, 3.3 Hz, 1H), 1.85 (dt, *J* = 10.8, 9.1 Hz, 1H), 1.74 (dddd, *J* = 10.7, 9.5, 3.3, 0.9 Hz, 1H), 1.39 (s, 3H), 1.14 (s, 3H).

^{13}C NMR δ 171.8, 148.3, 138.6, 136.4, 134.7, 128.1, 127.6, 121.7, 121.3, 116.4, 51.0, 40.4, 32.3, 30.9, 23.4, 17.4.

FTIR (NaCl, thin film) 3353, 3047, 2952, 2861, 1685, 1595, 1577, 1526, 1485, 1460, 1424, 1385, 1324, 1261, 1239, 1187, 1169, 1153, 825, 791,756 cm.$^{-1}$

HRMS (MM) calc'd for $C_{16}H_{19}N_2O$ $[M+H]^+$ 255.1492, found 255.1501.

1.5.6 Optimized Scale-Up Protocol for Enantioenriched Amides 73–76

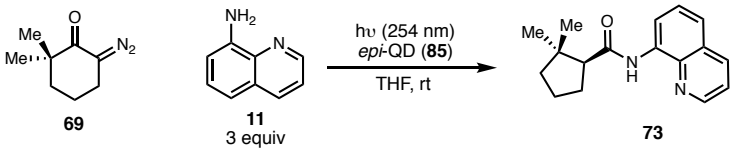

(**73**) 0.2 mmol scale: An oven-dried quartz tube was charged with aminoquinoline (**11**) (86.5 mg, 0.600 mmol, 3.00 equiv) and *epi*-QD (**85**) (32.5 mg, 0.100 mmol, 0.500 equiv) and brought into a N_2 filled glovebox. Diazoketone (**69**) (33.2 mg, 0.200 mmol, 1.00 equiv) was added as a solution in 2.00 mL THF and the tube was sealed with a 19/38 rubber septum and secured with electrical tape. The reaction was removed from the glovebox and

placed in a bottomless test tube rack in front of a Honeywell 254 nm lamp for 48 hours. The reaction mixture was then concentrated *in vacuo*. The crude residue was purified via silica gel flash chromatography (6% EtOAc/hexanes) to afford **73** (37.5 mg, 77% yield) as a brown oil. The enantiomeric excess was determined to be 71% by chiral SFC analysis (AD-H, 2.5 mL/min, 20% IPA in CO_2, λ = 254 nm): t_R (major) = 4.28 min, t_R (minor) = 5.41 min.

(**73**) 1 mmol scale (CRL-1-218): An oven-dried quartz tube was charged with aminoquinoline (**11**) (433 mg, 3.00 mmol, 3.00 equiv) and *epi*-QD (**85**) (64.9 mg, 0.200 mmol, 0.200 equiv) and brought into a N_2-filled glovebox. Diazoketone (**69**) (166 mg, 1.00 mmol, 1.00 equiv) was added as a solution in 10.0 mL THF and the tube was sealed with a 19/38 rubber septum and secured with electrical tape. The reaction was removed from the glovebox and placed in a bottomless test tube rack in front of a Honeywell 254 nm lamp for 48 hours. The reaction mixture was then concentrated *in vacuo*. The crude residue was purified via silica gel flash chromatography (6% EtOAc/hexanes) to afford **73** (215 mg, 80% yield) as a brown oil. The enantiomeric excess was determined to be 67% by chiral SFC analysis (AD-H, 2.5 mL/min, 20% IPA in CO_2, λ = 254 nm): t_R (major) = 4.28 min, t_R (minor) = 5.41 min.

The same procedure was used for 5.0 mmol scale in a 250 mL quartz flask. Irradiated for 5 days instead of 2. 81% yield, 68% ee (CRL-1-241)

$[\alpha]_D^{25.0}$ = –32.5° (c = 2.075, $CHCl_3$).

^{1}H NMR (400 MHz, $CDCl_3$) δ 9.80 (s, 1H), 8.81 (d, *J* = 1.7 Hz, 1H), 8.80 (dd, *J* = 3.0, 1.7 Hz, 1H), 8.16 (dd, *J* = 8.3, 1.7 Hz, 1H), 7.57 – 7.47 (m, 2H), 7.45 (dd, *J* = 8.3, 4.2 Hz, 1H),

2.61 (t, *J* = 8.4 Hz, 1H), 2.38 – 2.22 (m, 1H), 2.02 (dtd, *J* = 13.2, 8.5, 4.4 Hz, 1H), 1.95 – 1.82 (m, 1H), 1.79 – 1.65 (m, 2H), 1.63 – 1.57 (m, 1H), 1.31 (s, 3H), 1.01 (s, 3H).

^{13}C NMR (101 MHz, $CDCl_3$) δ 173.1, 148.3, 138.6, 136.5, 134.8, 128.1, 127.6, 121.7, 121.3, 116.4, 58.1, 43.2, 42.1, 29.7, 27.9, 24.0, 22.5.

FTIR (NaCl, thin film) 3362, 2957, 2924, 2854, 1729, 1690, 1525, 1486, 1464, 1424, 1381, 1325, 1262, 1164, 1145, 1132, 1072, 825, 791, 720 cm.$^{-1}$

HRMS (MM) calc'd for $C_{17}H_{21}N_2O$ $[M+H]^+$ 269.1648, found 269.1645.

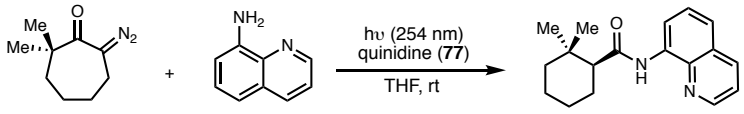

70 11 (3 equiv) 74

(**74**) 0.2 mmol scale: An oven-dried quartz tube was charged with 8-aminoquinoline (**11**) (86.5 mg, 0.600 mmol, 3.00 equiv) and quinidine (**77**) (32.5 mg, 0.100 mmol, 0.500 equiv) and brought into a N_2-filled glovebox. Diazoketone (**70**) (31.0 mg, 0.200 mmol, 1.00 equiv) was added as a solution in 2.00 mL THF and the tube was sealed with a 19/38 rubber septum and secured with electrical tape. The reaction was removed from the glovebox and placed in a bottomless test tube rack in front of a Honeywell 254 nm lamp for 48 hours. The reaction mixture was then concentrated *in vacuo*. The crude residue was purified via silica gel flash chromatography (6% EtOAc/hexanes) to afford **74** (33.3 mg, 59% yield) as a brown oil. The enantiomeric excess was determined to be 71% by chiral SFC analysis (AD-H, 2.5 mL/min, 12% IPA in CO_2, λ = 254 nm): t_R (major) = 9.67 min, t_R (minor) = 10.34 min.

(**74**) 1 mmol scale (CRL-1-228): An oven-dried quartz tube was charged with 8-aminoquinoline (**11**) (433 mg, 3.00 mmol, 3.00 equiv) and quinidine (**77**) (64.9 mg, 0.200 mmol, 0.200 equiv) and brought into a N_2-filled glovebox. Diazoketone (**70**) (152 mg, 1.00

mmol, 1.00 equiv) was added as a solution in 10.0 mL THF and the tube was sealed with a 19/38 rubber septum and secured with electrical tape. The reaction was removed from the glovebox and placed in a bottomless test tube rack in front of a Honeywell 254 nm lamp for 48 hours. The reaction mixture was then concentrated *in vacuo*. The crude residue was purified via silica gel flash chromatography (6% EtOAc/hexanes) to afford **74** (189 mg, 67% yield) as a brown oil. The enantiomeric excess was determined to be 67% by chiral SFC analysis (AD-H, 2.5 mL/min, 12% IPA in CO_2, λ = 254 nm): t_R (major) = 9.67 min, t_R (minor) = 10.34 min.

$[\alpha]_D^{25.0}$ = –17.3° (c = 1.68, $CHCl_3$).

^{1}H NMR (400 MHz, CDCl3) δ 9.79 (s, 1H), 8.82 (d, *J* = 1.7 Hz, 1H), 8.80 (dd, *J* = 2.7, 1.7 Hz, 1H), 8.16 (dd, *J* = 8.3, 1.7 Hz, 1H), 7.57 – 7.47 (m, 2H), 7.45 (dd, *J* = 8.3, 4.2 Hz, 1H), 2.30 (dd, *J* = 11.8, 3.5 Hz, 1H), 1.99 – 1.78 (m, 3H), 1.55 – 1.47 (m, 2H), 1.39 – 1.27 (m, 3H), 1.13 (s, 3H), 1.10 (s, 3H).

^{13}C NMR (101 MHz, $CDCl_3$) δ 173.6, 148.3, 138.6, 136.5, 134.7, 128.1, 127.6, 121.7, 121.3, 116.5, 56.5, 41.6, 33.4, 31.5, 25.7, 25.7, 22.1, 21.2.

FTIR (NaCl, thin film) 3364, 2956, 2923, 2852, 1729, 1691, 1523, 1486, 1462, 1424, 1378, 1326, 1273, 1129, 1072, 825, 790 cm.$^{-1}$

HRMS (MM) calc'd for $C_{18}H_{23}N_2O$ $[M+H]^+$ 283.1805, found 283.1796.

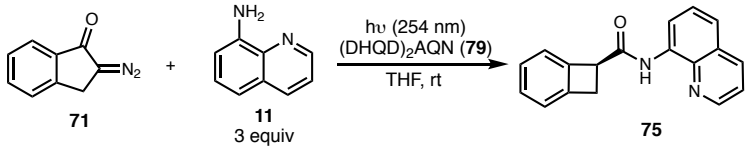

(**75**) 0.2 mmol: An oven-dried quartz tube was charged with aminoquinoline (**11**) (86.5 mg, 0.600 mmol, 3.00 equiv) and $(DHQD)_2AQN$ (**79**) (85.7 mg, 0.100 mmol, 0.500 equiv) and brought into a N_2-filled glovebox. Diazoketone (**71**) (31.6 mg, 0.200 mmol, 1.00 equiv)

was added as a solution in 2.00 mL THF and the tube was sealed with a 19/38 rubber septum and secured with electrical tape. The reaction was removed from the glovebox and placed in a bottomless test tube rack in front of a Honeywell 254 nm lamp for 48 hours. The reaction mixture was then concentrated *in vacuo*. The crude residue was purified via silica gel flash chromatography (5–50 % EtOAc/hexanes followed by 0–1% Et_2O/CH_2Cl_2) to afford **75** (16.8 mg, 31% yield). The enantiomeric excess was determined to be 34% by chiral SFC analysis (AD-H, 2.5 mL/min, 30% IPA in CO_2, λ = 254 nm): t_R (major) = 5.06 min, t_R (minor) = 6.89 min.

$[\alpha]_D^{25.0}$ = –4.1° (c = 0.565, $CHCl_3$).

^{1}H NMR (400 MHz, $CDCl_3$) δ 10.21 (s, 1H), 8.79 (dd, *J* = 11.5, 1.7 Hz, 1H), δ 8.78 (d, *J* = 1.7 Hz, 1H), 8.15 (dd, *J* = 8.3, 1.7 Hz, 1H), 7.54 (dd, *J* = 8.3, 7.2 Hz, 1H), 7.50 (dd, *J* = 8.3, 1.8 Hz, 1H), 7.46 – 7.41 (m, 2H), 7.38 – 7.29 (m, 2H), 7.22 – 7.16 (m, 1H), 4.56 (ddt, *J* = 5.8, 2.9, 0.8 Hz, 1H), 3.69 (ddd, *J* = 14.2, 5.7, 0.7 Hz, 1H), 3.60 (ddd, *J* = 14.2, 2.9, 0.8 Hz, 1H).

^{13}C NMR (101 MHz, CDCl3) δ 170.6, 148.4, 144.7, 142.9, 138.7, 136.4, 134.5, 128.6, 128.0, 127.8, 127.5, 123.5, 122.7, 121.7, 121.7, 116.5, 49.3, 35.2.

FTIR (NaCl, thin film) 3347, 3066, 2928, 2851, 1680, 1596, 1578, 1526, 1485, 1458, 1424, 1386, 1328, 1262, 1240, 1202, 1162, 1132, 869, 826, 791, 759, 734, 707, 679 cm.$^{-1}$

HRMS (MM) calc'd for $C_{18}H_{15}N_2O$ $[M+H]^+$ 275.1179, found 275.1178.

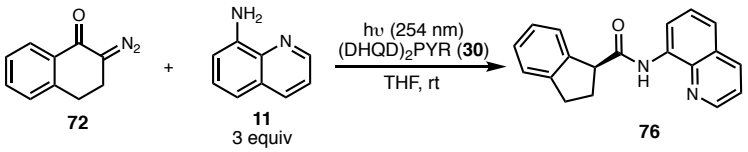

(**76**) 0.2 mmol: An oven-dried quartz tube was charged with diazoketone (**72**) (34.4 mg, 0.200 mmol, 1.00 equiv), aminoquinoline (**11**) (86.5 mg, 0.600 mmol, 3.00 equiv), and

$(DHQD)_2PYR$ (**30**) (88.1 mg, 0.100 mmol, 0.500 equiv), and brought into a N_2-filled glovebox. The mixture was suspended in 2.00 mL THF and the tube was sealed with a 19/38 rubber septum and secured with electrical tape. The reaction was removed from the glovebox and placed in a bottomless test tube rack in front of a Honeywell 254 nm lamp for 48 hours. The reaction mixture was then concentrated *in vacuo*. The crude residue was purified via silica gel flash chromatography (5–10% EtOAc/hexanes) to afford **76** (24.1 mg, 42% yield) as a brown oil. The enantiomeric excess was determined to be 75% by chiral SFC analysis (AD-H, 2.5 mL/min, 30% IPA in CO_2, λ = 254 nm): t_R (major) = 5.73 min, t_R (minor) = 4.86 min.

$[\alpha]_D^{25.0}$ = 65.0° (c = 0.91, $CHCl_3$).

^{1}H NMR (400 MHz, $CDCl_3$) δ 10.06 (s, 1H), 8.79 (dd, *J* = 7.1, 1.9 Hz, 1H), 8.75 (dd, *J* = 4.2, 1.7 Hz, 1H), 8.15 (dd, *J* = 8.3, 1.7 Hz, 1H), 7.56 – 7.46 (m, 3H), 7.44 (dd, *J* = 8.3, 4.2 Hz, 1H), 7.33 (d, *J* = 7.2 Hz, 1H), 7.31 – 7.18 (m, 2H), 4.27 (dd, *J* = 8.4, 6.1 Hz, 1H), 3.23 (dt, *J* = 15.2, 7.4 Hz, 1H), 3.09 – 2.95 (m, 1H), 2.69 – 2.48 (m, 2H).

^{13}C NMR (101 MHz, $CDCl_3$) δ 172.7, 148.4, 144.8, 141.5, 138.7, 136.4, 134.7, 128.0, 127.9, 127.53, 126.9, 125.1, 125.0, 121.7, 121.7, 116.6, 54.0, 32.1, 30.4.

FTIR (NaCl, thin film) 3347, 2957, 2923, 2852, 1728, 1689, 1524, 1484, 1461, 1424, 1380, 1325, 1272, 1163, 1132, 1072, 826, 791, 743 $cm.^{-1}$

HRMS (MM) calc'd for $C_{19}H_{17}N_2O$ $[M+H]^+$ 289.1335, found 289.1334.

1.5.7 C_{sp}^3–H arylation

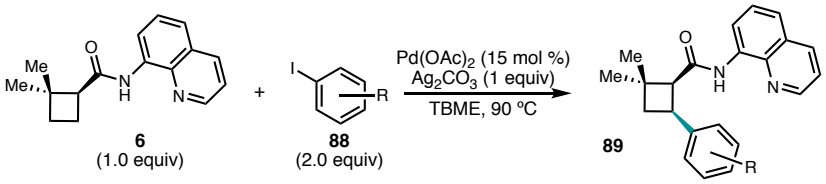

General Procedure 3

On the bench-top, a 2-dram vial equipped with a stir bar was charged with $Pd(OAc)_2$ (15 mol %, 0.03 mmol), Ag_2CO_3 (1 equiv, 0.2 mmol), cyclobutamide (**6**) (1 equiv, 0.2 mmol), and aryl iodide (2 equiv, 0.4 mmol). TBME (0.2 M, 1 mL) was added to the vial, then the vial was sealed with a Teflon cap and electrical tape and submerged in an oil bath at 90 °C. After approximately 5 minutes for aryl iodide substrates and 30 minutes for heteroaryl iodide substrates, the olive-green mixture became black. The reaction mixture was stirred at 90 °C additional 16 hours, at which point the vial is allowed to cool to room temperature over 15 minutes. The black reaction mixture was diluted with CH_2Cl_2 and filtered over a pad of 20 grams of tightly packed celite. The celite plug was eluted with an additional 100 mL of CH_2Cl_2. Following this, the resultant orange solution was concentrated *in vacuo* and subsequently purified by silica gel column chromatography to give the arylated cyclobutane products. (Note: some substrates required purification with basic alumina as the stationary phase).

1.5.8 Characterization of Arylation Products

89a

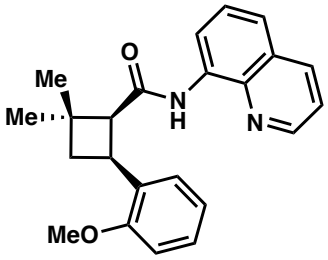

Prepared from cyclobutamide **6** (1 equiv, 50.8 mg, 0.2 mmol) and 2-iodoanisole (2 equiv, 93.6 mg, 0.4 mmol). The crude residue was purified by column chromatography (10 → 15 → 20% EtOAc/Hexanes) to give a colorless foam.

Run 1: (54.4 mg, 75%), Run 2: (61.2 mg, 84%)

R_f = 0.48 (silica gel, 30% EtOAc/Hex, UV, *p*-anisaldehyde).

$[\alpha]_D^{25}$ = +84.8° (c = 3.3, $CHCl_3$).

^{1}H NMR (400 MHz, $CDCl_3$): δ 9.57 (s, 1H), 8.77 (dd, *J* = 4.2, 1.7 Hz, 1H), 8.60 (dd, *J* = 4.9, 4.2 Hz, 1H), 8.10 (dd, *J* = 8.3, 1.7 Hz, 1H), 7.44 – 7.36 (m, 3H), 7.24 (dt, *J* = 7.4, 1.5 Hz, 1H), 7.09 (dddd, *J* = 8.2, 7.4, 1.8, 0.8 Hz, 1H), 6.96 (tdd, *J* = 7.5, 1.1, 0.4 Hz, 1H), 6.61 (dd, *J* = 8.1, 1.1 Hz, 1H), 4.09 – 3.95 (m, 1H), 3.62 (s, 3H), 3.46 (ddd, *J* = 8.6, 2.9, 0.8 Hz, 1H), 2.74 (t, *J* = 10.8 Hz, 1H), 2.13 (ddd, *J* = 10.4, 8.4, 2.9 Hz, 1H), 1.53 (s, 3H), 1.22 (s, 3H).

^{13}C NMR (101 MHz, $CDCl_3$): δ 171.13, 157.19, 147.90, 138.41, 136.31, 134.88, 130.18, 127.92, 127.66, 127.54, 127.00, 121.45, 120.75, 120.43, 116.27, 109.43, 58.05, 55.05, 37.10, 35.89, 32.81, 30.33, 25.14.

FTIR (NaCl, thin film, cm^{-1}): 3366, 2952, 5927, 2863, 2361, 1685, 1523, 1485, 1464, 1424, 1324, 1241, 1161, 1132, 1161, 1029, 826, 792, 751.

HRMS (ESI-TOF, *m/z*): calc'd for $C_{23}H_{25}N_2O_2$ $[M+H]^+$: 361.1911; found: 361.1925.

89b

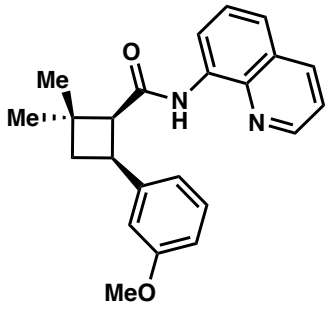

Prepared from cyclobutamide **6** (1 equiv, 50.8 mg, 0.2 mmol) and 3-iodoanisole (2 equiv, 93.6 mg, 0.4 mmol). The crude residue was purified by column chromatography (10 → 15 → 20% EtOAc/Hexanes) to give a white solid.

Run 1: (59.0 mg, 82%), Run 2: (58.3 mg, 81%)

R_f = 0.36 (silica gel, 20% EtOAc/Hex, UV, *p*-anisaldehyde).

$[\alpha]_D^{25}$ = +61.6° (c = 0.4, $CHCl_3$).

^{1}H NMR (400 MHz, $CDCl_3$): δ 9.62 (s, 1H), 8.75 (dd, *J* = 4.2, 1.7 Hz, 1H), 8.64 (p, *J* = 4.3 Hz, 1H), 8.11 (dd, *J* = 8.3, 1.7 Hz, 1H), 7.45 – 7.38 (m, 3H), 7.13 (t, *J* = 7.9 Hz, 1H), 6.82 (ddt, *J* = 7.6, 1.8, 1.0 Hz, 1H), 6.77 (dt, *J* = 2.7, 1.3 Hz, 1H), 6.63 (ddt, *J* = 8.2, 2.6, 0.9 Hz, 1H), 4.03 (dtd, *J* = 11.0, 8.6, 1.1 Hz, 1H), 3.67 (s, 3H), 3.39 (ddd, *J* = 8.7, 2.9, 0.8 Hz, 1H), 2.76 (t, *J* = 10.7 Hz, 1H), 2.16 (ddd, *J* = 10.4, 8.5, 3.0 Hz, 1H), 1.51 (s, 3H), 1.22 (s, 3H).

^{13}C NMR (101 MHz, $CDCl_3$): δ 170.5, 159.5, 148.0, 143.7, 138.4, 136.4, 134.6, 129.1, 127.9, 127.5, 121.5, 121.2, 119.1, 116.5, 112.3, 111.3, 57.7, 55.1, 37.8, 36.0, 35.8, 30.2, 25.1.

FTIR (NaCl, thin film, cm^{-1}): 3357, 2952, 2925, 1684, 1600, 1582, 1521, 1485, 1424, 1386, 1323, 1259, 1160, 1049, 878, 826, 790, 756, 694.

HRMS (ESI-TOF, *m/z*): calc'd for $C_{23}H_{25}N_2O_2$ $[M+H]^+$: 361.1911; found: 361.1915.

89c

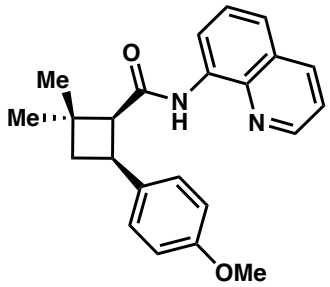

Prepared from cyclobutamide **6** (1 equiv, 50.8 mg, 0.2 mmol) and 4-iodoanisole (2 equiv, 93.6 mg, 0.4 mmol). The crude residue was purified by column chromatography (10 → 15% EtOAc/Hexanes) to give a white, amorphous solid.

Run 1: (47.7 mg, 66%), Run 2: (51.2 mg, 71%)

R_f = 0.23 (silica gel, 20% EtOAc/Hex, UV, *p*-anisaldehyde).

$[\alpha]_D^{25}$ = +59.8° (c = 1.3, $CHCl_3$).

^{1}H NMR (400 MHz, $CDCl_3$): δ 9.58 (s, 1H), 8.75 (dd, *J* = 4.2, 1.7 Hz, 1H), 8.63 (p, *J* = 4.4 Hz, 1H), 8.10 (dd, *J* = 8.3, 1.7 Hz, 1H), 7.45 – 7.38 (m, 3H), 7.20 – 7.13 (m, 2H), 6.80 – 6.73 (m, 2H), 4.00 (q, *J* = 11.1, 8.6 Hz, 1H), 3.70 (s, 3H), 3.34 (ddd, *J* = 8.7, 3.0, 0.8 Hz, 1H), 2.75 (t, *J* = 10.8 Hz, 1H), 2.13 (ddd, *J* = 10.4, 8.6, 3.0 Hz, 1H), 1.51 (s, 3H), 1.23 (s, 3H).

^{13}C NMR (101 MHz, $CDCl_3$): δ 170.6, 157.7, 148.0, 138.4, 136.4, 134.6, 133.7, 127.9, 127.5, 121.5, 121.1, 116.5, 113.6, 57.7, 55.3, 37.9, 35.7, 35.5, 30.2, 25.2.

FTIR (NaCl, thin film, cm^{-1}): 2926, 2361, 1685, 1523, 1485, 1288, 1324, 1247, 1160, 1038, 826, 772.

HRMS (ESI-TOF, *m/z*): calc'd for $C_{23}H_{25}N_2O_2$ $[M+H]^+$: 361.1911; found: 361.1921.

89d

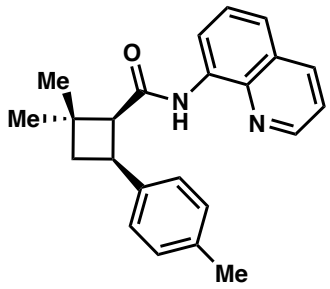

Prepared from cyclobutamide **6** (1 equiv, 50.8 mg, 0.2 mmol) and 4-iodotoluene (2 equiv, 87.2 mg, 0.4 mmol). The crude residue was purified by column chromatography (10 → 15 → 20% EtOAc/Hexanes) to give a white, amorphous solid.

Run 1: (54.1 mg, 79%), Run 2: (55.9 mg, 81%)

R_f = 0.29 (silica gel, 20% EtOAc/Hex, UV, *p*-anisaldehyde).

$[\alpha]_D^{25}$ = +54.2° (c = 2.0, $CHCl_3$).

^{1}H NMR (400 MHz, $CDCl_3$): δ 9.60 (s, 1H), 8.76 (dd, *J* = 4.2, 1.7 Hz, 1H), 8.65 (h, *J* = 4.2 Hz, 1H), 8.11 (dd, *J* = 8.2, 1.7 Hz, 1H), 7.50 – 7.36 (m, 3H), 7.14 (d, *J* = 7.8 Hz, 2H), 7.02 (d, *J* = 7.4 Hz, 2H), 4.01 (td, *J* = 10.8, 8.1 Hz, 1H), 3.37 (ddd, *J* = 8.7, 2.9, 0.8 Hz, 1H), 2.76 (t, *J* = 10.8 Hz, 1H), 2.24 (s, 3H), 2.14 (ddd, *J* = 10.4, 8.6, 2.9 Hz, 1H), 1.51 (s, 3H), 1.22 (s, 3H).

^{13}C NMR (101 MHz, $CDCl_3$): δ 170.6, 148.0, 138.7, 138.4, 136.4, 135.0, 134.7, 128.9, 127.9, 127.5, 126.7, 121.5, 121.1, 116.5, 57.7, 37.8, 35.8, 35.7, 30.2, 25.2, 21.2.

FTIR (NaCl, thin film, cm^{-1}): 3360, 2924, 2359, 1686, 1522 1485, 1424, 1386, 1324, 1160, 826, 792.

HRMS (ESI-TOF, *m/z*): calc'd for $C_{23}H_{25}N_2O$ $[M+H]^+$: 345.1961; found: 345.1971.

89e

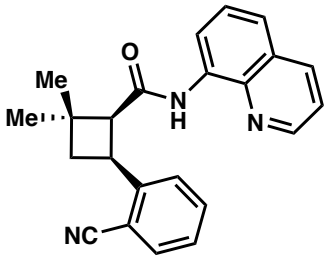

Prepared from cyclobutamide **6** (1 equiv, 50.8 mg, 0.2 mmol) and 2-iodobenzonitrile (2 equiv, 91.8 mg, 0.4 mmol). The crude residue was purified by column chromatography (10 → 15% EtOAc/Hexanes) to give a pale, yellow foam.

Run 1: (57.6 mg, 81%), Run 2: (64.7 mg, 91%)

R_f = 0.55 (silica gel, 30% EtOAc/Hex, UV, *p*-anisaldehyde).

$[\alpha]_D^{25}$ = –24.4° (c = 5.4, $CHCl_3$).

^{1}H NMR (400 MHz, $CDCl_3$): δ 9.76 (s, 1H), 8.81 (dd, *J* = 4.2, 1.7 Hz, 1H), 8.53 (dd, *J* = 7.4, 1.7 Hz, 1H), 8.10 (dd, *J* = 8.3, 1.7 Hz, 1H), 7.56 (td, *J* = 8.0, 7.6, 1.2 Hz, 1H), 7.51 – 7.35 (m, 5H), 7.21 (tdd, *J* = 7.6, 1.3, 0.7 Hz, 1H), 4.21 (dt, *J* = 11.1, 8.3, 7.8 Hz, 1H), 3.74 (ddd, *J* = 8.3, 3.0, 0.8 Hz, 1H), 2.87 (t, *J* = 10.7 Hz, 1H), 2.16 (ddd, *J* = 10.4, 8.3, 3.1 Hz, 1H), 1.57 (s, 3H), 1.20 (s, 3H).

^{13}C NMR (101 MHz, $CDCl_3$): δ 170.0, 148.3, 146.9, 138.5, 136.3, 134.5, 132.6, 128.1, 127.9, 127.2, 126.3, 121.7, 121.4, 118.8, 116.3, 110.6, 57.7, 36.6, 36.1, 35.2, 29.8, 25.1.

FTIR (NaCl, thin film, cm^{-1}): 3353, 2954, 2361, 2222, 1683, 1523, 1485, 1424, 1388, 1323, 1260, 1161, 826, 791, 755, 668.

HRMS (ESI-TOF, *m/z*): calc'd for $C_{23}H_{21}N_3O$ $[M+H]^+$: 356.1757; found: 356.1773.

89f

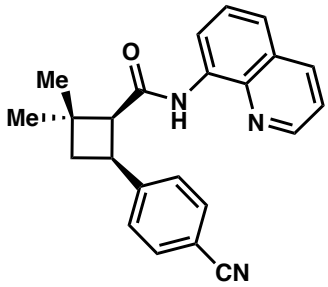

Prepared from cyclobutamide **6** (1 equiv, 50.8 mg, 0.2 mmol) and 4-iodobenzonitrile (2 equiv, 91.8 mg, 0.4 mmol). The crude residue was purified by column chromatography (10 → 15 → 20 →25 % EtOAc/Hexanes) to give a pale, yellow foam.

Run 1: (50.5 mg, 71%), Run 2: (53.3 mg, 75%)

R_f = 0.32 (silica gel, 30% EtOAc/Hex, UV, *p*-anisaldehyde).

$[\alpha]_D^{25}$ = +102.7° (c = 5.1, $CHCl_3$).

^{1}H NMR (400 MHz, $CDCl_3$): δ 9.66 (s, 1H), 8.79 (dd, *J* = 4.2, 1.7 Hz, 1H), 8.56 (dd, *J* = 7.2, 1.8 Hz, 1H), 8.14 (dd, *J* = 8.3, 1.7 Hz, 1H), 7.50 (dt, *J* = 8.3, 1.8 Hz, 2H), 7.49 – 7.37 (m, 3H), 7.33 – 7.24 (m, 2H), 4.02 (dt, *J* = 10.8, 8.3 Hz, 1H), 3.43 (ddd, *J* = 8.5, 3.0, 0.8 Hz, 1H), 2.77 (t, *J* = 10.7 Hz, 1H), 2.18 (ddd, *J* = 10.4, 8.5, 3.0 Hz, 1H), 1.53 (s, 3H), 1.20 (s, 3H).

^{13}C NMR (101 MHz, $CDCl_3$): δ 169.9, 148.4, 148.2, 138.3, 136.5, 134.2, 131.9, 128.0, 127.5, 127.3, 121.7, 121.6, 119.5, 116.5, 109.3, 57.7, 37.5, 36.1, 36.0, 29.9, 25.0.

FTIR (NaCl, thin film, cm^{-1}): 3353, 2954, 2930, 2361, 2226, 1684, 1608, 1524, 1486, 1424, 1288, 1323, 1161, 826, 792, 755, 668.

HRMS (ESI-TOF, *m/z*): calc'd for $C_{23}H_{22}N_3O$ $[M+H]^+$: 356.1757; found: 356.1752.

89g

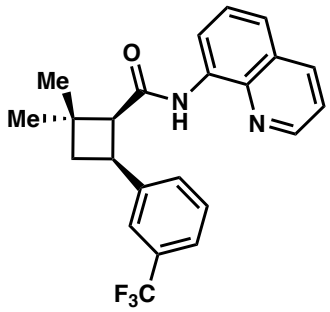

Prepared from cyclobutamide **6** (1 equiv, 50.8 mg, 0.2 mmol) and 3-iodotrifluorotoluene (2 equiv, 109.1 mg, 0.4 mmol). The crude residue was purified by column chromatography (10% EtOAc/Hexanes) to give a colorless oil.

Run 1: (67.7 mg, 85%), Run 2: (62.9 mg, 79%)

R_f = 0.23 (silica gel, 20% EtOAc/Hex, UV, *p*-anisaldehyde).

$[\alpha]_D^{25}$ = +47.3° (c = 3.3, $CHCl_3$).

^{1}H NMR (400 MHz, $CDCl_3$): δ 9.63 (s, 1H), 8.77 (dd, *J* = 4.2, 1.7 Hz, 1H), 8.57 (dd, *J* = 6.6, 2.4 Hz, 1H), 8.12 (dd, *J* = 8.3, 1.7 Hz, 1H), 7.50 – 7.36 (m, 5H), 7.39 – 7.26 (m, 2H), 4.05 (dt, *J* = 11.0, 8.7 Hz, 1H), 3.42 (ddd, *J* = 8.6, 3.0, 0.8 Hz, 1H), 2.80 (t, *J* = 10.8 Hz, 1H), 2.20 (ddd, *J* = 10.4, 8.5, 3.0 Hz, 1H), 1.53 (s, 3H), 1.23 (s, 3H).

^{13}C NMR (101 MHz, $CDCl_3$): δ 170.2, 148.2, 143.2, 138.5, 136.6, 134.5, 130.4 (q, $J_{C–F}$ = 32 Hz), 130.3, 128.5, 128.1, 127.6, 125.9, 123.7 (q, $J_{C–F}$ = 3.7 Hz), 123.2, 122.8 (q, $J_{C–F}$ = 3.8 Hz), 121.7, 121.5, 116.6, 57.8, 37.8, 36.1, 36.0, 30.2, 30.0, 25.2.

^{19}F NMR (376 MHz, $CDCl_3$) δ -63.50.

FTIR (NaCl, thin film, cm^{-1}): 3355, 2931, 2360, 1684, 1523, 1486, 1425, 1388, 1324, 1162, 1122, 1072, 901, 826, 793, 756, 701, 659.

HRMS (ESI-TOF, *m/z*): calc'd for $C_{23}H_{22}F_3N_2O$ $[M+H]^+$: 399.1679; found: 399.1679.

89h

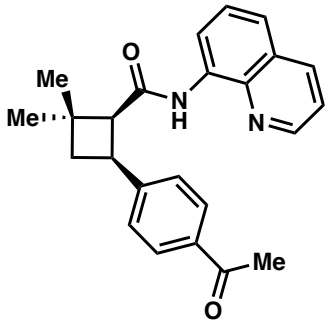

Prepared from cyclobutamide **6** (1 equiv, 50.8 mg, 0.2 mmol) and 4-iodoacetophenone (2 equiv, 98.7 mg, 0.4 mmol). The crude residue was purified by column chromatography (20% EtOAc/Hexanes) to give a white, amorphous solid.

Run 1: (57.3 mg, 77%), Run 2: (56.6 mg, 76%)

R_f = 0.41 (silica gel, 40% EtOAc/Hex, UV, *p*-anisaldehyde).

$[\alpha]_D^{25}$ = +95.0° (c = 3.0, $CHCl_3$).

^{1}H NMR (400 MHz, $CDCl_3$): δ 9.73 (s, 1H), 8.85 (dd, *J* = 4.3, 1.7 Hz, 1H), 8.66 (dd, *J* = 7.1, 1.8 Hz, 1H), 8.20 (dd, *J* = 8.3, 1.7 Hz, 1H), 7.94 – 7.87 (m, 2H), 7.51 (dd, *J* = 8.5, 4.1 Hz, 2H), 7.48 (q, *J* = 9.2, 8.2, 8.2 Hz, 1H), 7.39 – 7.33 (m, 2H), 4.12 (td, *J* = 11.3, 9.7, 8.4 Hz, 1H), 3.51 (ddd, *J* = 8.6, 2.9, 0.8 Hz, 1H), 2.88 (t, *J* = 10.7 Hz, 1H), 2.58 (s, 3H), 2.26 (ddd, *J* = 10.3, 8.5, 3.0 Hz, 1H), 1.61 (s, 3H), 1.29 (s, 3H).

^{13}C NMR (101 MHz, $CDCl_3$): δ 198.1, 170.1, 148.5, 148.1, 138.4, 136.5, 134.8, 134.4, 128.4, 128.0, 127.5, 126.7, 121.6, 121.4, 116.5, 57.8, 37.7, 36.1, 36.0, 30.0, 26.7, 25.1.

FTIR (NaCl, thin film, cm^{-1}): 3354, 2954, 2928, 2866, 1678, 1606, 1523, 1485, 1424, 1387, 1323, 1267, 1161, 956, 826, 792, 754, 657.

HRMS (ESI-TOF, *m/z*): calc'd for $C_{24}H_{25}N_2O_2$ $[M+H]^+$: 373.1911; found: 373.1900.

89i

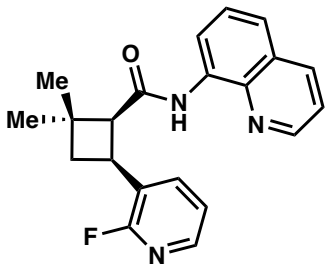

Prepared from cyclobutamide **6** (1 equiv, 50.8 mg, 0.2 mmol) and 2-fluoro-3-iodopyridine (2 equiv, 89.2 mg, 0.4 mmol). The crude residue was purified by column chromatography using silica gel basified with 4 mL of aqueous ammonium hydroxide (10% EtOAc/2% Et_3N/88% hexanes → 15% EtOAc/2% Et_3N/83% hexanes → 20% EtOAc/2% Et_3N/78% hexanes → 35% EtOAc/2% Et_3N/63% hexanes) to give a white foam.

Run 1: (56.1 mg, 80%), Run 2: (56.4 mg, 81%)

R_f = 0.22 (silica gel, 20% EtOAc/Hex, UV, p-Anisaldehyde).

$[\alpha]_D^{25}$ = +60.8° (c = 0.415, $CHCl_3$).

^{1}H NMR (400 MHz, $CDCl_3$): δ 9.66 (s, 1H), 8.77 (dd, *J* = 4.3, 1.7 Hz, 1H), 8.54 (dd, *J* = 7.0, 2.1 Hz, 1H), 8.09 (dd, *J* = 8.3, 1.7 Hz, 1H), 7.96 (ddt, *J* = 4.9, 2.0, 1.0 Hz, 1H), 7.72 (ddq, *J* = 9.9, 7.5, 1.2, 0.7 Hz, 1H), 7.45 – 7.34 (m, 3H), 7.15 (ddd, *J* = 7.1, 4.9, 1.9 Hz, 1H), 3.99 (dtd, *J* = 11.0, 8.6, 1.1 Hz, 1H), 3.44 (ddt, *J* = 8.4, 2.5, 1.3 Hz, 1H), 2.76 (t, *J* = 10.7 Hz, 1H), 2.11 (ddd, *J* = 10.4, 8.4, 3.0 Hz, 1H), 1.53 (s, 3H), 1.19 (s, 3H).

^{13}C NMR (101 MHz, $CDCl_3$): δ 170.2, 161.5 (d, J_{C-F} = 237 Hz), 148.2, 144.6 (d, J_{C-F} = 14.7 Hz), 139.3 (d, J_{C-F} = 6.1 Hz), 138.4, 136.3, 134.4, 127.9, 127.3, 124.2 (d, J_{C-F} = 31.2 Hz), 121.6, 121.4, 121.3 (d, J_{C-F} = 4.0 Hz), 116.4, 57.0, 36.4 (d, J_{C-F} = 14.8 Hz), 30.8, 30.7, 29.8, 25.0.

^{19}F NMR (376 MHz, $CDCl_3$): δ -71.52 (d, *J* = 10.1 Hz).

FTIR (NaCl, thin film, cm^{-1}): 3355, 3058, 2954, 2930, 2866, 1682, 1605, 1577, 1524, 1486, 1431, 1388, 1372, 1324, 1261, 1240, 1162, 1132, 1112, 826, 793, 758.

HRMS (ESI-TOF, *m/z*): calc'd for $C_{21}H_{21}FN_3O$ $[M+H]^+$: 350.1663; found: 350.1659.

89j

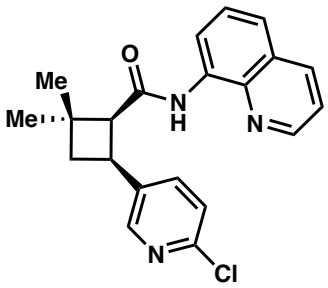

Prepared from cyclobutamide **6** (1 equiv, 50.8 mg, 0.2 mmol) and 5-iodo-2-chloropyridine (2 equiv, 95.8 mg, 0.4 mmol). The crude residue was purified by column chromatography using basic alumina as the stationary phase (0 → 1% MeOH/CH_2Cl_2) to give a colorless foam.

Run 1: (50.6 mg, 69%), Run 2: (49.7 mg, 68%)

R_f = 0.24 (silica gel, 40% EtOAc/Hex, UV).

$[\alpha]_D^{25}$ = +81.1° (c = 4.3, $CHCl_3$).

^{1}H NMR (500 MHz, $CDCl_3$): δ 9.64 (s, 1H), 8.76 (dd, *J* = 4.2, 1.7 Hz, 1H), 8.58 (dd, *J* = 6.8, 2.2 Hz, 1H), 8.22 (dt, *J* = 2.6, 0.8 Hz, 1H), 8.11 (dd, *J* = 8.3, 1.7 Hz, 1H), 7.56 (ddd, *J* = 8.2, 2.5, 0.9 Hz, 1H), 7.46 – 7.38 (m, 3H), 7.17 (d, *J* = 8.2 Hz, 1H), 3.96 (q, *J* = 11.0, 8.5 Hz, 1H), 3.38 (ddd, *J* = 8.5, 3.0, 0.8 Hz, 1H), 2.76 (t, *J* = 10.7 Hz, 1H), 2.15 (ddd, *J* = 10.4, 8.5, 3.0 Hz, 1H), 1.52 (s, 3H), 1.22 (s, 3H).

^{13}C NMR (101 MHz, $CDCl_3$): δ 169.8, 148.8, 148.5, 148.1, 138.3, 137.7, 136.5, 136.3, 134.2, 127.9, 127.4, 123.5, 121.7, 121.6, 116.5, 57.4, 37.4, 36.3, 33.3, 29.8, 29.8, 25.0.

FTIR (NaCl, thin film, cm^{-1}): 3350, 2954, 1682, 1524, 1485, 1460, 1424, 1386, 1324, 1260, 1162, 1133, 1104, 826, 792, 755, 666.

HRMS (ESI-TOF, *m/z*): calc'd for $C_{21}H_{21}ClN_3O$ $[M+H]^+$: 366.1368; found: 366.1370.

89k

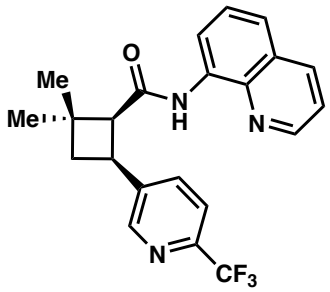

Prepared from cyclobutamide **6** (1 equiv, 50.8 mg, 0.2 mmol) and 5-iodo-2-trifluoromethylpyridine (2 equiv, 95.8 mg, 0.4 mmol). The crude residue was purified by column chromatography using silica gel basified with 5 mL of aqueous ammonium hydroxide (5% EtOAc/2% Et_3N/93% hexanes → 10% EtOAc/2% Et_3N/88% hexanes → 15% EtOAc/2% Et_3N/83% hexanes → 20% EtOAc/2% Et_3N/78% hexanes) to give a pale, yellow foam.

Run 1: (71.6 mg, 90%), Run 2: (68.2 mg, 85%)

R_f = 0.19 (silica gel, 20% EtOAc/Hex, UV).

$[\alpha]_D^{25}$ = +67.7° (c = 4.2, $CHCl_3$).

^{1}H NMR (400 MHz, $CDCl_3$): δ 9.61 (s, 1H), 8.69 (dd, *J* = 4.2, 1.7 Hz, 1H), 8.52 – 8.41 (m, 2H), 8.04 (dd, *J* = 8.3, 1.7 Hz, 1H), 7.70 – 7.62 (m, 1H), 7.46 (dd, *J* = 8.1, 0.7 Hz, 1H), 7.41 – 7.28 (m, 3H), 3.95 (q, *J* = 11.0, 8.5 Hz, 1H), 3.37 (ddd, *J* = 8.4, 2.9, 0.9 Hz, 1H), 2.73 (t, *J* = 10.7 Hz, 1H), 2.12 (ddd, *J* = 10.4, 8.5, 3.0 Hz, 1H).

^{13}C NMR (101 MHz, $CDCl_3$): δ 169.7, 148.8, 148.2, 145.5 (q, J_{C-F} = 35 Hz), 141.2, 138.3, 136.5, 135.7, 134.1, 128.0, 127.4, 123.2, 121.7, 120.5, 119.9, 119.9, 119.8, 119.8, 116.5, 57.4, 37.3, 36.5, 33.7, 29.8, 25.0.

^{19}F NMR (282 MHz, $CDCl_3$): δ -68.6.

FTIR (NaCl, thin film, cm^{-1}): 3351, 2957, 1682, 1524, 1486, 1425, 1387, 1340, 1261, 1164, 1134, 1088, 1030, 826, 792, 756, 667.

HRMS (ESI-TOF, *m/z*): calc'd for $C_{22}H_{21}F_3N_3O$ $[M+H]^+$: 400.1631; found: 400.1621.

89l

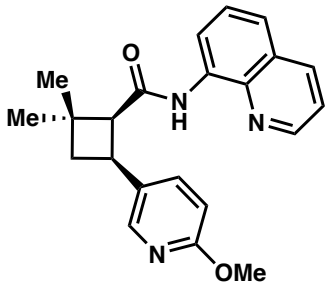

Prepared from cyclobutamide **6** (1 equiv, 50.8 mg, 0.2 mmol) and 5-iodo-2-methoxypyridine (2 equiv, 94.0 mg, 0.4 mmol). The crude residue was purified by column chromatography using silica gel basified with 4 mL of aqueous ammonium hydroxide (10% EtOAc/2% Et_3N/88% hexanes → 15% EtOAc/2% Et_3N/83% hexanes → 20% EtOAc/2% Et_3N/78% hexanes → 30% EtOAc/2% Et_3N/68% hexanes) to give a white solid.

Run 1: (34.9 mg, 48%), Run 2: (36.1 mg, 50%)

R_f = 0.14 (silica gel, 20% EtOAc/Hex, UV, *p*-anisaldehyde).

$[\alpha]_D^{25}$ = +61.1° (c = 0.415, $CHCl_3$).

^{1}H NMR (400 MHz, $CDCl_3$): δ 9.60 (s, 1H), 8.76 (dd, *J* = 4.2, 1.7 Hz, 1H), 8.62 (dd, *J* = 5.3, 3.7 Hz, 1H), 8.12 (dd, *J* = 8.3, 1.7 Hz, 1H), 8.01 (dt, *J* = 2.5, 0.9 Hz, 1H), 7.54 (ddd, *J* = 8.6, 2.5, 0.7 Hz, 1H), 7.46 – 7.39 (m, 3H), 6.61 (dd, *J* = 8.6, 0.7 Hz, 1H), 3.96 (qd, *J* = 11.0, 8.6, 1.1 Hz, 1H), 3.84 (s, 3H), 3.33 (ddd, *J* = 8.7, 2.9, 0.8 Hz, 1H), 2.76 (t, *J* = 10.8 Hz, 1H), 2.14 (ddd, *J* = 10.4, 8.6, 3.0 Hz, 1H), 1.51 (s, 3H), 1.23 (s, 3H).

^{13}C NMR (101 MHz, $CDCl_3$): δ 170.3, 162.7, 148.1, 145.3, 138.4, 138.0, 136.4, 134.5, 129.6, 128.0, 127.5, 121.6, 121.4, 116.5, 110.1, 57.6, 53.4, 37.7, 36.1, 33.4, 30.1, 25.1.

FTIR (NaCl, thin film, cm^{-1}): 3352, 2922, 2850, 2351, 1682, 1606, 1574, 1523, 1494, 1486, 1424, 1385, 1324, 1285, 1259, 1160, 1132, 1032, 826, 792, 756.

HRMS (ESI-TOF, *m/z*): calc'd for $C_{22}H_{24}N_3O_2$ $[M+H]^+$: 362.1863; found: 362.1856

89m

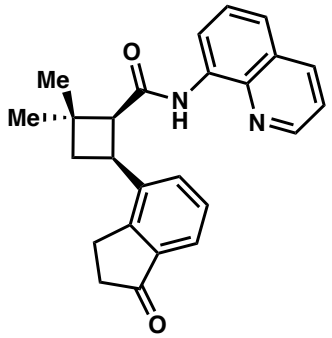

Prepared from cyclobutamide **6** (1 equiv, 50.8 mg, 0.2 mmol) and 4-iodo-1-indanone (2 equiv, 103.5 mg, 0.4 mmol). The crude residue was purified by column chromatography (30% EtOAc/Hexanes) to give a pale, yellow foam.

Run 1: (43.4 mg, 56%), Run 2: (39.7 mg, 52%)

R_f = 0.32 (silica gel, 40% EtOAc/Hex, UV, *p*-anisaldehyde).

$[\alpha]_D^{25}$ = +2.0° (c = 5.0, $CHCl_3$).

^{1}H NMR (400 MHz, $CDCl_3$): δ 9.57 (s, 1H), 8.74 (dd, *J* = 4.3, 1.7 Hz, 1H), 8.54 (dd, *J* = 7.1, 2.0 Hz, 1H), 8.10 (dd, *J* = 8.3, 1.7 Hz, 1H), 7.56 (ddt, *J* = 17.3, 7.6, 1.1 Hz, 2H), 7.46 – 7.33 (m, 4H), 4.07 (dt, *J* = 11.2, 8.4 Hz, 1H), 3.47 (ddd, *J* = 8.4, 3.0, 0.9 Hz, 1H), 3.10 (ddd, *J* = 17.1, 7.8, 3.8 Hz, 1H), 2.98 (ddd, *J* = 17.1, 7.6, 3.9 Hz, 1H), 2.92 (t, *J* = 10.8 Hz, 1H), 2.57 (dddd, *J* = 32.0, 19.4, 7.8, 3.7 Hz, 2H), 2.18 (ddd, *J* = 10.5, 8.4, 3.1 Hz, 1H), 1.58 (s, 3H), 1.23 (s, 3H).

^{13}C NMR (101 MHz, $CDCl_3$): δ 207.3, 170.1, 153.3, 148.1, 139.5, 138.3, 136.8, 136.5, 134.2, 132.9, 127.9, 127.5, 127.4, 121.6, 121.5, 121.4, 116.6, 57.2, 37.0, 36.5, 36.2, 34.1, 30.1, 25.2, 25.1.

FTIR (NaCl, thin film, cm^{-1}): 3353, 3012, 2954, 2927, 2866, 2359, 1709, 1587, 1523, 1485, 1425, 1386, 1324, 1265, 1162, 1055, 827, 790, 754, 666.

HRMS (ESI-TOF, *m/z*): calc'd for $C_{25}H_{25}N_2O_2$ $[M+H]^+$: 385.1911; found: 385.1921.

89n

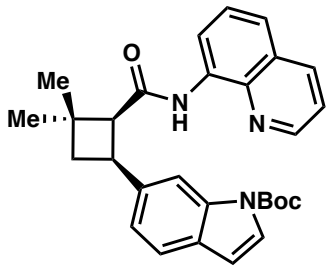

Prepared from cyclobutamide **6** (1 equiv, 50.8 mg, 0.2 mmol) and 6-iodo-N-Boc-indole (2 equiv, 137 mg, 0.4 mmol). The crude residue was purified by column chromatography (10% → 15% EtOAc/hexanes) to give a colorless foam.

Run 1: (56.1 mg, 60%), Run 2: (62.8 mg, 67%)

R_f = 0.36 (silica gel, 20% EtOAc/Hex, UV, *p*-anisaldehyde).

$[\alpha]_D^{25}$ = +114.7° (c = 5.7, $CHCl_3$).

^{1}H NMR (400 MHz, $CDCl_3$): δ 9.64 (s, 1H), 8.65 (dd, *J* = 4.2, 1.7 Hz, 1H), 8.60 (dd, *J* = 6.3, 2.8 Hz, 1H), 8.08 (dd, *J* = 8.3, 1.7 Hz, 1H), 8.03 (s, 1H), 7.47 (d, *J* = 3.7 Hz, 1H), 7.43 – 7.32 (m, 4H), 7.09 (dt, *J* = 8.1, 1.1 Hz, 1H), 6.44 (dd, *J* = 3.7, 0.8 Hz, 1H), 4.19 (dt, *J* = 10.9, 8.6 Hz, 1H), 3.44 (dd, *J* = 8.7, 2.9 Hz, 1H), 2.85 (t, *J* = 10.7 Hz, 1H), 2.25 (ddd, *J* = 10.3, 8.6, 3.0 Hz, 1H), 1.61 (s, 9H), 1.54 (s, 3H), 1.23 (s, 3H).

^{13}C NMR (101 MHz, $CDCl_3$): δ 170.6, 150.0, 147.9, 138.6, 138.4, 136.3, 135.5, 134.7, 128.7, 127.9, 127.5, 125.3, 121.6, 121.5, 121.1, 120.5, 116.5, 113.4, 107.4, 83.4, 57.9, 38.2, 36.4, 35.9, 30.2, 28.3, 25.3.

FTIR (NaCl, thin film, cm^{-1}): 3358, 3008, 2954, 2929, 2866, 1730, 1686, 1618, 1578, 1523, 1485, 1424, 1386, 1370, 1338, 1253, 1214, 1151, 117, 1077, 1022, 826, 816, 756.

HRMS (ESI-TOF, *m/z*): calc'd for $C_{29}H_{32}N_3O_3$ $[M+H]^+$: 470.2438; found: 470.2449.

89o

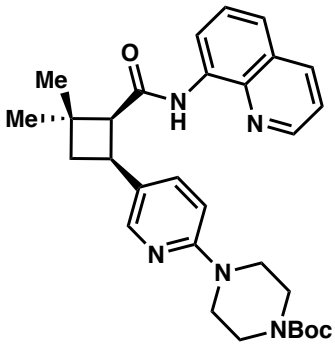

Prepared from cyclobutamide **6** (1 equiv, 50.8 mg, 0.2 mmol) and 4-(5-iodopyrin-2-yl)piperazine-1-carboxylic acid *tert*-butyl ester (2 equiv, 156 mg, 0.4 mmol). The crude residue was purified by column chromatography using silica gel basified with 5 mL of aqueous ammonium hydroxide (20% EtOAc/2% Et_3N/78% hexanes → 30% EtOAc/2% Et_3N/68% hexanes → 40% EtOAc/2% Et_3N/58% hexanes) to give a pale, yellow foam.

Run 1: (79.9 mg, 77%), Run 2: (84.6 mg, 82%)

R_f = 0.27 (silica gel, 40% EtOAc/Hex, UV, *p*-anisaldehyde).

$[\alpha]_D^{25}$ = +69.2° (c = 5.1, $CHCl_3$).

^{1}H NMR (500 MHz, $CDCl_3$): δ 9.58 (s, 1H), 8.74 (dd, *J* = 4.2, 1.7 Hz, 1H), 8.62 (p, *J* = 4.4 Hz, 1H), 8.10 (dd, *J* = 8.2, 1.7 Hz, 1H), 8.06 (dt, *J* = 2.5, 0.8 Hz, 1H), 7.50 (ddd, *J* = 8.7, 2.5, 0.7 Hz, 1H), 7.46 – 7.37 (m, 3H), 6.53 (dd, *J* = 8.8, 0.8 Hz, 1H), 3.93 (dt, *J* = 11.0, 8.6 Hz, 1H), 3.45 (dd, *J* = 6.6, 3.5 Hz, 4H), 3.39 (dd, *J* = 6.3, 3.6 Hz, 4H), 3.30 (dd, *J* = 8.4, 2.9 Hz, 1H), 2.74 (t, *J* = 10.8 Hz, 1H), 2.10 (ddd, *J* = 10.4, 8.5, 2.9 Hz, 1H), 1.51 (s, 4H), 1.47 (s, 9H), 1.24 (s, 3H).

^{13}C NMR (101 MHz, $CDCl_3$): δ 170.4, 158.0, 154.9, 148.0, 146.8, 138.4, 137.0, 136.4, 134.5, 127.9, 127.4, 126.4, 121.6, 121.2, 116.4, 106.9, 79.9, 57.7, 45.5, 37.6, 35.9, 33.5, 30.1, 28.5, 25.1.

FTIR (NaCl, thin film, cm^{-1}): 3357, 3007, 2973, 2928, 2864, 2360, 1686, 1605, 1560, 1524, 1486, 1424, 1391, 1324, 1241, 1166, 1129, 1084, 1000, 934, 864, 826, 792, 756, 686, 666.

HRMS (ESI-TOF, *m/z*): calc'd for $C_{30}H_{38}N_5O_3$ $[M+H]^+$: 516.2969; found: 516.2955.

89p

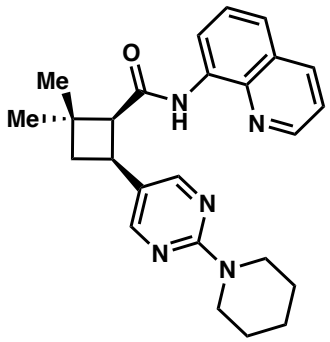

Prepared from cyclobutamide **6** (1 equiv, 50.8 mg, 0.2 mmol) and 5-iodo-2-(1-piperidinyl)pyrimidine (2 equiv, 116 mg, 0.4 mmol). The crude residue was purified by column chromatography using silica gel basified with 5 mL of aqueous ammonium hydroxide (10% EtOAc/2% Et_3N/88% hexanes → 20% EtOAc/2% Et_3N/78% hexanes → 30% EtOAc/2% Et_3N/68% hexanes) to give a pale yellow foam.

Run 1: (63.0 mg, 76%), Run 2: (60.6 mg, 73%)

R_f = 0.44 (silica gel, 40% EtOAc/Hex, UV).

$[\alpha]_D^{25}$ = +83.3° (c = 3.1, $CHCl_3$).

^{1}H NMR (400 MHz, $CDCl_3$): δ 9.59 (s, 1H), 8.74 (dd, *J* = 4.2, 1.7 Hz, 1H), 8.67 (dd, *J* = 6.6, 2.4 Hz, 1H), 8.25 (s, 2H), 8.10 (dd, *J* = 8.2, 1.7 Hz, 1H), 7.47 – 7.42 (m, 2H), 7.40 (dd, *J* = 8.2, 4.2 Hz, 2H), 3.81 (dt, *J* = 11.0, 8.6 Hz, 1H), 3.67 (dd, *J* = 6.2, 4.9 Hz, 4H), 3.27 (dd, *J* = 8.6, 2.9 Hz, 1H), 2.74 (t, *J* = 10.8 Hz, 1H), 2.07 (ddd, *J* = 10.6, 8.5, 2.9 Hz, 1H), 1.60 (p, *J* = 5.5 Hz, 2H), 1.52 (qd, *J* = 5.6, 5.1, 2.3 Hz, 4H), 1.49 (s, 3H), 1.24 (s, 3H).

^{13}C NMR (101 MHz, $CDCl_3$): δ 170.2, 160.8, 157.1, 148.1, 138.4, 136.4, 134.5, 127.9, 127.5, 121.6, 121.3, 120.8, 116.5, 57.4, 45.0, 37.3, 36.1, 31.8, 30.0, 25.8, 25.1, 25.0.

FTIR (NaCl, thin film, cm^{-1}): 3355, 2031, 2853, 1682, 1603, 1524, 1485, 1462, 1447, 1366, 1324, 1274, 1256, 1160, 1025, 946, 826, 792, 754.

HRMS (ESI-TOF, *m/z*): calc'd for $C_{25}H_{30}N_5O$ $[M+H]^+$: 416.2445; found: 416.2440.

1.5.9 Chiral SFC Traces of Racemic and Enantioenriched Products

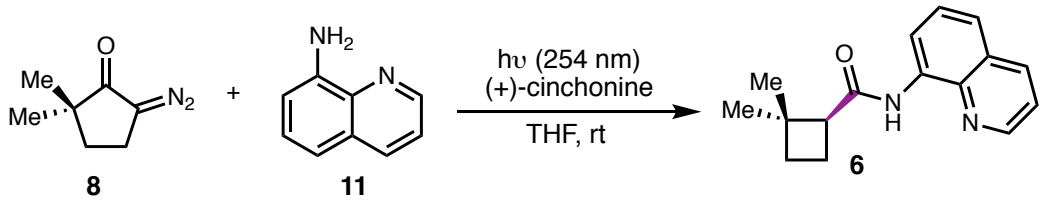

8 **11** **6**

SFC data for racemic 6

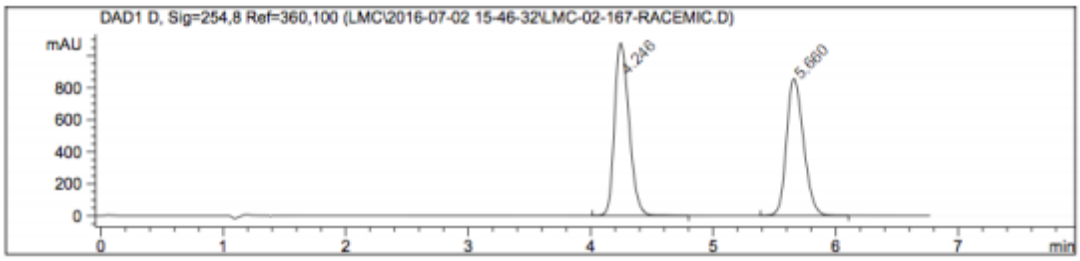

Peak #	RetTime [min]	Type	Width [min]	Area [mAU*s]	Height [mAU]	Area %
1	4.246	BB	0.1286	8934.03320	1078.74268	51.8271
2	5.660	BB	0.1532	8304.11426	855.84570	48.1729

Enantioenriched 6 before recrystallization

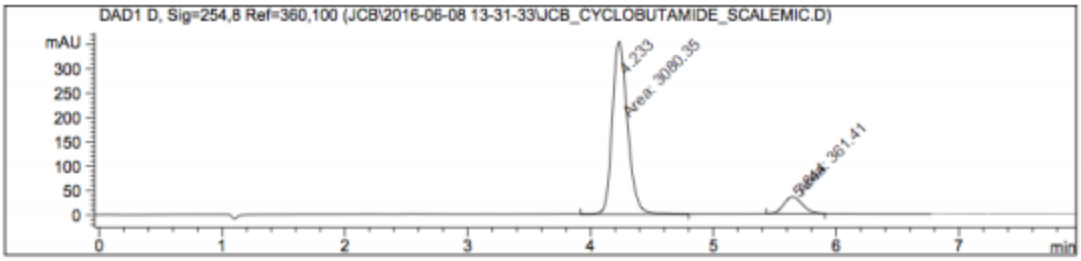

Peak #	RetTime [min]	Type	Width [min]	Area [mAU*s]	Height [mAU]	Area %
1	4.233	MM	0.1444	3080.35034	355.58780	89.4993
2	5.644	MM	0.1739	361.41000	34.64573	10.5007

Enantiopure 6 after a single recrystallization

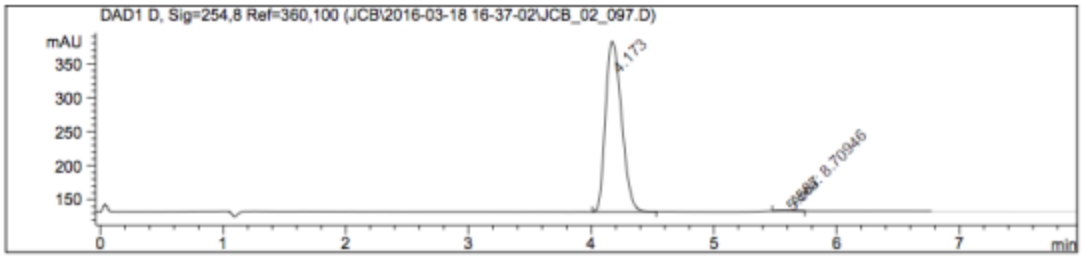

Peak #	RetTime [min]	Type	Width [min]	Area [mAU*s]	Height [mAU]	Area %
1	4.173	BB	0.1464	2285.16455	250.58836	99.6203
2	5.587	MM	0.1518	8.70946	9.55969e-1	0.3797

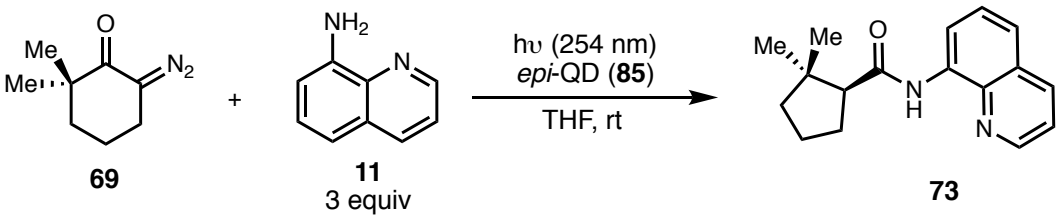

SFC data for racemic 73

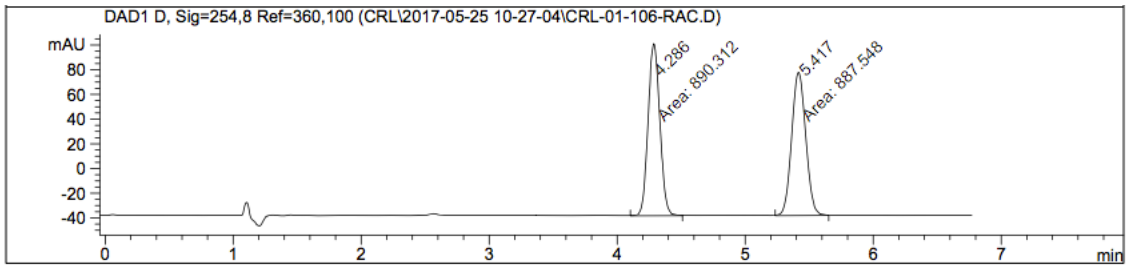

Peak #	RetTime [min]	Type	Width [min]	Area [mAU*s]	Area %
1	4.286	MM	0.1063	890.31165	50.0777
2	5.417	MM	0.1274	887.54810	49.9223

Enantioenriched 73

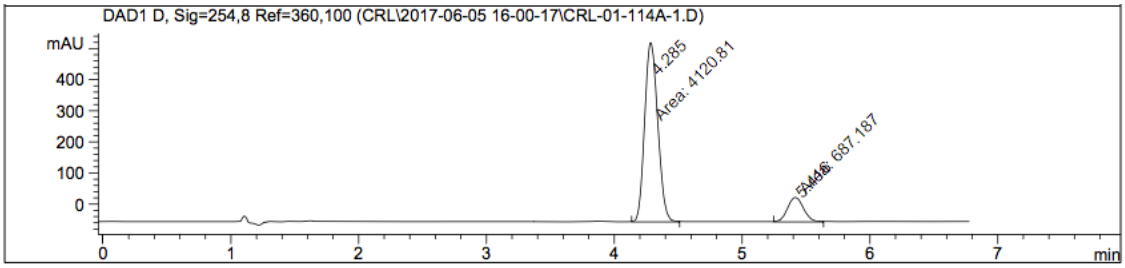

Peak #	RetTime [min]	Type	Width [min]	Area [mAU*s]	Area %
1	4.285	MM	0.1189	4120.80518	85.7074
2	5.416	MM	0.1449	687.18732	14.2926

Enantioenriched 73 with 20 mol % catalyst loading

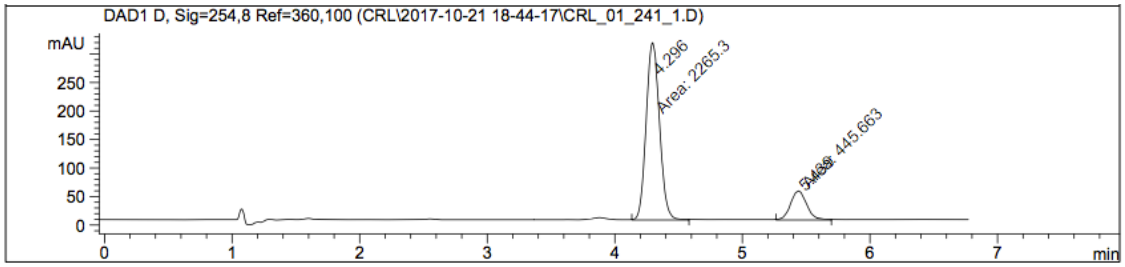

Peak #	RetTime [min]	Type	Width [min]	Area [mAU*s]	Area %
1	4.296	MM	0.1212	2265.30225	83.5607
2	5.439	MM	0.1461	445.66309	16.4393

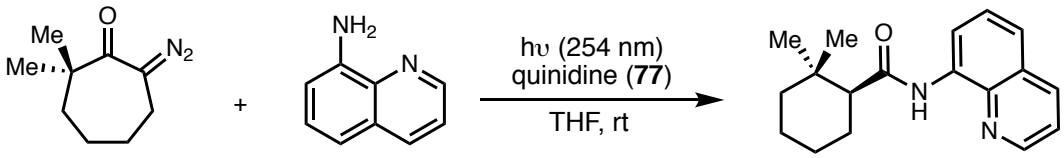

70 + **11** 3 equiv → **74**

SFC data for racemic 74 (12 min run, the rest for 74 are 15 min)

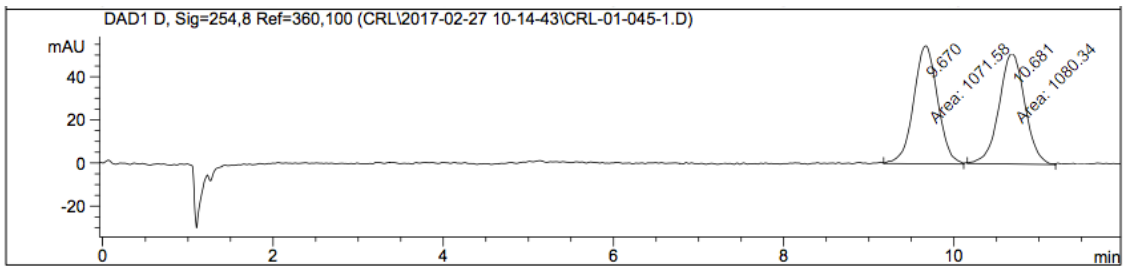

Peak #	RetTime [min]	Type	Width [min]	Area [mAU*s]	Area %
1	9.670	MM	0.3268	1071.58496	49.7965
2	10.681	MM	0.3511	1080.34424	50.2035

Enantioenriched 74

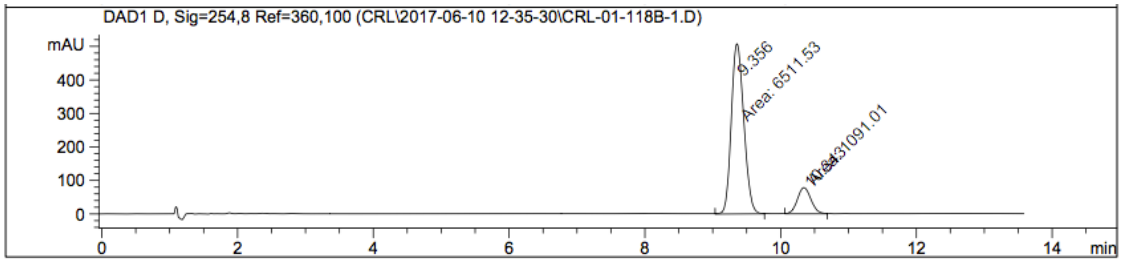

Peak #	RetTime [min]	Type	Width [min]	Area [mAU*s]	Area %
1	9.356	MM	0.2135	6511.52734	85.6494
2	10.343	MM	0.2316	1091.00696	14.3506

Enantioenriched 74 with 20 mol % catalyst loading

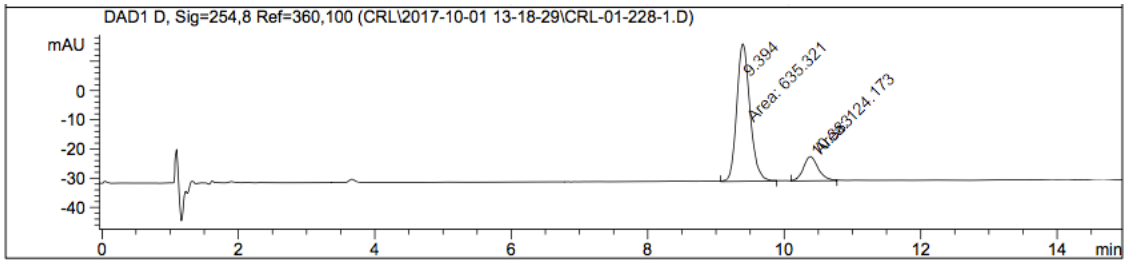

Peak #	RetTime [min]	Type	Width [min]	Area [mAU*s]	Area %
1	9.394	MM	0.2252	635.32117	83.6505
2	10.383	MM	0.2495	124.17338	16.3495

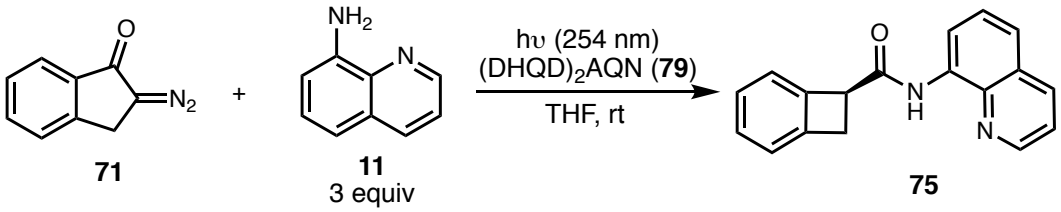

SFC data for racemic 75

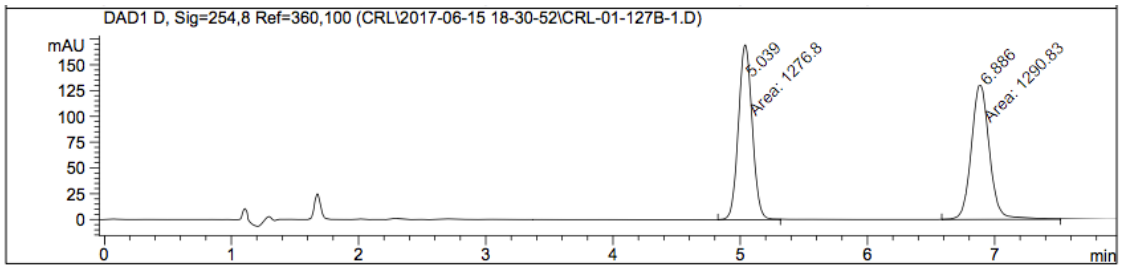

Peak #	RetTime [min]	Type	Width [min]	Area [mAU*s]	Area %
1	5.039	MM	0.1254	1276.80469	49.7268
2	6.886	MM	0.1641	1290.83447	50.2732

Enantioenriched 75

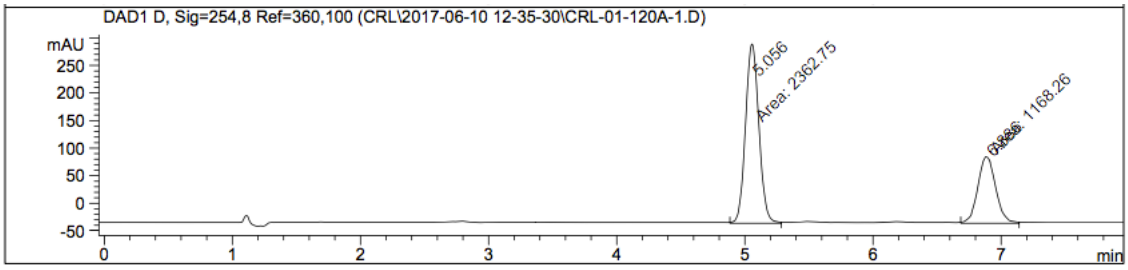

Peak #	RetTime [min]	Type	Width [min]	Area [mAU*s]	Area %
1	5.056	MM	0.1210	2362.74805	66.9143
2	6.886	MM	0.1605	1168.25940	33.0857

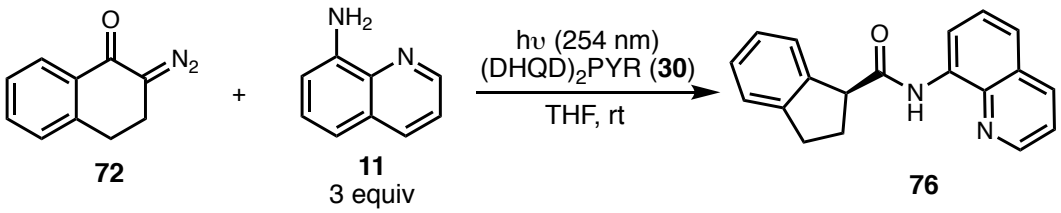

SFC data for racemic 76

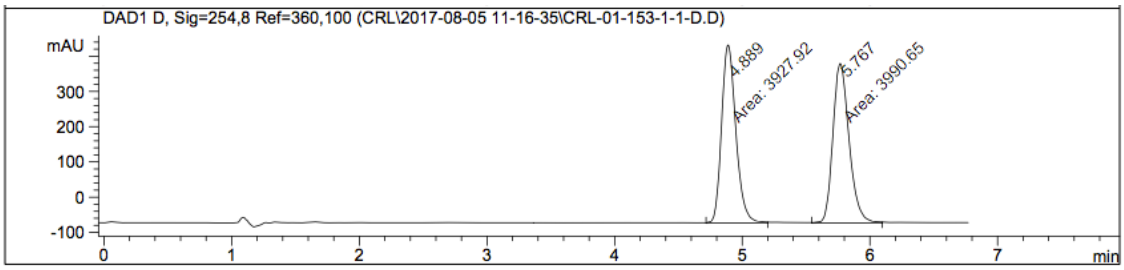

Peak #	RetTime [min]	Type	Width [min]	Area [mAU*s]	Area %
1	4.889	MM	0.1294	3927.92065	49.6039
2	5.767	MM	0.1468	3990.65186	50.3961

Enantioenriched 76

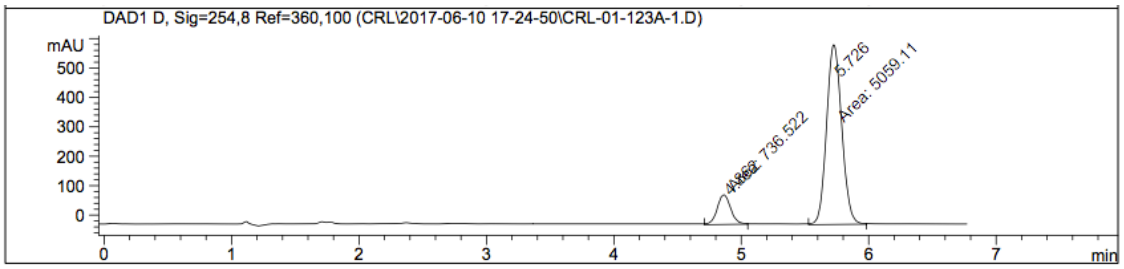

Peak #	RetTime [min]	Type	Width [min]	Area [mAU*s]	Area %
1	4.862	MM	0.1218	736.52246	12.7082
2	5.726	MM	0.1379	5059.11182	87.2918

1.5.10 C–H Proof of Enantiopurity

89m, racemic sample. Chiral SFC: (OD-H, 2.5 mL/min, 20% IPA in CO_2, λ = 254 nm):

t_R(minor) = 9.7 min, t_R(major) = 11.1 min.

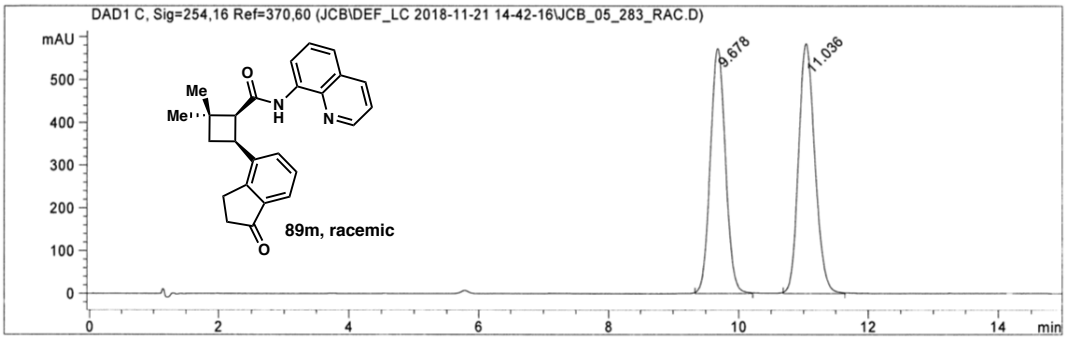

Peak #	RetTime [min]	Type	Width [min]	Area [mAU*s]	Height [mAU]	Area %
1	9.678	BB	0.2468	9170.02637	572.63605	47.0183
2	11.036	BB	0.2746	1.03331e4	583.59204	52.9817

9m, enantioenriched sample. Chiral SFC: (OD-H, 2.5 mL/min, 20% IPA in CO_2, λ = 254 nm): t_R(minor) = 9.7 min, t_R(major) = 11.1 min.

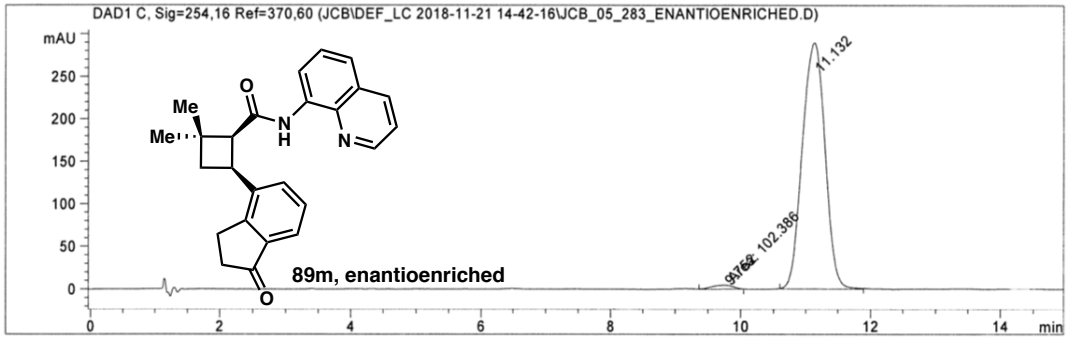

Peak #	RetTime [min]	Type	Width [min]	Area [mAU*s]	Height [mAU]	Area %
1	9.752	MM	0.3621	102.38605	4.71307	1.4187
2	11.132	BB	0.3991	7114.58105	289.14011	98.5813

1.6 REFERENCES

(1) Shao, M.; Wang, Y.; Liu, Z.; Zhang, D.-M.; Cao, H.-H.; Jiang, R.-W.; Fan, C.-L.; Zhang, X.-Q.; Chen, H.-R.; Yao, X.-S.; Ye, W.-C. *Org. Lett.* **2010**, *12* (21), 5040–5043.

(2) Dembitsky, V. M. *J. Nat. Med.* **2008**, *62* (1), 1–33.

(3) Chung, H.-M.; Chen, Y.-H.; Lin, M.-R.; Su, J.-H.; Wang, W.-H.; Sung, P.-J. *Tetrahedron Lett.* **2010**, *51* (46), 6025–6027.

(4) Wang, Y.-H.; Hou, A.-J.; Chen, D.-F.; Weiller, M.; Wendel, A.; Staples, R. J. *Eur. J. Org. Chem.* **2006**, *2006* (15), 3457–3463.

(5) Takao, K.; Hayakawa, N.; Yamada, R.; Yamaguchi, T.; Morita, U.; Kawasaki, S.; Tadano, K. *Angew. Chem. Int. Ed.* **2008**, *47* (18), 3426–3429.

(6) Magnan, R. F.; Rodrigues-Fo, E.; Daolio, C.; Ferreira, A. G.; Souza, A. Q. L. de. *Z. Für Naturforschung C* **2003**, *58* (5–6), 319–324.

(7) Fructos, M. R.; Prieto, A. *Tetrahedron* **2016**, *72* (3), 355–369.

(8) Chapman, L. M.; Beck, J. C.; Wu, L.; Reisman, S. E. *J. Am. Chem. Soc.* **2016**, *138* (31), 9803–9806.

(9) Chapman, L. M.; Beck, J. C.; Lacker, C. R.; Wu, L.; Reisman, S. E. *J. Org. Chem.* **2018**.

(10) Ghosh, A.; Banerjee, U. K.; Venkateswaran, R. V. *Tetrahedron* **1990**, *46* (8), 3077–3088.

(11) Banerjes, U. K.; Venkateswaran, R. V. *Tetrahedron Lett.* **1983**, *24* (4), 423–424.

(12) Hodous, B. L.; Fu, G. C. *J. Am. Chem. Soc.* **2002**, *124* (8), 1578–1579.

(13) Hodous, B. L.; Fu, G. C. *J. Am. Chem. Soc.* **2002**, *124* (34), 10006–10007.

(14) Wiskur, S. L.; Fu, G. C. *J. Am. Chem. Soc.* **2005**, *127* (17), 6176–6177.

(15) Dai, X.; Nakai, T.; Romero, J. A. C.; Fu, G. C. *Angew. Chem. Int. Ed.* **2007**, *46* (23), 4367–4369.

(16) Fu, G. C. *Acc. Chem. Res.* **2004**, *37* (8), 542–547.

(17) He, L.; Lv, H.; Zhang, Y.-R.; Ye, S. *J. Org. Chem.* **2008**, *73* (20), 8101–8103.

(18) France, S.; Wack, H.; Taggi, A. E.; Hafez, A. M.; Wagerle, T. R.; Shah, M. H.; Dusich, C. L.; Lectka, T. *J. Am. Chem. Soc.* **2004**, *126* (13), 4245–4255.

(19) Wang, J.; Hou, Y. *J. Chem. Soc. Perkin 1* **1998**, No. 12, 1919–1924.

(20) Chapman, L. M. (2017) Development of a Synthetic Strategy Toward Trans-Cyclobutane-Containing Natural Products: Enantioselective Total Synthesis of (+)-Psiguadial B. Dissertation (Ph.D.), California Institute of Technology. doi:10.7907/Z90G3H5M. https://resolver.caltech.edu/CaltechTHESIS:06052017-010024254

(21) Pracejus, H. *Justus Liebigs Ann. Chem.* **1960**, *634* (1), 9–22.

(22) Wynberg, H.; Staring, E. G. J. *J. Am. Chem. Soc.* **1982**, *104* (1), 166–168.

(23) Wynberg, H.; Staring, E. G. J. *J. Org. Chem.* **1985**, *50* (11), 1977–1979.

(24) Calter, M. A. *J. Org. Chem.* **1996**, *61* (23), 8006–8007.

(25) Dogo-Isonagie, C.; Bekele, T.; France, S.; Wolfer, J.; Weatherwax, A.; Taggi, A. E.; Paull, D. H.; Dudding, T.; Lectka, T. *Eur. J. Org. Chem.* **2007**, *2007* (7), 1091–1100.

(26) Paull, D. H.; Weatherwax, A.; Lectka, T. *Tetrahedron* **2009**, *65* (34), 6771–6803.

(27) Zaitsev, V. G.; Shabashov, D.; Daugulis, O. *J. Am. Chem. Soc.* **2005**, *127* (38), 13154–13155.

(28) Shabashov, D.; Daugulis, O. *J. Am. Chem. Soc.* **2010**, *132* (11), 3965–3972.

(29) Parella, R.; Gopalakrishnan, B.; Babu, S. A. *J. Org. Chem.* **2013**, *78* (23), 11911–11934.

(30) Chen, T.; Barton, L. M.; Lin, Y.; Tsien, J.; Kossler, D.; Bastida, I.; Asai, S.; Bi, C.; Chen, J. S.; Shan, M.; Fang, H.; Fang, F. G.; Choi, H.; Hawkins, L.; Qin, T.; Baran, P. S. *Nature* **2018**.

(31) Xiao, K.-J.; Lin, D. W.; Miura, M.; Zhu, R.-Y.; Gong, W.; Wasa, M.; Yu, J.-Q. *J. Am. Chem. Soc.* **2014**, *136* (22), 8138–8142.

(32) Wu, Q.-F.; Wang, X.-B.; Shen, P.-X.; Yu, J.-Q. *ACS Catal.* **2018**, *8* (3), 2577–2581.

(33) Gutekunst, W. R.; Baran, P. S. *J. Am. Chem. Soc.* **2011**, *133* (47), 19076–19079.

(34) Gutekunst, W. R.; Gianatassio, R.; Baran, P. S. *Angew. Chem. Int. Ed.* **2012**, *51* (30), 7507–7510.

(35) Gutekunst, W. R.; Baran, P. S. *J. Org. Chem.* **2014**, *79* (6), 2430–2452.

(36) Ting, C. P.; Maimone, T. J. *Angew. Chem. Int. Ed.* **2014**, *53* (12), 3115–3119.

(37) Lian, M.; Li, Z.; Du, J.; Meng, Q.; Gao, Z. *Eur. J. Org. Chem.* **2010**, *2010* (34), 6525–6530.

(38) Hiratake, J.; Inagaki, M.; Yamamoto, Y.; Oda, J. *J. Chem. Soc. Perkin 1* **1987**, No. 0, 1053–1058.

(39) Beck, J. C.; Lacker, C. R.; Chapman, L. M.; Reisman, S. E. *Chem. Sci.* **2019**, *10* (8), 2315–2319.

(40) Liu, H.; Drizin, I.; Koenig, J.; Cowart, M.; Zhao, C.; Wakefield, B.; Black, L.; Altenbach, R. 5,6,7,8-Tetrahydroquinazolin-2-Amine Derivatives and Related Compoundsa as Histamine H4 Receptor Modulators for the Treatment of Asthma. US Patent WO 0029123967, October 8, 2009.

(41) Cernijenko, A.; Risgaard, R.; Baran, P. S. *J. Am. Chem. Soc.* **2016**, *138* (30), 9425–9428.

(42) Rosenfeld, M. J.; Shankar, B. K. R.; Shechter, H. *J. Org. Chem.* **1988**, *53* (12), 2699–2705.

(43) Sato, Y.; Fujisawa, H.; Mukaiyama, T. *Bull. Chem. Soc. Jpn.* **2006**, *79* (8), 1275–1287.

(44) Vuluga, D.; Legros, J.; Crousse, B.; Bonnet-Delpon, D. *Green Chem.* **2009**, *11* (2), 156–159.

(45) Drizin, I.; Koenig, J. R.; Cowart, M. D. Macrocyclic Benzofused Pyrimidine Derivatives. US Patent US20080188452A1, October 2, 2006.

Appendix 1

Spectra Relevant to Chapter 1:

Enantioselective Ketene Trapping and Diastereoselective C–H Activation: Methods Developed from the Total Synthesis of (+)-Psiguadial B

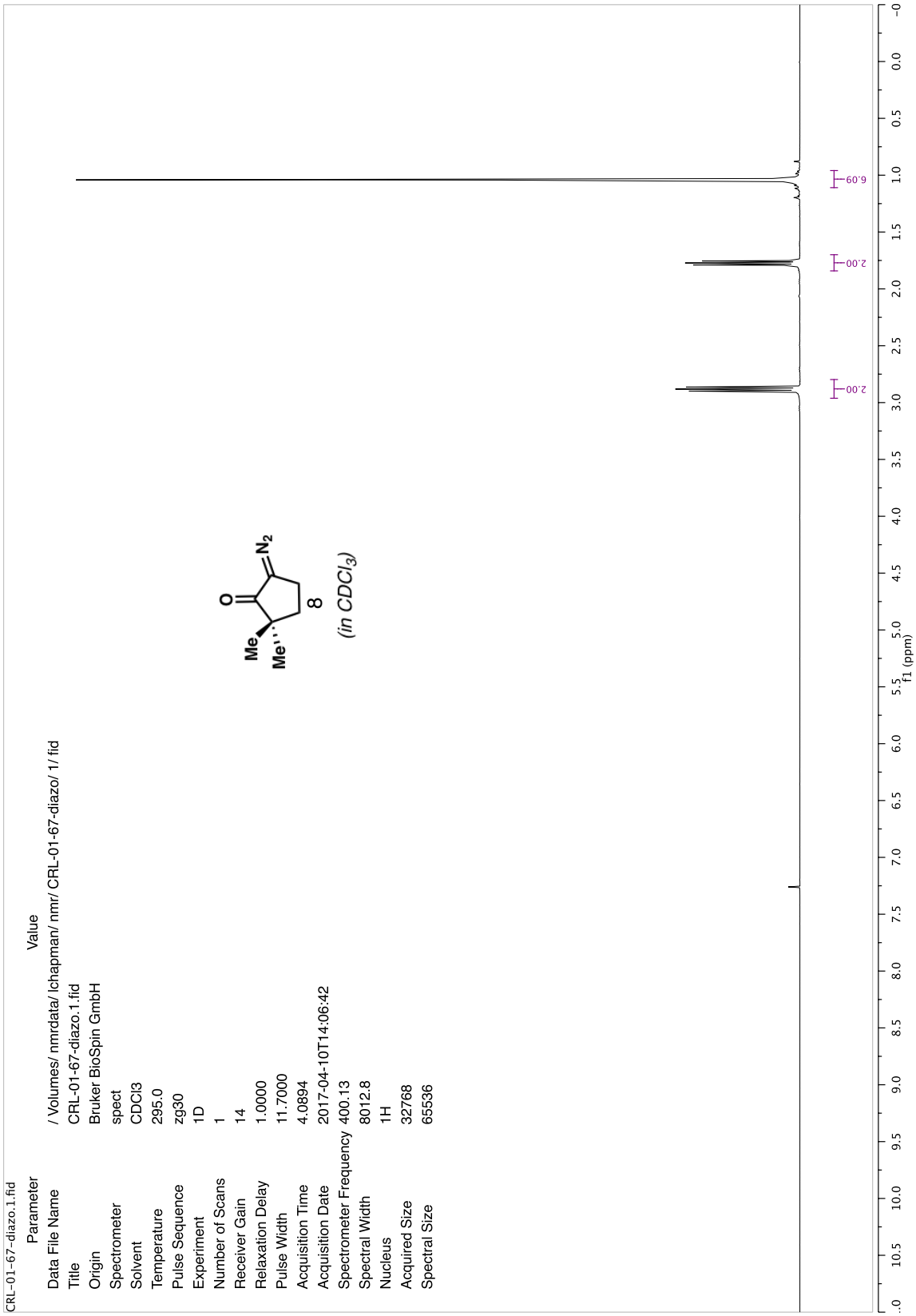
CRL-01-67-diazo.1.fid
Parameter Value
Data File Name / Volumes/ nmrdata/ lchapman/ nmr/ CRL-01-67-diazo/ 1/ fid
Title CRL-01-67-diazo.1.fid
Origin Bruker BioSpin GmbH
Spectrometer spect
Solvent CDCl3
Temperature 295.0
Pulse Sequence zg30
Experiment 1D
Number of Scans 1
Receiver Gain 14
Relaxation Delay 1.0000
Pulse Width 11.7000
Acquisition Time 4.0894
Acquisition Date 2017-04-10T14:06:42
Spectrometer Frequency 400.13
Spectral Width 8012.8
Nucleus 1H
Acquired Size 32768
Spectral Size 65536
O
N2
Me
Me
8
(in CDCl3)
6.09
2.00
2.00
f1 (ppm)

S32

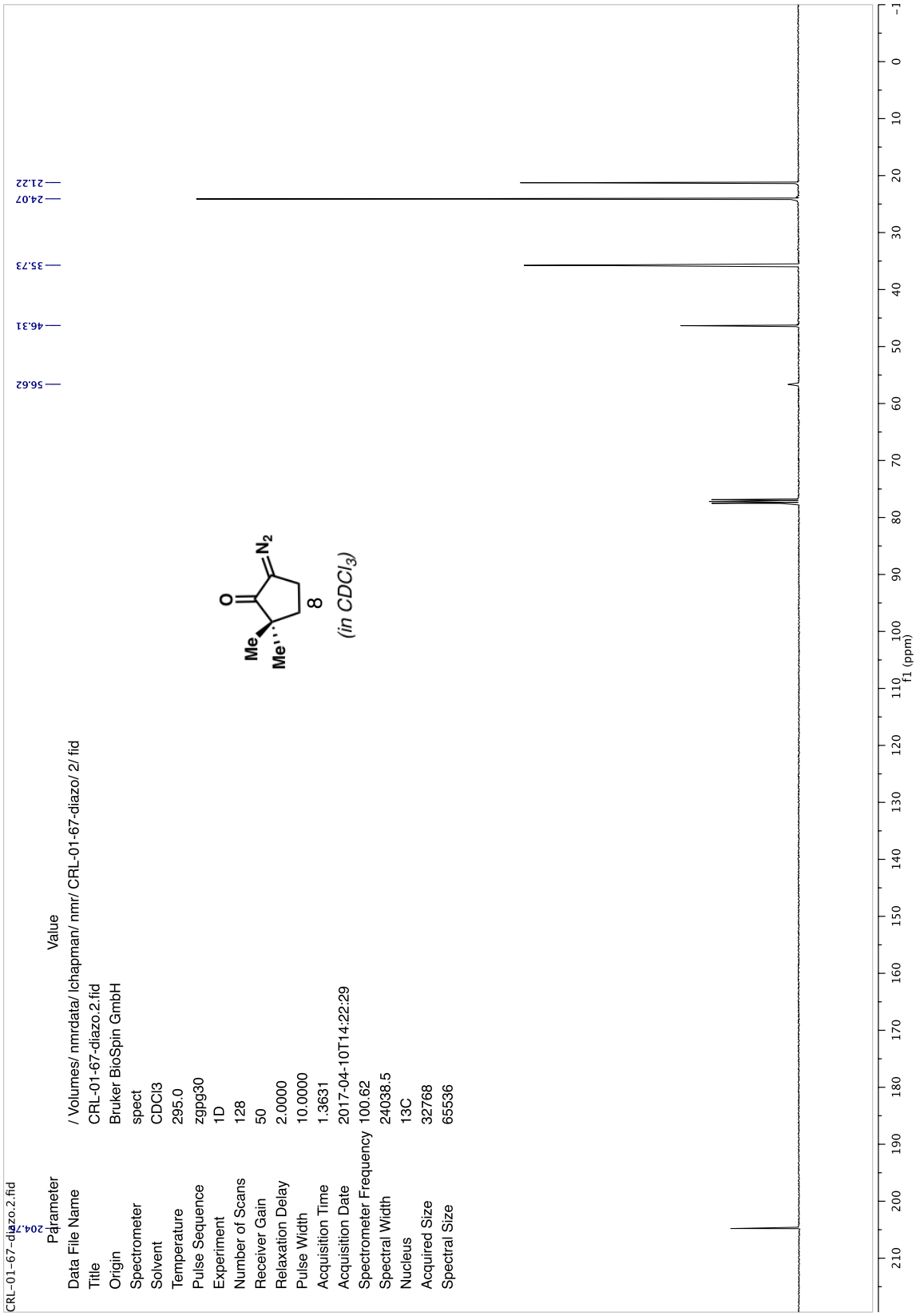

Parameter	Value
Data File Name	/ Volumes/ nmrdata/ lchapman/ nmr/ CRL-01-67-diazo/ 2/ fid
Title	CRL-01-67-diazo.2.fid
Origin	Bruker BioSpin GmbH
Spectrometer	spect
Solvent	CDCl3
Temperature	295.0
Pulse Sequence	zgpg30
Experiment	1D
Number of Scans	128
Receiver Gain	50
Relaxation Delay	2.0000
Pulse Width	10.0000
Acquisition Time	1.3631
Acquisition Date	2017-04-10T14:22:29
Spectrometer Frequency	100.62
Spectral Width	24038.5
Nucleus	13C
Acquired Size	32768
Spectral Size	65536

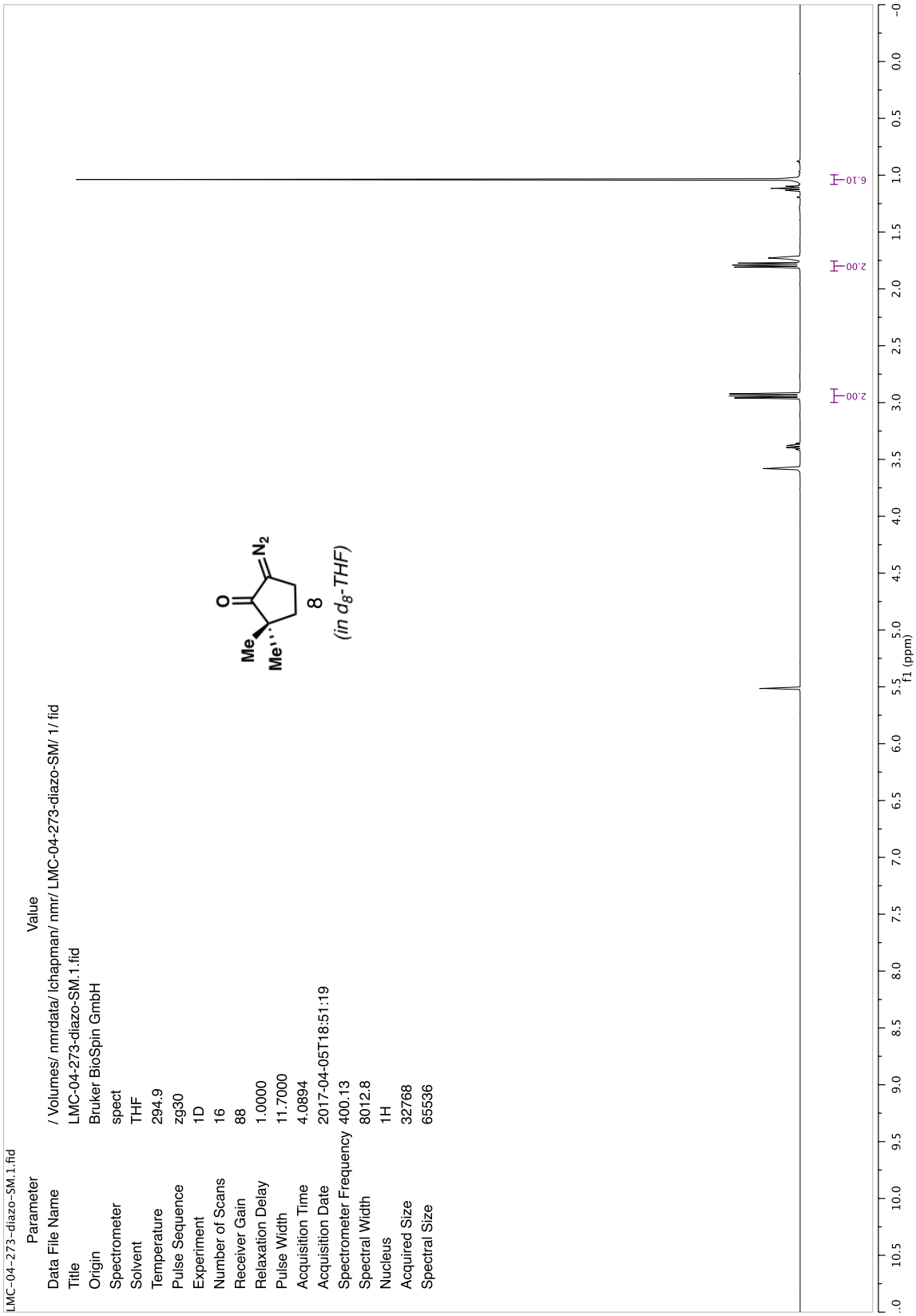
LMC-04-273-diazo-SM.1.fid
Parameter Value
Data File Name / Volumes/ nmrdata/ lchapman/ nmr/ LMC-04-273-diazo-SM/ 1/ fid
Title LMC-04-273-diazo-SM.1.fid
Origin Bruker BioSpin GmbH
Spectrometer spect
Solvent THF
Temperature 294.9
Pulse Sequence zg30
Experiment 1D
Number of Scans 16
Receiver Gain 88
Relaxation Delay 1.0000
Pulse Width 11.7000
Acquisition Time 4.0894
Acquisition Date 2017-04-05T18:51:19
Spectrometer Frequency 400.13
Spectral Width 8012.8
Nucleus 1H
Acquired Size 32768
Spectral Size 65536
O
N2
Me
Me
8
(in d8-THF)
6.10
2.00
2.00
f1 (ppm)

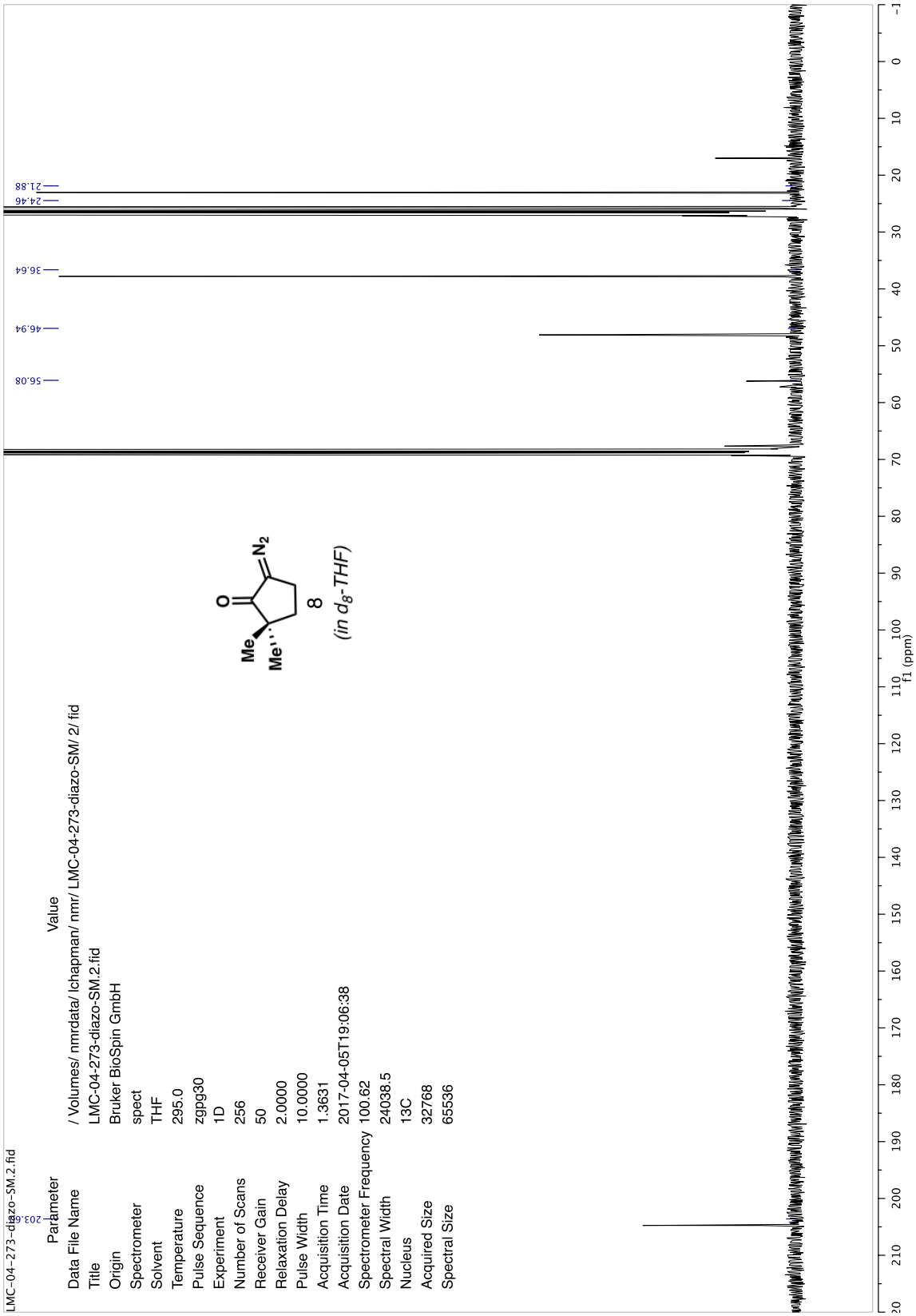
LMC-04-273-diazo-SM.2.fid
203.69
21.88
24.46
36.64
46.94
56.08
f1 (ppm)
Parameter Value
Data File Name / Volumes/ nmrdata/ lchapman/ nmr/ LMC-04-273-diazo-SM/ 2/ fid
Title LMC-04-273-diazo-SM.2.fid
Origin Bruker BioSpin GmbH
Spectrometer spect
Solvent THF
Temperature 295.0
Pulse Sequence zgpg30
Experiment 1D
Number of Scans 256
Receiver Gain 50
Relaxation Delay 2.0000
Pulse Width 10.0000
Acquisition Time 1.3631
Acquisition Date 2017-04-05T19:06:38
Spectrometer Frequency 100.62
Spectral Width 24038.5
Nucleus 13C
Acquired Size 32768
Spectral Size 65536
O
N2
Me
Me
8
(in d8-THF)

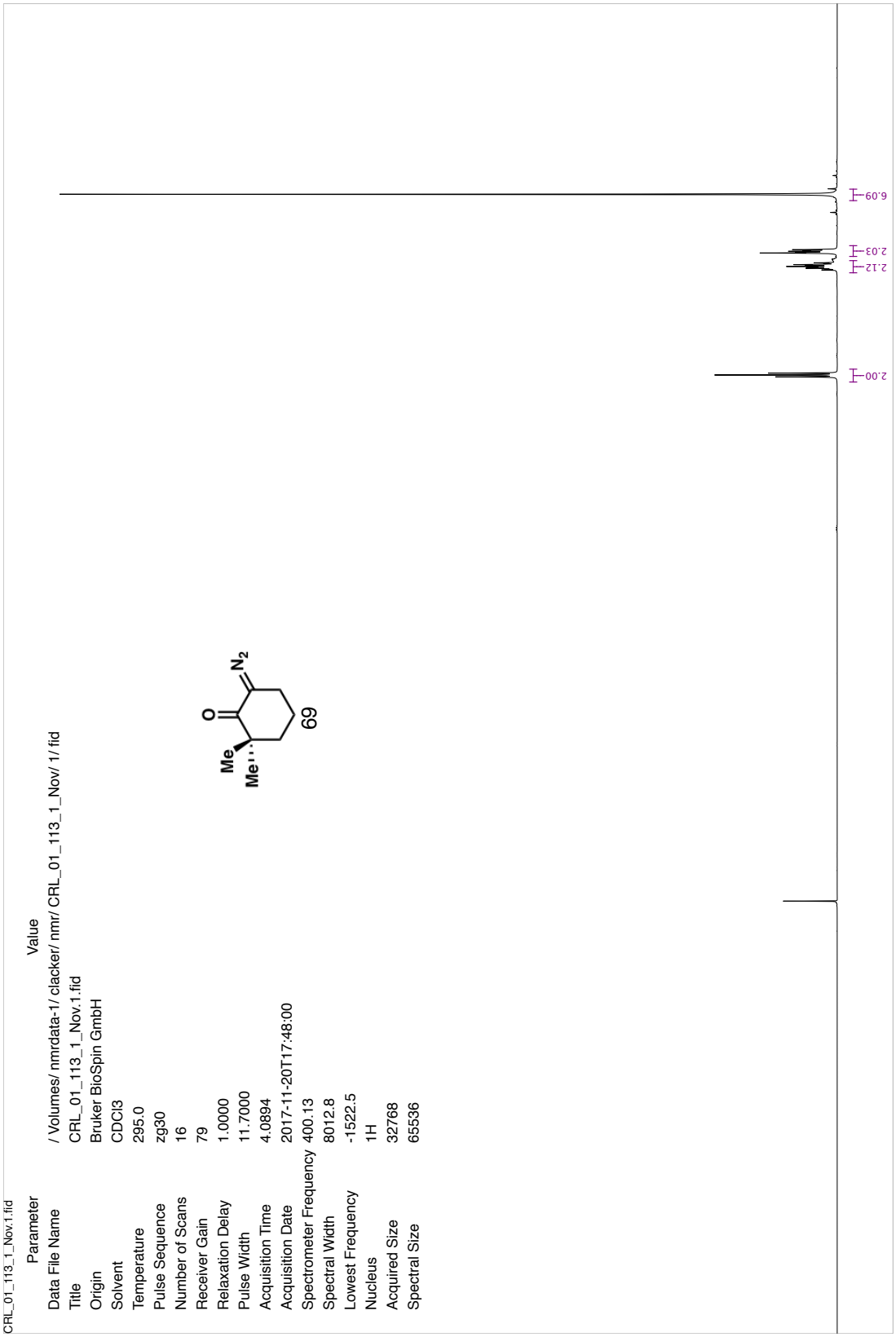
CRL_01_113_1_Nov1.fid
Parameter
Value
Data File Name / Volumes/ nmrdata-1/ clacker/ nmr/ CRL_01_113_1_Nov/ 1/ fid
Title CRL_01_113_1_Nov.1.fid
Origin Bruker BioSpin GmbH
Solvent CDCl3
Temperature 295.0
Pulse Sequence zg30
Number of Scans 16
Receiver Gain 79
Relaxation Delay 1.0000
Pulse Width 11.7000
Acquisition Time 4.0894
Acquisition Date 2017-11-20T17:48:00
Spectrometer Frequency 400.13
Spectral Width 8012.8
Lowest Frequency -1522.5
Nucleus 1H
Acquired Size 32768
Spectral Size 65536
Me
Me
O
N2
69
6.09
2.03
2.12
2.00
f1 (ppm)

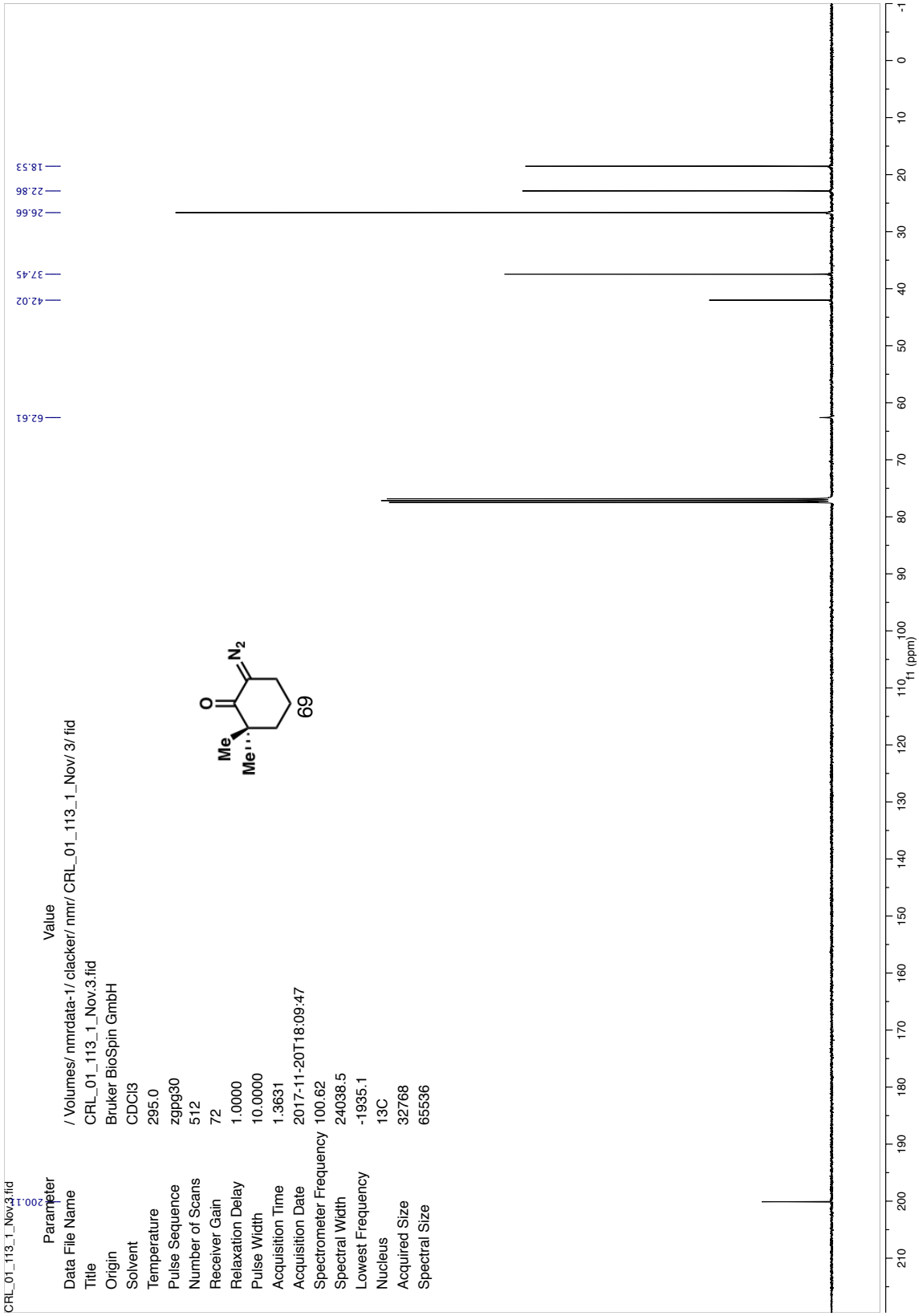
CRL_01_113_1_Nov3.fid
200.1
Parameter
Value
Data File Name / Volumes/ nmrdata-1/ clacker/ nmr/ CRL_01_113_1_Nov/ 3/ fid
Title CRL_01_113_1_Nov.3.fid
Origin Bruker BioSpin GmbH
Solvent CDCl3
Temperature 295.0
Pulse Sequence zgpg30
Number of Scans 512
Receiver Gain 72
Relaxation Delay 1.0000
Pulse Width 10.0000
Acquisition Time 1.3631
Acquisition Date 2017-11-20T18:09:47
Spectrometer Frequency 100.62
Spectral Width 24038.5
Lowest Frequency -1935.1
Nucleus 13C
Acquired Size 32768
Spectral Size 65536
18.53
22.86
26.66
37.45
42.02
62.61
Me
Me
O
N2
69
f1 (ppm)

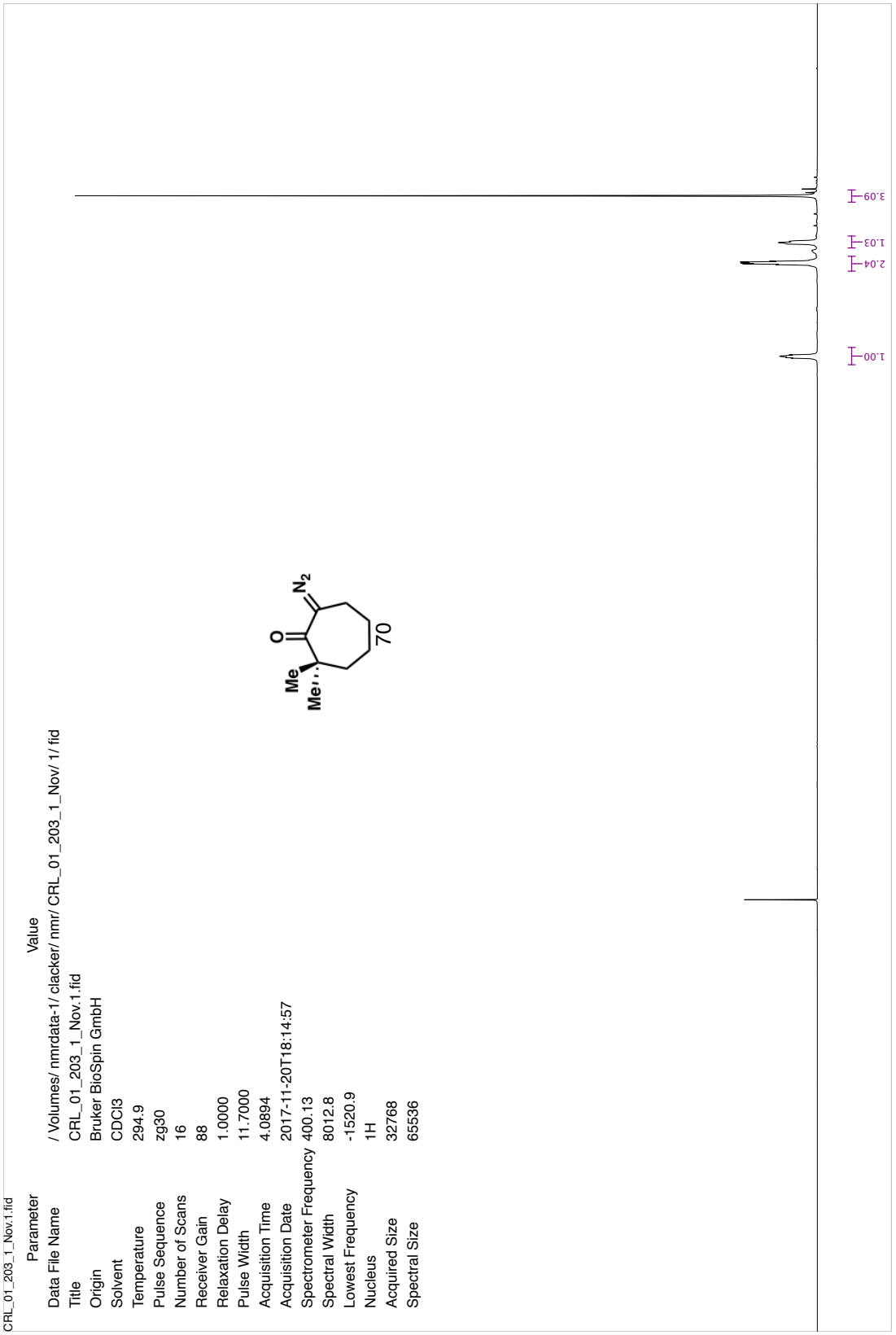
CRL_01_203_1_Nov.1.fid
Parameter Value
Data File Name / Volumes/ nmrdata-1/ clacker/ nmr/ CRL_01_203_1_Nov/ 1/ fid
Title CRL_01_203_1_Nov.1.fid
Origin Bruker BioSpin GmbH
Solvent CDCl3
Temperature 294.9
Pulse Sequence zg30
Number of Scans 16
Receiver Gain 88
Relaxation Delay 1.0000
Pulse Width 11.7000
Acquisition Time 4.0894
Acquisition Date 2017-11-20T18:14:57
Spectrometer Frequency 400.13
Spectral Width 8012.8
Lowest Frequency -1520.9
Nucleus 1H
Acquired Size 32768
Spectral Size 65536
Me
Me
O
N2
70
1.00
2.04
1.03
3.09
f1 (ppm)

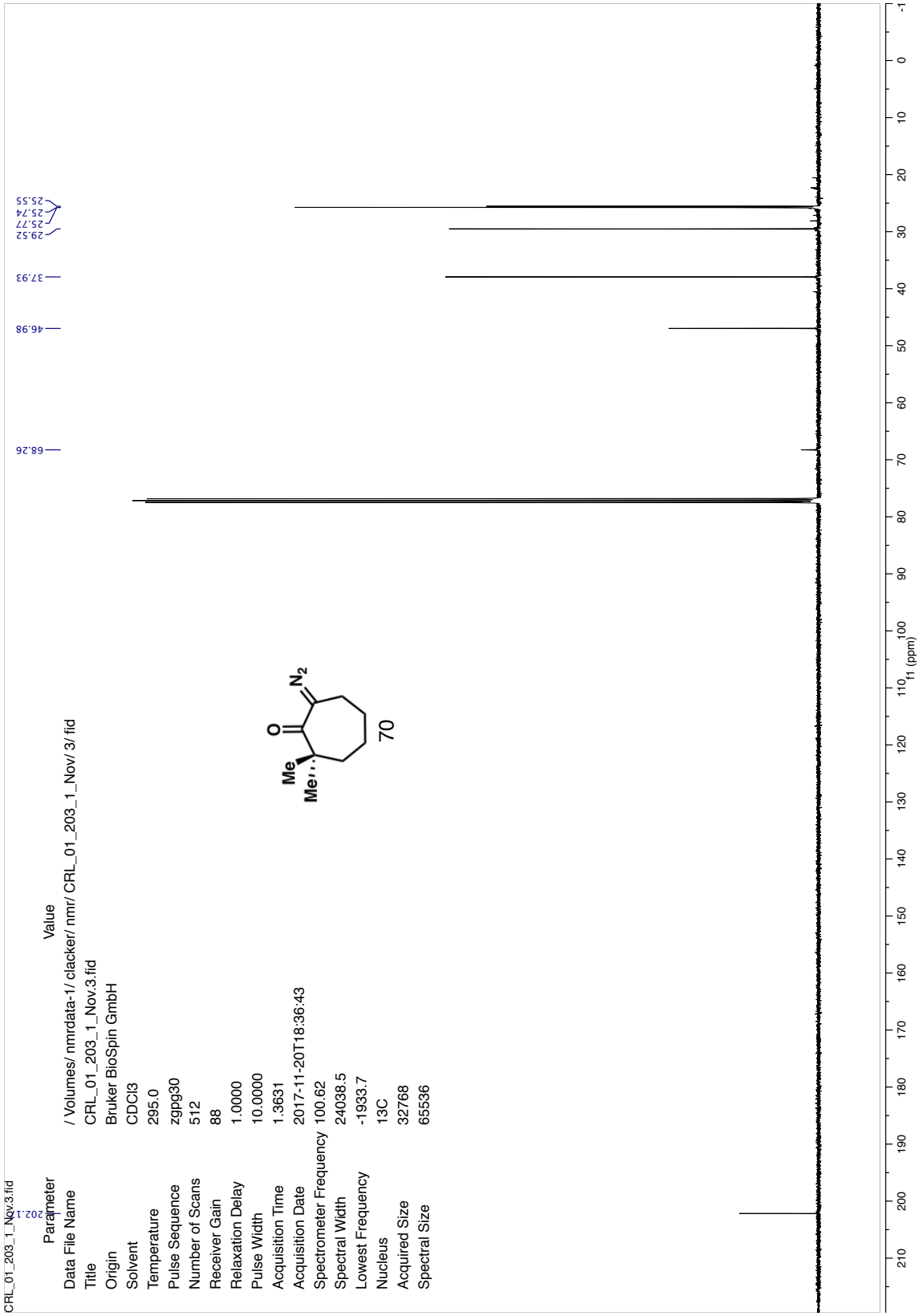
CRL_01_203_1_Nov3.fid
202.1
Parameter Value
Data File Name / Volumes/ nmrdata-1/ clacker/ nmr/ CRL_01_203_1_Nov/ 3/ fid
Title CRL_01_203_1_Nov.3.fid
Origin Bruker BioSpin GmbH
Solvent CDCl3
Temperature 295.0
Pulse Sequence zgpg30
Number of Scans 512
Receiver Gain 88
Relaxation Delay 1.0000
Pulse Width 10.0000
Acquisition Time 1.3631
Acquisition Date 2017-11-20T18:36:43
Spectrometer Frequency 100.62
Spectral Width 24038.5
Lowest Frequency -1933.7
Nucleus 13C
Acquired Size 32768
Spectral Size 65536
68.26
46.98
37.93
29.52
25.77
25.74
25.55
Me
Me
O
N2
70
f1 (ppm)

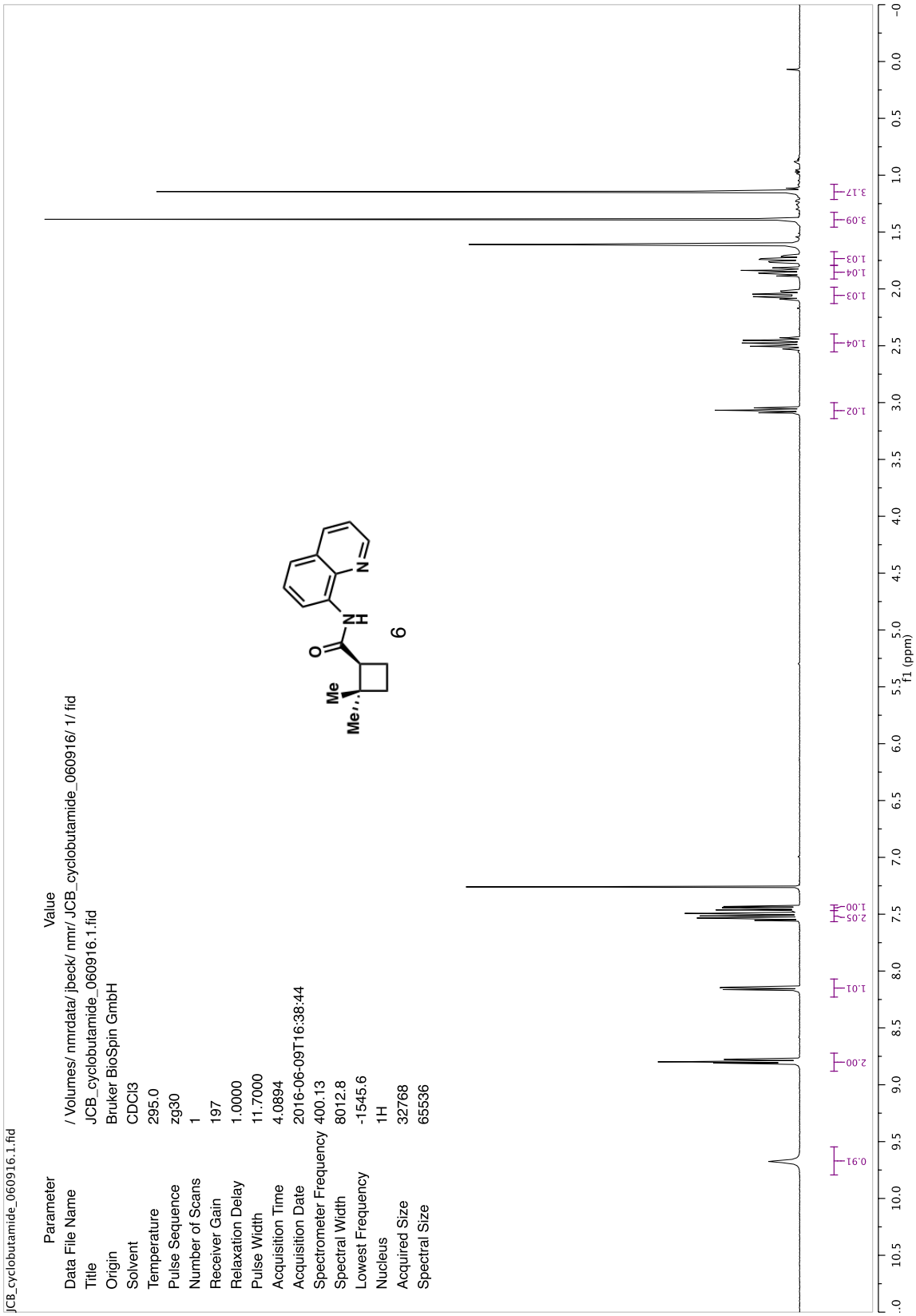
JCB_cyclobutamide_060916.1.fid
Parameter Value
Data File Name / Volumes/ nmrdata/ jbeck/ nmr/ JCB_cyclobutamide_060916/ 1/ fid
Title JCB_cyclobutamide_060916.1.fid
Origin Bruker BioSpin GmbH
Solvent CDCl3
Temperature 295.0
Pulse Sequence zg30
Number of Scans 1
Receiver Gain 197
Relaxation Delay 1.0000
Pulse Width 11.7000
Acquisition Time 4.0894
Acquisition Date 2016-06-09T16:38:44
Spectrometer Frequency 400.13
Spectral Width 8012.8
Lowest Frequency -1545.6
Nucleus 1H
Acquired Size 32768
Spectral Size 65536
Me
Me
O
N
H
N
6
0.91
2.00
1.01
2.05
1.00
1.02
1.04
1.03
1.04
1.03
3.09
3.17
f1 (ppm)

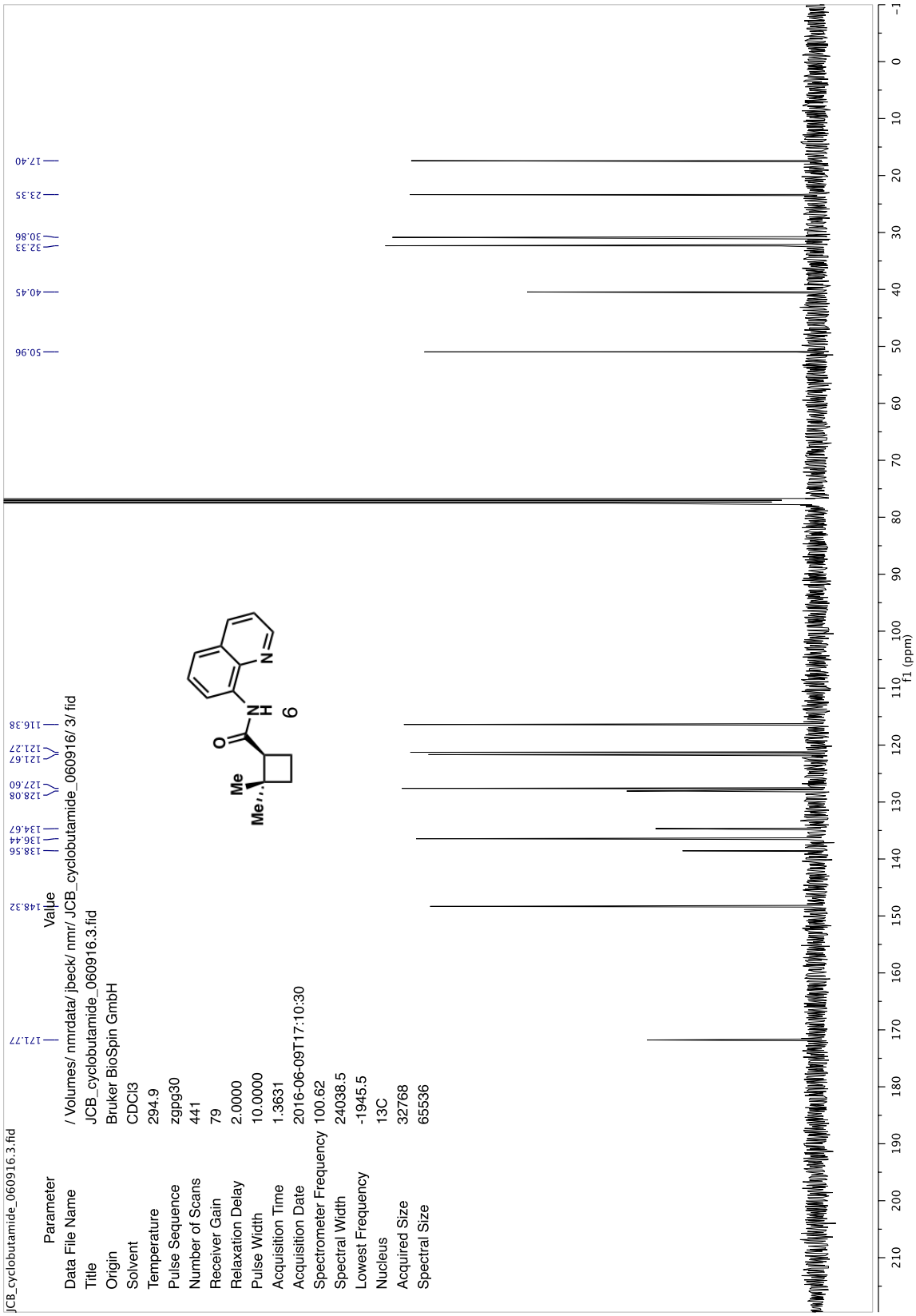
JCB_cyclobutamide_060916.3.fid
Parameter Value
Data File Name / Volumes/ nmrdata/ jbeck/ nmr/ JCB_cyclobutamide_060916/ 3/ fid
Title JCB_cyclobutamide_060916.3.fid
Origin Bruker BioSpin GmbH
Solvent CDCl3
Temperature 294.9
Pulse Sequence zgpg30
Number of Scans 441
Receiver Gain 79
Relaxation Delay 2.0000
Pulse Width 10.0000
Acquisition Time 1.3631
Acquisition Date 2016-06-09T17:10:30
Spectrometer Frequency 100.62
Spectral Width 24038.5
Lowest Frequency -1945.5
Nucleus 13C
Acquired Size 32768
Spectral Size 65536
171.77
148.32
138.56
136.44
134.67
128.08
127.60
121.67
121.27
116.38
50.96
40.45
32.33
30.86
23.35
17.40
Me
Me
O
H
N
N
6
f1 (ppm)

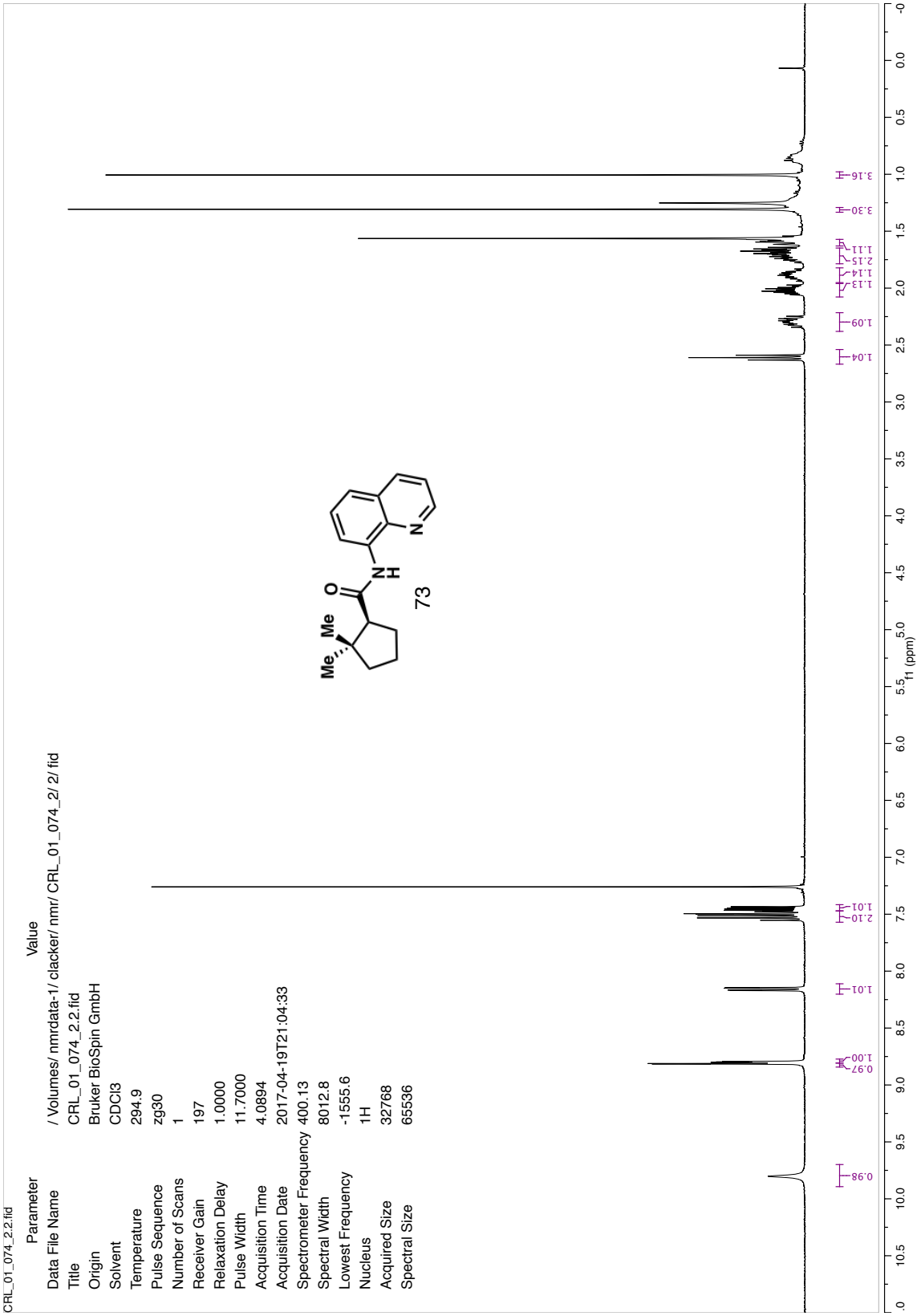
CRL_01_074_2.2.fid
Parameter Value
Data File Name / Volumes/ nmrdata-1/ clacker/ nmr/ CRL_01_074_2/ 2/ fid
Title CRL_01_074_2.2.fid
Origin Bruker BioSpin GmbH
Solvent CDCl3
Temperature 294.9
Pulse Sequence zg30
Number of Scans 1
Receiver Gain 197
Relaxation Delay 1.0000
Pulse Width 11.7000
Acquisition Time 4.0894
Acquisition Date 2017-04-19T21:04:33
Spectrometer Frequency 400.13
Spectral Width 8012.8
Lowest Frequency -1555.6
Nucleus 1H
Acquired Size 32768
Spectral Size 65536
Me
Me
Me
O
N
H
N
73
0.98
1.00
0.97
1.01
1.01
2.10
1.04
1.09
1.13
1.14
2.15
1.11
3.30
3.16
f1 (ppm)

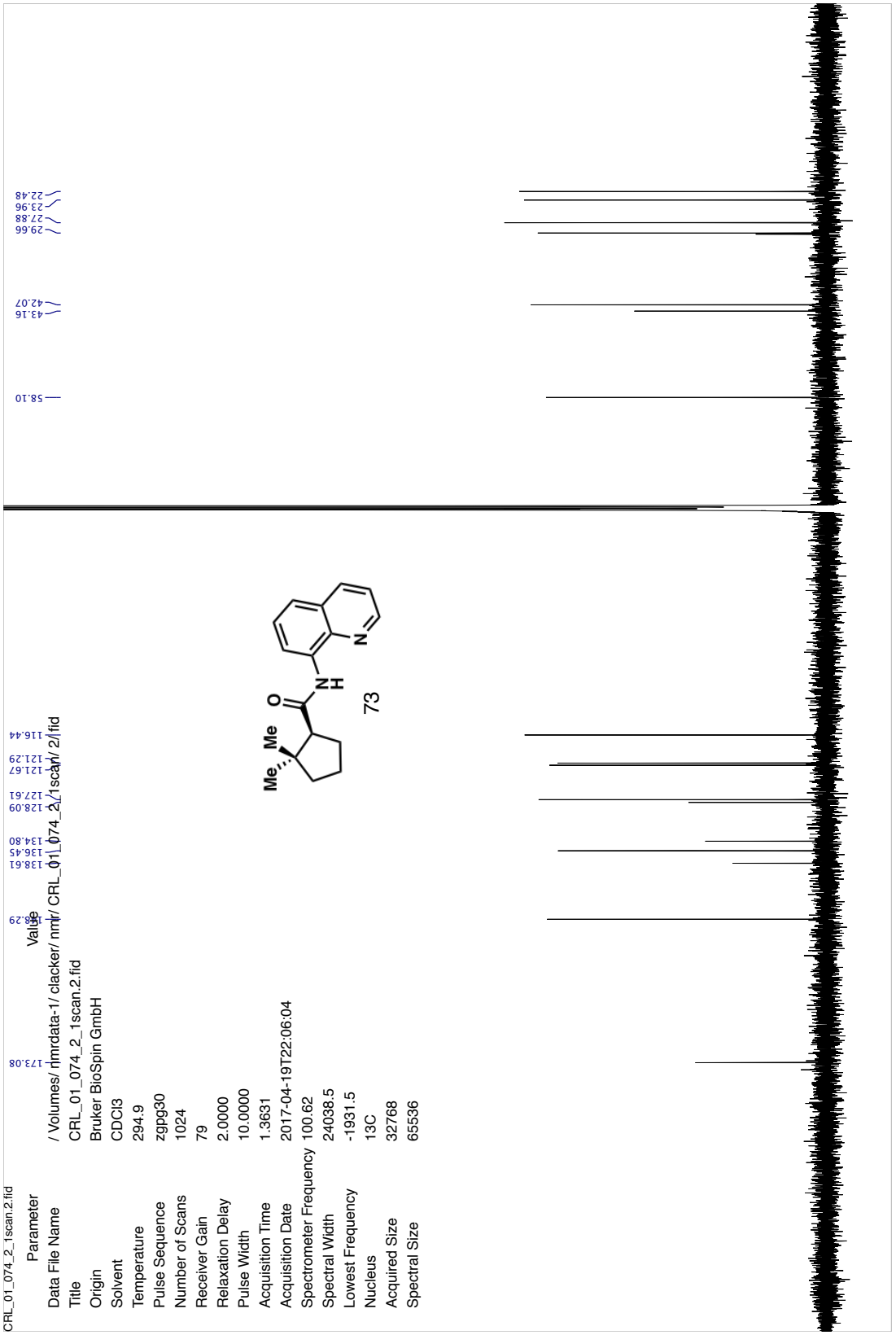
CRL_01_074_2_1scan.2.fid
Parameter Value
Data File Name / Volumes/ nmrdata-1/ clacker/ nmr/ CRL_01_074_2_1scan/ 2/fid
Title CRL_01_074_2_1scan.2.fid
Origin Bruker BioSpin GmbH
Solvent CDCl3
Temperature 294.9
Pulse Sequence zgpg30
Number of Scans 1024
Receiver Gain 79
Relaxation Delay 2.0000
Pulse Width 10.0000
Acquisition Time 1.3631
Acquisition Date 2017-04-19T22:06:04
Spectrometer Frequency 100.62
Spectral Width 24038.5
Lowest Frequency -1931.5
Nucleus 13C
Acquired Size 32768
Spectral Size 65536
173.08
138.29
138.61
136.45
134.80
128.09
127.61
121.67
121.29
116.44
58.10
43.16
42.07
29.66
27.88
23.96
22.48
Me
Me
O
N
H
N
73
f1 (ppm)

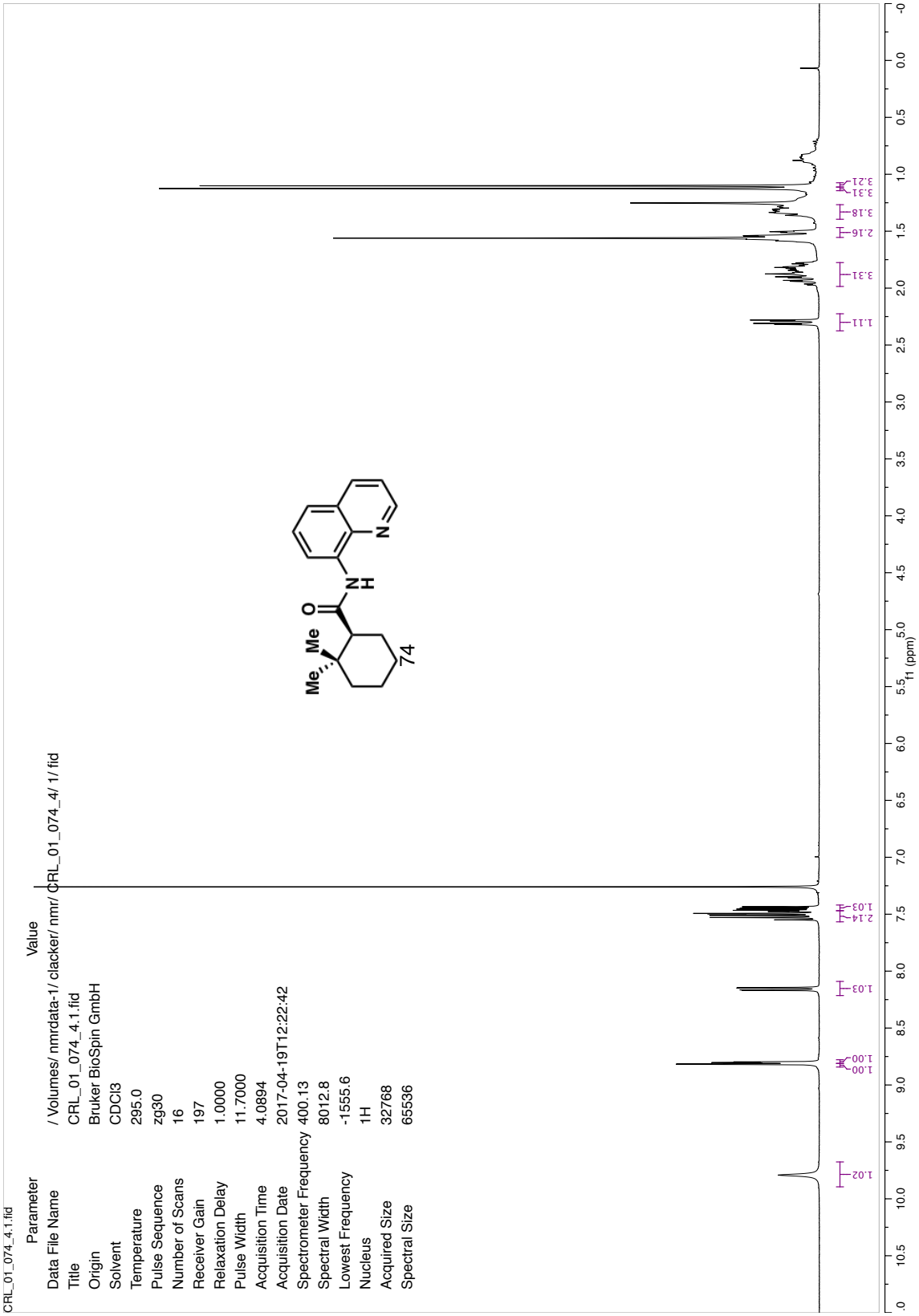
CRL_01_074_4.1.fid
Parameter Value
Data File Name / Volumes/ nmrdata-1/ clacker/ nmr/ CRL_01_074_4/ 1/ fid
Title CRL_01_074_4.1.fid
Origin Bruker BioSpin GmbH
Solvent CDCl3
Temperature 295.0
Pulse Sequence zg30
Number of Scans 16
Receiver Gain 197
Relaxation Delay 1.0000
Pulse Width 11.7000
Acquisition Time 4.0894
Acquisition Date 2017-04-19T12:22:42
Spectrometer Frequency 400.13
Spectral Width 8012.8
Lowest Frequency -1555.6
Nucleus 1H
Acquired Size 32768
Spectral Size 65536
Me
Me
O
N
H
N
74
1.02
1.00
1.03
2.14
1.03
1.11
3.31
2.16
3.18
3.31
3.21
f1 (ppm)

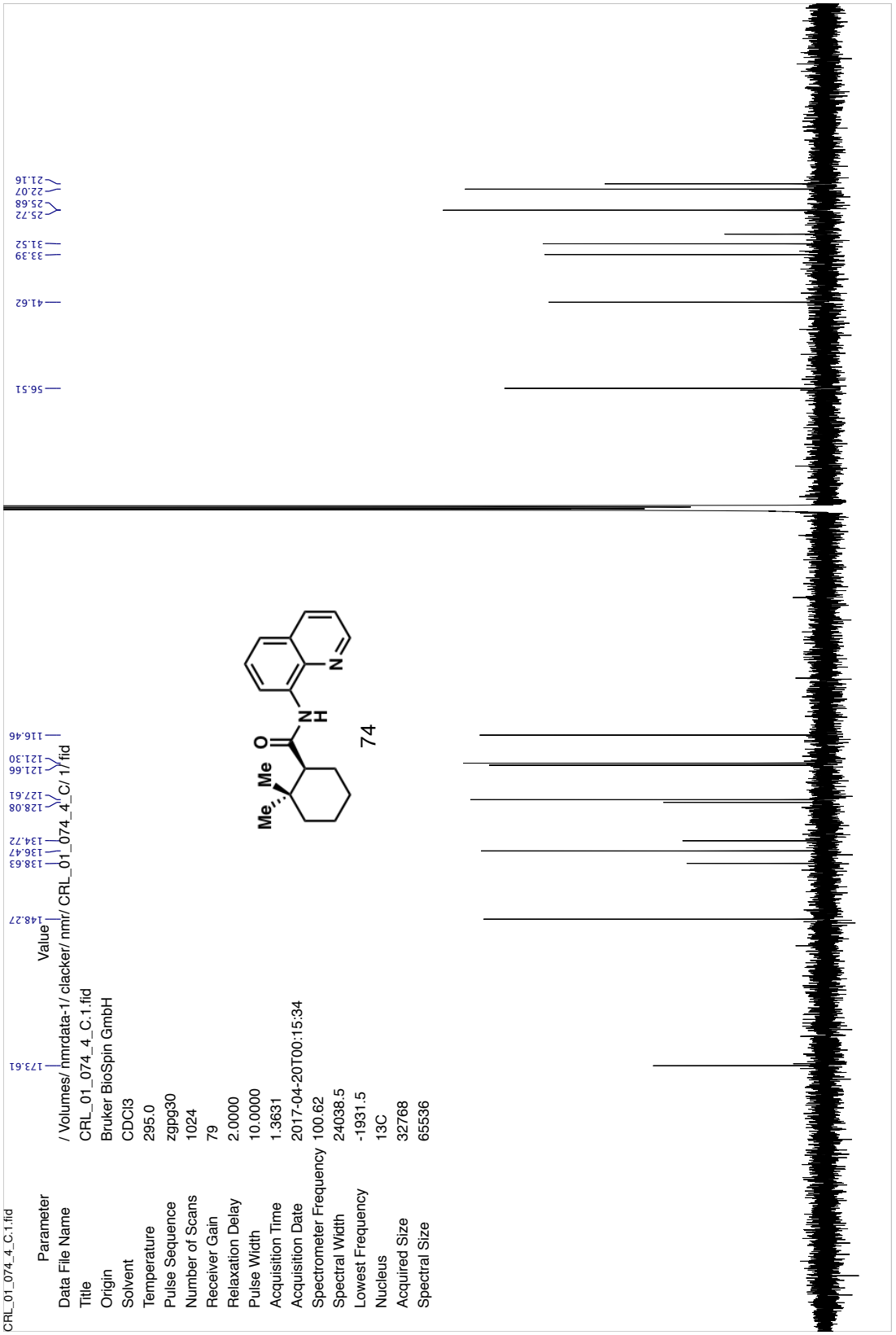
CRL_01_074_4_C.1.fid
Parameter Value
Data File Name / Volumes/ nmrdata-1/ clacker/ nmr/ CRL_01_074_4_C/ 1/ fid
Title CRL_01_074_4_C.1.fid
Origin Bruker BioSpin GmbH
Solvent CDCl3
Temperature 295.0
Pulse Sequence zgpg30
Number of Scans 1024
Receiver Gain 79
Relaxation Delay 2.0000
Pulse Width 10.0000
Acquisition Time 1.3631
Acquisition Date 2017-04-20T00:15:34
Spectrometer Frequency 100.62
Spectral Width 24038.5
Lowest Frequency -1931.5
Nucleus 13C
Acquired Size 32768
Spectral Size 65536
173.61
148.27
138.63
136.47
134.72
128.08
127.61
121.66
121.30
116.46
56.51
41.62
33.39
31.52
25.72
25.68
22.07
21.16
Me
Me
O
N
H
N
74
f1 (ppm)

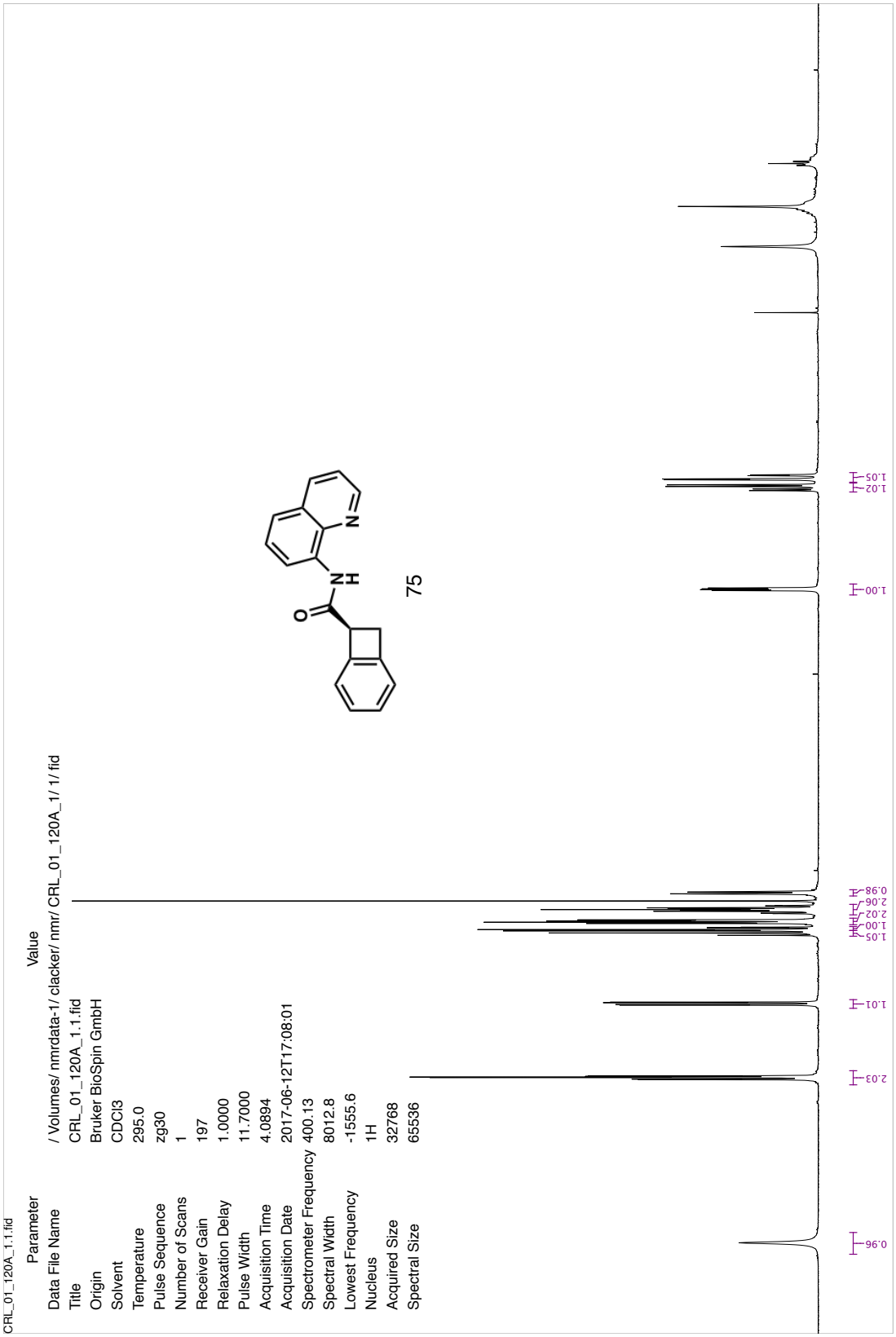
CRL_01_120A_1.1.fid
Parameter Value
Data File Name / Volumes/ nmrdata-1/ clacker/ nmr/ CRL_01_120A_1/ 1/ fid
Title CRL_01_120A_1.1.fid
Origin Bruker BioSpin GmbH
Solvent CDCl3
Temperature 295.0
Pulse Sequence zg30
Number of Scans 1
Receiver Gain 197
Relaxation Delay 1.0000
Pulse Width 11.7000
Acquisition Time 4.0894
Acquisition Date 2017-06-12T17:08:01
Spectrometer Frequency 400.13
Spectral Width 8012.8
Lowest Frequency -1555.6
Nucleus 1H
Acquired Size 32768
Spectral Size 65536
0.96
2.03
1.01
1.05
2.00
2.02
2.06
0.98
1.00
1.02
1.05
f1 (ppm)

75

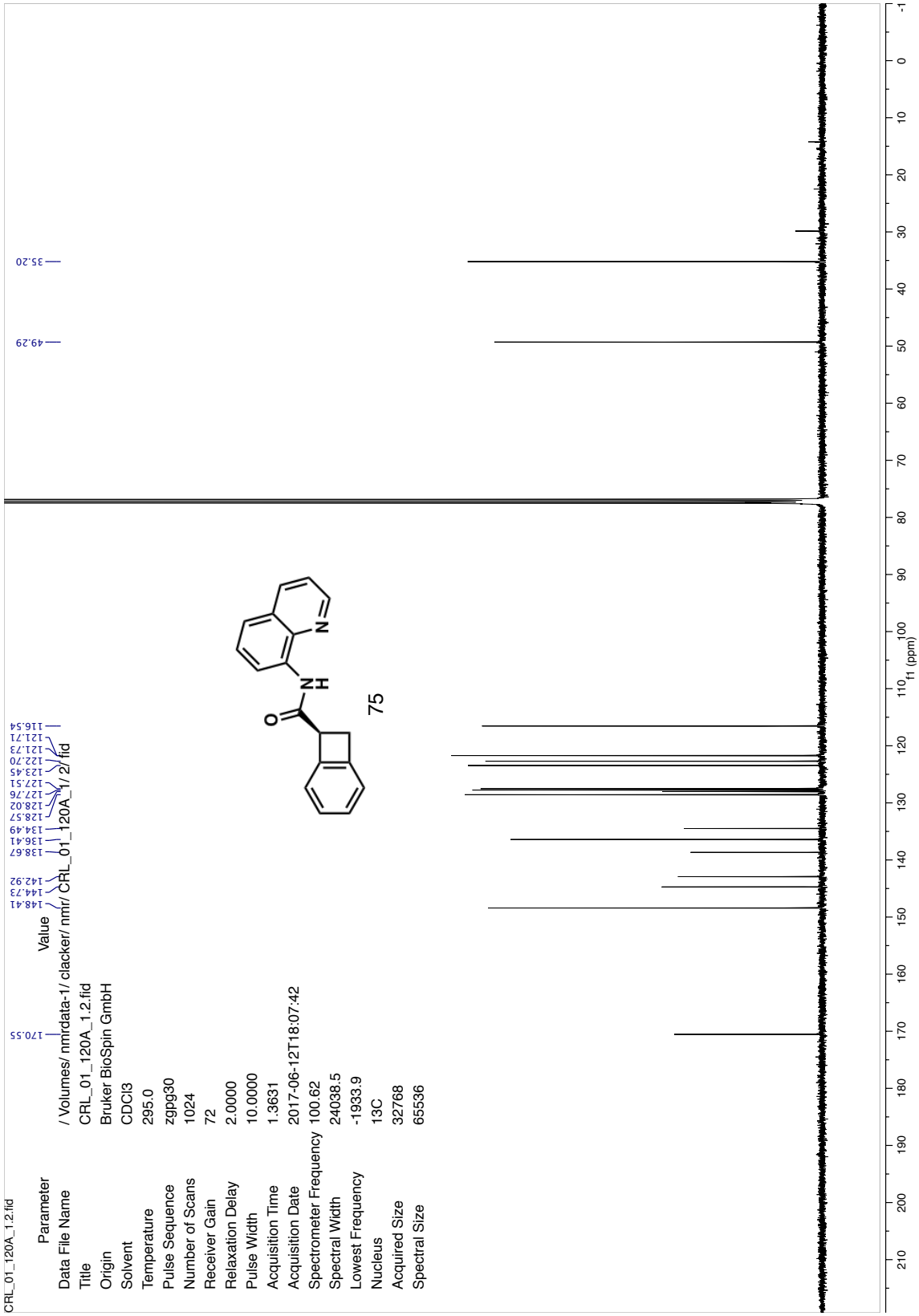
CRL_01_120A_1.2.fid
Parameter
Value
Data File Name / Volumes/ nmrdata-1/ clacker/ nmr/ CRL_01_120A_1/ 2/ fid
Title CRL_01_120A_1.2.fid
Origin Bruker BioSpin GmbH
Solvent CDCl3
Temperature 295.0
Pulse Sequence zgpg30
Number of Scans 1024
Receiver Gain 72
Relaxation Delay 2.0000
Pulse Width 10.0000
Acquisition Time 1.3631
Acquisition Date 2017-06-12T18:07:42
Spectrometer Frequency 100.62
Spectral Width 24038.5
Lowest Frequency -1933.9
Nucleus 13C
Acquired Size 32768
Spectral Size 65536
170.55
148.41
144.73
142.92
138.67
136.41
134.49
128.57
128.02
127.76
127.51
123.45
122.70
121.73
121.71
116.54
49.29
35.20
O
N
H
N
75
f1 (ppm)

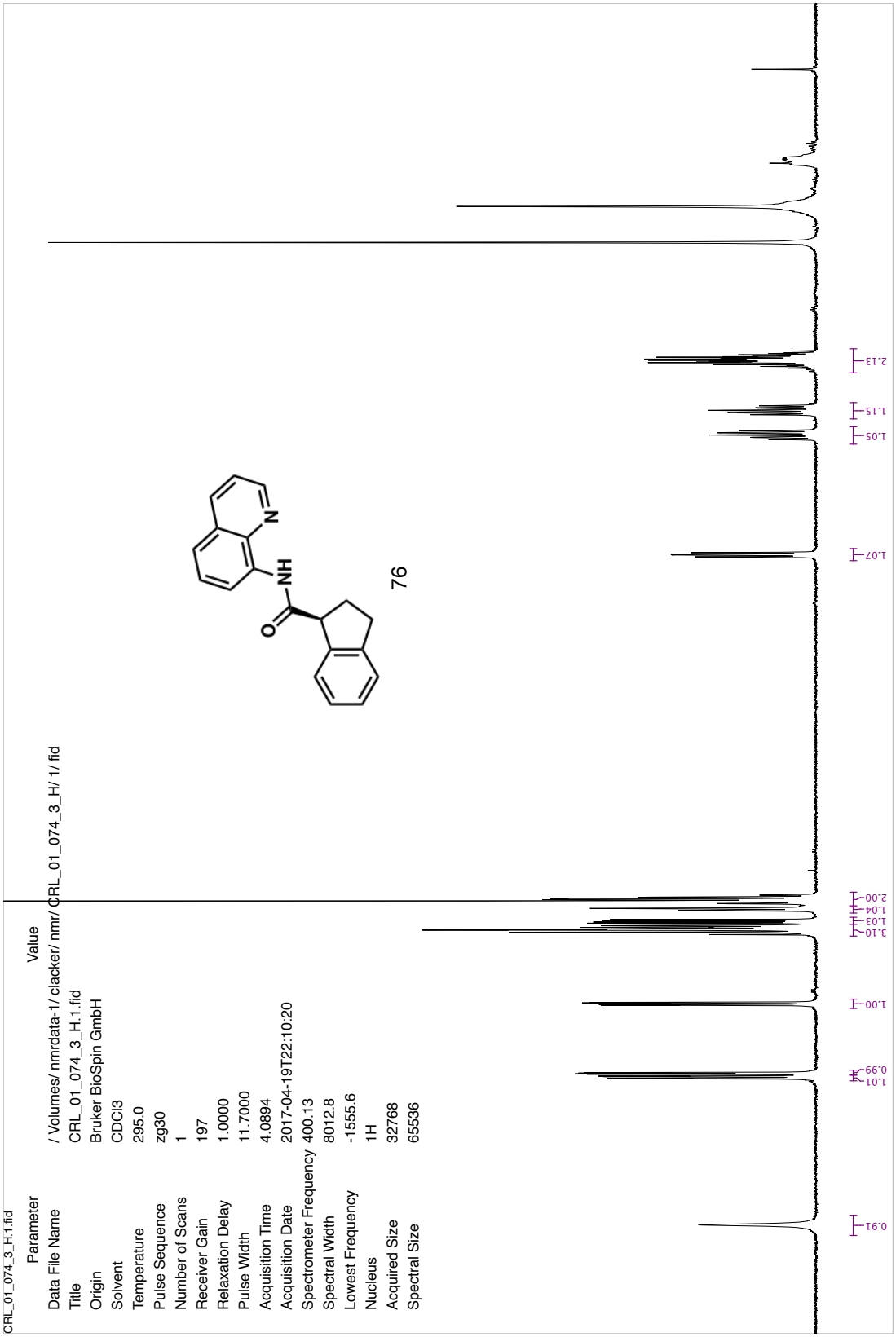
CRL_01_074_3_H.1.fid
Parameter Value
Data File Name / Volumes/ nmrdata-1/ clacker/ nmr/ CRL_01_074_3_H/ 1/ fid
Title CRL_01_074_3_H.1.fid
Origin Bruker BioSpin GmbH
Solvent CDCl3
Temperature 295.0
Pulse Sequence zg30
Number of Scans 1
Receiver Gain 197
Relaxation Delay 1.0000
Pulse Width 11.7000
Acquisition Time 4.0894
Acquisition Date 2017-04-19T22:10:20
Spectrometer Frequency 400.13
Spectral Width 8012.8
Lowest Frequency -1555.6
Nucleus 1H
Acquired Size 32768
Spectral Size 65536
NH
O
N
76
0.91
1.01
0.99
1.00
3.10
1.03
1.04
2.00
1.07
2.13
1.15
1.05
f1 (ppm)

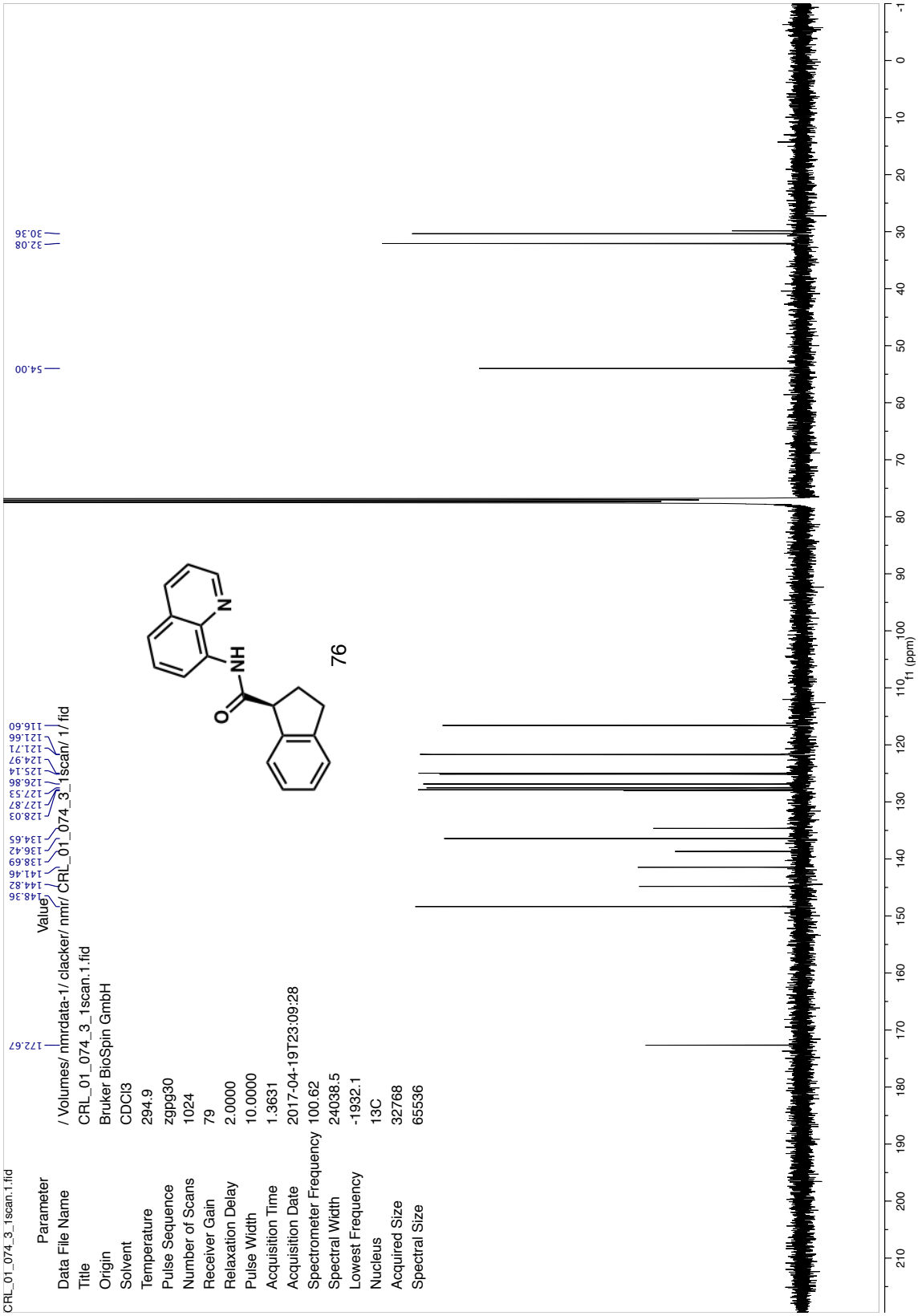
CRL_01_074_3_1scan.1.fid
Parameter Value
Data File Name / Volumes/ nmrdata-1/ clacker/ nmr/ CRL_01_074_3_1scan/ 1/ fid
Title CRL_01_074_3_1scan.1.fid
Origin Bruker BioSpin GmbH
Solvent CDCl3
Temperature 294.9
Pulse Sequence zgpg30
Number of Scans 1024
Receiver Gain 79
Relaxation Delay 2.0000
Pulse Width 10.0000
Acquisition Time 1.3631
Acquisition Date 2017-04-19T23:09:28
Spectrometer Frequency 100.62
Spectral Width 24038.5
Lowest Frequency -1932.1
Nucleus 13C
Acquired Size 32768
Spectral Size 65536
172.67
148.36
144.82
141.46
138.69
136.42
134.65
128.03
127.87
127.53
126.86
125.14
124.97
121.71
121.66
116.60
54.00
32.08
30.36
NH
O
N
76
f1 (ppm)

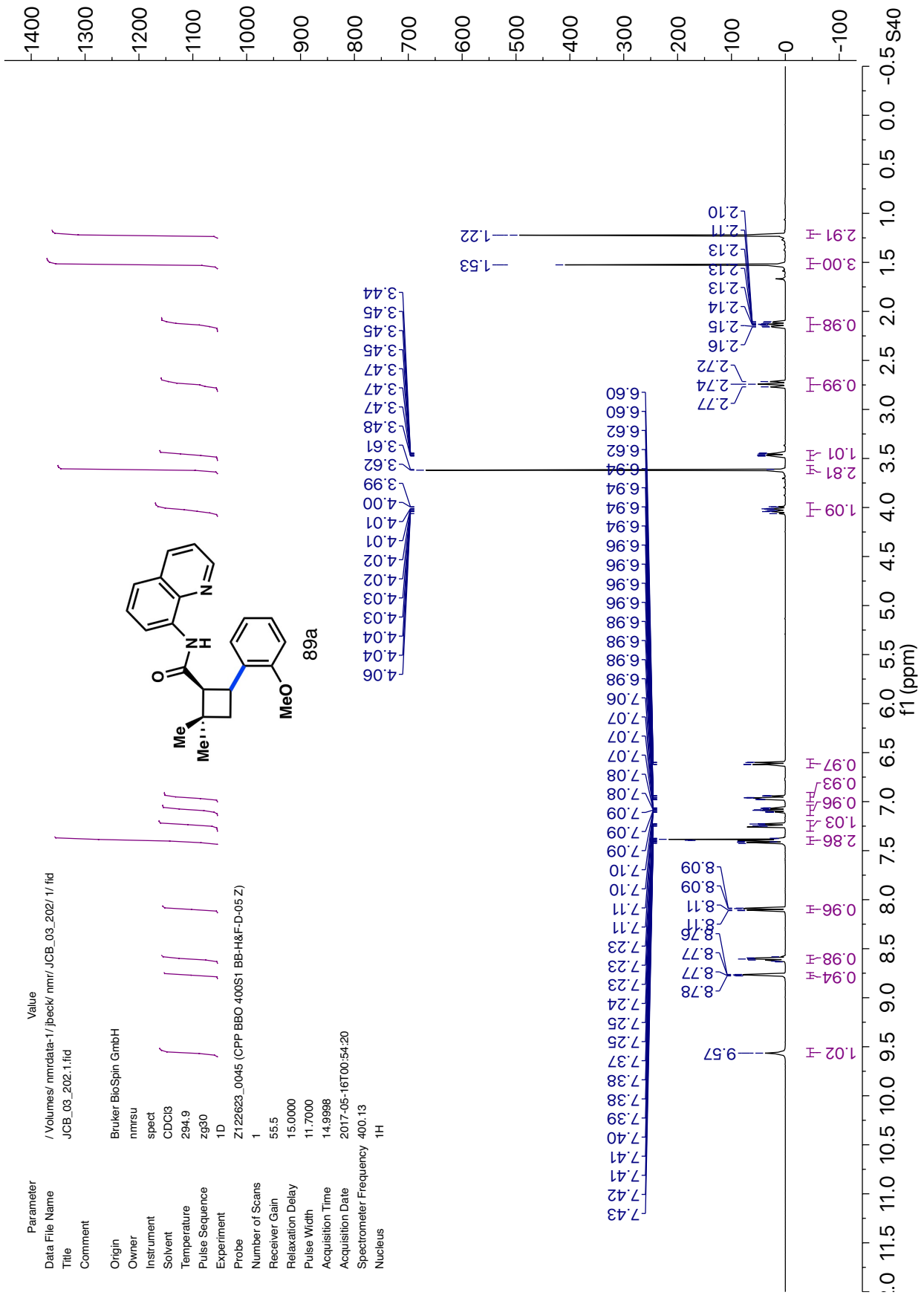
Parameter Value
Data File Name / Volumes/ nmrdata-1/ jbeck/ nmr/ JCB_03_202/ 1/ fid
Title JCB_03_202.1.fid
Comment
Origin Bruker BioSpin GmbH
Owner nmrsu
Instrument spect
Solvent CDCl3
Temperature 294.9
Pulse Sequence zg30
Experiment 1D
Probe Z122623_0045 (CPP BBO 400S1 BB-H&F-D-05 Z)
Number of Scans 1
Receiver Gain 55.5
Relaxation Delay 15.0000
Pulse Width 11.7000
Acquisition Time 14.9998
Acquisition Date 2017-05-16T00:54:20
Spectrometer Frequency 400.13
Nucleus 1H
89a
Me
MeO
f1 (ppm)

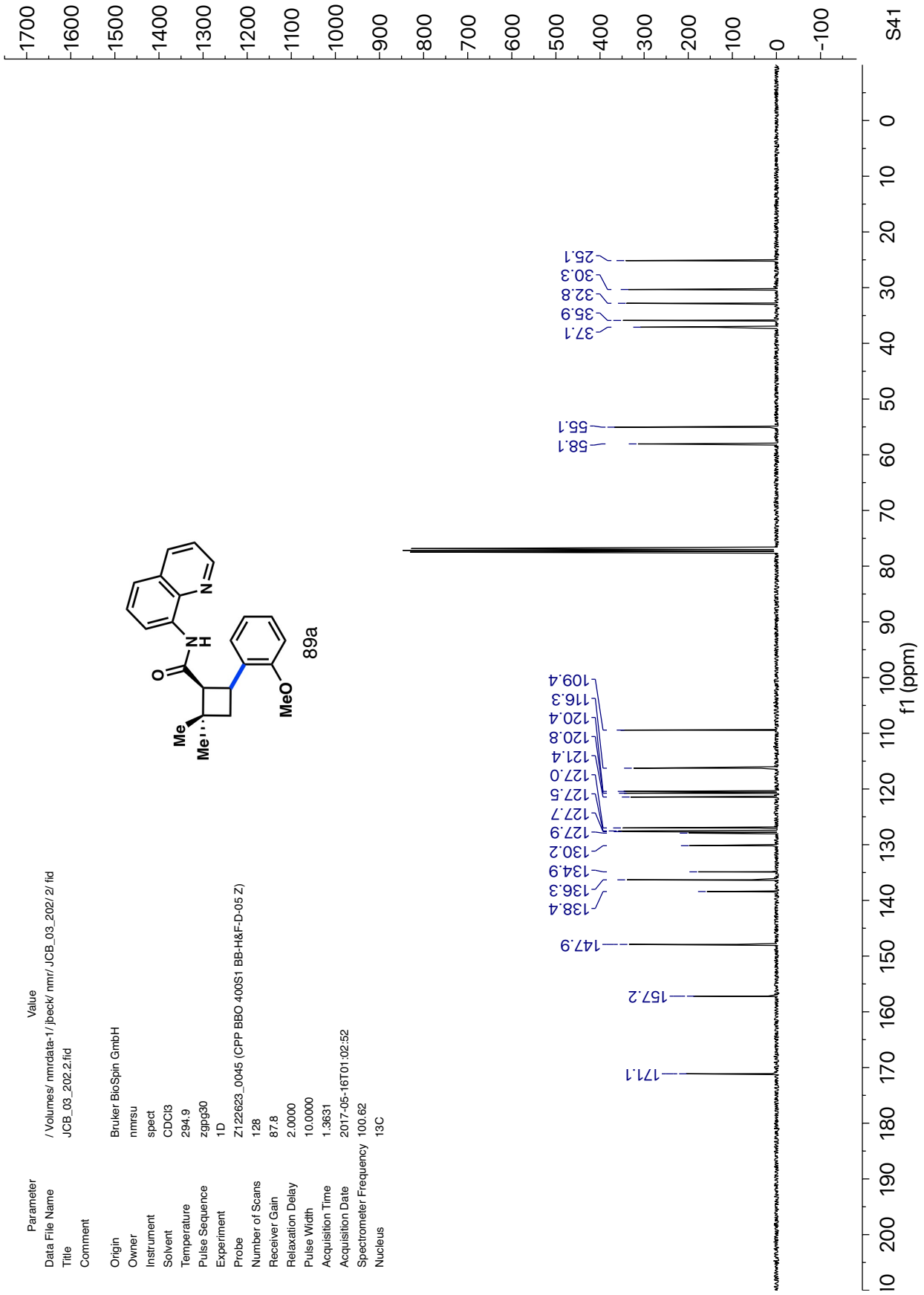
Parameter Value
Data File Name / Volumes/ nmrdata-1/ jbeck/ nmr/ JCB_03_202/ 2/ fid
Title JCB_03_202.2.fid
Comment
Origin Bruker BioSpin GmbH
Owner nmrsu
Instrument spect
Solvent CDCl3
Temperature 294.9
Pulse Sequence zgpg30
Experiment 1D
Probe Z122623_0045 (CPP BBO 400S1 BB-H&F-D-05 Z)
Number of Scans 128
Receiver Gain 87.8
Relaxation Delay 2.0000
Pulse Width 10.0000
Acquisition Time 1.3631
Acquisition Date 2017-05-16T01:02:52
Spectrometer Frequency 100.62
Nucleus 13C
89a
MeO
Me
Me
O
N
H
N
171.1
157.2
147.9
138.4
136.3
134.9
130.2
127.9
127.7
127.5
127.0
121.4
120.8
120.4
116.3
109.4
58.1
55.1
37.1
35.9
32.8
30.3
25.1
f1 (ppm)
S41

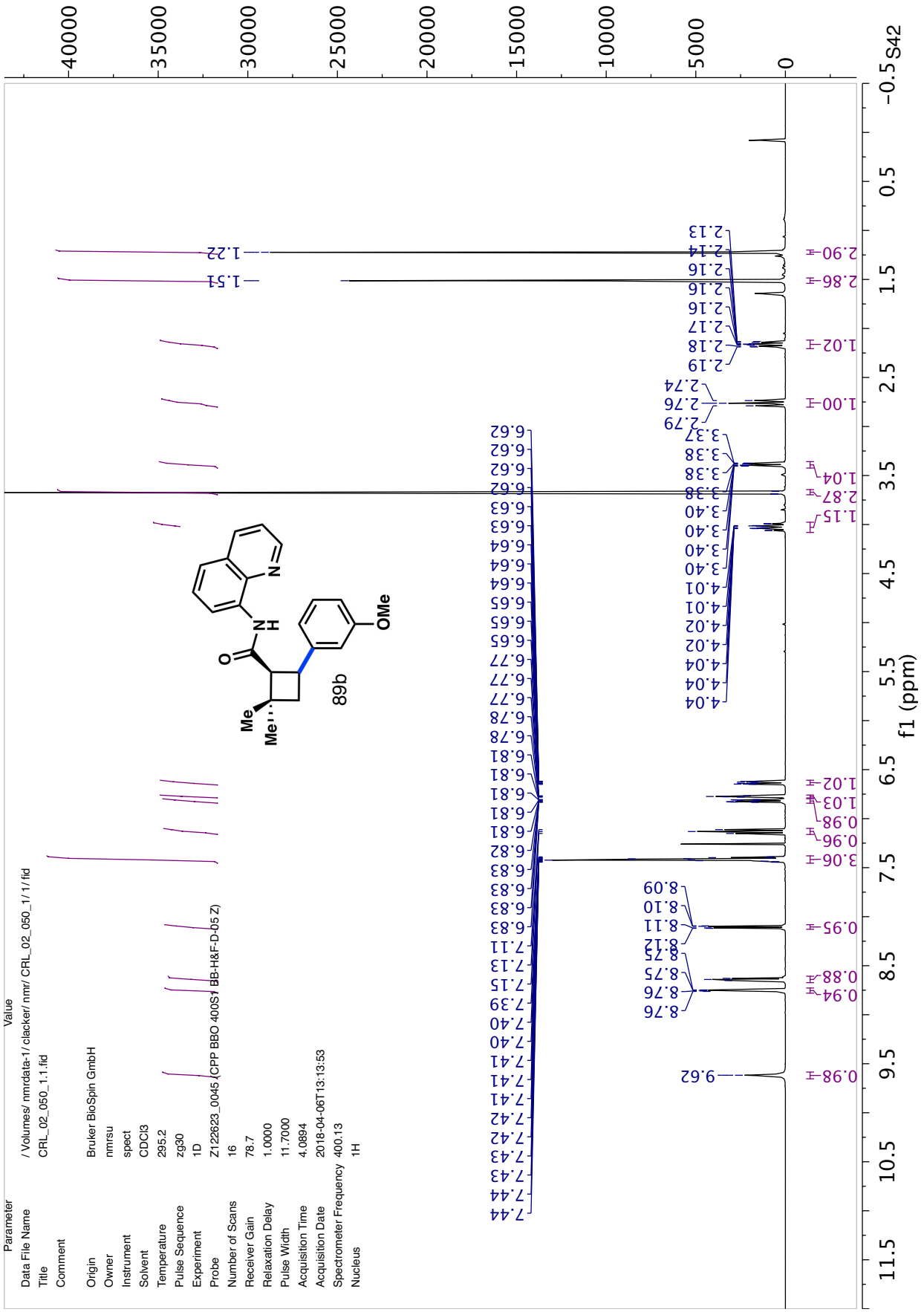
Parameter Value
Data File Name / Volumes/ nmrdata-1/ clacker/ nmr/ CRL_02_050_1/1/1/fid
Title CRL_02_050_1.1.fid
Comment
Origin Bruker BioSpin GmbH
Owner nmrsu
Instrument spect
Solvent CDCl3
Temperature 295.2
Pulse Sequence zg30
Experiment 1D
Probe Z122623_0045 (CPP BBO 400S1 BB-H&F-D-05 Z)
Number of Scans 16
Receiver Gain 78.7
Relaxation Delay 1.0000
Pulse Width 11.7000
Acquisition Time 4.0894
Acquisition Date 2018-04-06T13:13:53
Spectrometer Frequency 400.13
Nucleus 1H
89b
f1 (ppm)
S42

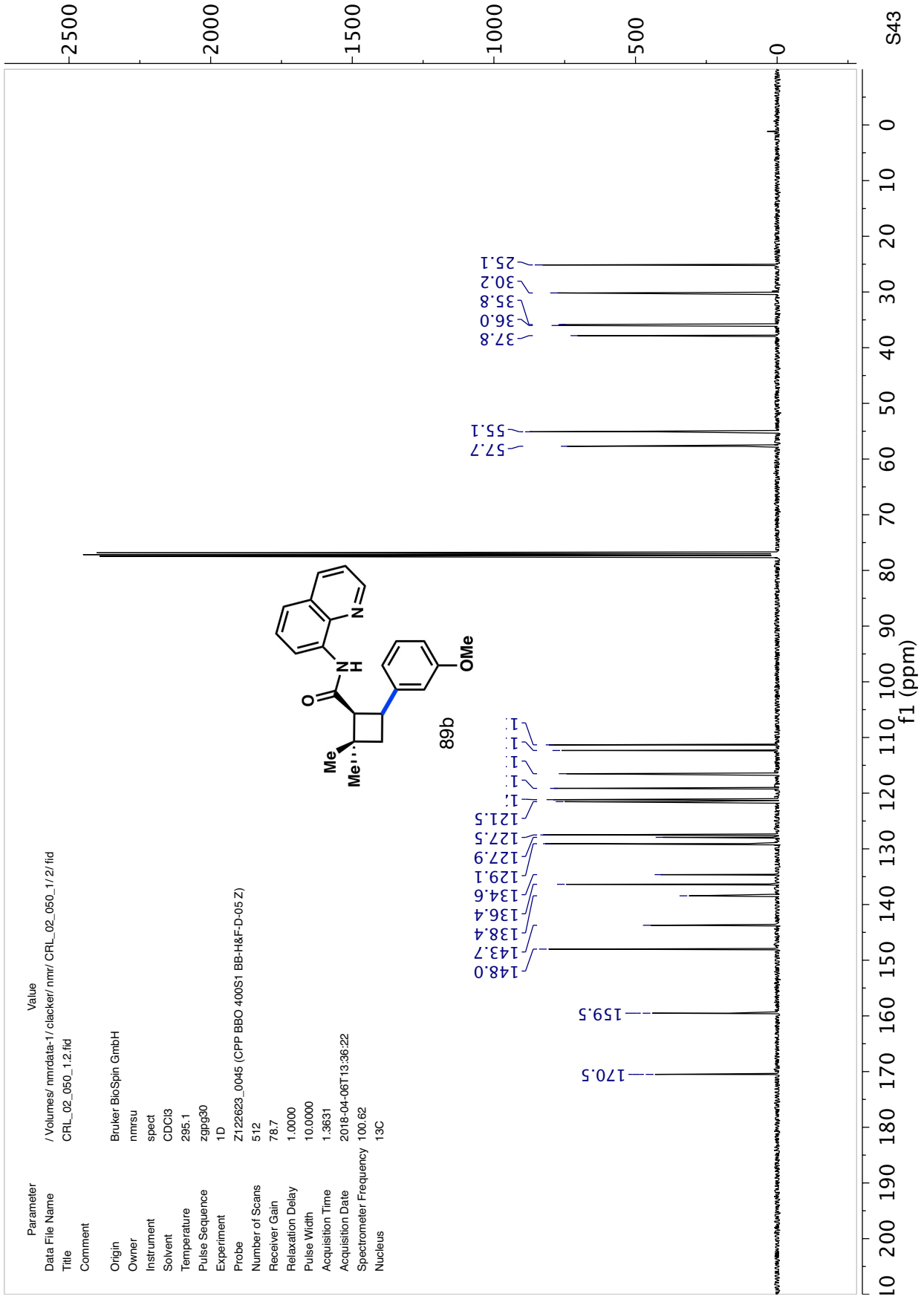
Parameter
Value
Data File Name
/ Volumes/ nmrdata-1/ clacker/ nmr/ CRL_02_050_1/ 2/ fid
Title
CRL_02_050_1.2.fid
Comment
Origin
Bruker BioSpin GmbH
Owner
nmrsu
Instrument
spect
Solvent
CDCl3
Temperature
295.1
Pulse Sequence
zgpg30
Experiment
1D
Probe
Z122623_0045 (CPP BBO 400S1 BB-H&F-D-05 Z)
Number of Scans
512
Receiver Gain
78.7
Relaxation Delay
1.0000
Pulse Width
10.0000
Acquisition Time
1.3631
Acquisition Date
2018-04-06T13:36:22
Spectrometer Frequency
100.62
Nucleus
13C
89b
Me
Me
OMe
N
H
O
N
170.5
159.5
148.0
143.7
138.4
136.4
134.6
129.1
127.9
127.5
121.5
57.7
55.1
37.8
36.0
35.8
30.2
25.1
f1 (ppm)
S43

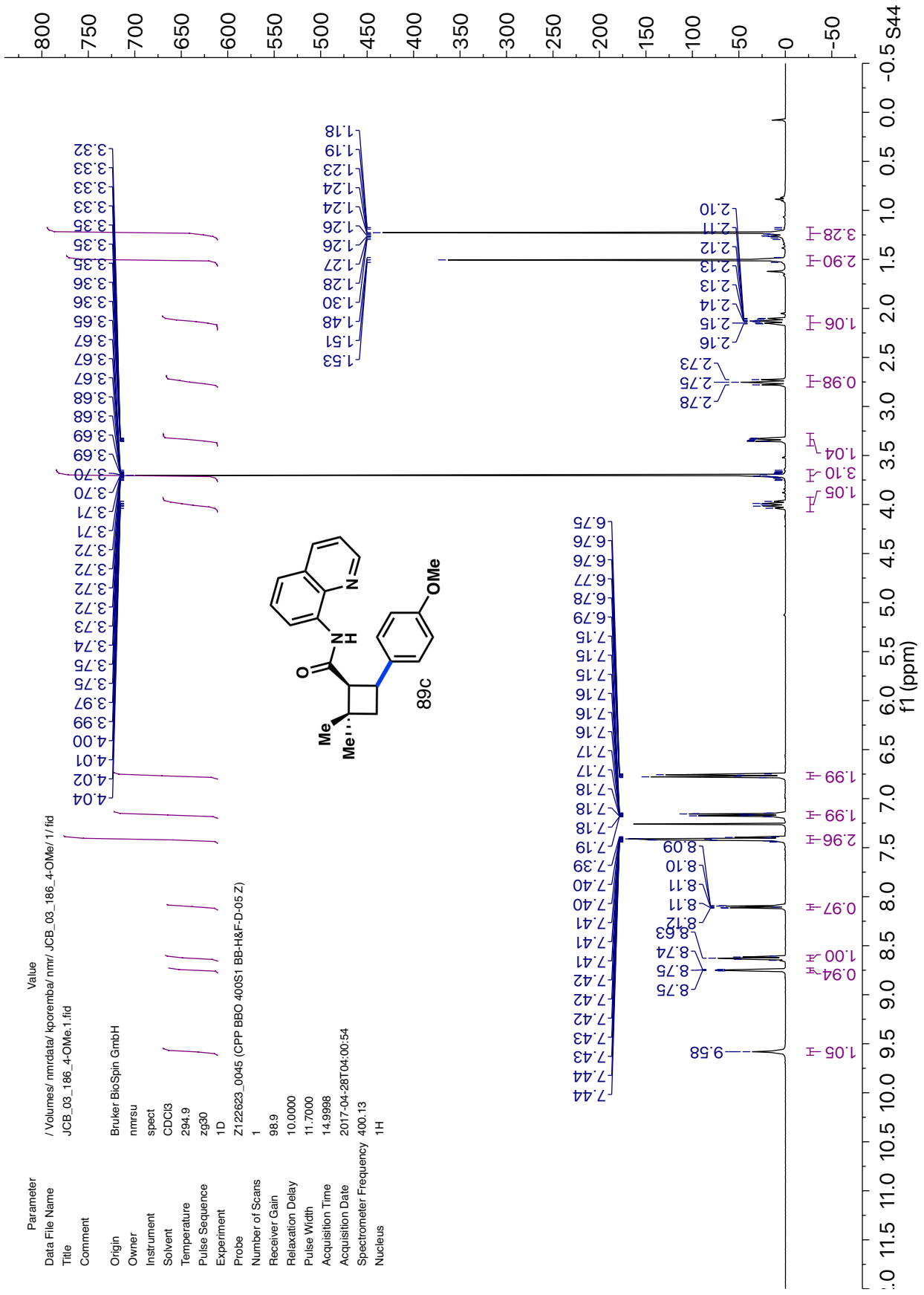
Parameter Value
Data File Name / Volumes/ nmrdata/ kporemba/ nmr/ JCB_03_186_4-OMe/ 1/ fid
Title JCB_03_186_4-OMe.1.fid
Comment
Origin Bruker BioSpin GmbH
Owner nmrsu
Instrument spect
Solvent CDCl3
Temperature 294.9
Pulse Sequence zg30
Experiment 1D
Probe Z122623_0045 (CPP BBO 400S1 BB-H&F-D-05 Z)
Number of Scans 1
Receiver Gain 98.9
Relaxation Delay 10.0000
Pulse Width 11.7000
Acquisition Time 14.9998
Acquisition Date 2017-04-28T04:00:54
Spectrometer Frequency 400.13
Nucleus 1H
OMe
Me
Me
89c
f1 (ppm)

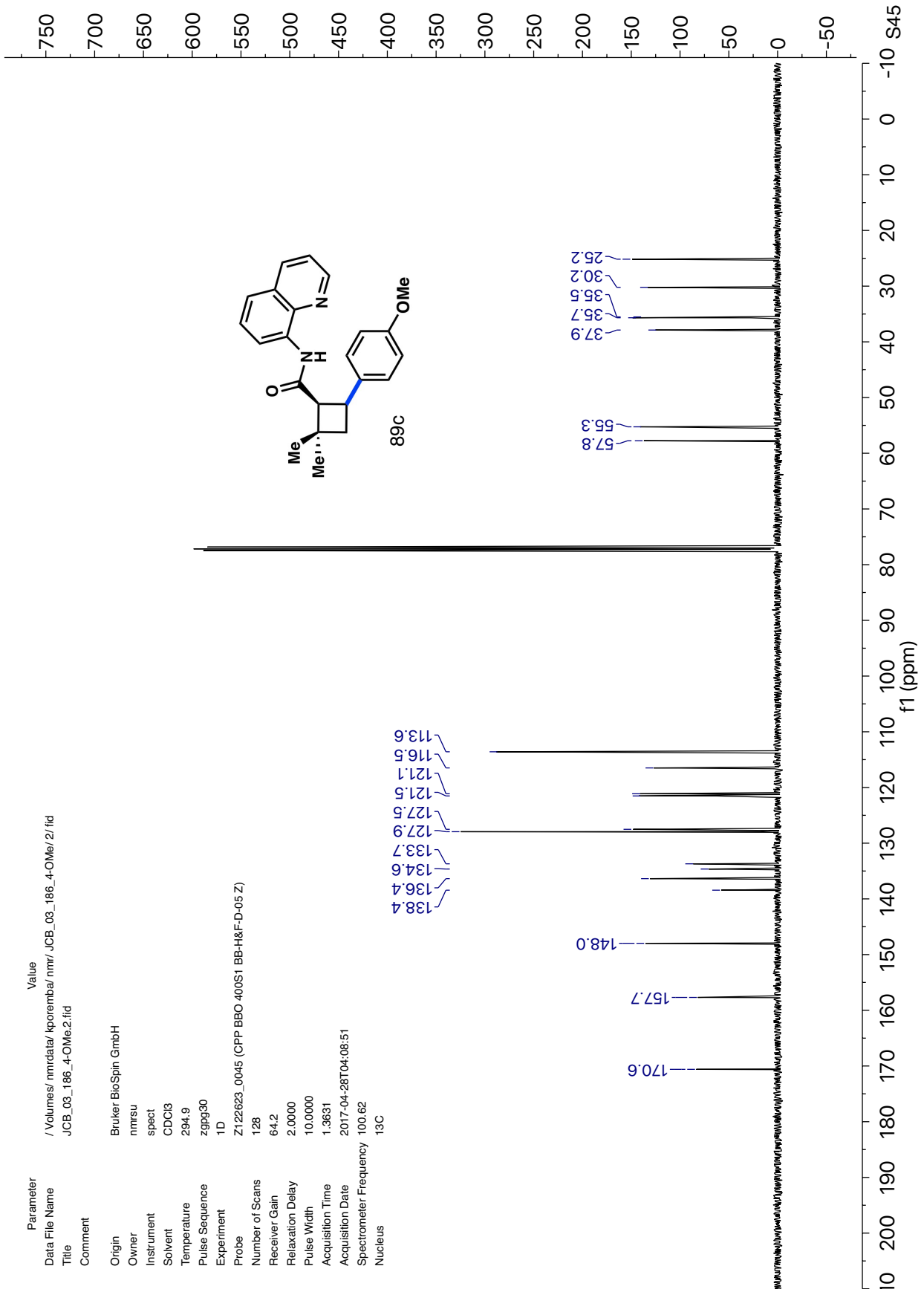
Parameter
Value
Data File Name / Volumes/ nmrdata/ kporemba/ nmr/ JCB_03_186_4-OMe/ 2/ fid
Title JCB_03_186_4-OMe.2.fid
Comment
Origin Bruker BioSpin GmbH
Owner nmrsu
Instrument spect
Solvent CDCl3
Temperature 294.9
Pulse Sequence zgpg30
Experiment 1D
Probe Z122623_0045 (CPP BBO 400S1 BB-H&F-D-05 Z)
Number of Scans 128
Receiver Gain 64.2
Relaxation Delay 2.0000
Pulse Width 10.0000
Acquisition Time 1.3631
Acquisition Date 2017-04-28T04:08:51
Spectrometer Frequency 100.62
Nucleus 13C
170.6
157.7
148.0
138.4
136.4
134.6
133.7
127.9
127.5
121.5
121.1
116.5
113.6
57.8
55.3
37.9
35.7
35.5
30.2
25.2
89c
Me
Me
OMe
O
N
H
N
f1 (ppm)

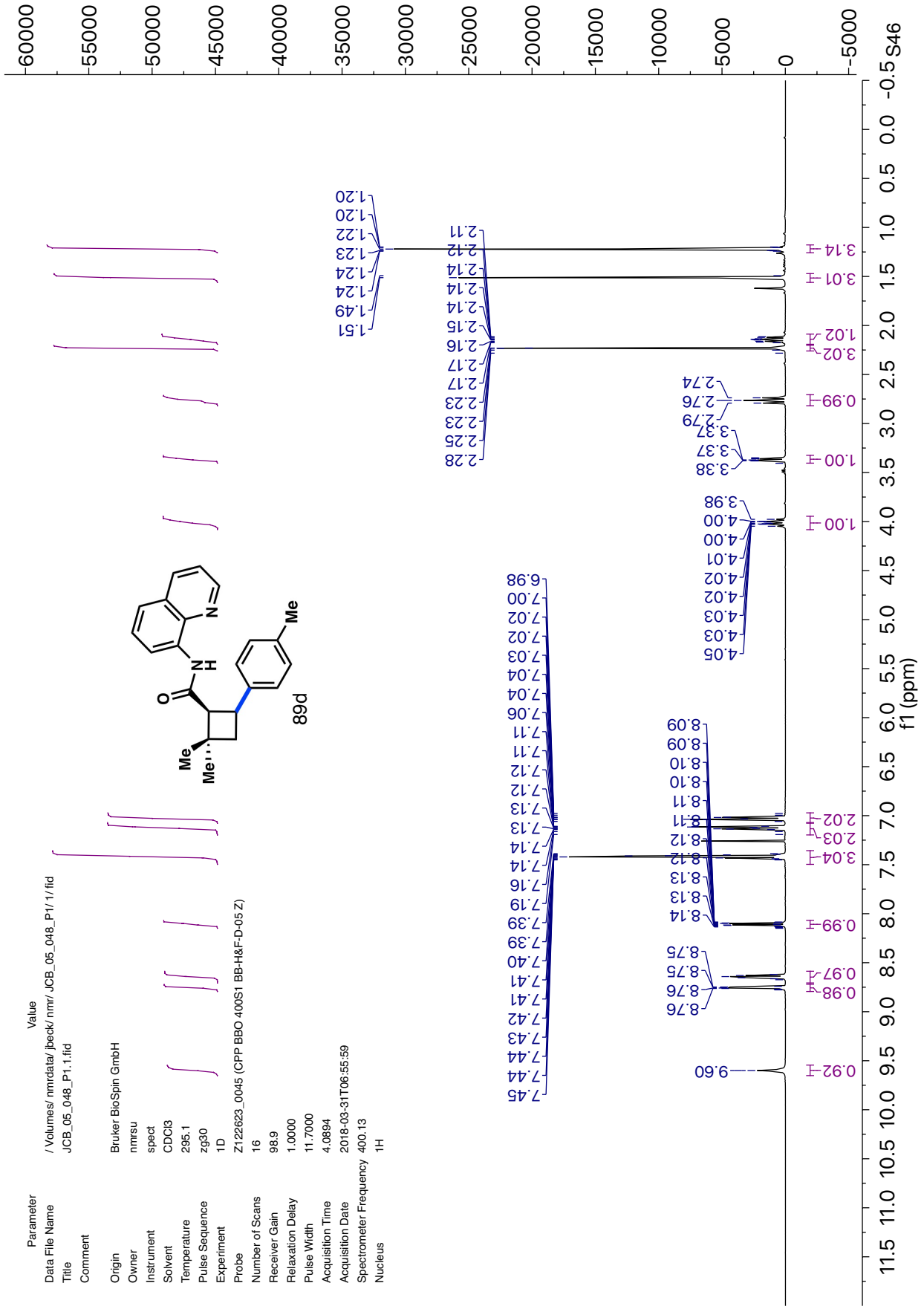
Parameter Value
Data File Name / Volumes/ nmrdata/ jbeck/ nmr/ JCB_05_048_P1/ 1/ fid
Title JCB_05_048_P1.1.fid
Comment
Origin Bruker BioSpin GmbH
Owner nmrsu
Instrument spect
Solvent CDCl3
Temperature 295.1
Pulse Sequence zg30
Experiment 1D
Probe Z122623_0045 (CPP BBO 400S1 BB-H&F-D-05 Z)
Number of Scans 16
Receiver Gain 98.9
Relaxation Delay 1.0000
Pulse Width 11.7000
Acquisition Time 4.0894
Acquisition Date 2018-03-31T06:55:59
Spectrometer Frequency 400.13
Nucleus 1H
89d
f1 (ppm)

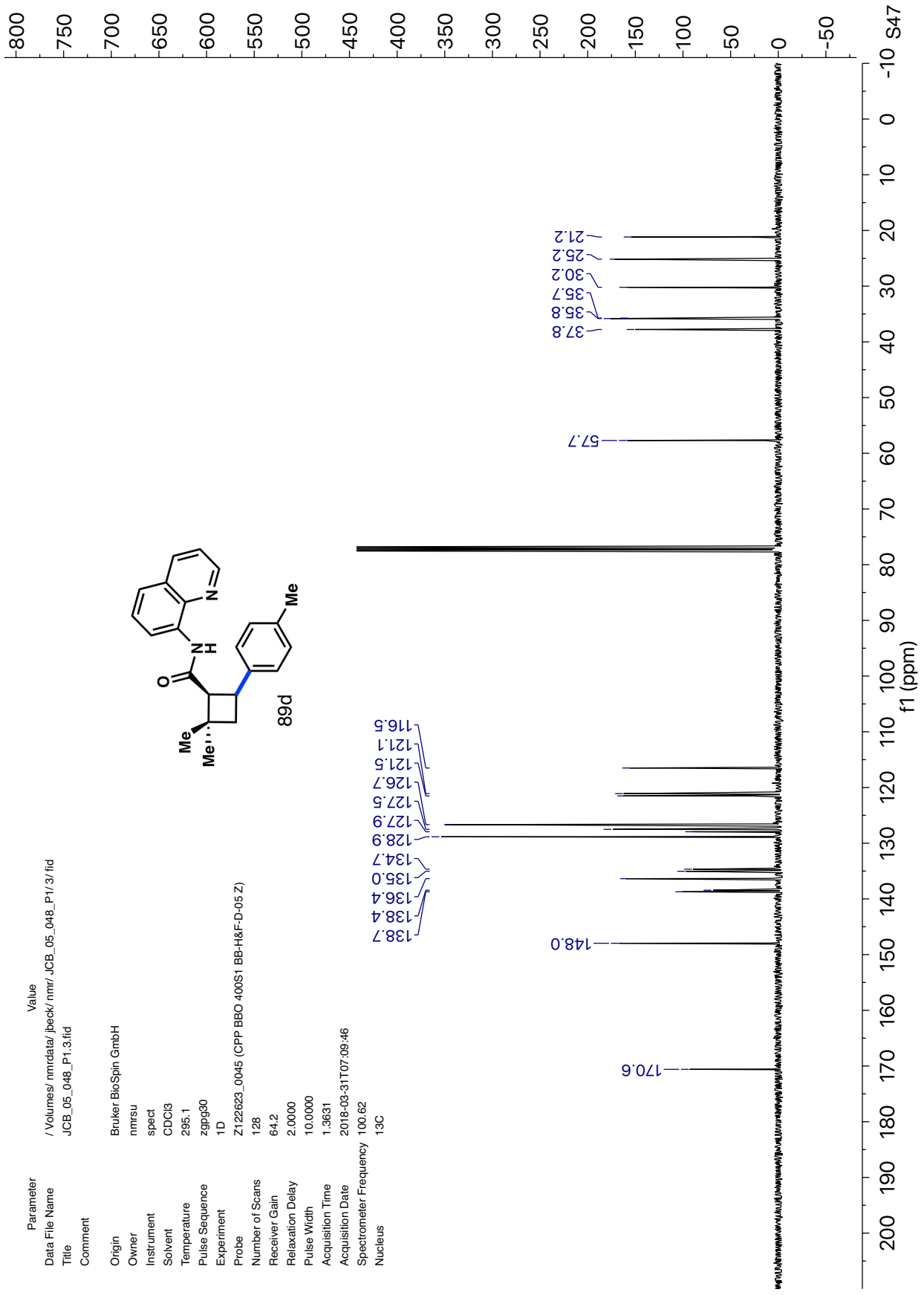
Parameter
Value
Data File Name
/ Volumes/ nmrdata/ jbeck/ nmr/ JCB_05_048_P1/ 3/ fid
Title
JCB_05_048_P1.3.fid
Comment
Origin
Bruker BioSpin GmbH
Owner
nmrsu
Instrument
spect
Solvent
CDCl3
Temperature
295.1
Pulse Sequence
zgpg30
Experiment
1D
Probe
Z122623_0045 (CPP BBO 400S1 BB-H&F-D-05 Z)
Number of Scans
128
Receiver Gain
64.2
Relaxation Delay
2.0000
Pulse Width
10.0000
Acquisition Time
1.3631
Acquisition Date
2018-03-31T07:09:46
Spectrometer Frequency
100.62
Nucleus
13C
89d
Me
Me
Me
N
H
O
N
170.6
148.0
138.7
138.4
136.4
135.0
134.7
128.9
127.9
127.5
126.7
121.5
121.1
116.5
57.7
37.8
35.8
35.7
30.2
25.2
21.2
f1 (ppm)

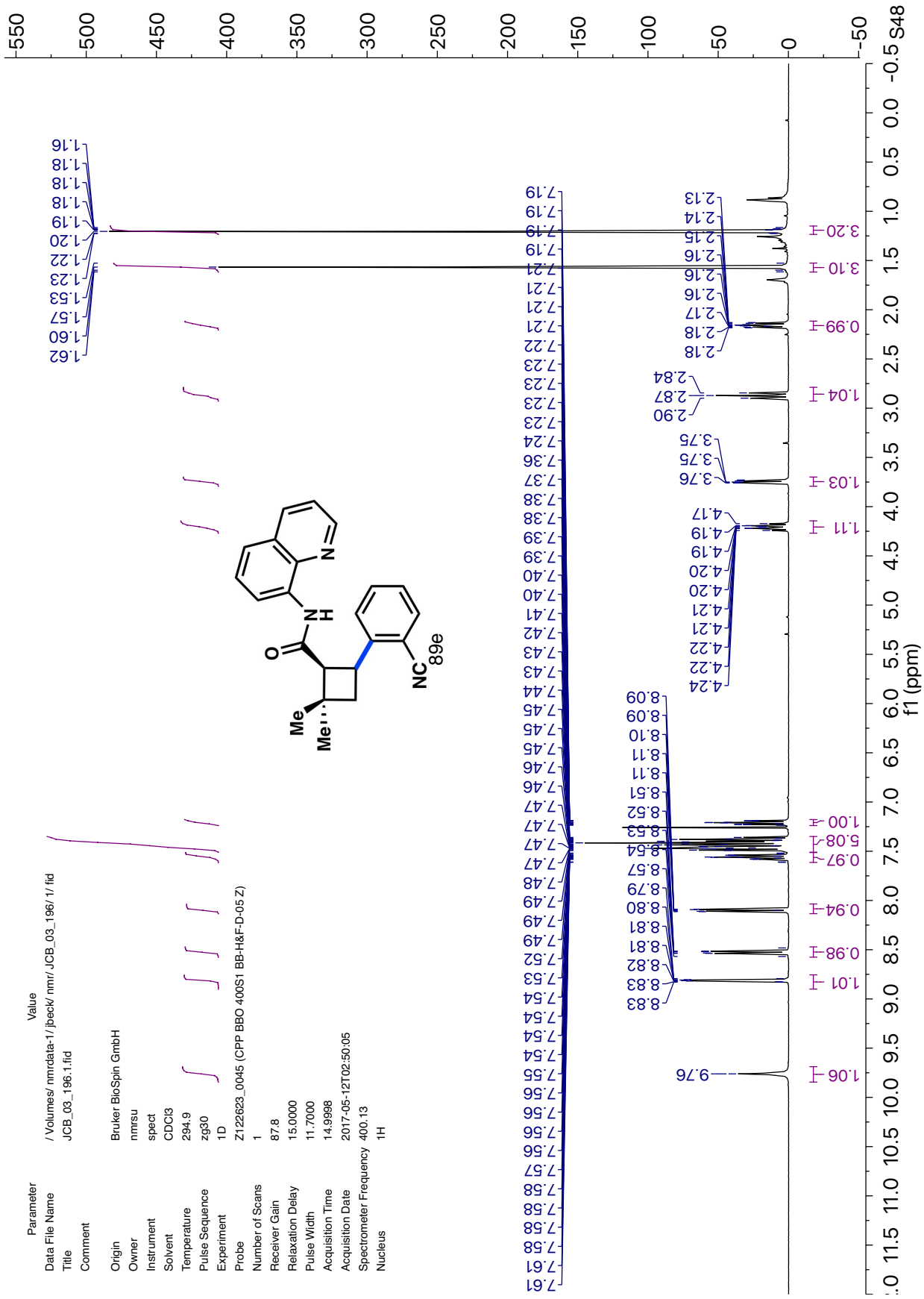
Parameter Value
Data File Name / Volumes/ nmrdata-1/ jbeck/ nmr/ JCB_03_196/ 1/ fid
Title JCB_03_196.1.fid
Comment
Origin Bruker BioSpin GmbH
Owner nmrsu
Instrument spect
Solvent CDCl3
Temperature 294.9
Pulse Sequence zg30
Experiment 1D
Probe Z122623_0045 (CPP BBO 400S1 BB-H&F-D-05 Z)
Number of Scans 1
Receiver Gain 87.8
Relaxation Delay 15.0000
Pulse Width 11.7000
Acquisition Time 14.9998
Acquisition Date 2017-05-12T02:50:05
Spectrometer Frequency 400.13
Nucleus 1H
f1 (ppm)
89e

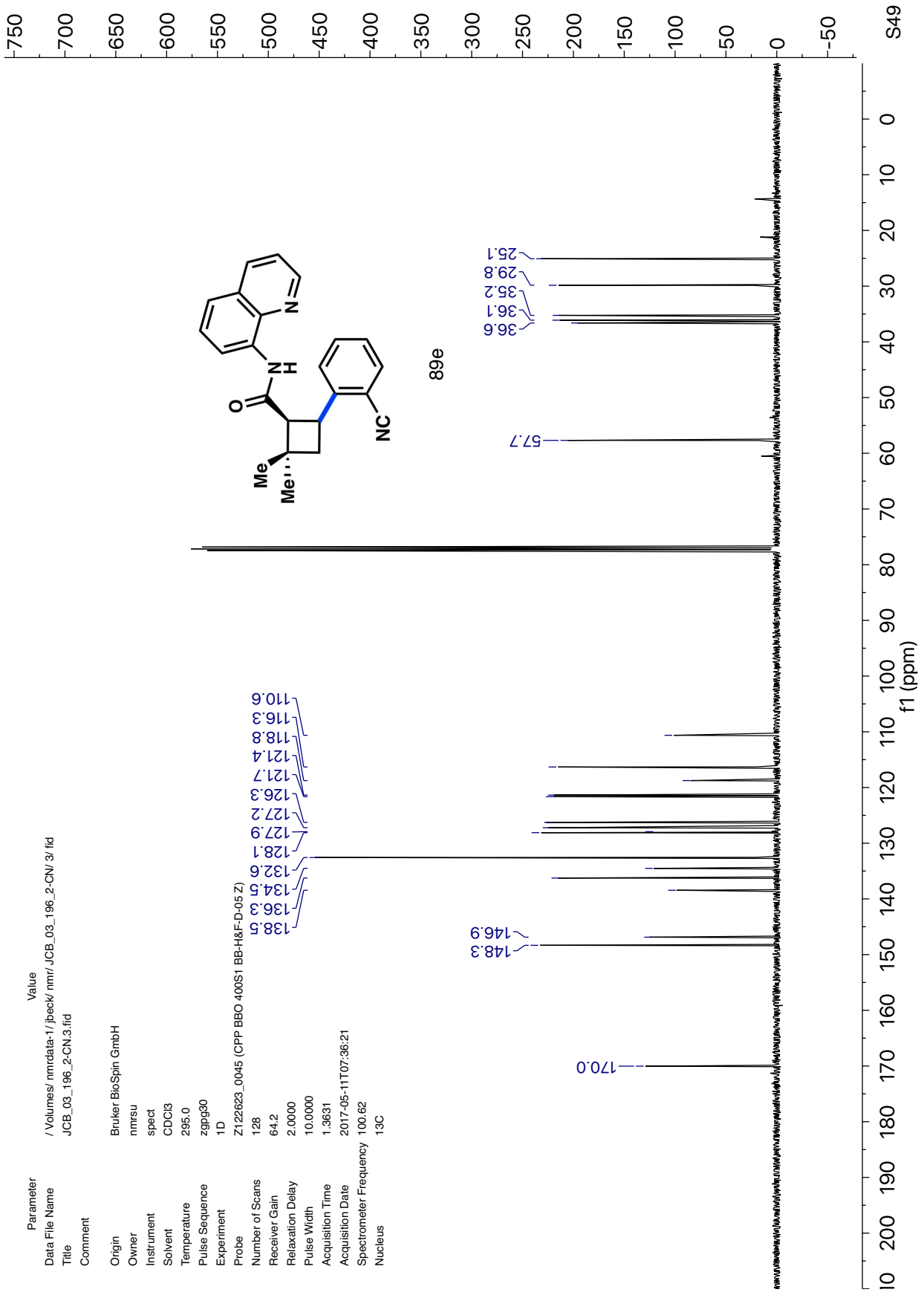
Parameter
Value
Data File Name / Volumes/ nmrdata-1/ jbeck/ nmr/ JCB_03_196_2-CN/ 3/ fid
Title JCB_03_196_2-CN.3.fid
Comment
Origin Bruker BioSpin GmbH
Owner nmrsu
Instrument spect
Solvent CDCl3
Temperature 295.0
Pulse Sequence zgpg30
Experiment 1D
Probe Z122623_0045 (CPP BBO 400S1 BB-H&F-D-05 Z)
Number of Scans 128
Receiver Gain 64.2
Relaxation Delay 2.0000
Pulse Width 10.0000
Acquisition Time 1.3631
Acquisition Date 2017-05-11T07:36:21
Spectrometer Frequency 100.62
Nucleus 13C
89e
170.0
148.3
146.9
138.5
136.3
134.5
132.6
128.1
127.9
127.2
126.3
121.7
121.4
118.8
116.3
110.6
57.7
36.6
36.1
35.2
29.8
25.1
f1 (ppm)
S49

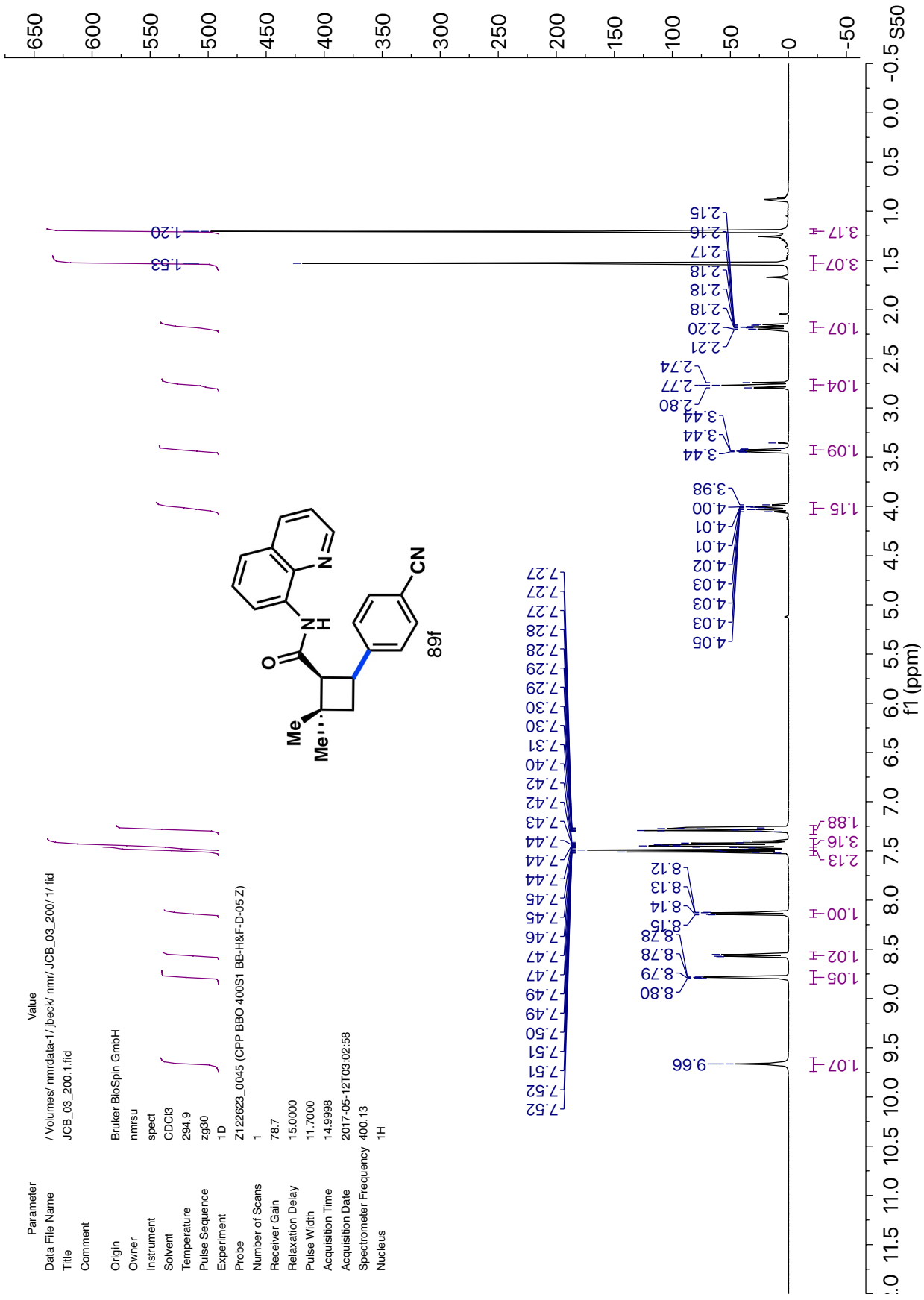
Parameter
Value
Data File Name / Volumes/ nmrdata-1/ jbeck/ nmr/ JCB_03_200/ 1/ fid
Title JCB_03_200_1.fid
Comment
Origin Bruker BioSpin GmbH
Owner nmrsu
Instrument spect
Solvent CDCl3
Temperature 294.9
Pulse Sequence zg30
Experiment 1D
Probe Z122623_0045 (CPP BBO 400S1 BB-H&F-D-05 Z)
Number of Scans 1
Receiver Gain 78.7
Relaxation Delay 15.0000
Pulse Width 11.7000
Acquisition Time 14.9998
Acquisition Date 2017-05-12T03:02:58
Spectrometer Frequency 400.13
Nucleus 1H
89f
f1 (ppm)

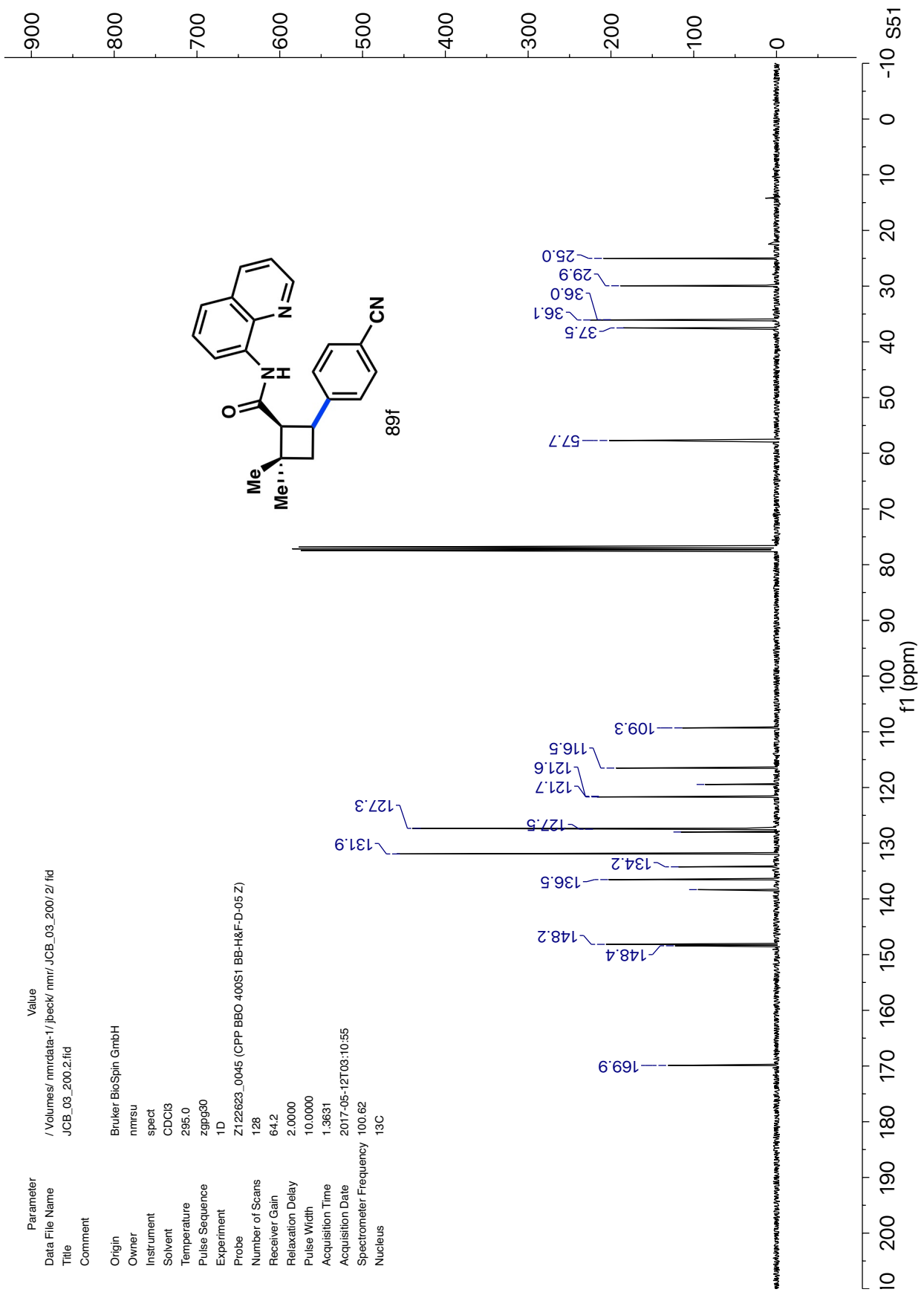
Parameter
Value
Data File Name
/ Volumes/ nmrdata-1/ jbeck/ nmr/ JCB_03_200/ 2/ fid
Title
JCB_03_200.2.fid
Comment
Origin
Bruker BioSpin GmbH
Owner
nmrsu
Instrument
spect
Solvent
CDCl3
Temperature
295.0
Pulse Sequence
zgpg30
Experiment
1D
Probe
Z122623_0045 (CPP BBO 400S1 BB-H&F-D-05 Z)
Number of Scans
128
Receiver Gain
64.2
Relaxation Delay
2.0000
Pulse Width
10.0000
Acquisition Time
1.3631
Acquisition Date
2017-05-12T03:10:55
Spectrometer Frequency
100.62
Nucleus
13C
169.9
148.4
148.2
136.5
134.2
131.9
127.3
127.5
121.7
121.6
116.5
109.3
57.7
37.5
36.1
36.0
29.9
25.0
89f
N
H
O
Me
Me
CN
f1 (ppm)
S51

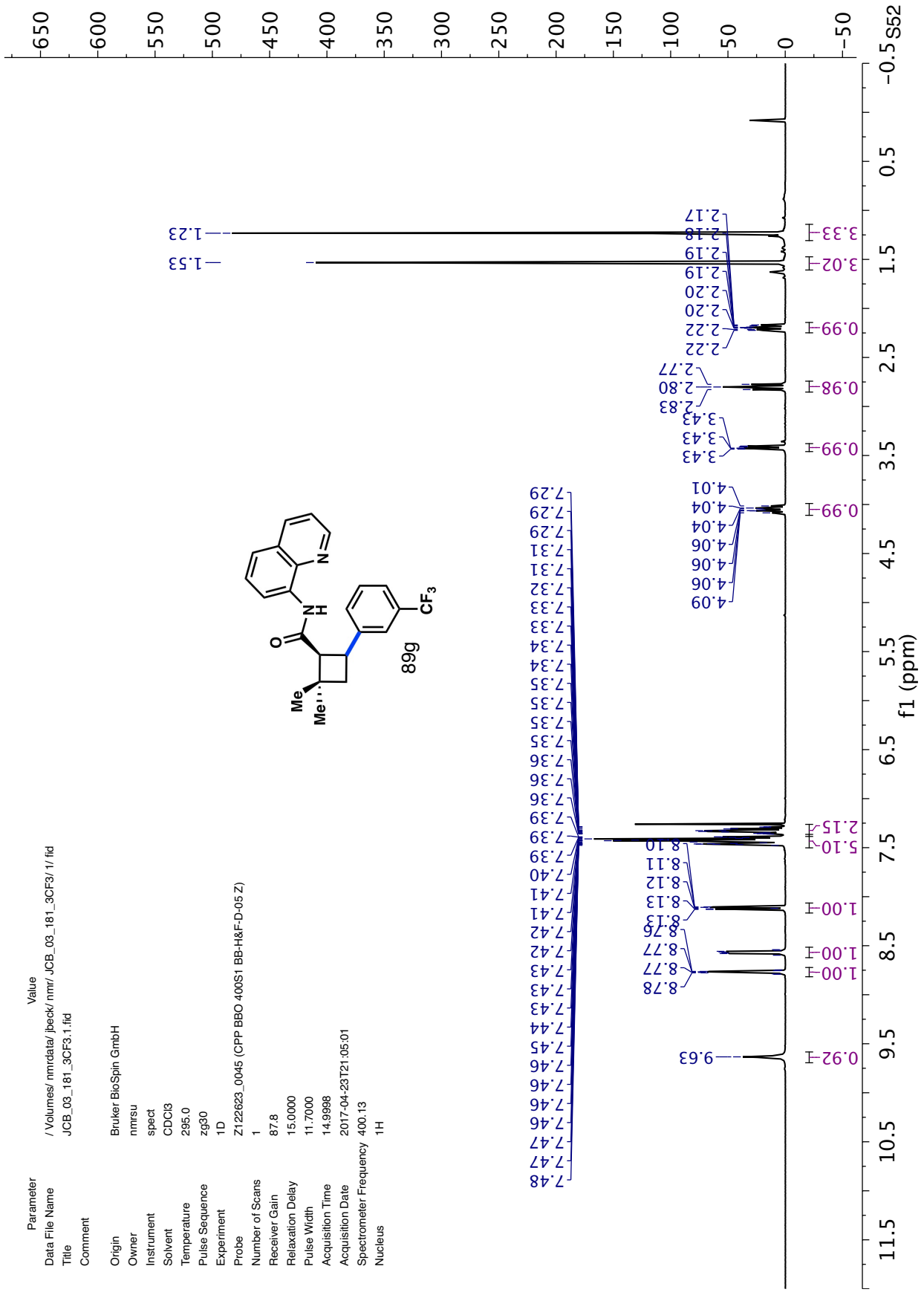
Parameter
Value
Data File Name / Volumes/ nmrdata/ jbeck/ nmr/ JCB_03_181_3CF3/ 1/ fid
Title JCB_03_181 _3CF3.1.fid
Comment
Origin Bruker BioSpin GmbH
Owner nmrsu
Instrument spect
Solvent CDCl3
Temperature 295.0
Pulse Sequence zg30
Experiment 1D
Probe Z122623_0045 (CPP BBO 400S1 BB-H&F-D-05 Z)
Number of Scans 1
Receiver Gain 87.8
Relaxation Delay 15.0000
Pulse Width 11.7000
Acquisition Time 14.9998
Acquisition Date 2017-04-23T21:05:01
Spectrometer Frequency 400.13
Nucleus 1H
89g
f1 (ppm)

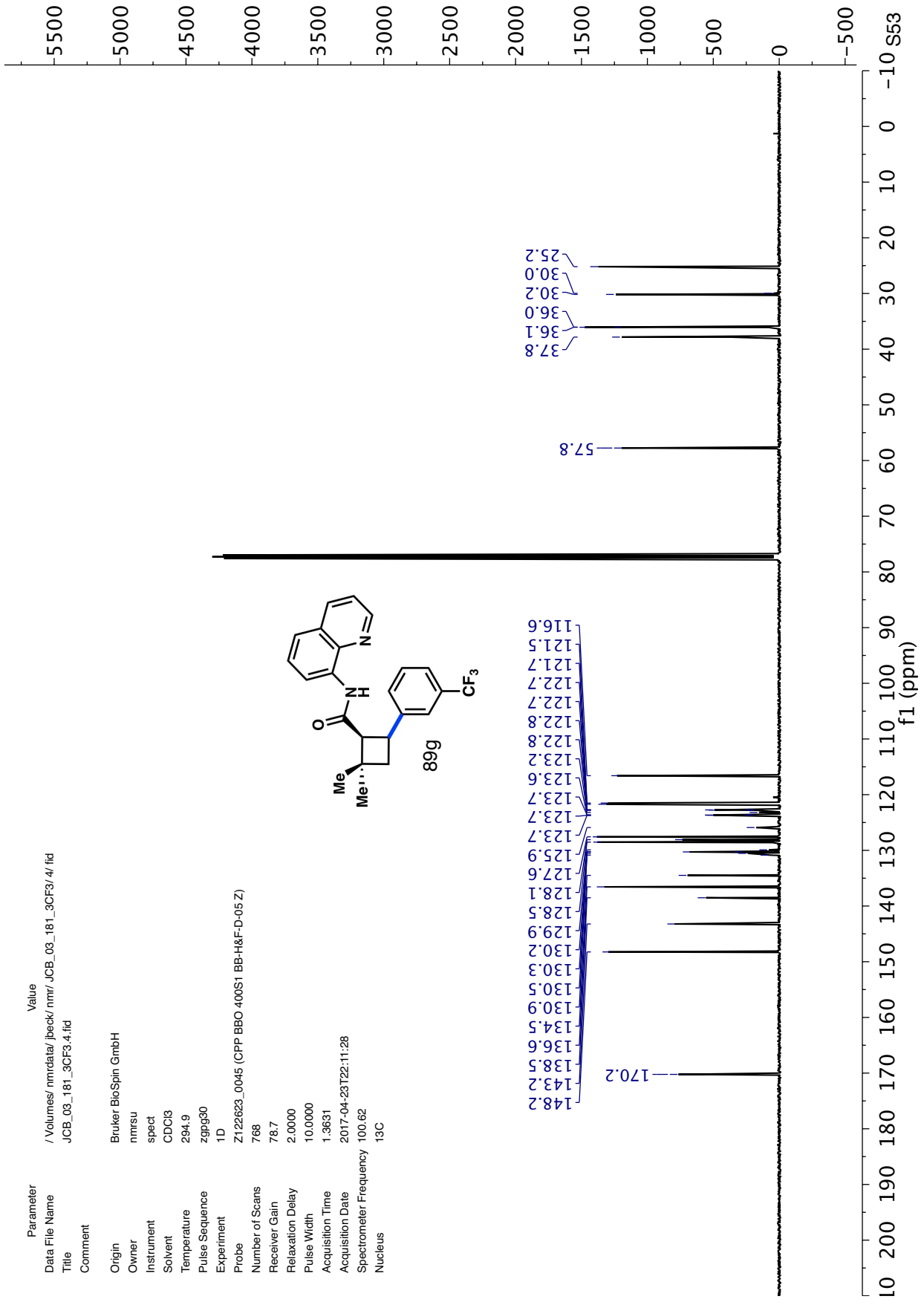
Parameter
Value
Data File Name / Volumes/ nmrdata/ jbeck/ nmr/ JCB_03_181_3CF3/ 4/ fid
Title JCB_03_181 _3CF3.4.fid
Comment
Origin Bruker BioSpin GmbH
Owner nmrsu
Instrument spect
Solvent CDCl3
Temperature 294.9
Pulse Sequence zgpg30
Experiment 1D
Probe Z122623_0045 (CPP BBO 400S1 BB-H&F-D-05 Z)
Number of Scans 768
Receiver Gain 78.7
Relaxation Delay 2.0000
Pulse Width 10.0000
Acquisition Time 1.3631
Acquisition Date 2017-04-23T22:11:28
Spectrometer Frequency 100.62
Nucleus 13C
89g
Me
Me
O
N
H
N
CF3
170.2
148.2
143.2
138.5
136.6
134.5
130.9
130.5
130.3
130.2
129.9
128.5
128.1
127.6
125.9
123.7
123.7
123.7
123.6
123.2
122.8
122.8
122.7
122.7
121.7
121.5
116.6
57.8
37.8
36.1
36.0
30.2
30.0
25.2
f1 (ppm)
S53

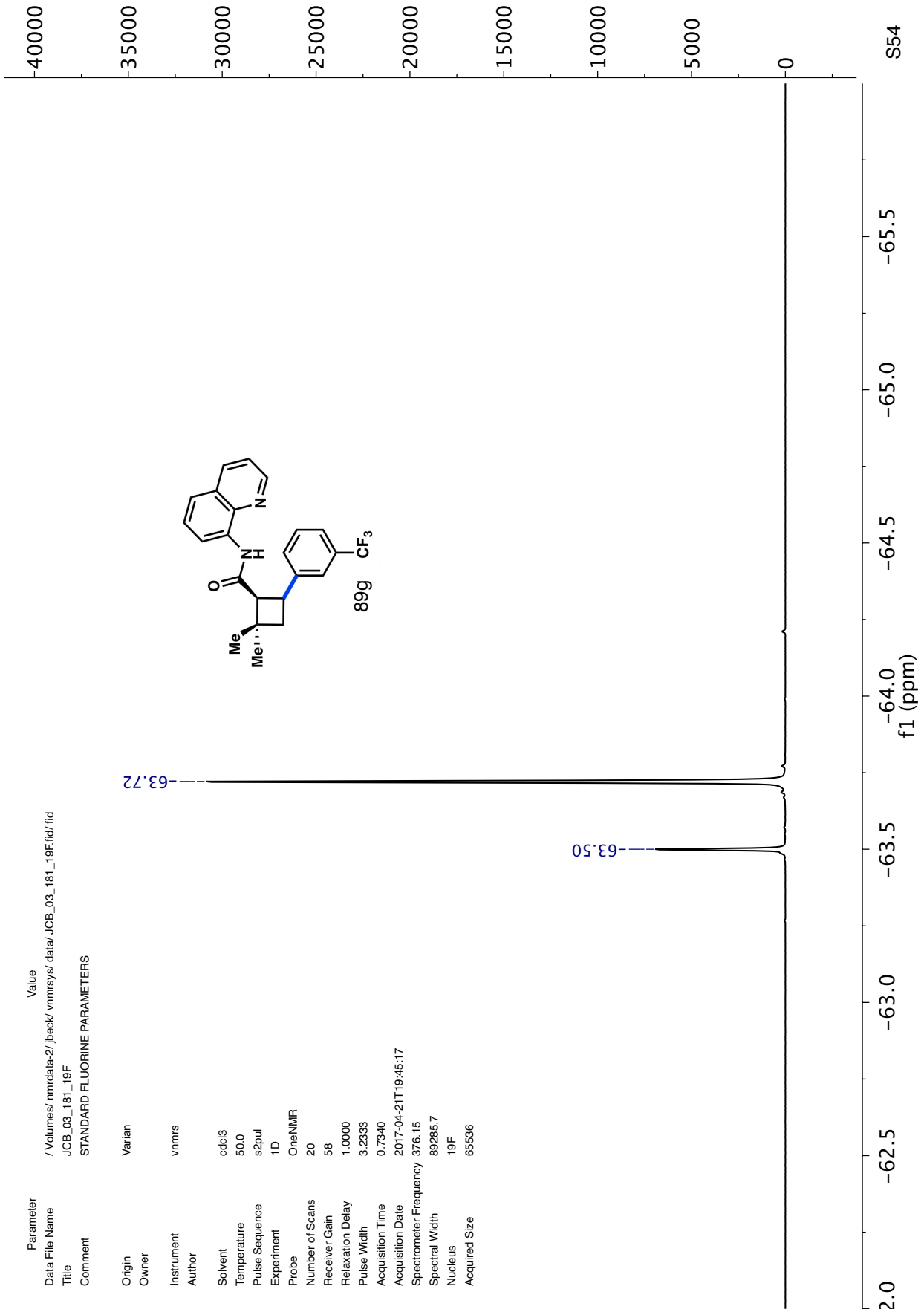
Parameter
Value
Data File Name
/ Volumes/ nmrdata-2/ jbeck/ vnmrsys/ data/ JCB_03_181_19F.fid/ fid
Title
JCB_03_181_19F
Comment
STANDARD FLUORINE PARAMETERS
Origin
Varian
Owner
Instrument
vnmrs
Author
Solvent
cdcl3
Temperature
50.0
Pulse Sequence
s2pul
Experiment
1D
Probe
OneNMR
Number of Scans
20
Receiver Gain
58
Relaxation Delay
1.0000
Pulse Width
3.2333
Acquisition Time
0.7340
Acquisition Date
2017-04-21T19:45:17
Spectrometer Frequency
376.15
Spectral Width
89285.7
Nucleus
19F
Acquired Size
65536
−63.72
−63.50
89g
CF3
Me
Me
O
N
H
N
40000
35000
30000
25000
20000
15000
10000
5000
0
−62.5
−63.0
−63.5
−64.0
−64.5
−65.0
−65.5
2.0
f1 (ppm)
S54

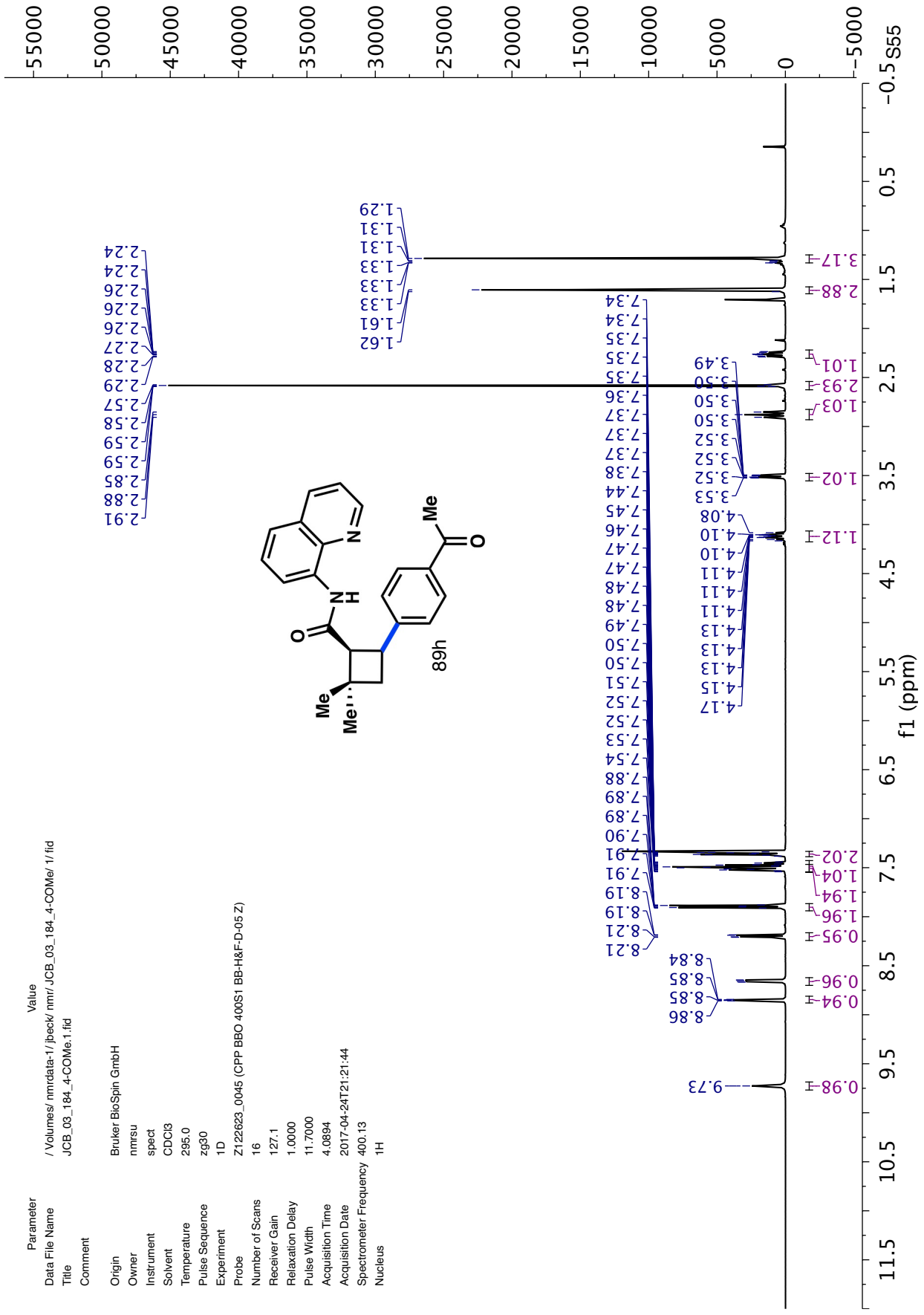
Parameter Value
Data File Name / Volumes/ nmrdata-1/ jbeck/ nmr/ JCB_03_184_4-COMe/ 1/ fid
Title JCB_03_184_4-COMe.1.fid
Comment
Origin Bruker BioSpin GmbH
Owner nmrsu
Instrument spect
Solvent CDCl3
Temperature 295.0
Pulse Sequence zg30
Experiment 1D
Probe Z122623_0045 (CPP BBO 400S1 BB-H&F-D-05 Z)
Number of Scans 16
Receiver Gain 127.1
Relaxation Delay 1.0000
Pulse Width 11.7000
Acquisition Time 4.0894
Acquisition Date 2017-04-24T21:21:44
Spectrometer Frequency 400.13
Nucleus 1H
89h
f1 (ppm)

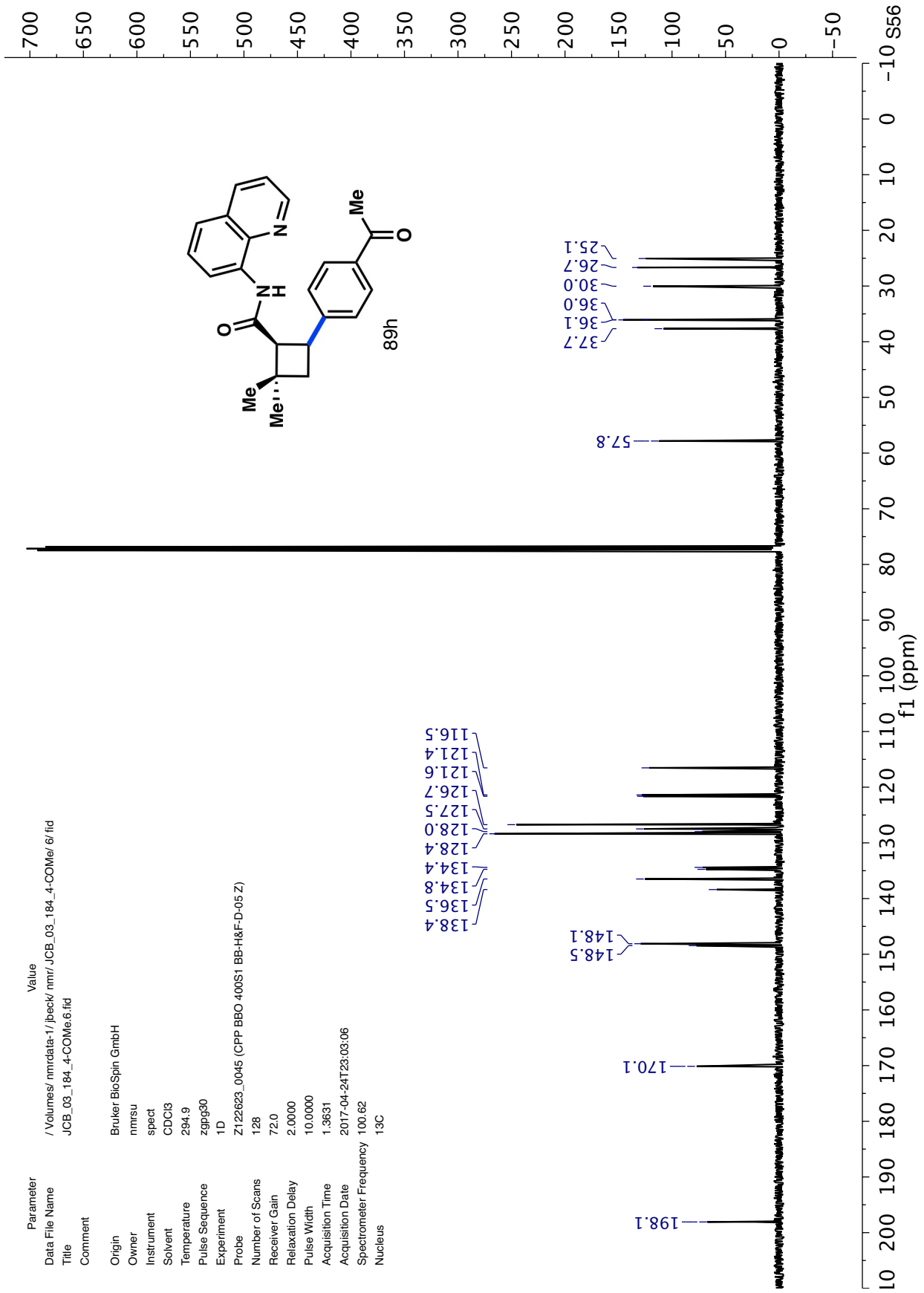
Parameter
Value
Data File Name
/ Volumes/ nmrdata-1/ jbeck/ nmr/ JCB_03_184_4-COMe/ 6/ fid
Title
JCB_03_184_4-COMe.6.fid
Comment
Origin
Bruker BioSpin GmbH
Owner
nmrsu
Instrument
spect
Solvent
CDCl3
Temperature
294.9
Pulse Sequence
zgpg30
Experiment
1D
Probe
Z122623_0045 (CPP BBO 400S1 BB-H&F-D-05 Z)
Number of Scans
128
Receiver Gain
72.0
Relaxation Delay
2.0000
Pulse Width
10.0000
Acquisition Time
1.3631
Acquisition Date
2017-04-24T23:03:06
Spectrometer Frequency
100.62
Nucleus
13C
198.1
170.1
148.5
148.1
138.4
136.5
134.8
134.4
128.4
128.0
127.5
126.7
121.6
121.4
116.5
57.8
37.7
36.1
36.0
30.0
26.7
25.1
89h
Me
Me
O
N
H
N
O
Me
f1 (ppm)
S56

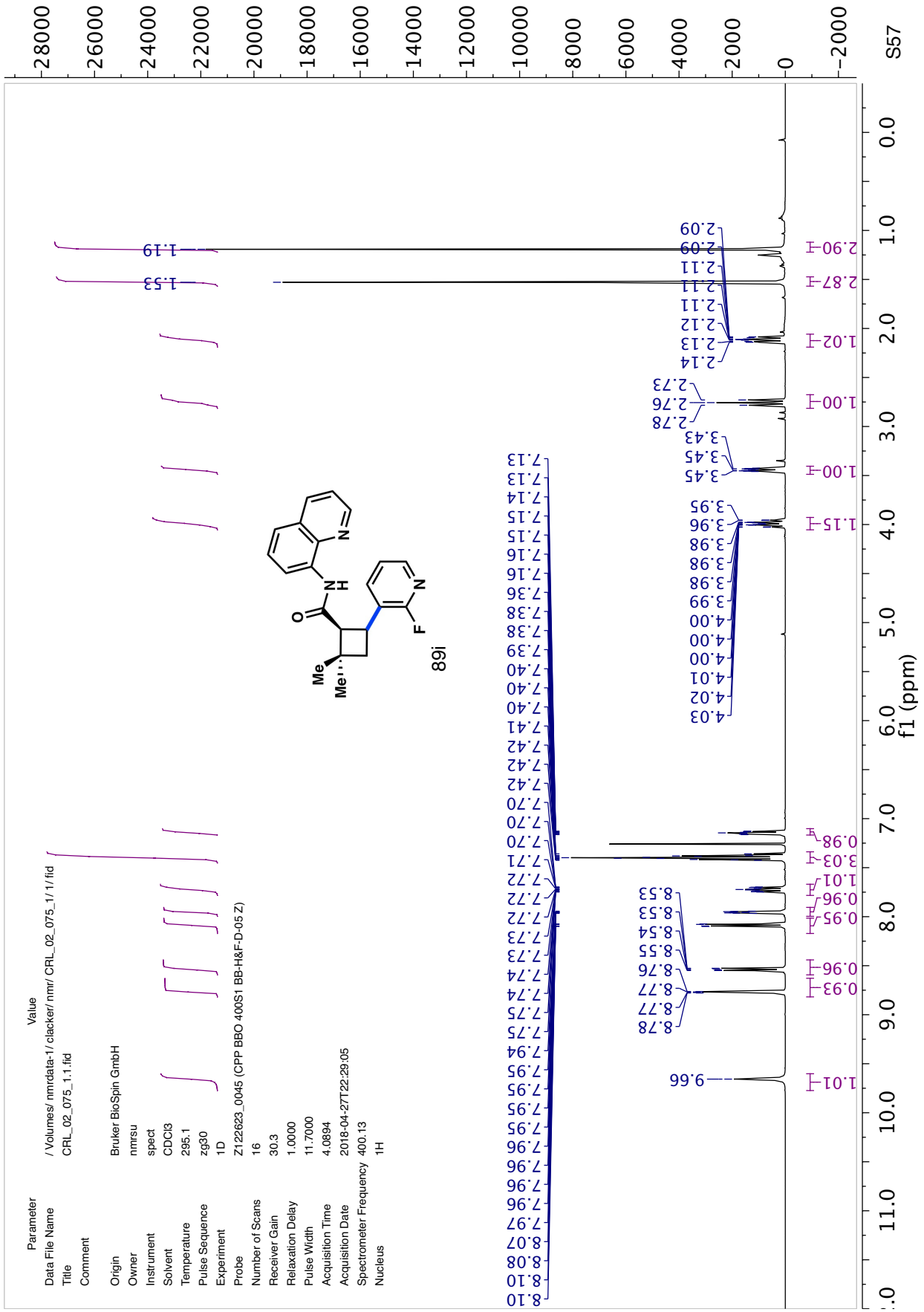
Parameter Value
Data File Name / Volumes/ nmrdata-1/ clacker/ nmr/ CRL_02_075_1/ 1/ fid
Title CRL_02_075_1.1.fid
Comment
Origin Bruker BioSpin GmbH
Owner nmrsu
Instrument spect
Solvent CDCl3
Temperature 295.1
Pulse Sequence zg30
Experiment 1D
Probe Z122623_0045 (CPP BBO 400S1 BB-H&F-D-05 Z)
Number of Scans 16
Receiver Gain 30.3
Relaxation Delay 1.0000
Pulse Width 11.7000
Acquisition Time 4.0894
Acquisition Date 2018-04-27T22:29:05
Spectrometer Frequency 400.13
Nucleus 1H
89i
f1 (ppm)
S57

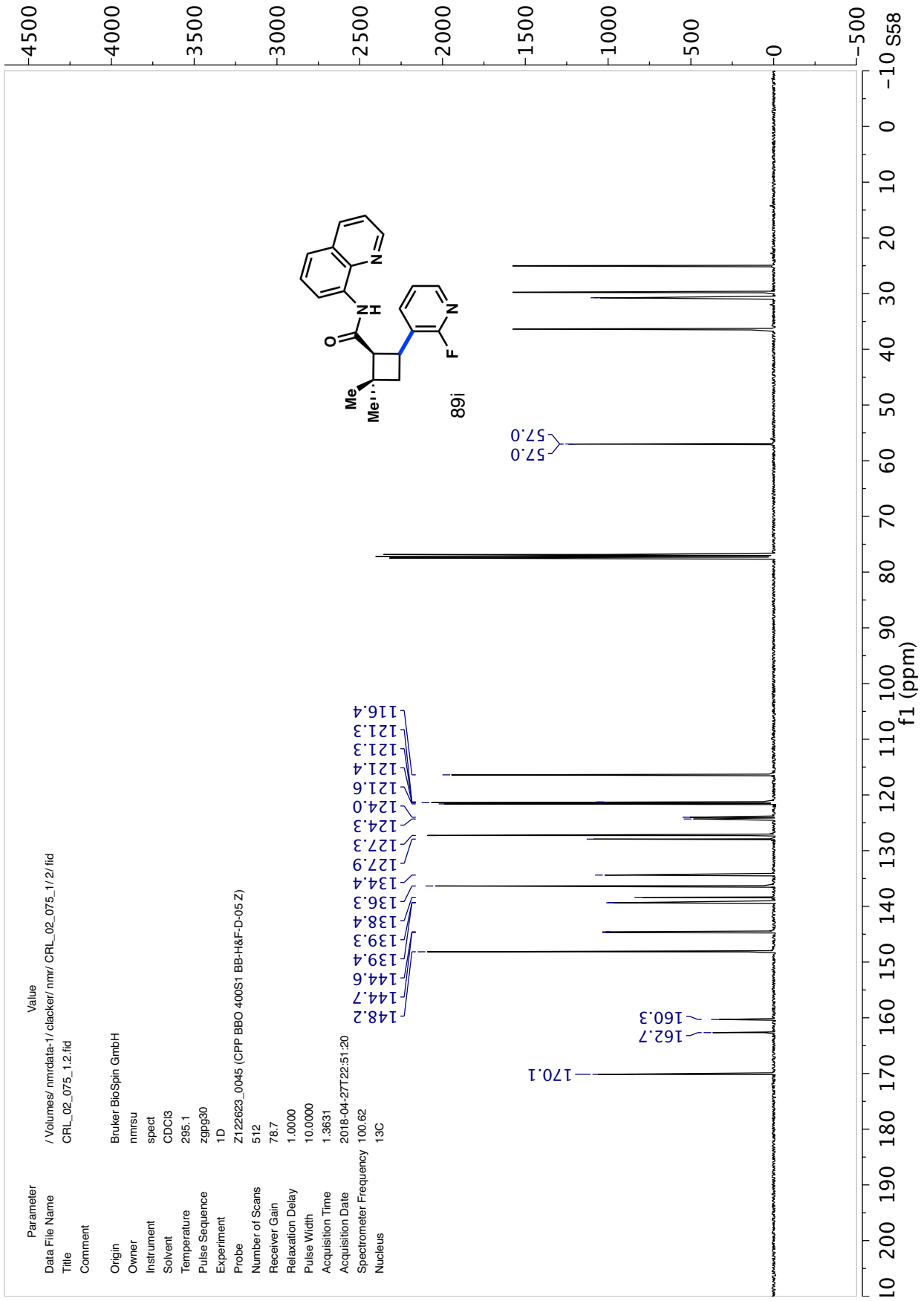
Parameter
Value
Data File Name
/ Volumes/ nmrdata-1/ clacker/ nmr/ CRL_02_075_1/ 2/ fid
Title
CRL_02_075_1.2.fid
Comment
Origin
Bruker BioSpin GmbH
Owner
nmrsu
Instrument
spect
Solvent
CDCl3
Temperature
295.1
Pulse Sequence
zgpg30
Experiment
1D
Probe
Z122623_0045 (CPP BBO 400S1 BB-H&F-D-05 Z)
Number of Scans
512
Receiver Gain
78.7
Relaxation Delay
1.0000
Pulse Width
10.0000
Acquisition Time
1.3631
Acquisition Date
2018-04-27T22:51:20
Spectrometer Frequency
100.62
Nucleus
13C
89i
Me
Me
O
N
H
N
F
N
170.1
162.7
160.3
148.2
144.7
144.6
139.4
139.3
138.4
136.3
134.4
127.9
127.3
124.3
124.0
121.6
121.4
121.3
121.3
116.4
57.0
57.0
f1 (ppm)

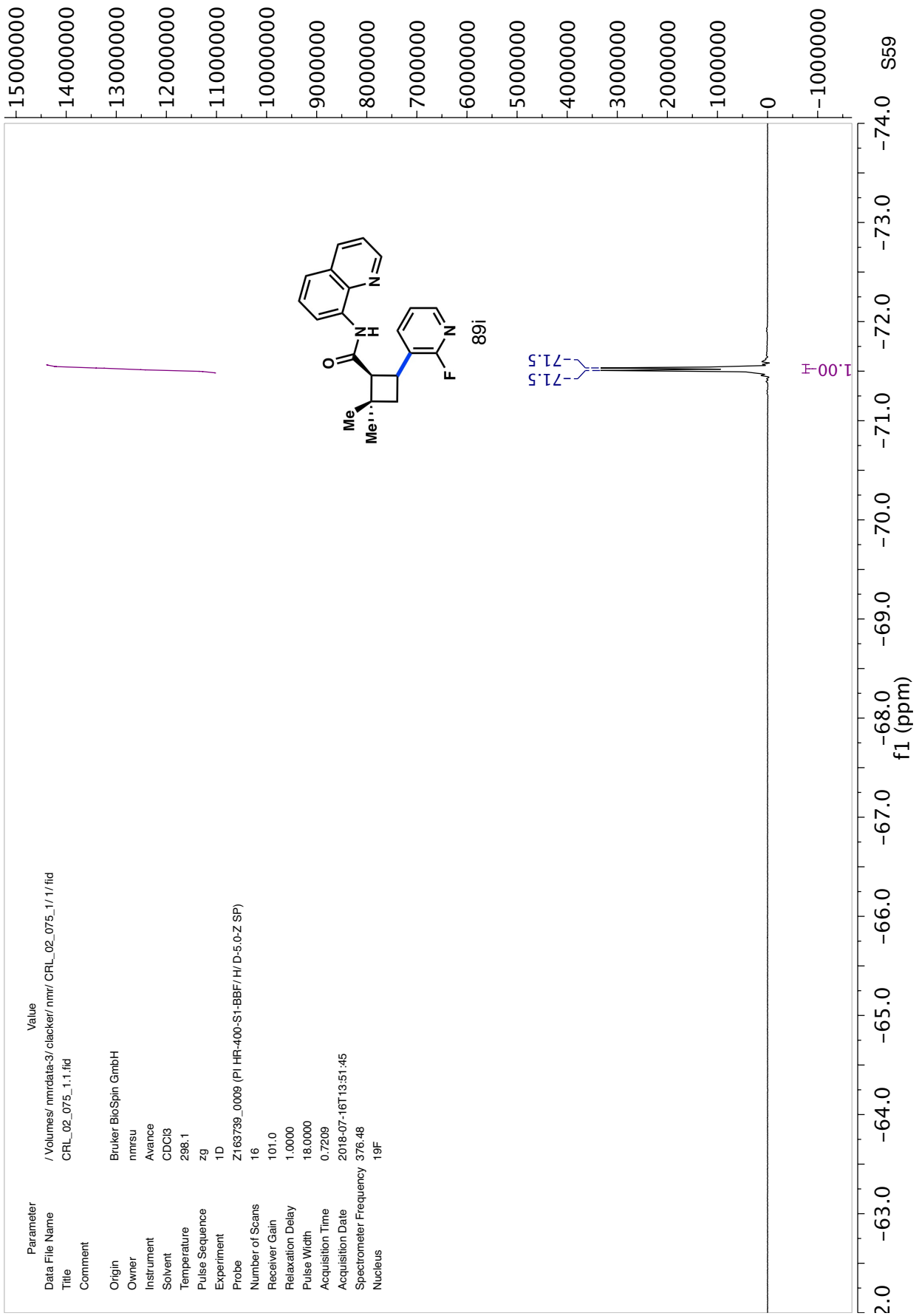
Parameter
Value
Data File Name
/ Volumes/ nmrdata-3/ clacker/ nmr/ CRL_02_075_1/ 1/ fid
Title
CRL_02_075_1.1.fid
Comment
Origin
Bruker BioSpin GmbH
Owner
nmrsu
Instrument
Avance
Solvent
CDCl3
Temperature
298.1
Pulse Sequence
zg
Experiment
1D
Probe
Z163739_0009 (PI HR-400-S1-BBF/ H/ D-5.0-Z SP)
Number of Scans
16
Receiver Gain
101.0
Relaxation Delay
1.0000
Pulse Width
18.0000
Acquisition Time
0.7209
Acquisition Date
2018-07-16T13:51:45
Spectrometer Frequency
376.48
Nucleus
19F
89i
-71.5
-71.5
1.00
f1 (ppm)
S59

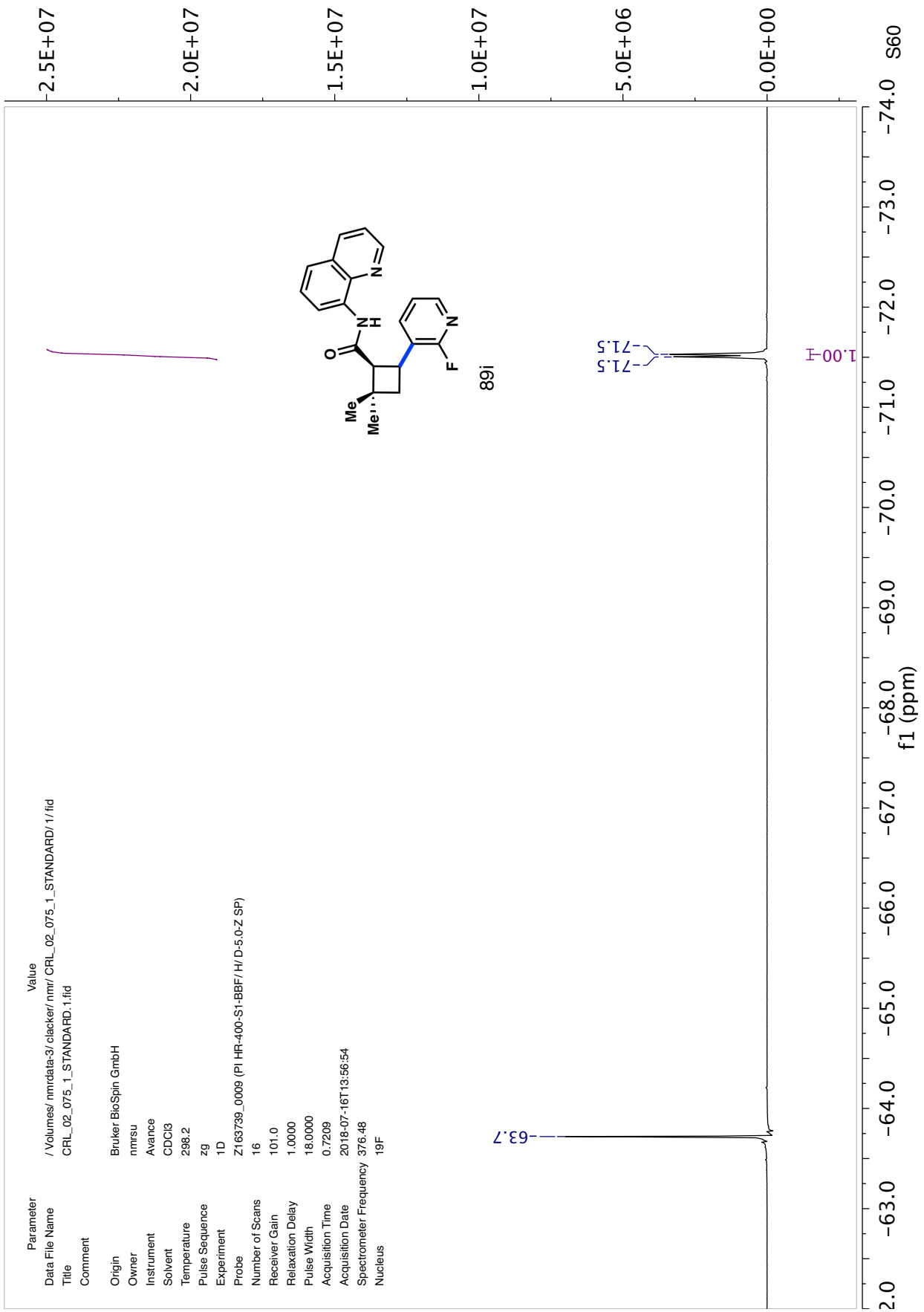
Parameter
Value
Data File Name
/ Volumes/ nmrdata-3/ clacker/ nmr/ CRL_02_075_1_STANDARD/ 1/ fid
Title
CRL_02_075_1_STANDARD.1.fid
Comment
Origin
Bruker BioSpin GmbH
Owner
nmrsu
Instrument
Avance
Solvent
CDCl3
Temperature
298.2
Pulse Sequence
zg
Experiment
1D
Probe
Z163739_0009 (PI HR-400-S1-BBF/ H/ D-5.0-Z SP)
Number of Scans
16
Receiver Gain
101.0
Relaxation Delay
1.0000
Pulse Width
18.0000
Acquisition Time
0.7209
Acquisition Date
2018-07-16T13:56:54
Spectrometer Frequency
376.48
Nucleus
19F
-63.7
-71.5
-71.5
1.00
89i
f1 (ppm)
S60

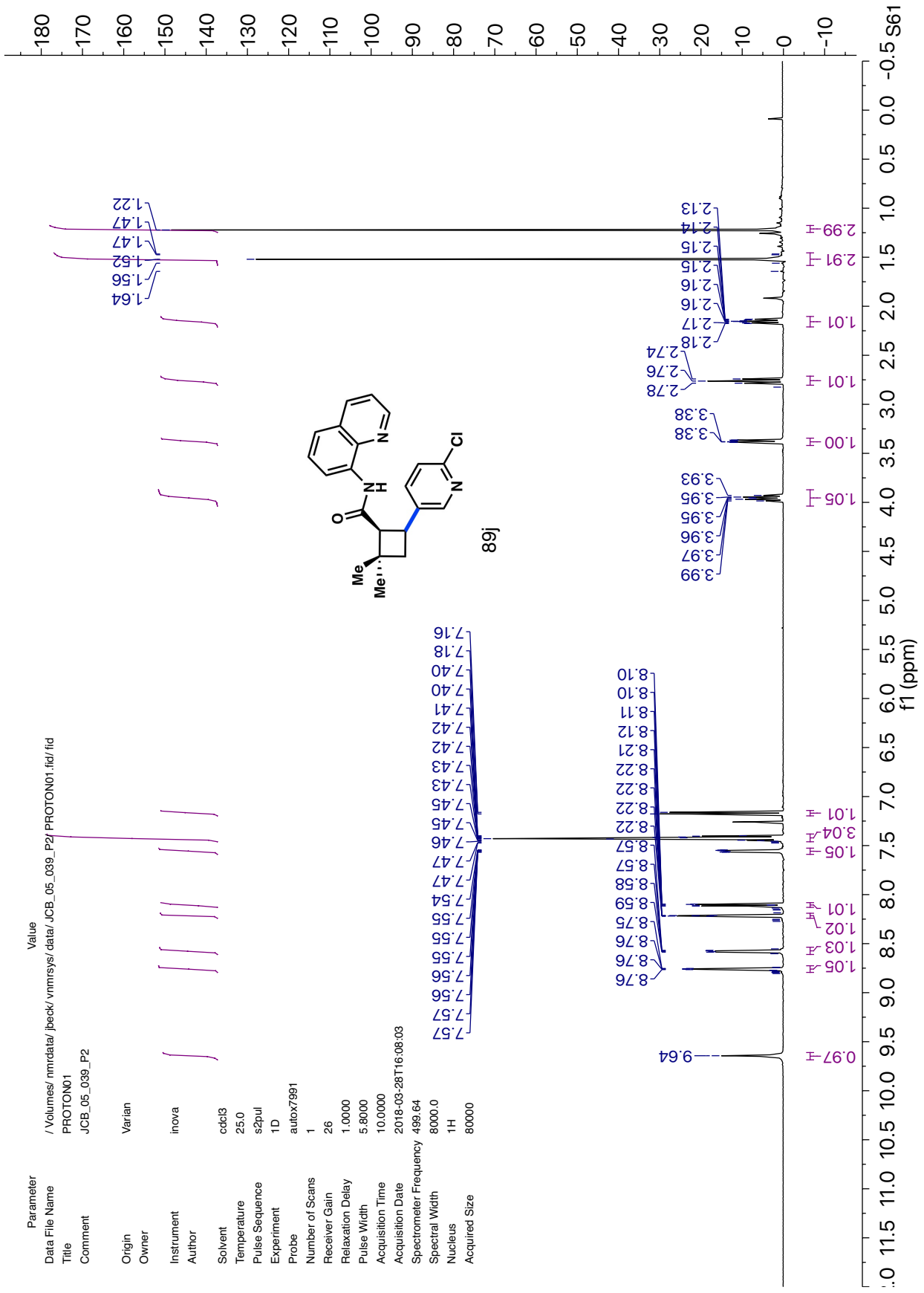
Parameter
Value
Data File Name / Volumes/ nmrdata/ jbeck/ vnmrsys/ data/ JCB_05_039_P2/ PROTON01.fid/ fid
Title PROTON01
Comment JCB_05_039_P2
Origin Varian
Owner
Instrument inova
Author
Solvent cdcl3
Temperature 25.0
Pulse Sequence s2pul
Experiment 1D
Probe autox7991
Number of Scans 1
Receiver Gain 26
Relaxation Delay 1.0000
Pulse Width 5.8000
Acquisition Time 10.0000
Acquisition Date 2018-03-28T16:08:03
Spectrometer Frequency 499.64
Spectral Width 8000.0
Nucleus 1H
Acquired Size 80000
89j
f1 (ppm)

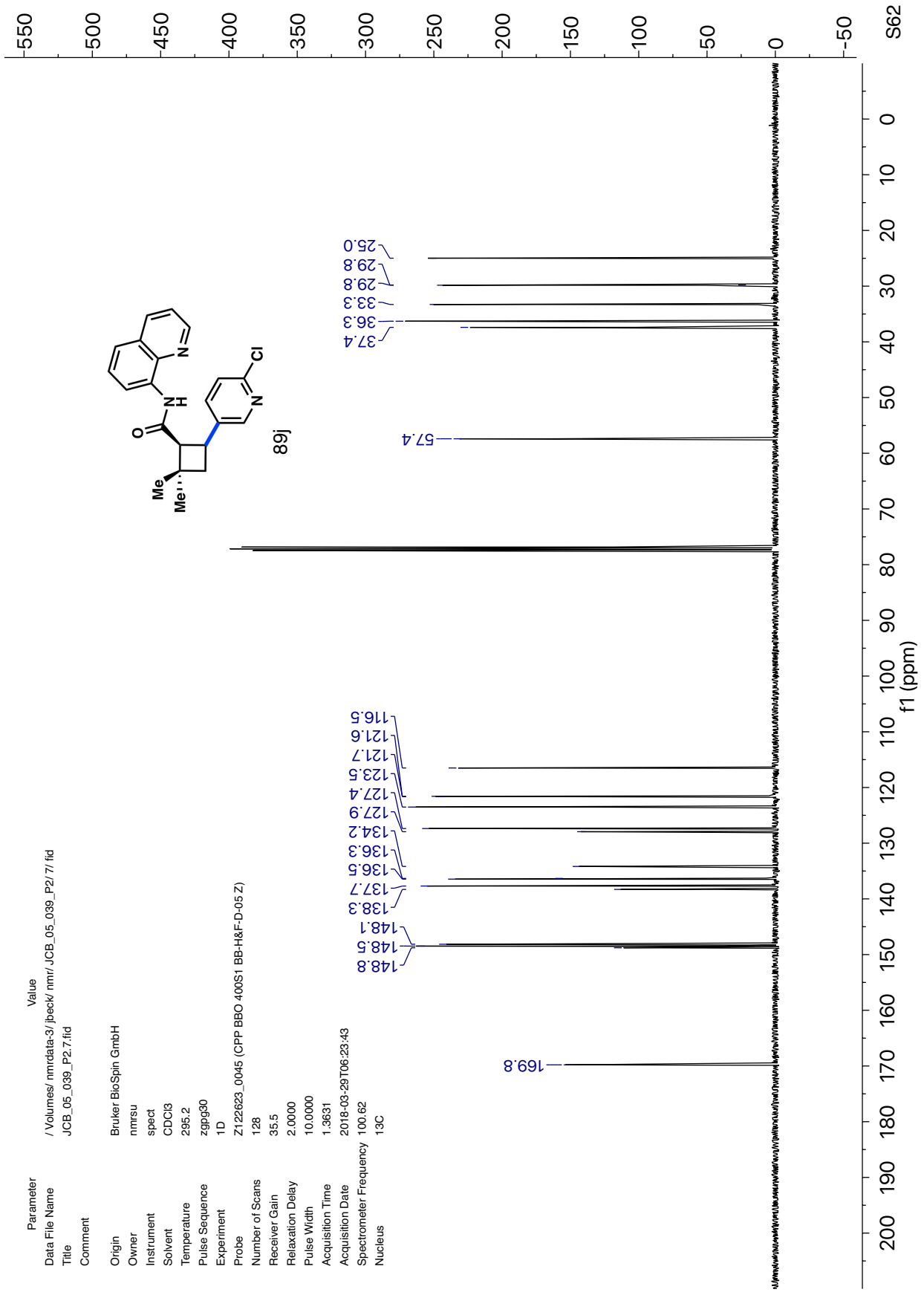
Parameter
Value
Data File Name / Volumes/ nmrdata-3/ jbeck/ nmr/ JCB_05_039_P2/ 7/ fid
Title JCB_05_039_P2.7.fid
Comment
Origin Bruker BioSpin GmbH
Owner nmrsu
Instrument spect
Solvent CDCl3
Temperature 295.2
Pulse Sequence zgpg30
Experiment 1D
Probe Z122623_0045 (CPP BBO 400S1 BB-H&F-D-05 Z)
Number of Scans 128
Receiver Gain 35.5
Relaxation Delay 2.0000
Pulse Width 10.0000
Acquisition Time 1.3631
Acquisition Date 2018-03-29T06:23:43
Spectrometer Frequency 100.62
Nucleus 13C
89j
169.8
148.8
148.5
148.1
138.3
137.7
136.5
136.3
134.2
127.9
127.4
123.5
121.7
121.6
116.5
57.4
37.4
36.3
33.3
29.8
29.8
25.0
f1 (ppm)

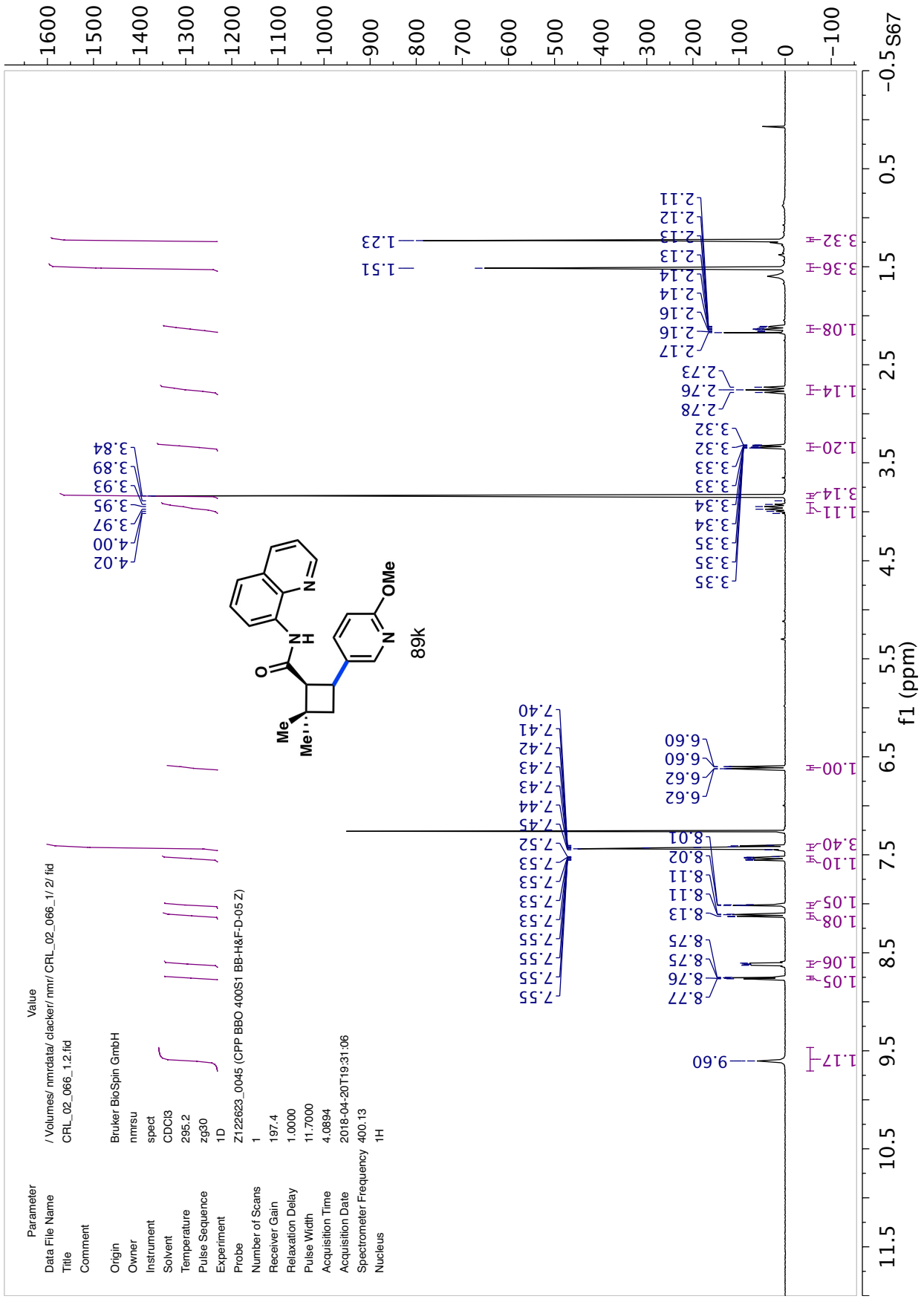
Parameter
Value
Data File Name
/ Volumes/ nmrdata/ clacker/ nmr/ CRL_02_066_1/ 2/ fid
Title
CRL_02_066_1.2.fid
Comment
Origin
Bruker BioSpin GmbH
Owner
nmrsu
Instrument
spect
Solvent
CDCl3
Temperature
295.2
Pulse Sequence
zg30
Experiment
1D
Probe
Z122623_0045 (CPP BBO 400S1 BB-H&F-D-05 Z)
Number of Scans
1
Receiver Gain
197.4
Relaxation Delay
1.0000
Pulse Width
11.7000
Acquisition Time
4.0894
Acquisition Date
2018-04-20T19:31:06
Spectrometer Frequency
400.13
Nucleus
1H
89k
f1 (ppm)
S67

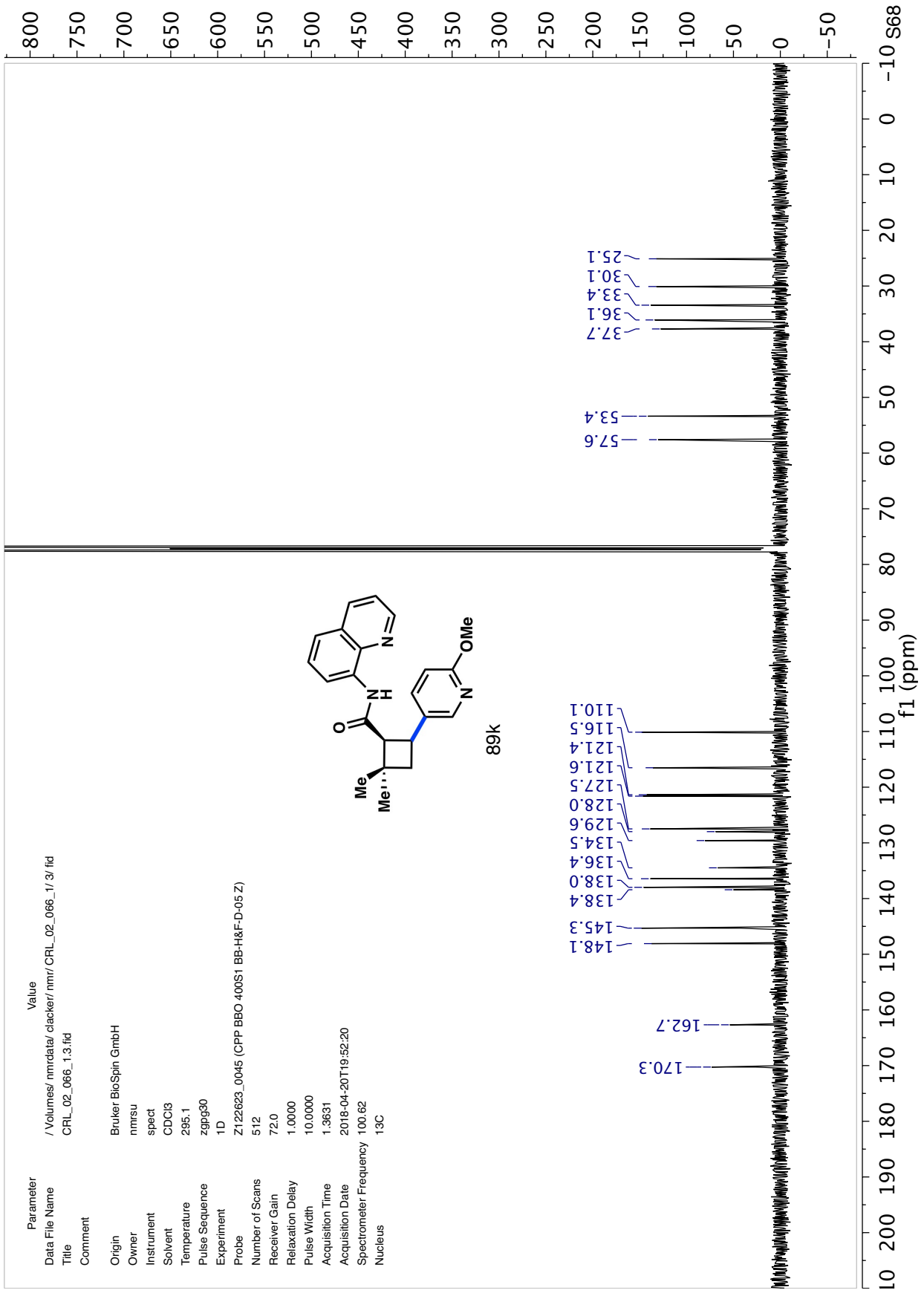
Parameter Value
Data File Name / Volumes/ nmrdata/ clacker/ nmr/ CRL_02_066_1/ 3/ fid
Title CRL_02_066_1.3.fid
Comment
Origin Bruker BioSpin GmbH
Owner nmrsu
Instrument spect
Solvent CDCl3
Temperature 295.1
Pulse Sequence zgpg30
Experiment 1D
Probe Z122623_0045 (CPP BBO 400S1 BB-H&F-D-05 Z)
Number of Scans 512
Receiver Gain 72.0
Relaxation Delay 1.0000
Pulse Width 10.0000
Acquisition Time 1.3631
Acquisition Date 2018-04-20T19:52:20
Spectrometer Frequency 100.62
Nucleus 13C
89k
OMe
Me
Me
25.1
30.1
33.4
36.1
37.7
53.4
57.6
110.1
116.5
121.4
121.6
127.5
128.0
129.6
134.5
136.4
138.0
138.4
145.3
148.1
162.7
170.3
f1 (ppm)

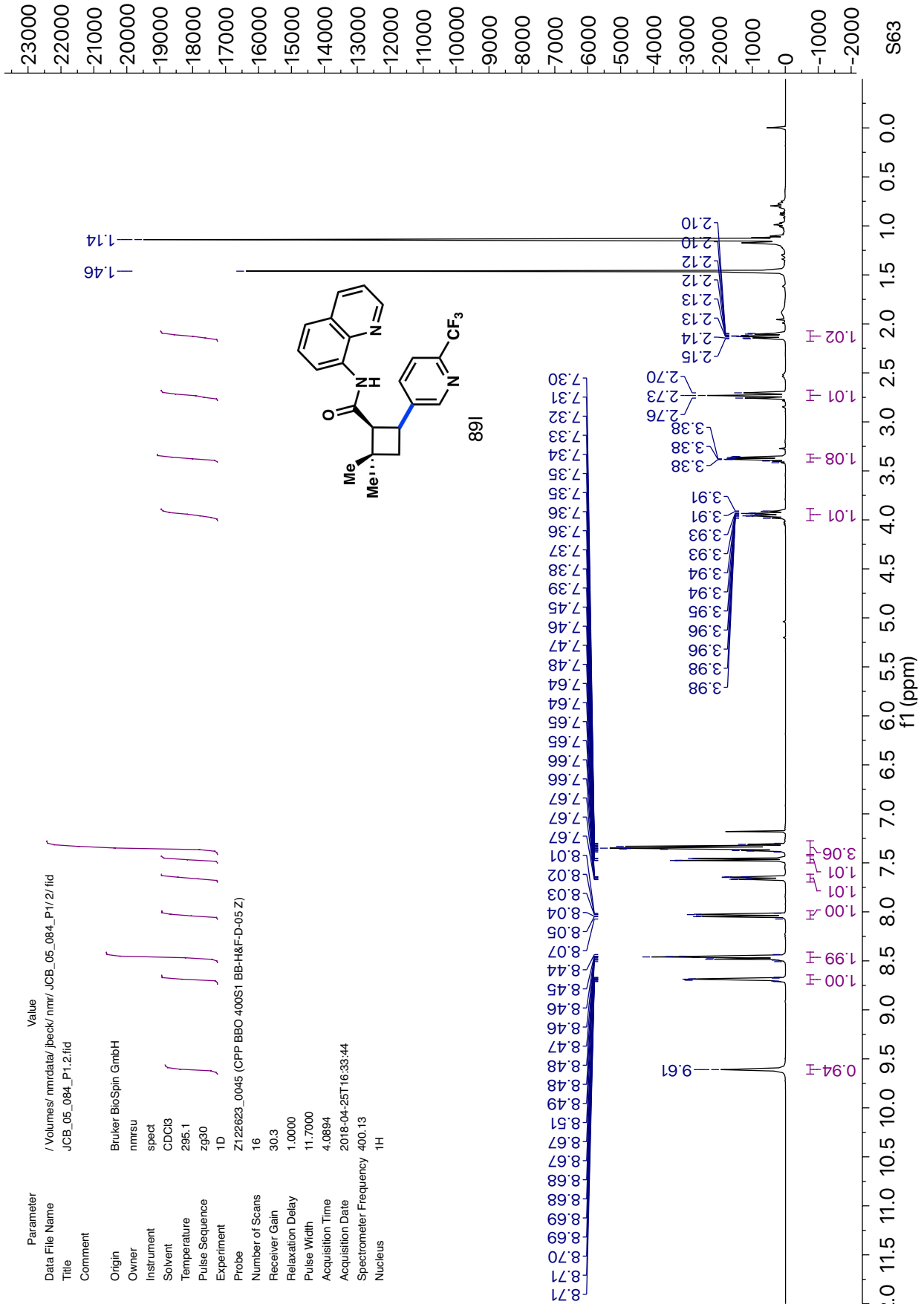
Parameter Value
Data File Name / Volumes/ nmrdata/ jbeck/ nmr/ JCB_05_084_P1/ 2/ fid
Title JCB_05_084_P1.2.fid
Comment
Origin Bruker BioSpin GmbH
Owner nmrsu
Instrument spect
Solvent CDCl3
Temperature 295.1
Pulse Sequence zg30
Experiment 1D
Probe Z122623_0045 (CPP BBO 400S1 BB-H&F-D-05 Z)
Number of Scans 16
Receiver Gain 30.3
Relaxation Delay 1.0000
Pulse Width 11.7000
Acquisition Time 4.0894
Acquisition Date 2018-04-25T16:33:44
Spectrometer Frequency 400.13
Nucleus 1H
1.14
1.46
9.61
0.94
1.02
1.01
1.08
1.01
3.06
1.01
1.01
1.00
1.99
1.00
Me
Me
O
N
H
N
N
CF3
I68
S63
f1 (ppm)

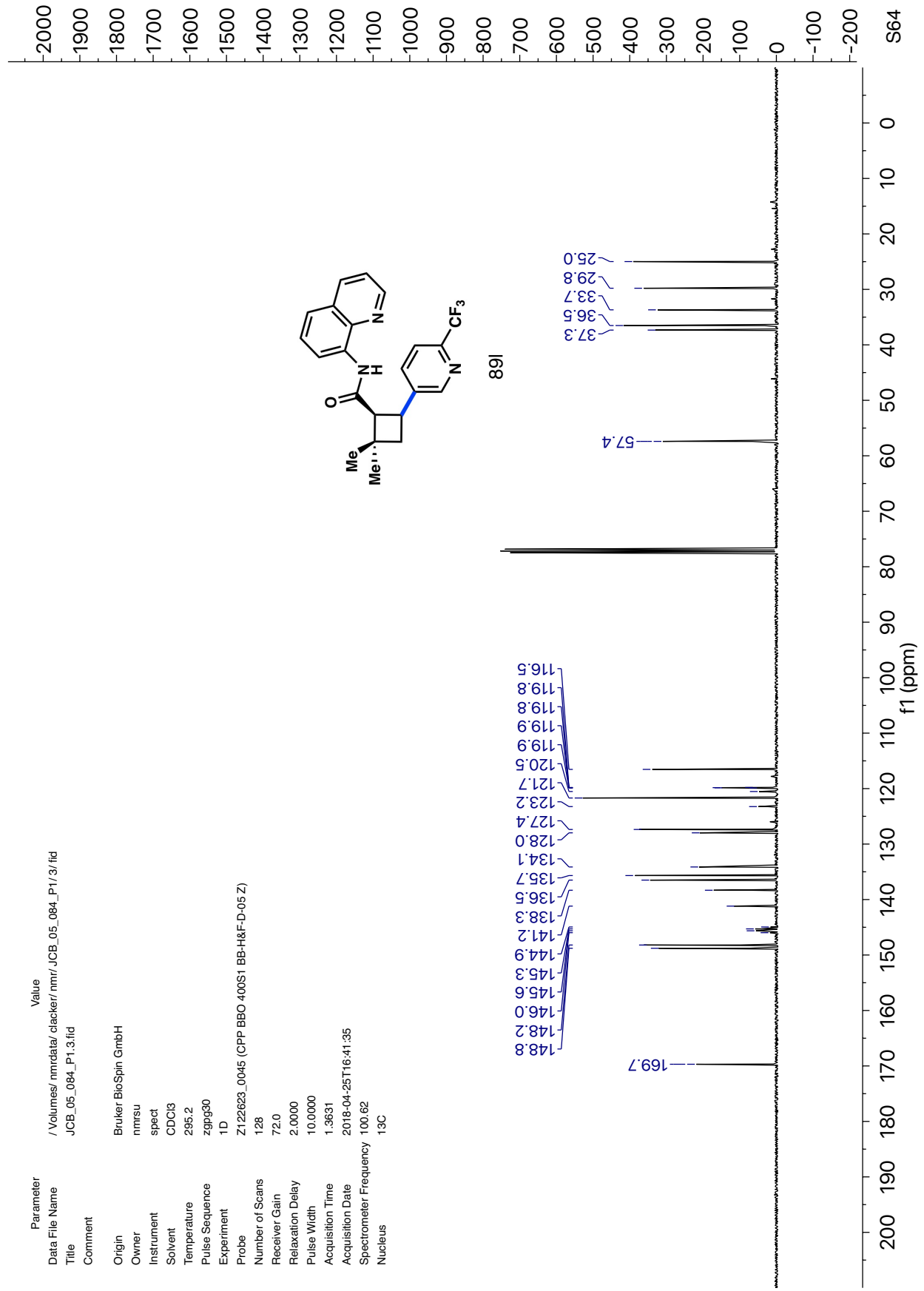
Parameter Value
Data File Name / Volumes/ nmrdata/ clacker/ nmr/ JCB_05_084_P1/ 3/ fid
Title JCB_05_084_P1.3.fid
Comment
Origin Bruker BioSpin GmbH
Owner nmrsu
Instrument spect
Solvent CDCl3
Temperature 295.2
Pulse Sequence zgpg30
Experiment 1D
Probe Z122623_0045 (CPP BBO 400S1 BB-H&F-D-05 Z)
Number of Scans 128
Receiver Gain 72.0
Relaxation Delay 2.0000
Pulse Width 10.0000
Acquisition Time 1.3631
Acquisition Date 2018-04-25T16:41:35
Spectrometer Frequency 100.62
Nucleus 13C
168
89l
Me
Me
O
N
H
N
N
CF3
169.7
148.8
148.2
146.0
145.6
145.3
144.9
141.2
138.3
136.5
135.7
134.1
128.0
127.4
123.2
121.7
120.5
119.9
119.9
119.8
119.8
116.5
57.4
37.3
36.5
33.7
29.8
25.0
f1 (ppm)
S64

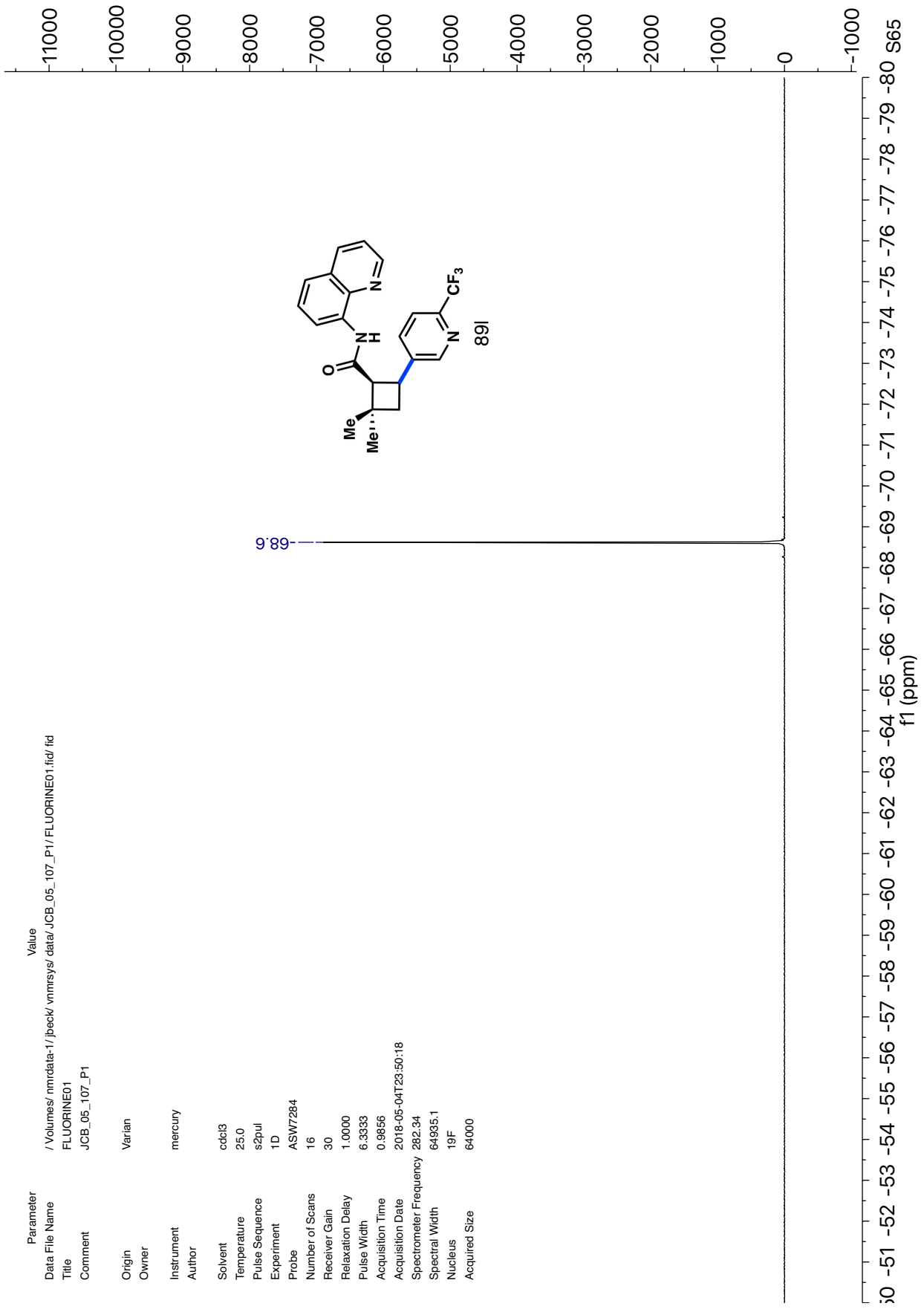
Parameter
Value
Data File Name
/ Volumes/ nmrdata-1/ jbeck/ vnmrsys/ data/ JCB_05_107_P1/ FLUORINE01.fid/ fid
Title
FLUORINE01
Comment
JCB_05_107_P1
Origin
Varian
Owner
Instrument
mercury
Author
Solvent
cdcl3
Temperature
25.0
Pulse Sequence
s2pul
Experiment
1D
Probe
ASW7284
Number of Scans
16
Receiver Gain
30
Relaxation Delay
1.0000
Pulse Width
6.3333
Acquisition Time
0.9856
Acquisition Date
2018-05-04T23:50:18
Spectrometer Frequency
282.34
Spectral Width
64935.1
Nucleus
19F
Acquired Size
64000
-68.6
Me
Me
O
N
H
N
N
CF3
89l
11000
10000
9000
8000
7000
6000
5000
4000
3000
2000
1000
0
-1000
-51 -52 -53 -54 -55 -56 -57 -58 -59 -60 -61 -62 -63 -64 -65 -66 -67 -68 -69 -70 -71 -72 -73 -74 -75 -76 -77 -78 -79 -80
f1 (ppm)

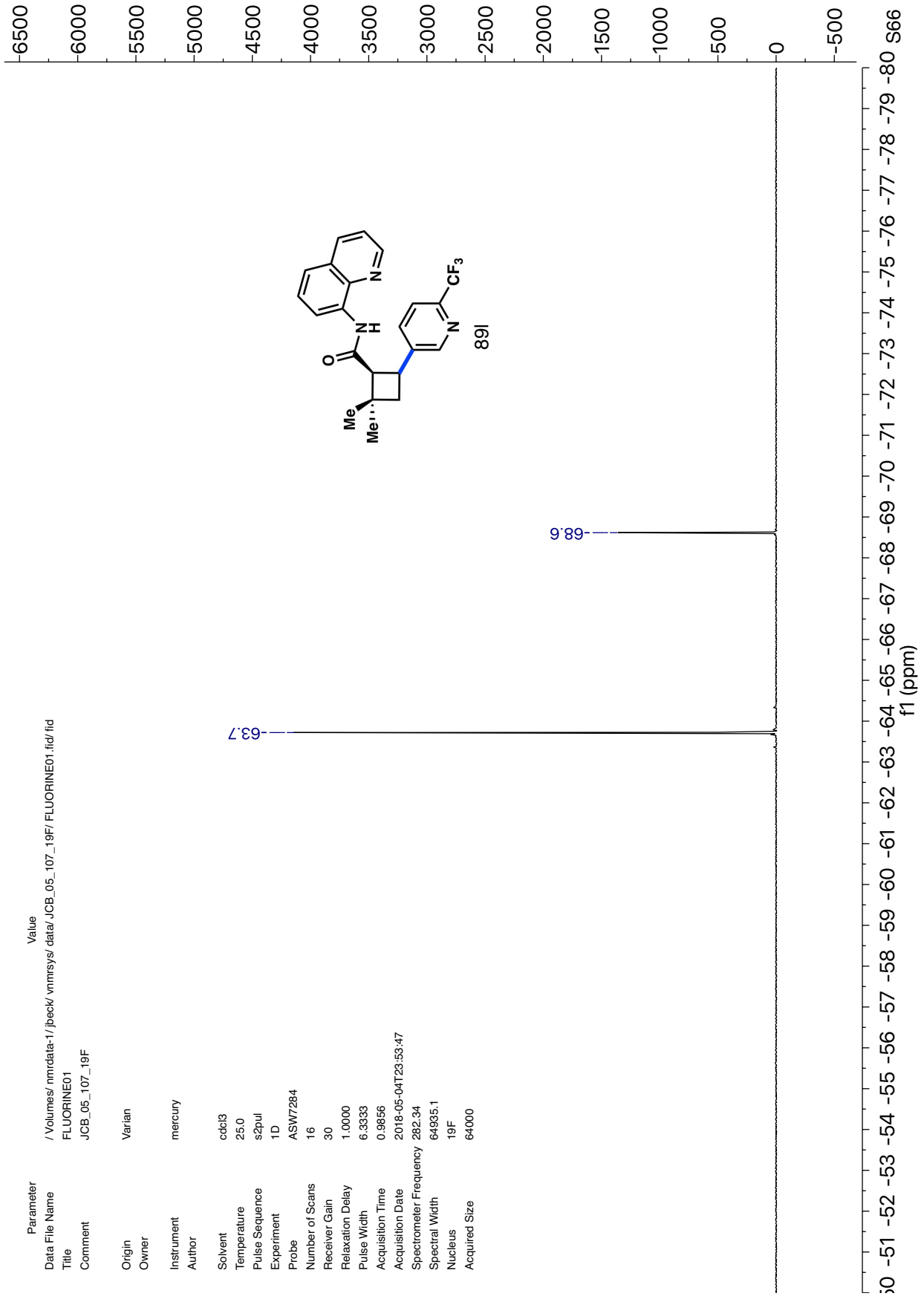
Parameter
Value
Data File Name
/ Volumes/ nmrdata-1/ jbeck/ vnmrsys/ data/ JCB_05_107_19F/ FLUORINE01.fid/ fid
Title
FLUORINE01
Comment
JCB_05_107_19F
Origin
Varian
Owner
Instrument
mercury
Author
Solvent
cdcl3
Temperature
25.0
Pulse Sequence
s2pul
Experiment
1D
Probe
ASW7284
Number of Scans
16
Receiver Gain
30
Relaxation Delay
1.0000
Pulse Width
6.3333
Acquisition Time
0.9856
Acquisition Date
2018-05-04T23:53:47
Spectrometer Frequency
282.34
Spectral Width
64935.1
Nucleus
19F
Acquired Size
64000
-63.7
-68.6
Me
Me
O
N
H
N
N
CF3
89l
f1 (ppm)

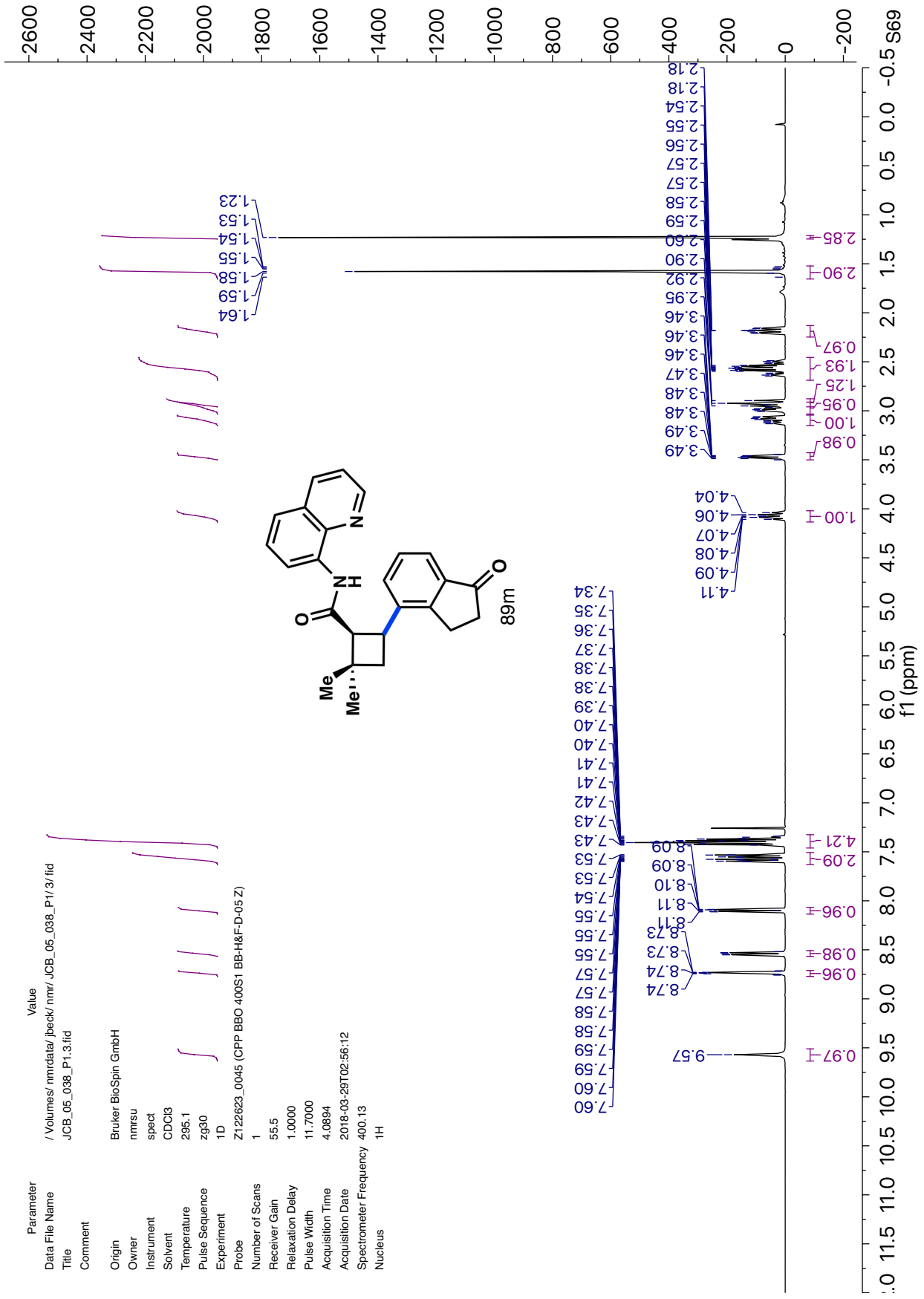
Parameter Value
Data File Name / Volumes/ nmrdata/ jbeck/ nmr/ JCB_05_038_P1/ 3/ fid
Title JCB_05_038_P1.3.fid
Comment
Origin Bruker BioSpin GmbH
Owner nmrsu
Instrument spect
Solvent CDCl3
Temperature 295.1
Pulse Sequence zg30
Experiment 1D
Probe Z122623_0045 (CPP BBO 400S1 BB-H&F-D-05 Z)
Number of Scans 1
Receiver Gain 55.5
Relaxation Delay 1.0000
Pulse Width 11.7000
Acquisition Time 4.0894
Acquisition Date 2018-03-29T02:56:12
Spectrometer Frequency 400.13
Nucleus 1H
89m
Me
Me
f1 (ppm)

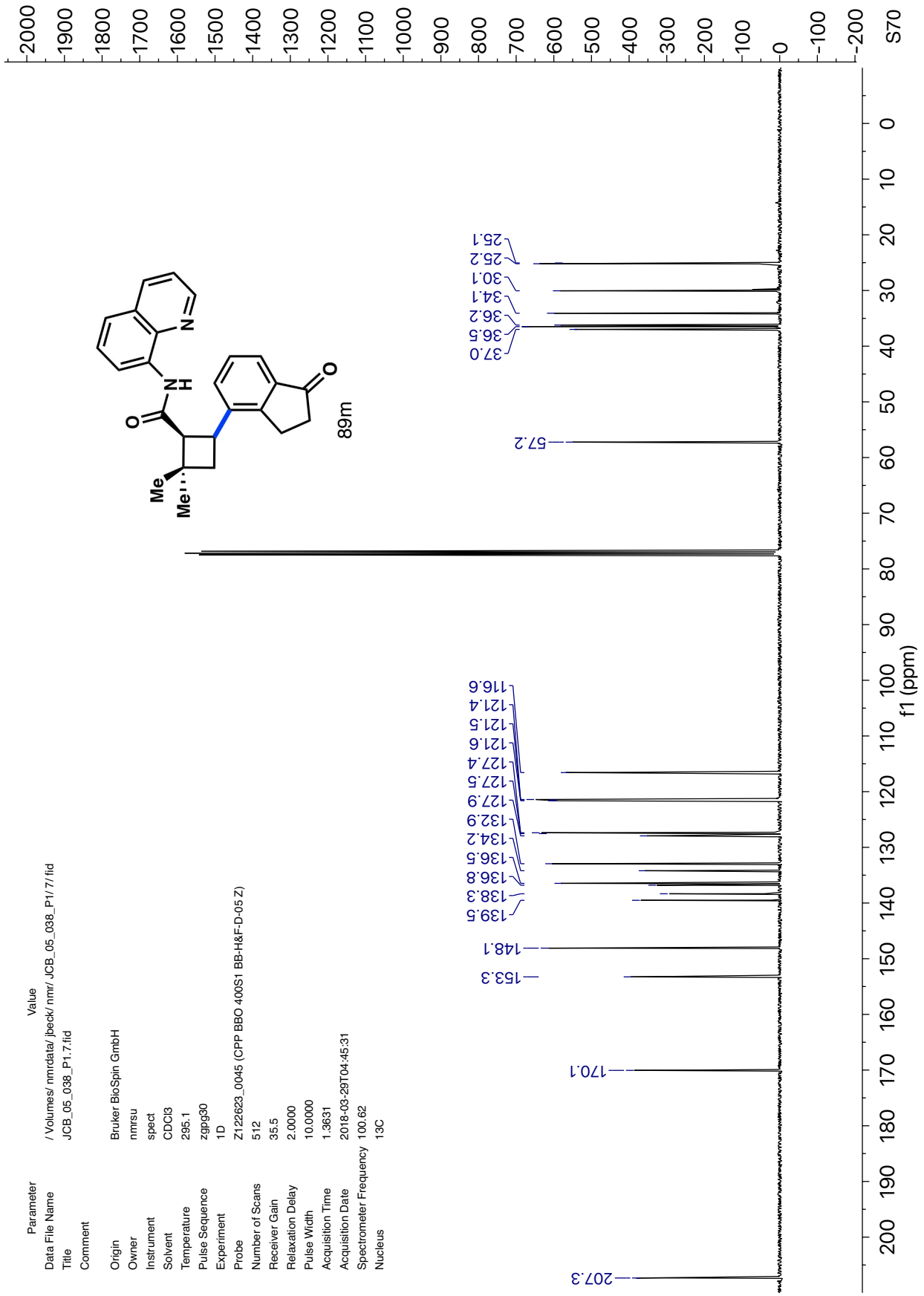
Parameter Value
Data File Name / Volumes/ nmrdata/ jbeck/ nmr/ JCB_05_038_P1/ 7/ fid
Title JCB_05_038_P1.7.fid
Comment
Origin Bruker BioSpin GmbH
Owner nmrsu
Instrument spect
Solvent CDCl3
Temperature 295.1
Pulse Sequence zgpg30
Experiment 1D
Probe Z122623_0045 (CPP BBO 400S1 BB-H&F-D-05 Z)
Number of Scans 512
Receiver Gain 35.5
Relaxation Delay 2.0000
Pulse Width 10.0000
Acquisition Time 1.3631
Acquisition Date 2018-03-29T04:45:31
Spectrometer Frequency 100.62
Nucleus 13C
89m
207.3
170.1
153.3
148.1
139.5
138.3
136.8
136.5
134.2
132.9
127.9
127.5
127.4
121.6
121.5
121.4
116.6
57.2
37.0
36.5
36.2
34.1
30.1
25.2
25.1
f1 (ppm)

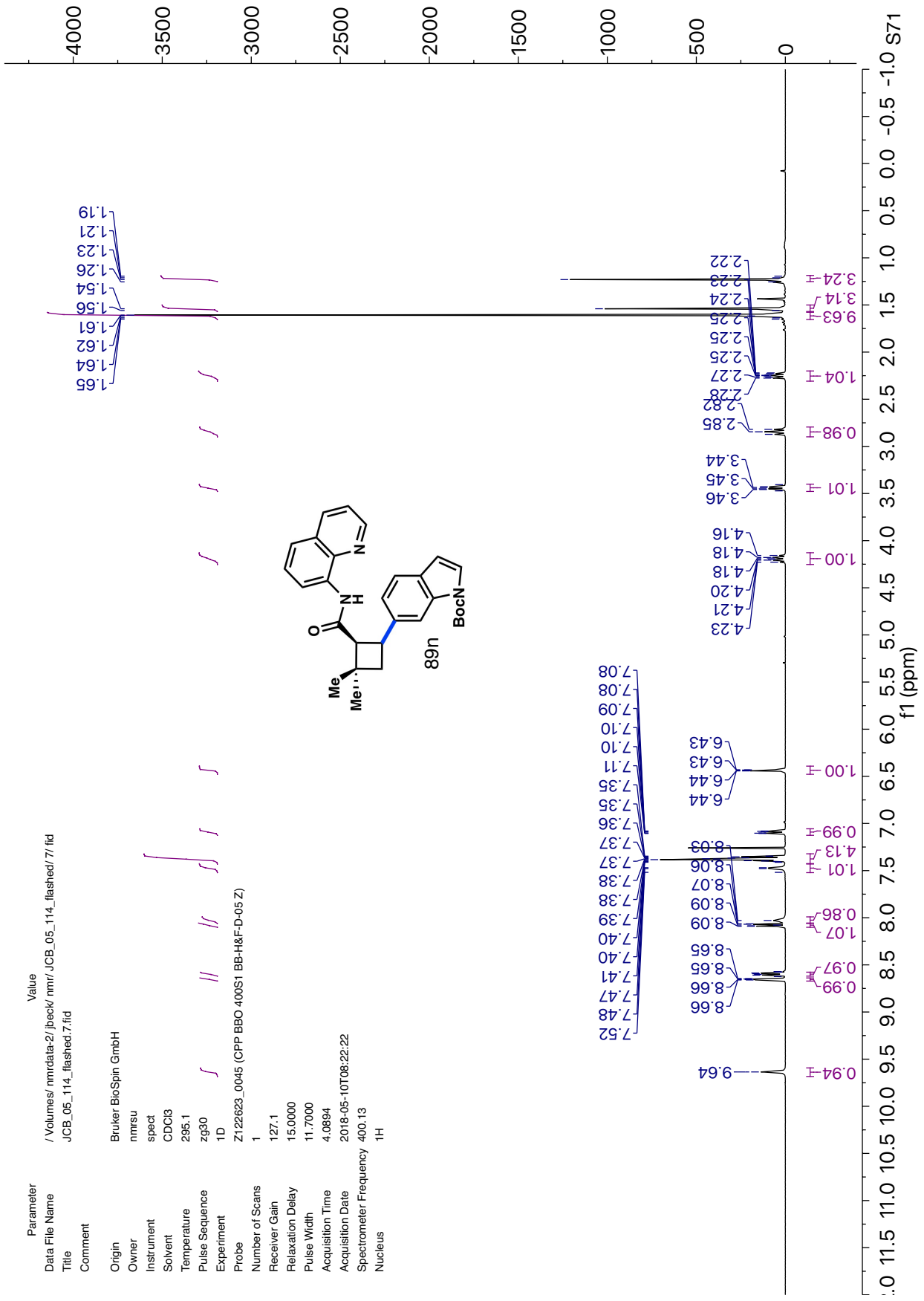
Parameter
Value
Data File Name / Volumes/ nmrdata-2/ jbeck/ nmr/ JCB_05_114_flashed/ 7/ fid
Title JCB_05_114_flashed.7.fid
Comment
Origin Bruker BioSpin GmbH
Owner nmrsu
Instrument spect
Solvent CDCl3
Temperature 295.1
Pulse Sequence zg30
Experiment 1D
Probe Z122623_0045 (CPP BBO 400S1 BB-H&F-D-05 Z)
Number of Scans 1
Receiver Gain 127.1
Relaxation Delay 15.0000
Pulse Width 11.7000
Acquisition Time 4.0894
Acquisition Date 2018-05-10T08:22:22
Spectrometer Frequency 400.13
Nucleus 1H
u68
Me
Me
BocN
f1 (ppm)
S71

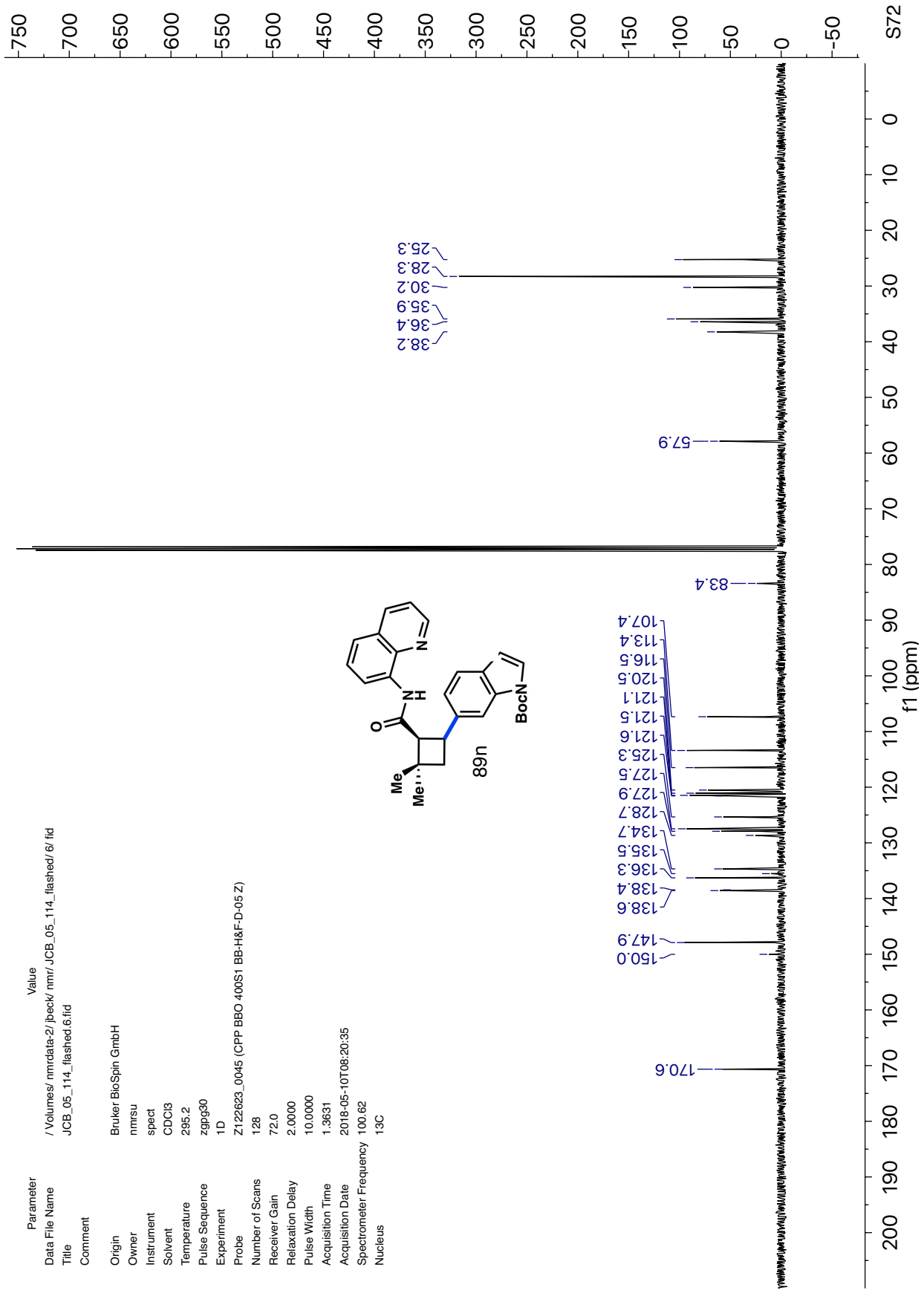
Parameter
Value
Data File Name / Volumes/ nmrdata-2/ jbeck/ nmr/ JCB_05_114_flashed/ 6/ fid
Title JCB_05_114_flashed.6.fid
Comment
Origin Bruker BioSpin GmbH
Owner nmrsu
Instrument spect
Solvent CDCl3
Temperature 295.2
Pulse Sequence zgpg30
Experiment 1D
Probe Z122623_0045 (CPP BBO 400S1 BB-H&F-D-05 Z)
Number of Scans 128
Receiver Gain 72.0
Relaxation Delay 2.0000
Pulse Width 10.0000
Acquisition Time 1.3631
Acquisition Date 2018-05-10T08:20:35
Spectrometer Frequency 100.62
Nucleus 13C
170.6
150.0
147.9
138.6
138.4
136.3
135.5
134.7
128.7
127.9
127.5
125.3
121.6
121.5
121.1
120.5
116.5
113.4
107.4
83.4
57.9
38.2
36.4
35.9
30.2
28.3
25.3
89n
f1 (ppm)

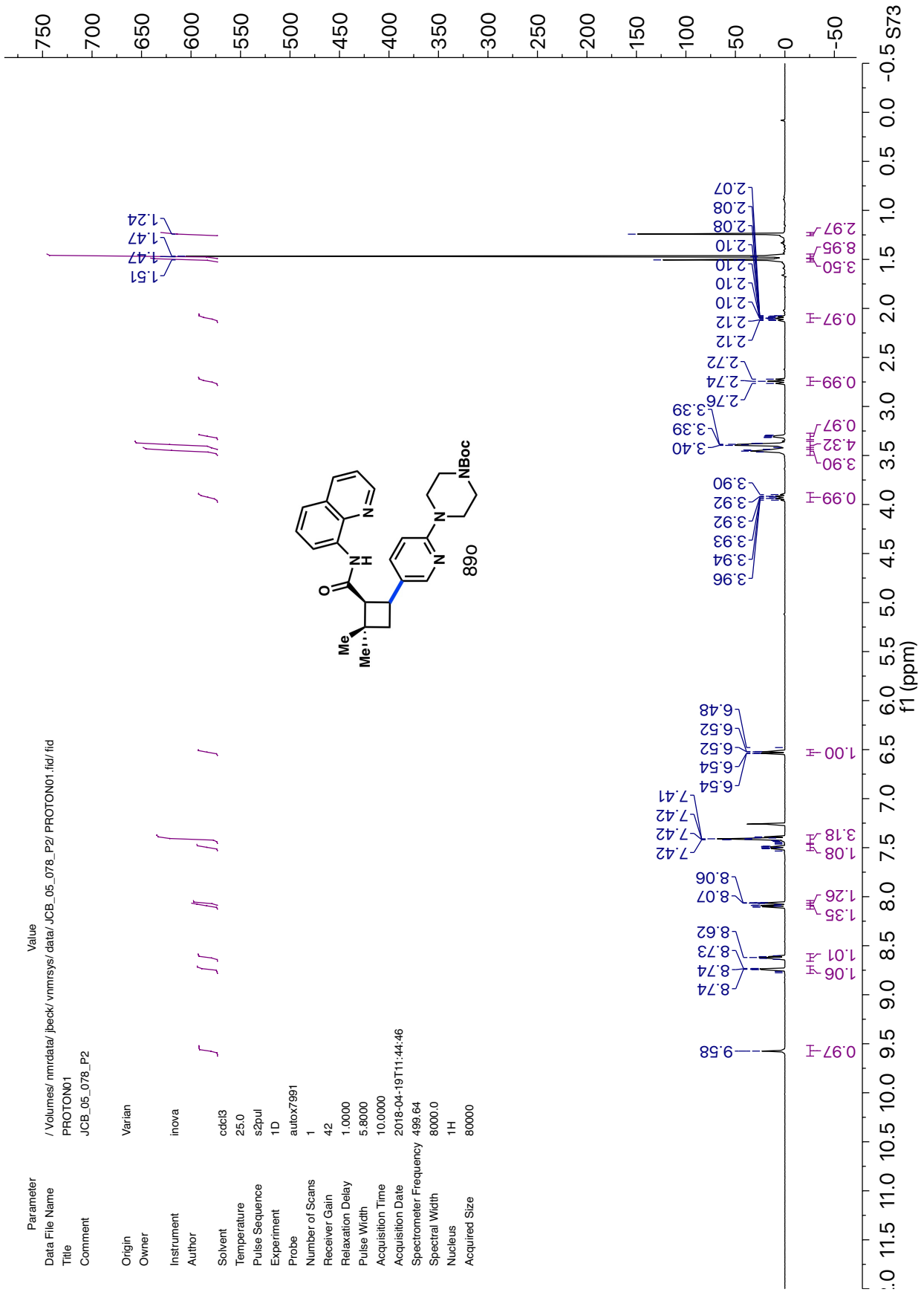
Parameter
Value
Data File Name / Volumes/ nmrdata/ jbeck/ vnmrsys/ data/ JCB_05_078_P2/ PROTON01.fid/ fid
Title PROTON01
Comment JCB_05_078_P2
Origin Varian
Owner
Instrument inova
Author
Solvent cdcl3
Temperature 25.0
Pulse Sequence s2pul
Experiment 1D
Probe autox7991
Number of Scans 1
Receiver Gain 42
Relaxation Delay 1.0000
Pulse Width 5.8000
Acquisition Time 10.0000
Acquisition Date 2018-04-19T11:44:46
Spectrometer Frequency 499.64
Spectral Width 8000.0
Nucleus 1H
Acquired Size 80000
NBoc
Me
Me
f1 (ppm)
S73

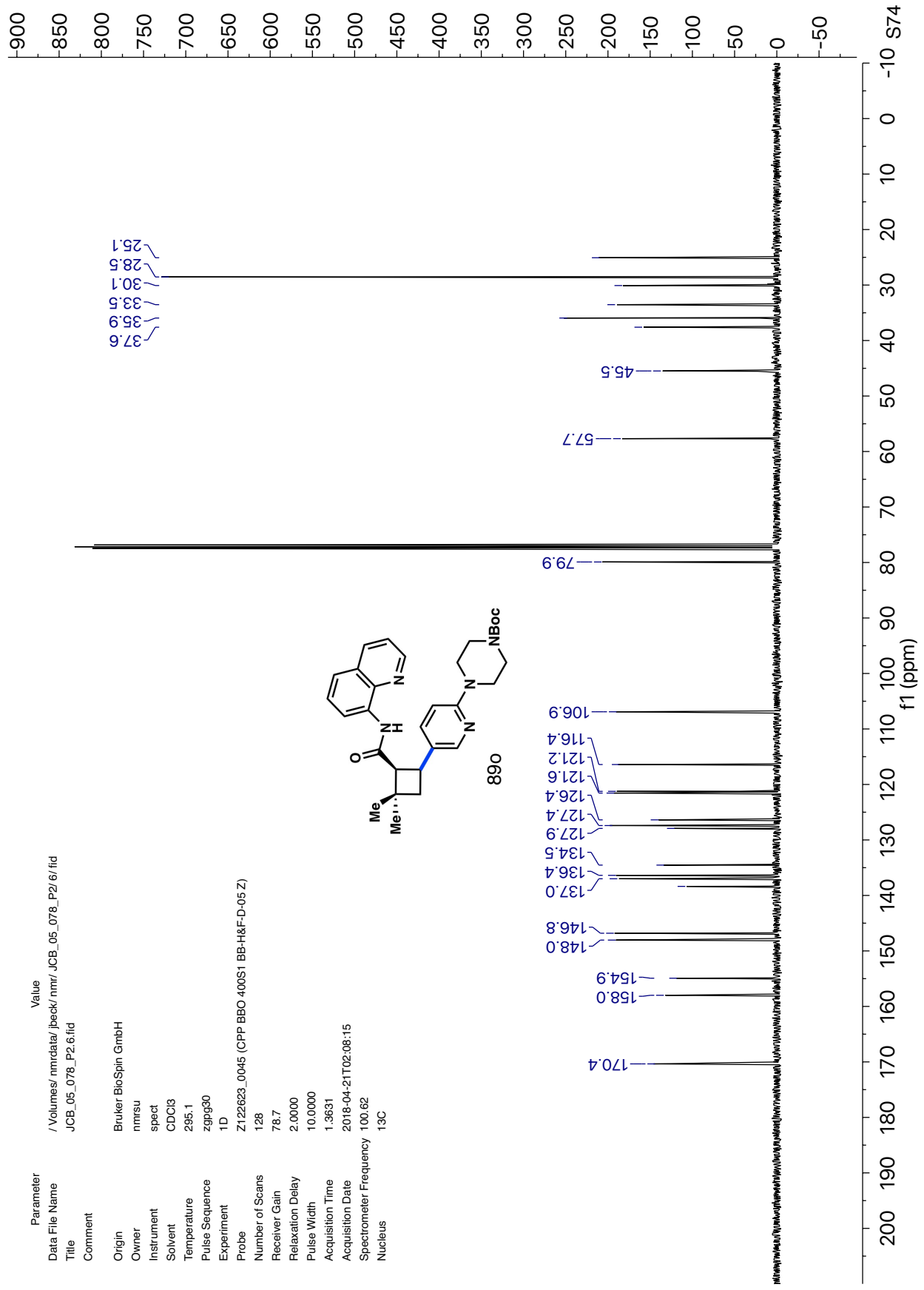
Parameter
Value
Data File Name
/ Volumes/ nmrdata/ jbeck/ nmr/ JCB_05_078_P2/ 6/ fid
Title
JCB_05_078_P2.6.fid
Comment
Origin
Bruker BioSpin GmbH
Owner
nmrsu
Instrument
spect
Solvent
CDCl3
Temperature
295.1
Pulse Sequence
zgpg30
Experiment
1D
Probe
Z122623_0045 (CPP BBO 400S1 BB-H&F-D-05 Z)
Number of Scans
128
Receiver Gain
78.7
Relaxation Delay
2.0000
Pulse Width
10.0000
Acquisition Time
1.3631
Acquisition Date
2018-04-21T02:08:15
Spectrometer Frequency
100.62
Nucleus
13C
170.4
158.0
154.9
148.0
146.8
137.0
136.4
134.5
127.9
127.4
126.4
121.6
121.2
116.4
106.9
79.9
57.7
45.5
37.6
35.9
33.5
30.1
28.5
25.1
f1 (ppm)
S74

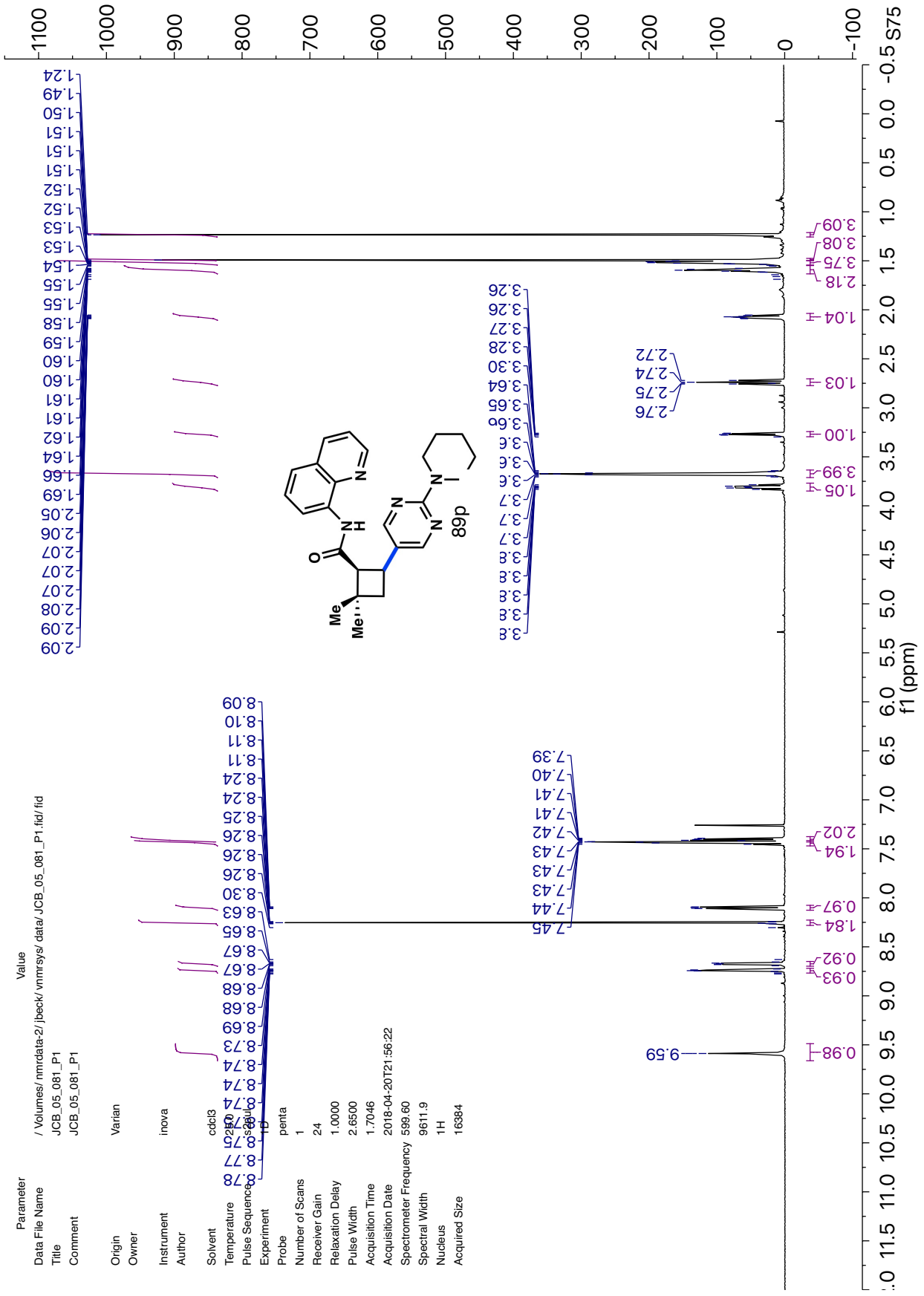
Parameter Value
Data File Name / Volumes/ nmrdata-2/ jbeck/ vnmrsys/ data/ JCB_05_081_P1.fid/ fid
Title JCB_05_081_P1
Comment JCB_05_081_P1
Origin Varian
Owner
Instrument inova
Author
Solvent cdcl3
Temperature 25.0
Pulse Sequence s2pul
Experiment 1D
Probe penta
Number of Scans 1
Receiver Gain 24
Relaxation Delay 1.0000
Pulse Width 2.6500
Acquisition Time 1.7046
Acquisition Date 2018-04-20T21:56:22
Spectrometer Frequency 599.60
Spectral Width 9611.9
Nucleus 1H
Acquired Size 16384
Me
Me
O
N
H
N
N
N
N
89p
f1 (ppm)

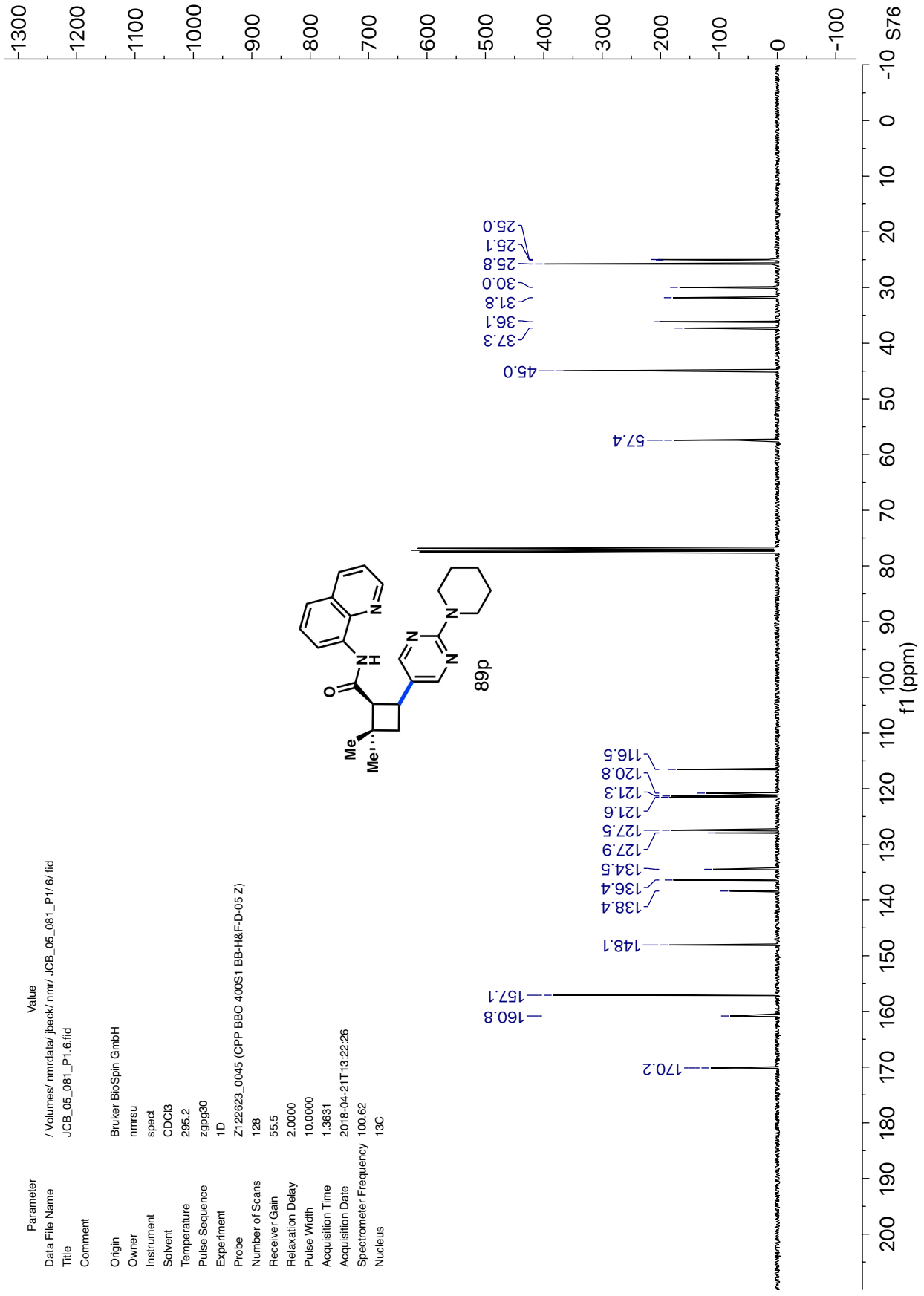
Parameter
Value
Data File Name
/ Volumes/ nmrdata/ jbeck/ nmr/ JCB_05_081_P1/ 6/ fid
Title
JCB_05_081_P1.6.fid
Comment
Origin
Bruker BioSpin GmbH
Owner
nmrsu
Instrument
spect
Solvent
CDCl3
Temperature
295.2
Pulse Sequence
zgpg30
Experiment
1D
Probe
Z122623_0045 (CPP BBO 400S1 BB-H&F-D-05 Z)
Number of Scans
128
Receiver Gain
55.5
Relaxation Delay
2.0000
Pulse Width
10.0000
Acquisition Time
1.3631
Acquisition Date
2018-04-21T13:22:26
Spectrometer Frequency
100.62
Nucleus
13C
170.2
160.8
157.1
148.1
138.4
136.4
134.5
127.9
127.5
121.6
121.3
120.8
116.5
89p
57.4
45.0
37.3
36.1
31.8
30.0
25.8
25.1
25.0
Me
Me
f1 (ppm)
S76

Chapter 2

Modular Synthesis of Enantioenriched Cyclobutanes: Applications Towards the Total Synthesis of (+)-Rumphellaone A[1]

2.1 INTRODUCTION

Figure 2.1 *A modular approach to enantioenriched trans cyclobutanes*

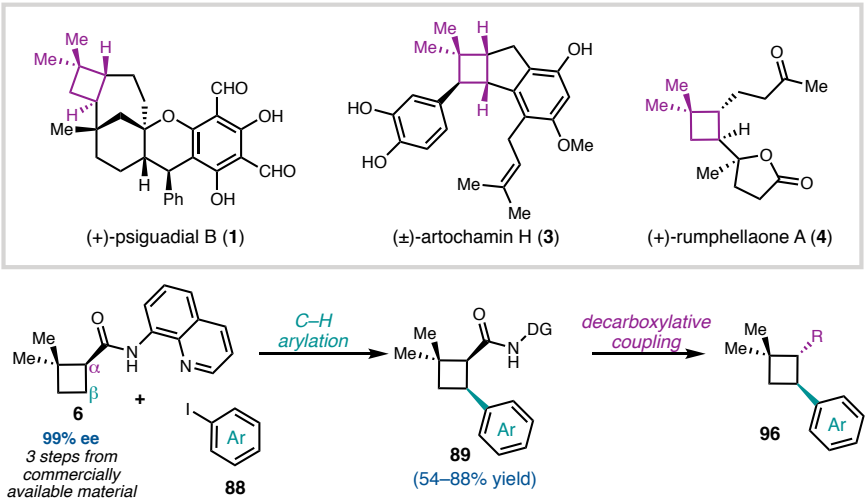

The cyclobutane structural motif is present in a variety of natural products and pharmaceuticals (**Figure 2.1**).[1–7] It is also a versatile synthetic intermediate, as the ring strain inherent to these structures engenders them with unique reactivity that can be leveraged in a variety of transformations to build complex frameworks.[8–11] Having developed a short, scalable method for the synthesis of enantioenriched cyclobutamide **6**, we sought to demonstrate the utility of this valuable building block.[12,13] Previously, our

[1] Portions of this chapter were adapted from the following communication: Beck, J. C.; Lacker, C. R.; Chapman, L. M.; Reisman, S. E. *Chem. Sci.* **2019**, *10*, 2315., DOI: 10.1039/C8SC05444D, copyright 2019, Royal Society of Chemistry. The research discussed in this chapter was completed in collaboration with Dr. Jordan C. Beck as well as Dr. Lauren M. Chapman, former graduate students in the Reisman Lab.

group had demonstrated that **6** could undergo subsequent C–H arylation with a variety of aryl iodides (**88**) (see Chapter 1), and we thought that we could derivatize these compounds further.

We envisioned that by starting from **6**, we could subsequently decorate the enantioenriched cyclobutane core by performing a diastereoselective C–H activation at the β position followed by a diastereoselective decarboxylative cross-coupling at the α position after hydrolysis of the directing group to afford *trans* cyclobutanes **96** (**Figure 2.1**). In this way, we hoped to demonstrate a strategy that would allow the expedient synthesis of a library of chiral, polyfunctionalized *trans* cyclobutanes from a single enantioenriched intermediate.

2.2 STRATEGIES TOWARDS ENANTIOENRICHED CYCLOBUTANES

2.2.1 Enantioselective [2+2] Cycloaddition

[2 + 2] cycloaddition reactions represent the most extensively developed approach to construct cyclobutanes and cyclobutenes; recent advances have given rise to elegant enantioselective reactions. In particular, the development of [2+2] cycloaddition reactions between alkenes to directly afford cyclobutanes is a growing area of research. One of the most effective methods for facilitating this transformation in an enantioselective fashion is photoactivation in the presence of a chiral Lewis acid (**Scheme 2.1**).[14–23] Bach and coworkers first demonstrated this in an intramolecular sense using chiral borane catalysis (**99**) to afford highly substituted, fused cyclobutanes **98** (**Scheme 2.1**a).[14–16] Yoon and coworkers have demonstrated a variety of enantioselective, intermolecular [2+2] cycloadditions of α,β unsaturated esters and activated alkenes to afford enantioenriched cyclobutanes **102** and **104** using photocatalysis (**Scheme 2.1**b,c). In 2014, Yoon

Scheme 2.1 *Photochemical enantioselective [2+2] cycloadditions*

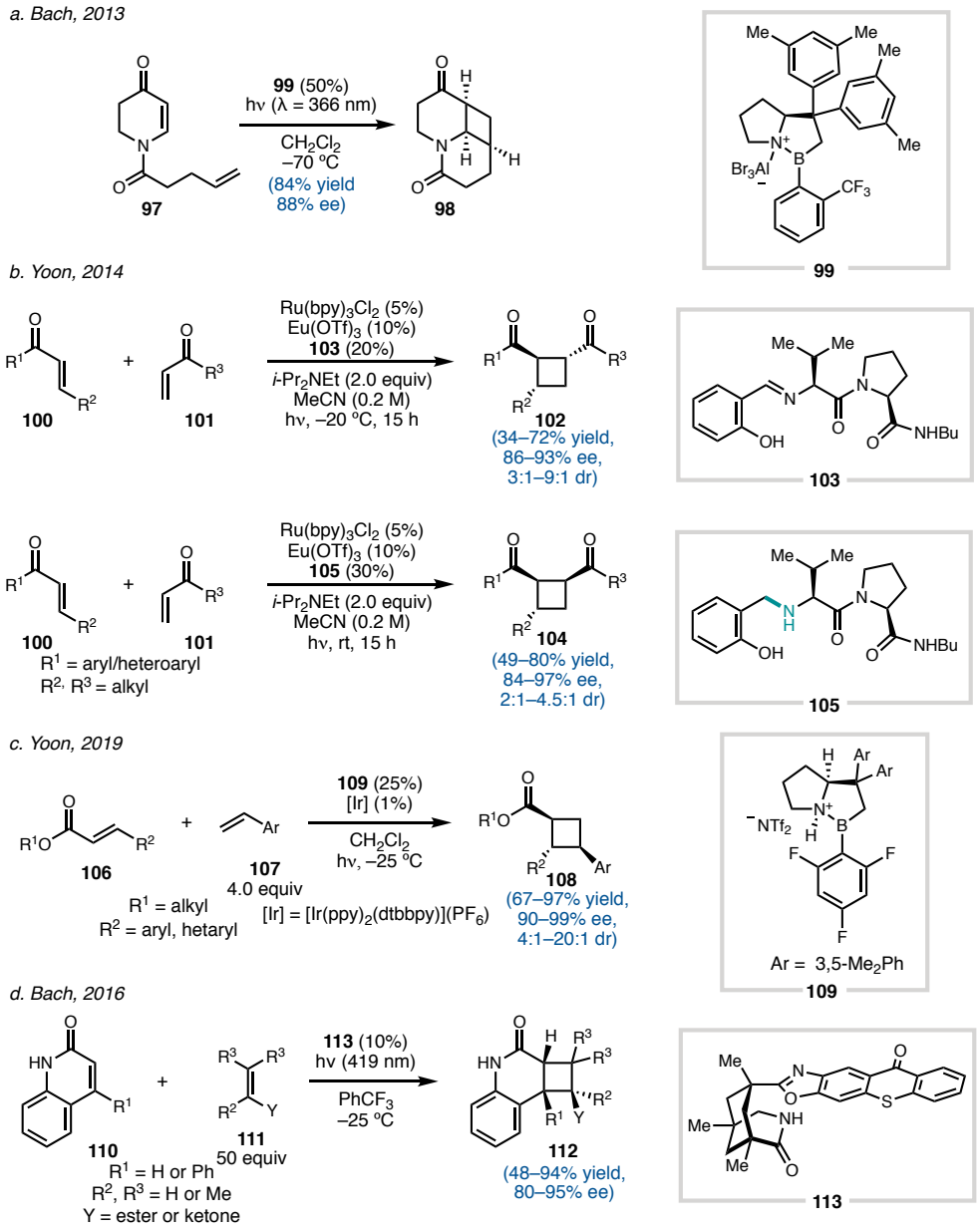

demonstrated this strategy using ruthenium and europium photocatalysis and a peptide-like Lewis acid (**103**, **105**). Interestingly, it was found that the diastereoselectivity depended on whether an imine (**103**) or amine (**105**) form of the catalyst was used.[17] In 2019, Yoon reported a similar reaction using iridium photocatalysis with a chiral borane catalyst (**109**) between α,β-unsaturated esters (**106**) and styrenes (**107**).[18] In 2016, Bach demonstrated the

use of enantioenriched photocatalyst (**113**) instead of an enantioenriched Lewis acid to afford enantioenriched cyclobutanes **112** in good yield and good ee (**Scheme 2.1**d).[19]

Scheme 2.2 *Transition metal-catalyzed enantioselective [2+2] cycloadditions*

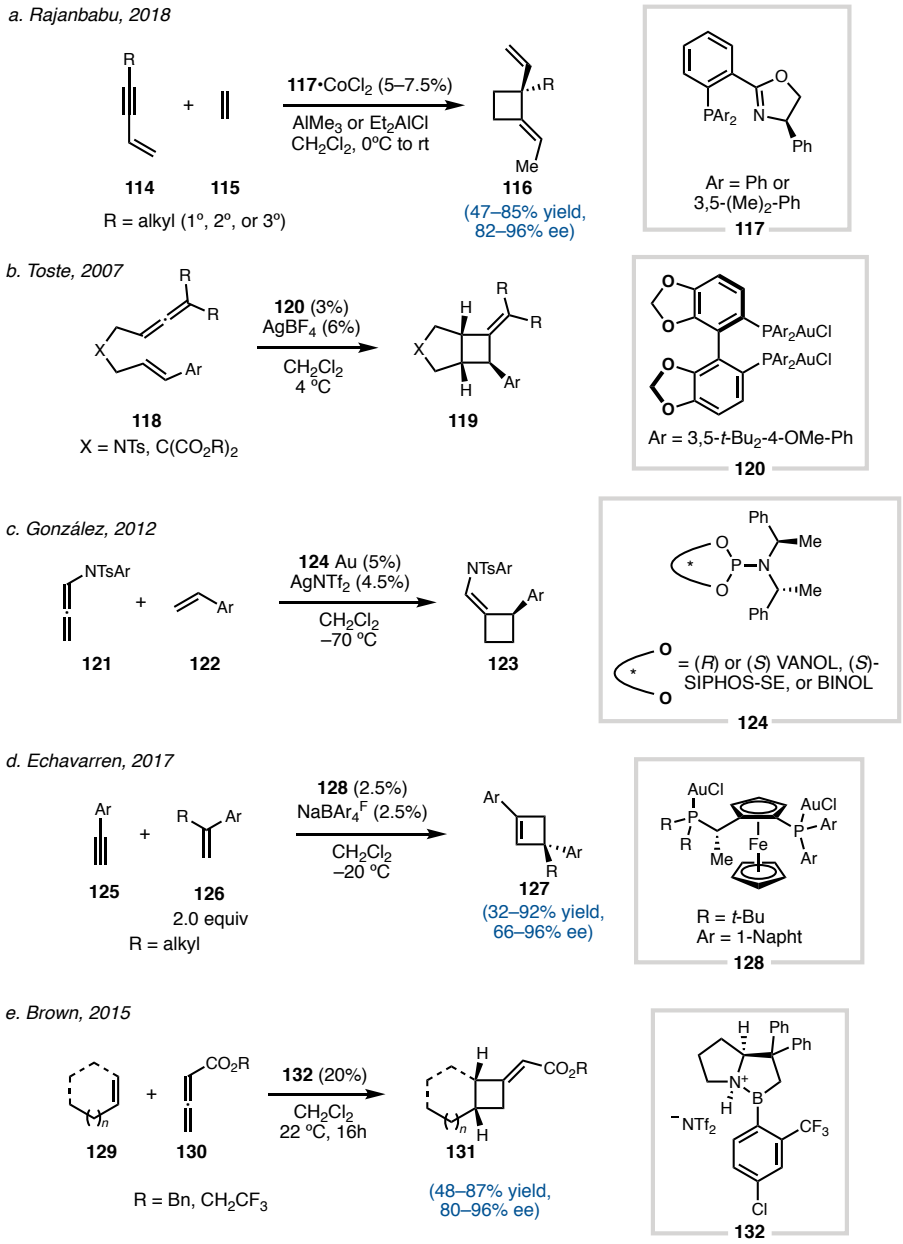

Cycloadditions between allenes or alkynes and alkenes to afford enantioenriched cyclobutanes and cyclobutenes has also been explored thoroughly in the literature by a variety of groups (**Scheme 2.2**).[24–35] RajanBabu and coworkers have shown that cobalt with

an aryl PHOX ligand (**117**) can be used to catalyze the enantioselective [2+2] cycloaddition of allylic alkynes (**114**) with ethylene in the presence of alkyl aluminum reagents to afford enantioenriched cyclobutanes containing an all-carbon quaternary center (**116**) (**Scheme 2.2**a).[24] Later, Rajanbabu also demonstrated that a similar cobalt and PHOX catalyst system in the absence of alkylaluminum reagents could also be used to afford enantioenriched cyclobutenes.[25] Toste, González, and Echavarren, as well as others, have showed the ability of gold catalysts to catalyze enantioselective [2+2] cycloadditions to afford enantioenriched cyclobutene products.[26,27,30,33] Toste demonstrated this in an intramolecular sense in 2007, utilizing an axially chiral gold catalyst (**120**) to facilitate this transformation (**Scheme 2.2**b).[26] González similarly showed that a chiral phosphoramidite gold complex (**124**) could facilitate this transformation in an intermolecular sense (**Scheme 2.2**c).[30] Recently, Echavarren and coworkers demonstrated that gold catalysis (**128**) could also be applied to alkynes and styrenes to afford enantioenriched cyclobutenes (**127**) (**Scheme 2.2**d).[32] In addition to transition metal catalysis, Brown and coworkers have demonstrated a variety of transition metal-free enantioselective [2+2] cycloadditions between alkenes and allenes in the presence of a chiral borane catalyst (**132**) (**Scheme 2.2**e).[35]

Though these reactions are powerful tools, they are not necessarily suited to developing a library of compounds. They are limited to specific types of activated substrates (such as allenes or α,β-unsaturated ketones), and enantioselectivity and diastereoselectivity can vary greatly from substrate to substrate. We hoped that by decorating a single easily accessed, scalable, enantioenriched building block, we could

divergently access a broader library of compounds, albeit potentially in a greater number of steps.

2.2.2 Divergent C–H Activation Strategies towards Cyclobutanes

Figure 2.2 *Baran's strategy towards cyclobutane natural products*

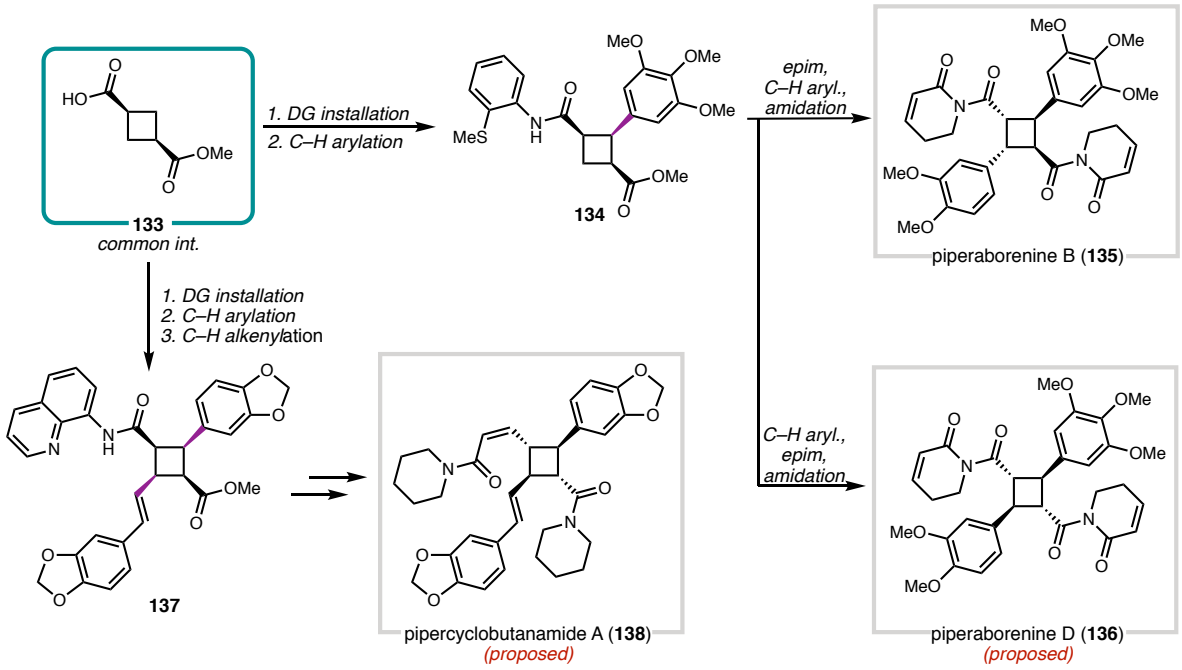

A divergent strategy to access various cyclobutanes has been demonstrated previously. Notably, the Baran lab utilized a similar strategy for their divergent syntheses of piperaborenine B (**135**) and the proposed structures of piperaborenine D (**136**) and pipercyclobutanamide A (**138**) (**Figure 2.2**).[36–38] These syntheses were derived from a common intermediate, cyclobutane **133**. By applying C–H activation methods to decorate the rest of the core, Baran was able to afford the desired products. However, this strategy was limited due to the achiral nature of the common intermediate and the choice of racemic C–H activation conditions.

Scheme 2.3 *C–H Activations of cyclobutanes*

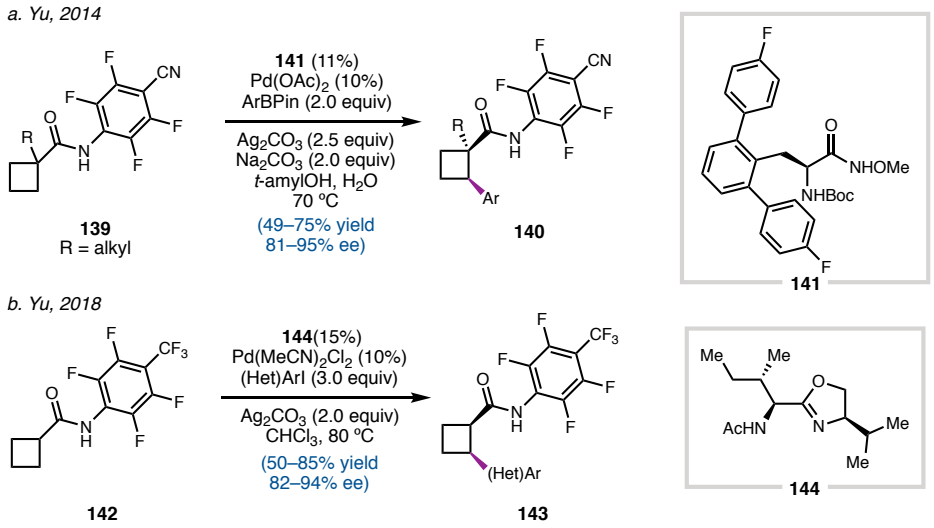

The Yu lab has effectively demonstrated the utility of enantioselective C–H activation methodologies to synthesize a variety of functionalized products from achiral starting materials.[39–44] In particular, they have been able to apply this strategy to both 3º (**139**) and 2º (**142**) cyclobutamide starting materials to afford arylated products in good yield and good enantioselectivity using specialized ligands (**141** and **144**) and directing groups (**Scheme 2.3a,b**).[39,41] Interestingly, the less substituted 3º aryl products **143** were observed in lower yield and ee than the 4º aryl products (**140**).

In 2018, Baran and coworkers published a strategy that allowed access to a variety of *bis*-functionalized carbocycles (**148**) in good yield and good ee starting from racemic anhydrides (**145**) (**Scheme 2.4a**).[45] After anhydride desymmetrization, sequential, diastereoselective decarboxylative cross-couplings afforded the bis-functionalized products (**148**). However, these reaction sequences were long and required multiple carboxylic acid activations and deprotections. Similarly, during the course of our investigations, Baran and Yu published a similar strategy towards a variety of functionalized, saturated heterocycles (**150**) by a doubly diastereoselective C–H

Scheme 2.4 *Baran and Yu's divergent strategies towards substituted chiral carbocycles and heterocycles*

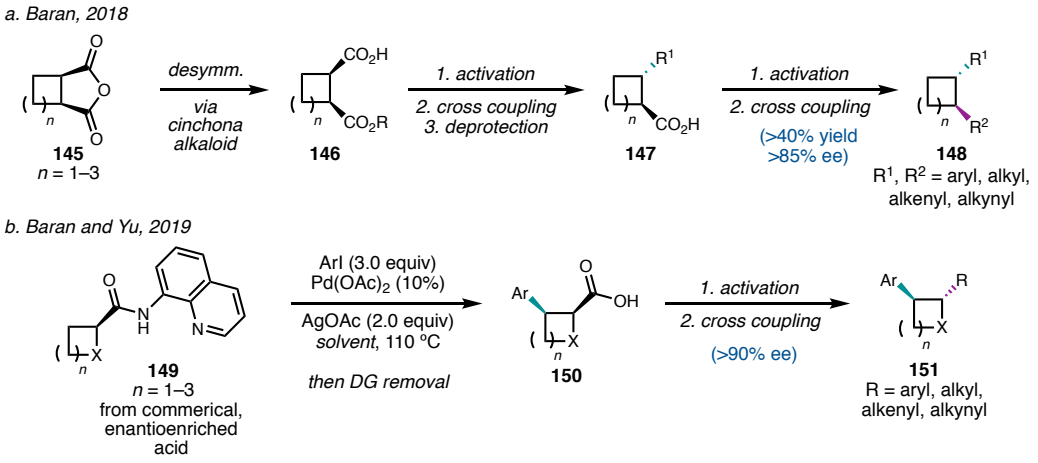

activation/decarboxylative cross coupling sequence of enantioenriched starting materials (**149**) (**Scheme 2.4b**).[46] Directing group installation of chiral acids followed by diastereoselective C–H activation and directing group removal afforded chiral acids **150**. Activation of the carboxylic acid to form the *N*-hydroxyphthalimide (NHP) or tetrachloro-*N*-hydroxyphthalimide (TCNHP) ester allowed for diastereoselective decarboxylative cross coupling to afford enantioenriched *trans* products **151**. This sequence is similar to what we proposed, but it is dependent on commercially available chiral acids and focuses on saturated heterocycles.

2.3 DECARBOXYLATIVE CROSS-COUPLINGS

Figure 2.3 *Modular approach towards enantioenriched cyclobutanes*

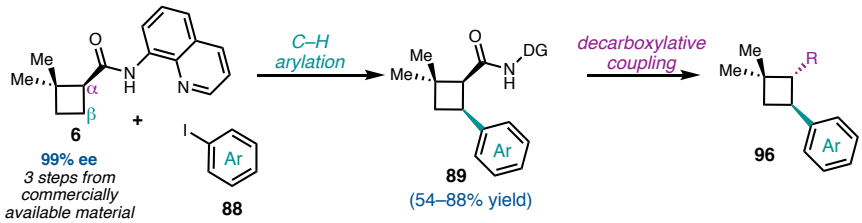

Having already developed a stereoselective C–H arylation of **6** to afford a variety of aryl- and heteroarylated products (**89**) in good yields, we sought to diastereoselectively functionalize the α-position of the resulting cyclobutanes after removal of the quinolinamide directing group using a variety of modern decarboxylative coupling techniques to synthesize a library of chiral *trans* cyclobutanes (**96**) (**Figure 2.3**). A number of powerful methods have been developed that leverage the decarboxylative formation of carbon-centered radicals for C–C and C–X bond formation. There were four main categories of decarboxylative cross-coupling reactions that we hoped to investigate: photochemical decarboxylative cross-couplings of free carboxylic acids, photochemical decarboxylative cross-couplings of redox-active esters, transition metal-mediated cross-couplings of activated redox-active esters, and reductive cross-couplings of redox-active esters.

Direct decarboxylative cross coupling of free carboxylic acids (**152**) through metallophotoredox catalysis has become a powerful tool in organic synthesis in recent years (**Scheme 2.5**).[47–62] Starting with MacMillan and Doyle's disclosure of the decarboxylative cross-coupling of amino acids and aryl bromides (**153**) in 2014, this field has grown dramatically (**Scheme 2.5**a).[60] MacMillan and coworkers have published decarboxylative alkenylation and alkylation methods with alkenyl (**155**) and alkyl halides (**157**), respectively (**Scheme 2.5b,c**).[58,61] Similarly, they disclosed a decarboxylative Giese-type reaction using a variety of electron-poor alkenes (**159**) (**Scheme 2.5**d).[63] Additional studies in this field have allowed for decarboxylative functionalization with a wide variety of cross-coupling partners. These methods often require stabilized radical intermediates and can be challenging to optimize for individual substrates.

Scheme 2.5 *Direct photochemical decarboxylative cross-couplings*

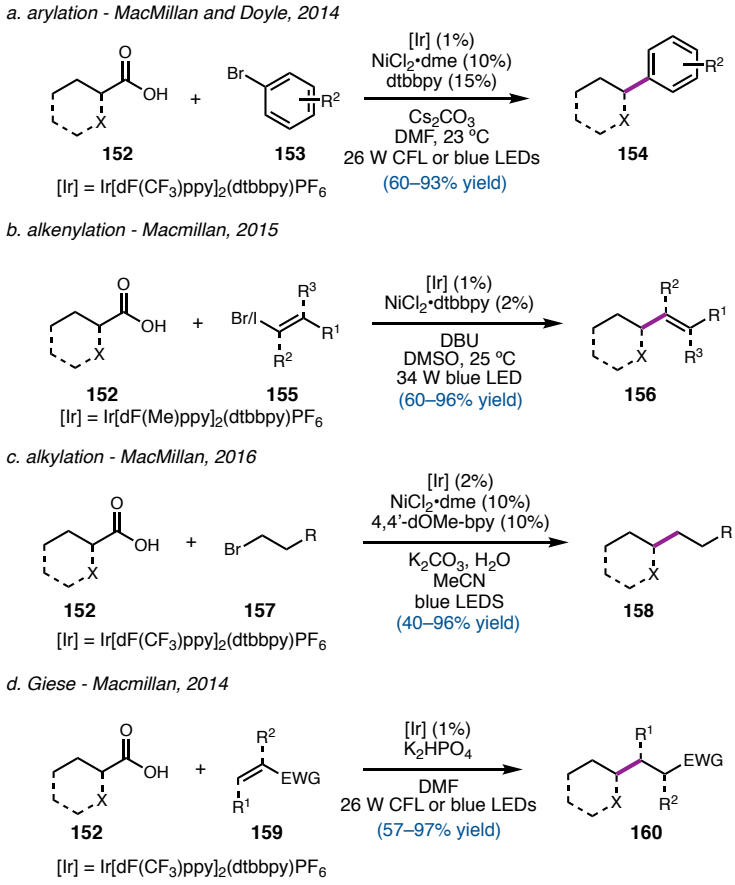

Scheme 2.6 *Photochemical decarboxylative cross-couplings of redox-active esters*

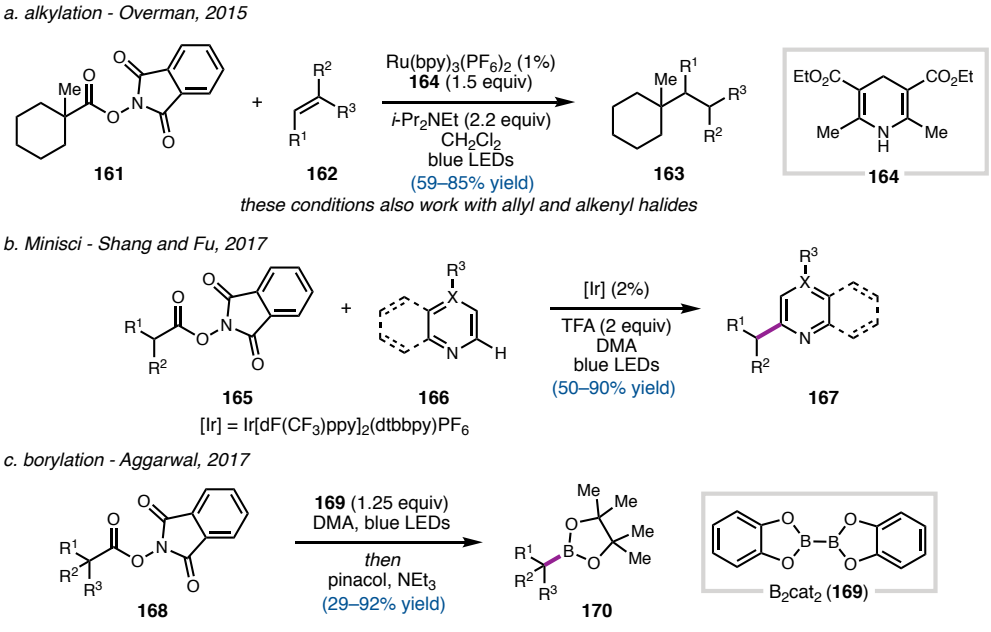

In addition to oxidative decarboxylation of carboxylic acids through photoredox chemistry, activated carboxylic acids such as NHP esters can undergo fragmentation through single electron reduction from a photocatalyst to afford a phthalimide anion and free alkyl radicals, which can then engage in further reactivity (**Scheme 2.6**).[64–69] Overman has demonstrated that this method is effective for forming all-carbon quaternary centers through Giese-type coupling of tertiary NHP esters **161** with alkenes, as well as allyl and alkenyl halides, in the presence of a Hantzch ester (**164**) reductant using a ruthenium photocatalyst (**Scheme 2.6**a).[66] Fu and Shang disclosed a photochemical Minisci-type reaction with NHP esters and a variety of nitrogen-containing heterocycles (**166**) using an iridium photocatalyst to afford heteroarylated products **167** (**Scheme 2.6**b).[68] In 2017, Aggarwal and coworkers published a photocatalyst-free, decarboxylative borylation of NHP esters that utilized B_2cat_2 (**169**) as a photosensitizer as well as a borylating agent, obviating the need for a traditional photocatalyst (**Scheme 2.6**c).[69] This type of reactivity can be challenging, however, as there is no catalyst to mediate the reaction upon radical formation.

Redox active esters can also be directly cleaved without the use of photochemistry through nickel catalysis, allowing for controlled entry of these radical intermediates into the catalytic cycle (**Scheme 2.7**).[45,70–80] In 2016, Baran and coworkers found that NHP esters (**171**) can be cross coupled with aryl zinc reagents (**172**) in a Negishi-type cross coupling to afford arylated products **173** (**Scheme 2.7**a).[79] Later in 2016 and 2017, it was found that this reactivity translates to both alkenyl (**175**) and alkyl (**178**) zinc species when using more activated *tetra*-chloro-*N*-hydroxyphthalimide(TCNHP) esters (**175**, **177**) to afford alkenylated (**176**) and alkylated (**179**) products, respectively (**Scheme 2.7**b,c).[70,74]

Scheme 2.7 *Ni-mediated decarboxylative cross-couplings of redox-active esters*

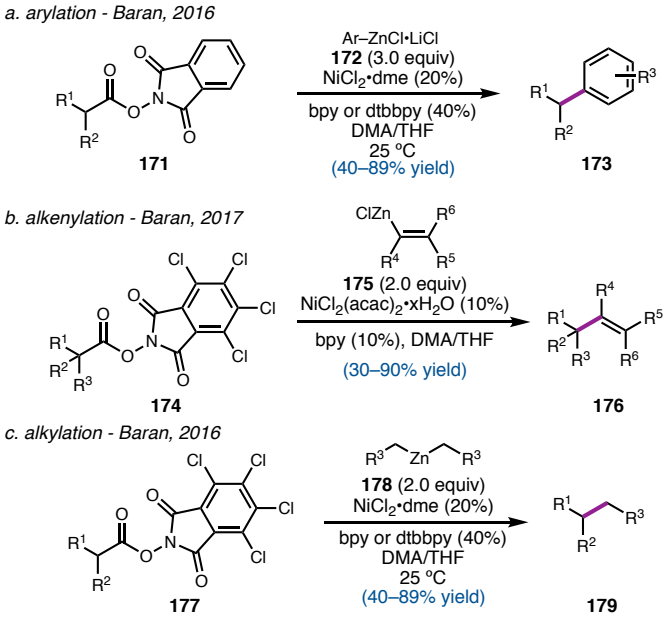

In addition to Negishi-type cross couplings, the Baran group has applied this strategy to a variety of organometallic cross coupling partners and other transition metal catalysts.[78,81,82]

In addition to traditional cross coupling, NHP esters can also be reductively cross coupled with a variety of halide cross-coupling partners in the presence of a nickel catalyst and a stoichiometric amount of a terminal reductant (**Scheme 2.8**). Weix and coworkers have shown that this strategy can be used for the arylation and alkynlation of NHP esters using zinc or manganese dust as the terminal reductant (**Scheme 2.8**a,b).[83–85] Our lab also has a particular interest in enantioselective Ni-mediated reductive cross coupling, and in 2017, we showed that benzylic NHP esters (**186**) can be enantioselectively cross-coupled with alkenyl halides (**187**) to afford enantioenriched products (**189**) in good yield and good ee using tetrakis(*N,N,*-dimethylamino)ethylene (TDAE) (**190**) as the homogenous, terminal reductant (**Scheme 2.8**c).[86] To the best of our knowledge, this work demonstrated the first example of NHP esters in enantioselective cross-coupling reactions.

Scheme 2.8 *Reductive decarboxylative cross-couplings of redox-active esters*

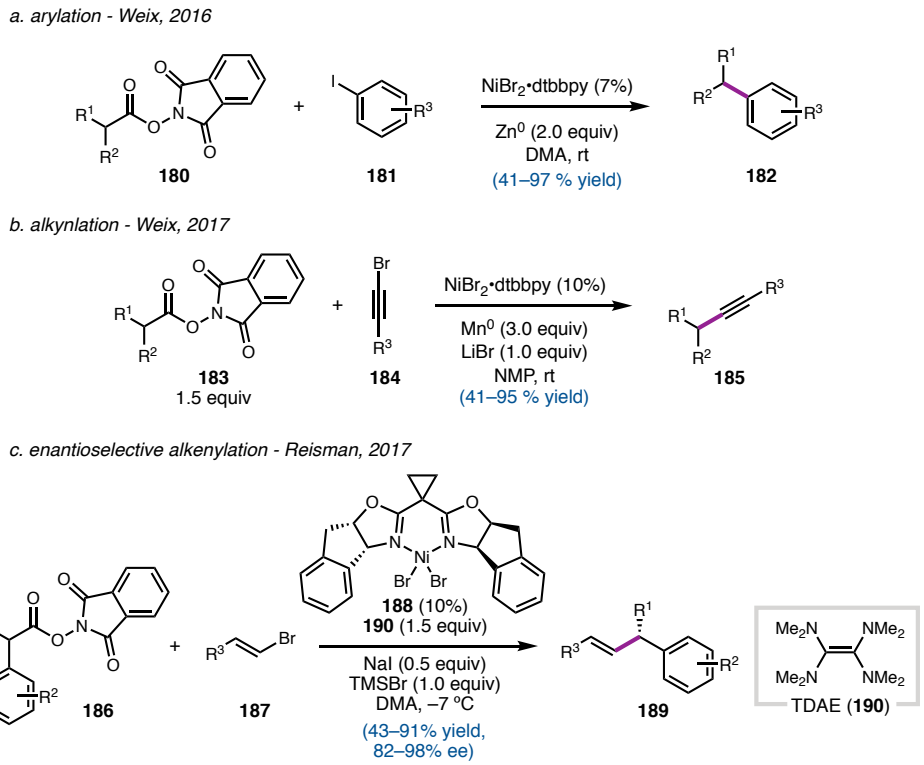

2.4 DIVERSIFICATION OF ENANTIOENRICHED CYCLOBUTANES

Scheme 2.9 *Carboxylic acid synthesis*

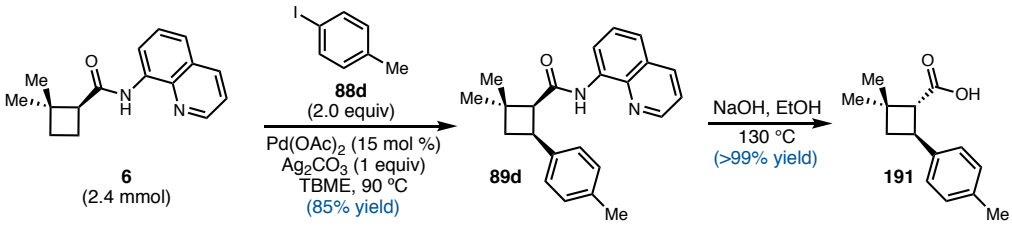

We next prepared to investigate a variety of decarboxylative cross-coupling reactions. Tolyl substrate **88d** was chosen due to its high yield and scalability for the C–H activation. Gratifyingly, simple base-mediated cleavage of the 8-aminoquinolinamide directing group afforded *trans* carboxylic acid **191** in excellent yields (**Scheme 2.9**).[87] With copious amounts of acid **191** in hand, we set out to derivatize this compound using known decarboxylative methods to synthesize a library of enantioenriched *trans* cyclobutanes.

Figure 2.4 *Direct decarboxylative cross-coupling challenges*

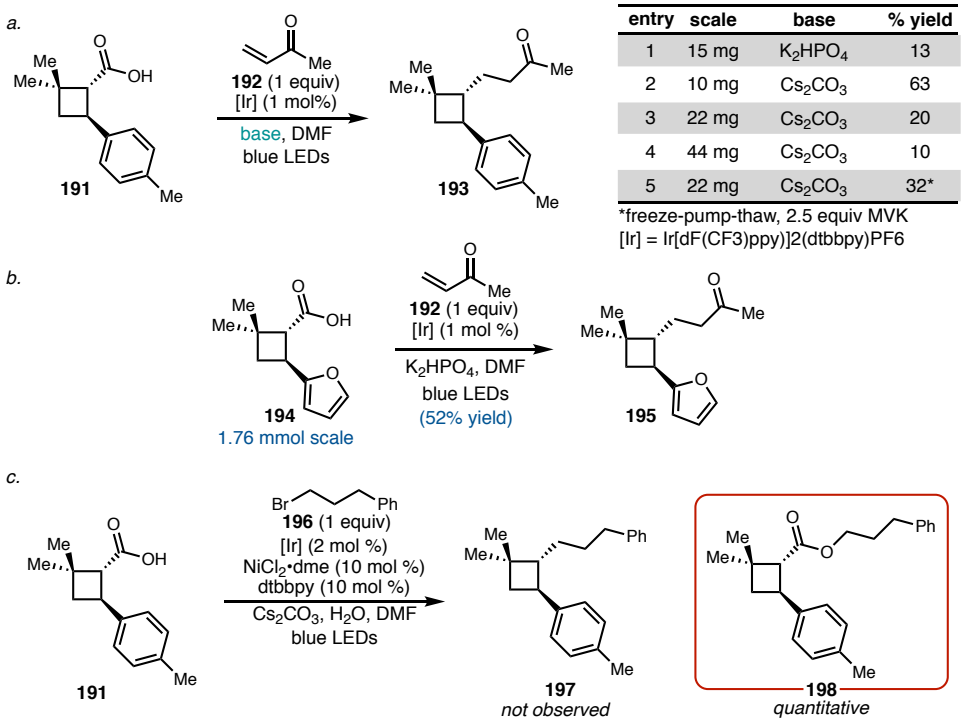

entry	scale	base	% yield
1	15 mg	K_2HPO_4	13
2	10 mg	Cs_2CO_3	63
3	22 mg	Cs_2CO_3	20
4	44 mg	Cs_2CO_3	10
5	22 mg	Cs_2CO_3	32*

*freeze-pump-thaw, 2.5 equiv MVK
[Ir] = Ir[dF(CF3)ppy)]2(dtbbpy)PF6

Initially, several direct decarboxylation methods of free carboxylic acid **191** were attempted. Unfortunately, there were a multitude of reproducibility and scalability issues. For example, a photochemical, decarboxylative Giese reaction with methyl vinyl ketone (MVK) (**192**) was attempted on tolyl carboxylic acid **191**, and, despite promising yields on 10 mg scale using Cs_2CO_3 (**Figure 2.4**a, entry 2), increasing the scale to 20 and 40 mg drastically decreased the yield of the desired product (entries 3, 4).[63] Even rigorous deoxygenation conditions afforded only a 12% recovery in yield (entry 5). Interestingly, this reaction afforded product **195** in good yields on up to 1.7 mmol scale using furan substrate **194** with K_2HPO_4 instead of tolyl-substituted acid **191** (**Figure 2.4**b). Attempts at a decarboxylative alkylation reaction only afforded esterified product **198** (**Figure 2.4**c).[61] Due to these irreproducibility issues and challenges with a variety of direct,

photochemical decarboxylation methods,[51,52,58,60] we chose to explore decarboxylative methods utilizing activated carboxylic acids.

Scheme 2.10 *Negishi-type decarboxylative cross-couplings of redox-active esters*

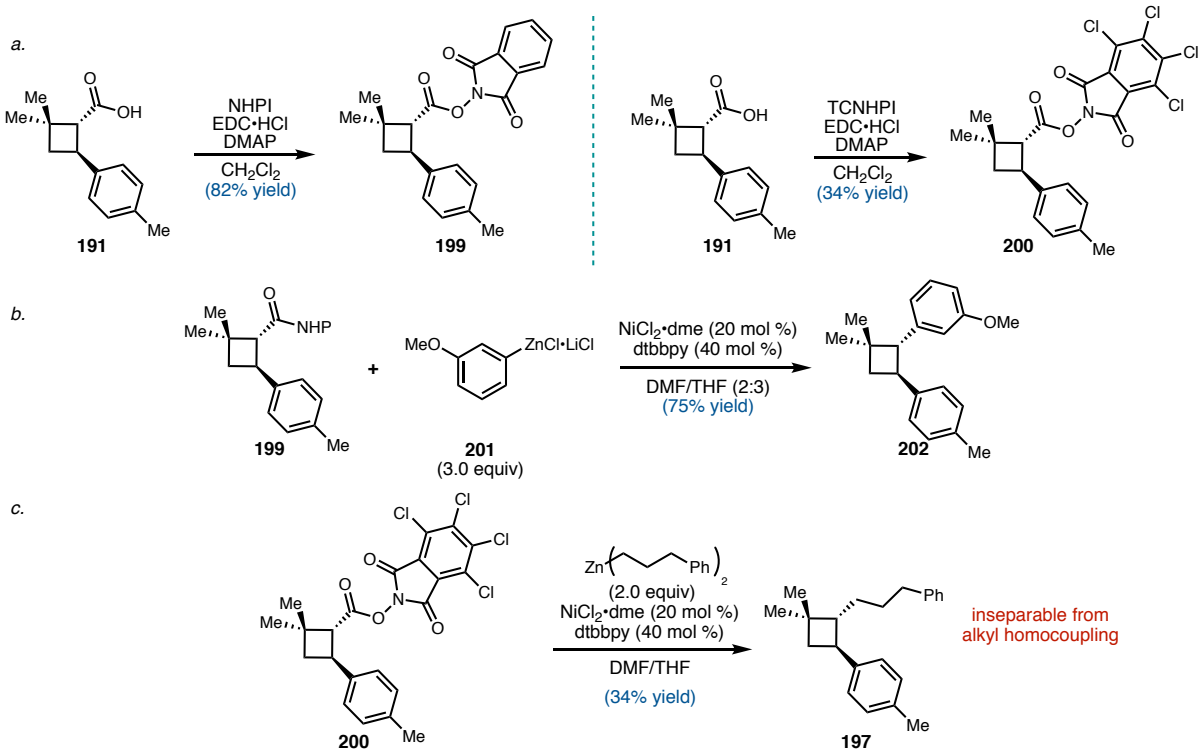

Simple EDC-mediated coupling of **191** with *N*-hydroxyphthalimide afforded NHP ester **199** in good yield (**Scheme 2.10**a). Similar conditions afforded TCNHP ester **200**, albeit in lower yield due to ester hydrolysis on silica gel during purification. We first attempted cross-coupling with organometallic reagents. Pleasingly, decarboxylative Negishi arylation conditions afforded *bis*-arylated compound **202** in 75% yield on up to 0.20 mmol scale (**Scheme 2.10**b).[79] However, attempts at decarboxylative alkylation with alkyl organozinc afforded only 34% alkylated cyclobutane **197**, which was found to be inseparable in our hands from primary alkyl homocoupling byproducts (**Scheme 2.10**c).[70]

Next were attempted several Ni-catalyzed reductive cross-coupling reactions using

Scheme 2.11 *Reductive cross-coupling of redox-active esters*

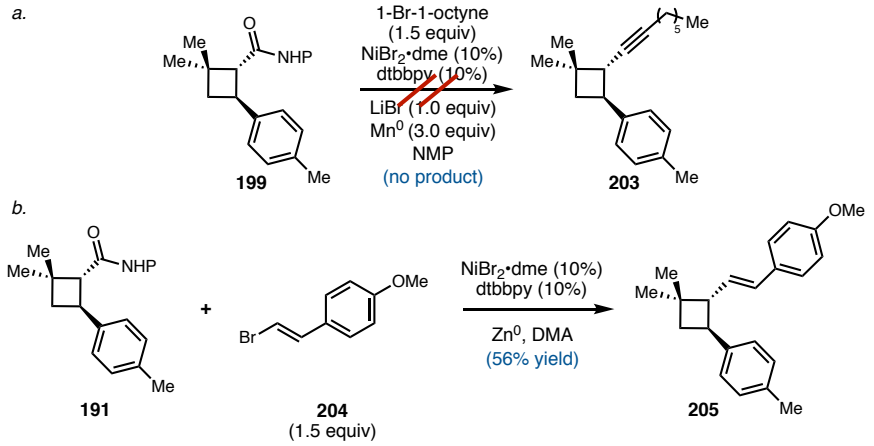

conditions developed by our lab and the Weix lab. Attempts at reductive alkynylation using 1-bromo-1-octyne with Mn^0 as the terminal reductant resulted in no formation of desired product **203** (**Scheme 2.11**a).[83] However, simple reductive alkenylation conditions using stoichiometric Zn^0 powder as the terminal reductant afforded the desired alkenylated product **205** in 56% yield on 0.20 mmol scale (**Scheme 2.11**b).[84,86]

Scheme 2.12 *Photochemical decarboxylative cross-coupling of redox-active esters*

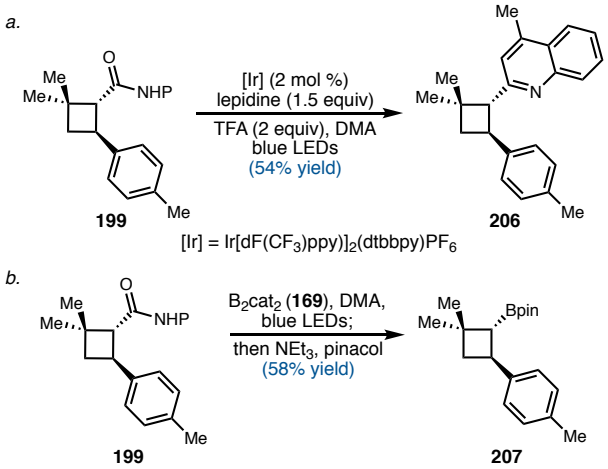

In addition to Ni-catalyzed decarboxylative methods, photochemical decarboxylative cross-couplings of NHP ester **199** were explored as well. *Bis*-arylated

product **206** was formed in 54% yield using Ir-catalyzed, photochemical Minisci-type conditions (**Scheme 2.12**a).[68] Interestingly, catalyst-free borylation conditions utilizing B_2cat_2 as both the photosensitizer and the coupling partner followed by treatment with pinacol and base afforded borylated product **207** in 58% yield (**Scheme 2.12**b).[69] These reactions were applied to furan NHP ester **S1** to afford arylated and borylated products in 36% and 47% yields, respectively, demonstrating that this strategy could potentially be applied to provide products with other substitution patterns (Section 2.8.2).

Scheme 2.13 *Carboxylic acid derivatization*

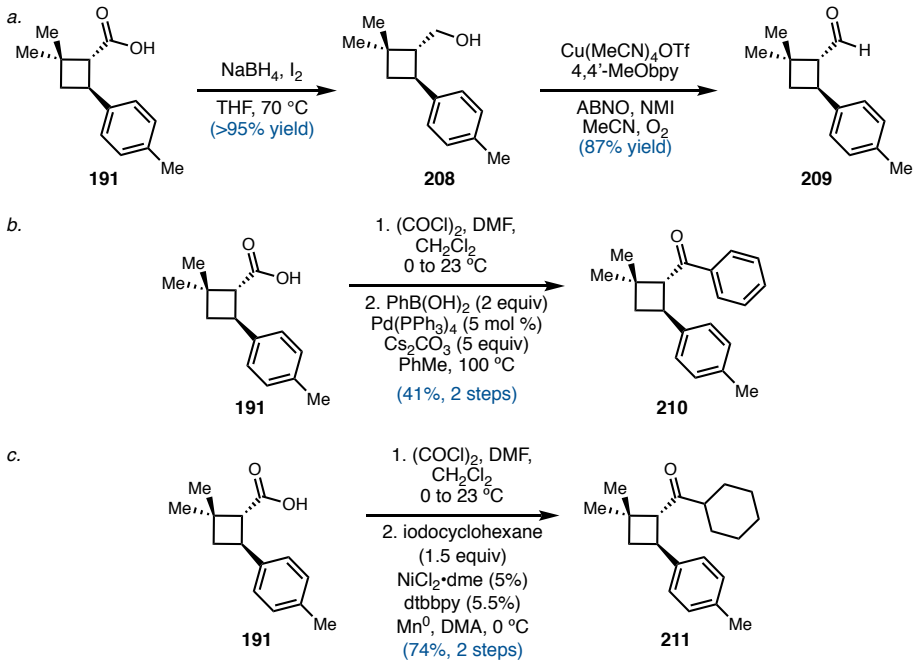

Modifications to the carboxylic acid itself were attempted as well. Simple borane reduction conditions afforded alcohol **208** in >95% crude yield (**Scheme 2.13**a). Stahl oxidation conditions were successfully applied, yielding aldehyde **209** in 87% yield, though a pure oxygen atmosphere and multiple additions of catalyst solution were required to facilitate full conversion of the starting alcohol.[88] Conversion to the acid chloride with oxalyl chloride followed by palladium-catalyzed cross-coupling afforded aryl ketone **210**

in 45% yield over 2 steps (**Scheme 2.13**b).[89] Returning to reductive cross-coupling, it was found that upon conversion to the acid chloride, treatment with $NiCl_2$•dme, di-*tert*-butylbipyridine (dtbbpy), stoichiometric Mn^0, and iodocyclohexane afforded cyclohexyl ketone **211** in 74% yield over two steps (**Scheme 2.13**c).[90]

Figure 2.5 *Summary of cyclobutane functionalizations*

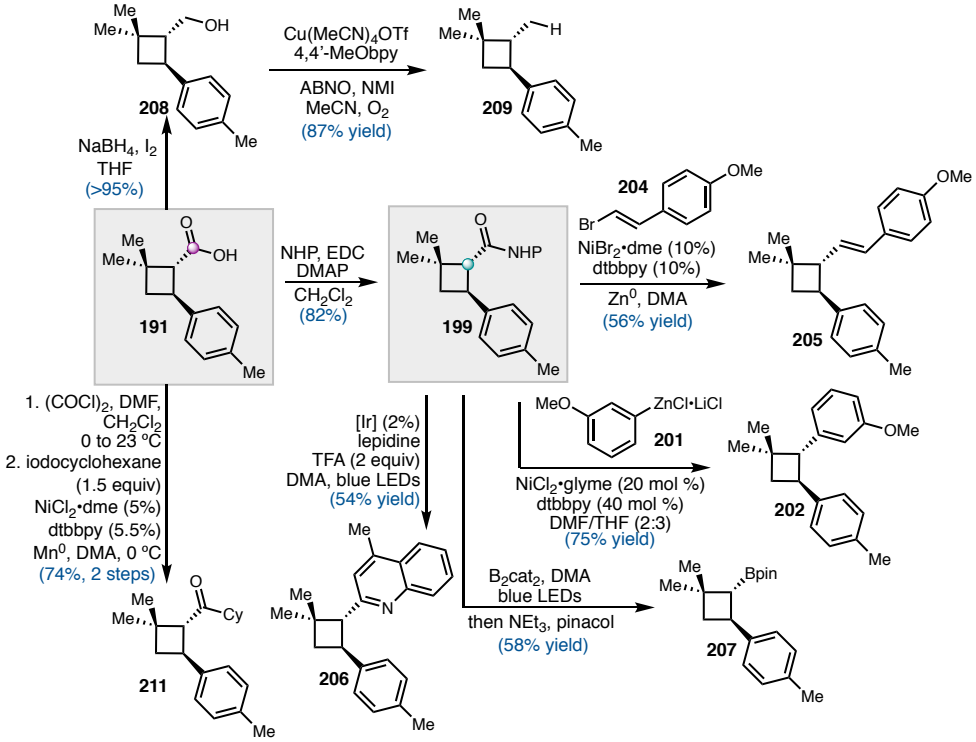

A summary of all successful cyclobutane functionalizations discussed is detailed in **Figure 2.5**. Notably, all decarboxylative cross-coupling reactions described here afforded the desired products with perfect *trans* selectivity. These data, in conjugation with our scope for the C–H arylation of cyclobutamide **6**, demonstrate the feasibility of a modular approach to *trans* cyclobutanes starting from a common, enantioenriched intermediate. We next hoped to demonstrate the utility of this strategy by applying it to the total synthesis of a natural product.

2.5 TOTAL SYNTHESIS OF (+)-RUMPHELLAONE A

2.5.1 Background and Biosynthesis

Figure 2.6 *A modular approach towards (+)-rumphellaone A*

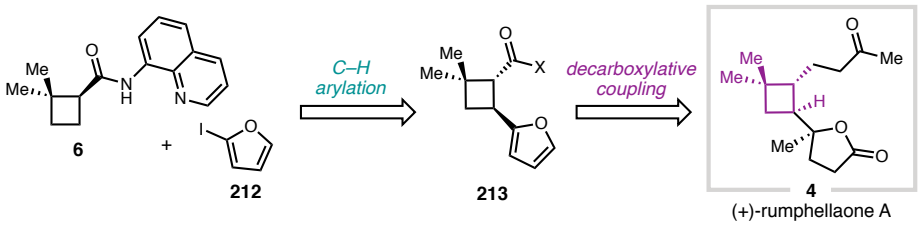

As this modular approach towards enantioenriched, trans-substituted cyclobutanes was being developed, we sought to apply this strategy towards the total synthesis of a natural product. (+)-Rumphellaone A (**4**), a 4,5-seco-caryophyllane sesquiterpenoid isolated in 2010 from the gorgonian coral *Rumphella antipathies*, was chosen as the target due to its *trans*-cyclobutane core and *gem*-dimethyl motif (**Figure 2.6**).[7] (+)-Rumphellaone A possesses anti-proliferative activity against human T-cell acute lymphoblastic leukemia tumor cells and contains a γ-lactone functionality.

Scheme 2.14 *Proposed biosynthesis of (+)-rumphellaone A*

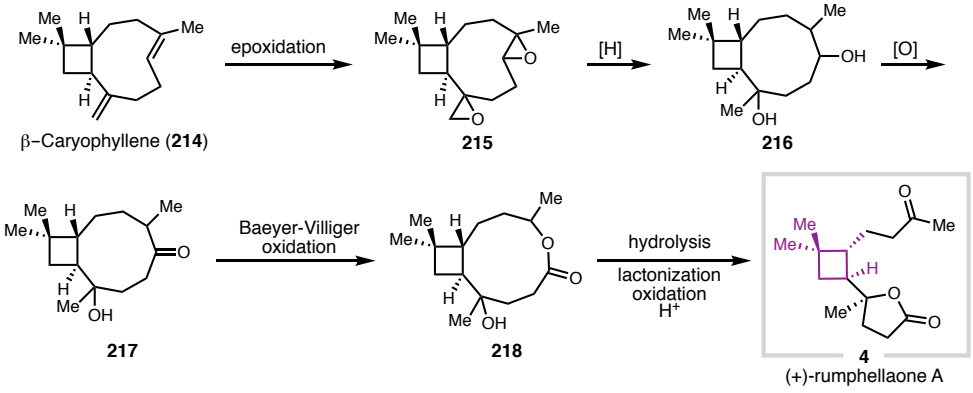

It is thought that (+)-rumphellaone A and its related compounds arise biosynthetically from β-caryophyllene (**214**).[7] It was hypothesized that after bisepoxidation

of **214**, a series of reductions would deliver diol **216**, which could then be oxidized to provide ketone **217**. Baeyer-Villiger-type oxidation of the ketone would lead to formation of the macrocyclic ester (**218**), and hydrolysis and secondary alcohol oxidation would afford the natural product (**4**).

2.5.2 Previous Syntheses

Scheme 2.15 *Kuwahara's enantioselective synthesis of (+)-rumphellaone A*

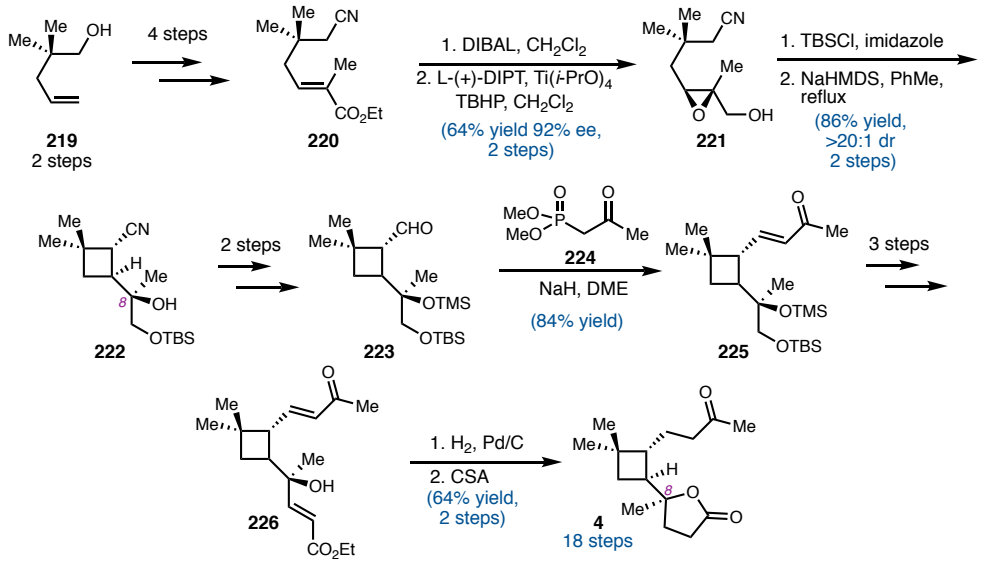

There have been several total syntheses of (+)-rumphellaone A since its isolation in 2010. In 2012, the Kuwahara lab published the first enantioselective total synthesis of (+)-rumphellaone A.[91,92] α,β-unsaturated ester **220** was synthesized in four steps from alcohol **219** (two steps from commercially available starting materials). Reduction followed by Sharpless asymmetric epoxidation afforded enantioenriched epoxide **221**, setting the stereochemistry at the particularly challenging C8 carbon. Silylation followed by epoxy nitrile cyclization of **221** afforded the *trans*-cyclobutane core (**222**) of rumphellaone A in good yield and diastereoselectivity. Alcohol protection and nitrile reduction afforded aldehyde **223**, which was elaborated to α,β-unsaturated ketone **225** via

a Horner-Wadsworth Emmons olefination. Further oxidations and olefinations yielded ester **226**, which, upon hydrogenation and treatment with acid, cyclized to form (+)-rumphellaone A, completing the 18-step total synthesis.

Scheme 2.16 *Echavarren's enantioselective synthesis of (+)-rumphellaone A*

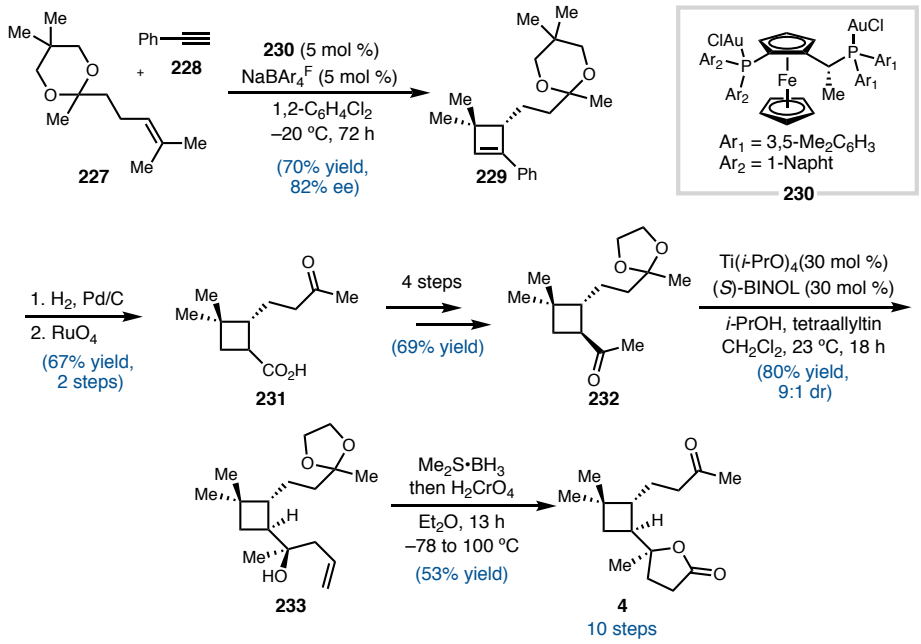

Echavarren and coworkers have published two total syntheses of (+)-rumphellaone A, both utilizing a [2+2] cycloaddition strategy to afford the core of the natural product.[93,32] Their most recent synthesis in 2017 utilized an enantioselective [2+2] cycloaddition to afford cyclobutene **229** in 70% yield and 82% ee (**Scheme 2.16**). From there, it took 6 steps to elaborate to *trans*-cyclobutane **232**. In order to set the C8 stereocenter, it was found that utilization of a chiral BINOL ligand with Ti(*i*-PrO)$_4$ allowed for the diastereoselective allylation of ketone **232** to afford tertiary alcohol **233** in 9:1 dr. Hydroboration-oxidation and cyclization afforded the natural product in 10 steps overall.

2.5.3 Our Strategy: Application of a Modular Approach

Scheme 2.17 *Retrosynthetic analysis of (+)-rumphellaone A*

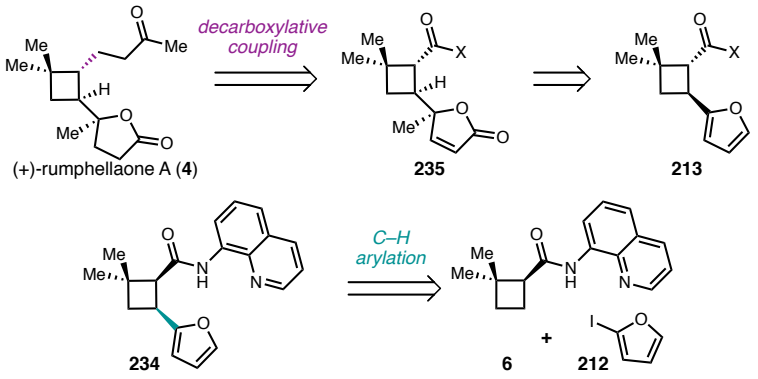

Having developed a modular strategy towards the synthesis of enantioenriched *trans* cyclobutanes utilizing two robust methods developed for the total synthesis of (+)-psiguadial B, we hoped to apply this approach towards the synthesis of (+)-rumphellaone A (**Scheme 2.17**). It was thought that the methyl ketone functionality could be installed at a late stage through a decarboxylative cross-coupling. We envisioned that the γ-lactone could be derived from oxidation and methylation of a furan (**213**), which could be installed through a diastereoselective C–H arylation with known enantioenriched cyclobutamide **6** and furanyl iodide **212**.*

2.5.4 C–H Activation Optimization

C–H activation with furanyl iodide **212** was first attempted. Iodides **212** and **236** were synthesized according to known literature conditions (**Table 2.1, Table 2.2**).[94,95] Unsubstituted iodofuran **212** performed well on small scale using 30% $Pd(OAc)_2$ and 3 equivalents of **212** (**Table 2.1**, entry 1). Attempts to lower the equivalents of **212** resulted

* An alternative approach using an alkenyl iodide was attempted with Dr. Lauren Chapman and is further detailed in Appendix 4 of her thesis.

Table 2.1 *C–H arylation with furan* ***212***

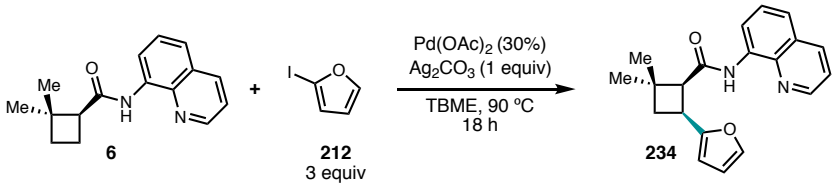

entry	scale (mg)	equiv iodide	% yield
1	20	3	70
2	20	2	54
3	200	3	59
4	300	3	55

[a]Reactions run in a pressure flask or a sealed vial with a Teflon cap under air. Yields determined by ^{1}H NMR analysis against an internal standard.

in lower yields (entry 2). Similarly, scaling up the reaction to 200 or 300 mg resulted in yields between 50–60% (entries 3 and 4). Notably, substrate **212** required double the catalytic loading of $Pd(OAc)_2$ compared to the standard reaction conditions.

Table 2.2 *C–H arylation optimization with TMS furan* ***236***

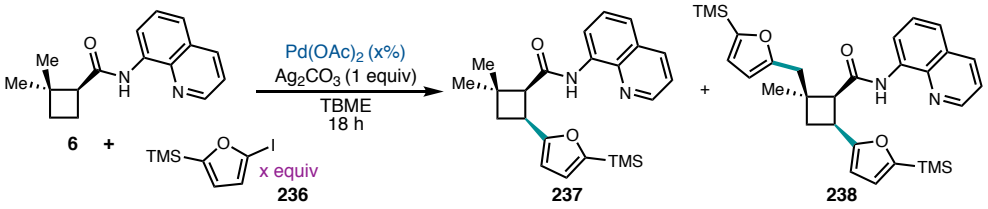

entry	scale (mg)	temp (°C)	cat loading (mol %)	equiv iodide	% yield **237**[a]	% yield **238**[a]	**237**:**238**
1	20	90	15	2	57	37	1.5:1
2	20	90	15	1.5	84	5	16:1
3	20	90	7.5	2	-	-	4:1
4	20	70	15	2	86	3	29:1
5	20	70	7.5	2	83	2	42:1
6	20	70	15	1.5	88	2	44:1
7	100	70	7.5	2	86[b]	trace	-
8	100	70	15	1.5	87[b]	2	44:1
9	300	70	7.5	2	91[b]	trace	-
10	400	70	7.5	2	90[b]	-	-
11	600	70	7.5	2	88[b]	-	-

[a]Reactions run in a pressure flask or a sealed vial with a Teflon cap under air. Yields determined by ^{1}H NMR analysis against an internal standard. [b] Isolated yield.

Similarly, TMS iodofuran **236** was submitted to the reaction conditions. However, in addition to 57% yield of the desired product **237**, an interesting bisarylation byproduct **238** arising from a second arylation at the β-face methyl was observed in 37% yield on 20 mg scale (**Table 2.2**, entry 1). This was particularly surprising as no such bisarylation product had been observed for any other substrates subjected to these arylation conditions (Chapter 1, section 1.3). A time course study revealed facile mono arylation (70% NMR yield after 1 hour) with further conversion to the bisarylated product as the reaction progressed (See 2.8.3, **Table S1**). Additionally, after 1 hour, 7% **238** was present in the reaction mixture. We therefore sought to optimize the reaction conditions to minimize formation of the undesired byproduct. It was found that reducing the temperature to 70 ºC and lowering the catalyst loading to 7.5% afforded the desired product in 88% yield with minimal formation of **238** (entry 6). Alternatively, if instead of reducing the catalyst loading, the amount of TMS furan **236** was reduced to 1.5 equivalents, similar results were observed (entry 5). We chose to move forward with lower catalyst loading. The reaction also scaled well, affording comparable yields of the product with minimal bisarylation on up to 600 mg scale (entries 7, 9–11). Due to the superior reactivity and scalability, TMS furan **236** was chosen for future study.

2.5.5 Directing Group Removal and Functionalization

Scheme 2.18 *Schwartz reduction and base-mediated epimerization*

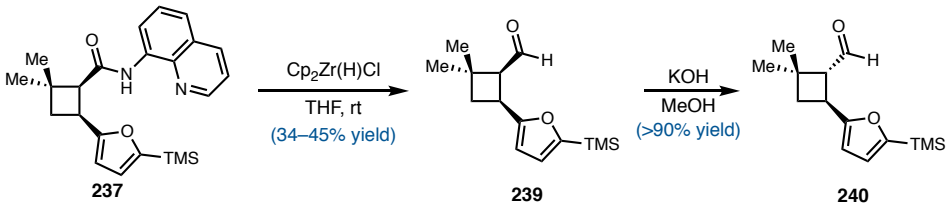

In order to afford the *trans*-cyclobutane core of (+)-rumphellaone A, the 8-aminoquinoline directing group had to be cleaved and the stereochemistry at the C1 carbon inverted. Early attempts focused on replicating conditions from the synthesis of (+)-psiguadial B, namely reductive cleavage of the amide to form aldehyde **239** using Schwartz's reagent followed by base-mediated epimerization (**Scheme 2.18**).[12,13] Though this process did yield the desired product (**240**), the amide reduction was low-yielding, the epimerization conditions were irreproducible, and the aldehyde (**240**) was unstable.

Scheme 2.19 *Single step directing group removal and epimerization*

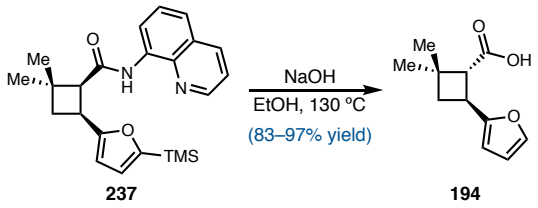

237 **194**

Due to these challenges, alternative methods to remove the quinolinamide directing group were investigated. Pleasingly, simple base-mediated conditions used previously (**Scheme 2.9**) not only cleaved the directing group, but also facilitated complete epimerization to afford the *trans*-cyclobutane carboxylic acid (**194**) in high yields (**Scheme 2.19**).[87] Surprisingly, these conditions resulted in cleavage of the furan TMS group, but it was decided to move forward with **194** due to the high yields and scalability. These reaction conditions increased the overall yield and afforded a substrate primed for direct decarboxylative coupling. Acid-mediated conditions were also attempted, but without success.[96]

2.5.6 Furan Oxidation and Diastereoselective Methylation

Next, we focused on the functionalization of the furan to afford the desired γ-lactone (**241**) found in the natural product. This required oxidation and diastereoselective

Scheme 2.20 *Summary of C8 methylation strategies*

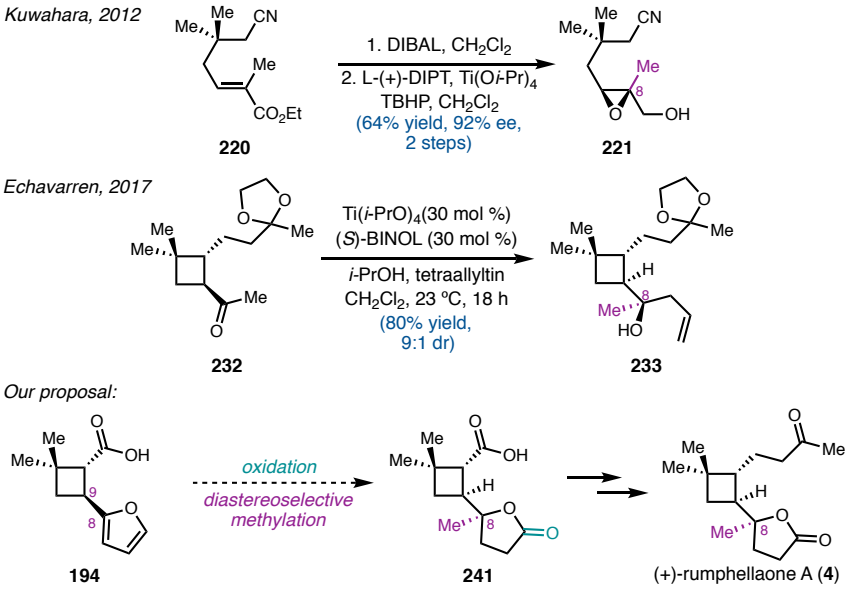

methylation of the furan. The diastereoselective methylation was thought to be challenging due to the free rotation around the C8–C9 bond and the unknown orientation of the furan in solution. Indeed, both previous syntheses of (+)-rumphellaone A relied on chiral catalysis to set the C8 stereocenter (**Scheme 2.20**).[32,91–93] We hoped that perhaps the presence of the carboxylic acid could afford some diastereoselectivity through either coordination of a methylating reagent or coordination to a Lewis acid resulting in facial blocking.

2.5.6.1 Cyclopropanation Strategy

It was thought that the C8 methyl group could be installed via a cyclopropanation followed by a ring opening. It was predicted that the cyclopropanation would be selective for the more substituted, electron rich alkene, and that the carboxylic acid could afford diastereoselectivity through coordination to a zinc carbenoid generated from diethyl zinc and diiodomethane (CH_2I_2).[97] Unfortunately, only *bis*-cyclopropanation product **241** was observed (**Scheme 2.21**). Iodomethyl ester product **242** was observed when excess CH_2I_2

Scheme 2.21 *Attempts at directed furan cyclopropanation*

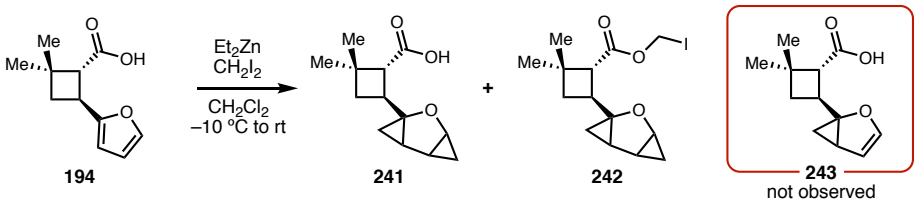

was used. Lowering to one equivalent of cyclopropanating reagents led to the formation of biscyclopropanated products and recovered starting material. These results suggested that after the first cyclopropanation, the loss of aromaticity and electron donation from the adjacent oxygen make the second cyclopropanation very facile, resulting in no observable formation of the mono-cyclopropanated product. Milder cyclopropanation conditions afforded no desired reactivity.[98] There are select examples of monocyclopropanation of furans in the literature using diazo carbene precursors, but we chose to turn our efforts elsewhere.[99–102]

2.5.6.2 Titanium-Mediated Diastereoselective Methylation

Scheme 2.22 *Titanium-mediated diastereoselective methylation of hydroxy-butenolides*

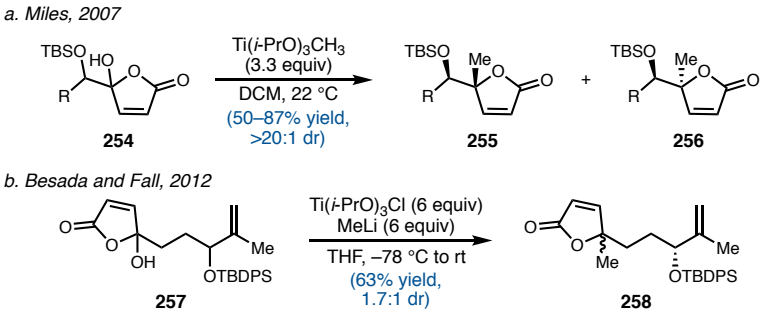

Inherent to our proposed strategy was the need for a diastereoselective addition of the methyl group to the furan or a furan derivative. In 2007, Miles and coworkers published a diastereoselective methylation of γ-hydroxybutenolides (**254**) using stoichiometric Ti(*i*-

PrO)$_3$CH$_3$ (**Scheme 2.22**a).[103] In 2012, Besada and Fall showed that they could generate Ti(*i*-PrO)$_3$CH$_3$ *in situ* by prestirring Ti(*i*-PrO)$_3$Cl and methyllithium (MeLi) to perform a similar methylation of a γ-hydroxybutenolide (**257**), though with lower diastereoselectivity (**Scheme 2.22**b).[104] It was proposed that these conditions could be applied to our system.

Scheme 2.23 *Furan oxidation and undesired diastereoselectivity*

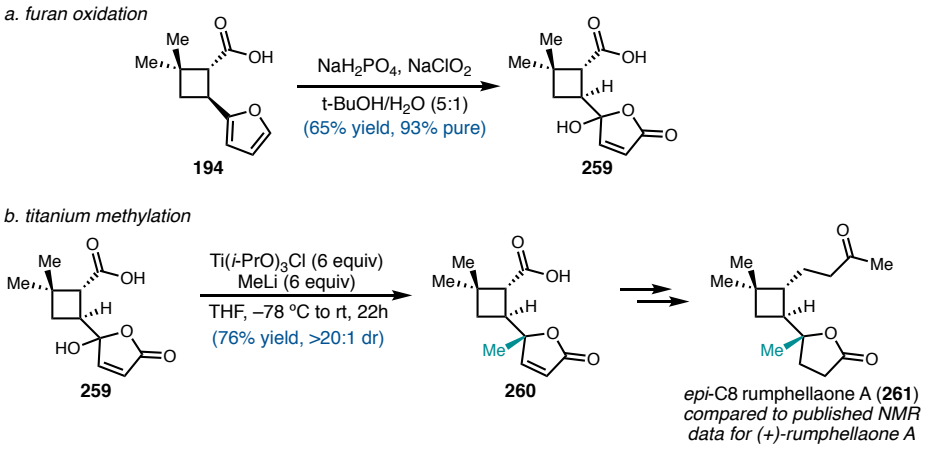

Gratifyingly, it was found that Pinnick-type oxidation conditions afforded γ-hydroxybutenolide **259** in 65% yield and 93% purity after column chromatography (**Scheme 2.23a**).[105] Lower purity material could be acquired in about 5% higher yield without chromatography, though we elected to move forward with cleaner material. Carboxylic acid butenolide **259** was investigated as opposed to **250**, which contained the ketone functionality, as it was envisioned that the carboxylic acid could act as a directing group. **259** was added to a preformed solution of Ti(*i*-PrO)$_3$CH$_3$ to afford γ-methylated product **260** in 76% yield and >20:1 dr (**Scheme 2.23b**). However, upon elaboration to **261**, it was found that this methylation favored the undesired diastereomer, as determined by comparing ^{1}H and ^{13}C NMR data with published isolation and synthetic NMR data for (+)-rumphellaone A.[7,32,91–93] Despite this disappointing result, we were pleased to find that

diastereoselective methylation was possible in good yields, despite being the undesired diastereomer. Investigations into reversing the diastereoselectivity were undertaken.

Scheme 2.24 *Additional methylation attempts*

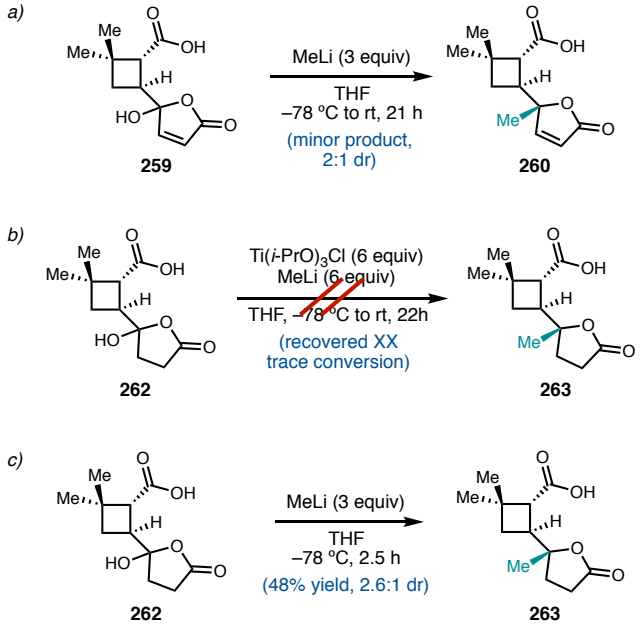

Attempts to perform the transformation with only MeLi resulted in poor reactivity for the desired methylation (**Scheme 2.24**a). Presumably, this is due to competitive 1,4 addition into butenolide **259**. Hydrogenated butenolide **262** was therefore submitted to both titanium-mediated and titanium-free reaction conditions (**Scheme 2.24**b,c). The titanium conditions led to poor conversion, while the MeLi conditions resulted in poor diastereoselectivity. At this point, efforts turned towards screening other Lewis acids that could facilitate this transformation to afford the desired diastereomer.

A wide variety of Lewis acids and organometallic reagents were screened in order to find conditions that afforded the desired product with the correct stereochemistry at the C8 carbon (**264**) (**Table 2.3**). Previous reaction conditions still afforded the methylated product in the best yield and was the most selective for a single diastereomer, albeit the

Table 2.3 *Lewis acid screen for methylation diastereoselectivity*

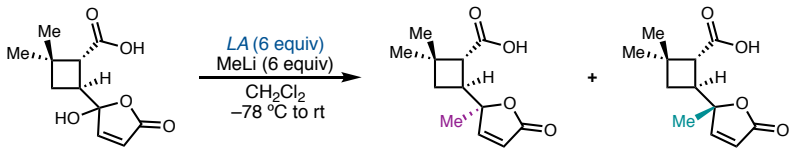

259 **264** **260**

entry	scale (mg)	conditions	prestir	% yield[a]	dr (**264**:**260**)[b]	time (h)
1	50	$TiCl(i\text{-}PrO)_3$	LA and MeLi	76	>1:20	21
2	20	$CeCl_3$, MeLi	LA and MeLi	33	1:2	21
3	10	$CeCl_3$, MeLi[c]	LA and MeLi	13	–	22
4	20	$BF_3{\cdot}Et_2O$, MeLi	LA and MeLi	24	1:2	21
5	10	$La(i\text{-}PrO)_3$, MeLi	LA and MeLi	6	1:1	4.25
6	10	$LaCl_3$, MeLi	LA and MeLi	31	1:2	4.25
7	10	$Sc(OTf)_3$, MeLi	LA and MeLi	4	1:5	21
8	10	$In(OTf)_3$, MeLi	LA and MeLi	–	–	21
9	10	$Ti(i\text{-}PrO)_4$, MeLi	LA and MeLi	–	–	22
10	10	$TiCl_4$, MeLi[d]	LA and MeLi	13	4:1	22
11	10	$CeCl_3$, MeLi	LA and sm	12	1:2	8.7
12	10	$BF_3{\cdot}Et_2O$, MeLi	LA and sm	12	1:2	6
13	10	$Ti(i\text{-}PrO)_4$, MeLi	LA and sm	10	1:3	22
14	10	MeMgBr	–	38	1:3	20
15	10	$AlMe_3$, then MeLi	–	–	–	41
16	10	$ZnMe_2$, then MeLi	–	–	–	41

[a,b]determined by ^1H NMR, [c]3 equiv. reagents, [d]CH_2Cl_2 instead of THF

undesired diastereomer (**260**) (entry 1). Most Lewis acids resulted in poor yields and diastereoselectivities (entries 2–9, 11–13). Simple methyl Grignard afforded the methylated product in 38% yield, but 1:3 dr (entry 14). Surprisingly, $AlMe_3$ and $ZnMe_2$ were ineffective methylating reagents, even after extensive stirring times (entries 15,16). Prestirring the Lewis acid with the starting material had little effect (entries 11–13). Interestingly, a combination of $TiCl_4$ and MeLi afforded the methylated product in 4:1 dr favoring the desired diastereomer (**264**), albeit in poor yield (entry 10). Due to the high reactivity of $TiCl_4$ with ethers, this reaction was run in CH_2Cl_2 instead of THF. These conditions were chosen for further investigation.

These conditions proved to be challenging to optimize (**Table 2.4**). Adjusting the reaction temperature, equivalents of reagents, and reaction setup afforded no improvements

Table 2.4 *$TiCl_4$ and MeLi methylation optimization*

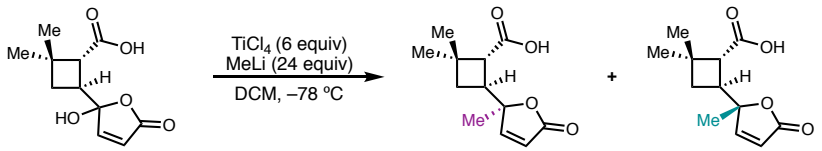

259 **264** **260**

entry[a]	scale (mg)	equiv $TiCl_4$	equiv MeLi	time (h)	% yield[b]	dr (xx:xx)[b]	notes
1	10	6	6	22[c]	13	1:4	–
2	25	6	6	23[c]	–	1:1.2	–
3	10	4	4	23[c]	–	–	–
4	10	6	6	22	trace	–	kept at –78ºC
5	10	6	6	22[c]	14	1:2	–40 ºC to rt
6	10	6	6	3	–	–	0 ºC
7	10	6	6	27[c]	–	–	reverse addition
8	10	6	12	6	11	1:2	–
9	10	6	24	5	54	1:1	–
10	30	6	24	2	35	1:3	–
11	35	6	24	4	61	9:1	sm cooled to –78 ºC, dropwise
12	100	6	24	4	46	1:2	sm cooled to –78 ºC, dropwise
13	50	6	24	4	60	9:1	sm cooled to –78 ºC, slow dropwise

[a]Reaction set up: $TiCl_4$ and MeLi prestirred at –78 ºC ~1h. Add xx as a room temperature solution in DCM via cannula, [b] determined by ^1H NMR, [c]reaction allowed to warm to room temerature

in yield or dr to the initial hit (entries 1–7). Indeed, upon scaling up the reaction, the dr decreased (entry 2). Finally, it was found that increasing the amount of MeLi to 24 equivalents (a 4:1 ratio of MeLi to $TiCl_4$) significantly increased reactivity, providing the product in 54% yield, albeit with 1:1 dr **264**:**260** (entry 9). Based on both the stoichiometry of the reagents and the abrupt change in color from brown to blue/green upon addition of the final equivalent of MeLi, this combination presumably forms $Ti(CH_3)_4$ *in situ*. Upon scaling up this reaction from 10 mg to 30 mg again however, the yield decreased and the diastereoselectivity reversed to favor the undesired diastereomer (entry 10). We hypothesized that this could be due to the increased volume of starting material being added to the reaction mixture, which could be warming up the reaction mixture too quickly. Indeed, upon cooling the solution of starting material to –78 ºC in a dry ice/acetone bath as it was added to the $Ti(CH_3)_4$ solution via cannula, the reaction not only increased in

yield, but the dr increased to 9:1 favoring the desired diastereomer (**264**) (entry 11). This reaction was scaled up to 100 mg, and, unfortunately, the diastereoselectivity again reversed to 1:2 and the yield dropped to 46%. It appeared that the internal temperature was more unstable than suspected. By monitoring the internal temperature of the reaction mixture as the cooled solution of starting material was added, it was found that even with cannula addition of the cooled starting material, the internal temperature could quickly increase if the starting material was added too quickly. To combat this, the reaction was set up on 50 mg scale, and the solution of starting material was added with a narrow cannula over the course of 20 minutes. This minimized internal temperature fluctuations and afforded the desired product in 60% yield and 9:1 dr after purification (entry 13). This method was found to be reproducible and allowed for independent synthesis of both butenolide diastereomers **264** and **260**.

2.5.6.3 Discussion of Diastereoselectivity

Figure 2.8 *Methylation diastereoselectivity*

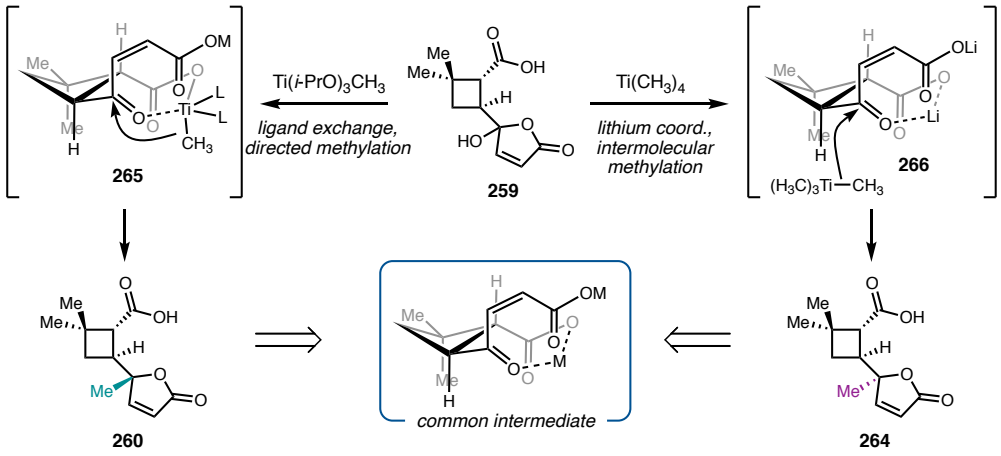

The current hypothesis for the diastereoselectivity observed for these reaction conditions hinges on the differences in reactivity between Ti(*i*-PrO)$_3$CH$_3$ and Ti(CH$_3$)$_4$. It

is proposed that under both sets of conditions, hydroxybutenolide **259** undergoes ring-opening to form the α,β-unsaturated ketone, which can undergo chelation to a metal species as shown in **Figure 2.8**. Due to the lability of isopropoxide, Ti(*i*-PrO)$_3$CH$_3$ could undergo ligand exchange with the carboxylate to afford intermediate **265**. The titanium species could then deliver the methyl group intramolecularly from the α face of the ketone, affording the undesired diastereomer (**260**) as observed under these conditions. On the other hand, Ti(CH$_3$)$_4$ would be unlikely to undergo ligand exchange. Instead, the carboxylate could coordinate to Li$^+$ to afford intermediate **X266**. Ti(CH$_3$)$_4$ could then deliver the methyl group intermolecularly to the β face of the ketone, which would result in the observed, desired diastereomer (**264**).

2.5.7 Ketone Installation

Scheme 2.25 *Ketone installation from aldehyde* ***239***

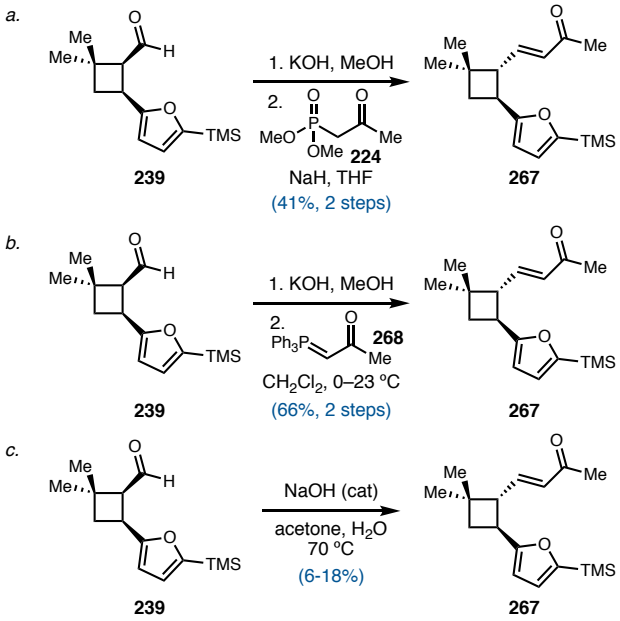

With a strategy to access the desired γ-methyl lactone in place, investigations were made into the installation of the methyl ketone. Early investigations into Horner-

Wadsworth-Emmons olefination of aldehyde **239** resulted in moderate yields of the desired product (**267**) with irreproducibility issues (**Scheme 2.25a**).[12,13] Upon switching to a commercially available Wittig reagent (**268**), the desired product could be obtained in higher yields with greater reproducibility (**Scheme 2.25b**). Attempts were made to combine the aldehyde epimerization and olefination through a base catalyzed aldol reaction, however this resulted in low yields (**Scheme 2.25c**). Though Wittig conditions afforded **267** in good yield, this procedure required a rigorous one-day, three-step sequence to cleave the directing group, epimerize the aldehyde, and install the ketone. In addition, the α,β unsaturated ketone in **267** would have to undergo hydrogenation to afford the desired product. Due to these restrictions, and in light of the successes with carboxylic acid **194**, investigations were turned toward ways to afford the saturated ketone directly through decarboxylative cross coupling.

Table 2.5 *Photochemical decarboxylative Giese to install the methyl ketone*

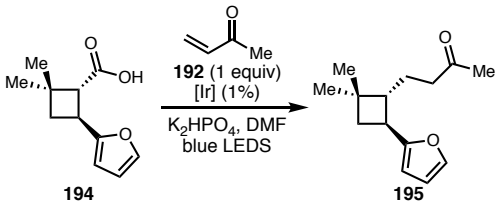

[Ir] = Ir[dF(CF$_3$)ppy)]$_2$(dtbbpy)PF$_6$

entry	scale (mg)	% yield	notes
1	16	31	–
2	80	29	–
3	100	40	dried K_2HPO_4
4	342	52	dried K_2HPO_4, dist MVK

As mentioned previously, several inherent reactivity challenges with direct decarboxylation methods in other aryl cyclobutane systems had been observed, manifesting in low yields and challenges with scalability. However, we were pleased to see promising activity on small scale for a photochemical, decarboxylative Giese reaction of carboxylic acid **194** with methyl vinyl ketone (MVK) (**192**) using conditions from MacMillan and coworkers (**Table 2.5**).[63] After some optimization, it was found that not

only could the desired product (**195**) be obtained in good yield, but that this reaction was scalable (entry 5). In light of this promising and robust reactivity, we sought to apply this reaction to the late-stage intermediates containing the γ-methyl lactone.

Scheme 2.26 *Final steps towards (+)-rumphellaone A and epi-C8-rumphellaone A*

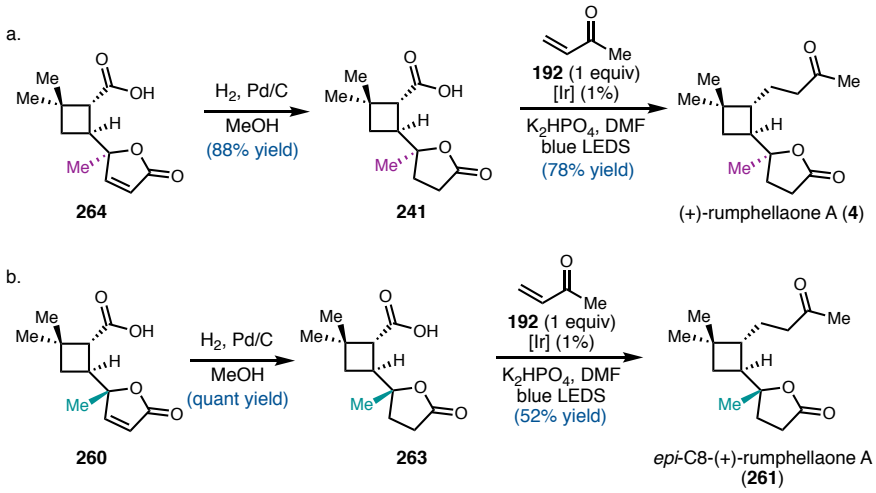

Hydrogenation of **264** and **260** under standard hydrogenation conditions was facile, affording γ-methyl lactones **241** and **263** (**Scheme 2.26**). Gratifyingly, both compounds successfully underwent a photochemical, decarboxylative Giese reaction with MVK to afford (+)-rumphellaone A (**4**) and *epi*-C8-(+)-rumphellaone A (**261**), respectively. This completed our total synthesis of (+)-rumphellaone A. We were pleased to be able to afford both the natural product and its C-8 epimer directly from the corresponding carboxylic acids under photochemical conditions in good yields.

2.6 SUMMARY

A robust, enantioselective total synthesis of the natural product (+)-rumphellaone A (**4**) was completed in 9 steps from commercially available starting materials, making it the shortest synthesis to date (**Scheme 2.27**).[106] Key to our strategy was the application of a modular approach to *trans* cyclobutanes, which allowed us to quickly access the

Scheme 2.27 *Enantioselective total synthesis of (+)-rumphellaone A*

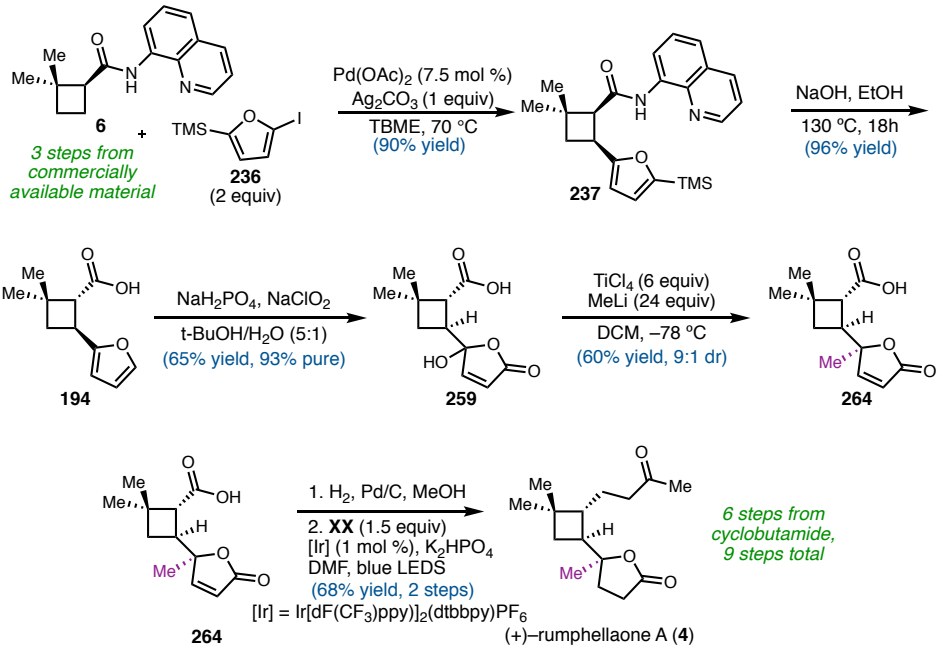

enantioenriched core of (+)-rumphellaone A. Concomitant directing group removal and epimerization allowed us access to key carboxylic acid **194**, which enabled diastereoselective installation of the C8 methyl group without the use of a chiral catalyst. Finally, the methyl ketone functionality was installed directly through a photochemical, decarboxylative Giese coupling with methyl vinyl ketone in good yield. This strategy allowed for independent access of both C8 methyl diastereomers of (+)-rumphellaone A. This efficient synthesis demonstrates the efficacy of our modular approach to *trans* cyclobutanes.

2.7 CONCLUSION

In conclusion, a modular strategy towards the synthesis of a library of enantioenriched cyclobutanes was developed, and this strategy was applied toward the enantioselective total synthesis of (+)-rumphellaone A (**4**). Application of two robust methods developed for the synthesis of (+)-psiguadial B (**1**) allowed for the development

Figure 2.10 *Summary of work to date*

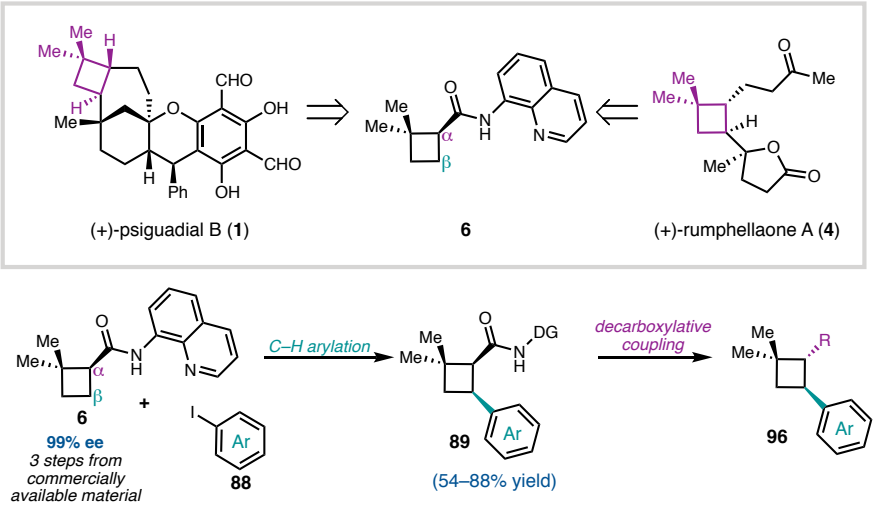

of this strategy.[12,13] Enantioenriched cyclobutamide **6** served as a common intermediate, allowing for the synthesis of a broad scope of arylated *cis* cyclobutanes (Chapter 1). These compounds could then be further functionalized upon directing group removal through a variety of decarboxylative cross-couplings, affording a variety of enantioenriched *trans* cyclobutanes. The strengths of this strategy include starting from a common, enantioenriched intermediate, as well as two divergence points, allowing for the synthesis of a library of *trans* cyclobutanes with different substitution at the α and β positions.

This strategy was applied towards the total synthesis of (+)-rumphellaone A. The use of a furanyl iodide allowed for the later installation of the distinct γ-lactone moiety, and a photochemical decarboxylative Giese was used to directly form the methyl ketone from the free carboxylic acid. The challenging C8 methyl group was installed diastereoselectively using $Ti(CH_3)_4$, marking the first time that this methyl group has been installed synthetically without the use of a chiral catalyst. Our strategy led to the shortest synthesis of (+)-rumphellaone A to date, affording the product in 9 steps from commercially available starting materials; 6 steps from known cyclobutamide **6**.

2.8 EXPERIMENTAL SECTION

2.8.1 Materials and methods

Unless otherwise stated, reactions were performed under a nitrogen atmosphere using freshly dried solvents. Methylene chloride (CH_2Cl_2), diethyl ether (Et_2O), tetrahydrofuran (THF), 1,4-dioxane, *tert*-butyl methyl ether (TBME), and toluene (PhMe) were dried by passing through activated alumina columns. Methanol (MeOH) was distilled over calcium hydride. Acetonitrile (MeCN), *tert*-butanol (*t*-BuOH), anhydrous *N,N*-dimethylformamide (DMF), anhydrous *N,N*-dimethylacetamide (DMA), chloroform ($CHCl_3$), and absolute ethanol (EtOH) were used as received from Fisher Scientific. Methyl vinyl ketone was dried over K_2CO_3 and $CaCl_2$ and then distilled immediately prior to use. K_2HPO_4 was flame-dried under vacuum and dried at 0.200 Torr overnight and stored in a dessicator. Aryl iodides were purchased from Sigma-Aldrich or Combi-Blocks or prepared according to literature procedures. $NiBr_2$•dme and $NiCl_2$•dme were purchased from Strem and stored in a N_2-filled glovebox. Zinc dust and $Pd(OAc)_2$ were purchased from Strem and stored in a dessicator. $Ir[dF(CF_3)ppy]_2(dtbbpy)PF_6$ was purchased from Oakwood chemicals and used as received. $Pd(PPh_3)_4$ and Cs_2CO_3 were purchased from Sigma-Aldrich and stored in a N_2-filled glovebox. All other commercially obtained reagents were purchased from Sigma-Aldrich and used as received unless specifically indicated. Photochemical reactions were conducted using either Kessil A160WE blue LED lamps positioned 3–6 cm from the reactions using a computer fan to keep the reactions at ambient temperature, or 12W blue LED strips lining a beaker wrapped in aluminum foil. All reactions were monitored by thin-layer chromatography using EMD/Merck silica gel 60 F254 pre-coated plates (0.25 mm). Silica gel and basic alumina column chromatography was performed as described by

Still et al. (W. C. Still, M. Kahn, A. Mitra, *J. Org. Chem*. **1978**, *43*, 2923.) using silica gel (particle size 0.032–0.063) purchased from Silicycle and aluminum oxide (activated, basic, Brockmann I, 58 Å pore size, powder) purchased from Sigma-Aldrich. ^{1}H and ^{13}C NMR were recorded on a Varian Inova 500 (at 500 MHz and 125 MHz, respectively) or a Bruker Avance III HD with Prodigy cyroprobe (at 400 MHz and 101 MHz, respectively). ^{19}F NMR spectra were recorded on a Varian Inova 400 (at 376 MHz). NMR data is reported relative to internal chloroform (^{1}H, $\delta = 7.26$, ^{13}C, $\delta = 77.2$) or to internal methanol (^{1}H, $\delta = 3.31$, ^{13}C, $\delta = 49.0$) and $PhCF_3$ (^{19}F, $\delta = -63.7$). Data for ^{1}H NMR spectra are reported as follows: chemical shift (δ ppm) (multiplicity, coupling constant (Hz), integration). Multiplicity and qualifier abbreviations are as follows: s = singlet, d = doublet, t = triplet, q = quartet, m = multiplet. IR spectra were recorded on a Perkin Elmer Paragon 1000 spectrometer and are reported in frequency of absorption (cm^{-1}). HRMS were acquired using either an Agilent 6200 Series TOF with an Agilent G1978A Multimode source in electrospray ionization (ESI), atmospheric pressure chemical ionization (APCI), or mixed (MM) ionization mode. Specific optical rotations were recorded on a Jasco P-2000 polarimeter using a 100 mm cell.

Abbreviations used: Et_2O – diethyl ether; CH_2Cl_2 – methylene chloride; PhMe – toluene; EtOAc – ethyl acetate; THF – tetrahydrofuran; *t*-BuOH – *tert*-butanol; $CHCl_3$ – chloroform; MeCN – acetonitrile; DMF – *N,N*-dimethylformamide; DMA – *N,N*-dimethylacetamide; dtbbpy – 4,4'-di*tert*butylbipyridine; dme – 1,2-dimethoxyethane; TBME – *tert*-butyl methyl ether; ABNO – 9-azabicyclo[3.3.1]nonane *N*-oxyl.

2.8.2 Carboxylic Acid Derivatization

Large-Scale Synthesis of 89d

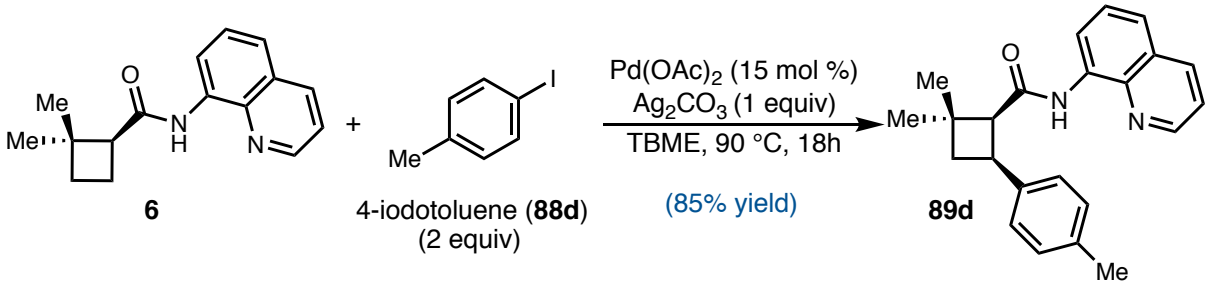

A 48 mL pressure flask was charged with cyclobutamide **6** (608 mg, 2.39 mmol, 1.00 equiv), Ag_2CO_3 (659 mg, 2.39 mmol, 1.00 equiv), and $Pd(OAc)_2$ (80.5 mg, 0.358 mmol, 15 mol%) followed by 4-iodotoluene (**88d**) (1.04 g, 4.78 mmol, 2.00 equiv). The solids were suspended in TBME (12 mL, 0.2 M). The vessel was sealed, placed in a pre-heated oil bath (90 ºC), and allowed to stir for 18 h. The reaction mixture was cooled to room temperature, diluted with CH_2Cl_2, and filtered through a 40 g celite plug with approx. 150 mL CH_2Cl_2. The solvent was removed *in vacuo*, and the crude oil was purified by silica gel flash chromatography (10 → 15% EtOAc/hexanes) to afford **89d** as a white solid (700. mg, 85% yield). *(See ch 1 for full characterization)*

Hydrolysis: Preparation of 191[87]

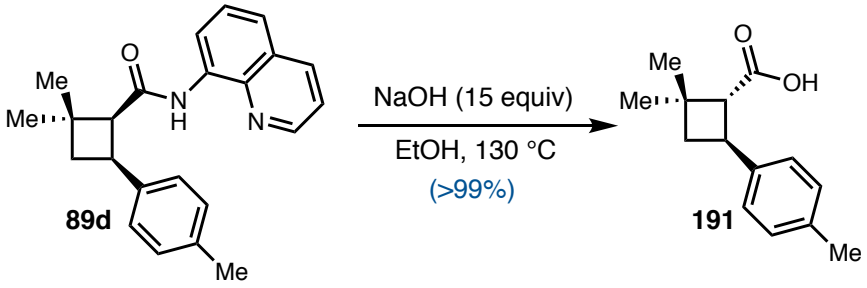

A 48 mL pressure flask was charged with *cis*-cyclobutamide **89d** (693 mg, 2.01 mmol, 1.00 equiv), sodium hydroxide (1.21 g, 30.2 mmol, 15 equiv), and absolute ethanol

(8.5 mL, 0.24 M). The flask was sealed and placed in a pre-heated oil bath (130 ºC) and stirred for 18 h. The reaction mixture was cooled to room temperature, and the solvent was removed *in vacuo*. The crude residue was diluted with 1 M aq HCl (38 mL) and EtOAc (38 mL). The organic and aqueous layers were separated, and the organic layer was washed with 1 M HCl (2 x 38 mL). The organic layer was dried over $MgSO_4$, filtered, and concentrated *in vacuo*. The crude reddish solid was purified by silica gel flash chromatography (15 → 20% EtOAc/hexanes) to afford **191** as an off-white solid (443 mg, >99% yield).

R_f = 0.31 (silica gel, 20% EtOAc/Hexanes, *p*-anisaldehyde)

$[\alpha]_D^{25}$ = +123.6° (c = 0.28, $CHCl_3$).

^{1}H NMR (400 MHz, $CDCl_3$): δ 7.13 (d, *J* = 1.1 Hz, 4H), 3.74 (q, *J* = 9.8 Hz, 1H), 2.91 (dd, *J* = 10.0, 0.8 Hz, 1H), 2.32 (s, 3H), 2.11 (ddd, *J* = 10.9, 8.9, 0.9 Hz, 1H), 1.95 (t, *J* = 10.5 Hz, 1H), 1.29 (s, 3H), 1.25 (s, 3H).

^{13}C NMR (101 MHz, $CDCl_3$): δ 178.8, 140.7, 135.9, 129.2, 126.6, 55.2, 39.4, 36.6, 35.1, 30.6, 23.6, 21.2.

FTIR (NaCl, thin film, cm^{-1}): 3021, 2957, 2927, 2867, 2731, 2647,1699, 1516, 1464, 1421 1370, 1281, 1238, 1162 1118, 937, 806, 716.

HRMS (ESI-TOF, *m/z*): calc'd for $C_{14}H_{22}NO_2$ $[M+NH_4]^+$: 236.1645; found: 236.1645.

Preparation of 195: Photochemical Giese with MVK[63]

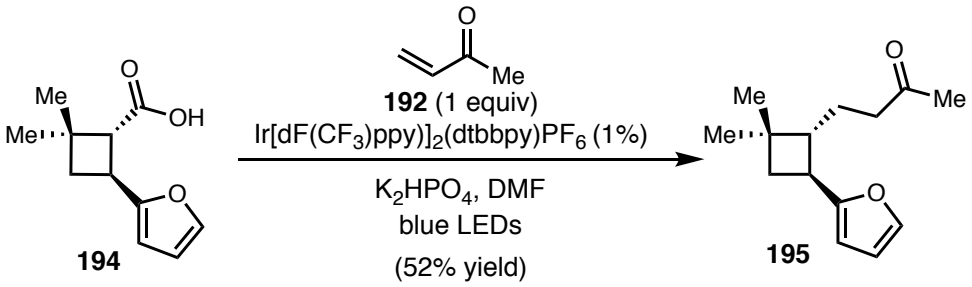

A 100 mL flame-dried round bottom flask was charged with carboxylic acid **194** (342 mg, 1.76 mmol, 1.00 equiv), $Ir[dF(CF_3)ppy]_2(dtbbpy)PF_6$ (19.7 mg, 0.0176 mmol, 0.01 equiv), and K_2HPO_4 (368 mg, 1.76 mmol, 1.00 equiv). The flask was evacuated and backfilled with N_2 three times. DMF (17.6 mL, 0.1 M) and freshly distilled methyl vinyl ketone (144 μL, 1.76 mmol, 1. equiv) were then added, and the reaction mixture was sparged with Ar for 5 minutes. The reaction flask was placed about 5 cm from a 34W blue LED lamp and was allowed to stir at room temperature under N_2. After 42 h, the reaction was quenched with sat aq $NaHCO_3$ and extracted with EtOAc (75 mL x 3). The combined organics were then dried with $MgSO_4$, filtered, and concentrated *in vacuo* to afford the product as a crude oil, which was then purified by silica gel flash chromatography (3 → 10% EtOAc/hexanes) to afford **195** as a white solid (201 mg, 52% yield).

$\mathbf{R_f}$ = 0.79 (silica gel, 20% EtOAc/Hexanes, UV, *p*-anisaldehyde)

$\mathbf{[\alpha]_D^{25}}$ = +57.8° (c = 1.07, $CHCl_3$).

^{1}H NMR (400 MHz, $CDCl_3$): δ 7.30 (dd, *J* = 1.8, 0.9 Hz, 1H), 6.27 (dd, *J* = 3.1, 1.9 Hz, 1H), 5.97 (dt, *J* = 3.2, 0.7 Hz, 1H), 2.97 (td, *J* = 9.6, 8.5 Hz, 1H), 2.41 – 2.21 (m, 2H), 2.09 – 1.97 (m, 4H), 1.93 (ddd, *J* = 10.7, 8.5, 0.7 Hz, 1H), 1.88 – 1.79 (m, 1H), 1.74 – 1.59 (m, 2H), 1.11 (s, 3H), 1.08 (s, 3H).

^{13}C NMR (101 MHz, $CDCl_3$): δ 209.1, 158.9, 140.9, 110.3, 104.0, 50.4, 41.5, 39.0, 34.6, 34.3, 30.6, 30.1, 24.2, 22.3.

FTIR (NaCl, thin film, cm^{-1}): 3114, 2953, 2933, 2863, 1717, 1593, 1506, 1451, 1411, 1368, 1360, 1235, 1159, 1150, 1009, 799, 729.

HRMS (ESI-TOF, *m/z*): calc'd for $C_{14}H_{20}O_2Na$ $[M+Na]^+$: 243.1356; found: 243.1359.

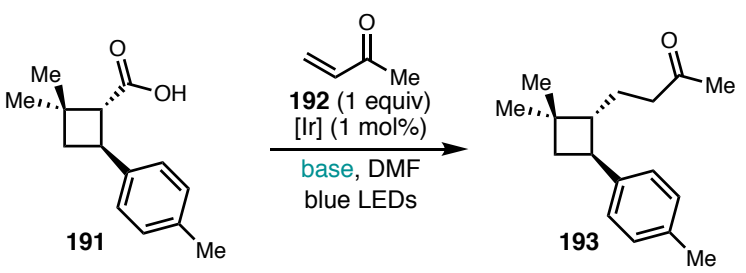

entry	scale	base	% yield
1	15 mg	K_2HPO_4	13
2	10 mg	Cs_2CO_3	63
3	22 mg	Cs_2CO_3	20
4	44 mg	Cs_2CO_3	10
5	22 mg	Cs_2CO_3	32*

*freeze-pump-thaw, 2.5 equiv MVK
[Ir] = Ir[dF(CF3)ppy)]2(dtbbpy)PF6

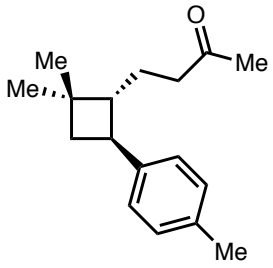

An analogous procedure was used for the investigation of the photochemical Giese of **191** with MVK to form **193**. This reaction was challenging to scale.

^{1}H NMR (400 MHz, Chloroform-*d*) δ 7.17 – 7.05 (m, 4H), 2.92 (td, *J* = 9.8, 8.5 Hz, 1H), 2.32 (s, 3H), 2.28 – 2.20 (m, 2H), 2.04 – 1.90 (m, 5H), 1.79 – 1.63 (m, 3H), 1.13 (s, 3H), 1.12 (s, 3H).

^{13}C NMR (101 MHz, $CDCl_3$) δ 209.16, 142.16, 135.54, 129.13, 126.93, 51.96, 41.81, 41.44, 41.33, 34.00, 30.95, 30.02, 24.68, 22.43, 21.14.

Undesired Formation of 198[61] (CRL-2-152)

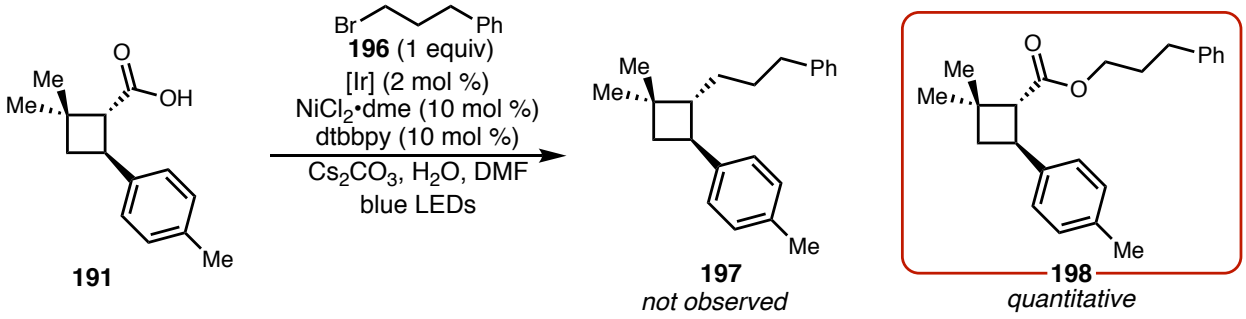

A flame-dried 25 mL round bottom flask was charged with carboxylic acid **191** (66 mg, 0.3 mmol, 1 equiv), and $Ir[dF(CF_3)ppy]_2(dtbbpy)PF_6$ (6.7 mg, 0.006 mmol, 0.02 equiv), $NiCl_2$•dme (6.6 mg, 0.030 mmol, 0.10 equiv), dtbbpy (8.1 mg, 0.030 mmol, 0.10 equiv), and Cs_2CO_3 (293 mg, 0.900 mmol, 3.00 equiv). Sealed with a septa cap and tape. The flask was evacuated and backfilled with N_2 x 3. DMF (6.0 mL, 0.05 M), H_2O (81 µL, 4.50 mmol, 15 equiv), and 1-bromo-3-phenyl propane (60 mg, 0.300 mmol, 1.0 equiv) were then added. Sparged with argon for about 20 minutes at 0 ºC and placed between 2 blue LEDs (~5 cm each). Let stir at room temperature overnight. Once the reaction was complete, the reaction mixture was diluted with sat aq NH_4Cl and EtOAc. The layers were separated, and the aqueous layer was extracted with EtOAc x 3. The combined organic layers were washed with aq. 1.0 M LiCl, dried over $MgSO_4$, filtered, and concentrated *in vacuo*. The crude oil was purified by silica gel chromatography, 2.5–5% EtOAc/hexanes to afford ester **198** as a white solid. (88.0 mg, 87% yield)

^{1}H NMR (400 MHz, Chloroform-*d*) δ 7.32 – 7.27 (m, 2H), 7.23 – 7.16 (m, 3H), 7.16 – 7.09 (m, 4H), 4.20 – 4.04 (m, 2H), 3.78 (q, *J* = 9.7 Hz, 1H), 2.86 (dd, *J* = 9.9, 0.8 Hz, 1H), 2.74 – 2.61 (m, 2H), 2.32 (s, 3H), 2.10 (ddd, *J* = 10.7, 8.9, 0.9 Hz, 1H), 2.01 – 1.90 (m, 3H), 1.29 (s, 3H), 1.19 (s, 3H).

^{13}C NMR (101 MHz, $CDCl_3$) δ 172.86, 141.36, 141.07, 135.79, 129.13, 128.58, 128.54, 126.62, 126.14, 63.57, 55.49, 39.35, 36.38, 35.25, 32.43, 30.70, 30.64, 23.74, 21.16.

Preparation of NHP Ester 199 (CRL-2-157)

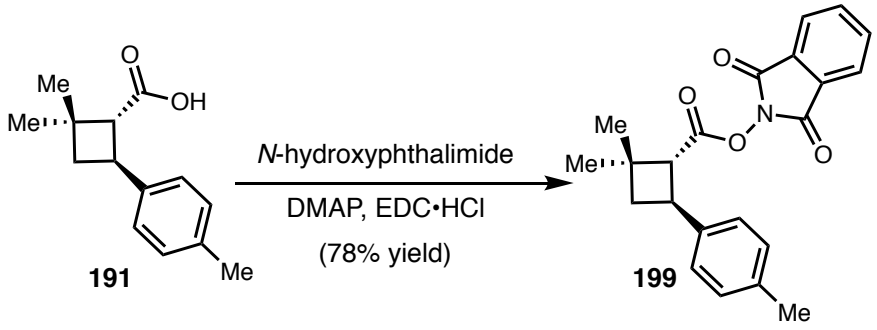

A 20 mL vial was charged with carboxylic acid **191** (208.9 mg, 0.957 mmol, 1.00 equiv), *N*-hydroxyphthalimide (156.1 mg, 0.957 mmol, 1.00 equiv), and 4-dimethylaminopyridine (11.7 mg, 0.096 mmol, 0.10 equiv). The vial was sealed with a rubber septum and evacuated and backfilled with N_2 three times. The solids were dissolved in CH_2Cl_2 (4 mL), and then EDC•HCl (201.8 mg, 1.05 mmol, 1.10 equiv) was added as a slurry in CH_2Cl_2 (1.3 mL). The reaction mixture was allowed to stir for 23 hours at room temperature. The reaction mixture was then transferred to a flask containing EtOAc (50 mL), and the resulting solids were removed by filtration. The filtrate was concentrated *in vacuo* and the crude oil was purified by silica gel flash chromatography (15 → 40% EtOAc/hexanes) to afford **199** as a white solid (272.8 mg, 78% yield).

R_f = 0.46 (silica gel, 20% EtOAc/Hexanes, UV, *p*-anisaldehyde)

$[\alpha]_D^{25}$ = +100.5° (c = 0.42, $CHCl_3$).

^{1}H NMR (400 MHz, $CDCl_3$): δ 7.94 – 7.83 (m, 2H), 7.83 – 7.73 (m, 2H), 7.14 (s, 4H), 3.87 (q, *J* = 9.8 Hz, 1H), 3.21 (dd, *J* = 9.9, 0.9 Hz, 1H), 2.33 (s, 3H), 2.20 (ddd, *J* = 10.8, 8.9, 0.9 Hz, 1H), 2.08 (t, *J* = 10.5 Hz, 1H), 1.42 (s, 3H), 1.39 (s, 3H).

^{13}C NMR (101 MHz, $CDCl_3$): δ 168.9, 162.2, 139.7, 136.3, 134.8, 129.3, 129.1, 126.5, 124.0, 52.5, 39.6, 37.5, 35.3, 30.5, 23.7, 21.2.

FTIR (NaCl, thin film, cm^{-1}): 3520, 3022, 2959, 2927, 2868, 1808, 1794, 1745, 1615, 1516, 1467, 1368, 1274, 1186, 1132, 1081, 1016, 972, 878, 811, 786, 696.

HRMS (ESI-TOF, *m/z*): calc'd for $C_{22}H_{21}NO_4$ $[M+NH_4]^+$: 381.1809; found: 381.1814.

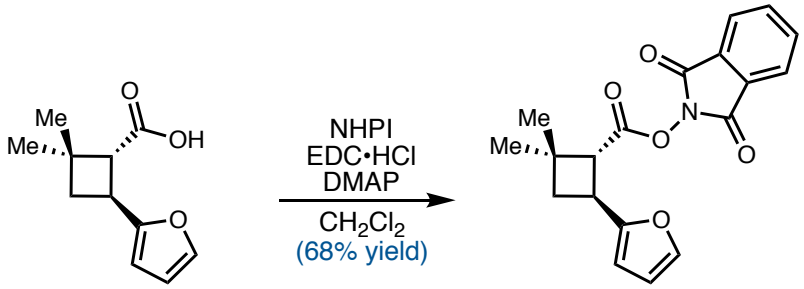

194 **S1**

An analogous procedure was used for the preparation of furan NHP ester **S1**. Concentrated the crude material onto celite and purified by silica gel chromatography, 5–20% EtOAc/hexanes to afford **S1** (26.4 mg, 68% yield)

R_f = 0.32 (silica gel, 20% EtOAc/Hexanes, UV, *p*-anisaldehyde)

^{1}H NMR (300 MHz, Chloroform-*d*) δ 7.87 (dt, *J* = 5.4, 2.7 Hz, 2H), 7.78 (dt, *J* = 5.6, 2.7 Hz, 2H), 7.35 (q, *J* = 1.5, 1.0 Hz, 1H), 6.29 (q, *J* = 2.3, 1.8 Hz, 1H), 6.10 (t, *J* = 2.6 Hz, 1H), 3.84 (qd, *J* = 9.6, 2.0 Hz, 1H), 3.41 (dd, *J* = 9.6, 2.0 Hz, 1H), 2.15 (ddt, *J* = 18.1, 11.1, 8.8 Hz, 2H), 1.42 (d, *J* = 2.0 Hz, 3H), 1.38 (d, *J* = 2.1 Hz, 3H).

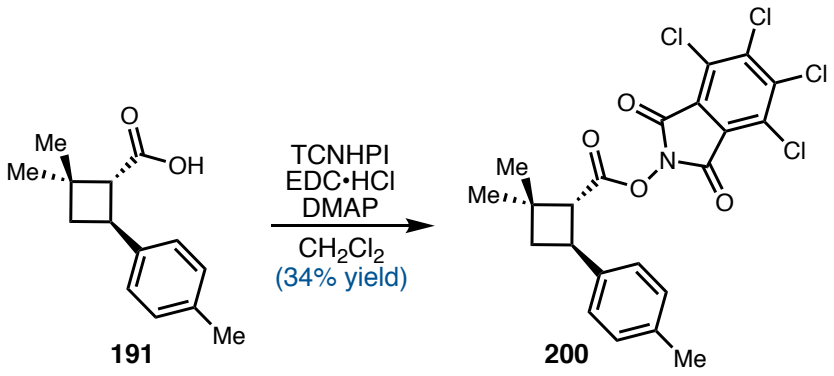

An analogous procedure 0.4 mmol scale was used for the preparation of tetrachloro NHP ester **200**. Dissolved in DCM, triterated with EtOAc to crash out EDC salts. Filter to remove the salts and concentrate the filtrate. Purify the resulting oil by fast silica plug, 10–30% EtOAc/hex. Isolated **200** (69 mg, 34% yield) plus 53 mg ~1:1 **200**/**191**.

$\mathbf{R}_f$ = 0.74 (silica gel, 20% EtOAc/Hexanes, UV, *p*-anisaldehyde)

^{1}H NMR (300 MHz, Chloroform-*d*) δ 7.19 – 7.03 (m, 4H), 3.87 (q, *J* = 9.8 Hz, 1H), 3.21 (d, *J* = 9.9 Hz, 1H), 2.34 (d, *J* = 1.3 Hz, 3H), 2.22 (dd, *J* = 10.7, 9.1 Hz, 1H), 2.09 (t, *J* = 10.5 Hz, 1H), 1.41 (dd, *J* = 7.0, 1.4 Hz, 6H).

Negishi Coupling to Form Diaryl Cyclobutane 202[79]

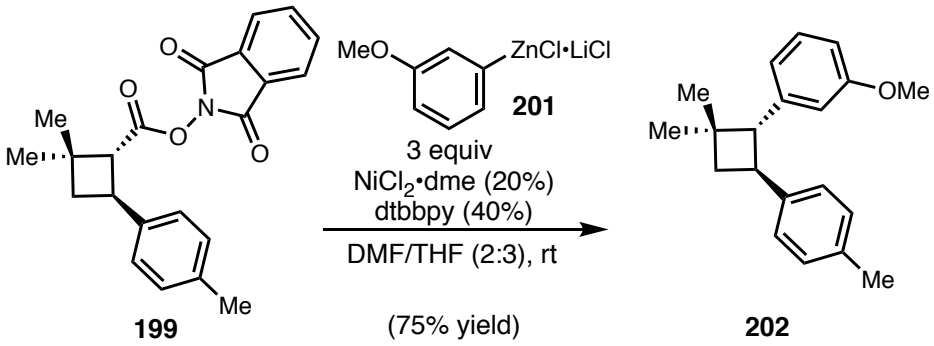

A 25 mL round bottom flask was charged with **199** (109 mg, 0.300 mmol, 1.00 equiv), $NiCl_2$•dme (13.2 mg, 0.060 mmol, 0.20 equiv), and dtbbpy (32.2 mg, 0.120 mmol, 0.40

equiv). The flask was sealed with a septum and then evacuated and backfilled with argon three times. DMF was then added (3.2 mL), forming a green solution. Freshly prepared aryl zinc reagent **201** (4.8 mL, 0.90 mmol, 3.0 equiv, 0.19 M in THF) was then added and the solution turned red. The reaction was allowed to stir for 18 h, at which point the reaction was quenched with 1 M HCl (10 mL) and diluted with EtOAc (10 mL). The organic and aqueous layers were separated, and the organic layer was washed with water (10 mL) and brine (10 mL). The organic layer was dried with $MgSO_4$, filtered, and concentrated *in vacuo* to afford a red oil. The crude material was then purified by silica gel flash chromatography (2.5 → 25% PhMe/hexanes) to afford **202** as a clear oil (63 mg, 75% yield).

R_f = 0.77 (silica gel, 20% EtOAc/Hexanes, UV, *p*-anisaldehyde)

$[\alpha]_D^{25}$ = +195° (c = 0.42, $CHCl_3$).

^{1}H NMR (500 MHz, $CDCl_3$): δ 7.26 – 7.17 (m, 1H), 7.14 (d, *J* = 8.0 Hz, 2H), 7.08 (d, *J* = 7.9 Hz, 2H), 6.81 (ddt, *J* = 7.6, 1.7, 0.9 Hz, 1H), 6.80 – 6.71 (m, 2H), 3.79 (s, 3H), 3.32 (d, *J* = 10.4 Hz, 1H), 2.30 (s, 3H), 2.16 (ddd, *J* = 10.3, 8.5, 0.7 Hz, 1H), 1.90 (t, *J* = 10.1 Hz, 1H), 1.28 (s, 3H), 0.88 (s, 3H).

^{13}C NMR (101 MHz, $CDCl_3$): δ 159.6, 142.8, 142.1, 135.5, 129.1, 129.0, 126.6, 120.0, 113.6, 111.0, 56.7, 55.2, 40.2, 37.4, 37.2, 30.9, 23.3, 21.1.

FTIR (NaCl, thin film, cm^{-1}): 3014, 2947, 2859, 1596, 1514, 1490, 1458, 1428, 1371, 1318, 1292, 1252, 1166, 1040, 832, 808, 797, 694.

HRMS (ESI-TOF, *m/z*): calc'd for $C_{15}H_{25}O_3$ $[M+H]^+$: 281.1900; found: 281.1899.

Attempted Preparation of 197 from 200[70]

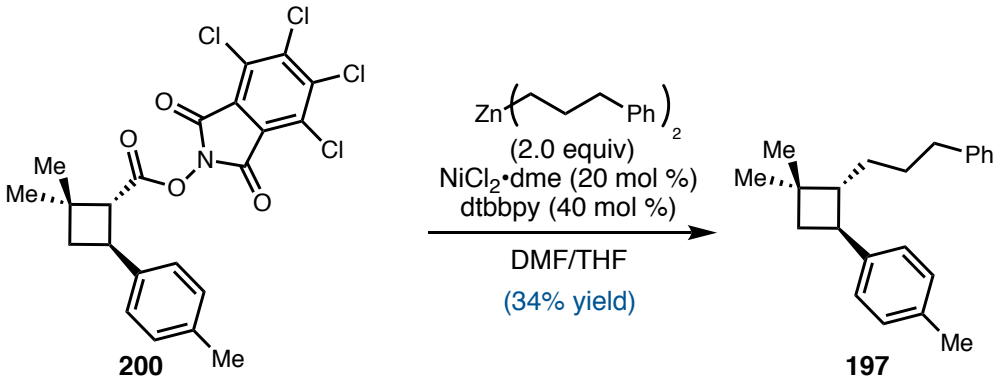

Alkyl zinc species prepared from 1-bromo-3-phenyl propane using known methods. To a 1-dram vial was added **200** (50.1 mg, 0.1 mmol, 1.0 equiv). The vial was evacuated and backfilled with argon x 3. $NiCl_2$•dme (4.4 mg, 0.02 mmol, 20 mol%) and dtbbpy (10.7 mg, 0.040 mmol, 40 mol%) were added as a stock solution in DMF (1.0 mL, 0.1 M). After stirrin for about 5 min, the alkyl zinc reagent (1.54 mL, 0.13 M in THF, 0.200 mmol, 2.00 equiv) was then added and the reaction mixture was allowed to stir overnight. Once complete, the reaction was quenched with 1M HCl. The aqueous layer was extract with EtOAc, and the organic layer was washed with water and saturated brine. The organic layer was dried over Na_2SO_4, filtered, and concentrated *in vacuo*. The crude oil was purified by silica gel chromatography, 1–50% EtOAc/hexanes. Fractions containing the product were isolated and repurified by prep TLC (10% EtOAc/hexanes, let run up the place twice). Isolated 19.4 mg 1:2.4 **197**:primary alkyl homocoupling.

R_f = 0.72 (silica gel, 10% EtOAc/Hexanes x 2, UV, *p*-anisaldehyde, prep plate)

1H NMR (400 MHz, Chloroform-d) δ 7.24 – 7.13 (m, 7H), 7.13 – 7.06 (m, 9H), 7.04 (d, J = 6.1 Hz, 3H), 7.02 – 6.96 (m, 3H), 2.82 (td, J = 9.8, 8.4 Hz, 1H), 2.56 – 2.48 (m, 5H), 2.43 (q, J = 6.9 Hz, 2H), 2.24 (s, 3H), 1.89 (ddd, J = 10.6, 8.5, 0.8 Hz, 1H), 1.64 (t, J = 10.4

Hz, 1H), 1.58 – 1.48 (m, 5H), 1.47 – 1.34 (m, 3H), 1.31 – 1.25 (m, 5H), 1.05 (s, 3H), 1.01 (s, 3H).

Reductive Coupling of NHP Ester 199 and Vinyl Bromide 204: Preparation of 205[84,86]

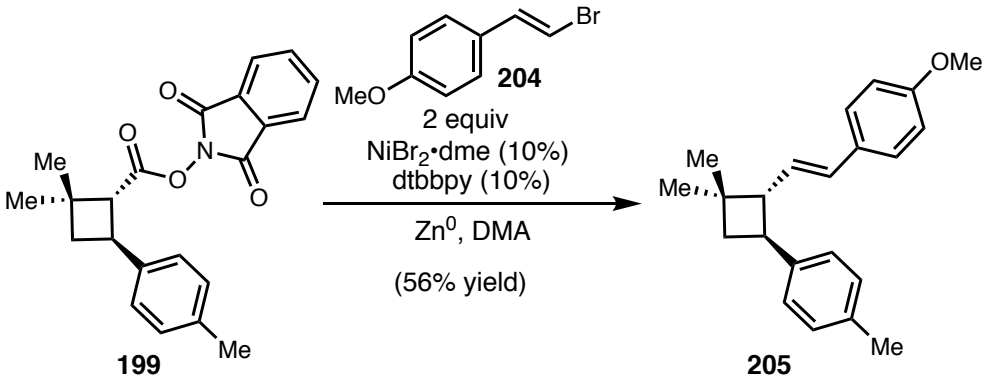

A 1-dram vial containing a 2-dram stir bar was charged with NHP ester **199** (75.7 mg, 0.208 mmol, 1.00 equiv) and vinyl bromide **204** (63.9 mg, 0.300 mmol, 1.50 equiv). A separate ½-dram vial containing a stir bar was charged with dtbbpy (5.4 mg, 0.020 mmol, 0.10 equiv). Both vials were brought into a N_2-filled glovebox. The vial containing dtbbpy was charged with $NiBr_2$•dme (6.2 mg, 0.020 mmol, 0.10 equiv) and DMA (0.200 mL, 1.0 M) and allowed to stir for 10 minutes. The vial containing **199** and **204** was charged with Zn powder (25.4 mg, 0.400 mmol, 2.00 equiv). Once the catalyst solution prestir was complete, the catalyst solution was added to the reaction vial via pipette. The vial was then sealed with a Teflon-lined cap, removed from the glovebox, placed in a pre-heated oil bath (28 °C), and allowed to stir for 15 h. Once the reaction was complete, the reaction mixture was diluted with Et_2O and passed through a short silica plug, eluting with Et_2O. The material was concentrated onto celite *in vacuo*, and the resulting powder was purified by silica gel flash chromatography (0 → 30% PhMe/hexanes) to afford **205** as a white solid (34.1 mg, 56% yield).

$\mathbf{R}_f$ = 0.71 (silica gel, 20% EtOAc/Hexanes, UV, *p*-anisaldehyde)

$[\alpha]_D^{25}$ = +238° (c = 1.66, $CHCl_3$).

^{1}H NMR (400 MHz, $CDCl_3$): δ 7.35 – 7.28 (m, 2H), 7.15 (d, *J* = 8.1 Hz, 2H), 7.11 (d, *J* = 8.0 Hz, 2H), 6.89 – 6.83 (m, 2H), 6.34 (d, *J* = 15.8 Hz, 1H), 6.22 (dd, *J* = 15.8, 7.8 Hz, 1H), 3.81 (s, 3H), 3.41 (q, J = 9.5 Hz, 1H), 2.73 (ddt, *J* = 9.5, 7.7, 0.9 Hz, 1H), 2.33 (s, 3H), 2.11 (ddd, *J* = 10.7, 8.5, 0.8 Hz, 1H), 1.87 (t, *J* = 10.3 Hz, 1H), 1.18 (s, 3H), 1.16 (s, 3H).

^{13}C NMR (101 MHz, $CDCl_3$): δ 158.9, 142.3, 135.3, 130.7, 130.0, 129.0, 128.1, 127.3, 126.6, 114.0, 55.9, 55.4, 40.0, 39.6, 36.9, 30.4, 23.6, 21.2.

FTIR (NaCl, thin film, cm^{-1}): 2999, 2951, 2921, 2860, 1607, 1511, 1462, 1370, 1249, 1174, 1106, 1036, 966, 806.

HRMS (ESI-TOF, *m/z*): calc'd for $C_{22}H_{27}O$ $[M+H]^+$: 307.2056; found: 307.2062.

Photochemical Minisci Arylation: Preparation of 206 and S2[68]

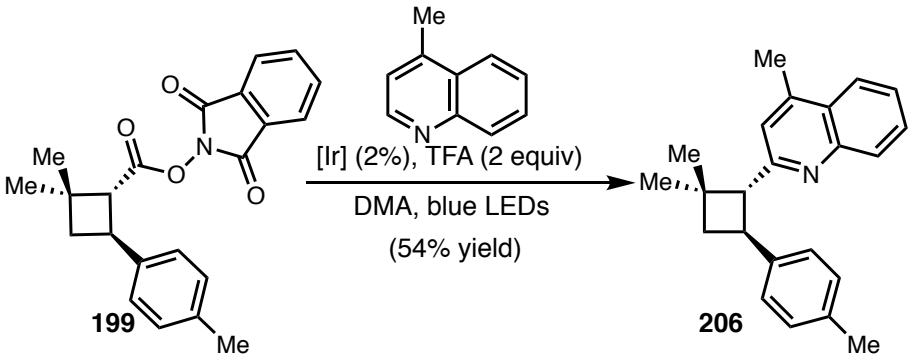

A flame-dried 2-dram vial was charged with NHP ester **199** (72.7, mg, 0.200 mmol, 1.00 equiv) and $Ir[dF(CF_3)ppy]_2(dtbbpy)PF_6$ (4.5 mg, 0.004 mmol, 0.02 equiv). The vial was evacuated and backfilled with Ar three times. DMA (2.0 mL, 0.1 M) and lepidine (43.0 mg, 0.300 mmol, 1.50 equiv) were then added, and the reaction mixture was cooled to 0 °C and sparged with Ar 10 minutes. The reaction vial was removed from the ice bath,

trifluoroacetic acid (30.6 μL, 0.400 mmol, 2.00 equiv) was added, and the reaction mixture was allowed to stir in front of a 34W blue LED lamp (~3 cm from the lamp). The reaction was monitored by TLC (20% EtOAc/hexanes). Once the reaction was complete (~4 h), the reaction was quenched with 1 mL NEt_3 and 2 mL H_2O. The aqueous layer was extracted with EtOAc (3 mL x 4), and the combined organics were washed with 1 M LiCl. The organic layer was then dried with Na_2SO_4, filtered, and concentrated onto celite *in vacuo*, and the resulting powder was purified by silica gel flash chromatography (0 → 5% EtOAc/hexanes) to afford **206** as a yellow solid (34.1 mg, 54% yield).

R_f = 0.76 (silica gel, 20% EtOAc/Hexanes, UV, *p*-anisaldehyde)

$[\alpha]_D^{25}$ = +305° (c = 1.47, $CHCl_3$).

^{1}H NMR (400 MHz, $CDCl_3$): δ 8.09 (d, *J* = 8.4 Hz, 1H), 7.95 (dd, *J* = 8.3, 1.4 Hz, 1H), 7.67 (ddd, *J* = 8.3, 6.7, 1.4 Hz, 1H), 7.50 (ddd, *J* = 8.1, 6.8, 1.3 Hz, 1H), 7.21 (d, *J* = 7.9 Hz, 2H), 7.08 (d, *J* = 8.1 Hz, 3H), 4.39 (q, *J* = 9.7 Hz, 1H), 3.52 (d, *J* = 10.1 Hz, 1H), 2.67 (s, 3H), 2.30 (s, 3H), 2.20 (dd, *J* = 10.4, 8.8 Hz, 1H), 2.04 (t, *J* = 10.3 Hz, 1H), 1.39 (s, 3H), 0.89 (s, 3H).

^{13}C NMR (101 MHz, $CDCl_3$): δ ^{13}C NMR (101 MHz, $CDCl_3$) δ 160.6, 148.0, 143.4, 142.6, 135.2, 130.2, 129.0, 128.9, 128.8, 128.7, 127.1, 126.9, 126.8, 125.4, 123.7, 121.7, 59.1, 39.7, 37.9, 35.4, 31.2, 23.7, 21.1, 18.9.

FTIR (NaCl, thin film, cm^{-1}): 3428, 3950, 2925, 2360, 1603, 1558, 1514, 1446, 1379, 1260, 1176, 1162, 1034, 809, 756.

HRMS (ESI-TOF, *m/z*): calc'd for $C_{23}H_{26}N$ $[M+H]^+$: 316.2060; found: 316.2063.

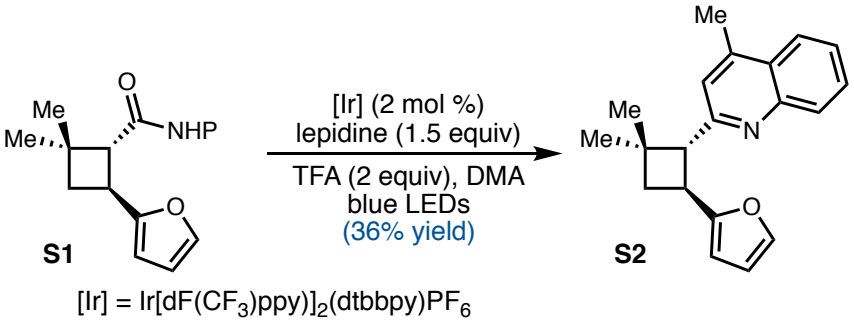

An analogous procedure was used for the preparation of **S2**. Crude material purified by silica gel chromatography. 5–20% EtOAc/hexanes. Isolated **S2** (10 mg, 36% yield).

R_f = 0.82 (silica gel, 20% EtOAc/Hexanes, UV, *p*-anisaldehyde)

^{1}H NMR (400 MHz, Chloroform-*d*) δ 8.01 (ddd, *J* = 8.5, 1.3, 0.6 Hz, 1H), 7.86 (ddd, *J* = 8.3, 1.5, 0.6 Hz, 1H), 7.58 (ddd, *J* = 8.4, 6.8, 1.4 Hz, 1H), 7.41 (ddd, *J* = 8.2, 6.8, 1.3 Hz, 1H), 7.23 (dd, *J* = 1.8, 0.9 Hz, 1H), 6.98 (d, *J* = 1.1 Hz, 1H), 6.19 (dd, *J* = 3.2, 1.8 Hz, 1H), 6.03 (dt, *J* = 3.2, 0.8 Hz, 1H), 4.38 – 4.15 (m, 1H), 3.58 (d, *J* = 9.9 Hz, 1H), 2.59 (d, *J* = 1.0 Hz, 3H), 2.10 – 1.98 (m, 2H), 1.34 (s, 3H), 0.78 (s, 3H).

^{13}C NMR (101 MHz, $CDCl_3$) δ 159.66, 158.38, 147.76, 143.28, 140.81, 129.97, 128.62, 126.91, 125.24, 123.43, 121.40, 110.04, 104.21, 56.83, 38.47, 37.72, 30.85, 29.61, 23.19, 18.70.

Photochemical Borylation: Preparation of 207 and S3[69]

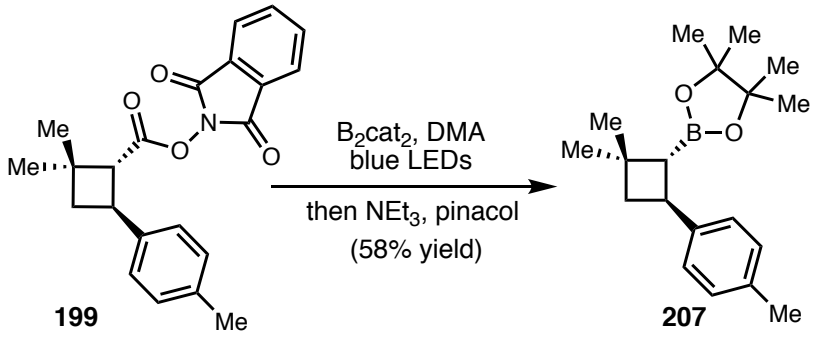

A flame-dried 2-dram vial was charged with NHP ester **199** (72.7, mg, 0.200 mmol, 1.00 equiv) and B_2cat_2 (59.5 mg, 0.250 mmol, 1.25 equiv). The vial was evacuated and backfilled with Ar three times. DMA (2.0 mL, 0.1 M) was then added, and the reaction mixture was cooled to 0 °C and sparged with Ar for 10 minutes. The reaction vial was removed from the ice bath and suspended inside a large beaker lined with 12W blue LED strips and covered with foil. After 21 h, pinacol (94.5 mg, 0.800 mmol, 4.00 equiv) was added as a solution in NEt_3 (700 μL, 5.04 mmol, 25.2 equiv). After 2 h, the reaction was quenched with H_2O, saturated aqueous NH_4Cl, and EtOAc. The organic and aqueous layers were separated, and the aqueous layer was extracted with EtOAc (2 mL x 3). The combined organics were then dried with Na_2SO_4, filtered, and concentrated onto celite *in vacuo*, and the resulting powder was purified by silica gel flash chromatography (0 → 5% EtOAc/hexanes) to afford **207** as a white solid (35.1 mg, 58% yield).

R_f = 0.81 (silica gel, 20% EtOAc/Hexanes, UV, *p*-anisaldehyde)

$[\alpha]_D^{25}$ = +77.5° (c = 1.47, $CHCl_3$).

^{1}H NMR (400 MHz, $CDCl_3$): δ 7.09 (s, 4H), 3.53 (td, *J* = 10.2, 8.2 Hz, 1H), 2.31 (s, 3H), 2.13 (ddd, *J* = 10.6, 8.2, 0.8 Hz, 1H), 2.02 (t, *J* = 10.3 Hz, 1H), 1.68 (d, *J* = 10.5 Hz, 1H), 1.26 (s, 6H), 1.24 (d, *J* = 1.1 Hz, 9H), 1.16 (s, 3H).

^{13}C NMR (101 MHz, $CDCl_3$): δ 144.1, 134.9, 128.9, 126.3, 83.2, 42.9, 34.3, 34.0, 32.4, 26.6, 25.3, 24.9, 21.1. (Note: the resonance from the carbon attached to the boron was not visible).

FTIR (NaCl, thin film, cm^{-1}): 3444, 2980, 2922, 2946, 2862, 2728, 1898, 1652, 1514, 1462, 1414, 1380, 1363, 1345, 1329, 1275, 1237, 1143, 1112, 1080, 1020, 967, 854, 809, 730.

HRMS (ESI-TOF, *m/z*): calc'd for $C_{19}H_{29}BO_2Na$ $[M+Na]^+$: 323.2158; found: 323.2174.

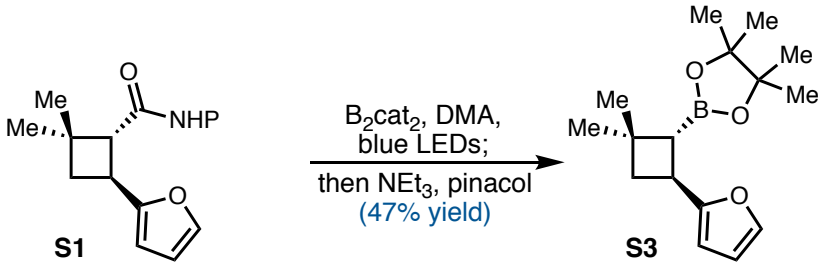

An analogous procedure was used for the preparation of **S3**. Crude material purified by silica gel chromatography, 5–20% EtOAc/hexanes. Isolated **S3** as a pale yellow oil (13.1 mg, 47% yield).

R_f = 0.74 (silica gel, 20% EtOAc/Hexanes, UV, *p*-anisaldehyde)

^{1}H NMR (400 MHz, Chloroform-*d*) δ 7.22 (dd, *J* = 1.8, 0.9 Hz, 1H), 6.19 (dd, *J* = 3.1, 1.9 Hz, 1H), 5.89 (dt, *J* = 3.1, 0.9 Hz, 1H), 3.49 – 3.29 (m, 1H), 2.06 – 2.00 (m, 1H), 2.00 – 1.94 (m, 1H), 1.76 (d, *J* = 10.1 Hz, 1H), 1.52 (s, 1H), 1.17 (d, *J* = 5.3 Hz, 13H), 1.13 (s, 3H), 1.11 (s, 3H).

^{13}C NMR (101 MHz, $CDCl_3$) δ 159.95, 140.58, 109.86, 103.26, 83.04, 41.48, 34.38, 31.98, 27.74, 26.33, 25.01, 24.76.

Reduction to Form Alcohol 208

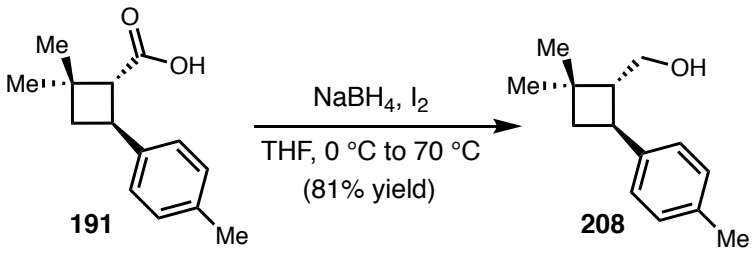

A 2-dram vial containing a stir bar was charged with **191** (87 mg, 0.400 mmol, 1.00 equiv) and $NaBH_4$ (37.8 mg, 1.00 mmol, 2.5 equiv). The vial was then evacuated and backfilled

with N_2 three times. THF (3.0 mL) was added and the reaction mixture was cooled to 0 °C. I_2 (121.8 mg, 0.480 mmol, 1.2 equiv) was then added as a solution in THF (1 mL) dropwise. The vial was then sealed with a Teflon-lined cap, placed in a pre-heated oil bath (70 ºC), and allowed to stir overnight. Once the reaction was complete, the reaction was cooled to room temperature and quenched with MeOH until bubbling stopped and the reaction mixture turned clear. The reaction mixture was then concentrated, then treated with 20% KOH (4 mL) and allowed to stir for 5 h at room temperature. The aqueous layer was then extracted with EtOAc (6 x 5 mL). The combined organic layers were dried over Na_2SO_4 and concentrated to afford **208** (82.2 mg, quant yield) as a white solid which was carried forward without further purification.

R_f = 0.38 (silica gel, 20% EtOAc/Hexanes, UV, *p*-anisaldehyde)

$[\alpha]_D^{25}$ = +57.0° (c = 0.42, $CHCl_3$).

^{1}H NMR (400 MHz, $CDCl_3$): δ 7.18 – 7.08 (m, 4H), 3.75 (qd, *J* = 11.0, 7.2 Hz, 2H), 3.06 (q, *J* = 9.5 Hz, 1H), 2.34 (s, 3H), 2.28 (dddd, *J* = 9.4, 8.3, 6.1, 0.7 Hz, 1H), 2.05 (ddd, *J* = 10.8, 8.7, 0.8 Hz, 1H), 1.82 (t, *J* = 10.3 Hz, 1H), 1.21 (s, 6H).

^{13}C NMR (101 MHz, $CDCl_3$): δ 141.9, 135.6, 129.1, 126.7, 63.6, 53.9, 40.6, 37.6, 33.7, 31.4, 22.5, 21.1.

FTIR (NaCl, thin film, cm^{-1}): 3248, 2954, 2926, 2896, 2864, 1896, 1514, 1453, 1413, 1379, 1368, 1326, 1260, 1218, 1190, 1110, 1092, 1033, 1013, 812, 772.

HRMS (ESI-TOF, *m/z*): calc'd for $C_{14}H_{24}NO$ $[M+NH_4]^+$: 222.1852; found: 222.1846.

Stahl Oxidation to Form Aldehyde 209[88]

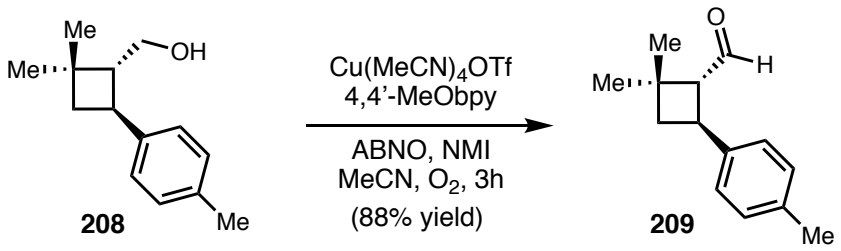

208 (0.400 mmol, 1.00 equiv) was dissolved in 1.2 mL MeCN in a 20 mL scintillation vial. In a separate vial $Cu(MeCN)_4OTf$ (7.5 mg, 0.02 mmol, 0.05 equiv) and 4,4'-MeObpy (4.3 mg, 0.02 mmol, 0.05 equiv)) were dissolved in 0.4 mL MeCN and allowed to stir until the solution turned an opaque blue. To this vial was added a solution of ABNO (0.6 mg, 0.004 mmol, 0.01 equiv) and *N*-methylimidazole (3.3 mg, 0.04 mmol, 0.10 equiv) in 0.4 mL MeCN. Once the catalyst solution turned green, it was added to the reaction mixuture and allowed to stir open to air. After 3 h and 6 h, additional portions of catalyst ($Cu(MeCN)_4OTf$ (7.5 mg, 0.02 mmol, 0.05 equiv), 4,4'-MeObpy (4.3 mg, 0.02 mmol, 0.05 equiv) ABNO (0.6 mg, 0.004 mmol, 0.01 equiv), and *N*-methylimidazole (3.3 mg, 0.04 mmol, 0.10 equiv) dissolved in 0.8 mL MeCN) were added. After the addition at 6 h, the reaction vessel was sealed with a rubber septum and the reaction mixture was sparged with $O_{2(g)}$ and allowed to stir under an O_2 atmosphere for an additional 15.5 h. When the reaction was judged to be done by TLC, the reaction mixture was filtered over a short silica plug, eluting with 20% EtOAc/hexanes, and the resulting solution was concentrated *in vacuo* to give **209** as a brown oil (71.1 mg, 87% yield).

$\mathbf{R}_f$ = 0.69 (silica gel, 20% EtOAc/Hexanes, UV, *p*-anisaldehyde)

$\mathbf{[\alpha]_D^{25}}$ = +62.9° (c = 1.66, $CHCl_3$).

^{1}H NMR (400 MHz, $CDCl_3$): δ 9.86 (d, *J* = 1.6 Hz, 1H), 7.21 – 7.01 (m, 5H), 3.88 (q, *J* = 9.6 Hz, 1H), 2.97 (ddd, *J* = 9.7, 1.7, 0.9 Hz, 1H), 2.34 (s, 3H), 2.12 (ddt, *J* = 10.5, 8.9, 0.8 Hz, 1H), 2.02 (t, *J* = 10.5 Hz, 1H), 1.36 (s, 3H), 1.26 (s, 3H).

^{13}C NMR (101 MHz, $CDCl_3$): δ 203.0, 140.8, 135.8, 129.1, 129.1, 126.5, 126.5, 62.5, 39.9, 37.5, 33.0, 31.3, 24.0, 23.6, 21.1, 21.1.

FTIR (NaCl, thin film, cm^{-1}): 3248, 2954, 2926, 2896, 2864, 1896, 1514, 1453, 1413, 1379, 1368, 1326, 1260, 1218, 1190, 1110, 1092, 1033, 1013, 812, 772.

HRMS (ESI-TOF, *m/z*): calc'd for $C_{14}H_{22}NO$ $[M+NH_4]^+$: 220.1696; found: 220.1691.

Acid Chloride Formation and Suzuki Cross-Coupling to Form Aryl Ketone 210[89]

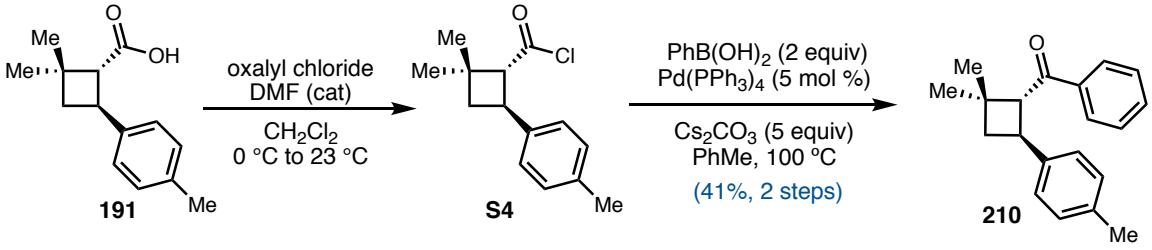

To a flame-dried 2-dram vial was added carboxylic acid **191** (87.3 mg, 0.400 mmol, 1 equiv). The vial was sealed with a septum vial cap and tape and was evacuated and backfilled with N_2 three times. CH_2Cl_2 (0.8 mL, 0.5 M) and 1-2 drops DMF were added, and the reaction mixture was cooled to 0 °C. Oxalyl chloride (0.040 mL, 0.480 mmol, 1.2 equiv) was then added dropwise. Once the addition was complete, the reaction was allowed to stir at room temperature for 1 h, at which point the solvent was removed *in vacuo* to afford acid chloride **S4** as a crude oil, 91 mg 96% yield. **S4** was taken forward without further purification. (characterization for **S4** is in the next section for the synthesis of alkyl ketone **211**)

A flame-dried 2-dram vial was charged with phenyl boronic acid (135 mg, 1.1 mmol, 3.0 equiv). The vial was brought into an N_2-filled glovebox and charged with Cs_2CO_3 (589 mg, 1.8 mmol, 5.0 equiv) and $Pd(PPh_3)_4$ (21.3 mg, 0.018 mmol, 5 mol%). **S4** (87.1 mg, 0.37 mmol, 1.0 equiv) was then added as a stock solution in PhMe (3.7 mg, 0.1 M). The reaction vessel was sealed with a septa cap and tape, brought out of the glovebox, and placed in a 100 ºC oil bath. The reaction was allowed to stir for 24 hours. Once the reaction was complete and allowed to cool, the reaction mixture was diluted with EtOAc, washed with H_2O, sat aq $NaHCO_3$ (goes from green to brown), and sat brine. The organic layer was dried over Na_2SO_4, filtered, and concentrated *in vacuo*. The crude material was purified by silica gel chromatography, 1–5% EtOAc/hexanes to afford **210** as a yellow solid (44 mg, 41% yield over 2 steps).

HRMS (ESI-TOF, *m/z*): calc'd for $C_{20}H_{26}NO$ $[M+NH_4]^+$: 296.2009; found: 296.2010.

^{1}H NMR (400 MHz, Chloroform-*d*) δ 8.00 – 7.90 (m, 2H), 7.60 – 7.51 (m, 1H), 7.46 (ddt, *J* = 8.1, 6.6, 1.1 Hz, 2H), 7.12 (t, *J* = 7.8 Hz, 3H), 4.16 (q, *J* = 9.5 Hz, 1H), 3.80 (d, *J* = 9.4 Hz, 1H), 2.30 (s, 3H), 2.17 – 2.07 (m, 2H), 1.36 (s, 3H), 0.98 (s, 3H).

^{13}C NMR (101 MHz, $CDCl_3$) δ 199.25, 141.60, 137.74, 135.61, 133.07, 129.10, 128.67, 128.47, 126.67, 59.12, 38.89, 37.67, 33.18, 30.74, 23.43, 21.13.

Reductive Coupling of Acid Chloride SX to Form Alkyl Ketone 211[90]

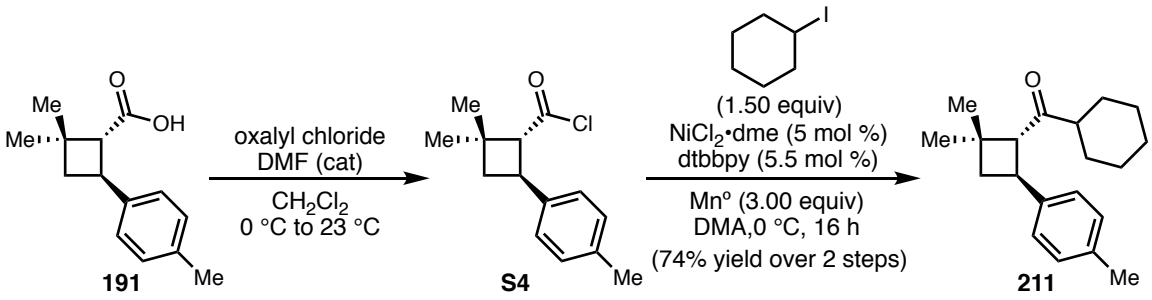

A 1-dram vial containing a stir bar was charged with carboxylic acid **191** (87.3 mg, 0.400 mmol, 1 equiv). The vial was sealed with a septum vial cap and tape and was evacuated and backfilled with N_2 three times. CH_2Cl_2 (0.8 mL, 0.5 M) and 1-2 drops DMF were added, and the reaction mixture was cooled to 0 °C. Oxalyl chloride (0.050 mL, 0.560 mmol, 1.4 equiv) was then added dropwise. Once the addition was complete, the reaction was allowed to stir at room temperature for 1 h, at which point the solvent was removed *in vacuo* to afford acid chloride **S4** as a crude oil. **S4** was taken forward without further purification.

^{1}H NMR (400 MHz, $CDCl_3$): δ 7.16 – 7.06 (m, 4H), 3.79 (q, *J* = 9.7 Hz, 1H), 3.29 (dd, *J* = 9.8, 0.9 Hz, 1H), 2.33 (s, 3H), 2.11 (ddd, *J* = 10.9, 9.1, 1.0 Hz, 1H), 2.01 – 1.88 (m, 1H), 1.41 (s, 3H), 1.31 (s, 3H).

^{13}C NMR (101 MHz, $CDCl_3$): δ 173.3, 139.2, 136.5, 129.4, 126.5, 66.1, 39.0, 37.0, 30.0, 23.2, 21.2.

A flame-dried 1-dram vial containing a 2-dram stir bar (tested before to ensure it would stir) was charged with $NiCl_2$•dme (4.4 mg, 0.020 mmol, 0.05 equiv), dtbbpy (5.9 mg, 0.022 mmol, 0.055 equiv), and Mn° powder (65.9 mg, 1.20 mmol, 3.00 equiv). The vial was sealed with a septa and tape and evacuated and backfilled with N_2 three times. 0.6 mL DMA was then added, and the reaction mixture was stirred vigorously (~1300 rpm) for about 30 min. The mixture should be a dark black color. The reaction mixture was then cooled to 0 °C in an ice bath. Iodocyclohexane (0.078 mL, 0.600 mmol, 1.50 equiv) was then added, followed by freshly prepared acid chloride **S4** (94.7 mg, 0.400 mmol, 1.0 equiv) dissolved in 0.8 mL DMA. The sealed vial was then placed in a cryocool set to 0 °C and allowed to stir for 16 h. The reaction mixture was then quenched with 1.0 mL H_2O and

extracted with CH_2Cl_2 (4 x 2.0 mL). The combined organic layers were filtered through a Na_2SO_4 plug and concentrated *in vacuo*. The resulting crude oil was purified by silica gel flash chromatography (0 → 5% EtOAc/hexanes) to afford **211** as a pale yellow, clear oil (84.6 mg, 74% yield over 2 steps).

R_f = 0.76 (silica gel, 20% EtOAc/Hexanes, UV, *p*-anisaldehyde)

$[\alpha]_D^{25}$ = +17.1° (c = 2.247, $CHCl_3$).

^{1}H NMR (400 MHz, $CDCl_3$): δ 7.11 – 7.05 (m, 2H), 7.02 (d, *J* = 8.0 Hz, 2H), 3.85 (q, *J* = 9.6 Hz, 1H), 3.13 (dd, *J* = 9.6, 0.8 Hz, 1H), 2.31 (s, 3H), 2.21 (tt, *J* = 11.3, 3.3 Hz, 1H), 2.02 (ddd, *J* = 10.6, 8.8, 0.8 Hz, 1H), 1.92 (t, *J* = 10.5 Hz, 1H), 1.88 – 1.62 (m, 3H), 1.44 (tdd, *J* = 13.0, 11.4, 3.6 Hz, 1H), 1.34 (s, 3H), 1.31 – 1.11 (m, 4H), 1.06 (s, 3H).

^{13}C NMR (101 MHz, $CDCl_3$): δ 212.7, 141.7, 135.5, 129.1, 126.5, 60.9, 50.8, 39.1, 37.4, 33.2, 31.3, 29.6, 26.9, 26.3, 26.0, 25.5, 24.0, 21.1.

FTIR (NaCl, thin film, cm^{-1}): 3380, 3048, 3020, 2929, 2855, 1894, 1698, 1515, 1449, 1370, 1331, 1288, 1244, 1183, 1145, 1066, 1021m 994, 952, 892, 829, 805, 759.

HRMS (ESI-TOF, *m/z*): calc'd for $C_{20}H_{32}NO$ $[M+NH_4]^+$: 302.2478; found: 302.2470.

2.8.3 Synthesis of (+)-Rumphellaone A

C–H Activation Procedure for the Preparation of 234

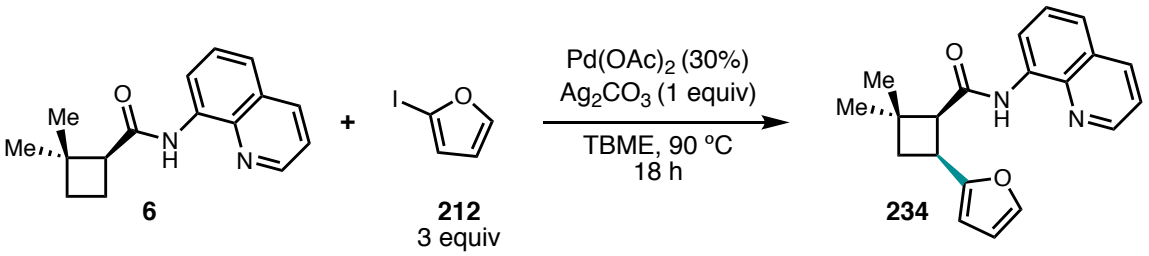

To a 15 mL flame-dried pressure flask was added cyclobutamide **6** (300 mg, 1.18 mmol, 1.0 equiv), $Pd(OAc)_2$ (79 mg, 0.35 mmol, 0.30 equiv), Ag_2CO_3 (325 mg, 1.18 mmol, 1 equiv), and 2-iodofuran (**212**) (686 mg, 3.54 mmol, 3.00 equiv), followed by TBME (6.0 mL, 0.2 M). Add a blanket of argon, seal, and place in 90 ºC oil bath. Let stir overnight. Purify by silica gel chromatography, 5–20% EtOAc/hexanes. **234** isolated (206 mg, 55% yield).

R_f = 0.52 (silica gel, 30% EtOAc/Hexanes, UV, *p*-anisaldehyde)

^{1}H NMR (500 MHz, Chloroform-*d*) δ 9.63 (s, 1H), 8.79 – 8.67 (m, 2H), 8.06 (dd, *J* = 8.3, 1.7 Hz, 1H), 7.47 – 7.35 (m, 3H), 7.23 (dd, *J* = 1.8, 0.8 Hz, 1H), 6.30 – 6.21 (m, 2H), 3.96 (q, *J* = 9.2 Hz, 1H), 3.32 (ddd, *J* = 8.9, 2.2, 0.8 Hz, 1H), 2.61 (dd, *J* = 10.9, 9.6 Hz, 1H), 2.18 (ddd, *J* = 11.1, 9.0, 2.3 Hz, 1H), 1.46 (s, 3H), 1.32 (s, 4H).

Table S1: Time Course Study for the Formation of 238

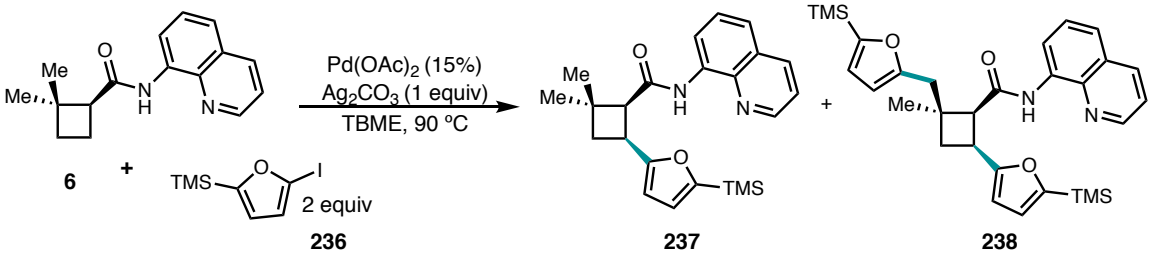

entry	time (h)	% yield pdt[a]	% yield bis aryl[a]	pdt:bis aryl
1	2	70	7	10:1
2	3	49	7	6.7:1
3	4	69	10	6.7:1
4	5	62	11	5.5:1
5	6	60	11	5.5:1

[a]Reactions run in a pressure flask or a sealed vial with a Teflon cap under air. Yields determined by ^{1}H NMR analysis against an internal standard.

Large-Scale C–H Activation Procedure for the Preparation of 237

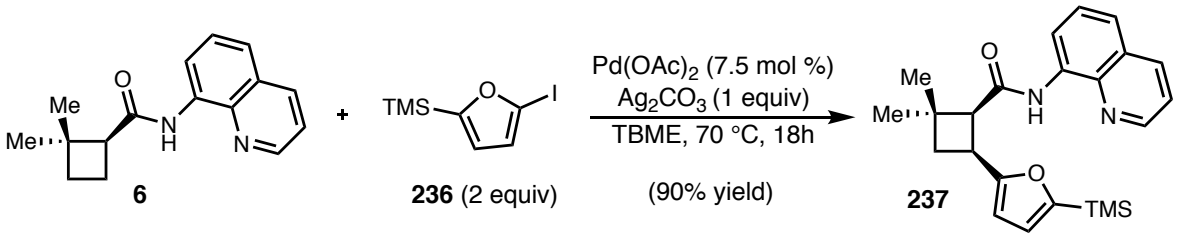

A 48 mL pressure flask was charged with cyclobutamide **6** (400 mg, 1.57 mmol, 1.00 equiv), Ag_2CO_3 (434 mg, 1.57 mmol, 1.00 equiv), and $Pd(OAc)_2$ (26.5 mg, 0.118 mmol, 7.5 mol %) followed by TMS-iodofuran **236** (834 mg, 3.15 mmol, 2.00 equiv). The mixture was then suspended in TBME (8.0 mL, 0.2 M). The vessel was sealed under ambient conditions and placed in a pre-heated oil bath (70 ºC). After about 10 minutes, the olive-green mixture becomes black, and the reaction mixture is stirred for an additional 18 h. The reaction mixture was then concentrated, diluted with toluene (3 mL), and loaded directly onto a silica gel column (0 → 20% EtOAc/hexanes) to afford **237** as a clear yellow oil (556 mg, 90% yield).

$\mathbf{R}_f$ = 0.56 (silica gel, 20% EtOAc/Hex, UV, *p*-anisaldehyde).

$\mathbf{[\alpha]_D^{25}}$ = –57.2° (c = 1.22, $CHCl_3$).

^{1}H NMR (400 MHz, $CDCl_3$): δ 9.61 (s, 1H), 8.77 (dd, *J* = 4.2, 1.7 Hz, 1H), 8.68 (dd, *J* = 6.7, 2.3 Hz, 1H), 8.11 (dd, *J* = 8.2, 1.7 Hz, 1H), 7.48 – 7.39 (m, 3H), 6.48 (d, *J* = 3.1 Hz, 1H), 6.23 (dd, *J* = 3.2, 1.1 Hz, 1H), 4.07 – 3.94 (m, 1H), 3.34 (ddd, *J* = 9.0, 2.2, 0.8 Hz, 1H), 2.61 – 2.50 (m, 1H), 2.19 (ddd, *J* = 11.0, 8.9, 2.3 Hz, 1H), 1.45 (s, 3H), 1.32 (s, 3H), -0.08 (s, 9H).

^{13}C NMR (101 MHz, $CDCl_3$): δ 170.1, 160.1, 158.7, 148.0, 138.5, 136.3, 134.8, 127.9, 127.6, 127.5, 121.5, 121.2, 121.1, 120.5, 120.5, 116.5, 106.8, 55.8, 38.1, 36.6, 32.3, 30.9, 30.7, 30.7, 24.9, –1.8.

FTIR (NaCl, thin film, cm^{-1}): 3360, 3109, 3049, 2954, 2866, 2613, 1944, 1878, 1687, 1595, 1578, 1522, 1485, 1424, 1385, 1324, 1249, 1161, 1131, 1009, 924, 842, 791, 757.

HRMS (ESI-TOF, *m/z*): calc'd for $C_{23}H_{29}N_2O_2Si$ $[M+H]^+$: 392.1993; found: 393.1990.

Schwartz Reduction and Base-Mediated Epimerization[12]

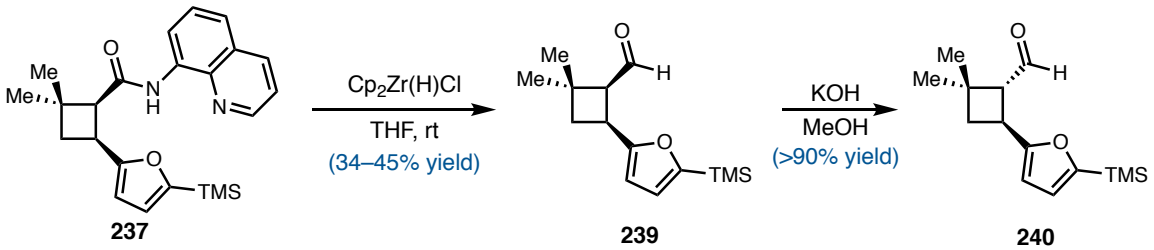

In an N_2-filled glovebox (lights off), Schwartz reagent (2.00 equiv) was added to a flame-dried flask. Added starting material **237** as a solution in THF (0.1 M). Removed from glovebox and let stir for 2h. Once the reaction was complete, quenched with sat aq $NaHCO_3$. Extracted aqueous layer with Et_2O, dried combined organic layers over Na_2SO_4, filter, and concentrated *in vacuo*. Purified crude by silica gel chromatography, 5–10% EtOAc/hexanes, isolated aldehyde **239**.

R_f = 0.69 (silica gel, 20% EtOAc/Hex, UV, *p*-anisaldehyde).

^{1}H NMR (300 MHz, Chloroform-*d*) δ 9.71 (d, *J* = 5.0 Hz, 1H), 6.51 (d, *J* = 3.1 Hz, 1H), 6.09 (dd, *J* = 3.2, 0.9 Hz, 1H), 3.88 (q, *J* = 9.0 Hz, 1H), 2.95 – 2.81 (m, 1H), 2.46 (dd, *J* = 11.6, 8.7 Hz, 1H), 2.30 (ddd, *J* = 11.6, 9.3, 2.2 Hz, 1H), 1.32 (s, 3H), 1.22 (s, 3H), 0.23 (d, *J* = 4.0 Hz, H).

To flask containing **239** was added KOH (20 equiv) followed by MeOH (0.1 M). Let the reaction stir, monitored by TLC, 10% EtOAc/hexanes. Once the reaction was complete, added pH 7 buffer, quenched with sat aq NH_4Cl, and diluted with water and EtOAc. Separated layers and extracted the aqueous layer with EtOAc. Dried the organic layer over $MgSO_4$, filtered, and concentrated *in vacuo*. Isolated epimerized aldehyde **240**, still some trace **239**.

^{1}H NMR (500 MHz, Chloroform-*d*) δ 9.79 (d, *J* = 1.6 Hz, 1H), 6.51 (d, *J* = 3.1 Hz, 1H), 6.02 (dd, *J* = 3.1, 0.6 Hz, 1H), 3.89 (q, *J* = 9.3 Hz, 1H), 3.15 – 3.10 (m, 1H), 1.38 (s, 3H), 1.20 (s, 3H), 0.28 – 0.19 (m, 20H).

Hydrolysis: Preparation of 194[87]

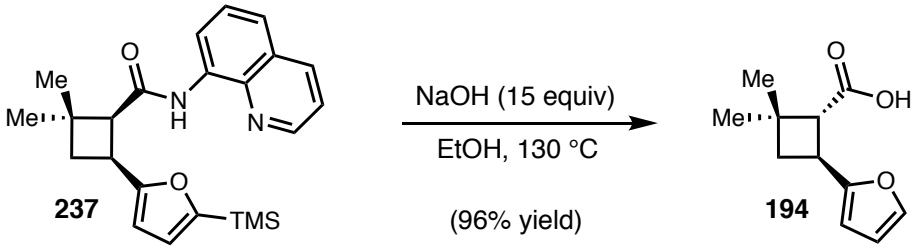

A 15 mL pressure flask was charged with *cis*-cyclobutamide **237** (532 mg, 1.36 mmol, 1.00 equiv), sodium hydroxide (813 mg, 20.33 mmol, 15 equiv), and absolute ethanol (5.7 mL, 0.24 M). The flask was sealed and placed in a pre-heated oil bath (130 ºC) and stirred for 18 h. The solvent was then concentrated *in vacuo*, and the crude residue was diluted with 1 M HCl (20 mL) and EtOAc (20 mL). The organic layer was separated and washed with 1 M HCl (2 x 20 mL). At this point, the aqueous layers should be yellow, and the organic layer should be faint brown. The combined aqueous layers were extracted with EtOAc (25 mL), and the second organic layer was washed with 1 M HCl (25 mL) until it was free of 8-aminoquinoline as indicated by TLC (usually 1-2 times). The organic layers were

combined, dried over $MgSO_4$, filtered, and concentrated *in vacuo*. The crude reddish solid was purified by silica gel flash chromatography (20 → 40 % EtOAc/hexanes) to afford **194** as an off-white solid (250 mg, 96 % yield).

R_f = 0.5 (silica gel, 30% EtOAc/Hex, *p*-anisaldehyde).

$[\alpha]_D^{25}$ = +133.0° (c = 0.85, $CHCl_3$).

^{1}H NMR (400 MHz, $CHCl_3$): δ 7.32 (dd, *J* = 1.9, 0.9 Hz, 1H), 6.28 (dd, *J* = 3.2, 1.8 Hz, 1H), 6.05 (dt, *J* = 3.2, 0.8 Hz, 1H), 3.72 (q, *J* = 9.5 Hz, 1H), 3.11 – 3.02 (m, 1H), 2.12 – 1.95 (m, 2H), 1.30 (s, 3H), 1.19 (s, 3H).

^{13}C NMR (101 MHz, $CDCl_3$): δ 178.3, 156.6, 141.5, 110.3, 105.0, 53.2, 38.3, 36.8, 30.4, 29.2, 23.4.

FTIR (NaCl, thin film, cm^{-1}): 3119, 2993, 2956, 2869, 1722, 1682, 1604, 1506, 1461, 1411, 1390, 1371, 1276, 1224, 1208, 1175, 1161, 1104, 1067, 1008, 946, 918, 884, 850, 804, 743, 730, 695.

HRMS (ESI-TOF, *m/z*): calc'd for $C_{11}H_{15}O_3$ $[M+H]^+$: 195.1016; found: 195.1019.

Attempts at Cyclopropanation[97,98]

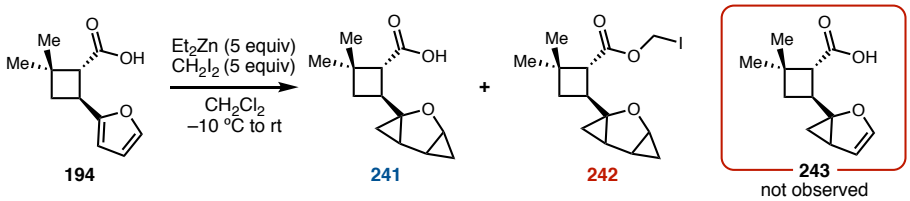

242 (confirmed by 1H NMR, 13 C NMR HSQC, LCMS, and Scott and Dave)

entry	scale	yield	notes
CRL-01-204	7 mg	2.4 mg **242**, 19 % yield; 0.9 mg **241**	5 equiv Zn and CH_2I_2; some xs CH_2I_2
CRL-01-205	23 mg	7.7 mg **241**, 30 % yield (tentative)	still sm, resubjected
CRL-01-207	11 mg	**194** and **241**	-
CRL-01-208	5 mg	mostly **194**	premixed reagent and added to sm
CRL-01-209	5 mg	4.6 mg ~1:1 **194**:**241**	added sm to premixed reagent
CRL-01-210	5 mg	2.7 mg **242**, 29 % yield; 0.9 mg **241**	2.5 equiv Zn and CH_2I_2 (xs CH_2I_2) on accident
CRL-01-213	20 mg	trace **242**; 10 mg **241**, 44 % yield	2 equiv Zn, 3 equiv CH_2I_2
CRL-01-214	20 mg	mostly sm, some **241**	2.5 equiv each Zn and CH_2I_2
CRL-01-216	20 mg	No A, only sm and **241**	1 equiv each Zn and CH_2I_2
CRL-01-217	20 mg	No A, only sm, **241**, and **242** (~1:1:0.3)	1.5 equiv each Zn and CH_2I_2

General procedure: To a 1-dram vial was added **194**. Evacuated and backfilled with N_2 x 3. Added DCM (0.1 M) and cooled to –10 ºC. Then added Et_2Zn (5.00 equiv) and CH_2I_2 (5.00 equiv) (*small volumes, easy to add too much*). Allowed and warm to room temperature, monitoring by TLC (20% EtOAc/hexanes). Once conversion was complete, quenched with sat aq NH_4Cl and diluted with EtOAc. Separated layers, washed organic with sat aq $Na_2S_2O_3$ and sat brine. Dried over Na_2SO_4, filtered, and concentrated *in vacuo*. Purify by prep TLC, 20% EtOAc/hexanes.

Unable to isolate **241**

242:

^{1}H NMR (400 MHz, Chloroform-*d*) δ 5.98 (d, *J* = 4.5 Hz, 1H), 5.82 (d, *J* = 4.6 Hz, 1H), 3.54 (td, *J* = 5.4, 2.1 Hz, 1H), 2.74 (dd, *J* = 9.8, 0.8 Hz, 1H), 2.46 (td, *J* = 9.8, 8.8 Hz, 1H), 1.77 – 1.66 (m, 1H), 1.65 – 1.58 (m, 2H), 1.60 – 1.52 (m, 2H), 1.43 (dd, *J* = 8.5, 4.5 Hz, 1H), 1.21 (s, 4H), 1.09 (s, 4H), 0.81 (ddd, *J* = 8.1, 5.7, 4.5 Hz, 1H), 0.59 (dd, *J* = 8.5, 5.7 Hz, 1H), 0.51 (ddd, *J* = 6.4, 4.4, 2.0 Hz, 1H), 0.48 – 0.33 (m, 1H).

^{13}C NMR (101 MHz, $CDCl_3$) δ 171.24, 67.93, 57.86, 49.84, 37.25, 34.41, 34.38, 30.72, 30.34, 26.40, 23.89, 22.30, 18.70, 14.65.

Pinnick Oxidation: Preparation of 259

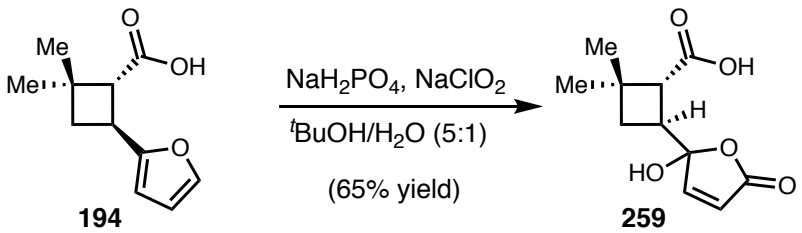

A 50 mL round bottom flask was charged with carboxylic acid **194 (**200 mg, 1.03 mmol, 1.00 equiv) and was evacuated and backfilled with N_2 three times. 5:1 ^{t}BuOH/H_2O (5.2

mL, 0.2 M) was added. Once the starting material was fully dissolved, $NaH_2PO_4 \bullet H_2O$ (213 mg, 1.54 mmol, 1.50 equiv) was added in one portion, followed by $NaClO_2$ (349 mg, 3.09 mmol, 3.00 equiv, 80%). The suspension turned bright yellow within the first 10-15 minutes. The reaction mixture was allowed to stir 2-3 hours, at which point the yellow color dissipated and no more starting material was observed by TLC. The reaction mixture was concentrated *in vacuo*, and the resulting solids were solubilized with a mixture of EtOAc and minimal H_2O. This crude mixture was concentrated onto 4 g SiO_2. The powder was applied to a silica gel column and purified by flash silica gel chromatography (0 → 5% MeOH/CH_2Cl_2, followed by flushing with 50% MeOH/CH_2Cl_2) to afford **259** as a white solid (151 mg, 65% yield, 93% pure by QNMR).

R_f = 0.20 (silica gel, 10% MeOH/CH_2Cl_2, UV, *p*-anisaldehyde)

$[\alpha]_D^{25}$ +62.6° (c = 0.22, MeOH).

^{1}H NMR (400 MHz, MeOD-*d*$_4$): δ 7.27 (d, *J* = 5.9 Hz, 1H), 6.12 (d, *J* = 5.8 Hz, 1H), 2.92 (q, *J* = 9.4 Hz, 1H), 2.72 (d, *J* = 9.6 Hz, 1H), 1.80 (t, *J* = 10.3 Hz, 1H), 1.70 (dd, *J* = 11.0, 9.0 Hz, 1H), 1.20 (s, 3H), 1.10 (s, 3H).

^{13}C NMR (101 MHz, MeOD-*d*$_4$): δ 175.7, 172.9, 155.7, 123.6, 51.5, 49.5, 37.8, 37.1, 36.9, 36.2, 33.7, 30.4, 30.3, 24.1, 23.7.

FTIR (NaCl, thin film, cm^{-1}): 3098, 2960, 2871, 1726, 1416, 1373, 1280, 1255, 1187, 1160, 1114, 1032, 1007, 935, 852, 829, 713.

(*i*-PrO)$_3$TiCH$_3$ Conditions for Methylation: Preparation of 260[103,104]

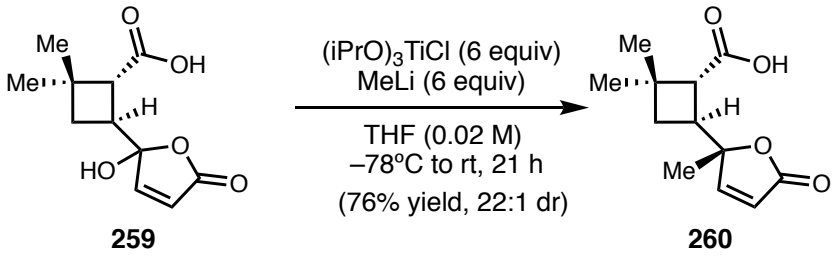

259 **260**

A flame-dried 50 mL round bottom flask was backfilled with N_2 and charged with THF (5 mL). The flask was cooled to –78 °C and (*i*-PrO)$_3$TiCl (1 M solution in hexanes; 1.33 mL, 1.33 mmol, 6.00 equiv) was added. MeLi (1.6 M solution in ether; 0.83 mL, 1.33 mmol, 6.00 equiv) was then added dropwise. This mixture was allowed to stir at –78 °C for 1 h. **259** (50 mg, 0.221 mmol, 1.00 equiv) was then added as a solution in THF (5.5 mL). The reaction mixture was slowly warmed to 23 °C over 21h. The reaction was then carefully quenched with 1 M HCl (11 mL) and stirred vigorously for 30 min. The organic and aqueous layers were then separated, and the aqueous layer was extracted with EtOAc (12 mL x 4). The combined organic layers were dried over $MgSO_4$, filtered, and concentrated *in vacuo*. The crude reaction mixture was purified by silica gel flash chromatography (0 → 4% MeOH/CH_2Cl_2) to afford **260** (37.5 mg, 76% yield, 22:1 dr)

R_f = 0.43 (silica gel, 10% MeOH/CH_2Cl_2, UV, *p*-anisaldehyde)

$[\alpha]_D^{25}$ = +120.4° (c = 1.20, $CHCl_3$).

^{1}H NMR (500 MHz, $CDCl_3$): δ 7.29 (d, *J* = 5.6 Hz, 1H), 5.97 (d, *J* = 5.6 Hz, 1H), 2.79 (td, *J* = 9.9, 8.9 Hz, 1H), 2.39 (dd, *J* = 9.8, 0.8 Hz, 1H), 1.93 (t, *J* = 10.4 Hz, 1H), 1.78 (ddd, *J* = 10.8, 8.9, 1.0 Hz, 1H), 1.39 (s, 3H), 1.21 (s, 3H), 1.11 (s, 3H).

^{13}C NMR (101 MHz, $CDCl_3$): δ 177.4, 172.9, 159.5, 120.5, 88.4, 46.9, 36.8, 35.5, 33.5, 29.9, 23.6, 21.6.

FTIR (NaCl, thin film, cm^{-1}): 3091, 2936, 2958, 1869, 1741, 1702, 1464, 1454, 1417, 1371, 1282, 1247, 1208, 1166, 1119, 1090, 1051, 956, 912, 820, 727, 661.

HRMS (ESI-TOF, *m/z*): calc'd for $C_{12}H_{20}NO_4$ $[M+NH_4]^+$: 242.1387; found: 242.1390.

Hydrogenation of butenolide 259

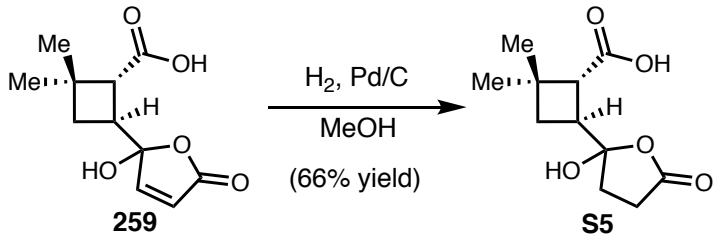

To a flame-dried 2-dram vial were added **259** (40 mg, 0.18 mmol, 1.00 equiv) and Pd/C (64 mg, 10 wt%, 0.34 equiv). The vial was evacuated and backfilled with N_2 x 3. Added MeOH (2.0 mL, 0.09M) and sparged with H_2 ballon for about 15 minutes. Allowed to stir under an H_2 atmosphere at room temperature. Monitored by TLC (10% MeOH/DCM). Once the reaction was complete, sparged with argon. Filtered through a celite plug, washing with methanol and ethyl acetate. Concentrated the crude *in vacuo*.Purified by silica gel chromatography, 1–10% MeOH/DCM. **S5** isolated (27 mg, 66% yield).

R_f = 0.16 (silica gel, 10% MeOH/CH_2Cl_2, *p*-anisaldehyde)

^{1}H NMR (300 MHz, Chloroform-*d*) δ 3.47 (s, 2H), 3.14 (d, *J* = 9.5 Hz, 0H), 3.07 (d, *J* = 9.4 Hz, 1H), 2.78 – 2.54 (m, 3H), 2.08 – 1.70 (m, 2H), 1.20 (s, 3H), 1.15 (s, 3H).

Ti(CH_3)$_4$ Conditions for Methylation: Preparation of 264

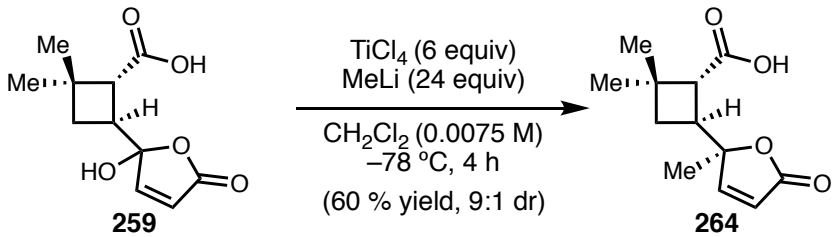

A 50 mL round bottom flask was flame-dried under vacuum and then backfilled with N_2. The flask was charged with CH_2Cl_2 (5 mL) and cooled to –78 ºC, at which point, $TiCl_4$ (142 μL, 1.33 mmol, 6.00 equiv) was added. The flask was then charged with MeLi (1.5 M in Et_2O; 4.00 mL, 5.30 mmol, ~24 equiv) dropwise via syringe, until the color of the solution changed from dark brown, to bright orange, and finally to dark green. The resulting solution was stirred for 1h at –78 ºC. A flame-dried 50 mL pear-shaped (pointed) flask was charged with **26** (49.0 mg, 0.217 mmol, 1.00 equiv) and then evacuated and backfilled with N_2 three times. The substrate was dissolved in CH_2Cl_2 (23 mL) and sonicated to dissolve any particulates. The solution was cooled to –78 ºC, then added to the reaction flask via a slow cannula transfer. If the addition proceeds too quickly or the solution of starting material is not sufficiently cooled, the reaction will favor the undesired diastereomer. The flask containing **26** was rinsed with 2 mL CH_2Cl_2 to complete the transfer. The resulting mixture was allowed to stir at –78 ºC. After 4 h the reaction was quenched with 1 M HCl (20 mL), allowed to warm to 23 °C, and stirred for 30 minutes during which time the aqueous layer became blue/green. The organic and aqueous layers were separated, and the aqueous layer was extracted with EtOAc (20 mL x 4), dried over $MgSO_4$, filtered, and concentrated *in vacuo*. The crude residue was purified by silica gel flash chromatography (0 → 10% MeOH/CH_2Cl_2) to afford **28** white solid (29 mg, 9:1 dr, 60% yield)

$\mathbf{R_f}$ = 0.43 (silica gel, 10% MeOH/CH_2Cl_2, UV, *p*-anisaldehyde)

$\mathbf{[\alpha]_D^{25}}$ = +43.0° (c = 0.46, $CHCl_3$).

^{1}H NMR (400 MHz, $CDCl_3$): 7.23 (d, *J* = 5.6 Hz, 1H), 6.01 (d, *J* = 5.6 Hz, 1H), 3.48 (s, 1H), 2.99 (dd, *J* = 9.4, 0.8 Hz, 1H), 2.92 – 2.78 (m, 1H), 1.46 – 1.41 (m, 1H), 1.39 (s, 3H), 1.35 (dd, *J* = 11.1, 9.9 Hz, 1H), 1.20 (s, 3H), 1.10 (s, 3H).

^{13}C NMR (101 MHz, $CDCl_3$): δ 178.3, 172.9, 172.8, 158.8, 121.1, 88.5, 49.1, 47.1, 36.4, 35.6, 35.5, 32.1, 29.9, 23.8, 21.7.

FTIR (NaCl, thin film, cm^{-1}): 3087, 2958, 2869, 1737, 1600, 1463, 1453, 1403, 1380, 1372, 1305, 1280, 1266, 1218, 1183, 1163, 1136, 1093, 1037, 961, 924, 880, 852, 824, 728, 711, 658.

HRMS (ESI-TOF, *m/z*): calc'd for $C_{12}H_{20}NO_4$ $[M+NH_4]^+$: 242.1387; found: 242.1394.

HWE Preparation of 267

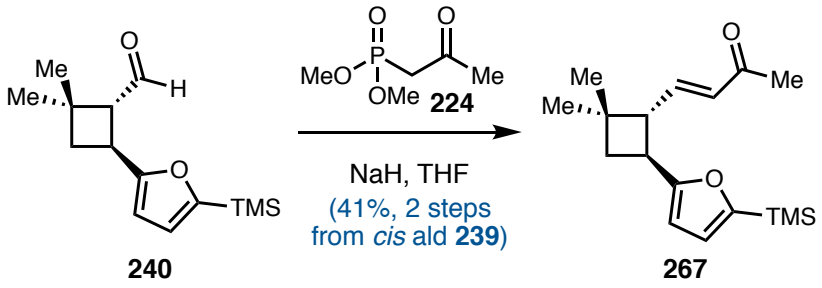

Preparation of ylide (0.181 M) from **224**: A flame-dried 10 mL round-bottom flask was pumped into an N_2-filled glovebox while still hot. Once inside the glovebox and cool, the flask was charged with NaH (25 mg, 95 wt%, 1.15 equiv) and THF (0.181 M, 5.0 mL). Sealed flask with rubber septa and tape and removed from the glovebox. Phosphonate **224** (0.125 mL, 1.0 equiv) was added to the reaction flask, and the slurry was allowed to stir for 3 hours.

Preparation of **267**: To a 25 mL round-bottom flask containing **240** (17.0 mg, 0.067 mmol, 1.00 equiv) under N_2 was added the ylide slurry (2.6 mL, 0.181M, 0.47 mmol, 7.00 equiv). Excess THF was used to rinse the sides of the flask. Let stir at room temperature under N_2 overnight. The next day, the reaction mixture had dried out. Dissolved in EtOAc and quenched with aq sat NH_4Cl. TLC (10% EtOAc/hex) showed still some aldehyde (**SX**)

remaining. Diluted further with water and EtOAc, separated layers, and extracted aqueous layer with EtOAc and DCM. Dry over $MgSO_4$, filter, and concentrate *in vacuo*. Added 4.9 mg pyrazine internal standard and calculated an NMR yield. 45% **267**, 13% **240** remaining. Combined with other reactions for purification. Purified by silica gel chromatography to afford clean **267**, 2–5% EtOAc/hexanes. *See Wittig prep for characterization of **267**.*

Wittig Preparation of 267[107]

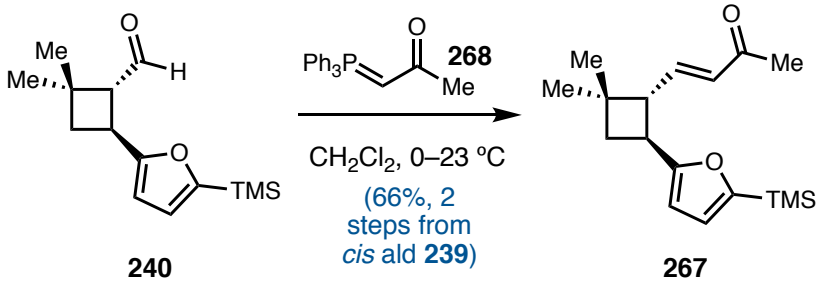

To a 2-dram vial under N_2 containing *trans* aldehyde **240** (20. mg, 0.08 mmol, 1.00 equiv) was added CH_2Cl_2 (0.18 mL, 0.44 M). Let the aldehyde dissolve. Cool to 0 ºC in an ice bath and add **268** (51 mg, 0.16 mmol, 2.0 equiv). Let stir overnight at room temperature. The next day, the reaction had dried out. Added CH_2Cl_2 (0.5 mL). TLC (20% EtOAc/hexanes) showed still some **SX** remaining. After ~ 6 hours, still **240** remaining, so added another equivalent **268** (27.3 mg). Purged with nitrogen, then sealed with a teflon cap instead of a rubber septa and let stir overnight. Almost complete conversion. The reaction was flushed through silica plug (20% EtOAc/hexanes). NMR yield was calculated by ^{1}H NMR vs an internal standard. 72% **267**, 11% **240**remaining. Combined with other reactions for purification. Purified by silica gel chromatography to afford clean **267**, 2–5% EtOAc/hexanes.

$\mathbf{R}_f$ = 0.63 (silica gel, 20% EtOAc/hexanes, UV, *p*-anisaldehyde)

^{1}H NMR (300 MHz, Chloroform-*d*) δ 6.83 (dd, *J* = 16.0, 6.9 Hz, 1H), 6.51 (d, *J* = 3.1 Hz, 1H), 6.11 (dd, *J* = 15.9, 1.4 Hz, 1H), 6.00 (d, *J* = 3.1 Hz, 1H), 3.44 (q, *J* = 9.4 Hz, 1H), 2.90 (dd, *J* = 9.4, 7.3 Hz, 1H), 2.25 (s, 3H), 2.08 – 1.96 (m, 2H), 1.19 (s, 3H), 1.11 (s, 3H), 0.24 (s, 9H).

Hydrogenation of Methylated Products: Preparation of 241 and 263

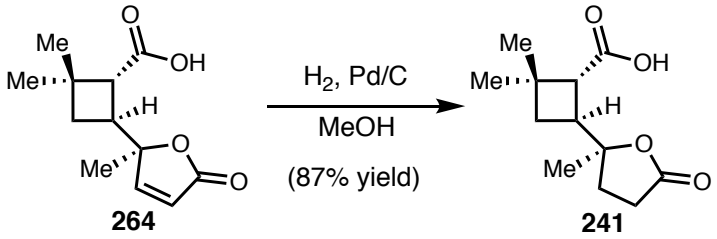

A 2-dram vial was charged with lactone **264** (29 mg, 0.129 mmol, 1.00 equiv) and Pd/C (10% by weight, 47 mg, 0.044 mmol, 0.34 equiv). The vial was then evacuated and backfilled with N_2 three times. The solids were suspended in MeOH (1.4 mL, 0.095 M), and the reaction mixture was sparged with a balloon of H_2 for 20 minutes at 0°C, at which point the balloon was replaced with a fresh balloon, and the reaction was allowed to warm to room temperature. The reaction mixture was then stirred for 7 h under an atmosphere of H_2. Once the reaction was complete, the reaction mixture was sparged with argon for 20 minutes, diluted with EtOAc (15 mL), and filtered through celite, and concentrated *in vacuo*. The crude residue was then purified by silica gel flash chromatography (5% MeOH/CH_2Cl_2) to afford **241** (25 mg, 88% yield) as a white solid.

R_f = 0.44 (silica gel, 10% MeOH/CH_2Cl_2, *p*-anisaldehyde)

$[\alpha]_D^{25}$ = +76.3° (c = 0.72, $CHCl_3$).

^{1}H NMR (400 MHz, $CDCl_3$): δ 2.91 (d, *J* = 9.7 Hz, 1H), 2.72 (t, *J* = 9.5 Hz, 1H), 2.70 – 2.59 (m, 1H), 2.53 (ddd, *J* = 18.2, 9.6, 5.0 Hz, 1H), 2.04 – 1.86 (m, 2H), 1.67 (s, 1H), 1.65 (s, 1H), 1.30 (s, 3H), 1.22 (s, 3H), 1.11 (s, 3H).

^{13}C NMR (101 MHz, $CDCl_3$): δ 178.4, 177.1, 86.3, 86.3, 48.7, 39.1, 35.3, 32.6, 30.9, 29.9, 29.3, 24.0, 23.7.

FTIR (NaCl, thin film, cm^{-1}): 2958, 2934, 2869, 1773, 1736, 1702, 1459, 1420, 1382, 1369, 1283, 1248, 1166, 1142, 1077, 940, 914, 802, 646.

HRMS (ESI-TOF, *m/z*): calc'd for $C_{12}H_{22}NO_4$ $[M+NH_4]^+$: 244.1543; found: 244.1541.

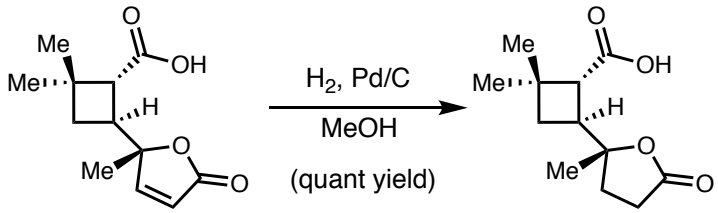

260 (31.0 mg, 0.138 mmol, 1.00 equiv) was subjected to analogous conditions to afford **263** (32.2 mg, quant yield), which was taken forward without further purification

R_f = 0.44 (silica gel, 10% MeOH/CH_2Cl_2, *p*-Anisaldehyde)

$[\alpha]_D^{25}$ = +51.2° (c = 0.53, $CHCl_3$).

^{1}H NMR (400 MHz, $CDCl_3$): δ 2.78 – 2.56 (m, 3H), 2.50 (ddd, *J* = 18.1, 9.9, 4.9 Hz, 1H), 2.17 – 2.06 (m, 1H), 1.91 (ddd, *J* = 13.1, 10.0, 4.9 Hz, 1H), 1.81 (td, *J* = 9.8, 1.2 Hz, 1H), 1.71 (dd, *J* = 10.8, 8.0 Hz, 1H), 1.29 (s, 3H), 1.21 (s, 3H), 1.11 (s, 3H).

^{13}C NMR (101 MHz, $CDCl_3$): δ 178.4, 177.2, 86.5, 48.1, 39.2, 35.5, 33.6, 30.9, 29.9, 29.3, 23.9, 23.7.

FTIR (NaCl, thin film, cm^{-1}): 2958, 2869, 1770, 1738, 1732, 1704, 1699, 1463, 1422, 1383, 1369, 1283, 1245, 1222, 1165, 1138, 1075, 1002, 965, 941, 914, 802, 757, 711, 648.

HRMS (ESI-TOF, *m/z*): calc'd for $C_{12}H_{22}NO_4$ $[M+NH_4]^+$: 244.1543; found: 244.1537.

Radical decarboxylative coupling to afford (+)-rumphellaone A (8) and *epi*-C8-rumphellaone A (29)[63]

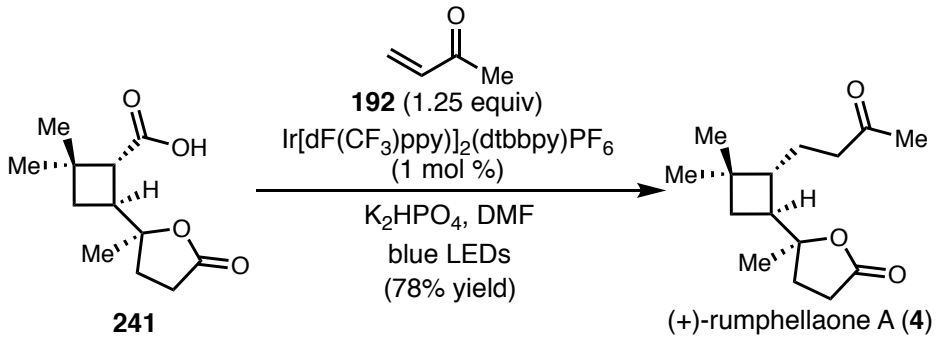

To a 2-dram vial charged with saturated lactone **241** (16 mg, 0.0707 mmol, 1.00 equiv) was added $Ir[dF(CF_3)ppy]_2(dtbbpy)PF_6$ (0.8 mg, 0.0007 mmol, 0.01 equiv) and K_2HPO_4 (14.8 mg, 0.0849 mmol, 1.20 equiv). The reaction vessel was evacuated and backfilled with N_2 three times. DMF (0.71 mL, 0.1 M) was then added, and the reaction mixture was cooled to 0 °C and sparged with argon for 15 minutes. Freshly distilled methyl vinyl ketone (7.2 μL, 0.0884 mmol, 1.25 equiv) was then added, and the reaction vessel was placed between two 34W blue LEDs (~5-6 cm away from each lamp) and stirred for 24 h with a small fan to keep the reactions at 23 ºC. Once complete, the reaction was diluted with sat. aq. $NaHCO_3$ (0.8 mL) and EtOAc (0.8 mL). The layers were separated, and the aqueous layer was extracted with EtOAc (4 x 1 mL). The combined organic layers were washed with 1 M LiCl (5 mL). The organic layer was then dried over Na_2SO_4, filtered, and concentrated *in vacuo.* The crude material was purified by silica gel flash chromatography (20 → 40% EtOAc/hexanes) to afford pure (+)-rumphellaone A (**4**) (15 mg, 78% yield) as a yellow solid.

R_f = 0.27 (silica gel, 40% EtOAc/Hexanes, UV, *p*-anisaldehyde)

$[\alpha]_D^{25}$ = +43.4° (c = 0.35, $CHCl_3$).

^{1}H NMR (400 MHz, $CDCl_3$): δ 2.63 (ddd, *J* =18.1, 10.0, 8.9 Hz, 1H), 2.53 (ddd, *J* = 18.1, 10.0, 5.0 Hz, 1H), 2.36 (t, *J* = 7.9 Hz, 2H), 2.12 (s, 3H), 2.09 – 2.02 (m, 2H), 2.03 – 1.97 (m, 1H), 1.90 (ddd, *J* = 10.2, 9.6, 5.3 Hz, 2H), 1.88 – 1.81 (m, 1H), 1.69 – 1.61 (m, 2H), 1.57 (ddd, *J* = 10.8, 8.6, 0.8 Hz, 1H), 1.42 (t, *J* = 10.3 Hz, 1H), 1.31 (s, 3H), 1.06 (s, 3H), 1.03 (s, 3H).

^{13}C NMR (101 MHz, $CDCl_3$): δ 208.8, 177.1, 87.4, 44.6, 44.4, 42.1, 33.7, 33.1, 31.1, 30.8, 30.1, 29.3, 25.2, 25.0, 22.6.

FTIR (NaCl, thin film, cm^{-1}): 2953, 2929, 2865, 1770, 1715, 1455, 1366, 1250, 1162, 1124, 1077, 938, 803, 645.

HRMS (ESI-TOF, *m/z*): calc'd for $C_{15}H_{25}O_3$ $[M+H]^+$: 253.1798; found: 253.1799.

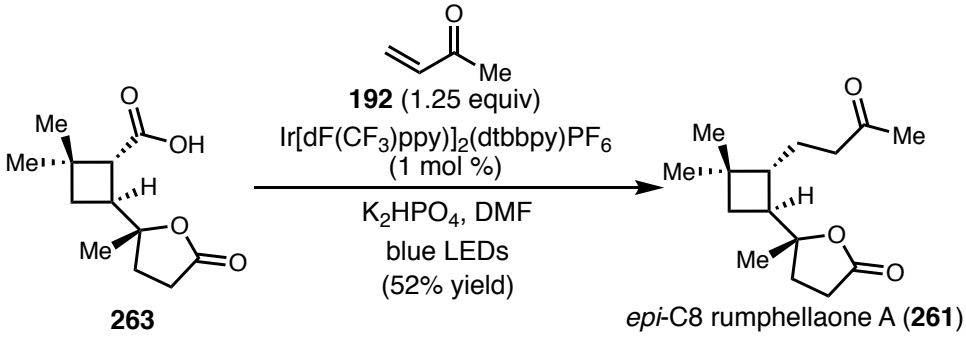

263 (15.0 mg, 0.066 mmol, 1.00 equiv) was subjected to an analogous procedure to afford *epi*-C8-rumphellaone A (**260**) (8.1 mg, 52% yield) as a white solid.

R_f = 0.33 (silica gel, 40% EtOAc/Hexanes, UV, *p*-anisaldehyde)

$[\alpha]_D^{25}$ = +38.5° (c = 0.41, $CHCl_3$).

^{1}H NMR (400 MHz, $CDCl_3$): δ 2.63 – 2.56 (m, 2H), 2.39 (dd, *J* = 8.6, 6.6 Hz, 2H), 2.13 (s, 3H), 2.10 – 1.96 (m, 2H), 1.90 (ddd, *J* = 13.0, 8.8, 7.2 Hz, 1H), 1.78 (tdd, *J* = 9.2, 6.6,

0.8 Hz, 1H), 1.71 – 1.57 (m, 3H), 1.51 (t, *J* = 10.4 Hz, 1H), 1.29 (s, 3H), 1.06 (s, 3H), 1.03 (s, 3H).

^{13}C NMR (101 MHz, $CDCl_3$): δ 208.7, 177.1, 87.3, 44.6, 44.1, 41.9, 34.5, 33.4, 31.6, 31.1, 30.2, 29.3, 25.0, 24.0, 22.6.

FTIR (NaCl, thin film, cm^{-1}): 2952, 2932, 2865, 1769, 1715, 1455, 1422, 1365, 1234, 1169, 1155, 1075, 963, 939, 801, 647.

HRMS (ESI-TOF, *m/z*): calc'd for $C_{15}H_{25}O_3$ $[M+H]^+$: 253.1798; found: 253.1799.

2.8.4 Comparison of ^{1}H NMR Spectroscopic Data for Natural and Synthetic (+)-Rumphellaone A (4) (carbon numbering as reported by Sung et al.)[7]

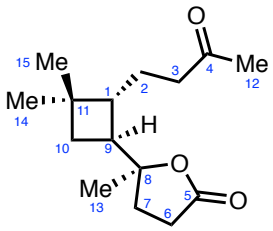

(+)-rumphellaone A (**4**)

Carbon Number	**Natural (+)-rumphellaone A** ^{1}H 400 MHz, $CDCl_3$	**Synthetic (+)-rumphellaone A** ^{1}H 400 MHz, $CDCl_3$
1	1.91 (ddd, *J* = 10.0, 9.2, 5.6 Hz, 2H)	1.90 (ddd, *J* = 10.2, 9.6, 5.3 Hz, 2H)
2	1.67 (m, 2H)	1.65 (m, 2H)
3	2.37 (t, *J* = 8.0 Hz, 2H)	2.36 (t, *J* = 7.9 Hz, 2H)
6α	2.63 (ddd, *J* = 18.0, 9.6, 8.8 Hz, 1H)	2.63 (ddd, *J* =18.1, 10.0, 8.9 Hz, 1H)
6β	2.54 (ddd, *J* = 18.0, 10.0, 4.8 Hz, 1H)	2.53 (ddd, *J* = 18.1, 10.0, 5.0 Hz, 1H)
7α	1.84 (m, 1H)	1.84 (m, 1H)
7β	2.01 (m, 1H)	2.01 (m, 1H)
9	2.06 (ddd, 10.4, 10.0, 10.0 Hz, 2H)	2.06 (m, 2H)
10α	1.57 (dd, *J* = 10.0, 10.0 Hz, 1H)	1.57 (ddd, *J* = 10.8, 8.6, 0.8 Hz, 1H)
10β	1.42 (dd, *J* = 10.4, 10.0 Hz, 1H))	1.42 (t, *J* = 10.3 Hz, 1H)
12	2.13 (s, 3H)	2.12 (s, 3H)
13	1.31 (s, 3H)	1.31 (s, 3H)
14	1.03 (s, 3H)	1.03 (s, 3H)
15	1.07 (s, 3H)	1.06 (s, 3H)

2.8.5 Comparison of ^{13}C NMR Spectroscopic Data for Natural and Synthetic (+)-Rumphellaone A (4)[7]

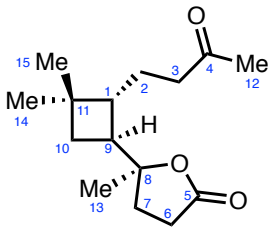

(+)-rumphellaone A (**4**)

Carbon Number	**Natural (+)-rumphellaone A** ^{13}C 100 MHz, $CDCl_3$	**Synthetic (+)-rumphellaone A** ^{13}C 101 MHz, $CDCl_3$	**Δ**
1	44.5	44.6	0.1
2	25.1	25.2	0.1
3	42.0	42.1	0.1
4	208.6	208.8	0.2
5	177.0	177.1	0.1
6	29.2	29.3	0.1
7	30.6	30.8	0.2
8	87.2	87.4	0.2
9	44.3	44.4	0.1
10	33.6	33.7	0.1
11	33.0	33.1	0.1
12	29.9	30.1	0.2
13	24.9	25.0	0.1
14	22.5	22.6	0.1
15	30.9	31.1	0.2

2.9 REFERENCES

(1) Dembitsky, V. M. *J. Nat. Med.* **2008**, *62* (1), 1–33.

(2) Hong, Y. J.; Tantillo, D. J. *Chem. Soc. Rev.* **2014**, *43* (14), 5042–5050.

(3) Ortuno, R.; Moglioni, A.; Moltrasio, G. *Curr. Org. Chem.* **2005**, *9* (3), 237–259.

(4) Shao, M.; Wang, Y.; Liu, Z.; Zhang, D.-M.; Cao, H.-H.; Jiang, R.-W.; Fan, C.-L.; Zhang, X.-Q.; Chen, H.-R.; Yao, X.-S.; Ye, W.-C. *Org. Lett.* **2010**, *12* (21), 5040–5043.

(5) Vinik, A.; Rosenstock, J.; Sharma, U.; Feins, K.; Hsu, C.; Merante, D. *Diabetes Care* **2014**, *37* (12), 3253–3261.

(6) Wang, Y.-H.; Hou, A.-J.; Chen, D.-F.; Weiller, M.; Wendel, A.; Staples, R. J. *Eur. J. Org. Chem.* **2006**, *2006* (15), 3457–3463.

(7) Chung, H.-M.; Chen, Y.-H.; Lin, M.-R.; Su, J.-H.; Wang, W.-H.; Sung, P.-J. *Tetrahedron Lett.* **2010**, *51* (46), 6025–6027.

(8) Seiser, T.; Saget, T.; Tran, D. N.; Cramer, N. *Angew. Chem. Int. Ed.* **2011**, *50* (34), 7740–7752.

(9) Namyslo, J. C.; Kaufmann, D. E. *Chem. Rev.* **2003**, *103* (4), 1485–1538.

(10) Lee-Ruff, E.; Mladenova, G. *Chem. Rev.* **2003**, *103* (4), 1449–1484.

(11) Wang, M.; Lu, P. *Org. Chem. Front.* **2018**, *5* (2), 254–259.

(12) Chapman, L. M.; Beck, J. C.; Wu, L.; Reisman, S. E. *J. Am. Chem. Soc.* **2016**, *138* (31), 9803–9806.

(13) Chapman, L. M.; Beck, J. C.; Lacker, C. R.; Wu, L.; Reisman, S. E. *J. Org. Chem.* **2018**.

(14) Guo, H.; Herdtweck, E.; Bach, T. *Angew. Chem. Int. Ed.* **2010**, *49* (42), 7782–7785.

(15) Brimioulle, R.; Guo, H.; Bach, T. *Chem. – Eur. J.* **2012**, *18* (24), 7552–7560.

(16) Brimioulle, R.; Bach, T. *Science* **2013**, *342* (6160), 840–843.

(17) Du, J.; Skubi, K. L.; Schultz, D. M.; Yoon, T. P. *Science* **2014**, *344* (6182), 392–396.

(18) Daub, M. E.; Jung, H.; Lee, B. J.; Won, J.; Baik, M.-H.; Yoon, T. P. *J. Am. Chem. Soc.* **2019**, *141* (24), 9543–9547.

(19) Tröster, A.; Alonso, R.; Bauer, A.; Bach, T. *J. Am. Chem. Soc.* **2016**, *138* (25), 7808–7811.

(20) Canales, E.; Corey, E. J. *J. Am. Chem. Soc.* **2007**, *129* (42), 12686–12687.

(21) Vallavoju, N.; Selvakumar, S.; Jockusch, S.; Sibi, M. P.; Sivaguru, J. *Angew. Chem. Int. Ed.* **2014**, *53* (22), 5604–5608.

(22) Kossler, D.; Cramer, N. *Chem. Sci.* **2017**, *8* (3), 1862–1866.

(23) Hörmann, F. M.; Chung, T. S.; Rodriguez, E.; Jakob, M.; Bach, T. *Angew. Chem. Int. Ed.* **2018**, *57* (3), 827–831.

(24) Pagar, V. V.; RajanBabu, T. V. *Science* **2018**, *361* (6397), 68–72.

(25) Parsutkar, M. M.; Pagar, V. V.; RajanBabu, T. V. *J. Am. Chem. Soc.* **2019**, *141* (38), 15367–15377.

(26) Luzung, M. R.; Mauleón, P.; Toste, F. D. *J. Am. Chem. Soc.* **2007**, *129* (41), 12402–12403.

(27) González, A. Z.; Benitez, D.; Tkatchouk, E.; Goddard, W. A.; Toste, F. D. *J. Am. Chem. Soc.* **2011**, *133* (14), 5500–5507.

(28) Teller, H.; Corbet, M.; Mantilli, L.; Gopakumar, G.; Goddard, R.; Thiel, W.; Fürstner, A. *J. Am. Chem. Soc.* **2012**, *134* (37), 15331–15342.

(29) Teller, H.; Flügge, S.; Goddard, R.; Fürstner, A. *Angew. Chem. Int. Ed.* **2010**, *49* (11), 1949–1953.

(30) Suárez-Pantiga, S.; Hernández-Díaz, C.; Rubio, E.; González, J. M. *Angew. Chem. Int. Ed.* **2012**, *51* (46), 11552–11555.

(31) Mascareñas, J. L.; Varela, I.; López, F. *Acc. Chem. Res.* **2019**, *52* (2), 465–479.

(32) García-Morales, C.; Ranieri, B.; Escofet, I.; López-Suarez, L.; Obradors, C.; Konovalov, A. I.; Echavarren, A. M. *J. Am. Chem. Soc.* **2017**, *139* (39), 13628–13631.

(33) Wiest, Johannes. M.; Conner, M. L.; Brown, M. K. *J. Am. Chem. Soc.* **2018**, *140* (46), 15943–15949.

(34) Conner, M. L.; Wiest, J. M.; Brown, M. K. *Tetrahedron* **2019**, *75* (24), 3265–3271.

(35) Conner, M. L.; Xu, Y.; Brown, M. K. *J. Am. Chem. Soc.* **2015**, *137* (10), 3482–3485.

(36) Gutekunst, W. R.; Baran, P. S. *J. Am. Chem. Soc.* **2011**, *133* (47), 19076–19079.

(37) Gutekunst, W. R.; Gianatassio, R.; Baran, P. S. *Angew. Chem. Int. Ed.* **2012**, *51* (30), 7507–7510.

(38) Gutekunst, W. R.; Baran, P. S. *J. Org. Chem.* **2014**, *79* (6), 2430–2452.

(39) Xiao, K.-J.; Lin, D. W.; Miura, M.; Zhu, R.-Y.; Gong, W.; Wasa, M.; Yu, J.-Q. *J. Am. Chem. Soc.* **2014**, *136* (22), 8138–8142.

(40) He, J.; Wasa, M.; Chan, K. S. L.; Shao, Q.; Yu, J.-Q. *Chem. Rev.* **2017**, *117* (13), 8754–8786.

(41) Wu, Q.-F.; Wang, X.-B.; Shen, P.-X.; Yu, J.-Q. *ACS Catal.* **2018**, *8* (3), 2577–2581.

(42) Shi, H.; Herron, A. N.; Shao, Y.; Shao, Q.; Yu, J.-Q. *Nature* **2018**, *558* (7711), 581–585.

(43) Park, H.; Verma, P.; Hong, K.; Yu, J.-Q. *Nat. Chem.* **2018**, *10* (7), 755–762.

(44) Shao, Q.; Wu, K.; Zhuang, Z.; Qian, S.; Yu, J.-Q. *Acc. Chem. Res.* **2020**.

(45) Chen, T.-G.; Barton, L. M.; Lin, Y.; Tsien, J.; Kossler, D.; Bastida, I.; Asai, S.; Bi, C.; Chen, J. S.; Shan, M.; Fang, H.; Fang, F. G.; Choi, H.; Hawkins, L.; Qin, T.; Baran, P. S. *Nature* **2018**, *560* (7718), 350–354.

(46) Shang, M.; Feu, K. S.; Vantourout, J. C.; Barton, L. M.; Osswald, H. L.; Kato, N.; Gagaring, K.; McNamara, C. W.; Chen, G.; Hu, L.; Ni, S.; Fernández-Canelas, P.; Chen, M.; Merchant, R. R.; Qin, T.; Schreiber, S. L.; Melillo, B.; Yu, J.-Q.; Baran, P. S. *Proc. Natl. Acad. Sci.* **2019**, *116* (18), 8721–8727.

(47) Yang, C.; Yang, J.-D.; Li, Y.-H.; Li, X.; Cheng, J.-P. *J. Org. Chem.* **2016**, *81* (24), 12357–12363.

(48) Bloom, S.; Liu, C.; Kölmel, D. K.; Qiao, J. X.; Zhang, Y.; Poss, M. A.; Ewing, W. R.; MacMillan, D. W. C. *Nat. Chem.* **2018**, *10* (2), 205–211.

(49) Zhou, Q.-Q.; Guo, W.; Ding, W.; Wu, X.; Chen, X.; Lu, L.-Q.; Xiao, W.-J. *Angew. Chem. Int. Ed.* **2015**, *54* (38), 11196–11199.

(50) Zuo, Z.; MacMillan, D. W. C. *J. Am. Chem. Soc.* **2014**, *136* (14), 5257–5260.

(51) Ventre, S.; Petronijevic, F. R.; MacMillan, D. W. C. *J. Am. Chem. Soc.* **2015**, *137* (17), 5654–5657.

(52) Till, N. A.; Smith, R. T.; MacMillan, D. W. C. *J. Am. Chem. Soc.* **2018**, *140* (17), 5701–5705.

(53) Liang, Y.; Zhang, X.; MacMillan, D. W. C. *Nature* **2018**, *559* (7712), 83–88.

(54) Kautzky, J. A.; Wang, T.; Evans, R. W.; MacMillan, D. W. C. *J. Am. Chem. Soc.* **2018**, *140* (21), 6522–6526.

(55) Martinez Alvarado, J. I.; Ertel, A. B.; Stegner, A.; Stache, E. E.; Doyle, A. G. *Org. Lett.* **2019**, *21* (24), 9940–9944.

(56) Zuo, Z.; Cong, H.; Li, W.; Choi, J.; Fu, G. C.; MacMillan, D. W. C. *J. Am. Chem. Soc.* **2016**, *138* (6), 1832–1835.

(57) Stache, E.; Ertel, A. B.; Rovis, T.; Doyle, A. G. *figshare* **2018**.

(58) Noble, A.; McCarver, S. J.; MacMillan, D. W. C. *J. Am. Chem. Soc.* **2015**, *137* (2), 624–627.

(59) Chu, L.; Lipshultz, J. M.; MacMillan, D. W. C. *Angew. Chem. Int. Ed.* **2015**, *54* (27), 7929–7933.

(60) Zuo, Z.; Ahneman, D. T.; Chu, L.; Terrett, J. A.; Doyle, A. G.; MacMillan, D. W. C. *Science* **2014**, *345* (6195), 437–440.

(61) Johnston, C. P.; Smith, R. T.; Allmendinger, S.; MacMillan, D. W. C. *Nature* **2016**, *536* (7616), 322–325.

(62) Le Vaillant, F.; Courant, T.; Waser, J. *Angew. Chem. Int. Ed.* **2015**, *54* (38), 11200–11204.

(63) Chu, L.; Ohta, C.; Zuo, Z.; MacMillan, D. W. C. *J. Am. Chem. Soc.* **2014**, *136* (31), 10886–10889.

(64) Lackner, G. L.; Quasdorf, K. W.; Overman, L. E. *J. Am. Chem. Soc.* **2013**, *135* (41), 15342–15345.

(65) Müller, D. S.; Untiedt, N. L.; Dieskau, A. P.; Lackner, G. L.; Overman, L. E. *J. Am. Chem. Soc.* **2015**, *137* (2), 660–663.

(66) Pratsch, G.; Lackner, G. L.; Overman, L. E. *J. Org. Chem.* **2015**, *80* (12), 6025–6036.

(67) Schnermann, M. J.; Overman, L. E. *Angew. Chem. Int. Ed.* **2012**, *51* (38), 9576–9580.

(68) Cheng, W.-M.; Shang, R.; Fu, M.-C.; Fu, Y. *Chem. – Eur. J.* **2017**, *23* (11), 2537–2541.

(69) Fawcett, A.; Pradeilles, J.; Wang, Y.; Mutsuga, T.; Myers, E. L.; Aggarwal, V. K. *Science* **2017**, *357* (6348), 283–286.

(70) Qin, T.; Cornella, J.; Li, C.; Malins, L. R.; Edwards, J. T.; Kawamura, S.; Maxwell, B. D.; Eastgate, M. D.; Baran, P. S. *Science* **2016**, *352* (6287), 801–805.

(71) Ni, S.; Garrido-Castro, A. F.; Merchant, R. R.; de Gruyter, J. N.; Schmitt, D. C.; Mousseau, J. J.; Gallego, G. M.; Yang, S.; Collins, M. R.; Qiao, J. X.; Yeung, K.-S.; Langley, D. R.; Poss, M. A.; Scola, P. M.; Qin, T.; Baran, P. S. *Angew. Chem. Int. Ed.* **2018**, *57* (44), 14560–14565.

(72) Ni, S.; Padial, N. M.; Kingston, C.; Vantourout, J. C.; Schmitt, D. C.; Edwards, J. T.; Kruszyk, M. M.; Merchant, R. R.; Mykhailiuk, P. K.; Sanchez, B. B.; Yang, S.; Perry, M. A.; Gallego, G. M.; Mousseau, J. J.; Collins, M. R.; Cherney, R. J.; Lebed, P. S.; Chen, J. S.; Qin, T.; Baran, P. S. *J. Am. Chem. Soc.* **2019**, *141* (16), 6726–6739.

(73) Sandfort, F.; O'Neill, M. J.; Cornella, J.; Wimmer, L.; Baran, P. S. *Angew. Chem. Int. Ed.* **2017**, *56* (12), 3319–3323.

(74) Edwards, J. T.; Merchant, R. R.; McClymont, K. S.; Knouse, K. W.; Qin, T.; Malins, L. R.; Vokits, B.; Shaw, S. A.; Bao, D.-H.; Wei, F.-L.; Zhou, T.; Eastgate, M. D.; Baran, P. S. *Nature* **2017**, *545* (7653), 213–218.

(75) Smith, J. M.; Qin, T.; Merchant, R. R.; Edwards, J. T.; Malins, L. R.; Liu, Z.; Che, G.; Shen, Z.; Shaw, S. A.; Eastgate, M. D.; Baran, P. S. *Angew. Chem. Int. Ed.* **2017**, *56* (39), 11906–11910.

(76) Li, C.; Wang, J.; Barton, L. M.; Yu, S.; Tian, M.; Peters, D. S.; Kumar, M.; Yu, A. W.; Johnson, K. A.; Chatterjee, A. K.; Yan, M.; Baran, P. S. *Science* **2017**, *356* (6342), eaam7355.

(77) Qin, T.; Malins, L. R.; Edwards, J. T.; Merchant, R. R.; Novak, A. J. E.; Zhong, J. Z.; Mills, R. B.; Yan, M.; Yuan, C.; Eastgate, M. D.; Baran, P. S. *Angew. Chem. Int. Ed.* **2017**, *56* (1), 260–265.

(78) Wang, J.; Qin, T.; Chen, T.-G.; Wimmer, L.; Edwards, J. T.; Cornella, J.; Vokits, B.; Shaw, S. A.; Baran, P. S. *Angew. Chem. Int. Ed.* **2016**, *55* (33), 9676–9679.

(79) Cornella, J.; Edwards, J. T.; Qin, T.; Kawamura, S.; Wang, J.; Pan, C.-M.; Gianatassio, R.; Schmidt, M.; Eastgate, M. D.; Baran, P. S. *J. Am. Chem. Soc.* **2016**, *138* (7), 2174–2177.

(80) Chen, T.-G.; Zhang, H.; Mykhailiuk, P. K.; Merchant, R. R.; Smith, C. A.; Qin, T.; Baran, P. S. *Angew. Chem. Int. Ed.* **2019**, *58* (8), 2454–2458.

(81) Wang, J.; Shang, M.; Lundberg, H.; Feu, K. S.; Hecker, S. J.; Qin, T.; Blackmond, D. G.; Baran, P. S. *ACS Catal.* **2018**, *8* (10), 9537–9542.

(82) Toriyama, F.; Cornella, J.; Wimmer, L.; Chen, T.-G.; Dixon, D. D.; Creech, G.; Baran, P. S. *J. Am. Chem. Soc.* **2016**, *138* (35), 11132–11135.

(83) Huang, L.; Olivares, A. M.; Weix, D. J. *Angew. Chem. Int. Ed.* **2017**, *56* (39), 11901–11905.

(84) Huihui, K. M. M.; Caputo, J. A.; Melchor, Z.; Olivares, A. M.; Spiewak, A. M.; Johnson, K. A.; DiBenedetto, T. A.; Kim, S.; Ackerman, L. K. G.; Weix, D. J. *J. Am. Chem. Soc.* **2016**, *138* (15), 5016–5019.

(85) Wang, J.; Cary, B. P.; Beyer, P. D.; Gellman, S. H.; Weix, D. J. *Angew. Chem. Int. Ed.* **2019**, *58* (35), 12081–12085.

(86) Suzuki, N.; Hofstra, J. L.; Poremba, K. E.; Reisman, S. E. *Org. Lett.* **2017**, *19* (8), 2150–2153.

(87) Derosa, J.; Tran, V. T.; Boulous, M. N.; Chen, J. S.; Engle, K. M. *J. Am. Chem. Soc.* **2017**, *139* (31), 10657–10660.

(88) Steves, J. E.; Stahl, S. S. *J. Am. Chem. Soc.* **2013**, *135* (42), 15742–15745.

(89) Haddach, M.; McCarthy, J. R. *Tetrahedron Lett.* **1999**, *40* (16), 3109–3112.

(90) Wotal, A. C.; Weix, D. J. *Org. Lett.* **2012**, *14* (6), 1476–1479.

(91) Hirokawa, T.; Nagasawa, T.; Kuwahara, S. *Tetrahedron Lett.* **2012**, *53* (6), 705–706.

(92) Hirokawa, T.; Kuwahara, S. *Tetrahedron* **2012**, *68* (24), 4581–4587.

(93) Ranieri, B.; Obradors, C.; Mato, M.; Echavarren, A. M. *Org. Lett.* **2016**, *18* (7), 1614–1617.

(94) Mongin, F.; Bucher, A.; Bazureau, J. P.; Bayh, O.; Awad, H.; Trécourt, F. *Tetrahedron Lett.* **2005**, *46* (46), 7989–7992.

(95) Huang, B.; Guo, L.; Jia, Y. *Angew. Chem. Int. Ed.* **2015**, *54* (46), 13599–13603.

(96) Gurak, J. A.; Yang, K. S.; Liu, Z.; Engle, K. M. *J. Am. Chem. Soc.* **2016**, *138* (18), 5805–5808.

(97) Charette, A. B.; Lebel, H. *J. Org. Chem.* **1995**, *60* (10), 2966–2967.

(98) Wender, P. A.; Dyckman, A. J.; Husfeld, C. O.; Scanio, M. J. C. *Org. Lett.* **2000**, *2* (11), 1609–1611.

(99) Monn, J. A.; Valli, M. J.; Massey, S. M.; Hansen, M. M.; Kress, T. J.; Wepsiec, J. P.; Harkness, A. R.; Grutsch, John L.; Wright, R. A.; Johnson, B. G.; Andis, S. L.; Kingston, A.; Tomlinson, R.; Lewis, R.; Griffey, K. R.; Tizzano, J. P.; Schoepp, D. D. *J. Med. Chem.* **1999**, *42* (6), 1027–1040.

(100) Kaschel, J.; Schneider, T. F.; Kratzert, D.; Stalke, D.; Werz, D. B. *Org. Biomol. Chem.* **2013**, *11* (21), 3494–3509.

(101) Herges, R.; Ugi, I. *Synthesis* **1986**, *1986* (12), 1059–1059.

(102) Meijere, A. de; Schulz, T.-J.; Kostikov, R. R.; Graupner, F.; Murr, T.; Bielfeldt, T. *Synthesis* **1991**, *1991* (07), 547–560.

(103) Miles, W.; Duca, D. G.; Freedman, J. T.; Goodzeit, E. O.; Hamman, K. B.; Palha De Sousa, C. A.; Selfridge, B. R. *Heterocycl. Commun.* **2007**, *13* (4), 195–198.

(104) Zúñiga, A.; Pazos, G.; Besada, P.; Fall, Y. *Tetrahedron Lett.* **2012**, *53* (33), 4293–4295.

(105) Annangudi, S. P.; Sun, M.; Salomon, R. G. *Synlett* **2005**, *2005* (9), 1468–1470.

(106) Beck, J. C.; Lacker, C. R.; Chapman, L. M.; Reisman, S. E. *Chem. Sci.* **2019**, *10* (8), 2315–2319.

(107) Lifchits, O.; Mahlau, M.; Reisinger, C. M.; Lee, A.; Farès, C.; Polyak, I.; Gopakumar, G.; Thiel, W.; List, B. *J. Am. Chem. Soc.* **2013**, *135* (17), 6677–6693.

Appendix 2

Spectra Relevant to Chapter 2:

Modular Synthesis of Enantioenriched Cyclobutanes: Applications

Towards the Total Synthesis of (+)-Rumphellaone A

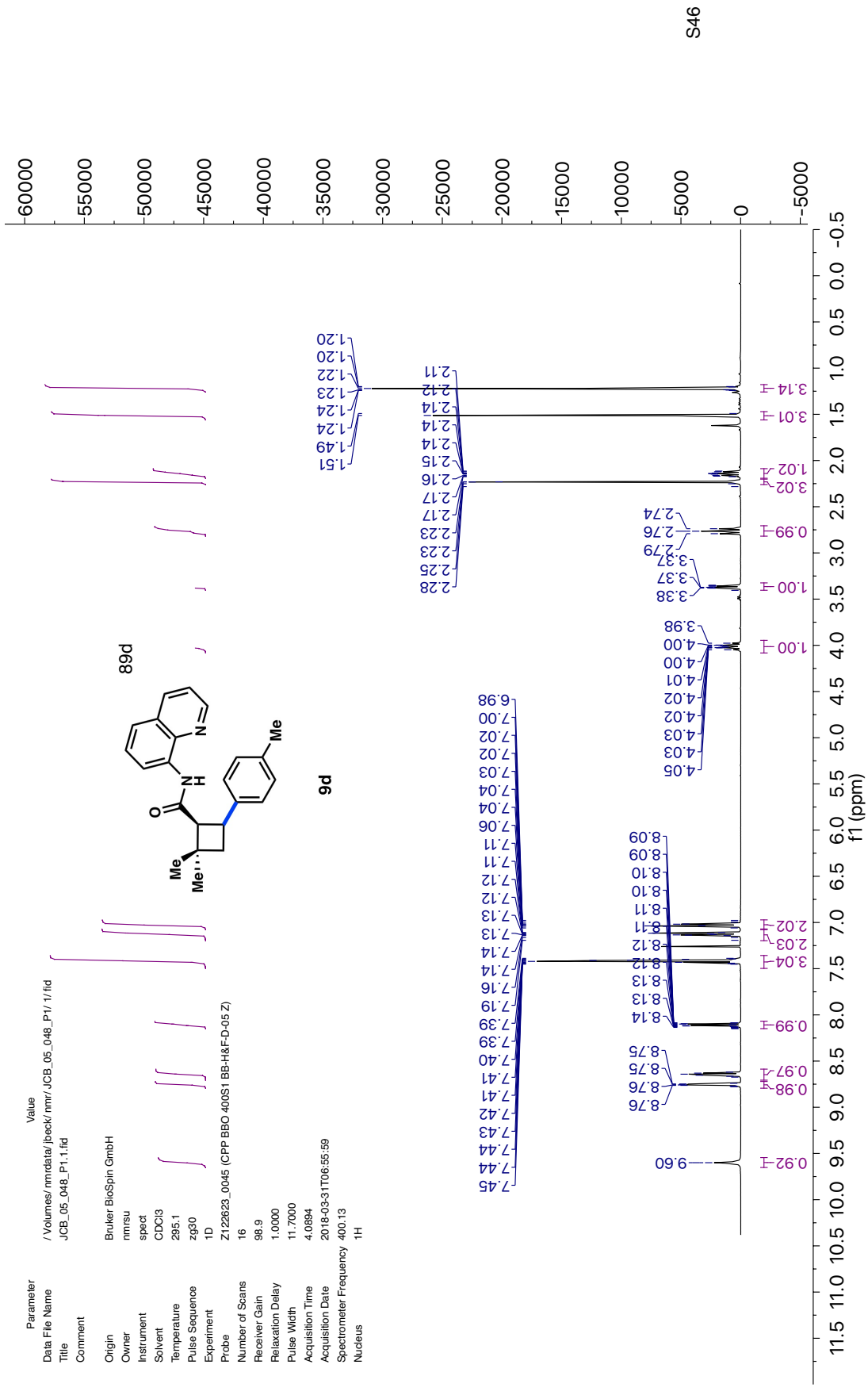
S46
89d
9d
Me
Me
Me
N
H
O
N
Parameter Value
Data File Name / Volumes/ nmrdata/ jbeck/ nmr/ JCB_05_048_P1/ 1/ fid
Title JCB_05_048_P1.1.fid
Comment
Origin Bruker BioSpin GmbH
Owner nmrsu
Instrument spect
Solvent CDCl3
Temperature 295.1
Pulse Sequence zg30
Experiment 1D
Probe Z122623_0045 (CPP BBO 400S1 BB-H&F-D-05 Z)
Number of Scans 16
Receiver Gain 98.9
Relaxation Delay 1.0000
Pulse Width 11.7000
Acquisition Time 4.0894
Acquisition Date 2018-03-31T06:55:59
Spectrometer Frequency 400.13
Nucleus 1H
f1 (ppm)

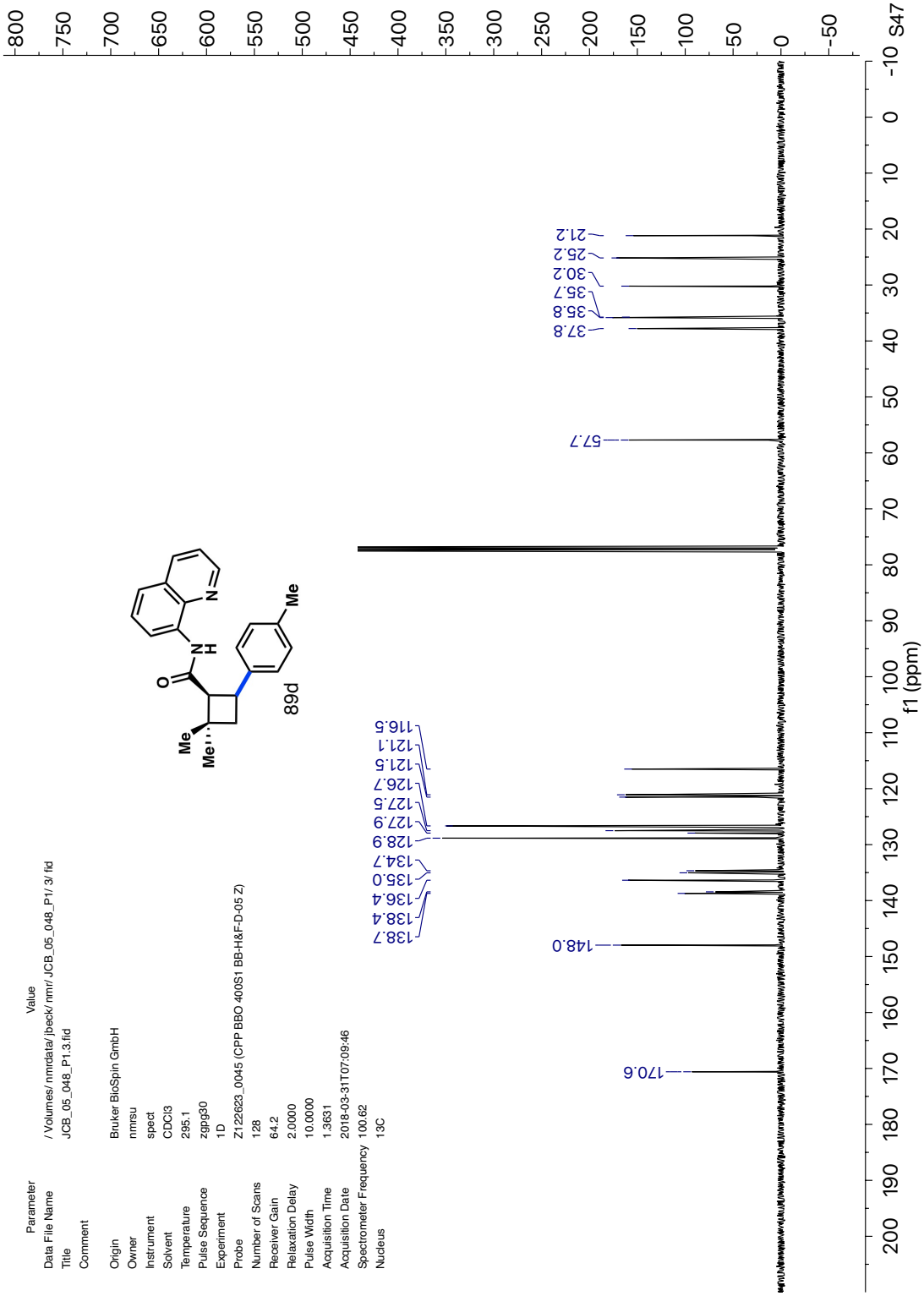
Parameter Value
Data File Name / Volumes/ nmrdata/ jbeck/ nmr/ JCB_05_048_P1/ 3/ fid
Title JCB_05_048_P1.3.fid
Comment
Origin Bruker BioSpin GmbH
Owner nmrsu
Instrument spect
Solvent CDCl3
Temperature 295.1
Pulse Sequence zgpg30
Experiment 1D
Probe Z122623_0045 (CPP BBO 400S1 BB-H&F-D-05 Z)
Number of Scans 128
Receiver Gain 64.2
Relaxation Delay 2.0000
Pulse Width 10.0000
Acquisition Time 1.3631
Acquisition Date 2018-03-31T07:09:46
Spectrometer Frequency 100.62
Nucleus 13C
89d
Me
Me
Me
N
H
N
O
170.6
148.0
138.7
138.4
136.4
135.0
134.7
128.9
127.9
127.5
126.7
121.5
121.1
116.5
57.7
37.8
35.8
35.7
30.2
25.2
21.2
f1 (ppm)
S47

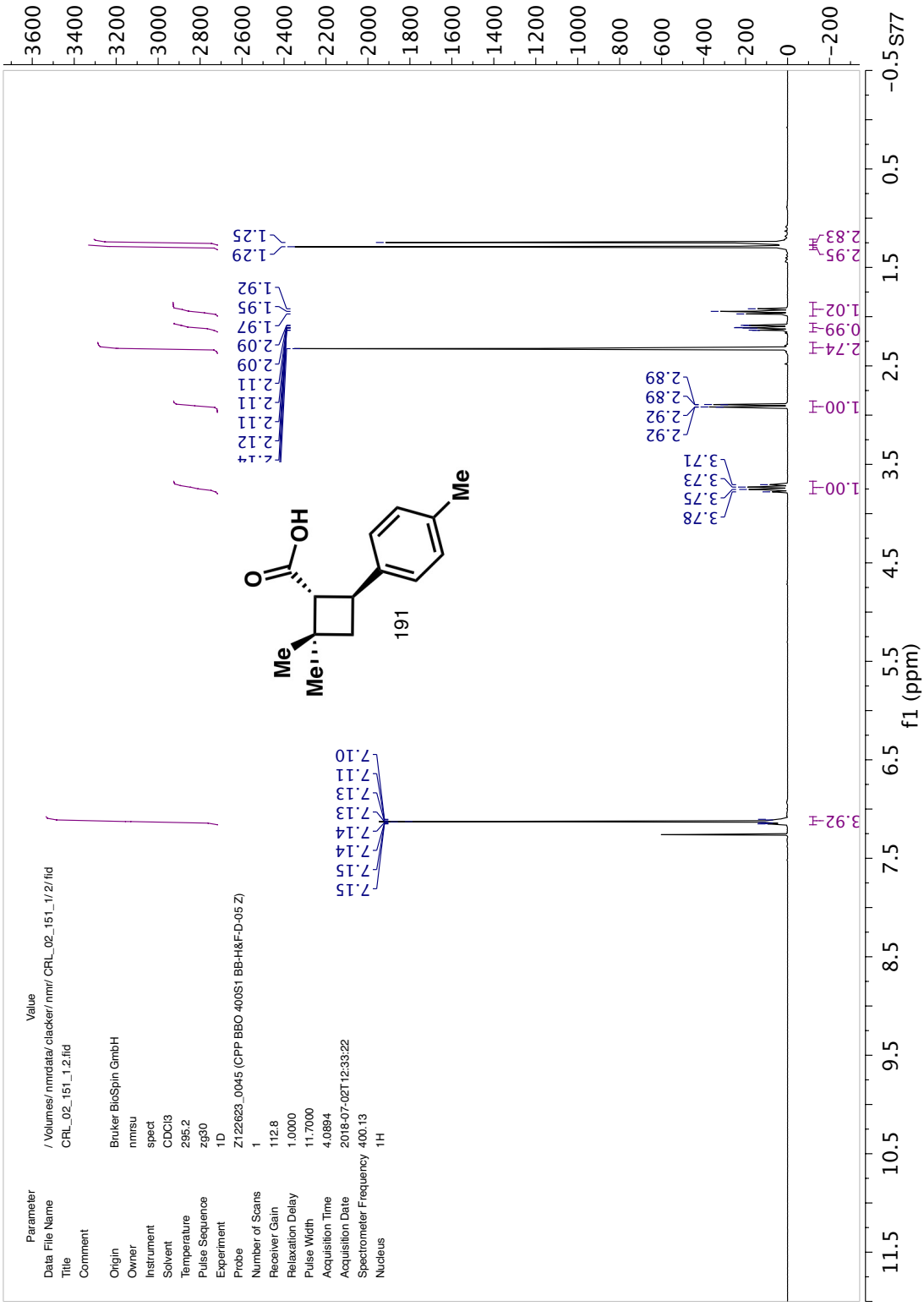
Parameter Value
Data File Name / Volumes/ nmrdata/ clacker/ nmr/ CRL_02_151_1/2/ fid
Title CRL_02_151_1.2.fid
Comment
Origin Bruker BioSpin GmbH
Owner nmrsu
Instrument spect
Solvent CDCl3
Temperature 295.2
Pulse Sequence zg30
Experiment 1D
Probe Z122623_0045 (CPP BBO 400S1 BB-H&F-D-05 Z)
Number of Scans 1
Receiver Gain 112.8
Relaxation Delay 1.0000
Pulse Width 11.7000
Acquisition Time 4.0894
Acquisition Date 2018-07-02T12:33:22
Spectrometer Frequency 400.13
Nucleus 1H
OH
O
Me
Me
191
f1 (ppm)
S77

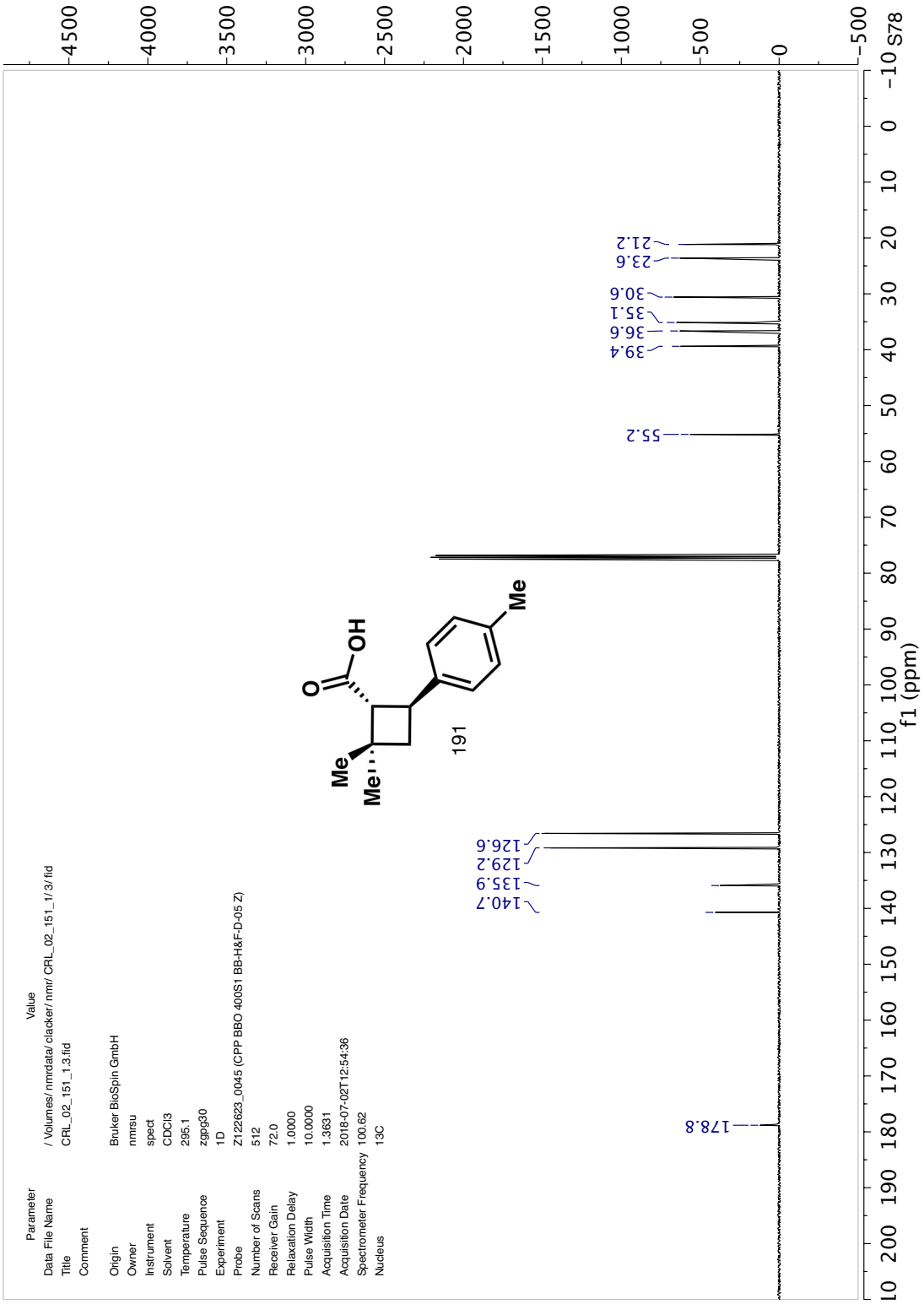
Parameter Value
Data File Name / Volumes/ nmrdata/ clacker/ nmr/ CRL_02_151_1/3/ fid
Title CRL_02_151_1.3.fid
Comment
Origin Bruker BioSpin GmbH
Owner nmrsu
Instrument spect
Solvent CDCl3
Temperature 295.1
Pulse Sequence zgpg30
Experiment 1D
Probe Z122623_0045 (CPP BBO 400S1 BB-H&F-D-05 Z)
Number of Scans 512
Receiver Gain 72.0
Relaxation Delay 1.0000
Pulse Width 10.0000
Acquisition Time 1.3631
Acquisition Date 2018-07-02T12:54:36
Spectrometer Frequency 100.62
Nucleus 13C
178.8
140.7
135.9
129.2
126.6
55.2
39.4
36.6
35.1
30.6
23.6
21.2
Me
Me
OH
O
191
f1 (ppm)
S78

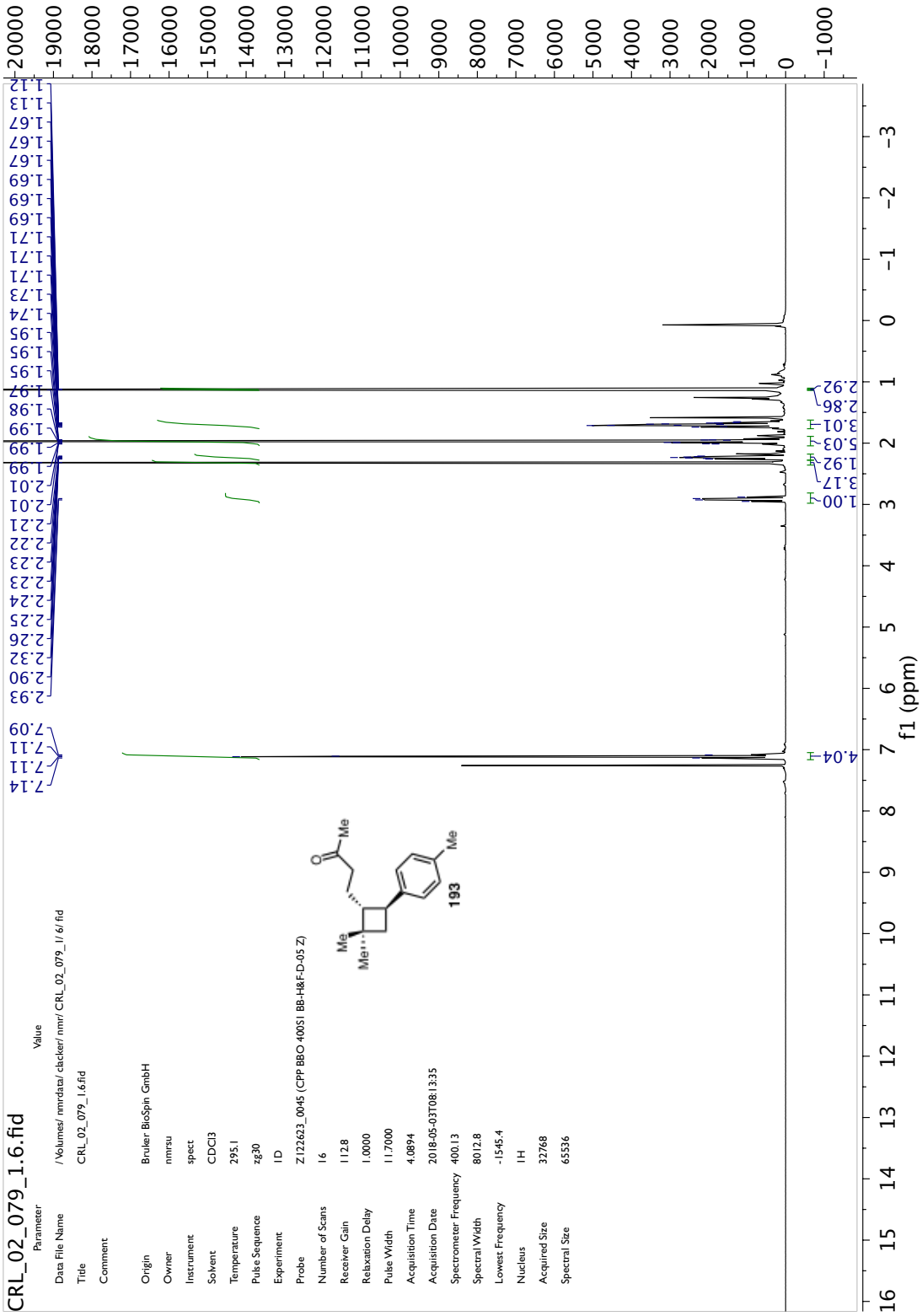
CRL_02_079_1.6.fid
Parameter
Value
Data File Name
/Volumes/ nmrdata/ clacker/ nmr/ CRL_02_079_1/ 6/ fid
Title
CRL_02_079_1.6.fid
Comment
Origin
Bruker BioSpin GmbH
Owner
nmrsu
Instrument
spect
Solvent
CDCl3
Temperature
295.1
Pulse Sequence
zg30
Experiment
1D
Probe
Z122623_0045 (CPP BBO 400SI BB-H&F-D-05 Z)
Number of Scans
16
Receiver Gain
1128
Relaxation Delay
1.0000
Pulse Width
11.7000
Acquisition Time
4.0894
Acquisition Date
2018-05-03T08:13:35
Spectrometer Frequency
400.13
Spectral Width
8012.8
Lowest Frequency
-1545.4
Nucleus
1H
Acquired Size
32768
Spectral Size
65536
Me
Me
Me
193
7.14
7.11
7.11
7.09
2.93
2.90
2.32
2.26
2.25
2.24
2.23
2.23
2.22
2.21
2.01
2.01
1.99
1.99
1.98
1.97
1.95
1.95
1.95
1.74
1.73
1.71
1.71
1.71
1.69
1.69
1.69
1.67
1.67
1.13
1.12
4.04
1.00
3.17
1.92
5.03
3.01
2.86
2.92
f1 (ppm)

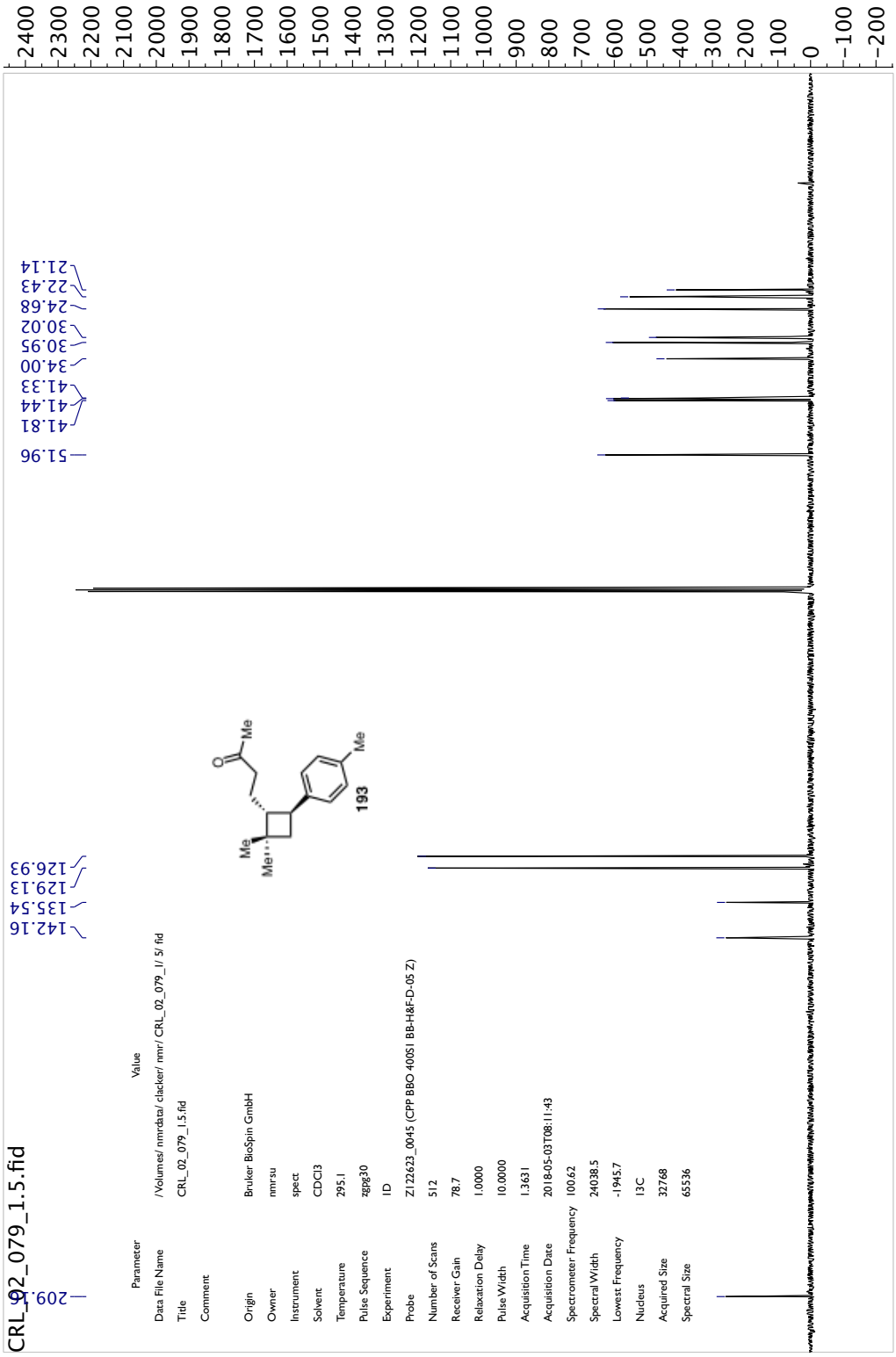
CRL_02_079_1.5.fid
209.16
142.16
135.54
129.13
126.93
51.96
41.81
41.44
41.33
34.00
30.95
30.02
24.68
22.43
21.14
Me
Me
Me
193
f1 (ppm)

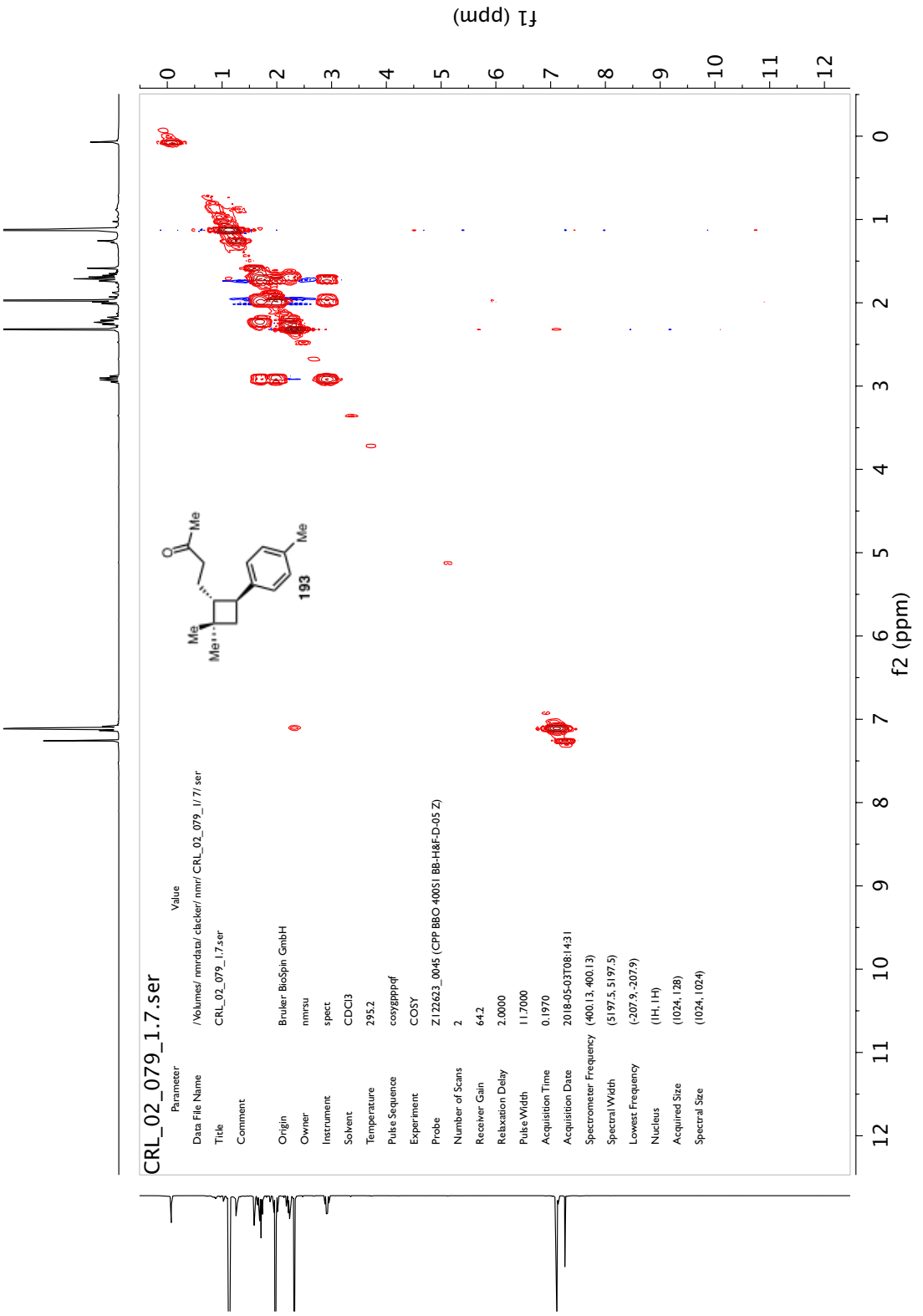
CRL_02_079_1.7.ser
Parameter Value
Data File Name /Volumes/ nmrdata/ clacker/ nmr/ CRL_02_079_1/7/ser
Title CRL_02_079_1.7.ser
Comment
Origin Bruker BioSpin GmbH
Owner nmrsu
Instrument spect
Solvent CDCl3
Temperature 295.2
Pulse Sequence cosygpppqf
Experiment COSY
Probe Z122623_0045 (CPP BBO 400SI BB-H&F-D-05 Z)
Number of Scans 2
Receiver Gain 64.2
Relaxation Delay 2.0000
Pulse Width 11.7000
Acquisition Time 0.1970
Acquisition Date 2018-05-03T08:14:31
Spectrometer Frequency (400.13, 400.13)
Spectral Width (5197.5, 5197.5)
Lowest Frequency (-207.9, -207.9)
Nucleus (1H, 1H)
Acquired Size (1024, 128)
Spectral Size (1024, 1024)
Me
Me
Me
Me
193
f1 (ppm)
f2 (ppm)

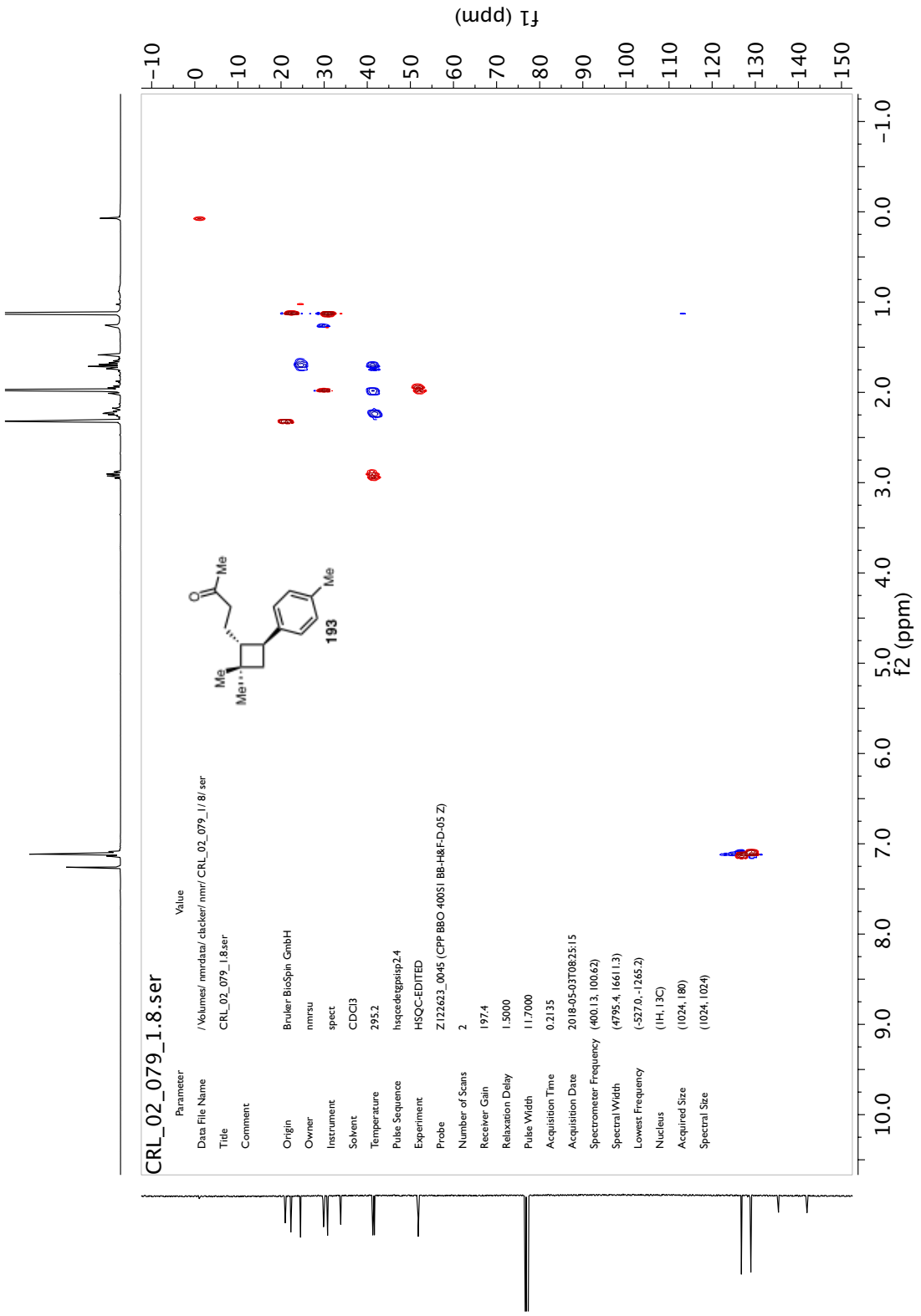
CRL_02_079_1.8.ser
Parameter Value
Data File Name /Volumes/nmrdata/clacker/nmr/CRL_02_079_1/8/ser
Title CRL_02_079_1.8.ser
Comment
Origin Bruker BioSpin GmbH
Owner nmrsu
Instrument spect
Solvent CDCl3
Temperature 295.2
Pulse Sequence hsqcedetgpsisp2.4
Experiment HSQC-EDITED
Probe Z122623_0045 (CPP BBO 400SI BB-H&F-D-05 Z)
Number of Scans 2
Receiver Gain 197.4
Relaxation Delay 1.5000
Pulse Width 11.7000
Acquisition Time 0.2135
Acquisition Date 2018-05-03T08:25:15
Spectrometer Frequency (400.13, 100.62)
Spectral Width (4795.4, 1661.3)
Lowest Frequency (-527.0, -1265.2)
Nucleus (1H, 13C)
Acquired Size (1024, 180)
Spectral Size (1024, 1024)
Me
Me
Me
Me
193
f1 (ppm)
f2 (ppm)

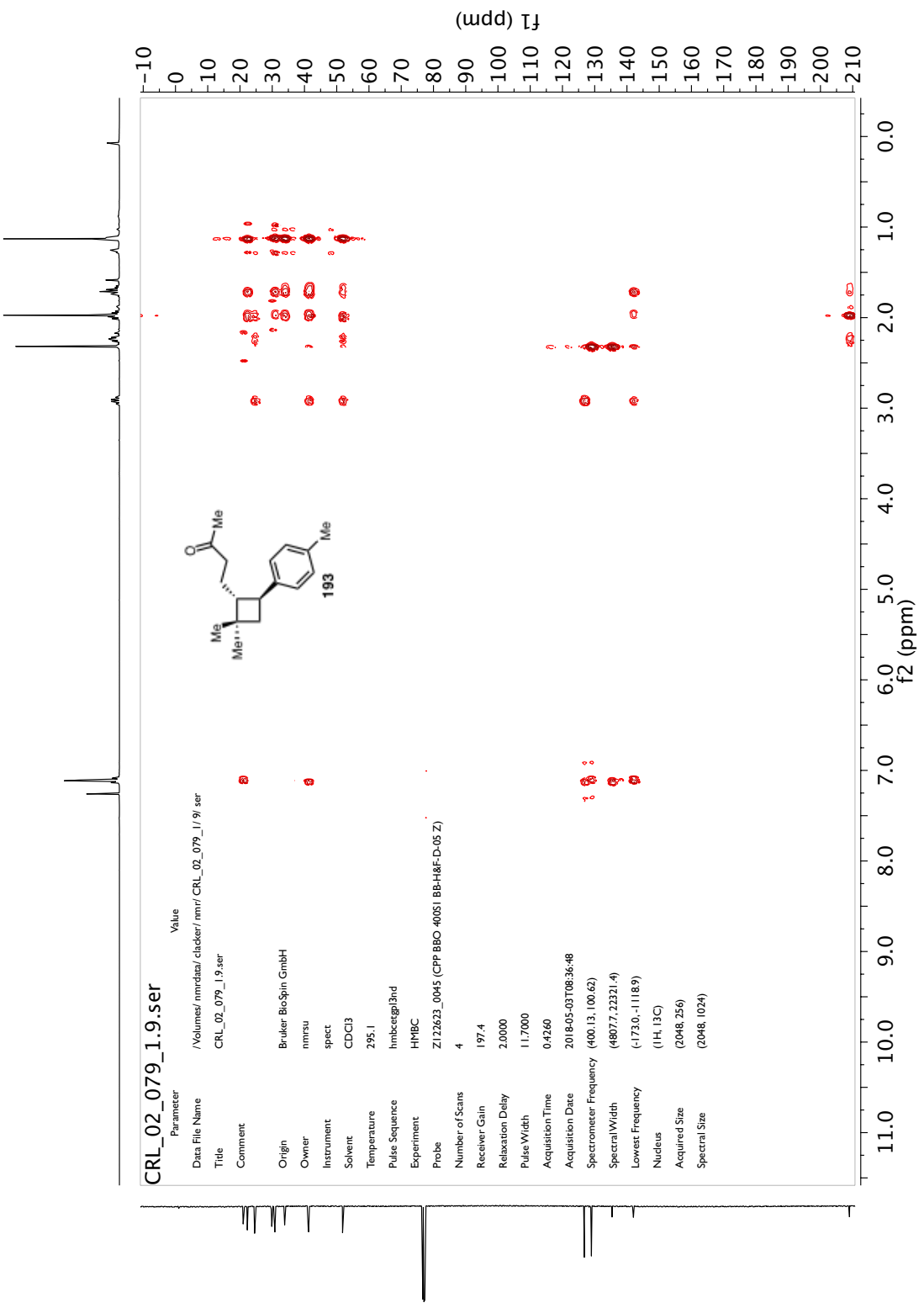
CRL_02_079_1.9.ser
Parameter Value
Data File Name /Volumes/ nmrdata/ clacker/ nmr/ CRL_02_079_1/ 9/ ser
Title CRL_02_079_1.9.ser
Comment
Origin Bruker BioSpin GmbH
Owner nmrsu
Instrument spect
Solvent CDCl3
Temperature 295.1
Pulse Sequence hmbcetgpl3nd
Experiment HMBC
Probe Z122623_0045 (CPP BBO 400S1 BB-H&F-D-05 Z)
Number of Scans 4
Receiver Gain 197.4
Relaxation Delay 2.0000
Pulse Width 11.7000
Acquisition Time 0.4260
Acquisition Date 2018-05-03T08:36:48
Spectrometer Frequency (400.13, 100.62)
Spectral Width (4807.7, 22321.4)
Lowest Frequency (-1730, -1118.9)
Nucleus (1H, 13C)
Acquired Size (2048, 256)
Spectral Size (2048, 1024)
Me
Me
Me
Me
193
f1 (ppm)
f2 (ppm)

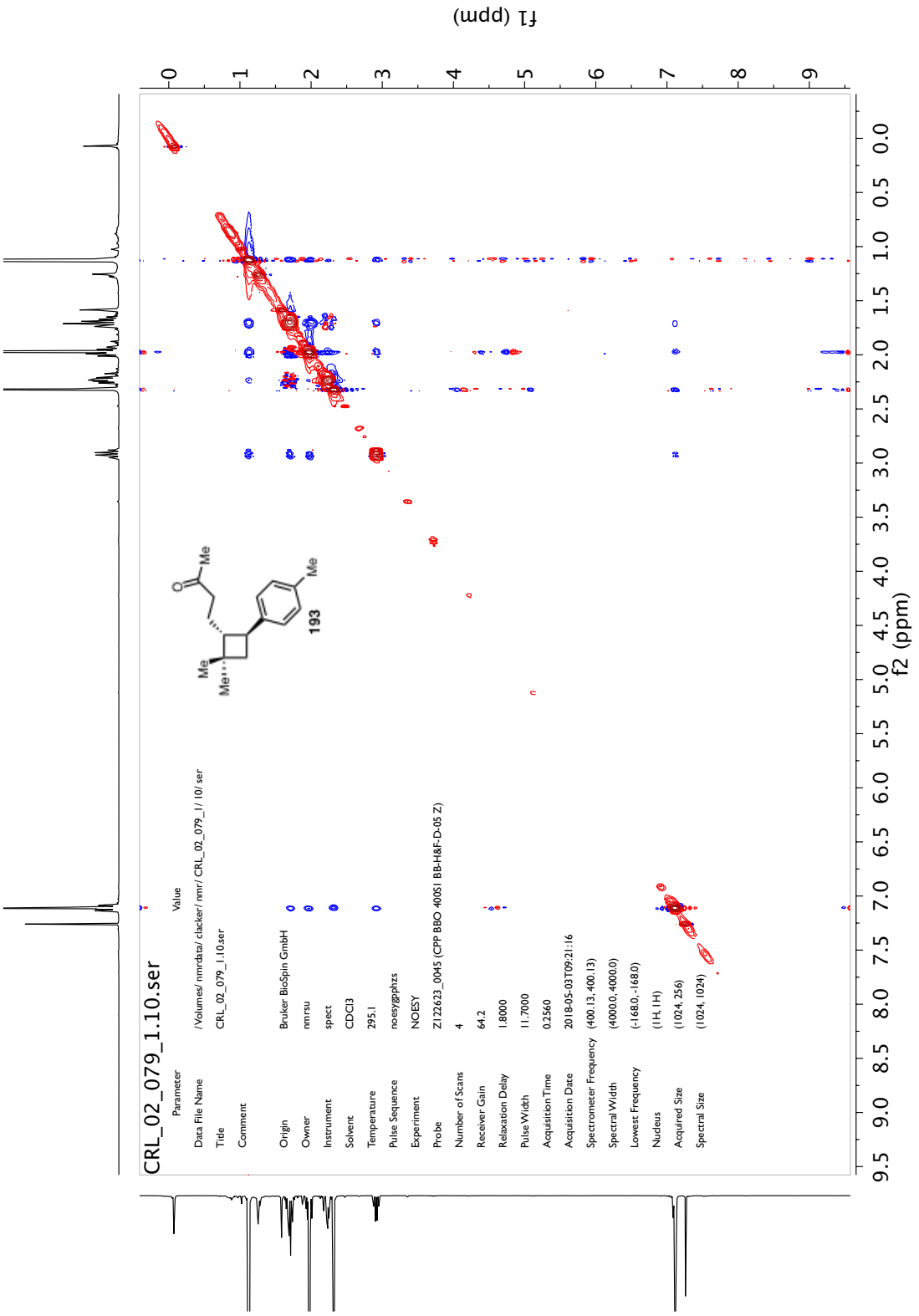
CRL_02_079_1.10.ser
Parameter Value
Data File Name /Volumes/ nmrdata/ clacker/ nmr/ CRL_02_079_1/ 10/ ser
Title CRL_02_079_1.10.ser
Comment
Origin Bruker BioSpin GmbH
Owner nmrsu
Instrument spect
Solvent CDCl3
Temperature 295.1
Pulse Sequence noesygpphzs
Experiment NOESY
Probe Z122623_0045 (CPP BBO 400SI BB-H&F-D-05 Z)
Number of Scans 4
Receiver Gain 64.2
Relaxation Delay 1.8000
Pulse Width 11.7000
Acquisition Time 0.2560
Acquisition Date 2018-05-03T09:21:16
Spectrometer Frequency (400.13, 400.13)
Spectral Width (4000.0, 4000.0)
Lowest Frequency (-168.0, -168.0)
Nucleus (1H, 1H)
Acquired Size (1024, 256)
Spectral Size (1024, 1024)
Me
Me
Me
Me
193
f2 (ppm)
f1 (ppm)

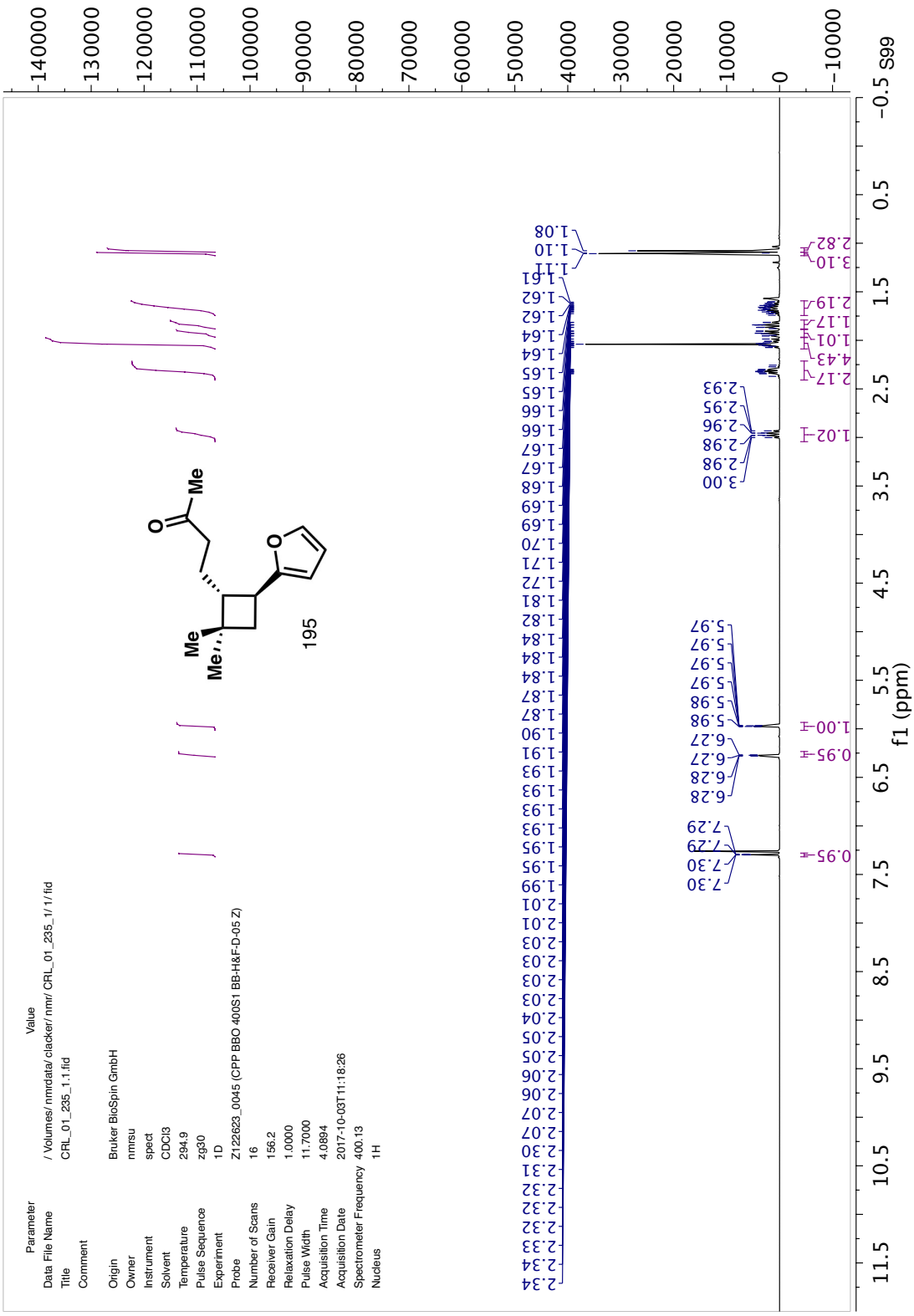
Parameter Value
Data File Name / Volumes/ nmrdata/ clacker/ nmr/ CRL_01_235_1/ 1/ fid
Title CRL_01_235_1.1.fid
Comment
Origin Bruker BioSpin GmbH
Owner nmrsu
Instrument spect
Solvent CDCl3
Temperature 294.9
Pulse Sequence zg30
Experiment 1D
Probe Z122623_0045 (CPP BBO 400S1 BB-H&F-D-05 Z)
Number of Scans 16
Receiver Gain 156.2
Relaxation Delay 1.0000
Pulse Width 11.7000
Acquisition Time 4.0894
Acquisition Date 2017-10-03T11:18:26
Spectrometer Frequency 400.13
Nucleus 1H
Me
O
Me
Me
O
195
f1 (ppm)

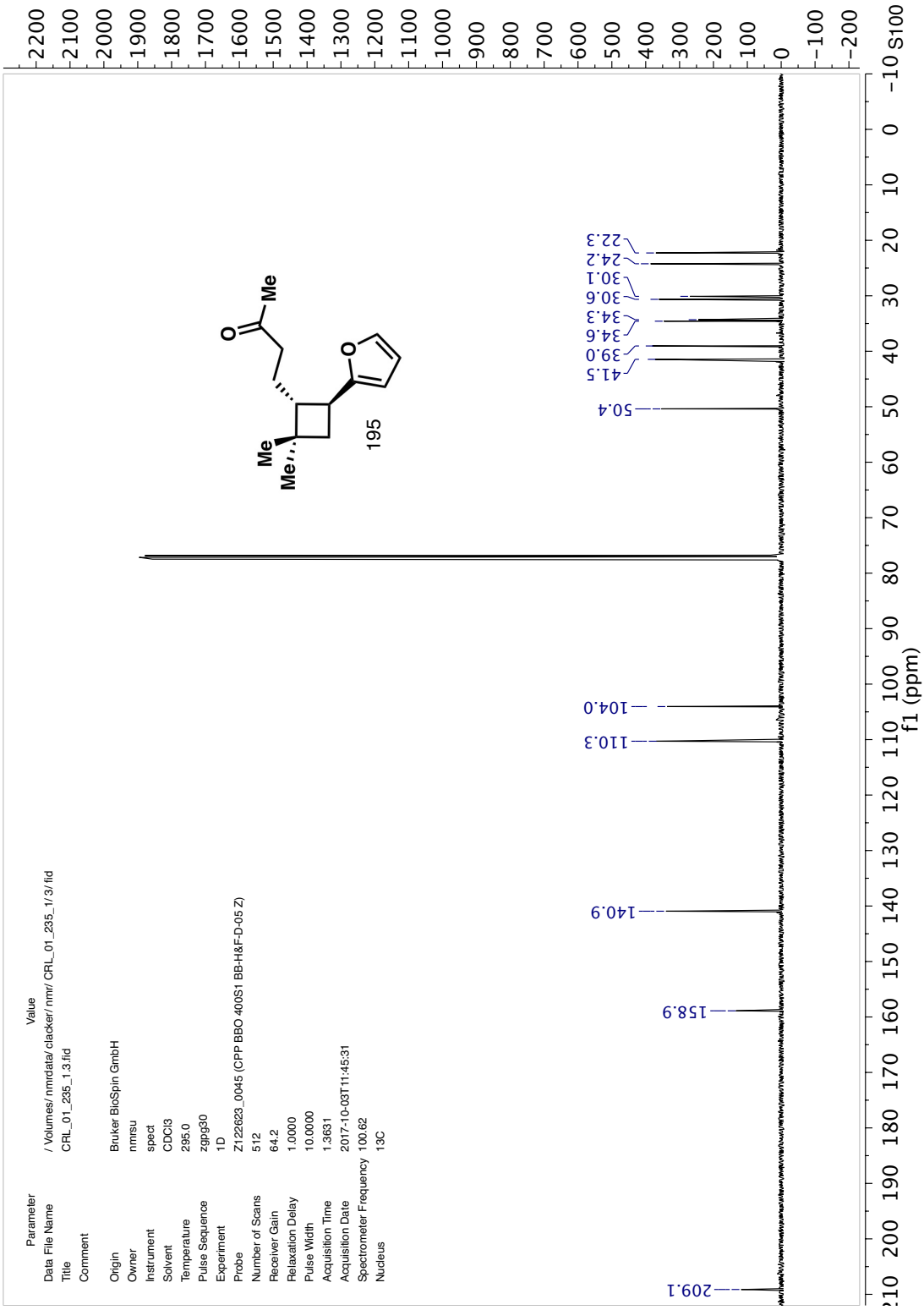
Parameter Value
Data File Name / Volumes/ nmrdata/ clacker/ nmr/ CRL_01_235_1/3/ fid
Title CRL_01_235_1.3.fid
Comment
Origin Bruker BioSpin GmbH
Owner nmrsu
Instrument spect
Solvent CDCl3
Temperature 295.0
Pulse Sequence zgpg30
Experiment 1D
Probe Z122623_0045 (CPP BBO 400S1 BB-H&F-D-05 Z)
Number of Scans 512
Receiver Gain 64.2
Relaxation Delay 1.0000
Pulse Width 10.0000
Acquisition Time 1.3631
Acquisition Date 2017-10-03T11:45:31
Spectrometer Frequency 100.62
Nucleus 13C
Me
O
Me
Me
O
195
209.1
158.9
140.9
110.3
104.0
50.4
41.5
39.0
34.6
34.3
30.6
30.1
24.2
22.3
f1 (ppm)

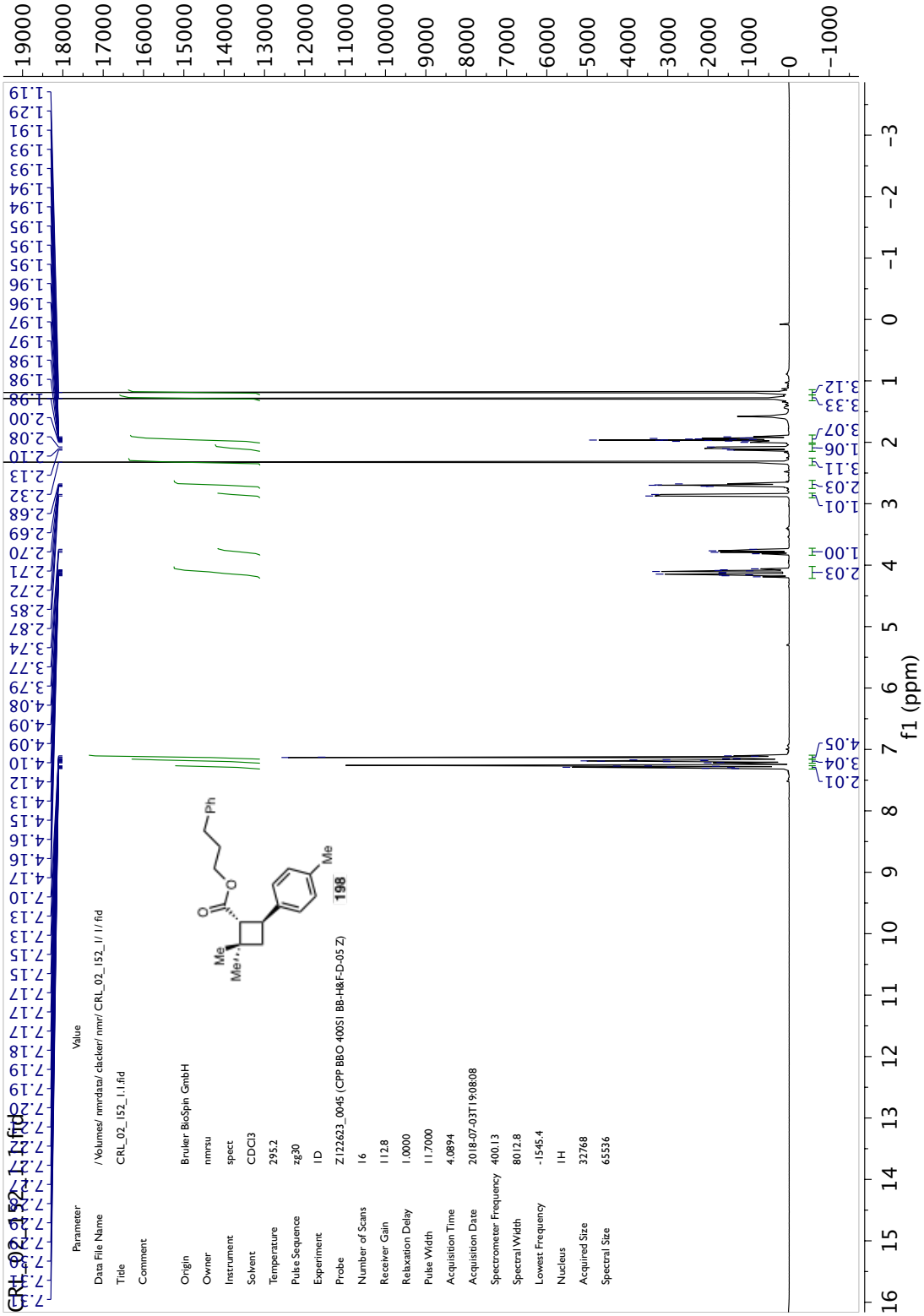
CRL_02_152_1_1.fid
Parameter Value
Data File Name /Volumes/ nmrdata/ clacker/ nmr/ CRL_02_152_1/ 1/ fid
Title CRL_02_152_1.1.fid
Comment
Origin Bruker BioSpin GmbH
Owner nmrsu
Instrument spect
Solvent CDCl3
Temperature 295.2
Pulse Sequence zg30
Experiment 1D
Probe Z122623_0045 (CPP BBO 400SI BB-H&F-D-05 Z)
Number of Scans 16
Receiver Gain 112.8
Relaxation Delay 1.0000
Pulse Width 11.7000
Acquisition Time 4.0894
Acquisition Date 2018-07-03T19:08:08
Spectrometer Frequency 400.13
Spectral Width 8012.8
Lowest Frequency -1545.4
Nucleus 1H
Acquired Size 32768
Spectral Size 65536
198
Ph
Me
Me
Me
f1 (ppm)

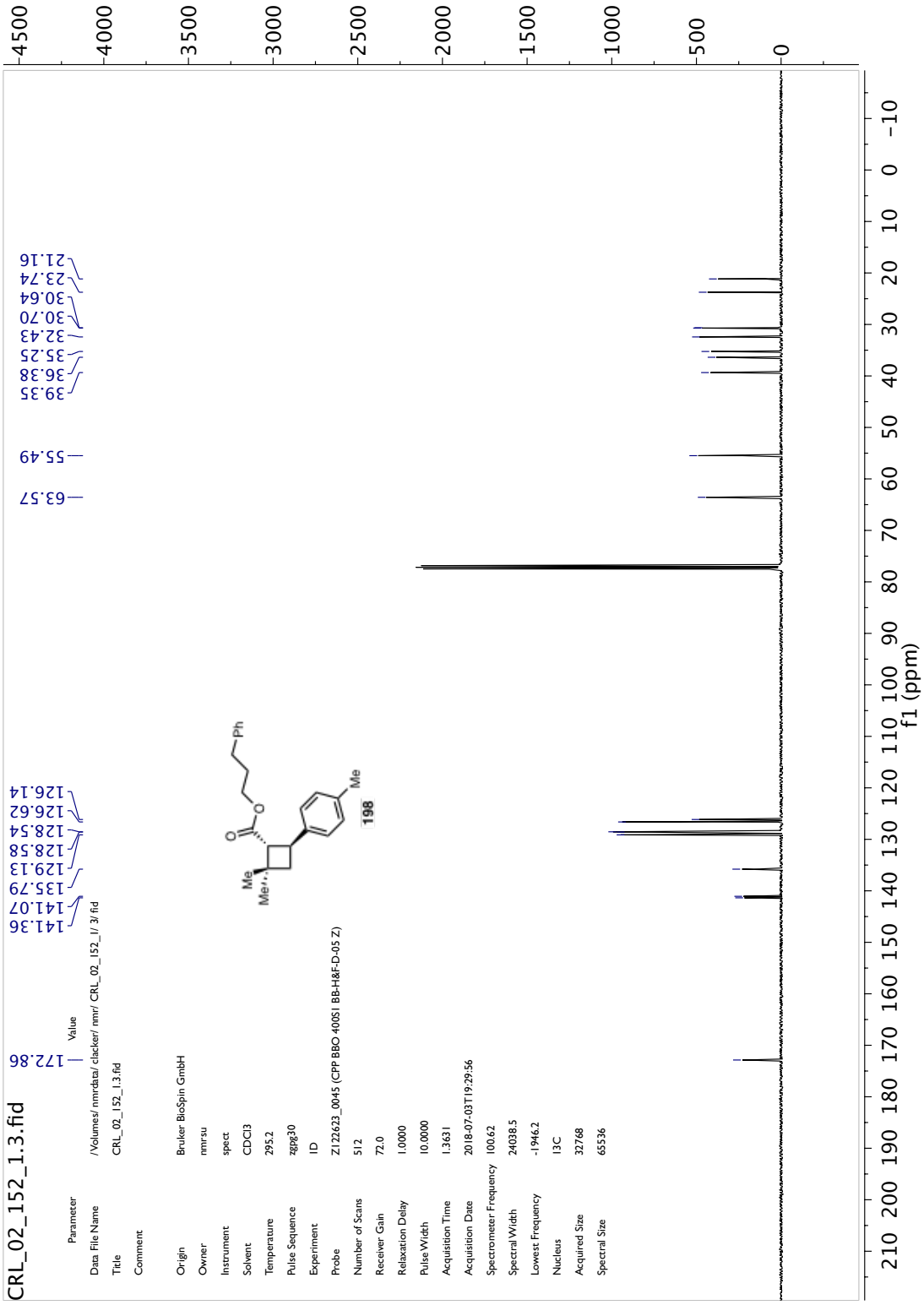
CRL_02_152_1.3.fid
Parameter
Value
Data File Name
/Volumes/ nmrdata/ clacker/ nmr/ CRL_02_152_1/ 3/ fid
Title
CRL_02_152_1.3.fid
Comment
Origin
Bruker BioSpin GmbH
Owner
nmrsu
Instrument
spect
Solvent
CDCl3
Temperature
295.2
Pulse Sequence
zgpg30
Experiment
1D
Probe
Z122623_0045 (CPP BBO 400SI BB-H&F-D-05 Z)
Number of Scans
512
Receiver Gain
72.0
Relaxation Delay
1.0000
Pulse Width
10.0000
Acquisition Time
1.3631
Acquisition Date
2018-07-03T19:29:56
Spectrometer Frequency
100.62
Spectral Width
24038.5
Lowest Frequency
-1946.2
Nucleus
13C
Acquired Size
32768
Spectral Size
65536
172.86
141.36
141.07
135.79
129.13
128.58
128.54
126.62
126.14
63.57
55.49
39.35
36.38
35.25
32.43
30.70
30.64
23.74
21.16
Ph
O
O
Me
Me
Me
198
f1 (ppm)

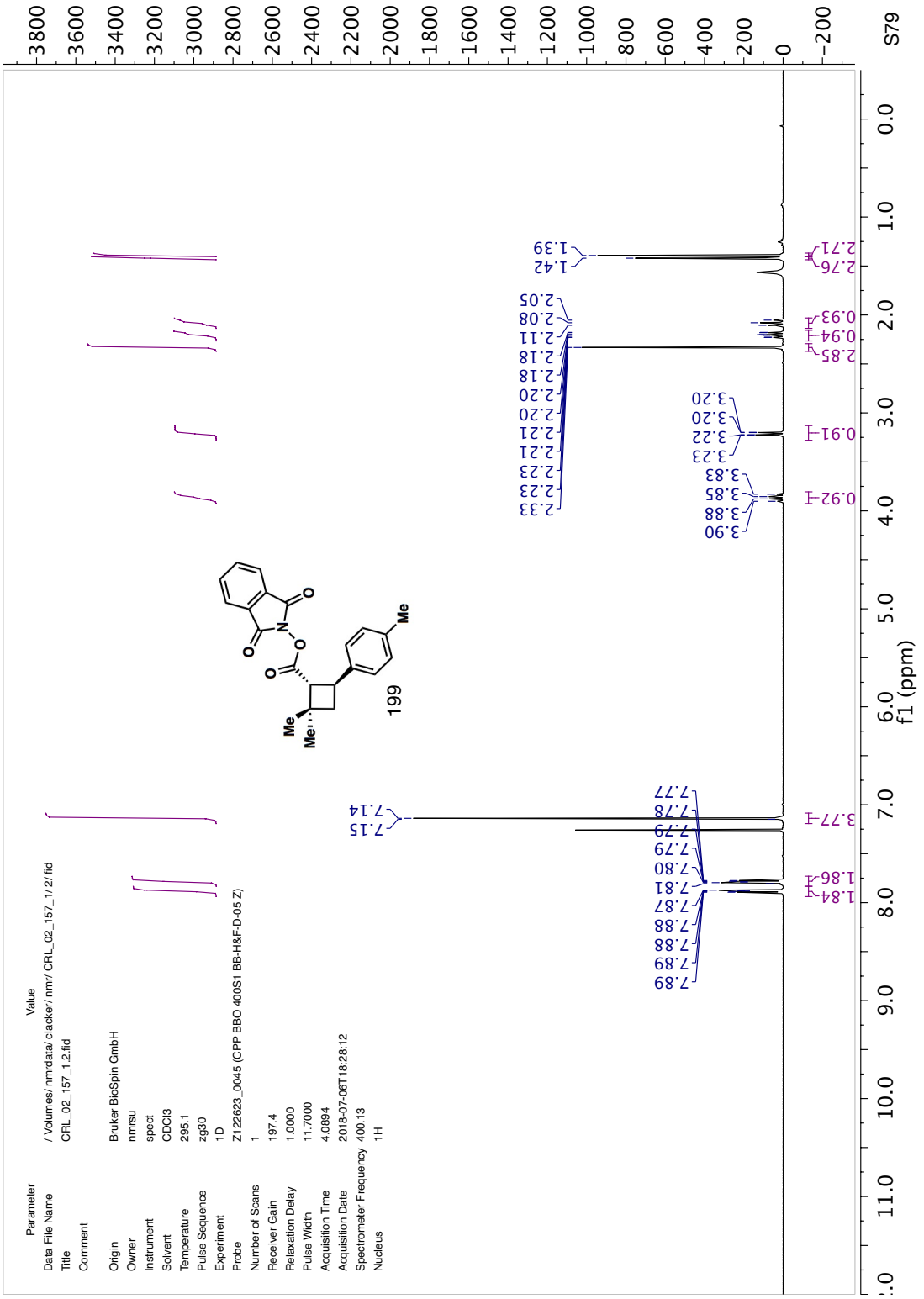
Parameter Value
Data File Name / Volumes/ nmrdata/ clacker/ nmr/ CRL_02_157_1/2/ fid
Title CRL_02_157_1.2.fid
Comment
Origin Bruker BioSpin GmbH
Owner nmrsu
Instrument spect
Solvent CDCl3
Temperature 295.1
Pulse Sequence zg30
Experiment 1D
Probe Z122623_0045 (CPP BBO 400S1 BB-H&F-D-05 Z)
Number of Scans 1
Receiver Gain 197.4
Relaxation Delay 1.0000
Pulse Width 11.7000
Acquisition Time 4.0894
Acquisition Date 2018-07-06T18:28:12
Spectrometer Frequency 400.13
Nucleus 1H
199
Me
Me
Me
S79
f1 (ppm)

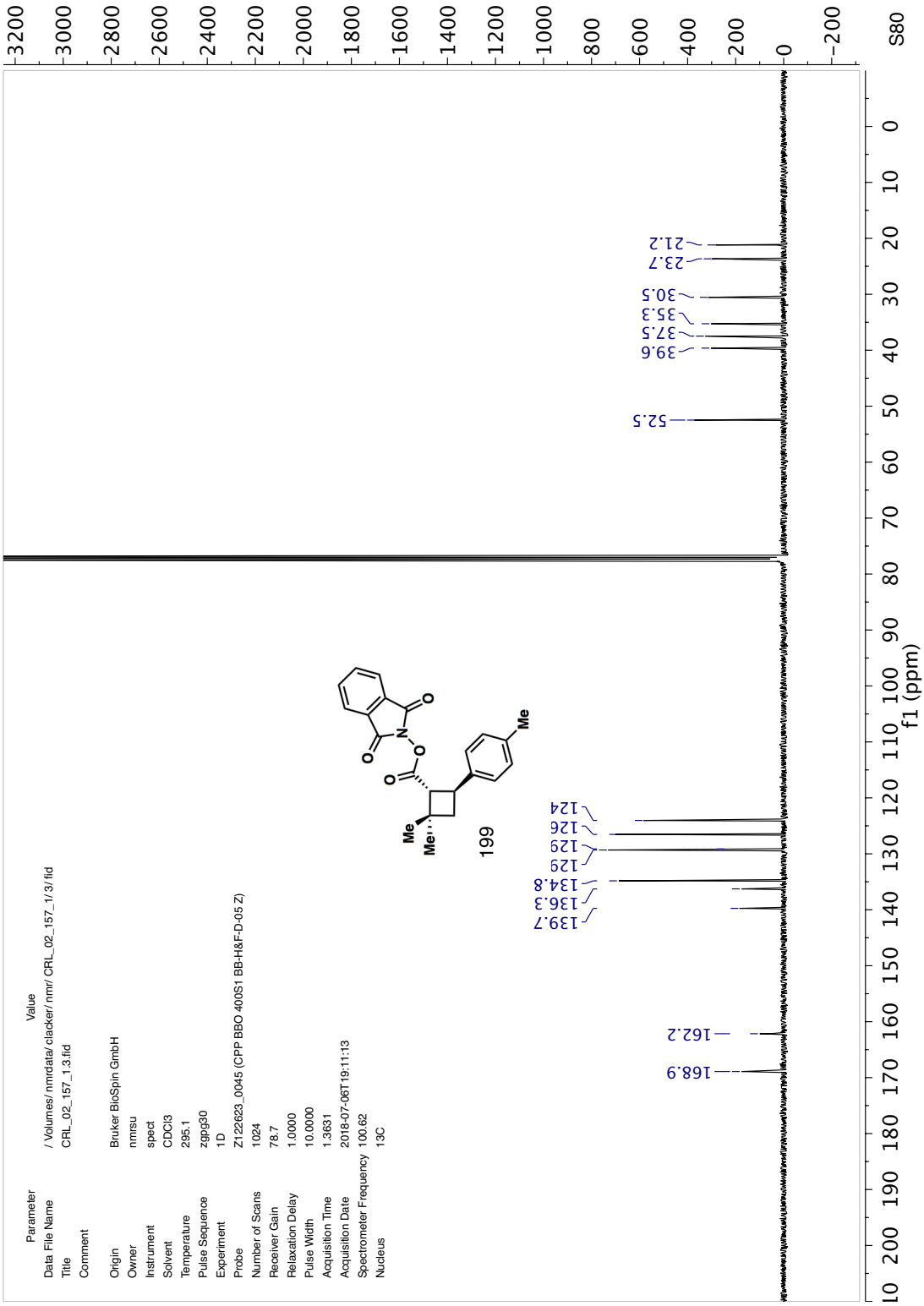
Parameter Value
Data File Name / Volumes/ nmrdata/ clacker/ nmr/ CRL_02_157_1/3/ fid
Title CRL_02_157_1.3.fid
Comment
Origin Bruker BioSpin GmbH
Owner nmrsu
Instrument spect
Solvent CDCl3
Temperature 295.1
Pulse Sequence zgpg30
Experiment 1D
Probe Z122623_0045 (CPP BBO 400S1 BB-H&F-D-05 Z)
Number of Scans 1024
Receiver Gain 78.7
Relaxation Delay 1.0000
Pulse Width 10.0000
Acquisition Time 1.3631
Acquisition Date 2018-07-06T19:11:13
Spectrometer Frequency 100.62
Nucleus 13C
199
Me
Me
Me
21.2
23.7
30.5
35.3
37.5
39.6
52.5
124
126
129
129
134.8
136.3
139.7
162.2
168.9
f1 (ppm)

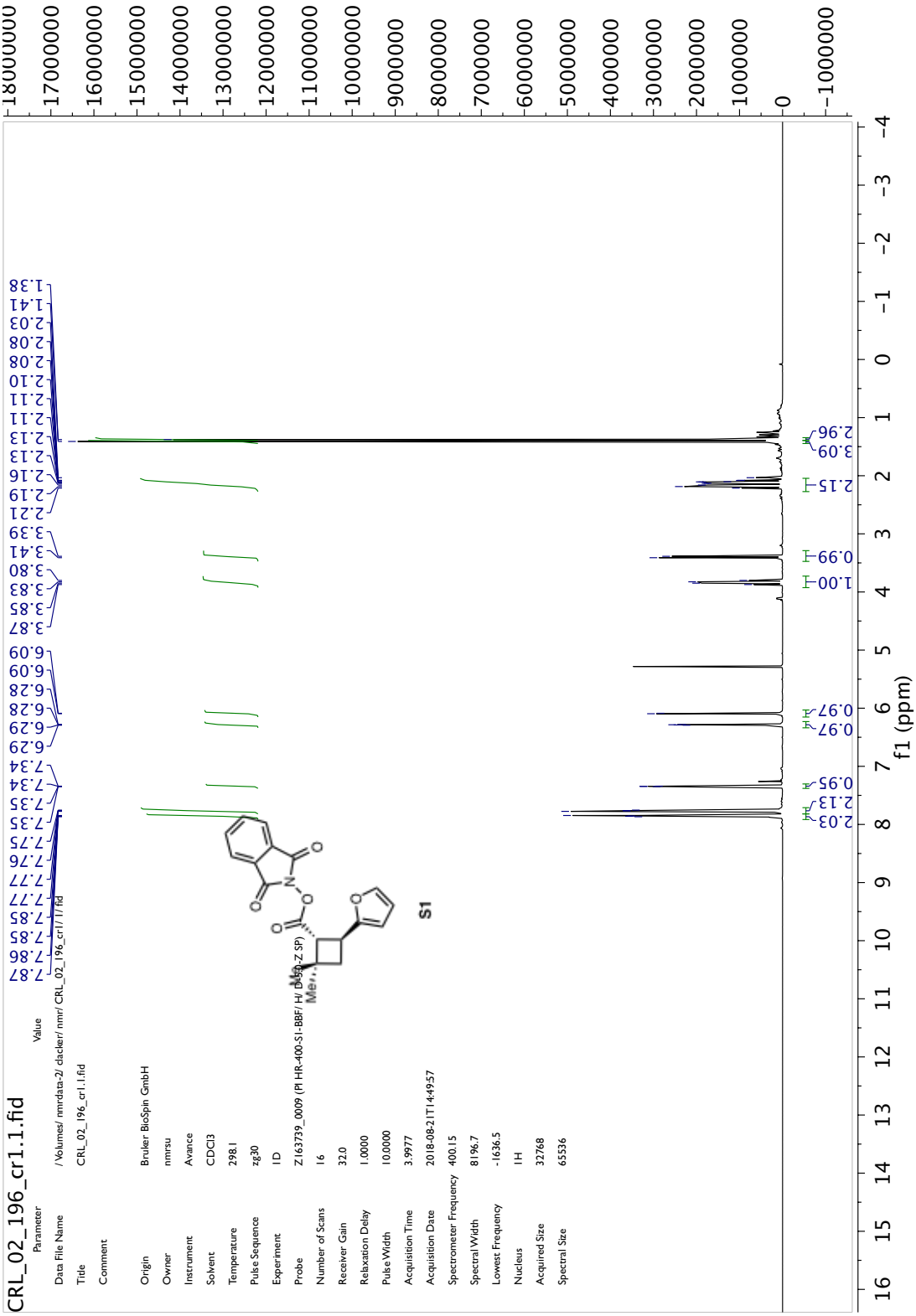
CRL_02_196_cr1.1.fid
Parameter
Value
Data File Name
/Volumes/ nmrdata-2/ dacker/ nmr/ CRL_02_196_cr1/ 1/ fid
Title
CRL_02_196_cr1.1.fid
Comment
Origin
Bruker BioSpin GmbH
Owner
nmrsu
Instrument
Avance
Solvent
CDCl3
Temperature
298.1
Pulse Sequence
zg30
Experiment
1D
Probe
Z163739_0009 (PI HR-400-S1-BBF/ H/ D-05 Z SP)
Number of Scans
16
Receiver Gain
32.0
Relaxation Delay
1.0000
Pulse Width
10.0000
Acquisition Time
3.9977
Acquisition Date
2018-08-21T14:49:57
Spectrometer Frequency
400.15
Spectral Width
8196.7
Lowest Frequency
-1636.5
Nucleus
1H
Acquired Size
32768
Spectral Size
65536
S1
f1 (ppm)

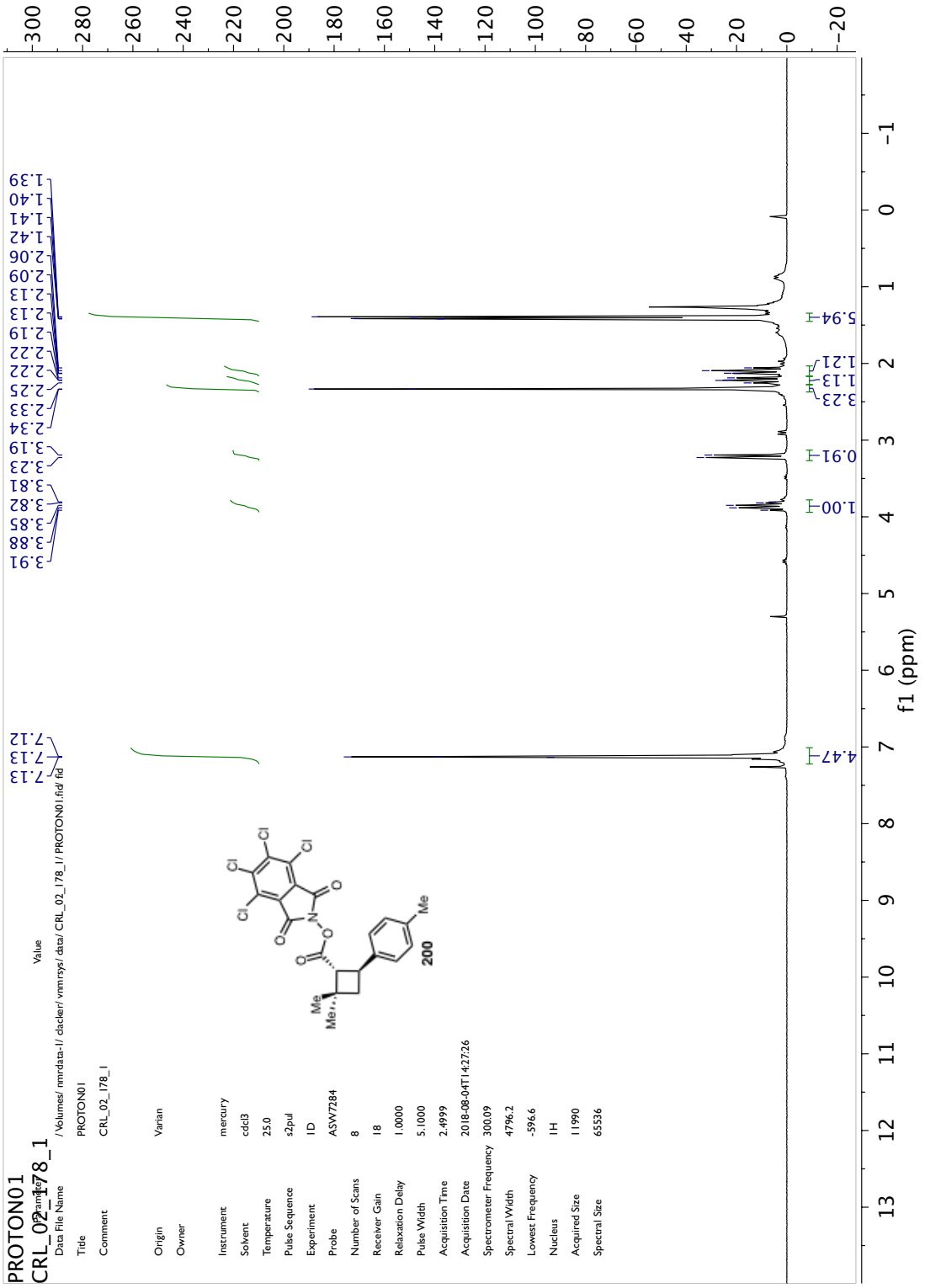
PROTON01
CRL_02_178_1
Parameter
Value
Data File Name /Volumes/ nmrdata-1/ dacker/ vnmrsys/ data/ CRL_02_178_1/ PROTON01.fid/ fid
Title PROTON01
Comment CRL_02_178_1
Origin Varian
Owner
Instrument mercury
Solvent cdcl3
Temperature 25.0
Pulse Sequence s2pul
Experiment ID
Probe ASW7284
Number of Scans 8
Receiver Gain 18
Relaxation Delay 1.0000
Pulse Width 5.1000
Acquisition Time 2.4999
Acquisition Date 2018-08-04T14:27:26
Spectrometer Frequency 300.09
Spectral Width 4796.2
Lowest Frequency -596.6
Nucleus 1H
Acquired Size 11990
Spectral Size 65536
7.13
7.13
7.12
3.91
3.88
3.85
3.82
3.81
3.23
3.19
2.34
2.33
2.25
2.22
2.22
2.19
2.13
2.13
2.09
2.06
1.42
1.41
1.40
1.39
4.47
1.00
0.91
3.23
1.13
1.21
5.94
f1 (ppm)

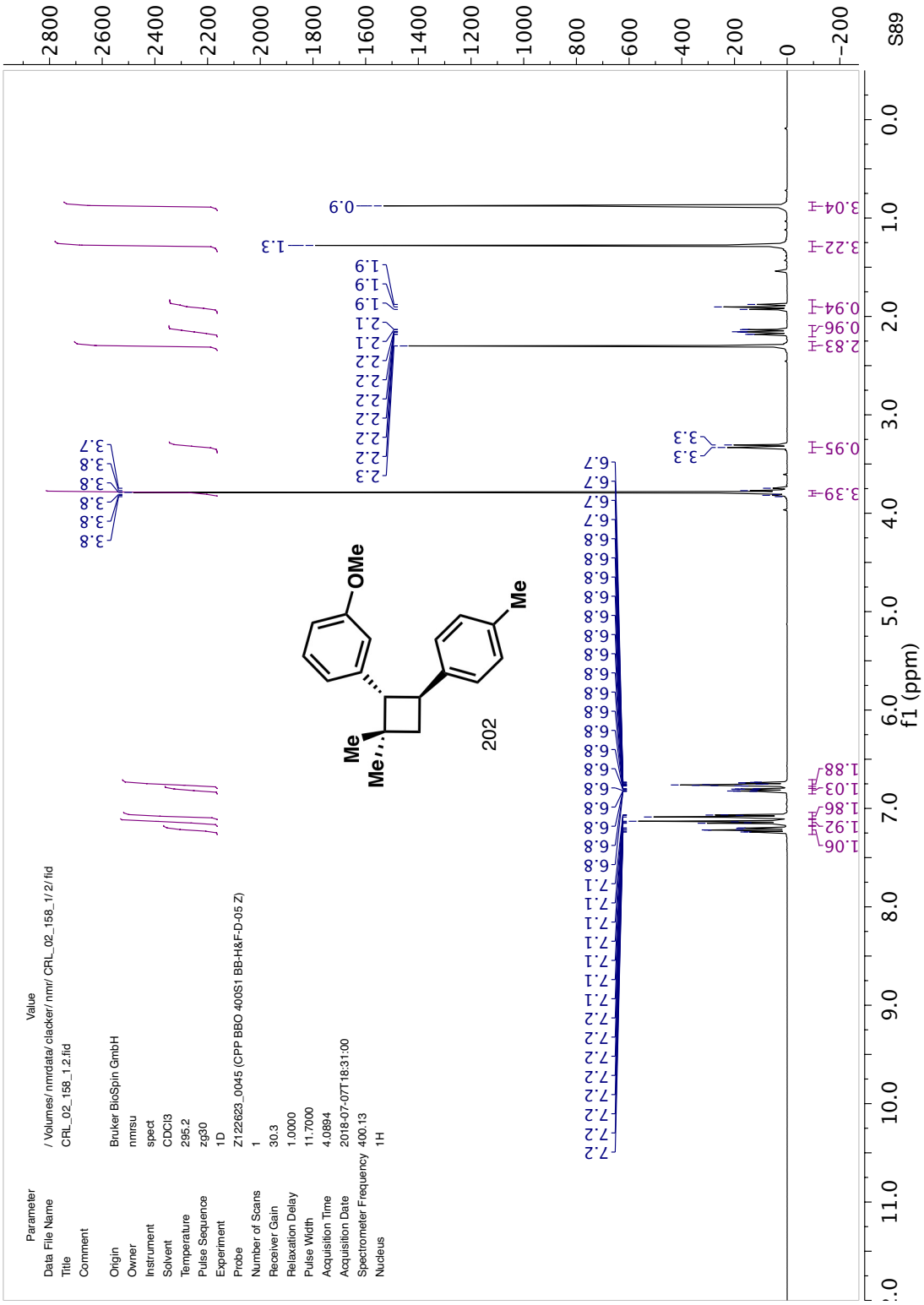
Parameter Value
Data File Name / Volumes/ nmrdata/ clacker/ nmr/ CRL_02_158_1/ 2/ fid
Title CRL_02_158_1.2.fid
Comment
Origin Bruker BioSpin GmbH
Owner nmrsu
Instrument spect
Solvent CDCl3
Temperature 295.2
Pulse Sequence zg30
Experiment 1D
Probe Z122623_0045 (CPP BBO 400S1 BB-H&F-D-05 Z)
Number of Scans 1
Receiver Gain 30.3
Relaxation Delay 1.0000
Pulse Width 11.7000
Acquisition Time 4.0894
Acquisition Date 2018-07-07T18:31:00
Spectrometer Frequency 400.13
Nucleus 1H
OMe
Me
Me
Me
202
f1 (ppm)
S89

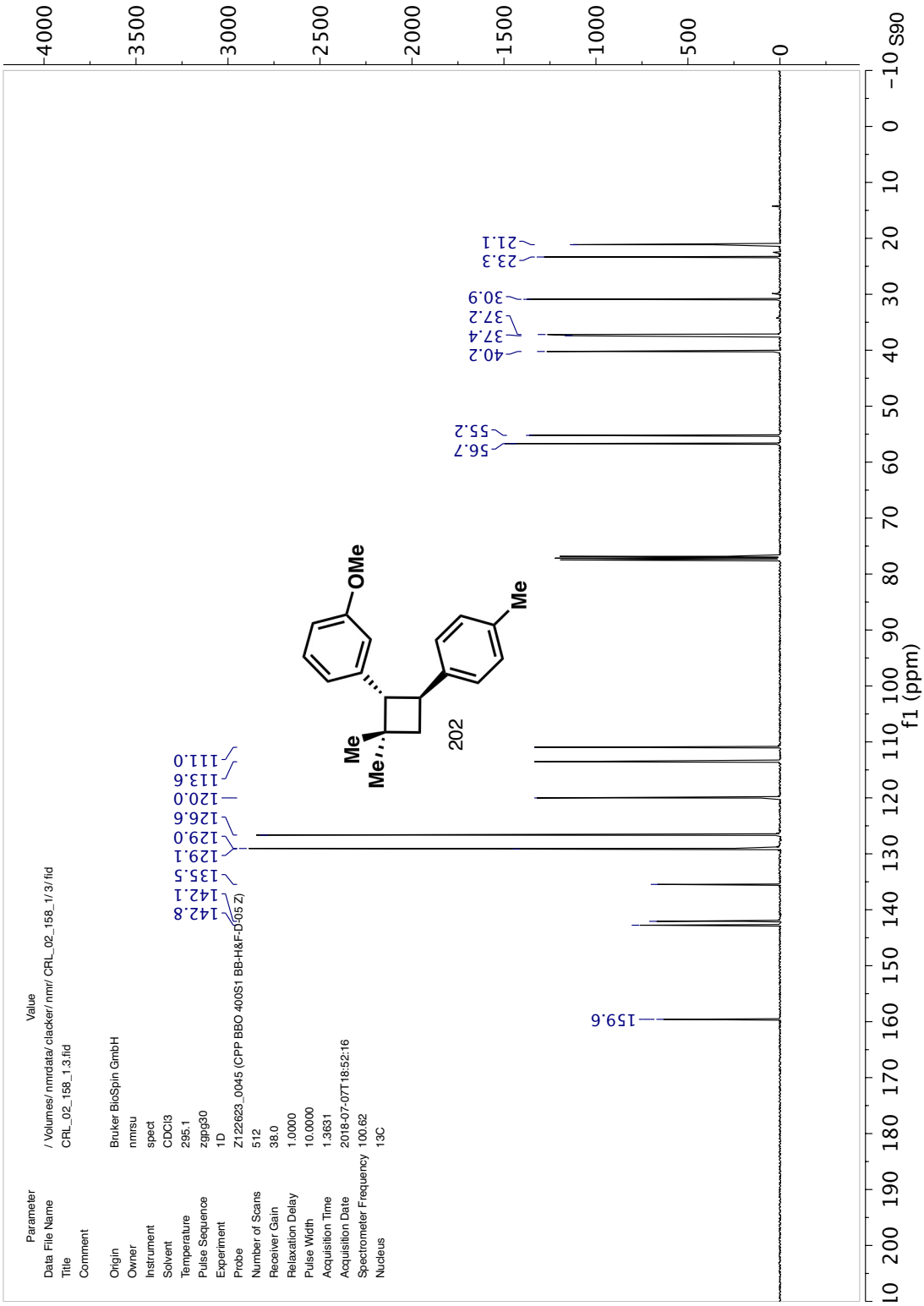
Parameter Value
Data File Name / Volumes/ nmrdata/ clacker/ nmr/ CRL_02_158_1/3/ fid
Title CRL_02_158_1.3.fid
Comment
Origin Bruker BioSpin GmbH
Owner nmrsu
Instrument spect
Solvent CDCl3
Temperature 295.1
Pulse Sequence zgpg30
Experiment 1D
Probe Z122623_0045 (CPP BBO 400S1 BB-H&F-D-05 Z)
Number of Scans 512
Receiver Gain 38.0
Relaxation Delay 1.0000
Pulse Width 10.0000
Acquisition Time 1.3631
Acquisition Date 2018-07-07T18:52:16
Spectrometer Frequency 100.62
Nucleus 13C
159.6
142.8
142.1
135.5
129.1
129.0
126.6
120.0
113.6
111.0
56.7
55.2
40.2
37.4
37.2
30.9
23.3
21.1
OMe
Me
Me
202
f1 (ppm)

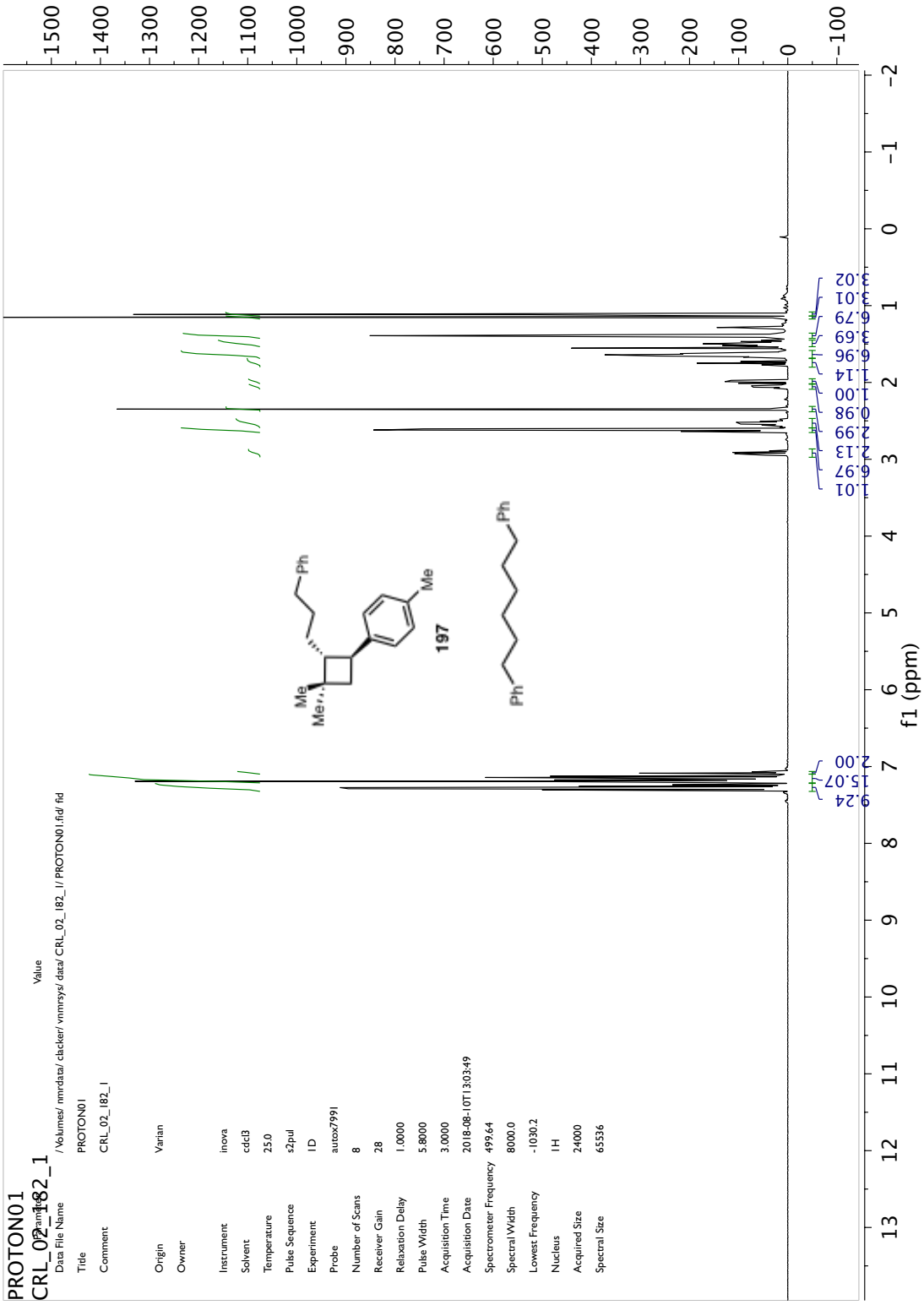
PROTON01
CRL_02_182_1
Parameter Value
Data File Name /Volumes/ nmrdata/ clacker/ vnmrsys/ data/ CRL_02_182_1/ PROTON01.fid/ fid
Title PROTON01
Comment CRL_02_182_1
Origin Varian
Owner
Instrument inova
Solvent cdcl3
Temperature 25.0
Pulse Sequence s2pul
Experiment ID
Probe autox7991
Number of Scans 8
Receiver Gain 28
Relaxation Delay 1.0000
Pulse Width 5.8000
Acquisition Time 3.0000
Acquisition Date 2018-08-10T13:03:49
Spectrometer Frequency 499.64
Spectral Width 8000.0
Lowest Frequency -1030.2
Nucleus 1H
Acquired Size 24000
Spectral Size 65536
Ph
Me
Me
197
Ph
Ph
9.24
15.07
2.00
1.01
6.97
2.13
2.99
0.98
1.00
1.14
6.96
3.69
6.79
3.01
3.02
f1 (ppm)

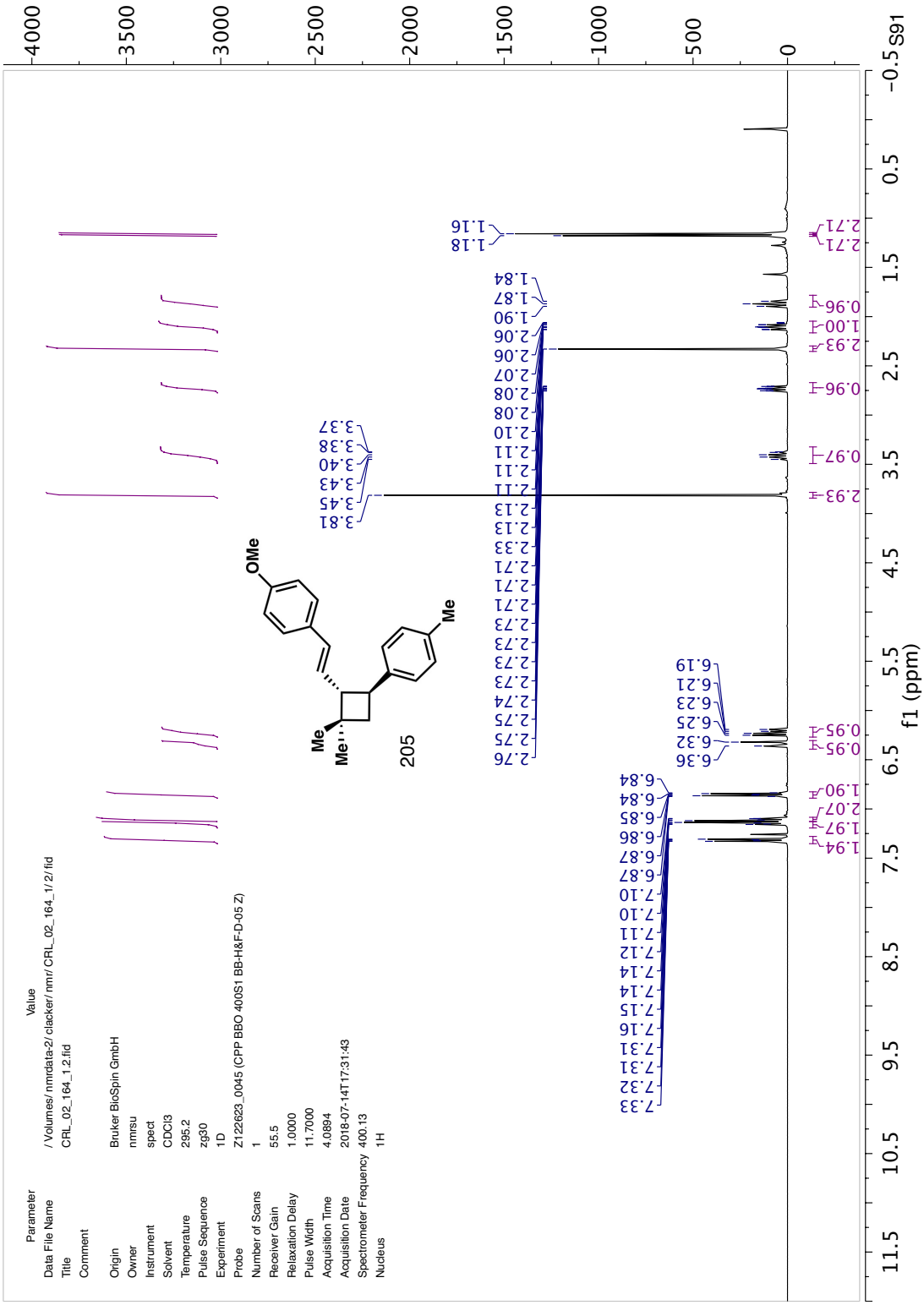
Parameter Value
Data File Name / Volumes/ nmrdata-2/ clacker/ nmr/ CRL_02_164_1/ 2/ fid
Title CRL_02_164_1.2.fid
Comment
Origin Bruker BioSpin GmbH
Owner nmrsu
Instrument spect
Solvent CDCl3
Temperature 295.2
Pulse Sequence zg30
Experiment 1D
Probe Z122623_0045 (CPP BBO 400S1 BB-H&F-D-05 Z)
Number of Scans 1
Receiver Gain 55.5
Relaxation Delay 1.0000
Pulse Width 11.7000
Acquisition Time 4.0894
Acquisition Date 2018-07-14T17:31:43
Spectrometer Frequency 400.13
Nucleus 1H
OMe
Me
Me
205
f1 (ppm)
S91

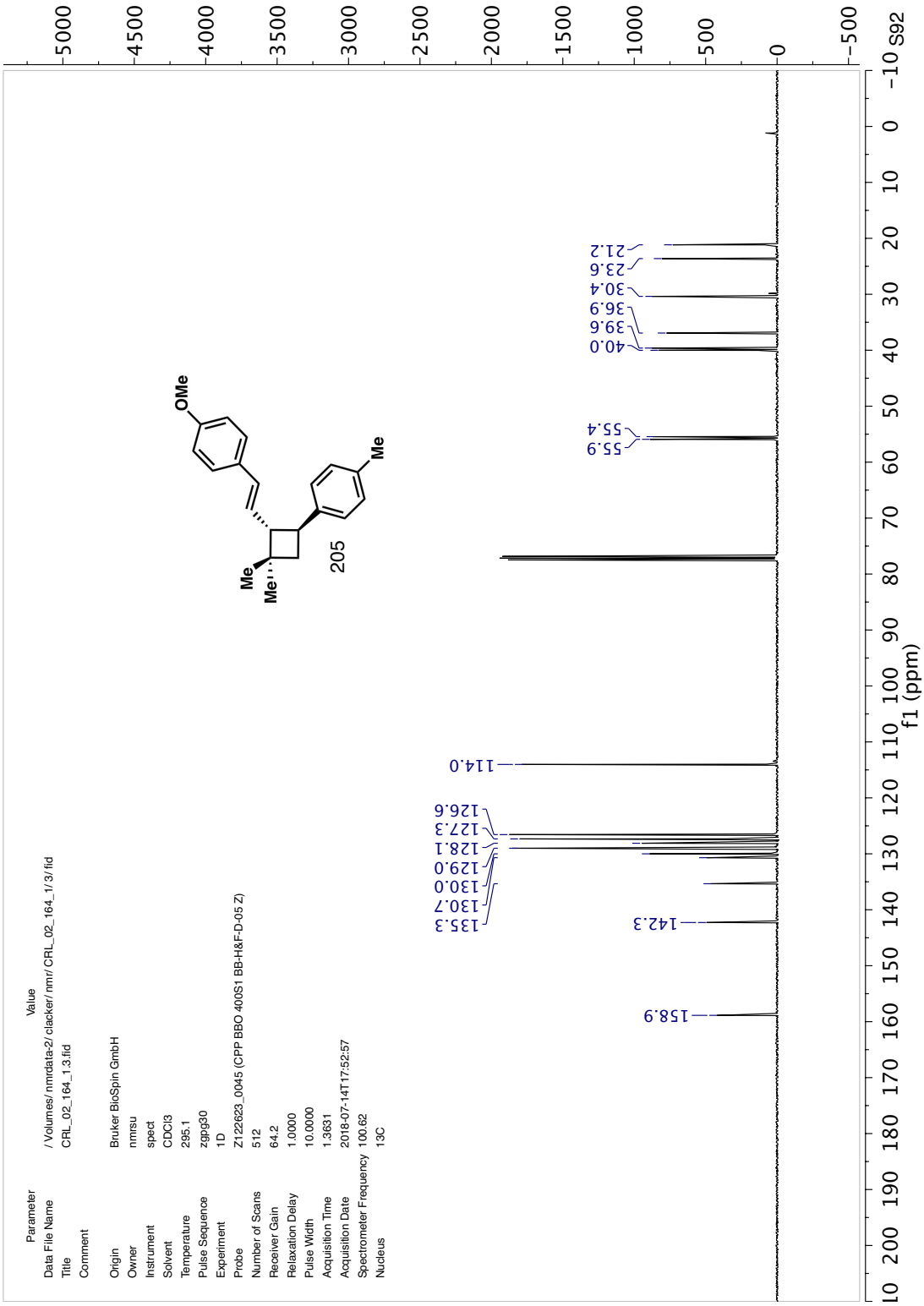
OMe
Me
Me
Me
205
Parameter Value
Data File Name / Volumes/ nmrdata-2/ clacker/ nmr/ CRL_02_164_1/3/ fid
Title CRL_02_164_1.3.fid
Comment
Origin Bruker BioSpin GmbH
Owner nmrsu
Instrument spect
Solvent CDCl3
Temperature 295.1
Pulse Sequence zgpg30
Experiment 1D
Probe Z122623_0045 (CPP BBO 400S1 BB-H&F-D-05 Z)
Number of Scans 512
Receiver Gain 64.2
Relaxation Delay 1.0000
Pulse Width 10.0000
Acquisition Time 1.3631
Acquisition Date 2018-07-14T17:52:57
Spectrometer Frequency 100.62
Nucleus 13C
158.9
142.3
135.3
130.7
130.0
129.0
128.1
127.3
126.6
114.0
55.9
55.4
40.0
39.6
36.9
30.4
23.6
21.2
f1 (ppm)
S92

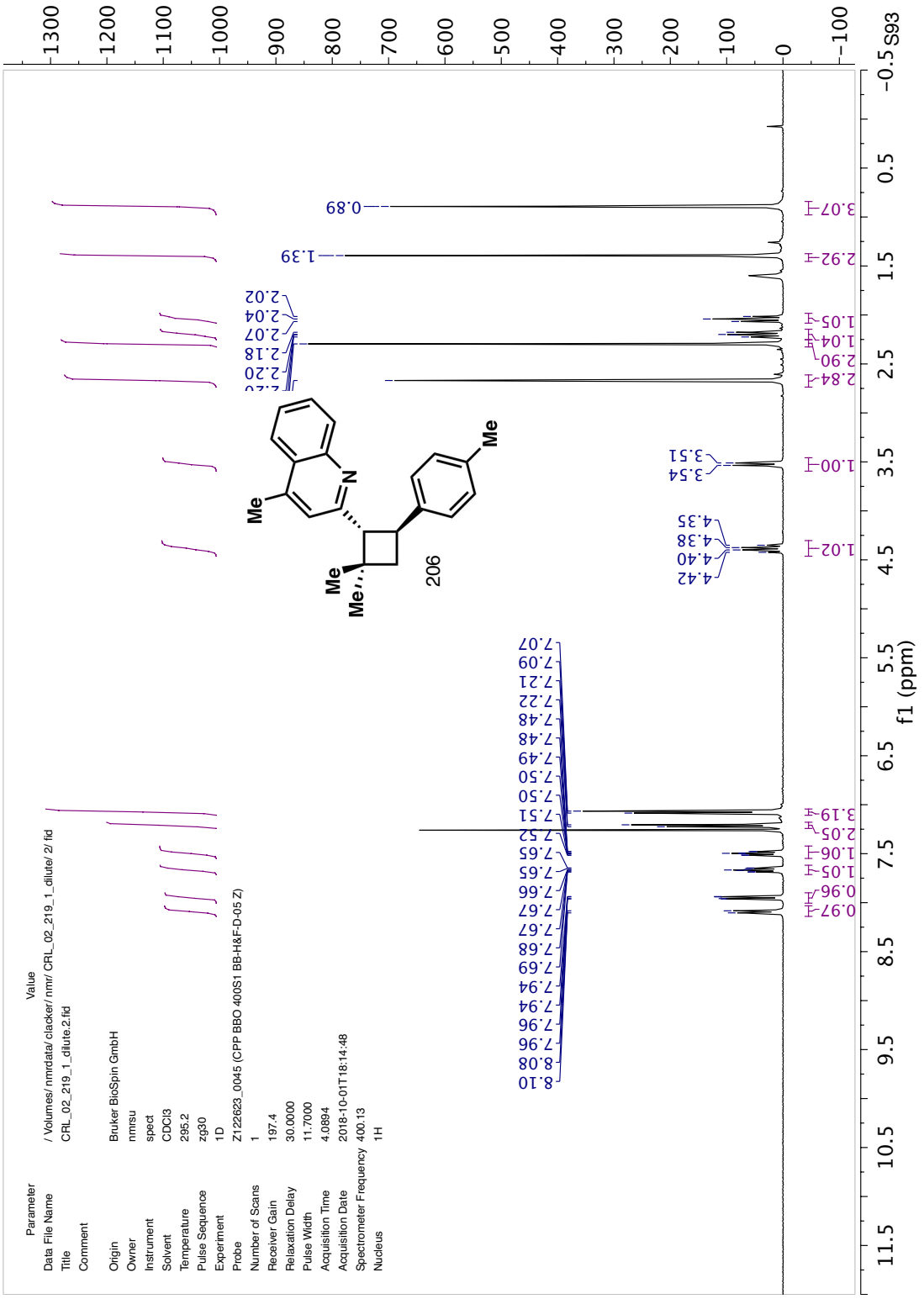
Parameter Value
Data File Name / Volumes/ nmrdata/ clacker/ nmr/ CRL_02_219_1_dilute/ 2/ fid
Title CRL_02_219_1_dilute.2.fid
Comment
Origin Bruker BioSpin GmbH
Owner nmrsu
Instrument spect
Solvent CDCl3
Temperature 295.2
Pulse Sequence zg30
Experiment 1D
Probe Z122623_0045 (CPP BBO 400S1 BB-H&F-D-05 Z)
Number of Scans 1
Receiver Gain 197.4
Relaxation Delay 30.0000
Pulse Width 11.7000
Acquisition Time 4.0894
Acquisition Date 2018-10-01T18:14:48
Spectrometer Frequency 400.13
Nucleus 1H
0.89
1.39
2.02
2.04
2.07
2.18
2.20
3.51
3.54
4.35
4.38
4.40
4.42
7.07
7.09
7.21
7.22
7.48
7.48
7.49
7.50
7.50
7.51
7.52
7.65
7.65
7.66
7.67
7.67
7.68
7.69
7.94
7.94
7.96
7.96
8.08
8.10
Me
Me
Me
N
206
3.07
2.92
1.05
1.04
2.90
2.84
1.00
1.02
3.19
2.05
1.06
1.05
0.96
0.97
f1 (ppm)
S93

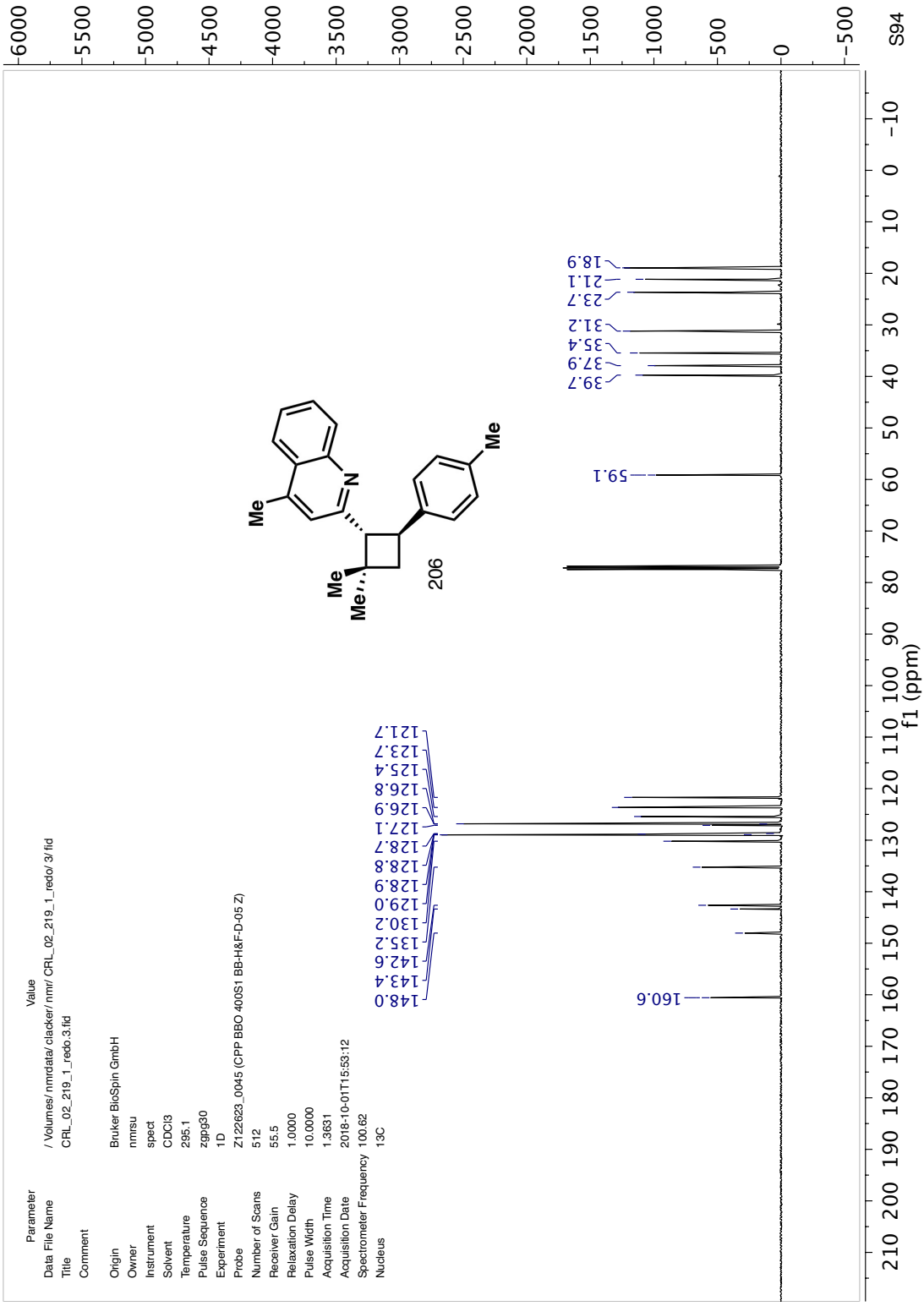
Parameter Value
Data File Name / Volumes/ nmrdata/ clacker/ nmr/ CRL_02_219_1_redo/ 3/ fid
Title CRL_02_219_1_redo.3.fid
Comment
Origin Bruker BioSpin GmbH
Owner nmrsu
Instrument spect
Solvent CDCl3
Temperature 295.1
Pulse Sequence zgpg30
Experiment 1D
Probe Z122623_0045 (CPP BBO 400S1 BB-H&F-D-05 Z)
Number of Scans 512
Receiver Gain 55.5
Relaxation Delay 1.0000
Pulse Width 10.0000
Acquisition Time 1.3631
Acquisition Date 2018-10-01T15:53:12
Spectrometer Frequency 100.62
Nucleus 13C
Me
N
Me
Me
Me
206
18.9
21.1
23.7
31.2
35.4
37.9
39.7
59.1
121.7
123.7
125.4
126.8
126.9
127.1
128.7
128.8
128.9
129.0
130.2
135.2
142.6
143.4
148.0
160.6
f1 (ppm)
S94

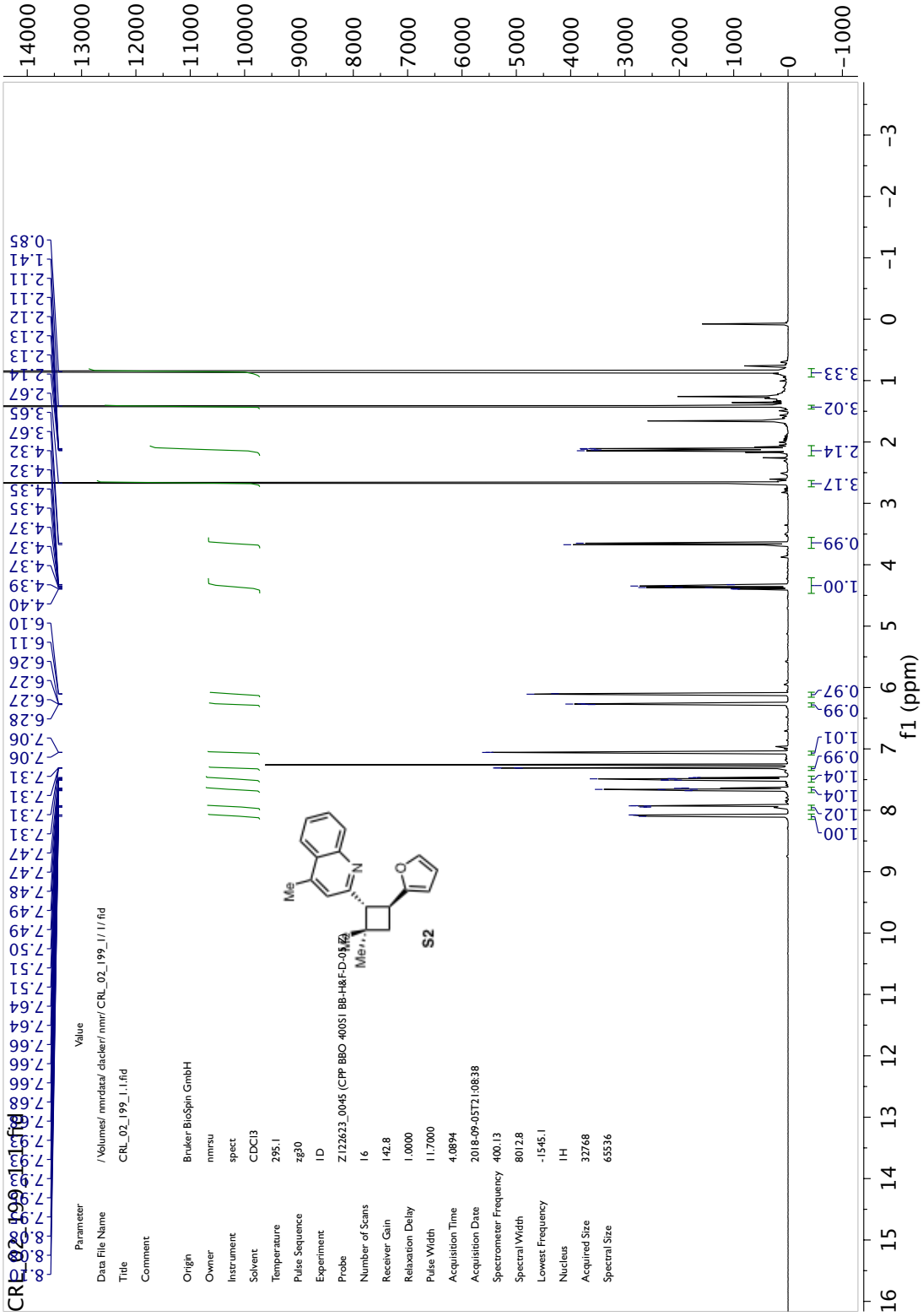
CRL_02_199_1_1.fid
Parameter Value
Data File Name /Volumes/ nmrdata/ clacker/ nmr/ CRL_02_199_1/ 1/ fid
Title CRL_02_199_1_1.fid
Comment
Origin Bruker BioSpin GmbH
Owner nmrsu
Instrument spect
Solvent CDCl3
Temperature 295.1
Pulse Sequence zg30
Experiment 1D
Probe Z122623_0045 (CPP BBO 400S1 BB-H&F-D-05-Z)
Number of Scans 16
Receiver Gain 142.8
Relaxation Delay 1.0000
Pulse Width 11.7000
Acquisition Time 4.0894
Acquisition Date 2018-09-05T21:08:38
Spectrometer Frequency 400.13
Spectral Width 8012.8
Lowest Frequency -1545.1
Nucleus 1H
Acquired Size 32768
Spectral Size 65536
Me
N
O
S2
f1 (ppm)

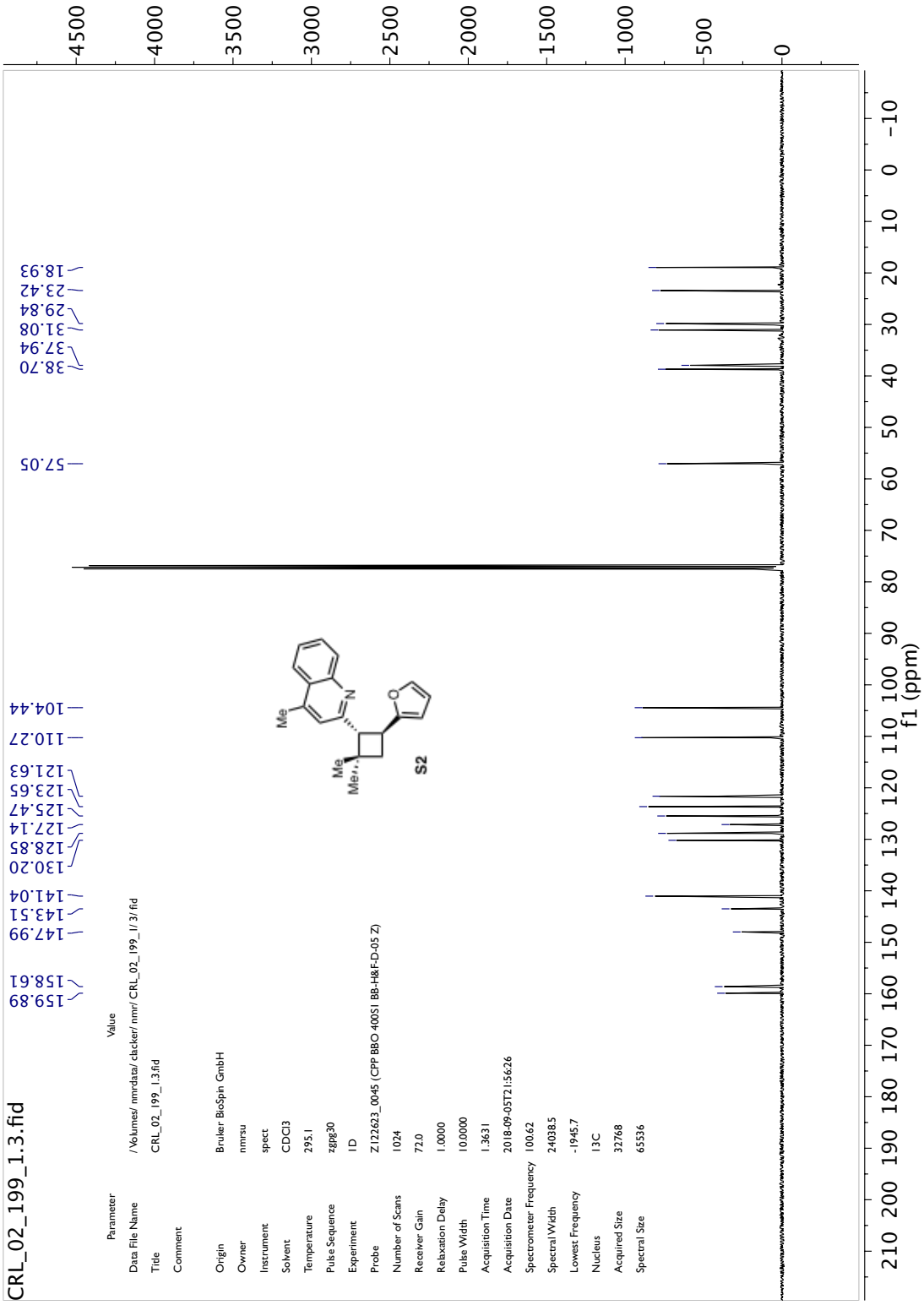
CRL_02_199_1.3.fid
Parameter
Value
Data File Name
/Volumes/ nmrdata/ clacker/ nmr/ CRL_02_199_1/ 3/ fid
Title
CRL_02_199_1.3.fid
Comment
Origin
Bruker BioSpin GmbH
Owner
nmrsu
Instrument
spect
Solvent
CDCl3
Temperature
295.1
Pulse Sequence
zgpg30
Experiment
1D
Probe
Z122623_0045 (CPP BBO 400SI BB-H&F-D-05 Z)
Number of Scans
1024
Receiver Gain
72.0
Relaxation Delay
1.0000
Pulse Width
10.0000
Acquisition Time
1.3631
Acquisition Date
2018-09-05T21:56:26
Spectrometer Frequency
100.62
Spectral Width
24038.5
Lowest Frequency
-1945.7
Nucleus
13C
Acquired Size
32768
Spectral Size
65536
159.89
158.61
147.99
143.51
141.04
130.20
128.85
127.14
125.47
123.65
121.63
110.27
104.44
57.05
38.70
37.94
31.08
29.84
23.42
18.93
Me
N
O
Me
Me
S2
f1 (ppm)

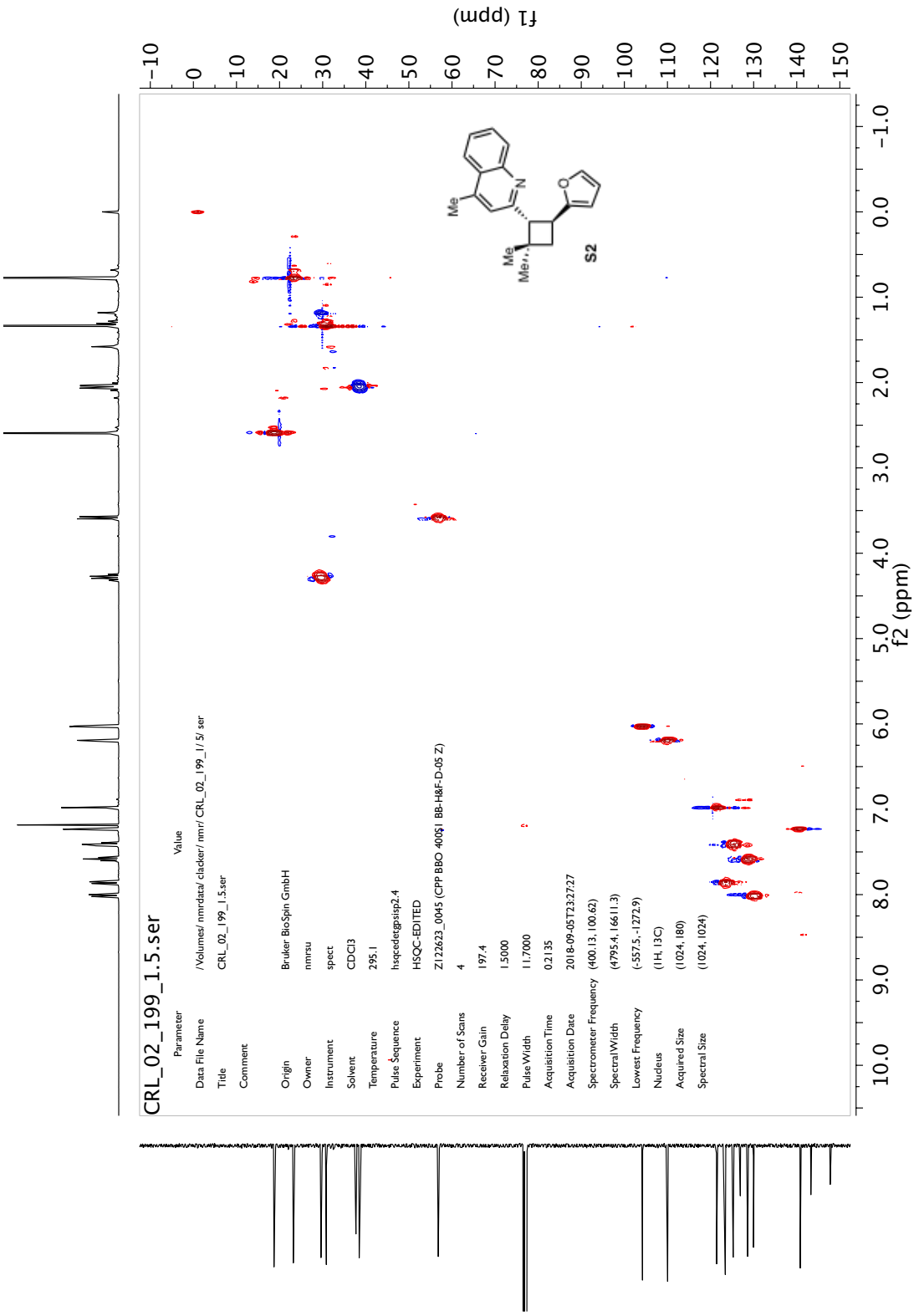
CRL_02_199_1.5.ser
Parameter Value
Data File Name /Volumes/ nmrdata/ clacker/ nmr/ CRL_02_199_1/ 5/ ser
Title CRL_02_199_1.5.ser
Comment
Origin Bruker BioSpin GmbH
Owner nmrsu
Instrument spect
Solvent CDCl3
Temperature 295.1
Pulse Sequence hsqcedetgpsisp2.4
Experiment HSQC-EDITED
Probe Z122623_0045 (CPP BBO 400SI BB-H&F-D-05 Z)
Number of Scans 4
Receiver Gain 197.4
Relaxation Delay 1.5000
Pulse Width 11.7000
Acquisition Time 0.2135
Acquisition Date 2018-09-05T23:27:27
Spectrometer Frequency (400.13, 100.62)
Spectral Width (4795.4, 16611.3)
Lowest Frequency (-557.5, -1272.9)
Nucleus (1H, 13C)
Acquired Size (1024, 180)
Spectral Size (1024, 1024)
Me
N
O
Me
Me
S2
f1 (ppm)
f2 (ppm)

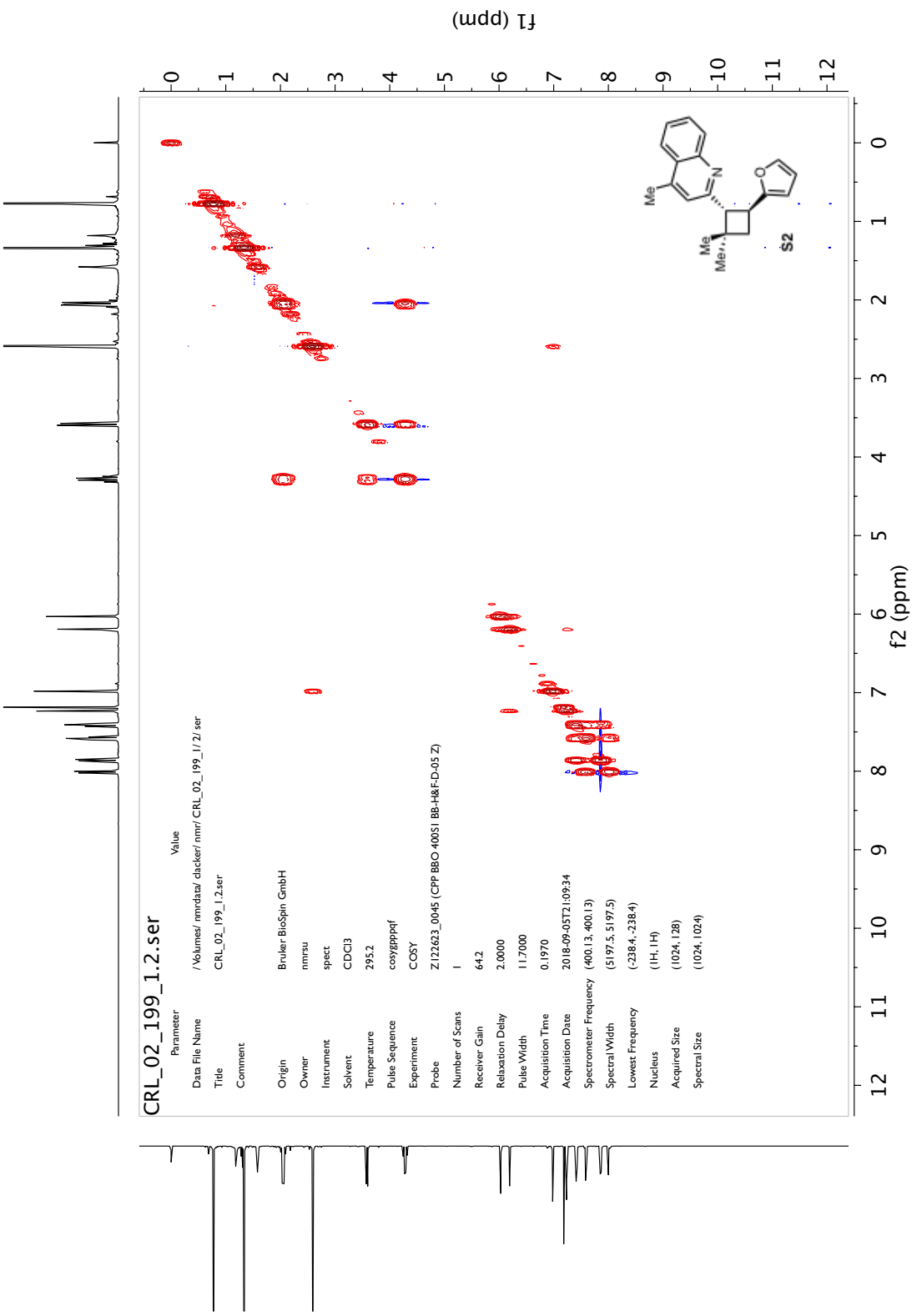
CRL_02_199_1.2.ser
Parameter Value
Data File Name /Volumes/ nmrdata/ clacker/ nmr/ CRL_02_199_1/ 2/ ser
Title CRL_02_199_1.2.ser
Comment
Origin Bruker BioSpin GmbH
Owner nmrsu
Instrument spect
Solvent CDCl3
Temperature 295.2
Pulse Sequence cosygpppqf
Experiment COSY
Probe Z122623_0045 (CPP BBO 400SI BB-H&F-D-05 Z)
Number of Scans 1
Receiver Gain 64.2
Relaxation Delay 2.0000
Pulse Width 11.7000
Acquisition Time 0.1970
Acquisition Date 2018-09-05T21:09:34
Spectrometer Frequency (400.13, 400.13)
Spectral Width (5197.5, 5197.5)
Lowest Frequency (-238.4, -238.4)
Nucleus (1H, 1H)
Acquired Size (1024, 128)
Spectral Size (1024, 1024)
Me
N
O
Me
Me
S2
f1 (ppm)
f2 (ppm)

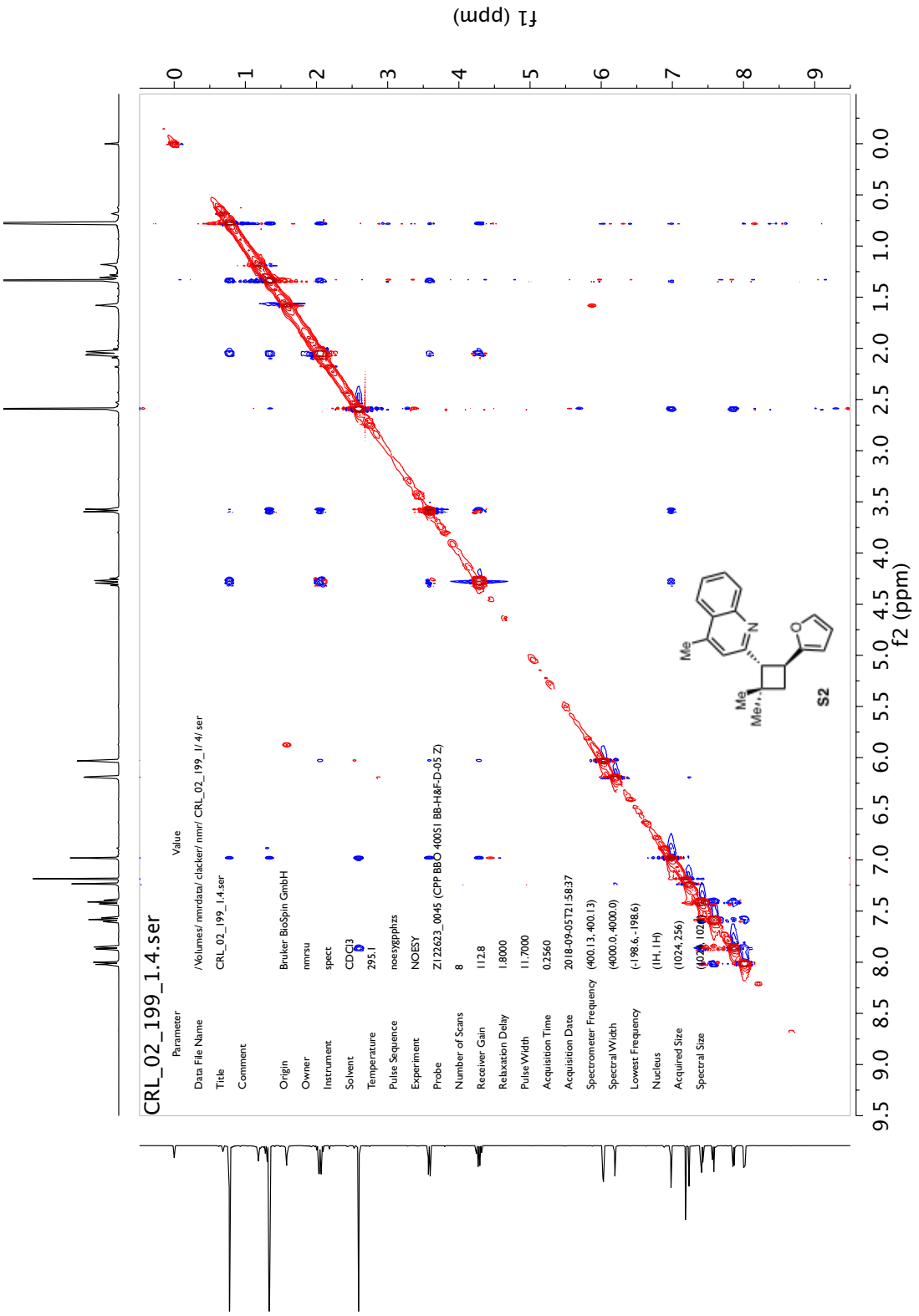
CRL_02_199_1.4.ser
Parameter Value
Data File Name /Volumes/ nmrdata/ clacker/ nmr/ CRL_02_199_1/ 4/ ser
Title CRL_02_199_1.4.ser
Comment
Origin Bruker BioSpin GmbH
Owner nmrsu
Instrument spect
Solvent CDCl3
Temperature 295.1
Pulse Sequence noesygpphzs
Experiment NOESY
Probe Z122623_0045 (CPP BBO 400SI BB-H&F-D-05 Z)
Number of Scans 8
Receiver Gain 112.8
Relaxation Delay 1.8000
Pulse Width 11.7000
Acquisition Time 0.2560
Acquisition Date 2018-09-05T21:58:37
Spectrometer Frequency (400.13, 400.13)
Spectral Width (4000.0, 4000.0)
Lowest Frequency (-198.6, -198.6)
Nucleus (1H, 1H)
Acquired Size (1024, 256)
Spectral Size (1024, 1024)
Me
N
O
Me
Me
S2
f2 (ppm)
f1 (ppm)

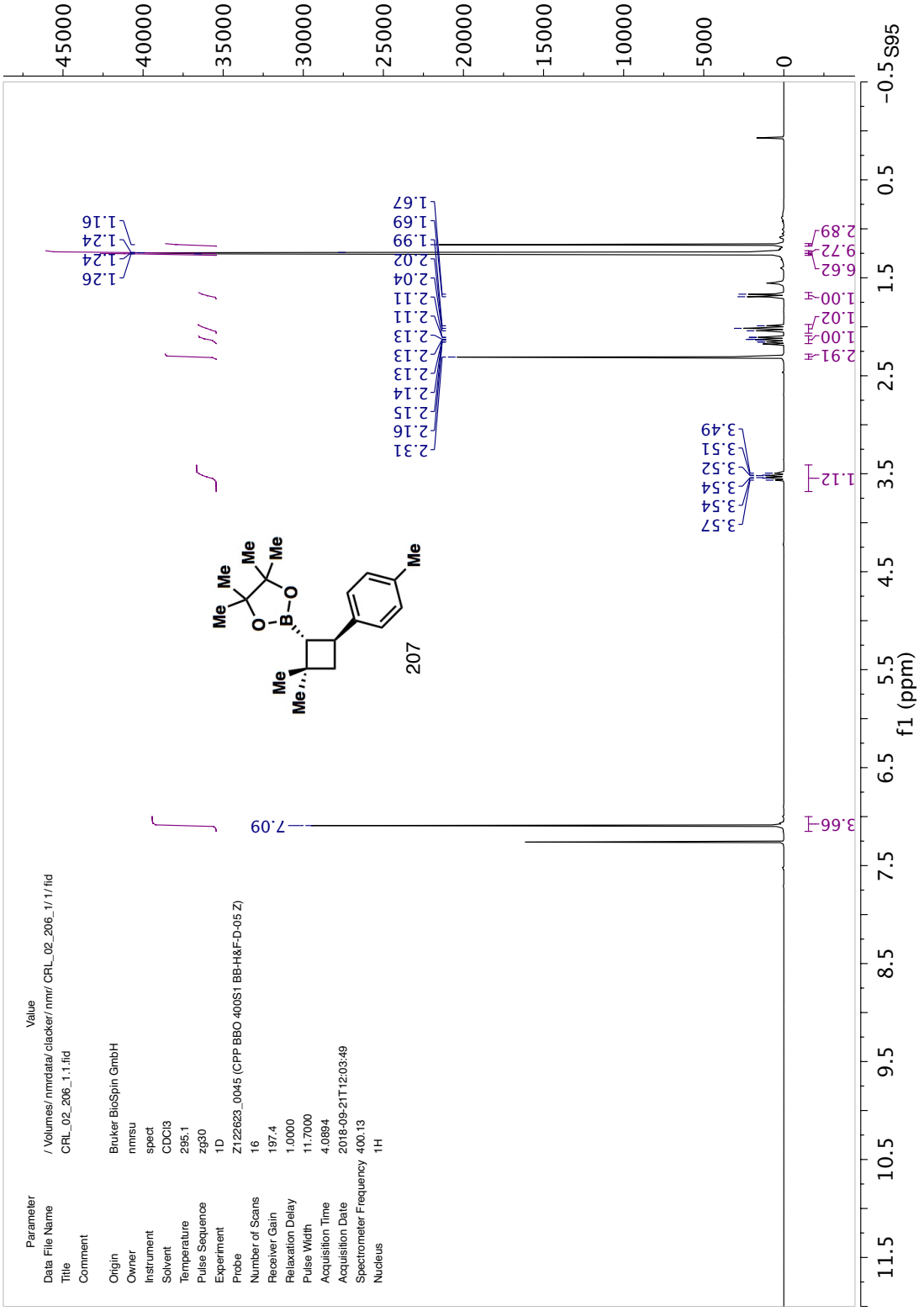
Parameter Value
Data File Name / Volumes/ nmrdata/ clacker/ nmr/ CRL_02_206_1/1/ fid
Title CRL_02_206_1.1.fid
Comment
Origin Bruker BioSpin GmbH
Owner nmrsu
Instrument spect
Solvent CDCl3
Temperature 295.1
Pulse Sequence zg30
Experiment 1D
Probe Z122623_0045 (CPP BBO 400S1 BB-H&F-D-05 Z)
Number of Scans 16
Receiver Gain 197.4
Relaxation Delay 1.0000
Pulse Width 11.7000
Acquisition Time 4.0894
Acquisition Date 2018-09-21T12:03:49
Spectrometer Frequency 400.13
Nucleus 1H
7.09
3.66
3.57
3.54
3.54
3.52
3.51
3.49
2.31
2.16
2.15
2.14
2.13
2.13
2.13
2.11
2.11
2.04
2.02
1.99
1.69
1.67
1.26
1.24
1.24
1.16
2.89
9.72
6.62
1.00
1.02
1.00
2.91
1.12
Me
Me
Me
Me
Me
Me
207
f1 (ppm)

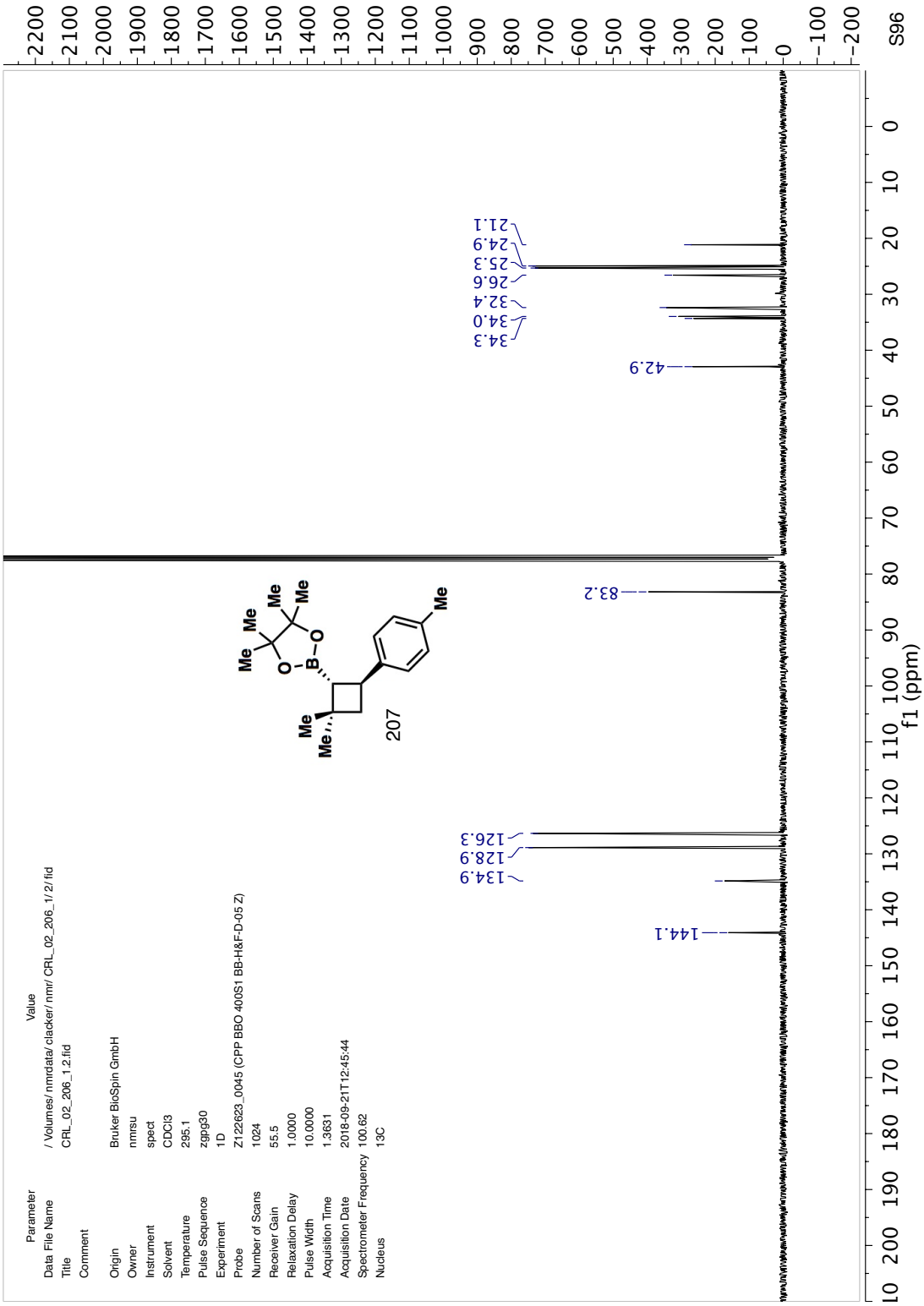
Parameter Value
Data File Name / Volumes/ nmrdata/ clacker/ nmr/ CRL_02_206_1/2/ fid
Title CRL_02_206_1.2.fid
Comment
Origin Bruker BioSpin GmbH
Owner nmrsu
Instrument spect
Solvent CDCl3
Temperature 295.1
Pulse Sequence zgpg30
Experiment 1D
Probe Z122623_0045 (CPP BBO 400S1 BB-H&F-D-05 Z)
Number of Scans 1024
Receiver Gain 55.5
Relaxation Delay 1.0000
Pulse Width 10.0000
Acquisition Time 1.3631
Acquisition Date 2018-09-21T12:45:44
Spectrometer Frequency 100.62
Nucleus 13C
144.1
134.9
128.9
126.3
83.2
42.9
34.3
34.0
32.4
26.6
25.3
24.9
21.1
Me
Me
Me
Me
Me
Me
O
O
B
207
f1 (ppm)
S96

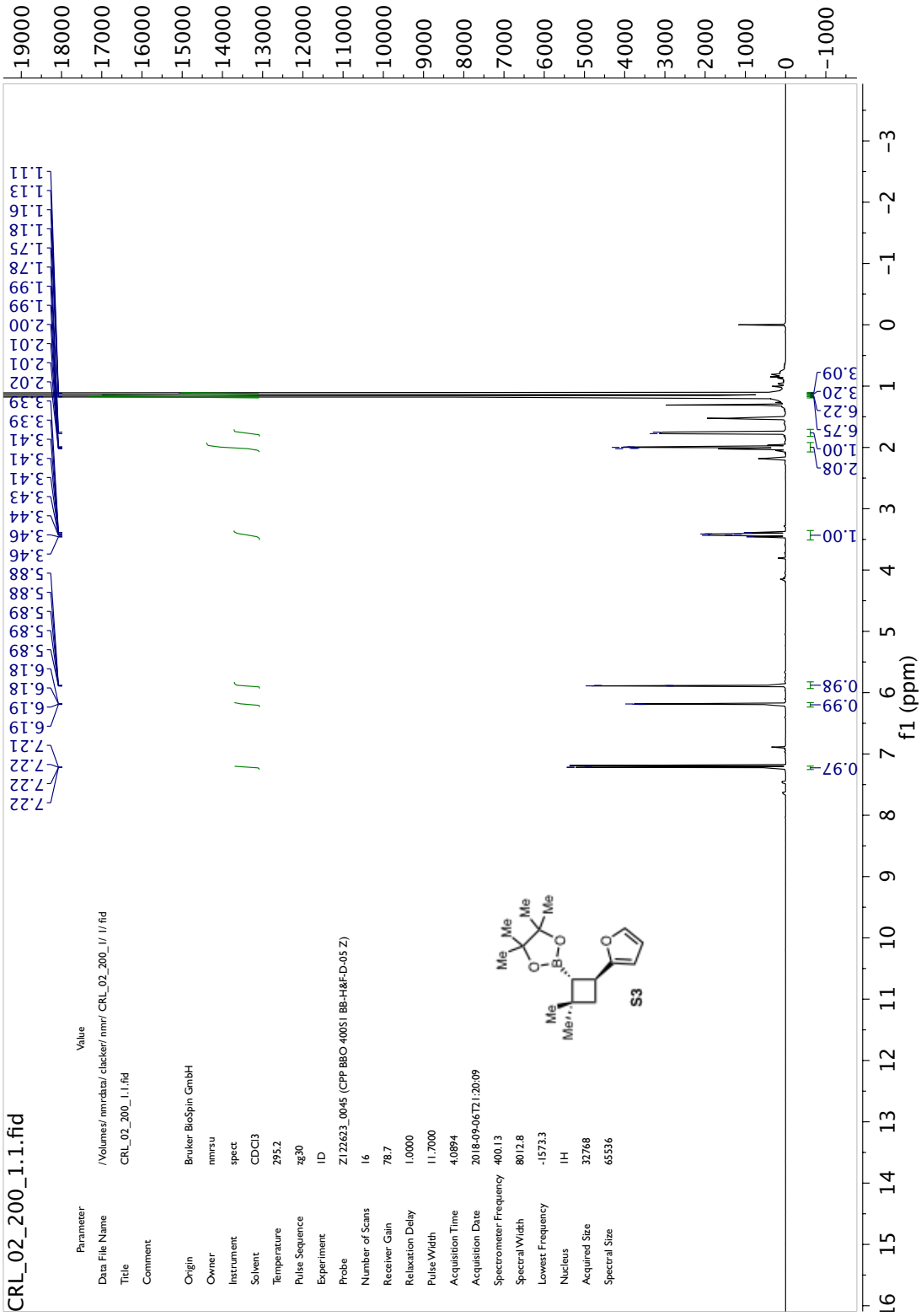
CRL_02_200_1.1.fid
Parameter
Value
Data File Name /Volumes/ nmrdata/ clacker/ nmr/ CRL_02_200_1/ 1/ fid
Title CRL_02_200_1.1.fid
Comment
Origin Bruker BioSpin GmbH
Owner nmrsu
Instrument spect
Solvent CDCl3
Temperature 295.2
Pulse Sequence zg30
Experiment ID
Probe Z122623_0045 (CPP BBO 400S1 BB-H&F-D-05 Z)
Number of Scans 16
Receiver Gain 78.7
Relaxation Delay 1.0000
Pulse Width 11.7000
Acquisition Time 4.0894
Acquisition Date 2018-09-06T21:20:09
Spectrometer Frequency 400.13
Spectral Width 8012.8
Lowest Frequency -1573.3
Nucleus 1H
Acquired Size 32768
Spectral Size 65536
S3
f1 (ppm)

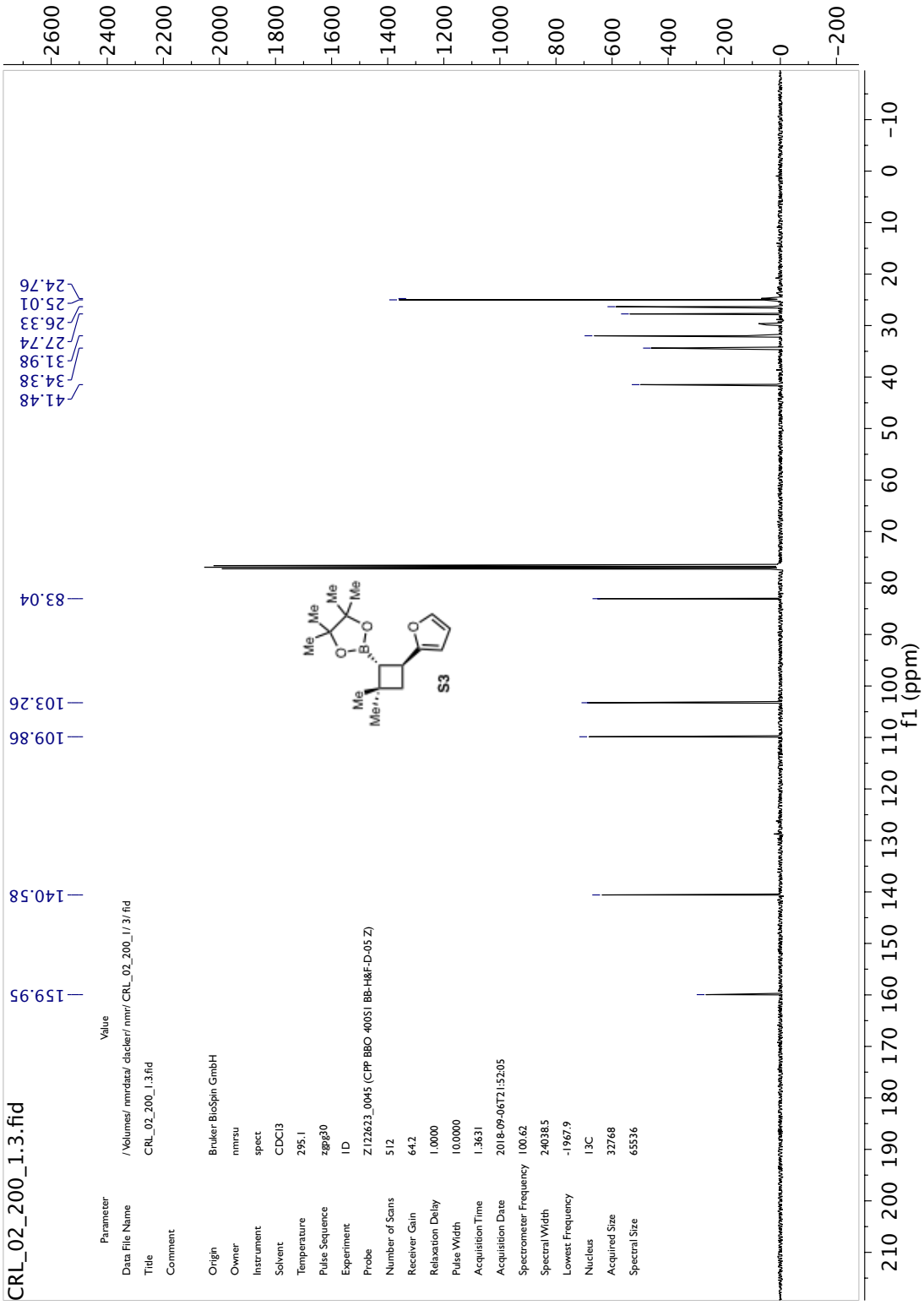
CRL_02_200_1.3.fid
Parameter
Value
Data File Name
/Volumes/ nmrdata/ dacker/ nmr/ CRL_02_200_1/ 3/ fid
Title
CRL_02_200_1.3.fid
Comment
Origin
Bruker BioSpin GmbH
Owner
nmrsu
Instrument
spect
Solvent
CDCl3
Temperature
295.1
Pulse Sequence
zgpg30
Experiment
1D
Probe
Z122623_0045 (CPP BBO 400S1 BB-H&F-D-05 Z)
Number of Scans
512
Receiver Gain
64.2
Relaxation Delay
1.0000
Pulse Width
10.0000
Acquisition Time
1.3631
Acquisition Date
2018-09-06T21:52:05
Spectrometer Frequency
100.62
Spectral Width
24038.5
Lowest Frequency
-1967.9
Nucleus
13C
Acquired Size
32768
Spectral Size
65536
159.95
140.58
109.86
103.26
83.04
41.48
34.38
31.98
27.74
26.33
25.01
24.76
S3
f1 (ppm)

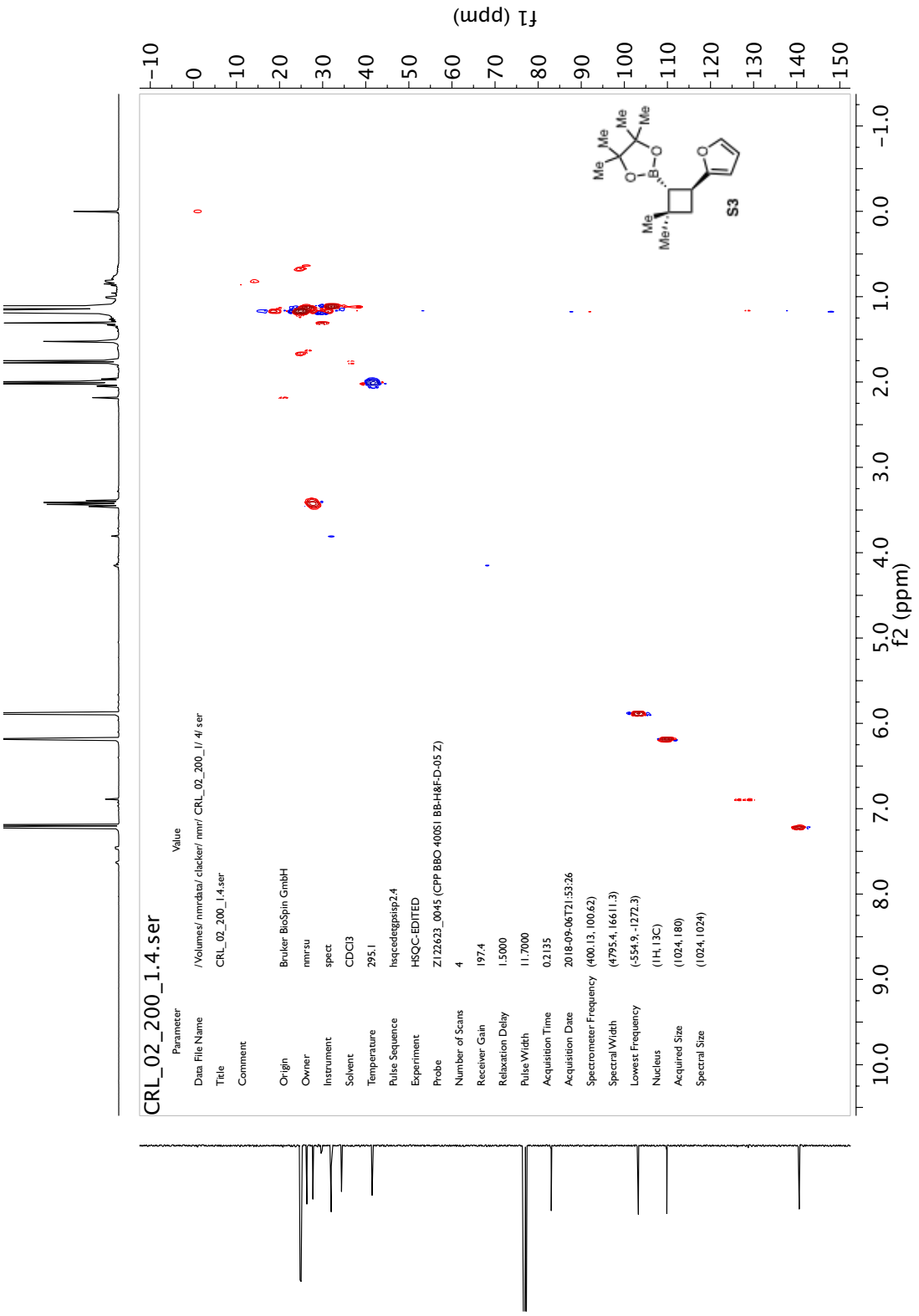
CRL_02_200_1.4.ser
Parameter Value
Data File Name /Volumes/ nmrdata/ clacker/ nmr/ CRL_02_200_1/ 4/ ser
Title CRL_02_200_1.4.ser
Comment
Origin Bruker BioSpin GmbH
Owner nmrsu
Instrument spect
Solvent CDCl3
Temperature 295.1
Pulse Sequence hsqcedetgpsisp2.4
Experiment HSQC-EDITED
Probe Z122623_0045 (CPP BBO 400SI BB-H&F-D-05 Z)
Number of Scans 4
Receiver Gain 197.4
Relaxation Delay 1.5000
Pulse Width 11.7000
Acquisition Time 0.2135
Acquisition Date 2018-09-06T21:53:26
Spectrometer Frequency (400.13, 100.62)
Spectral Width (4795.4, 16611.3)
Lowest Frequency (-554.9, -1272.3)
Nucleus (1H, 13C)
Acquired Size (1024, 180)
Spectral Size (1024, 1024)
Me
Me
Me
Me
Me
Me
S3
f1 (ppm)
f2 (ppm)

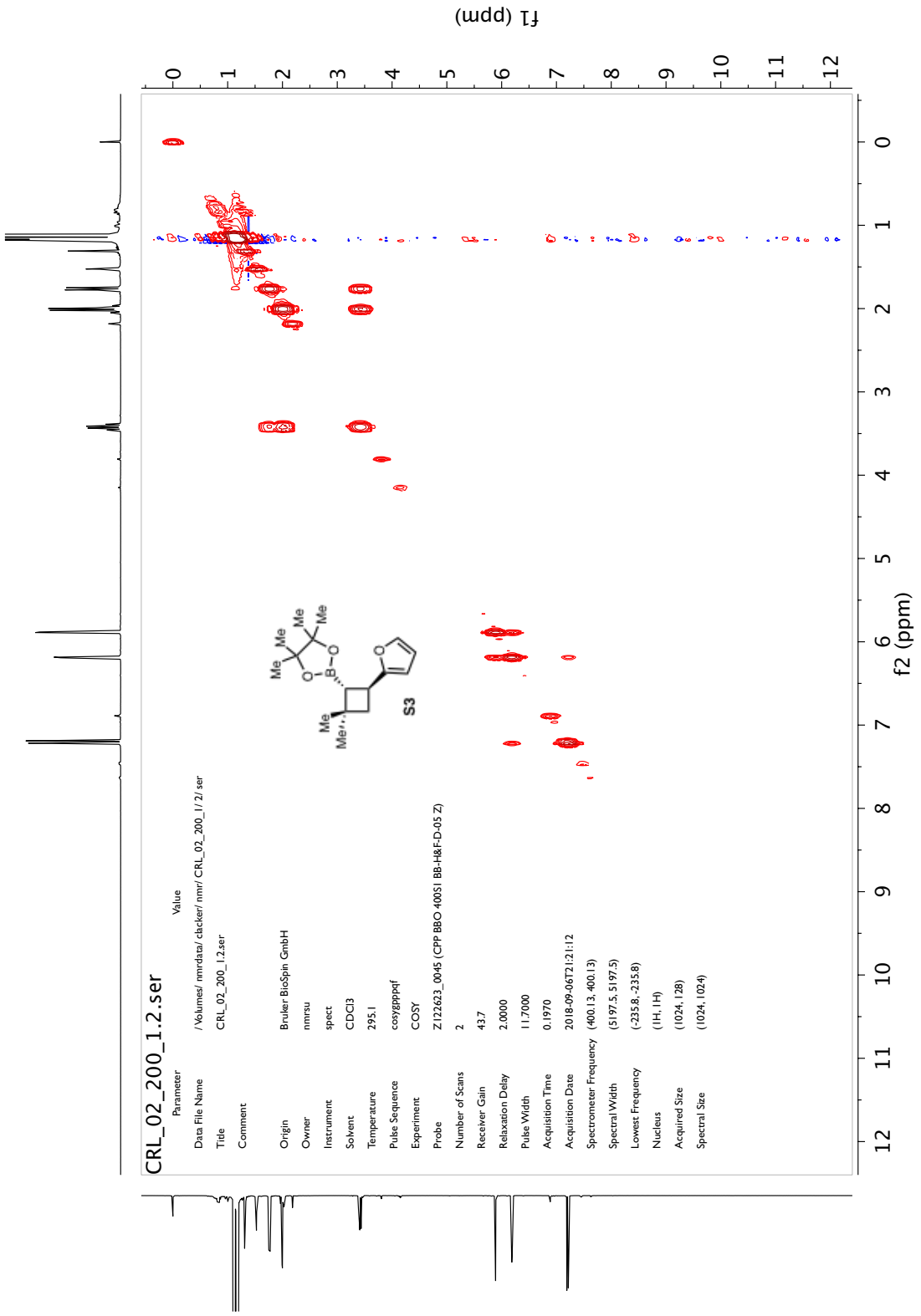
f1 (ppm)
f2 (ppm)
CRL_02_200_1.2.ser
Parameter Value
Data File Name /Volumes/nmrdata/clacker/nmr/CRL_02_200_1/2/ser
Title CRL_02_200_1.2.ser
Comment
Origin Bruker BioSpin GmbH
Owner nmrsu
Instrument spect
Solvent CDCl3
Temperature 295.1
Pulse Sequence cosygpppqf
Experiment COSY
Probe Z122623_0045 (CPP BBO 400SI BB-H&F-D-05 Z)
Number of Scans 2
Receiver Gain 43.7
Relaxation Delay 2.0000
Pulse Width 11.7000
Acquisition Time 0.1970
Acquisition Date 2018-09-06T21:21:12
Spectrometer Frequency (400.13, 400.13)
Spectral Width (5197.5, 5197.5)
Lowest Frequency (-235.8, -235.8)
Nucleus (1H, 1H)
Acquired Size (1024, 128)
Spectral Size (1024, 1024)
Me
Me
Me
Me
Me
B
O
O
O
S3

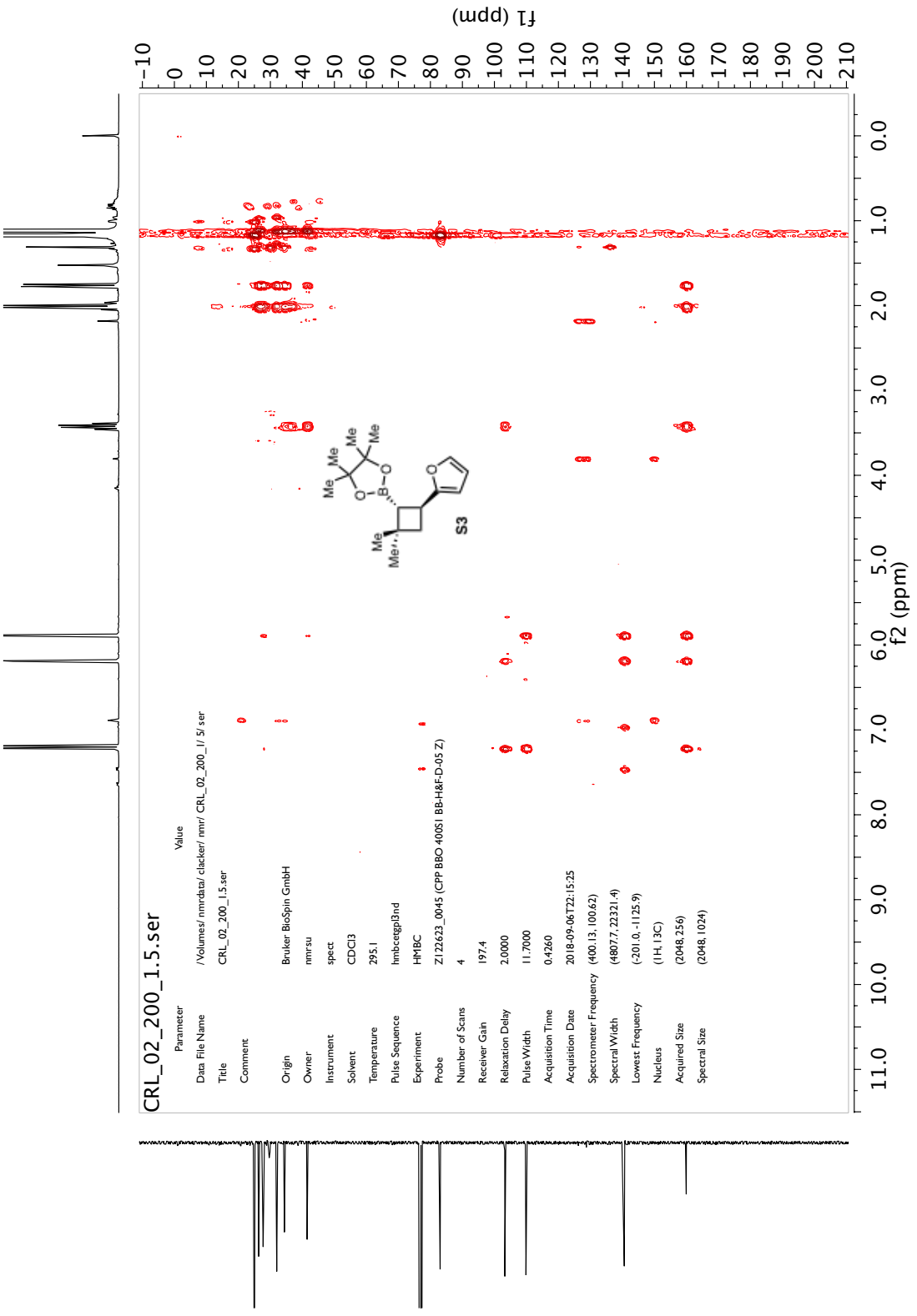
CRL_02_200_1.5.ser
Parameter Value
Data File Name /Volumes/ nmrdata/ clacker/ nmr/ CRL_02_200_1/ 5/ ser
Title CRL_02_200_1.5.ser
Comment
Origin Bruker BioSpin GmbH
Owner nmrsu
Instrument spect
Solvent CDCl3
Temperature 295.1
Pulse Sequence hmbcetgpl3nd
Experiment HMBC
Probe Z122623_0045 (CPP BBO 400SI BB-H&F-D-05 Z)
Number of Scans 4
Receiver Gain 197.4
Relaxation Delay 2.0000
Pulse Width 11.7000
Acquisition Time 0.4260
Acquisition Date 2018-09-06T22:15:25
Spectrometer Frequency (400.13, 100.62)
Spectral Width (4807.7, 22321.4)
Lowest Frequency (-201.0, -1125.9)
Nucleus (1H, 13C)
Acquired Size (2048, 256)
Spectral Size (2048, 1024)
Me
Me
Me
Me
Me
O
O
B
O
S3
f1 (ppm)
f2 (ppm)

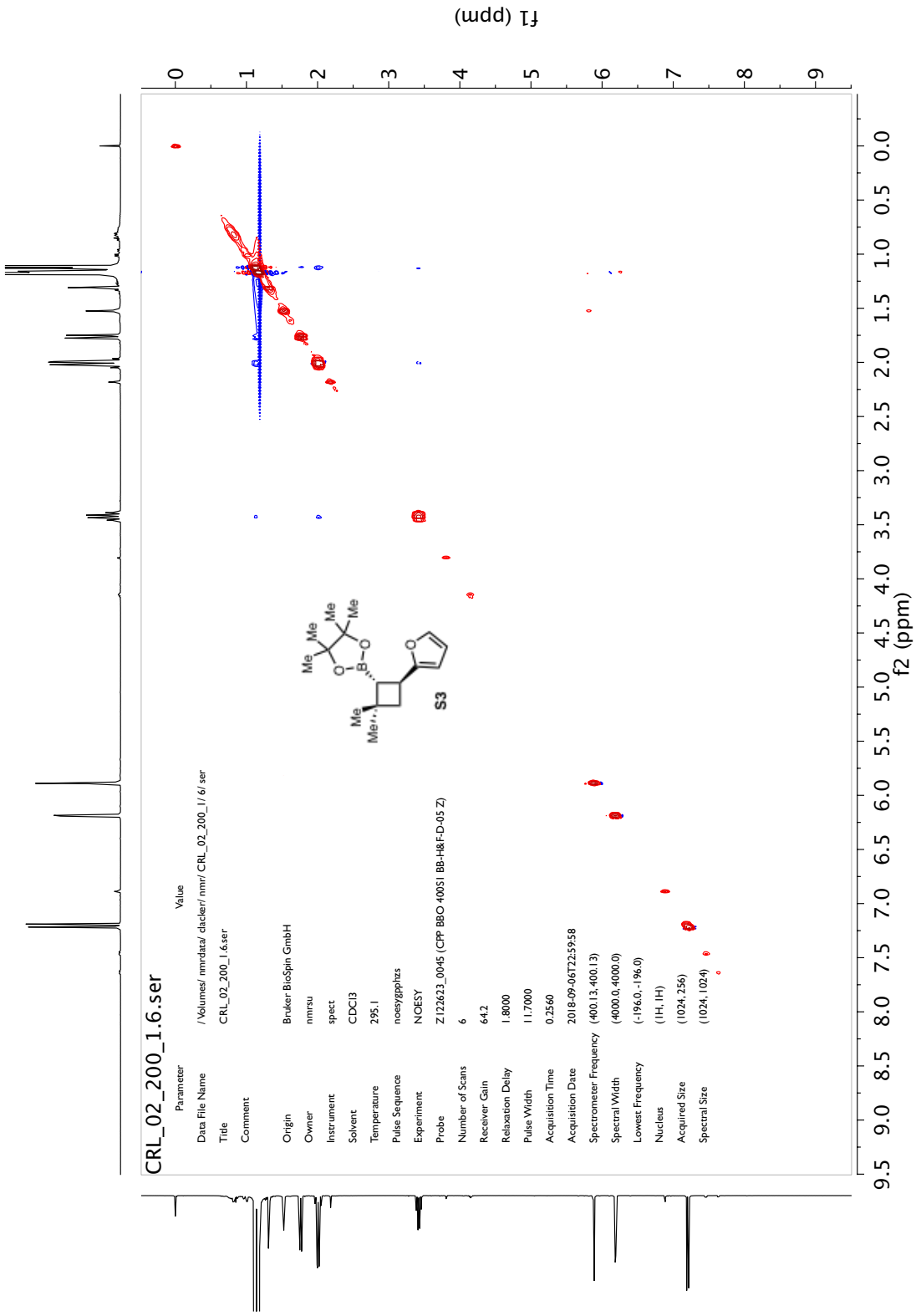
CRL_02_200_1.6.ser
Parameter Value
Data File Name /Volumes/ nmrdata/ dacker/ nmr/ CRL_02_200_1/ 6/ ser
Title CRL_02_200_1.6.ser
Comment
Origin Bruker BioSpin GmbH
Owner nmrsu
Instrument spect
Solvent CDCl3
Temperature 295.1
Pulse Sequence noesygpphzs
Experiment NOESY
Probe Z122623_0045 (CPP BBO 400SI BB-H&F-D-05 Z)
Number of Scans 6
Receiver Gain 64.2
Relaxation Delay 1.8000
Pulse Width 11.7000
Acquisition Time 0.2560
Acquisition Date 2018-09-06T22:59:58
Spectrometer Frequency (400.13, 400.13)
Spectral Width (4000.0, 4000.0)
Lowest Frequency (-196.0, -196.0)
Nucleus (1H, 1H)
Acquired Size (1024, 256)
Spectral Size (1024, 1024)
S3
f2 (ppm)
f1 (ppm)

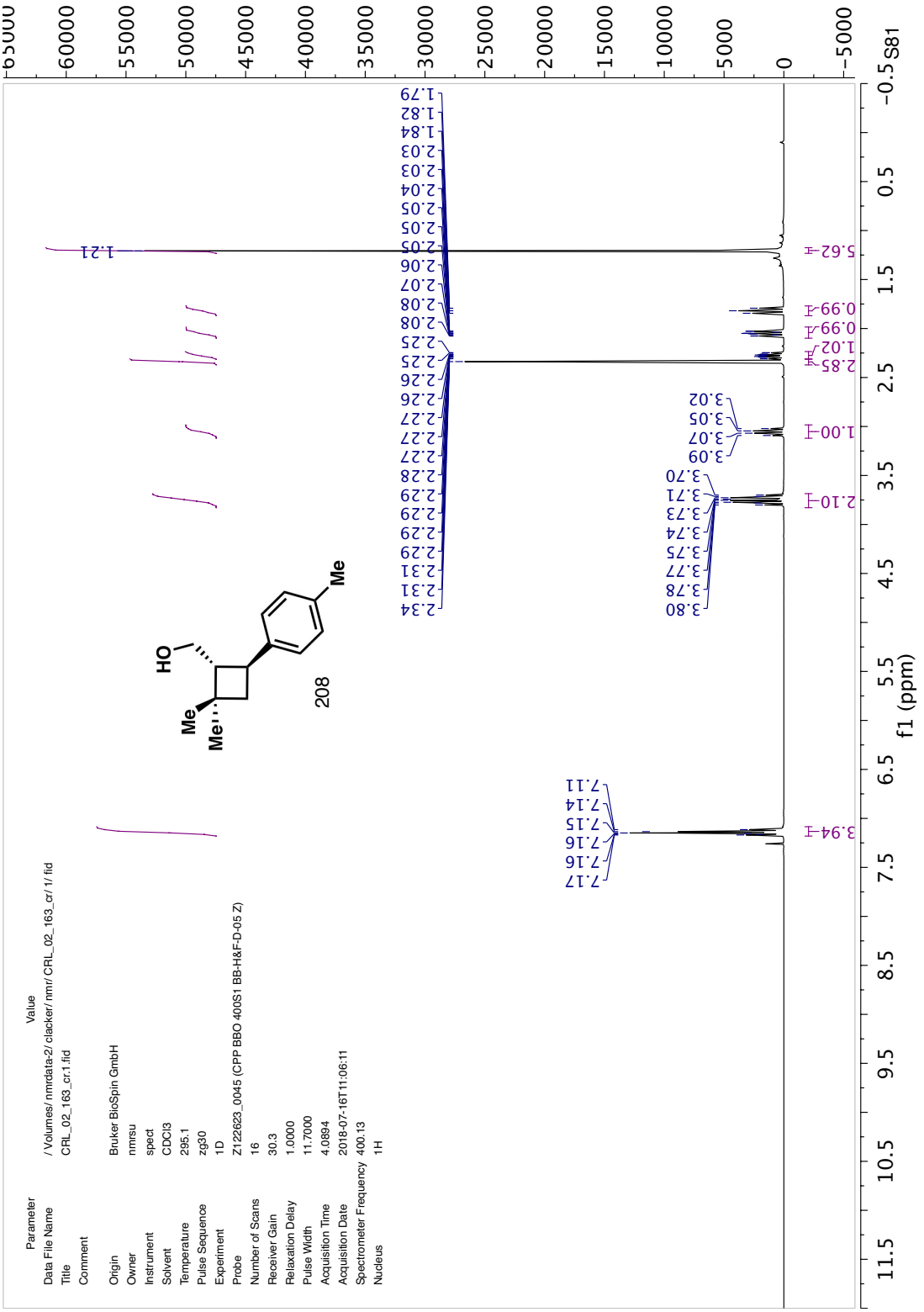
Parameter Value
Data File Name / Volumes/ nmrdata-2/ clacker/ nmr/ CRL_02_163_cr/ 1/ fid
Title CRL_02_163_cr.1.fid
Comment
Origin Bruker BioSpin GmbH
Owner nmrsu
Instrument spect
Solvent CDCl3
Temperature 295.1
Pulse Sequence zg30
Experiment 1D
Probe Z122623_0045 (CPP BBO 400S1 BB-H&F-D-05 Z)
Number of Scans 16
Receiver Gain 30.3
Relaxation Delay 1.0000
Pulse Width 11.7000
Acquisition Time 4.0894
Acquisition Date 2018-07-16T11:06:11
Spectrometer Frequency 400.13
Nucleus 1H
HO
Me
Me
Me
208
f1 (ppm)
S81

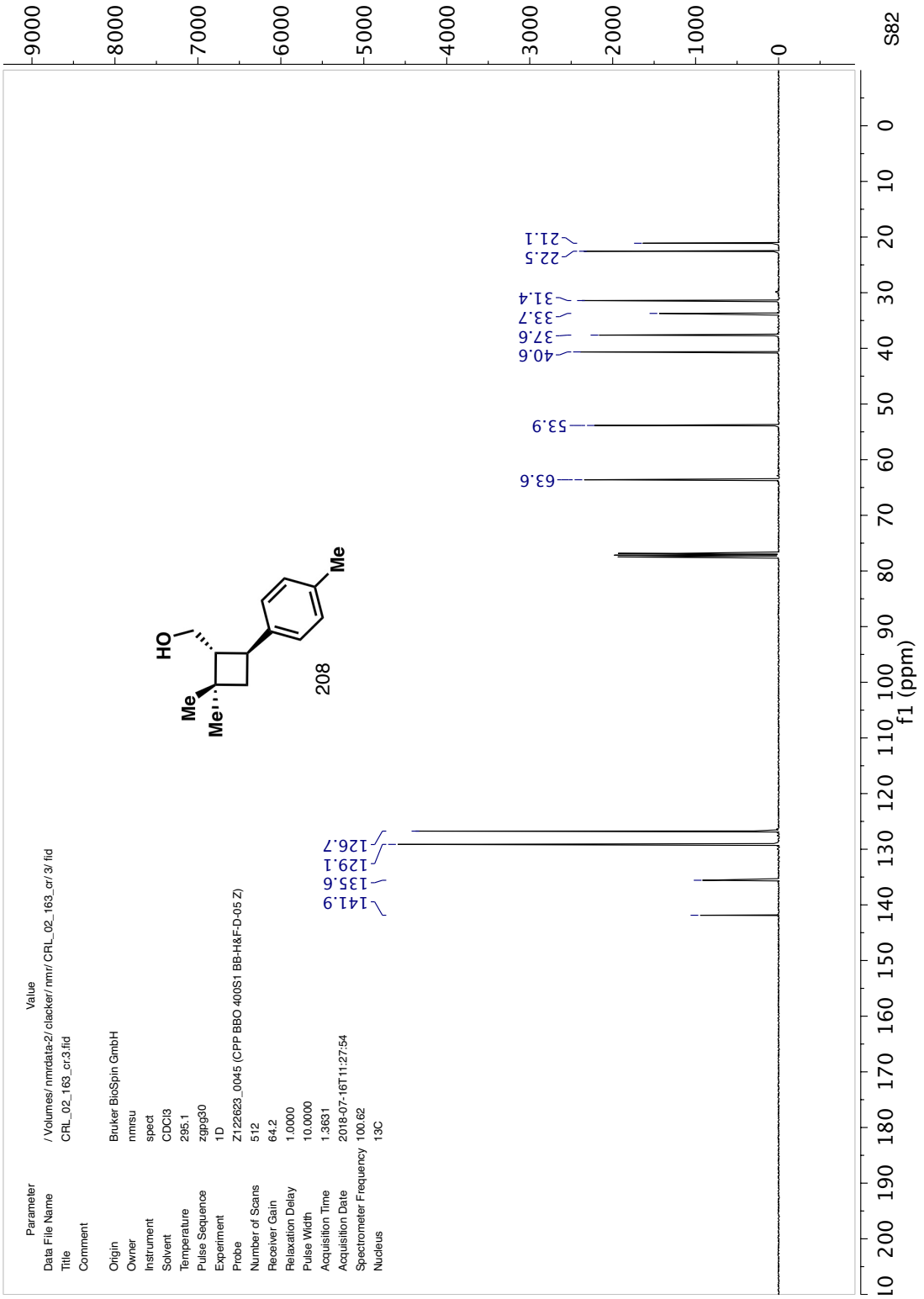
Parameter Value
Data File Name / Volumes/ nmrdata-2/ clacker/ nmr/ CRL_02_163_cr/ 3/ fid
Title CRL_02_163_cr.3.fid
Comment
Origin Bruker BioSpin GmbH
Owner nmrsu
Instrument spect
Solvent CDCl3
Temperature 295.1
Pulse Sequence zgpg30
Experiment 1D
Probe Z122623_0045 (CPP BBO 400S1 BB-H&F-D-05 Z)
Number of Scans 512
Receiver Gain 64.2
Relaxation Delay 1.0000
Pulse Width 10.0000
Acquisition Time 1.3631
Acquisition Date 2018-07-16T11:27:54
Spectrometer Frequency 100.62
Nucleus 13C
HO
Me
Me
Me
208
141.9
135.6
129.1
126.7
63.6
53.9
40.6
37.6
33.7
31.4
22.5
21.1
f1 (ppm)
S82

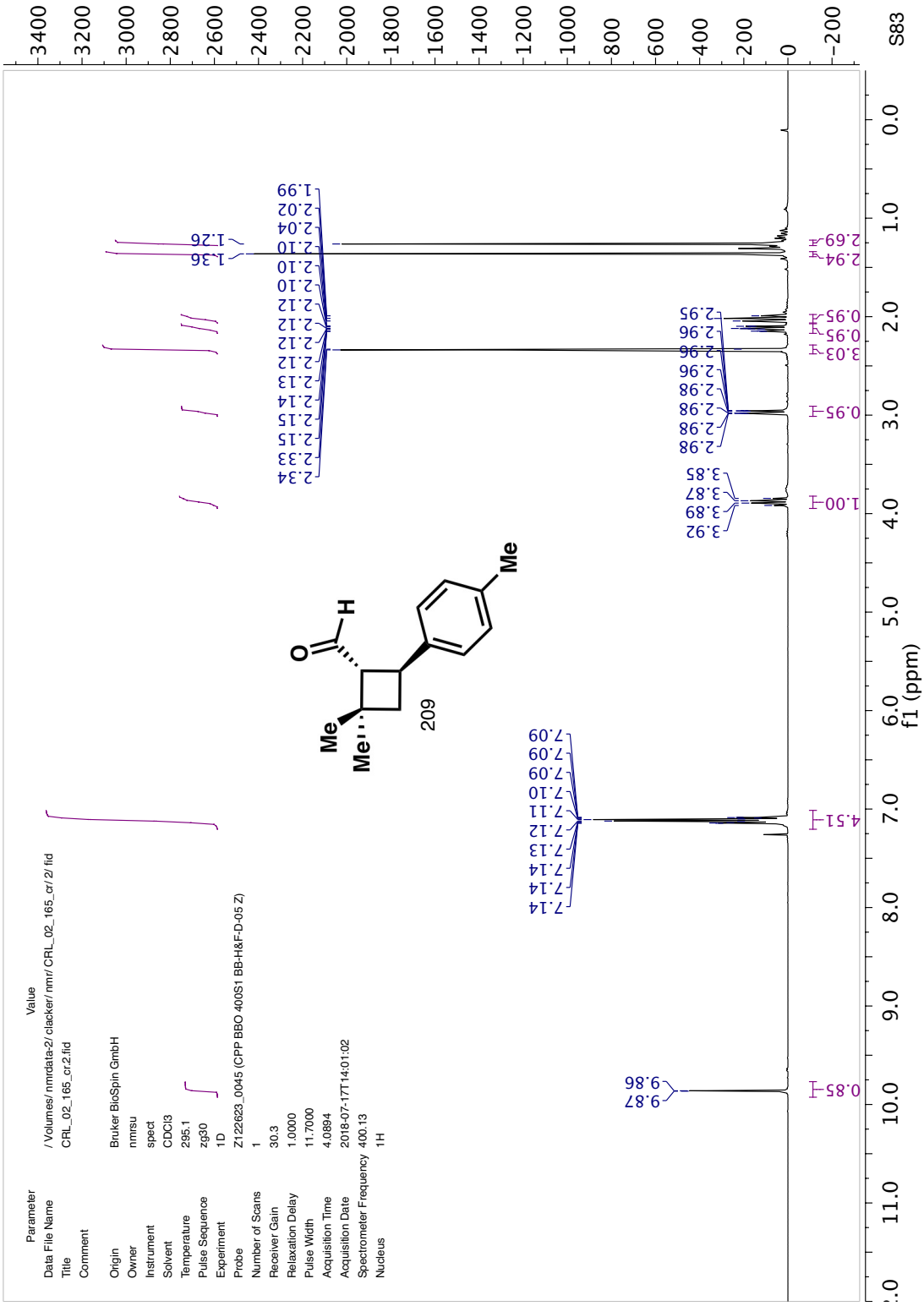
Parameter Value
Data File Name / Volumes/ nmrdata-2/ clacker/ nmr/ CRL_02_165_cr/ 2/ fid
Title CRL_02_165_cr.2.fid
Comment
Origin Bruker BioSpin GmbH
Owner nmrsu
Instrument spect
Solvent CDCl3
Temperature 295.1
Pulse Sequence zg30
Experiment 1D
Probe Z122623_0045 (CPP BBO 400S1 BB-H&F-D-05 Z)
Number of Scans 1
Receiver Gain 30.3
Relaxation Delay 1.0000
Pulse Width 11.7000
Acquisition Time 4.0894
Acquisition Date 2018-07-17T14:01:02
Spectrometer Frequency 400.13
Nucleus 1H
209
Me
Me
H
O
f1 (ppm)
S83

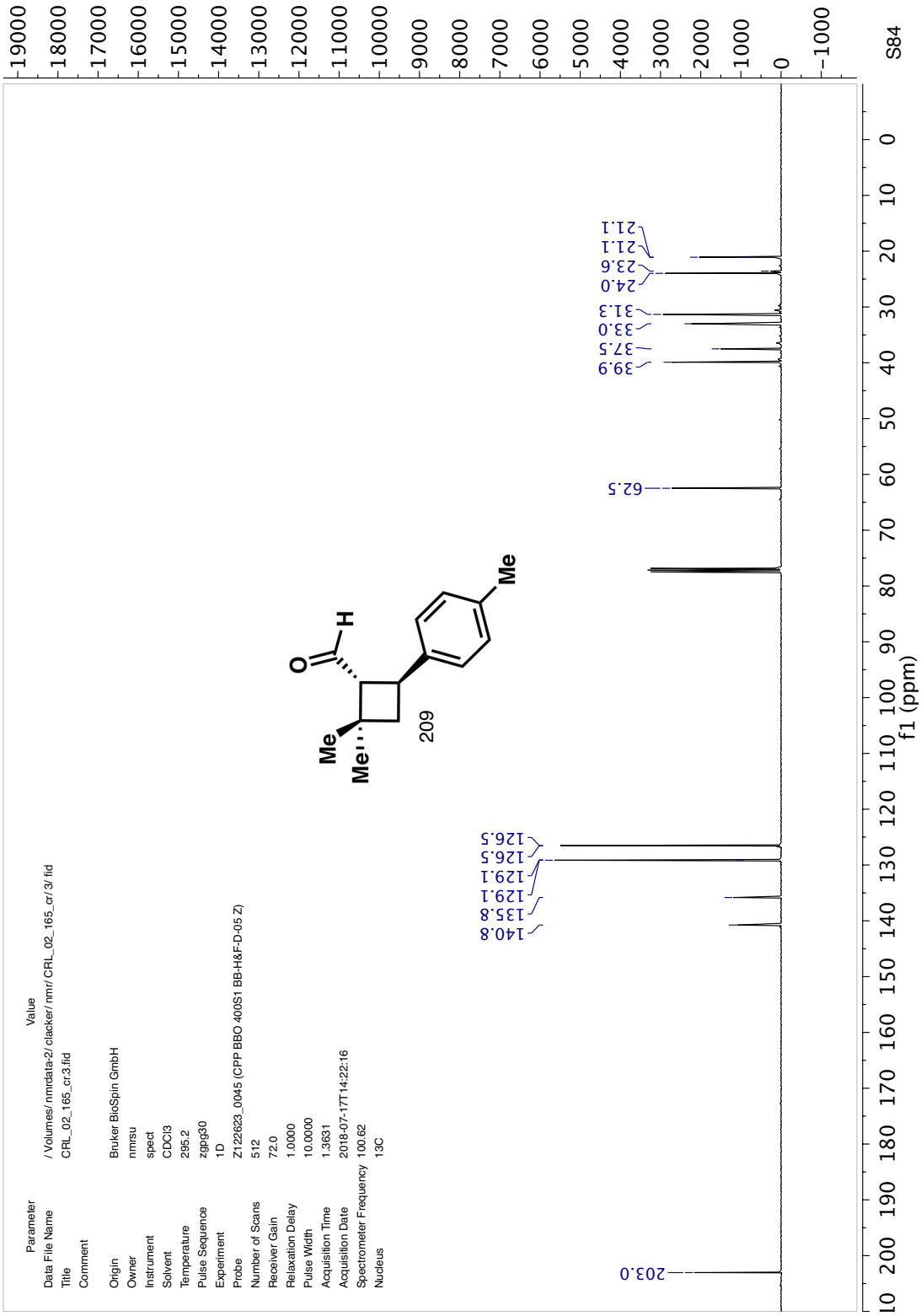
Parameter Value
Data File Name / Volumes/ nmrdata-2/ clacker/ nmr/ CRL_02_165_cr/ 3/ fid
Title CRL_02_165_cr.3.fid
Comment
Origin Bruker BioSpin GmbH
Owner nmrsu
Instrument spect
Solvent CDCl3
Temperature 295.2
Pulse Sequence zgpg30
Experiment 1D
Probe Z122623_0045 (CPP BBO 400S1 BB-H&F-D-05 Z)
Number of Scans 512
Receiver Gain 72.0
Relaxation Delay 1.0000
Pulse Width 10.0000
Acquisition Time 1.3631
Acquisition Date 2018-07-17T14:22:16
Spectrometer Frequency 100.62
Nucleus 13C
203.0
140.8
135.8
129.1
129.1
126.5
126.5
62.5
39.9
37.5
33.0
31.3
24.0
23.6
21.1
21.1
O
H
Me
Me
Me
209
S84
f1 (ppm)

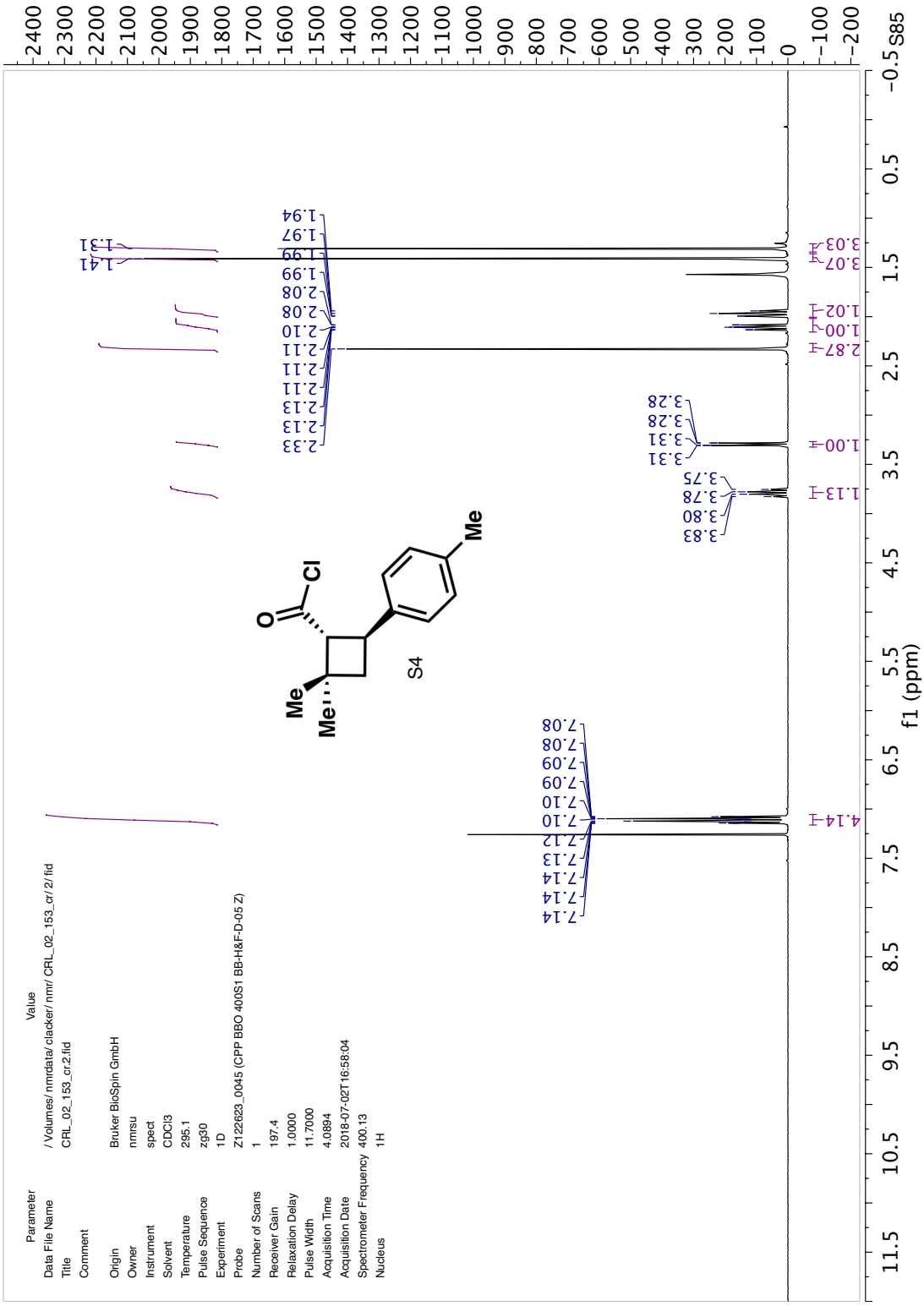
Parameter Value
Data File Name / Volumes/ nmrdata/ clacker/ nmr/ CRL_02_153_cr/ 2/ fid
Title CRL_02_153_cr.2.fid
Comment
Origin Bruker BioSpin GmbH
Owner nmrsu
Instrument spect
Solvent CDCl3
Temperature 295.1
Pulse Sequence zg30
Experiment 1D
Probe Z122623_0045 (CPP BBO 400S1 BB-H&F-D-05 Z)
Number of Scans 1
Receiver Gain 197.4
Relaxation Delay 1.0000
Pulse Width 11.7000
Acquisition Time 4.0894
Acquisition Date 2018-07-02T16:58:04
Spectrometer Frequency 400.13
Nucleus 1H
S4
Me
Me
Cl
O
f1 (ppm)

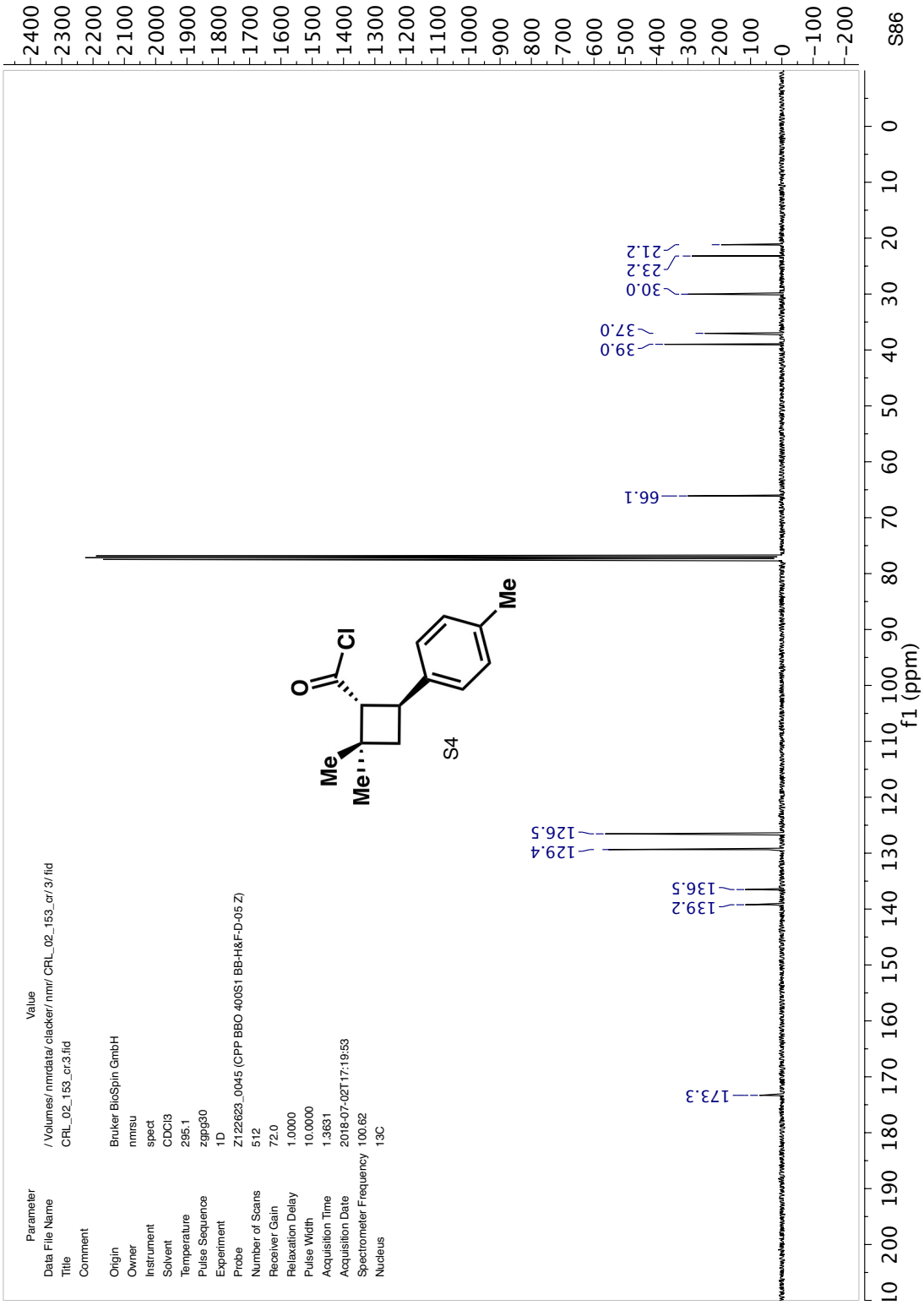
Parameter Value
Data File Name / Volumes/ nmrdata/ clacker/ nmr/ CRL_02_153_cr/ 3/ fid
Title CRL_02_153_cr.3.fid
Comment
Origin Bruker BioSpin GmbH
Owner nmrsu
Instrument spect
Solvent CDCl3
Temperature 295.1
Pulse Sequence zgpg30
Experiment 1D
Probe Z122623_0045 (CPP BBO 400S1 BB-H&F-D-05 Z)
Number of Scans 512
Receiver Gain 72.0
Relaxation Delay 1.0000
Pulse Width 10.0000
Acquisition Time 1.3631
Acquisition Date 2018-07-02T17:19:53
Spectrometer Frequency 100.62
Nucleus 13C
173.3
139.2
136.5
129.4
126.5
66.1
39.0
37.0
30.0
23.2
21.2
O
Cl
Me
Me
Me
S4
f1 (ppm)
S86

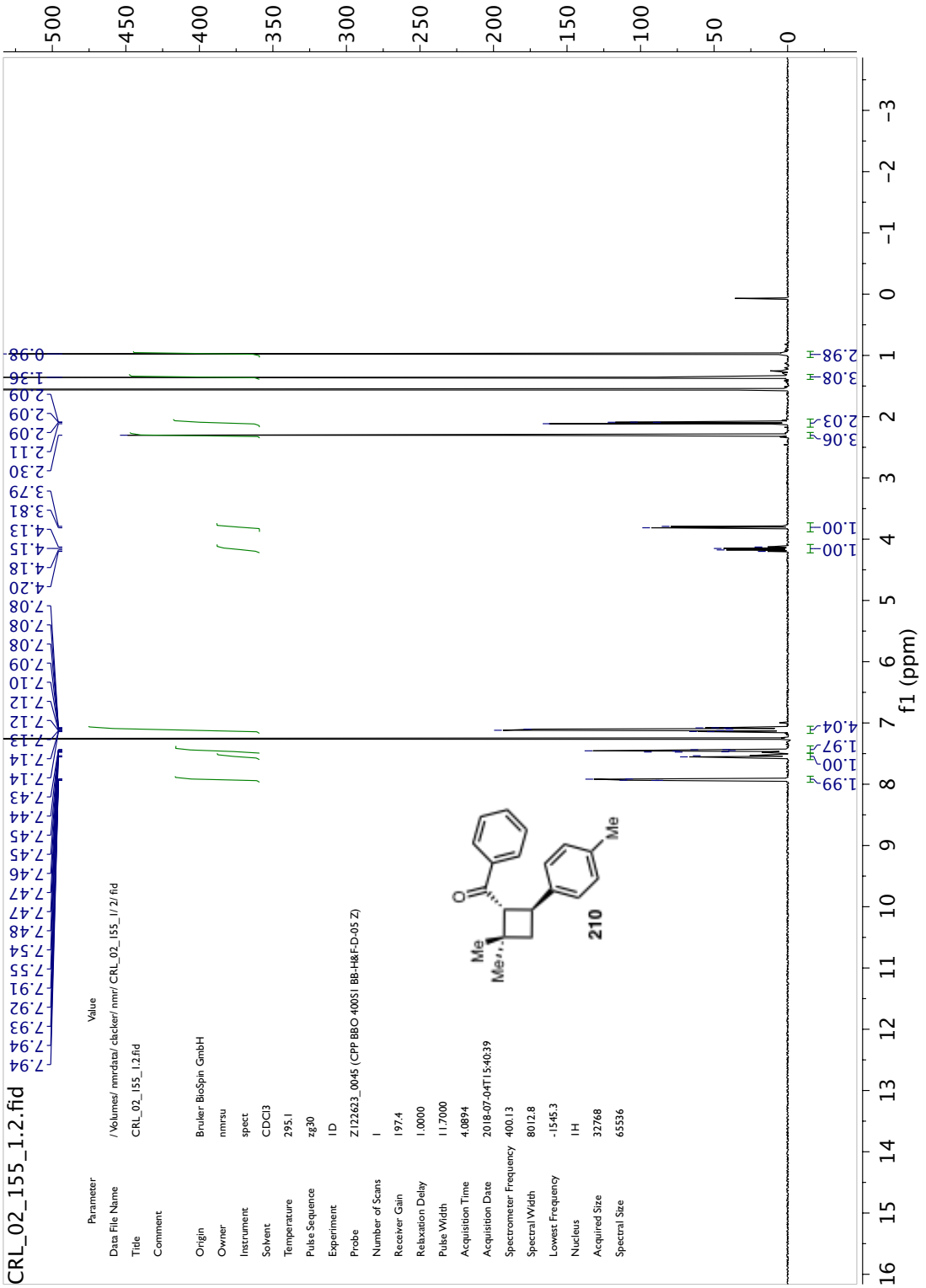
CRL_02_155_1.2.fid
f1 (ppm)
210
Me
Me
O
Me
Parameter Value
Data File Name /Volumes/ nmrdata/ clacker/ nmr/ CRL_02_155_1/2/fid
Title CRL_02_155_1.2.fid
Comment
Origin Bruker BioSpin GmbH
Owner nmrsu
Instrument spect
Solvent CDCl3
Temperature 295.1
Pulse Sequence zg30
Experiment 1D
Probe Z122623_0045 (CPP BBO 400S1 BB-H&F-D-05 Z)
Number of Scans 1
Receiver Gain 197.4
Relaxation Delay 1.0000
Pulse Width 11.7000
Acquisition Time 4.0894
Acquisition Date 2018-07-04T15:40:39
Spectrometer Frequency 400.13
Spectral Width 8012.8
Lowest Frequency -1545.3
Nucleus 1H
Acquired Size 32768
Spectral Size 65536

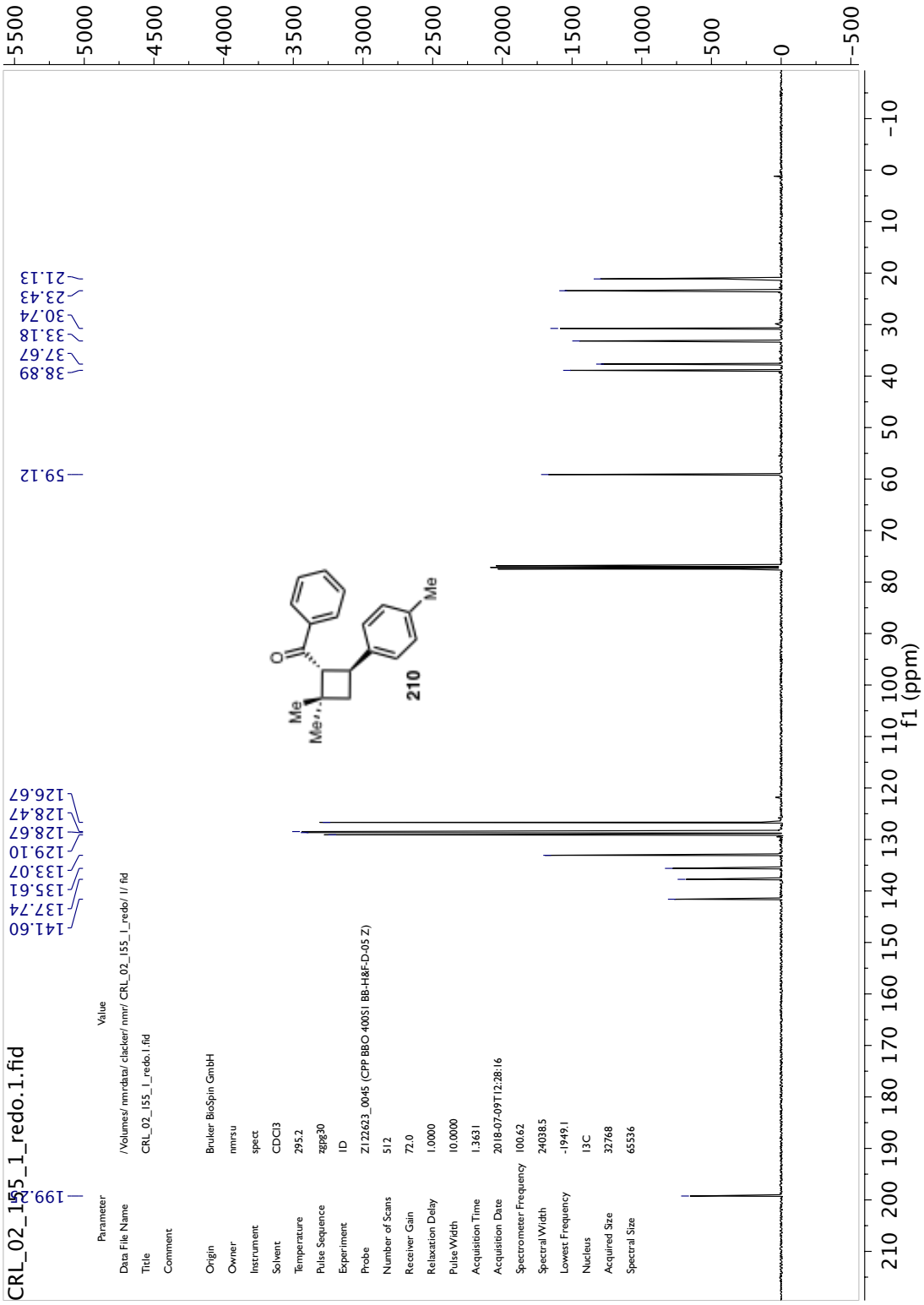
CRL_02_155_1_redo.1.fid
Parameter Value
Data File Name /Volumes/ nmrdata/ clacker/ nmr/ CRL_02_155_1_redo/ 1/ fid
Title CRL_02_155_1_redo.1.fid
Comment
Origin Bruker BioSpin GmbH
Owner nmrsu
Instrument spect
Solvent CDCl3
Temperature 295.2
Pulse Sequence zgpg30
Experiment 1D
Probe Z122623_0045 (CPP BBO 400SI BB-H&F-D-05 Z)
Number of Scans 512
Receiver Gain 72.0
Relaxation Delay 1.0000
Pulse Width 10.0000
Acquisition Time 1.3631
Acquisition Date 2018-07-09T12:28:16
Spectrometer Frequency 100.62
Spectral Width 24038.5
Lowest Frequency -1949.1
Nucleus 13C
Acquired Size 32768
Spectral Size 65536
199.22
141.60
137.74
135.61
133.07
129.10
128.67
128.47
126.67
59.12
38.89
37.67
33.18
30.74
23.43
21.13
Me
Me
Me
O
210
f1 (ppm)

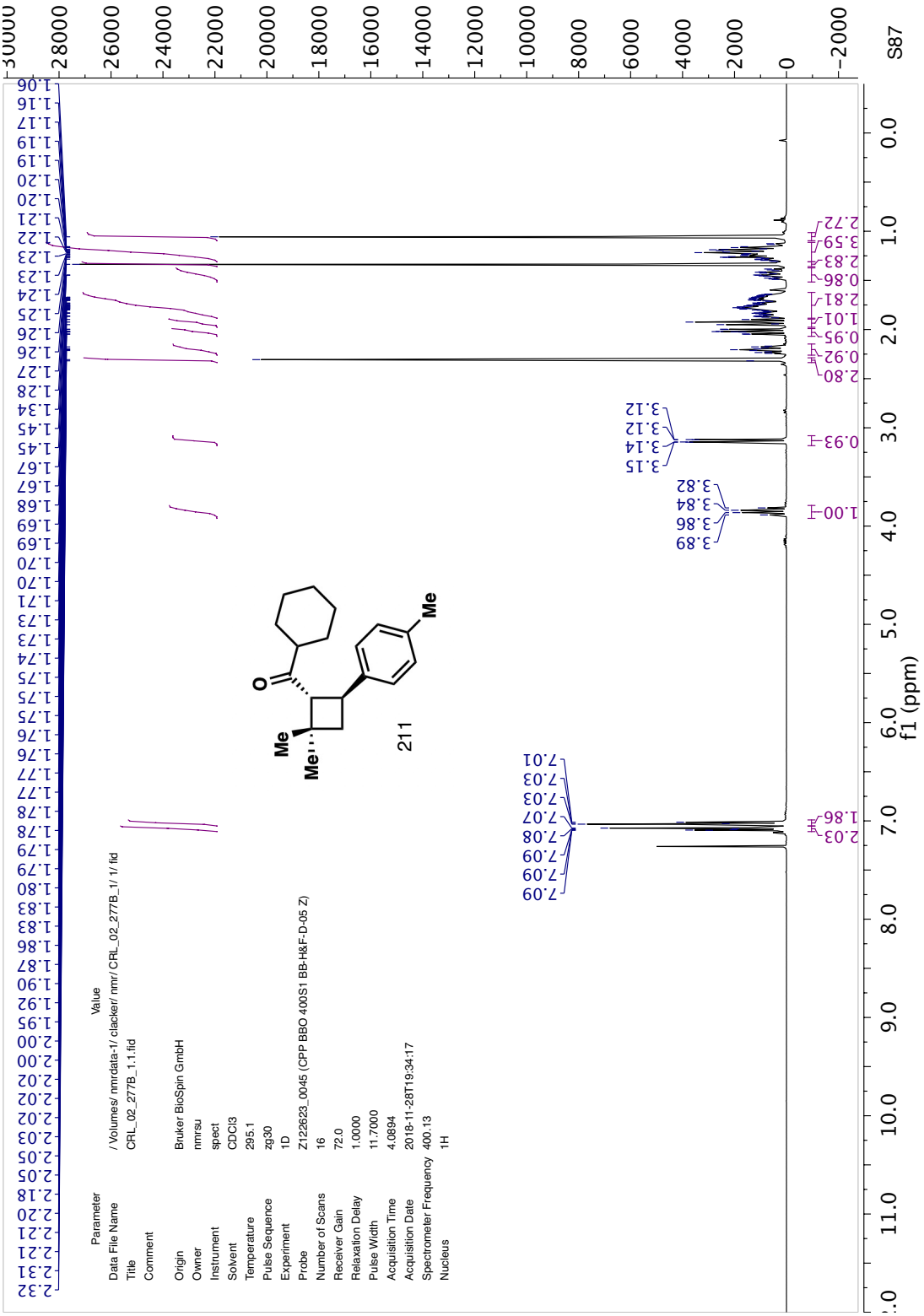
Parameter
Value
Data File Name
/ Volumes/ nmrdata-1/ clacker/ nmr/ CRL_02_277B_1/ 1/ fid
Title
CRL_02_277B_1.1.fid
Comment
Origin
Bruker BioSpin GmbH
Owner
nmrsu
Instrument
spect
Solvent
CDCl3
Temperature
295.1
Pulse Sequence
zg30
Experiment
1D
Probe
Z122623_0045 (CPP BBO 400S1 BB-H&F-D-05 Z)
Number of Scans
16
Receiver Gain
72.0
Relaxation Delay
1.0000
Pulse Width
11.7000
Acquisition Time
4.0894
Acquisition Date
2018-11-28T19:34:17
Spectrometer Frequency
400.13
Nucleus
1H
Me
Me
O
211
f1 (ppm)
S87

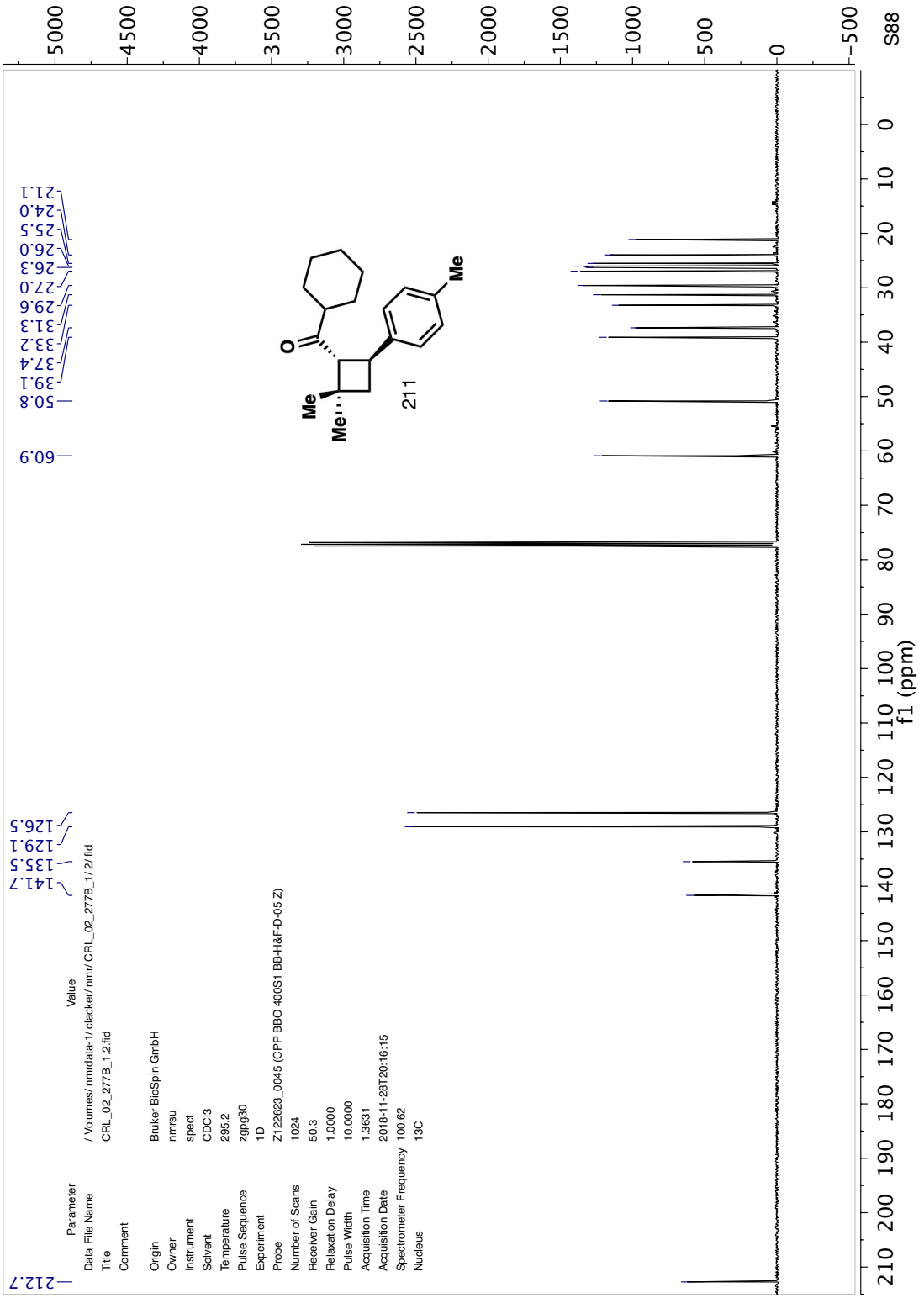
212.7
141.7
135.5
129.1
126.5
60.9
50.8
39.1
37.4
33.2
31.3
29.6
27.0
26.3
26.0
25.5
24.0
21.1
Me
Me
O
211
Me
f1 (ppm)
S88

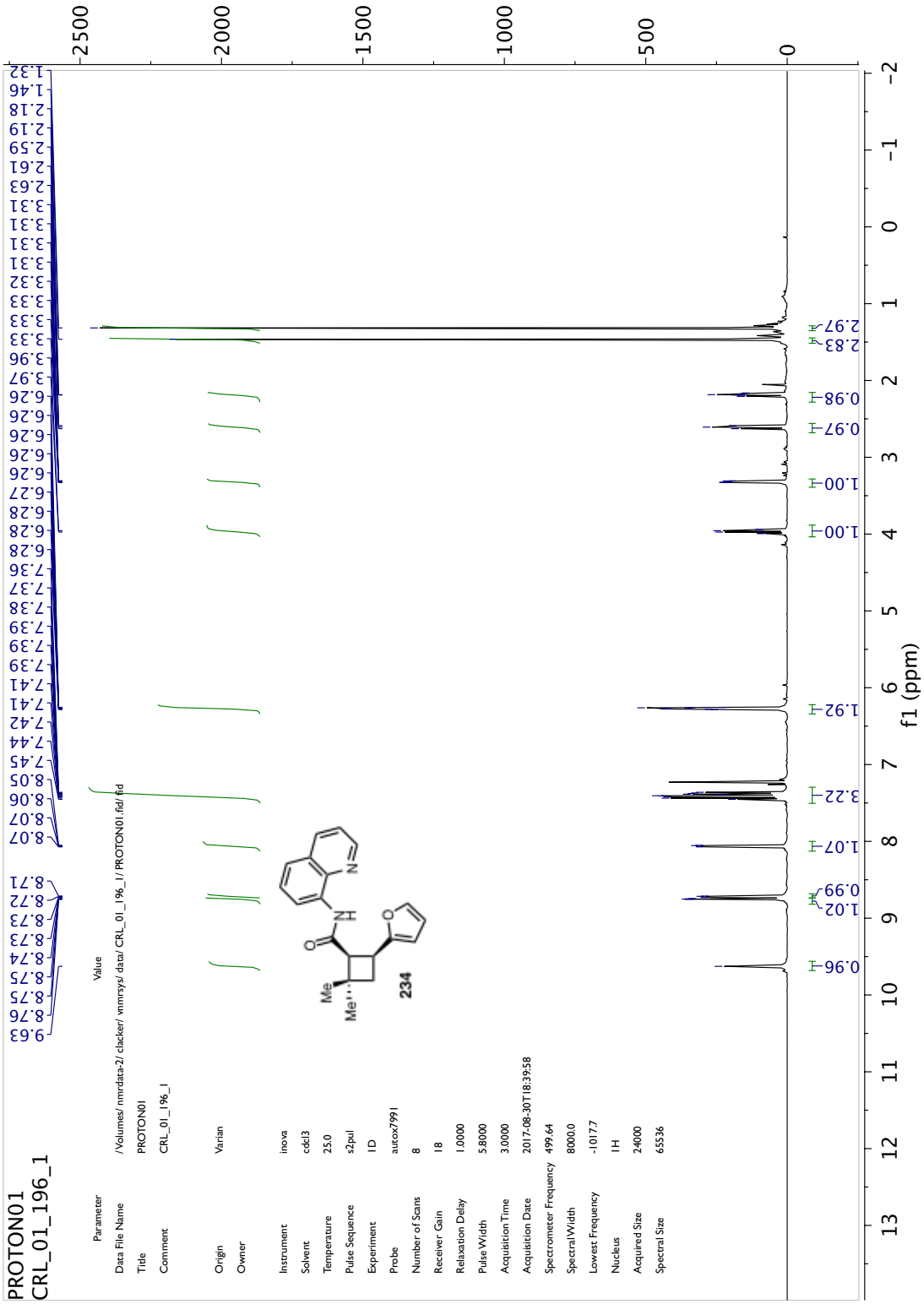
PROTON01
CRL_01_196_1
Parameter
Value
Data File Name
/Volumes/ nmrdata-2/ clacker/ vnmrsys/ data/ CRL_01_196_1/ PROTON01.fid/ fid
Title
PROTON01
Comment
CRL_01_196_1
Origin
Varian
Owner
Instrument
inova
Solvent
cdcl3
Temperature
25.0
Pulse Sequence
s2pul
Experiment
1D
Probe
autox7991
Number of Scans
8
Receiver Gain
18
Relaxation Delay
1.0000
Pulse Width
5.8000
Acquisition Time
3.0000
Acquisition Date
2017-08-30T18:39:58
Spectrometer Frequency
499.64
Spectral Width
8000.0
Lowest Frequency
-1017.7
Nucleus
1H
Acquired Size
24000
Spectral Size
65536
234
f1 (ppm)

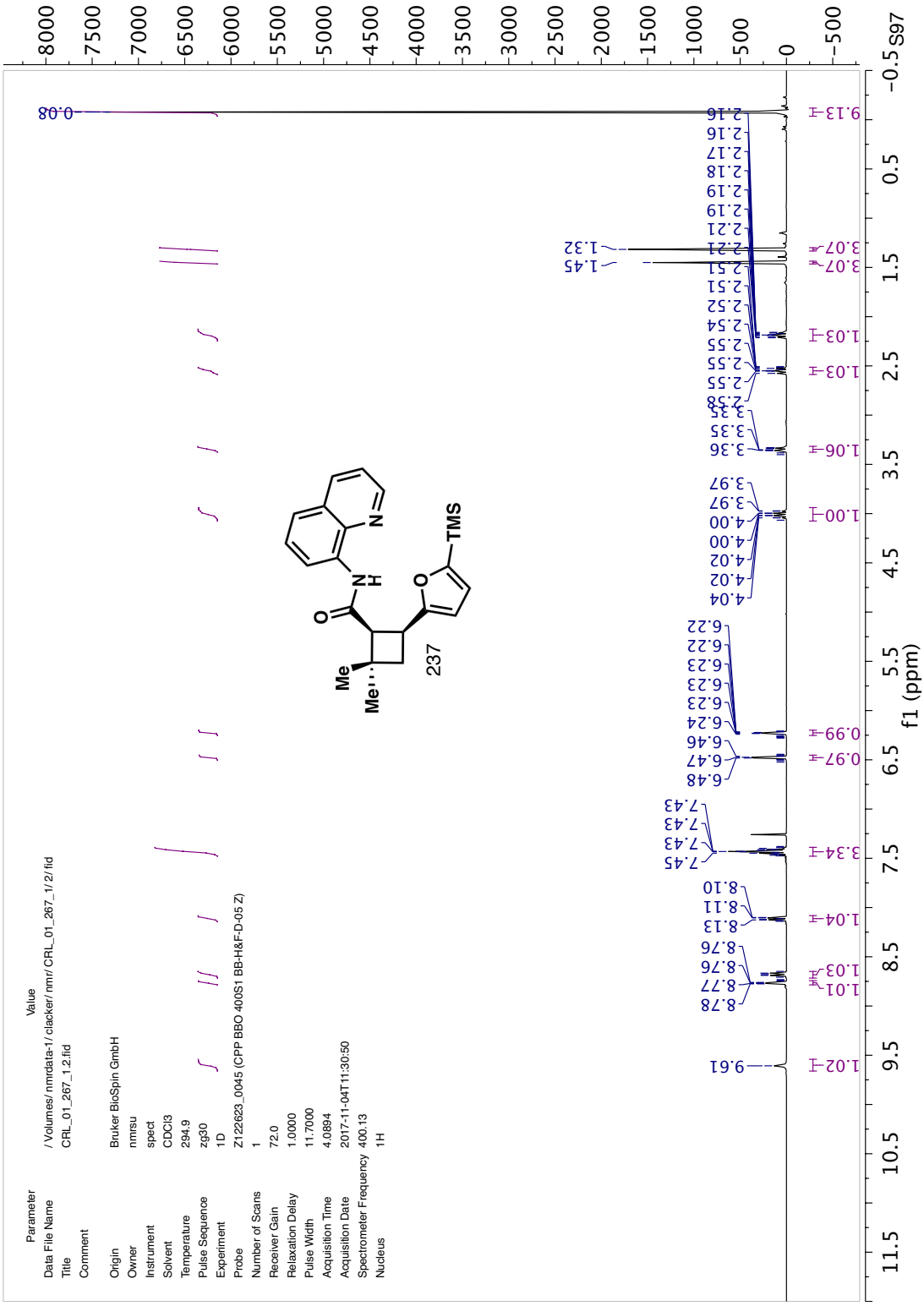
Parameter Value
Data File Name / Volumes/ nmrdata-1/ clacker/ nmr/ CRL_01_267_1/ 2/ fid
Title CRL_01_267_1.2.fid
Comment
Origin Bruker BioSpin GmbH
Owner nmrsu
Instrument spect
Solvent CDCl3
Temperature 294.9
Pulse Sequence zg30
Experiment 1D
Probe Z122623_0045 (CPP BBO 400S1 BB-H&F-D-05 Z)
Number of Scans 1
Receiver Gain 72.0
Relaxation Delay 1.0000
Pulse Width 11.7000
Acquisition Time 4.0894
Acquisition Date 2017-11-04T11:30:50
Spectrometer Frequency 400.13
Nucleus 1H
Me
Me
TMS
237
f1 (ppm)
S97

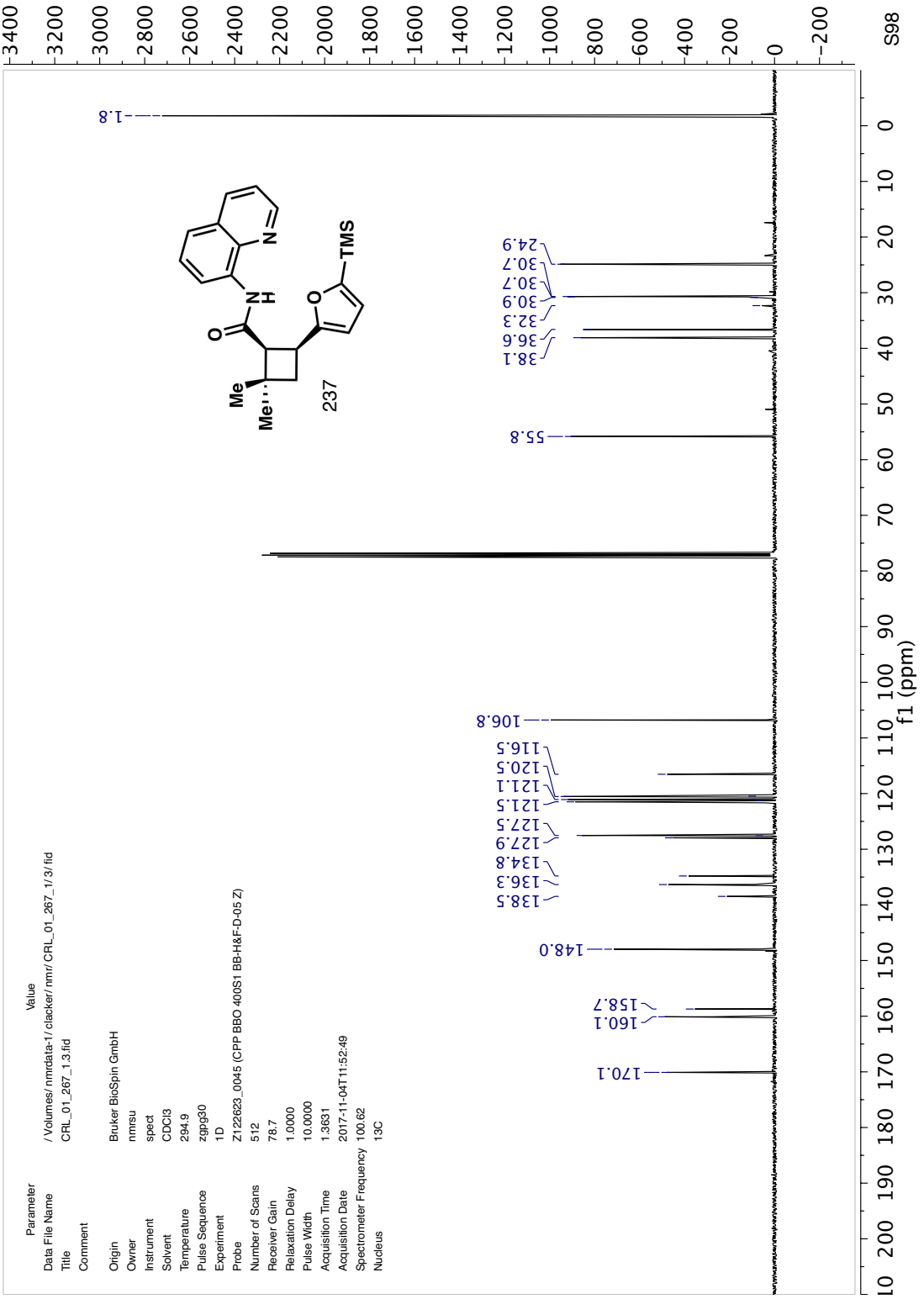
Parameter Value
Data File Name / Volumes/ nmrdata-1/ clacker/ nmr/ CRL_01_267_1/3/ fid
Title CRL_01_267_1.3.fid
Comment
Origin Bruker BioSpin GmbH
Owner nmrsu
Instrument spect
Solvent CDCl3
Temperature 294.9
Pulse Sequence zgpg30
Experiment 1D
Probe Z122623_0045 (CPP BBO 400S1 BB-H&F-D-05 Z)
Number of Scans 512
Receiver Gain 78.7
Relaxation Delay 1.0000
Pulse Width 10.0000
Acquisition Time 1.3631
Acquisition Date 2017-11-04T11:52:49
Spectrometer Frequency 100.62
Nucleus 13C
1.8
24.9
30.7
30.7
30.9
32.3
36.6
38.1
55.8
106.8
116.5
120.5
121.1
121.5
127.5
127.9
134.8
136.3
138.5
148.0
158.7
160.1
170.1
Me
Me
237
TMS
S98
f1 (ppm)

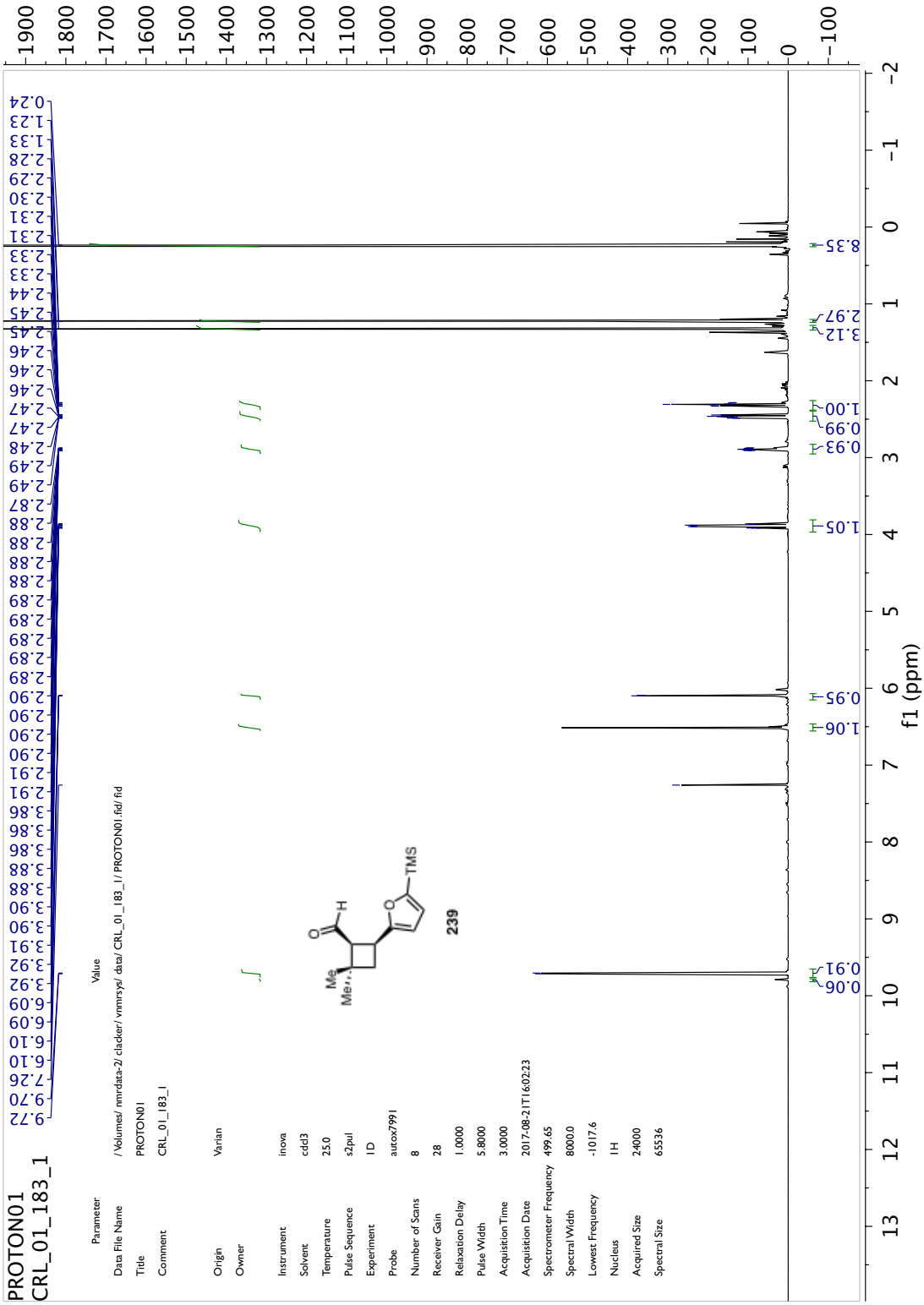
PROTON01
CRL_01_183_1
Parameter
Value
Data File Name
/Volumes/ nmrdata-2/ clacker/ vnmrsys/ data/ CRL_01_183_1/ PROTON01.fid/ fid
Title
PROTON01
Comment
CRL_01_183_1
Origin
Varian
Owner
Instrument
inova
Solvent
cdd3
Temperature
25.0
Pulse Sequence
s2pul
Experiment
1D
Probe
autox7991
Number of Scans
8
Receiver Gain
28
Relaxation Delay
1.0000
Pulse Width
5.8000
Acquisition Time
3.0000
Acquisition Date
2017-08-21T16:02:23
Spectrometer Frequency
499.65
Spectral Width
8000.0
Lowest Frequency
-1017.6
Nucleus
1H
Acquired Size
24000
Spectral Size
65536
239
Me
Me
H
O
TMS
O
8.35
2.97
3.12
1.00
0.99
0.93
1.05
0.95
1.06
0.91
0.06
f1 (ppm)

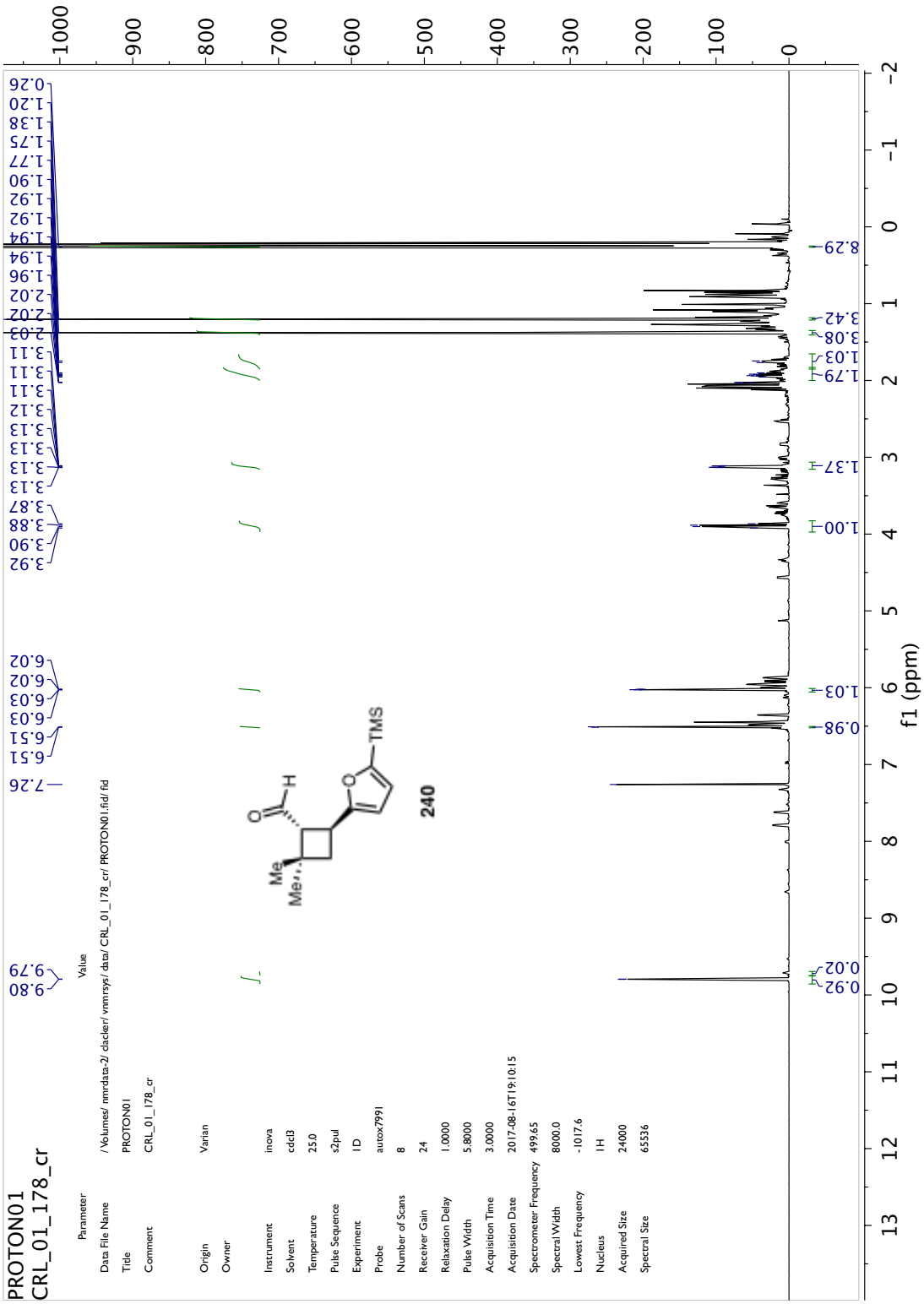
PROTON01
CRL_01_178_cr
Parameter
Value
Data File Name /Volumes/ nmrdata-2/ dacker/ vnmrsys/ data/ CRL_01_178_cr/ PROTON01.fid/ fid
Title PROTON01
Comment CRL_01_178_cr
Origin Varian
Owner
Instrument inova
Solvent cdcl3
Temperature 25.0
Pulse Sequence s2pul
Experiment 1D
Probe autox7991
Number of Scans 8
Receiver Gain 24
Relaxation Delay 1.0000
Pulse Width 5.8000
Acquisition Time 3.0000
Acquisition Date 2017-08-16T19:10:15
Spectrometer Frequency 499.65
Spectral Width 8000.0
Lowest Frequency -1017.6
Nucleus 1H
Acquired Size 24000
Spectral Size 65536
240
TMS
Me
Me
f1 (ppm)

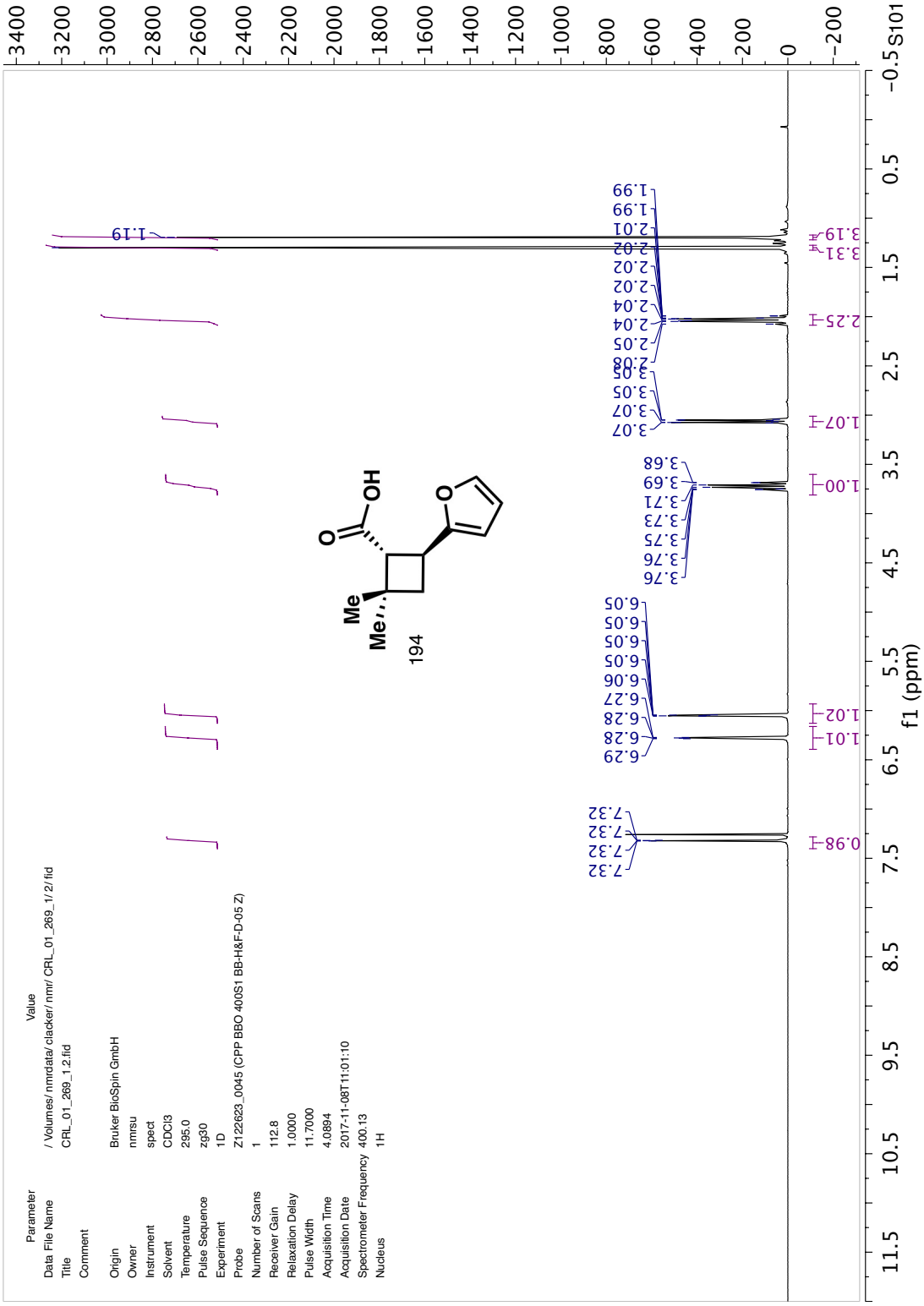
Parameter Value
Data File Name / Volumes/ nmrdata/ clacker/ nmr/ CRL_01_269_1/2/ fid
Title CRL_01_269_1.2.fid
Comment
Origin Bruker BioSpin GmbH
Owner nmrsu
Instrument spect
Solvent CDCl3
Temperature 295.0
Pulse Sequence zg30
Experiment 1D
Probe Z122623_0045 (CPP BBO 400S1 BB-H&F-D-05 Z)
Number of Scans 1
Receiver Gain 112.8
Relaxation Delay 1.0000
Pulse Width 11.7000
Acquisition Time 4.0894
Acquisition Date 2017-11-08T11:01:10
Spectrometer Frequency 400.13
Nucleus 1H
OH
O
Me
Me
194
f1 (ppm)

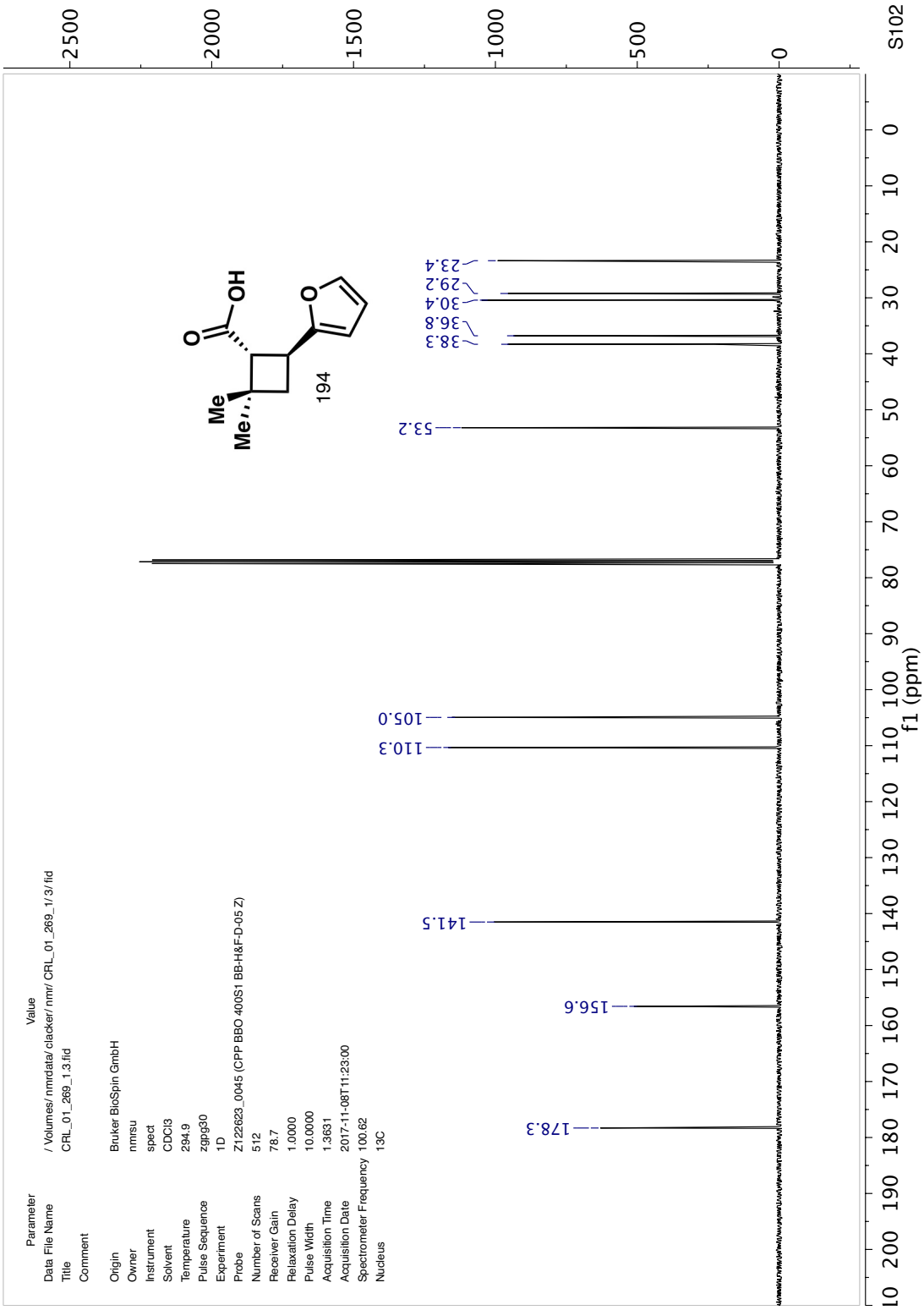
Parameter Value
Data File Name / Volumes/ nmrdata/ clacker/ nmr/ CRL_01_269_1/3/ fid
Title CRL_01_269_1.3.fid
Comment
Origin Bruker BioSpin GmbH
Owner nmrsu
Instrument spect
Solvent CDCl3
Temperature 294.9
Pulse Sequence zgpg30
Experiment 1D
Probe Z122623_0045 (CPP BBO 400S1 BB-H&F-D-05 Z)
Number of Scans 512
Receiver Gain 78.7
Relaxation Delay 1.0000
Pulse Width 10.0000
Acquisition Time 1.3631
Acquisition Date 2017-11-08T11:23:00
Spectrometer Frequency 100.62
Nucleus 13C
178.3
156.6
141.5
110.3
105.0
53.2
38.3
36.8
30.4
29.2
23.4
Me
Me
O
OH
O
194
f1 (ppm)
S102

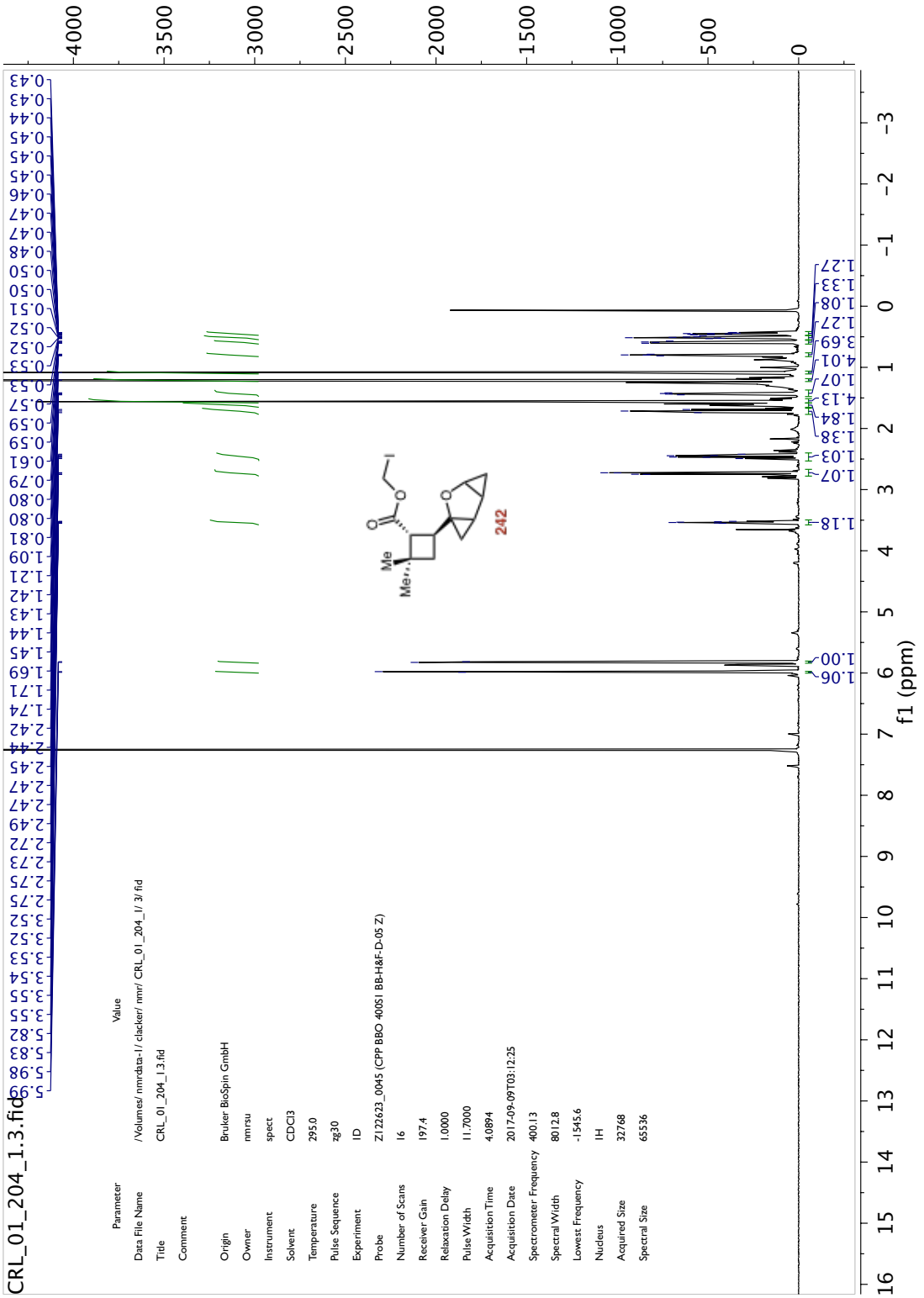
CRL_01_204_1.3.fid
Parameter Value
Data File Name /Volumes/ nmrdata-1/ clacker/ nmr/ CRL_01_204_1/ 3/ fid
Title CRL_01_204_1.3.fid
Comment
Origin Bruker BioSpin GmbH
Owner nmrsu
Instrument spect
Solvent CDCl3
Temperature 295.0
Pulse Sequence zg30
Experiment ID
Probe Z122623_0045 (CPP BBO 400S1 BB-H&F-D-05 Z)
Number of Scans 16
Receiver Gain 197.4
Relaxation Delay 1.0000
Pulse Width 11.7000
Acquisition Time 4.0894
Acquisition Date 2017-09-09T03:12:25
Spectrometer Frequency 400.13
Spectral Width 8012.8
Lowest Frequency -1545.6
Nucleus 1H
Acquired Size 32768
Spectral Size 65536
242
1.06
1.00
1.18
1.07
1.03
1.38
1.84
4.13
1.07
4.01
3.69
1.27
1.08
1.33
1.27
f1 (ppm)

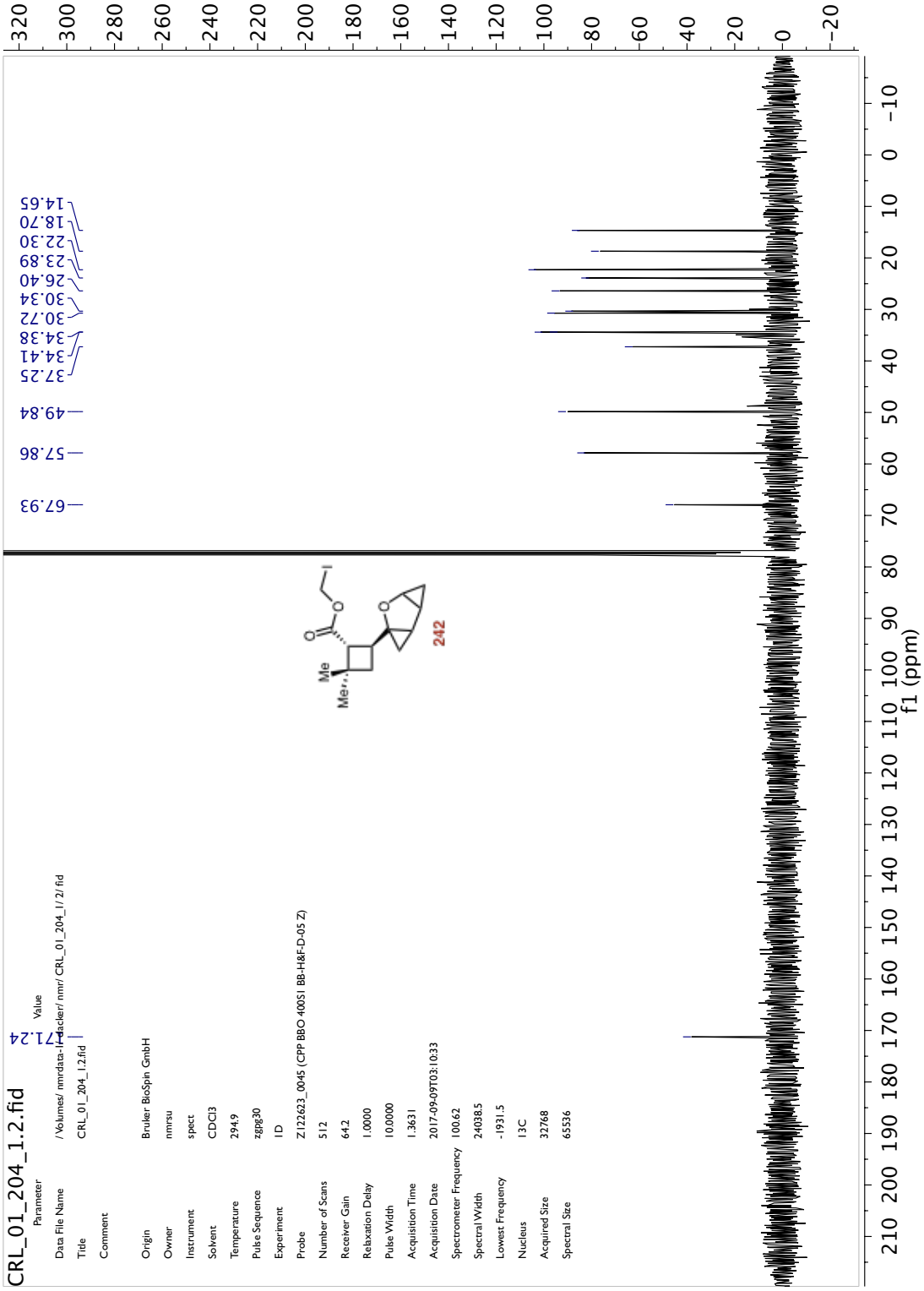
CRL_01_204_1.2.fid
Parameter
Value
Data File Name
/Volumes/ nmrdata-lhacker/ nmr/ CRL_01_204_1/ 2/ fid
Title
CRL_01_204_1.2.fid
Comment
Origin
Bruker BioSpin GmbH
Owner
nmrsu
Instrument
spect
Solvent
CDCl3
Temperature
294.9
Pulse Sequence
zgpg30
Experiment
1D
Probe
Z122623_0045 (CPP BBO 400SI BB-H&F-D-05 Z)
Number of Scans
512
Receiver Gain
64.2
Relaxation Delay
1.0000
Pulse Width
10.0000
Acquisition Time
1.3631
Acquisition Date
2017-09-09T03:10:33
Spectrometer Frequency
100.62
Spectral Width
24038.5
Lowest Frequency
-1931.5
Nucleus
13C
Acquired Size
32768
Spectral Size
65536
171.24
67.93
57.86
49.84
37.25
34.41
34.38
30.72
30.34
26.40
23.89
22.30
18.70
14.65
Me
Me
I
O
O
O
242
f1 (ppm)

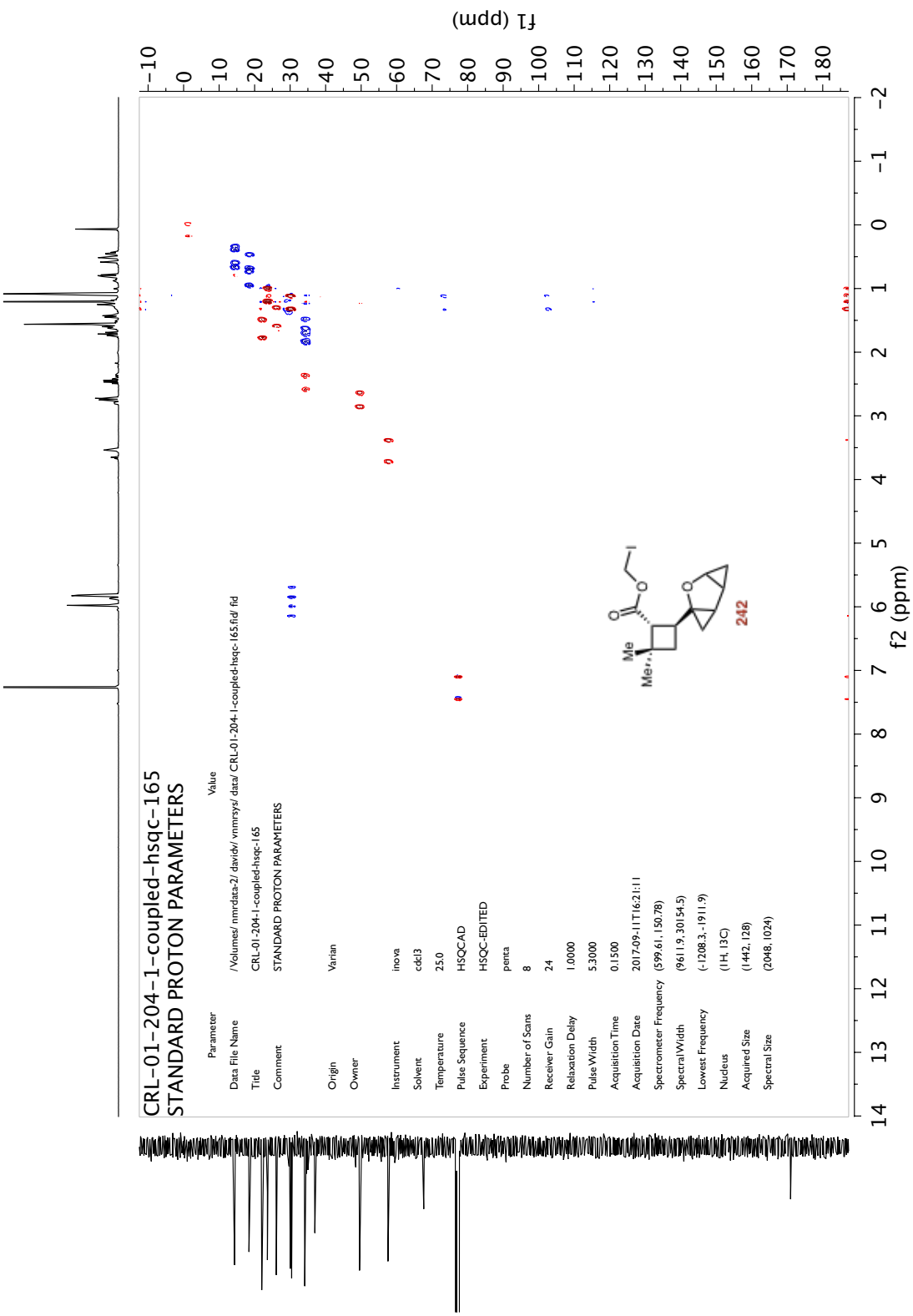
CRL-01-204-1-coupled-hsqc-165
STANDARD PROTON PARAMETERS
Parameter Value
Data File Name /Volumes/ nmrdata-2/ davidv/ vnmrsys/ data/ CRL-01-204-1-coupled-hsqc-165.fid/ fid
Title CRL-01-204-1-coupled-hsqc-165
Comment STANDARD PROTON PARAMETERS
Origin Varian
Owner
Instrument inova
Solvent cdcl3
Temperature 25.0
Pulse Sequence HSQCAD
Experiment HSQC-EDITED
Probe penta
Number of Scans 8
Receiver Gain 24
Relaxation Delay 1.0000
Pulse Width 5.3000
Acquisition Time 0.1500
Acquisition Date 2017-09-11T16:21:11
Spectrometer Frequency (599.61, 150.78)
Spectral Width (9611.9, 30154.5)
Lowest Frequency (-1208.3, -1911.9)
Nucleus (1H, 13C)
Acquired Size (1442, 128)
Spectral Size (2048, 1024)
Me
Me
242
f1 (ppm)
f2 (ppm)

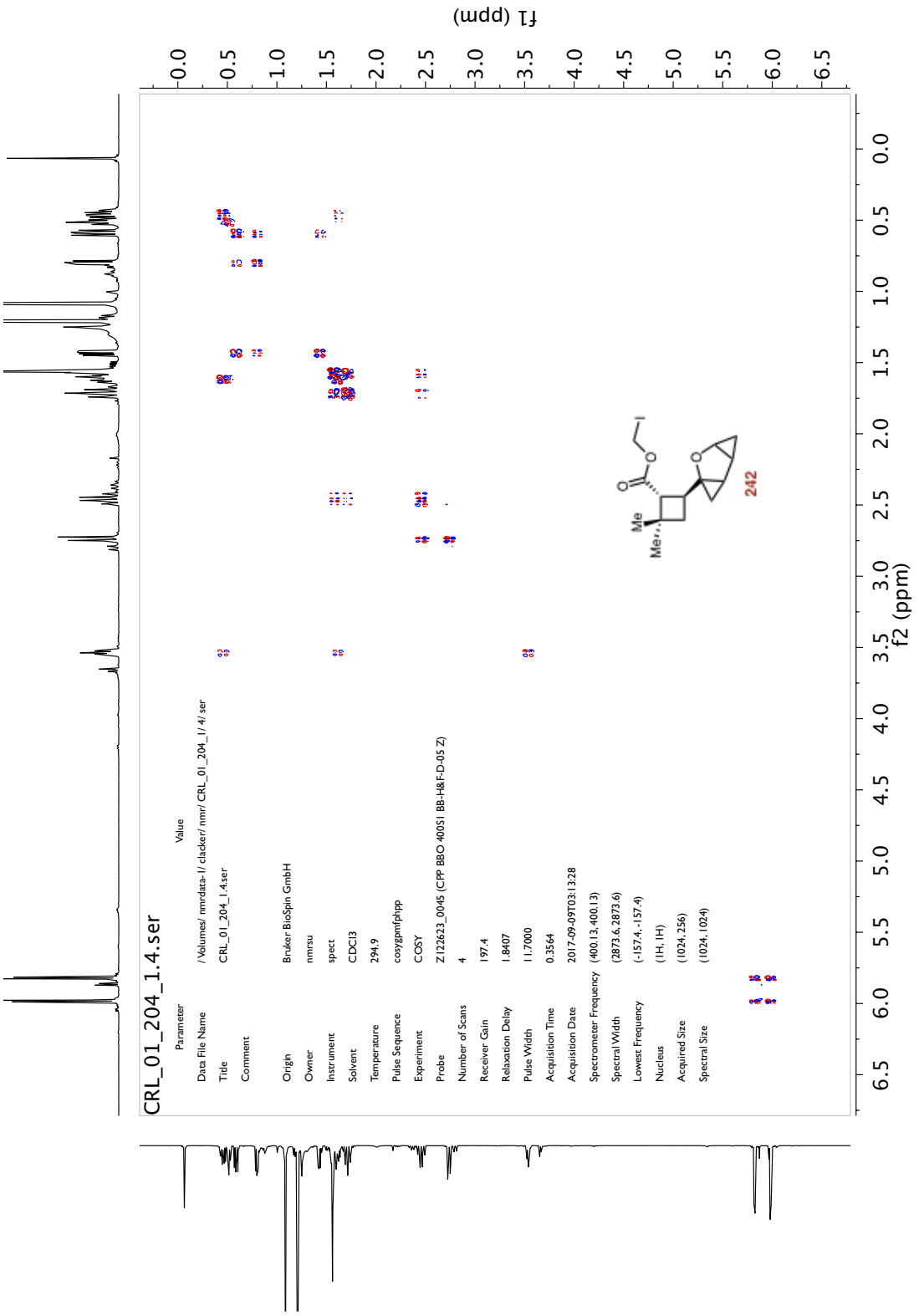
CRL_01_204_1.4.ser
Parameter Value
Data File Name /Volumes/ nmrdata-1/ clacker/ nmr/ CRL_01_204_1/ 4/ ser
Title CRL_01_204_1.4.ser
Comment
Origin Bruker BioSpin GmbH
Owner nmrsu
Instrument spect
Solvent CDCl3
Temperature 294.9
Pulse Sequence cosygpmfphpp
Experiment COSY
Probe Z122623_0045 (CPP BBO 400SI BB-H&F-D-05 Z)
Number of Scans 4
Receiver Gain 197.4
Relaxation Delay 1.8407
Pulse Width 11.7000
Acquisition Time 0.3564
Acquisition Date 2017-09-09T03:13:28
Spectrometer Frequency (400.13, 400.13)
Spectral Width (2873.6, 2873.6)
Lowest Frequency (-157.4, -157.4)
Nucleus (1H, 1H)
Acquired Size (1024, 256)
Spectral Size (1024, 1024)
Me
Me
242
f1 (ppm)
f2 (ppm)

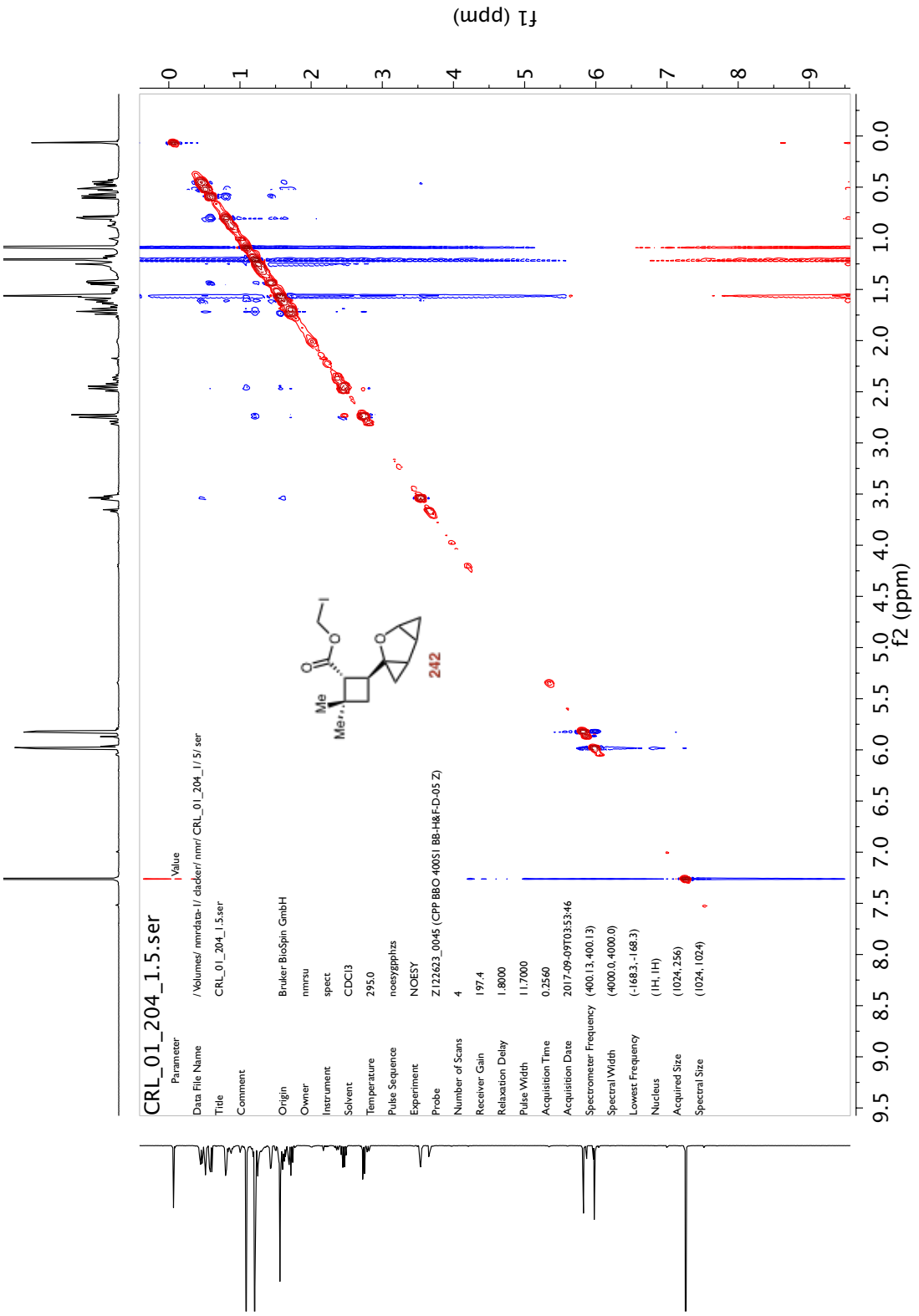
CRL_01_204_1.5.ser
Parameter
Value
Data File Name /Volumes/ nmrdata-1/ dacker/ nmr/ CRL_01_204_1/ 5/ ser
Title CRL_01_204_1.5.ser
Comment
Origin Bruker BioSpin GmbH
Owner nmrsu
Instrument spect
Solvent CDCl3
Temperature 295.0
Pulse Sequence noesygpphzs
Experiment NOESY
Probe Z122623_0045 (CPP BBO 400S1 BB-H&F-D-05 Z)
Number of Scans 4
Receiver Gain 197.4
Relaxation Delay 1.8000
Pulse Width 11.7000
Acquisition Time 0.2560
Acquisition Date 2017-09-09T03:53:46
Spectrometer Frequency (400.13, 400.13)
Spectral Width (4000.0, 4000.0)
Lowest Frequency (-168.3, -168.3)
Nucleus (1H, 1H)
Acquired Size (1024, 256)
Spectral Size (1024, 1024)
Me
Me
242
f2 (ppm)
f1 (ppm)

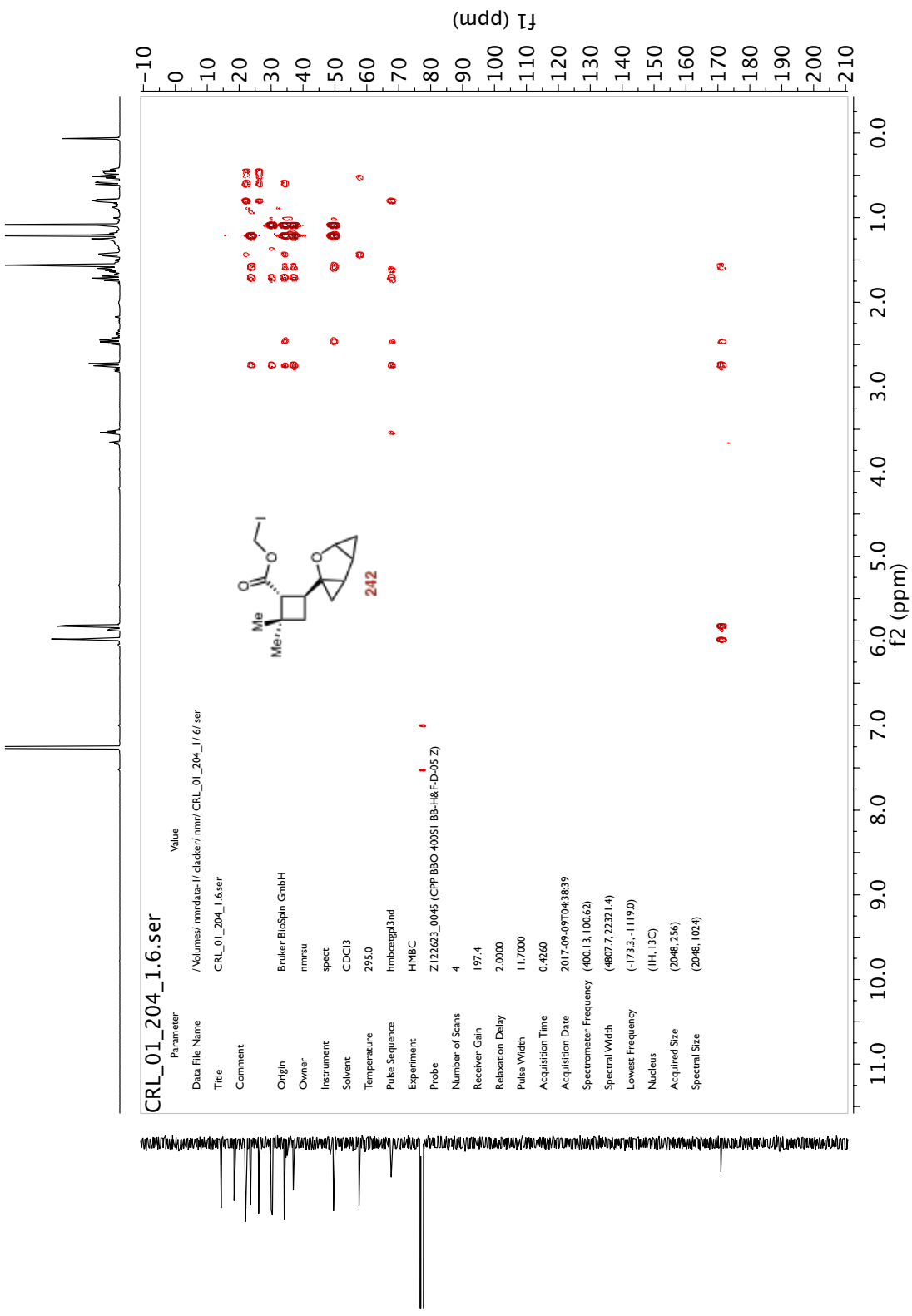
CRL_01_204_1.6.ser
Parameter Value
Data File Name /Volumes/nmrdata-1/clacker/nmr/CRL_01_204_1/6/ser
Title CRL_01_204_1.6.ser
Comment
Origin Bruker BioSpin GmbH
Owner nmrsu
Instrument spect
Solvent CDCl3
Temperature 295.0
Pulse Sequence hmbcetgpl3nd
Experiment HMBC
Probe Z122623_0045 (CPP BBO 400SI BB-H&F-D-05 Z)
Number of Scans 4
Receiver Gain 197.4
Relaxation Delay 2.0000
Pulse Width 11.7000
Acquisition Time 0.4260
Acquisition Date 2017-09-09T04:38:39
Spectrometer Frequency (400.13, 100.62)
Spectral Width (4807.7, 22321.4)
Lowest Frequency (-173.3, -1119.0)
Nucleus (1H, 13C)
Acquired Size (2048, 256)
Spectral Size (2048, 1024)
Me
Me
242
f1 (ppm)
f2 (ppm)

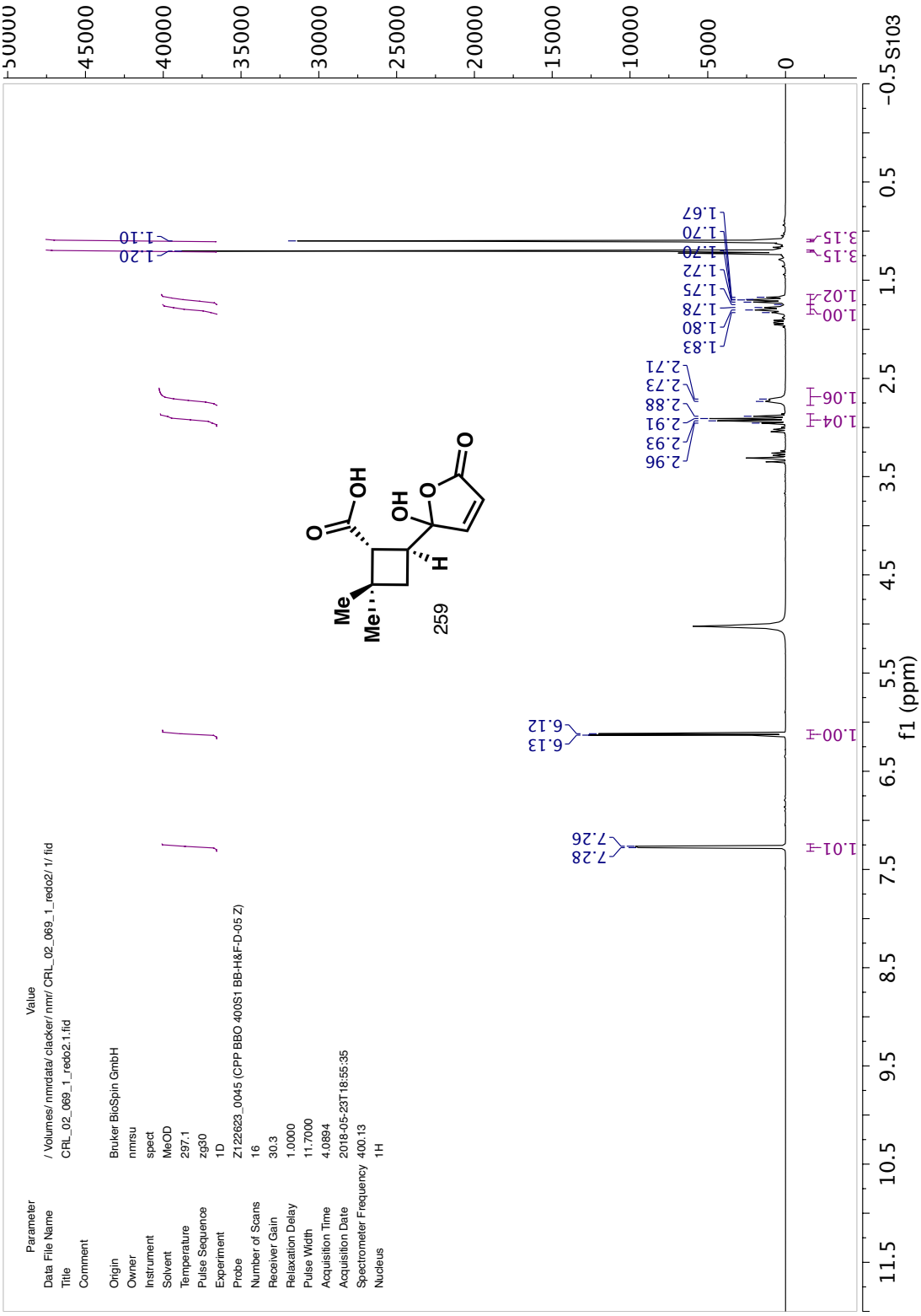
Parameter Value
Data File Name / Volumes/ nmrdata/ clacker/ nmr/ CRL_02_069_1_redo2/ 1/ fid
Title CRL_02_069_1_redo2.1.fid
Comment
Origin Bruker BioSpin GmbH
Owner nmrsu
Instrument spect
Solvent MeOD
Temperature 297.1
Pulse Sequence zg30
Experiment 1D
Probe Z122623_0045 (CPP BBO 400S1 BB-H&F-D-05 Z)
Number of Scans 16
Receiver Gain 30.3
Relaxation Delay 1.0000
Pulse Width 11.7000
Acquisition Time 4.0894
Acquisition Date 2018-05-23T18:55:35
Spectrometer Frequency 400.13
Nucleus 1H
259
f1 (ppm)
S103

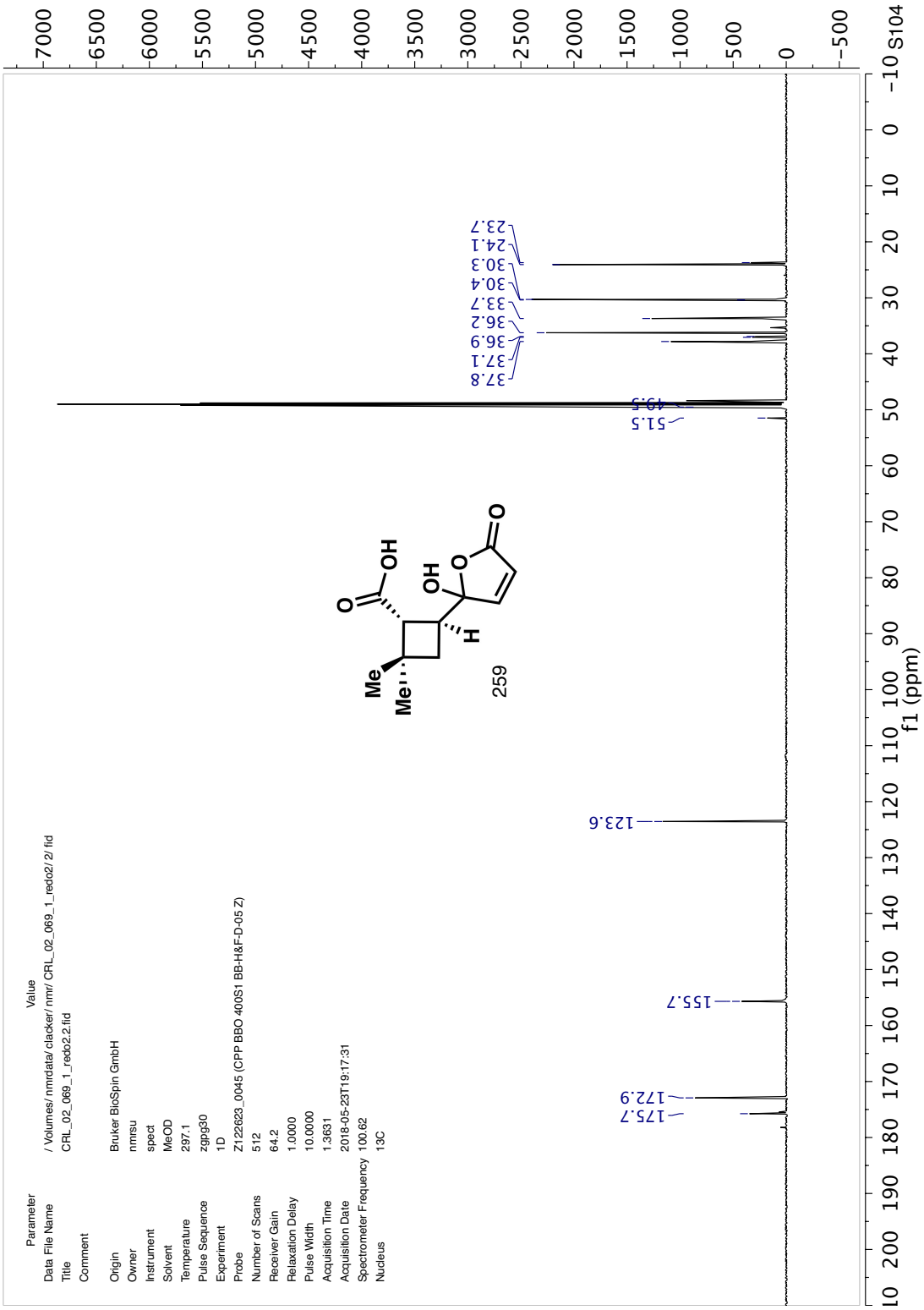
Parameter Value
Data File Name / Volumes/ nmrdata/ clacker/ nmr/ CRL_02_069_1_redo2/ 2/ fid
Title CRL_02_069_1_redo2.2.fid
Comment
Origin Bruker BioSpin GmbH
Owner nmrsu
Instrument spect
Solvent MeOD
Temperature 297.1
Pulse Sequence zgpg30
Experiment 1D
Probe Z122623_0045 (CPP BBO 400S1 BB-H&F-D-05 Z)
Number of Scans 512
Receiver Gain 64.2
Relaxation Delay 1.0000
Pulse Width 10.0000
Acquisition Time 1.3631
Acquisition Date 2018-05-23T19:17:31
Spectrometer Frequency 100.62
Nucleus 13C
259
175.7
172.9
155.7
123.6
51.5
49.5
37.8
37.1
36.9
36.2
33.7
30.4
30.3
24.1
23.7
f1 (ppm)
S104

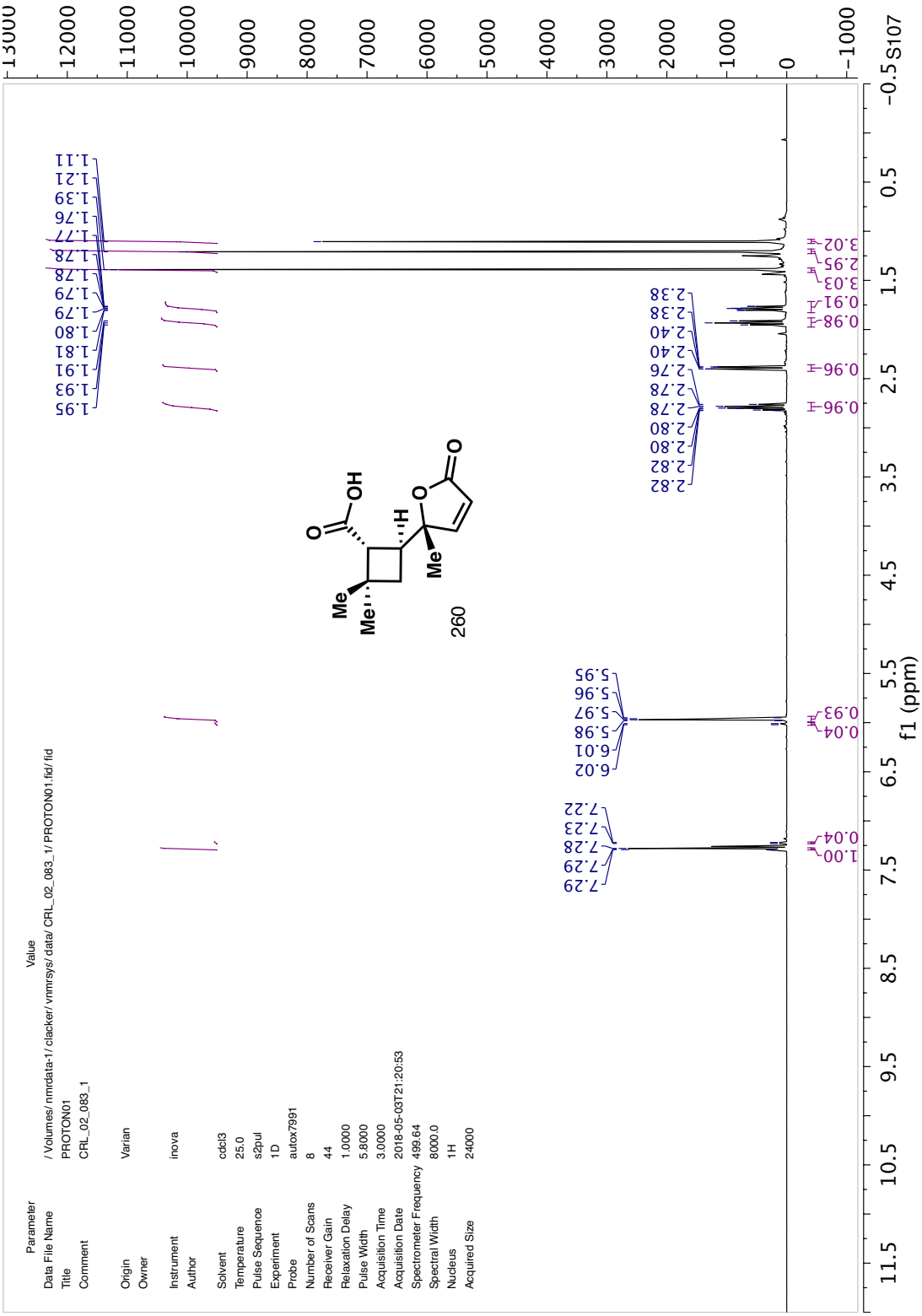
Parameter Value
Data File Name / Volumes/ nmrdata-1/ clacker/ vnmrsys/ data/ CRL_02_083_1/ PROTON01.fid/ fid
Title PROTON01
Comment CRL_02_083_1
Origin Varian
Owner
Instrument inova
Author
Solvent cdcl3
Temperature 25.0
Pulse Sequence s2pul
Experiment 1D
Probe autox7991
Number of Scans 8
Receiver Gain 44
Relaxation Delay 1.0000
Pulse Width 5.8000
Acquisition Time 3.0000
Acquisition Date 2018-05-03T21:20:53
Spectrometer Frequency 499.64
Spectral Width 8000.0
Nucleus 1H
Acquired Size 24000
260
f1 (ppm)
S107

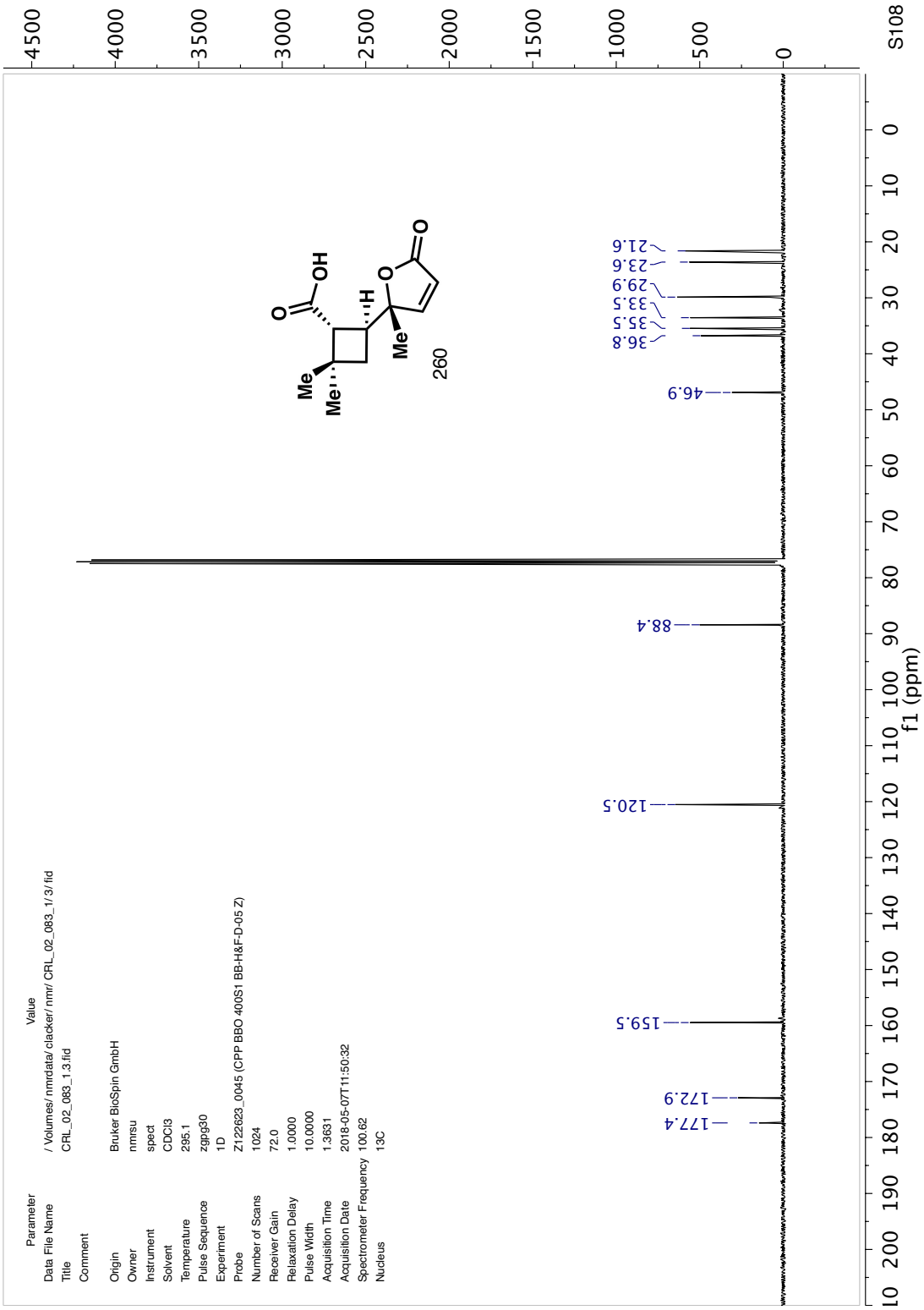
Parameter Value
Data File Name / Volumes/ nmrdata/ clacker/ nmr/ CRL_02_083_1/3/ fid
Title CRL_02_083_1.3.fid
Comment
Origin Bruker BioSpin GmbH
Owner nmrsu
Instrument spect
Solvent CDCl3
Temperature 295.1
Pulse Sequence zgpg30
Experiment 1D
Probe Z122623_0045 (CPP BBO 400S1 BB-H&F-D-05 Z)
Number of Scans 1024
Receiver Gain 72.0
Relaxation Delay 1.0000
Pulse Width 10.0000
Acquisition Time 1.3631
Acquisition Date 2018-05-07T11:50:32
Spectrometer Frequency 100.62
Nucleus 13C
177.4
172.9
159.5
120.5
88.4
46.9
36.8
35.5
33.5
29.9
23.6
21.6
Me
Me
H
O
OH
O
O
Me
260
f1 (ppm)
S108

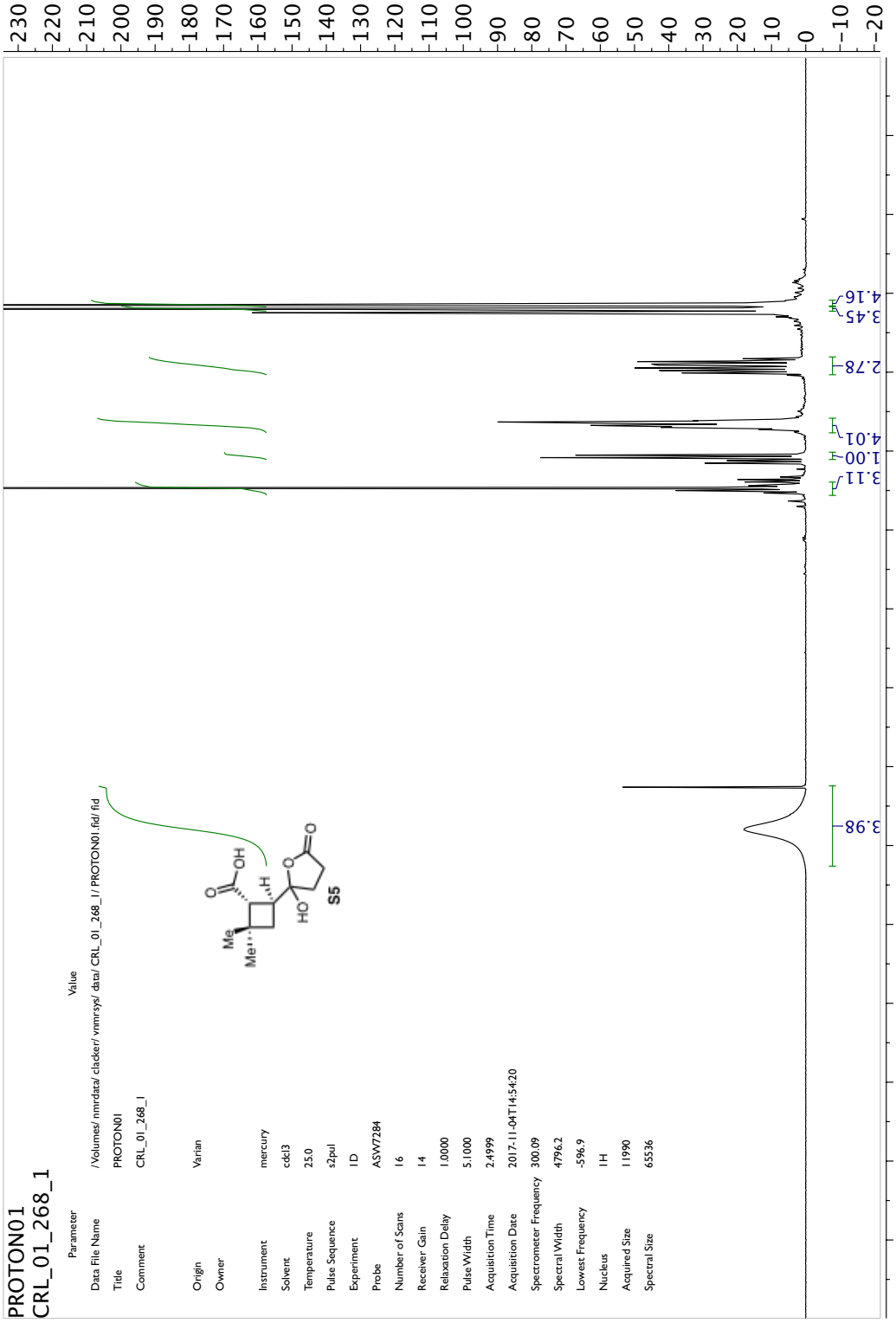
PROTON01
CRL_01_268_1
Parameter Value
Data File Name /Volumes/ nmrdata/ clacker/ vnmrsys/ data/ CRL_01_268_1/ PROTON01.fid/ fid
Title PROTON01
Comment CRL_01_268_1
Origin Varian
Owner
Instrument mercury
Solvent cdcl3
Temperature 25.0
Pulse Sequence s2pul
Experiment 1D
Probe ASW7284
Number of Scans 16
Receiver Gain 14
Relaxation Delay 1.0000
Pulse Width 5.1000
Acquisition Time 2.4999
Acquisition Date 2017-11-04T14:54:20
Spectrometer Frequency 300.09
Spectral Width 4796.2
Lowest Frequency -596.9
Nucleus 1H
Acquired Size 11990
Spectral Size 65536
S5
3.98
3.11
1.00
4.01
2.78
3.45
4.16
f1 (ppm)

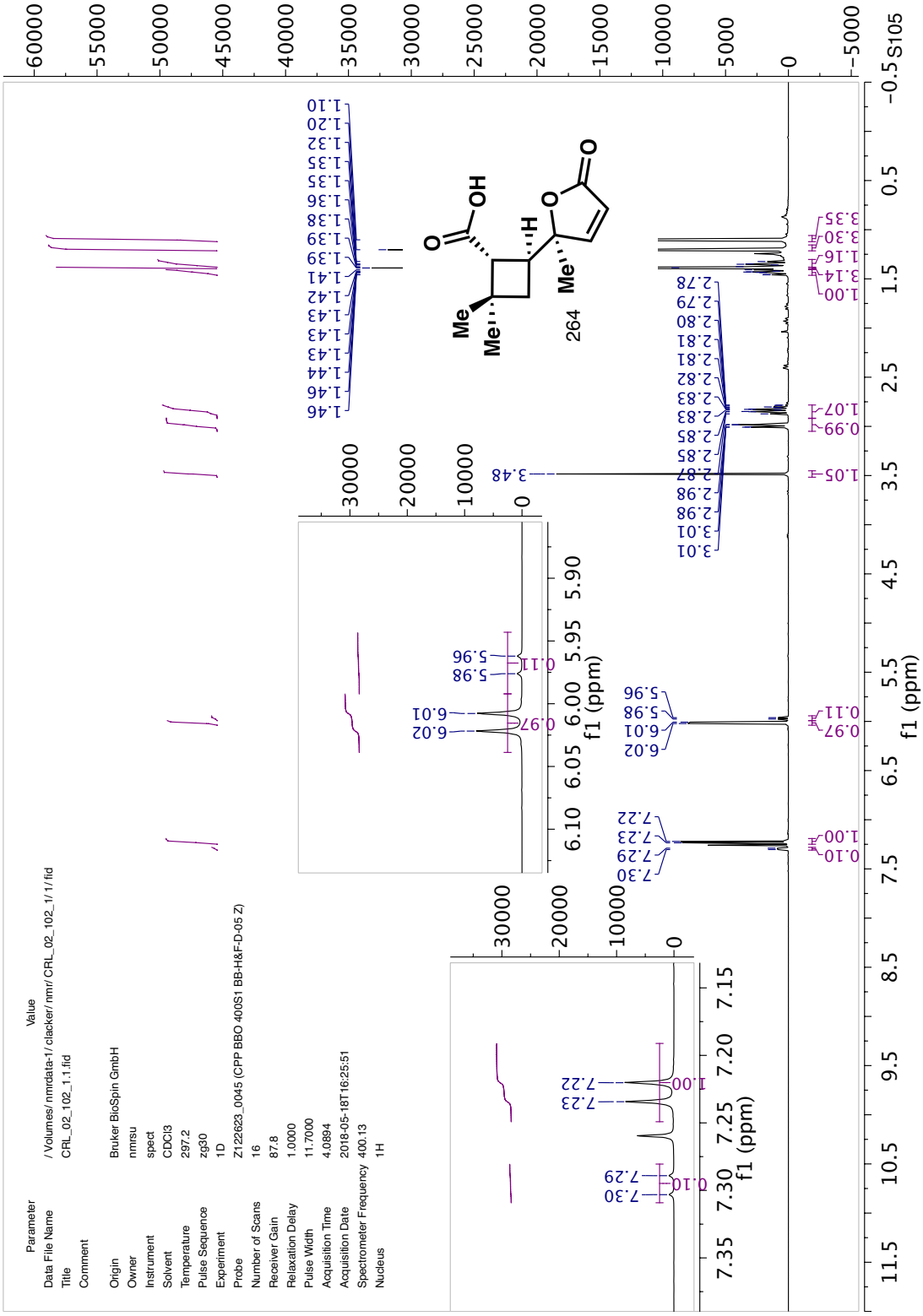
Parameter Value
Data File Name / Volumes/ nmrdata-1/ clacker/ nmr/ CRL_02_102_1/ 1/ fid
Title CRL_02_102_1.1.fid
Comment
Origin Bruker BioSpin GmbH
Owner nmrsu
Instrument spect
Solvent CDCl3
Temperature 297.2
Pulse Sequence zg30
Experiment 1D
Probe Z122623_0045 (CPP BBO 400S1 BB-H&F-D-05 Z)
Number of Scans 16
Receiver Gain 87.8
Relaxation Delay 1.0000
Pulse Width 11.7000
Acquisition Time 4.0894
Acquisition Date 2018-05-18T16:25:51
Spectrometer Frequency 400.13
Nucleus 1H
Me
Me
H
O
OH
O
O
264
f1 (ppm)
S105

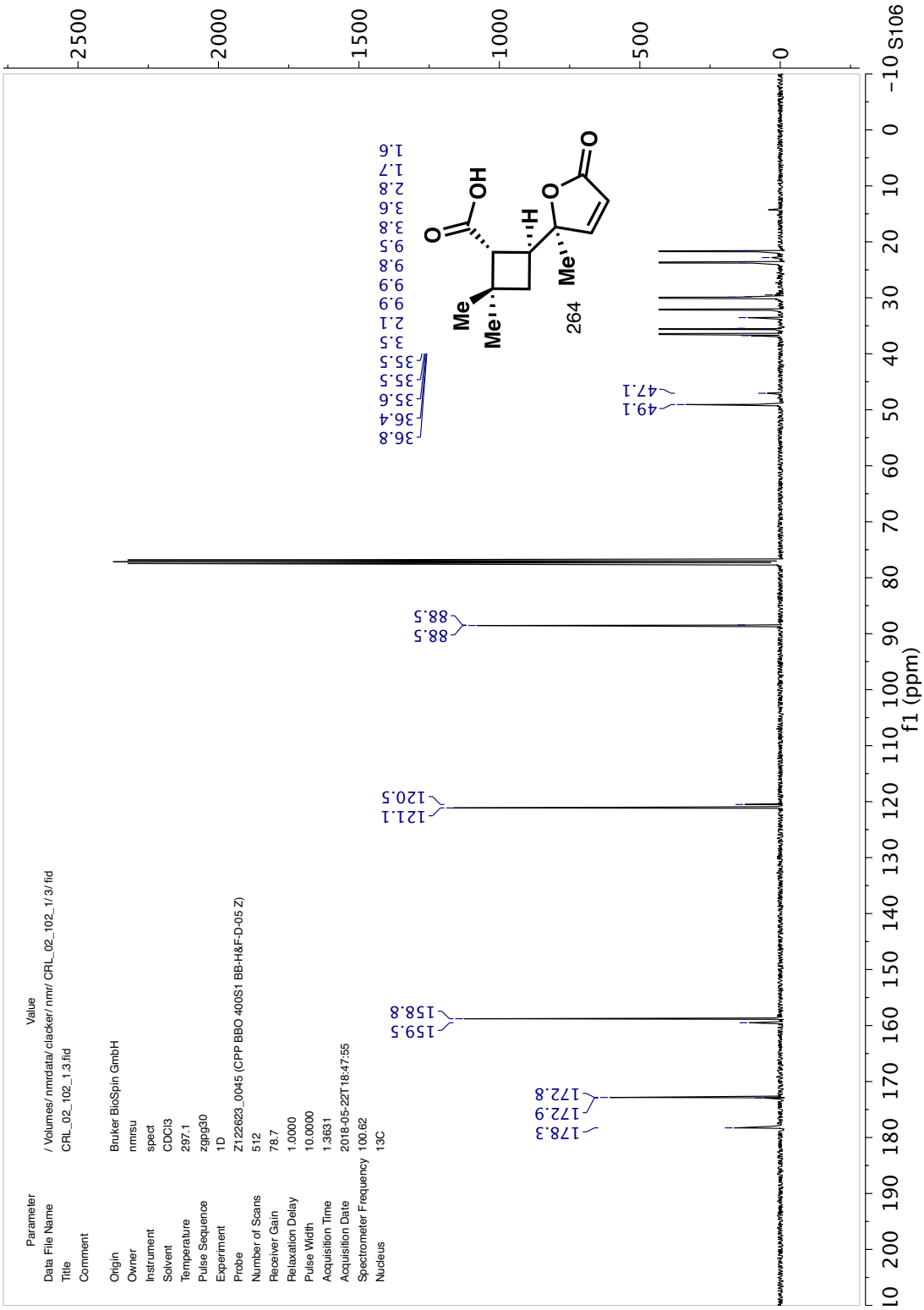
Parameter Value
Data File Name / Volumes/ nmrdata/ clacker/ nmr/ CRL_02_102_1/3/ fid
Title CRL_02_102_1.3.fid
Comment
Origin Bruker BioSpin GmbH
Owner nmrsu
Instrument spect
Solvent CDCl3
Temperature 297.1
Pulse Sequence zgpg30
Experiment 1D
Probe Z122623_0045 (CPP BBO 400S1 BB-H&F-D-05 Z)
Number of Scans 512
Receiver Gain 78.7
Relaxation Delay 1.0000
Pulse Width 10.0000
Acquisition Time 1.3631
Acquisition Date 2018-05-22T18:47:55
Spectrometer Frequency 100.62
Nucleus 13C
178.3
172.9
172.8
159.5
158.8
121.1
120.5
88.5
88.5
49.1
47.1
36.8
36.4
35.6
35.5
35.5
3.5
2.1
9.9
9.9
9.8
9.5
3.8
3.6
2.8
1.7
1.6
Me
Me
Me
H
O
OH
O
O
264
f1 (ppm)

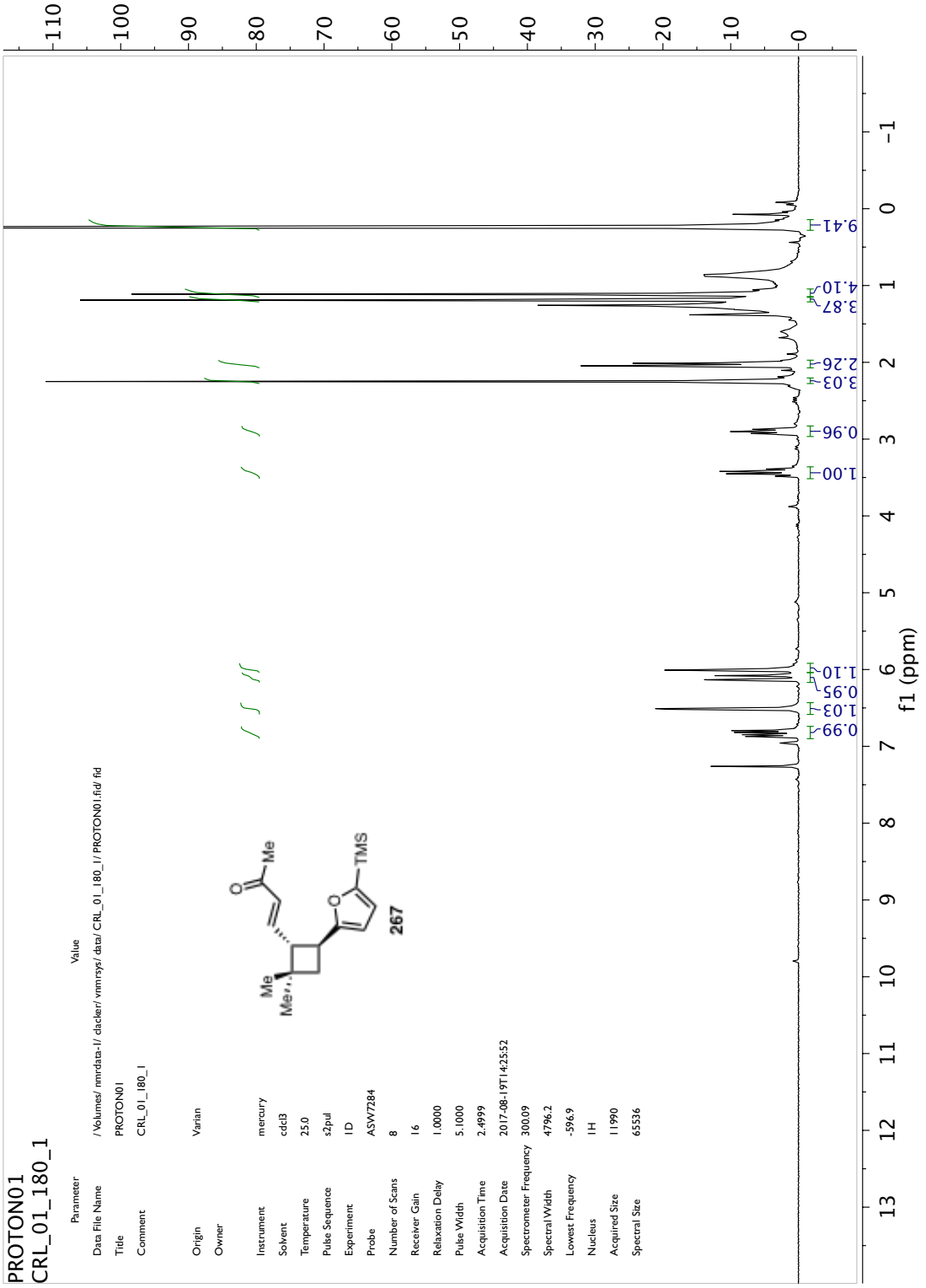
PROTON01
CRL_01_180_1
Parameter
Value
Data File Name /Volumes/ nmrdata-1/ dacker/ vnmrsys/ data/ CRL_01_180_1/ PROTON01.fid/ fid
Title PROTON01
Comment CRL_01_180_1
Origin Varian
Owner
Instrument mercury
Solvent cdcl3
Temperature 25.0
Pulse Sequence s2pul
Experiment 1D
Probe ASW7284
Number of Scans 8
Receiver Gain 16
Relaxation Delay 1.0000
Pulse Width 5.1000
Acquisition Time 2.4999
Acquisition Date 2017-08-19T14:25:52
Spectrometer Frequency 300.09
Spectral Width 4796.2
Lowest Frequency -596.9
Nucleus 1H
Acquired Size 11990
Spectral Size 65536
Me
Me
Me
O
O
TMS
267
9.41
4.10
3.87
3.03
2.26
0.96
1.00
1.10
0.95
1.03
0.99
f1 (ppm)

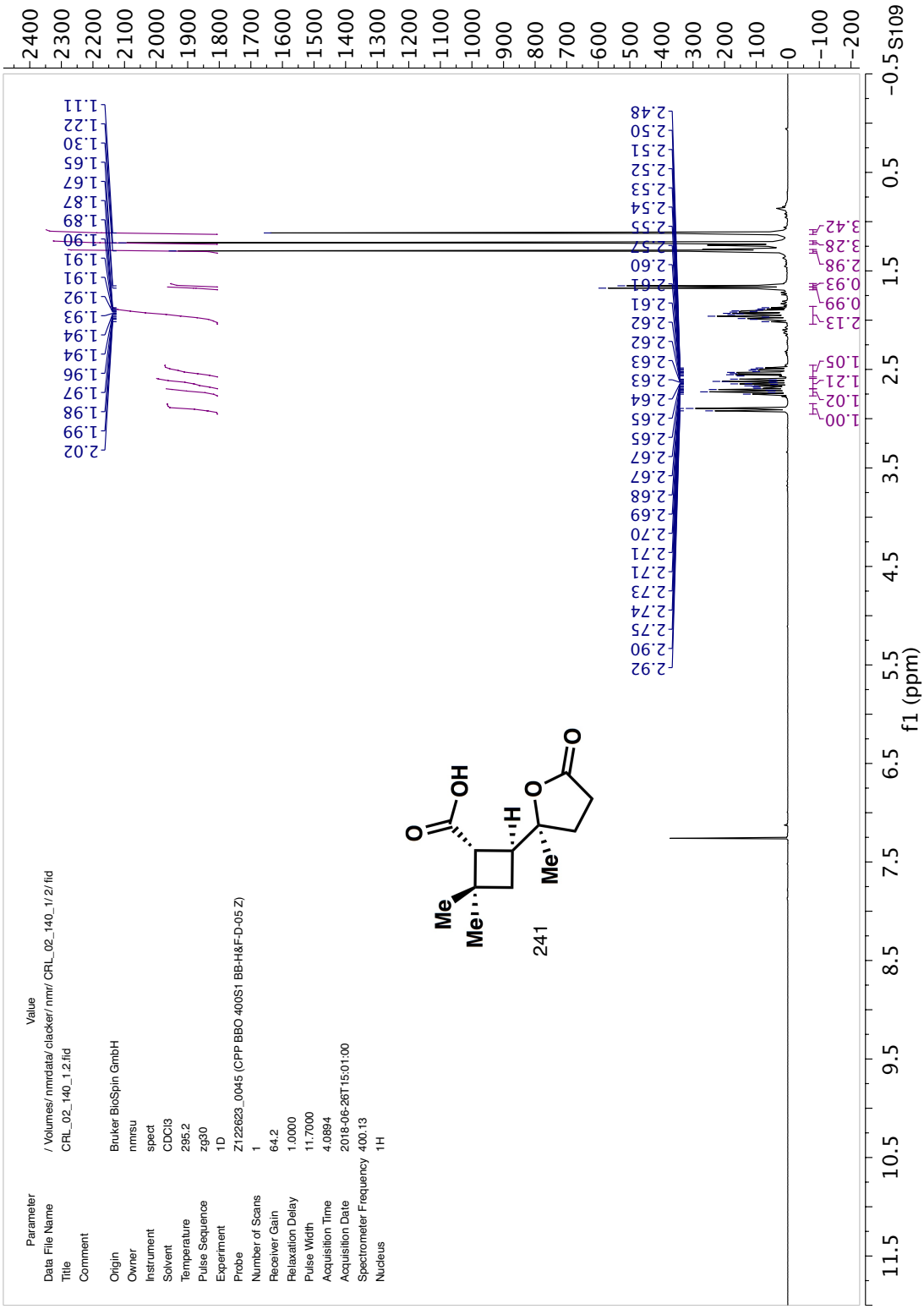
Parameter Value
Data File Name / Volumes/ nmrdata/ clacker/ nmr/ CRL_02_140_1/2/ fid
Title CRL_02_140_1.2.fid
Comment
Origin Bruker BioSpin GmbH
Owner nmrsu
Instrument spect
Solvent CDCl3
Temperature 295.2
Pulse Sequence zg30
Experiment 1D
Probe Z122623_0045 (CPP BBO 400S1 BB-H&F-D-05 Z)
Number of Scans 1
Receiver Gain 64.2
Relaxation Delay 1.0000
Pulse Width 11.7000
Acquisition Time 4.0894
Acquisition Date 2018-06-26T15:01:00
Spectrometer Frequency 400.13
Nucleus 1H
241
f1 (ppm)

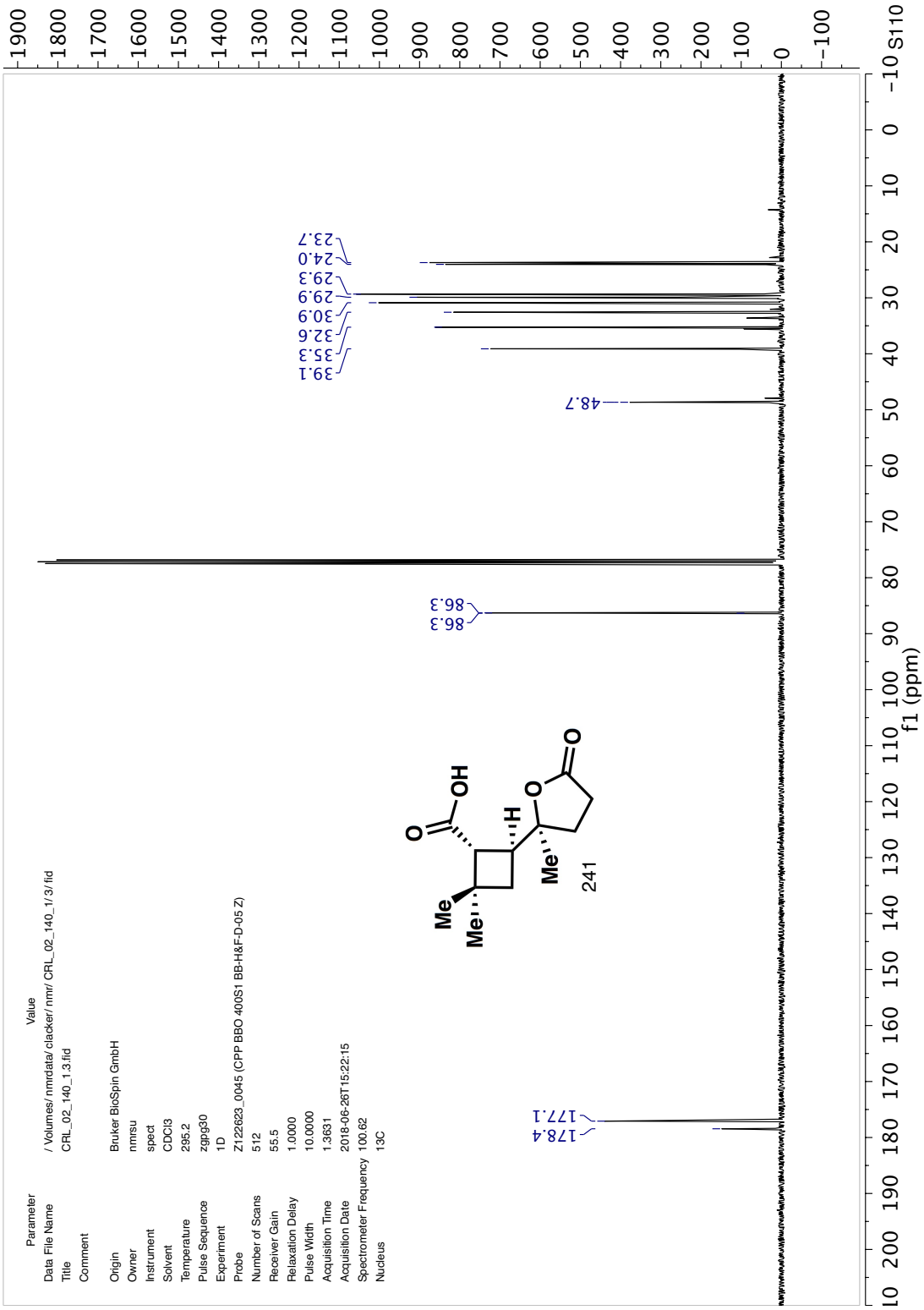
Parameter Value
Data File Name / Volumes/ nmrdata/ clacker/ nmr/ CRL_02_140_1/3/ fid
Title CRL_02_140_1.3.fid
Comment
Origin Bruker BioSpin GmbH
Owner nmrsu
Instrument spect
Solvent CDCl3
Temperature 295.2
Pulse Sequence zgpg30
Experiment 1D
Probe Z122623_0045 (CPP BBO 400S1 BB-H&F-D-05 Z)
Number of Scans 512
Receiver Gain 55.5
Relaxation Delay 1.0000
Pulse Width 10.0000
Acquisition Time 1.3631
Acquisition Date 2018-06-26T15:22:15
Spectrometer Frequency 100.62
Nucleus 13C
177.1
178.4
86.3
86.3
48.7
39.1
35.3
32.6
30.9
29.9
29.3
24.0
23.7
Me
Me
H
O
OH
O
Me
241
f1 (ppm)

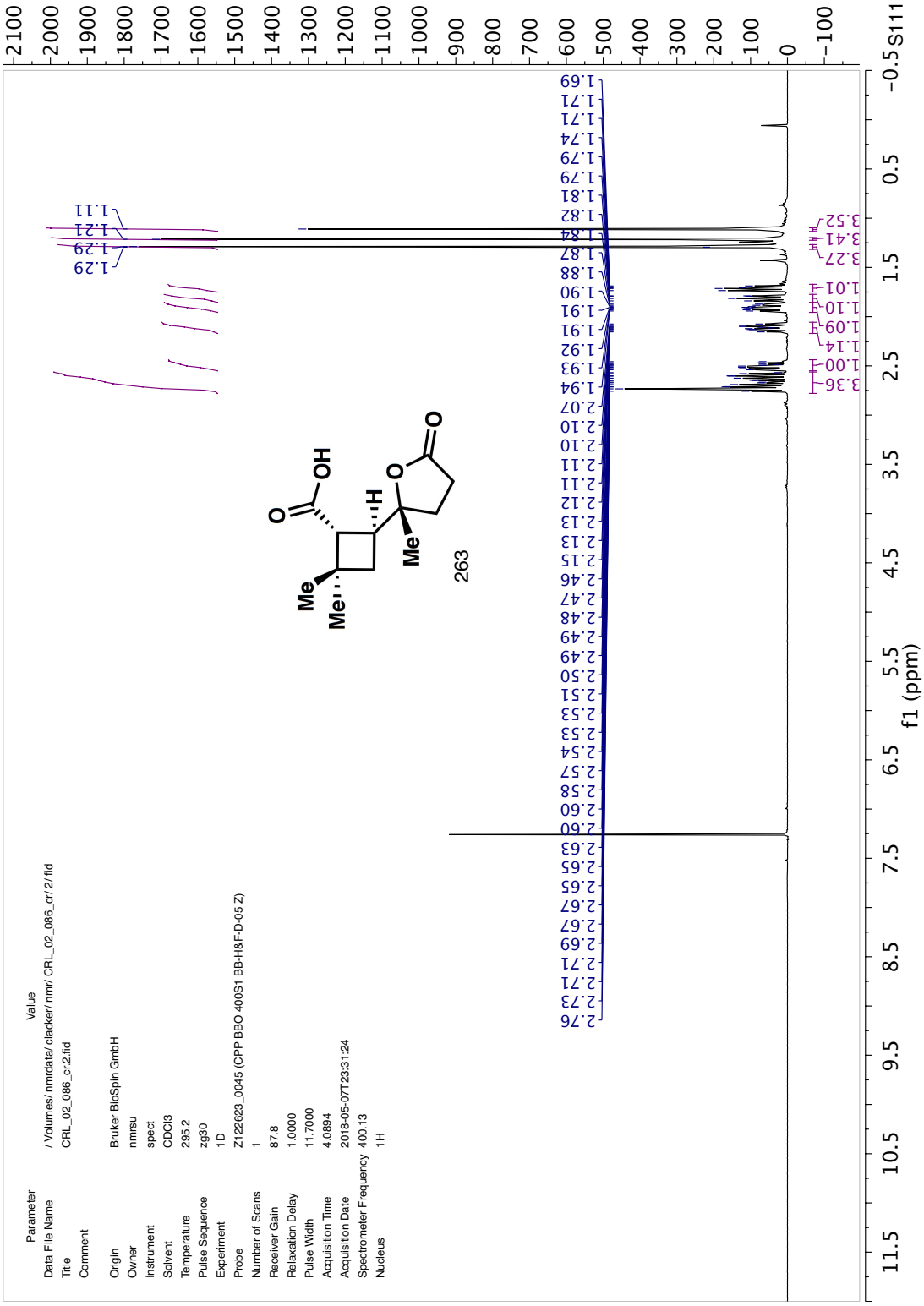
Parameter Value
Data File Name / Volumes/ nmrdata/ clacker/ nmr/ CRL_02_086_cr/ 2/ fid
Title CRL_02_086_cr.2.fid
Comment
Origin Bruker BioSpin GmbH
Owner nmrsu
Instrument spect
Solvent CDCl3
Temperature 295.2
Pulse Sequence zg30
Experiment 1D
Probe Z122623_0045 (CPP BBO 400S1 BB-H&F-D-05 Z)
Number of Scans 1
Receiver Gain 87.8
Relaxation Delay 1.0000
Pulse Width 11.7000
Acquisition Time 4.0894
Acquisition Date 2018-05-07T23:31:24
Spectrometer Frequency 400.13
Nucleus 1H
263
f1 (ppm)

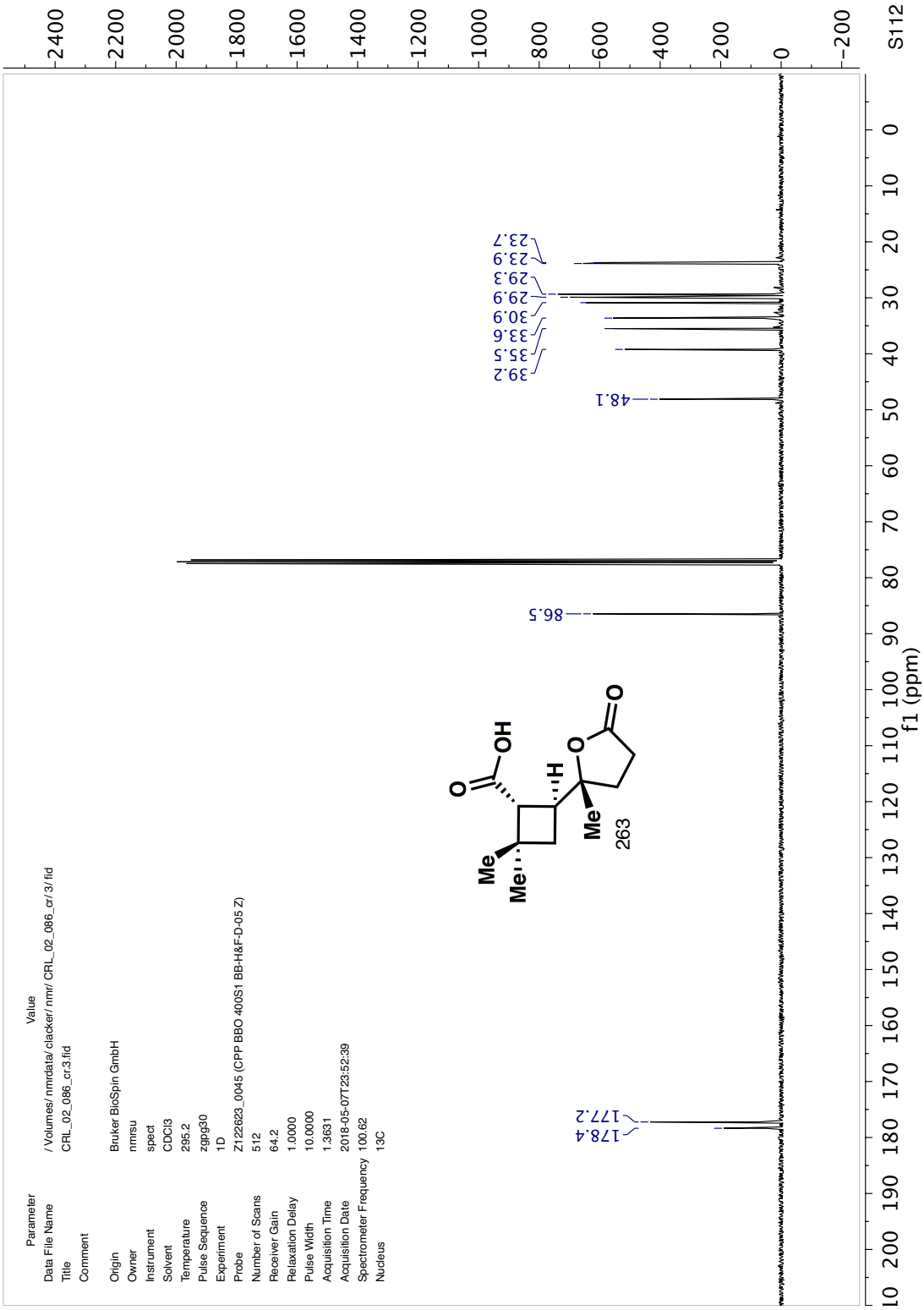
Parameter Value
Data File Name / Volumes/ nmrdata/ clacker/ nmr/ CRL_02_086_cr/ 3/ fid
Title CRL_02_086_cr.3.fid
Comment
Origin Bruker BioSpin GmbH
Owner nmrsu
Instrument spect
Solvent CDCl3
Temperature 295.2
Pulse Sequence zgpg30
Experiment 1D
Probe Z122623_0045 (CPP BBO 400S1 BB-H&F-D-05 Z)
Number of Scans 512
Receiver Gain 64.2
Relaxation Delay 1.0000
Pulse Width 10.0000
Acquisition Time 1.3631
Acquisition Date 2018-05-07T23:52:39
Spectrometer Frequency 100.62
Nucleus 13C
177.2
178.4
86.5
48.1
39.2
35.5
33.6
30.9
29.9
29.3
23.9
23.7
Me
Me
Me
H
O
O
OH
O
263
f1 (ppm)
S112

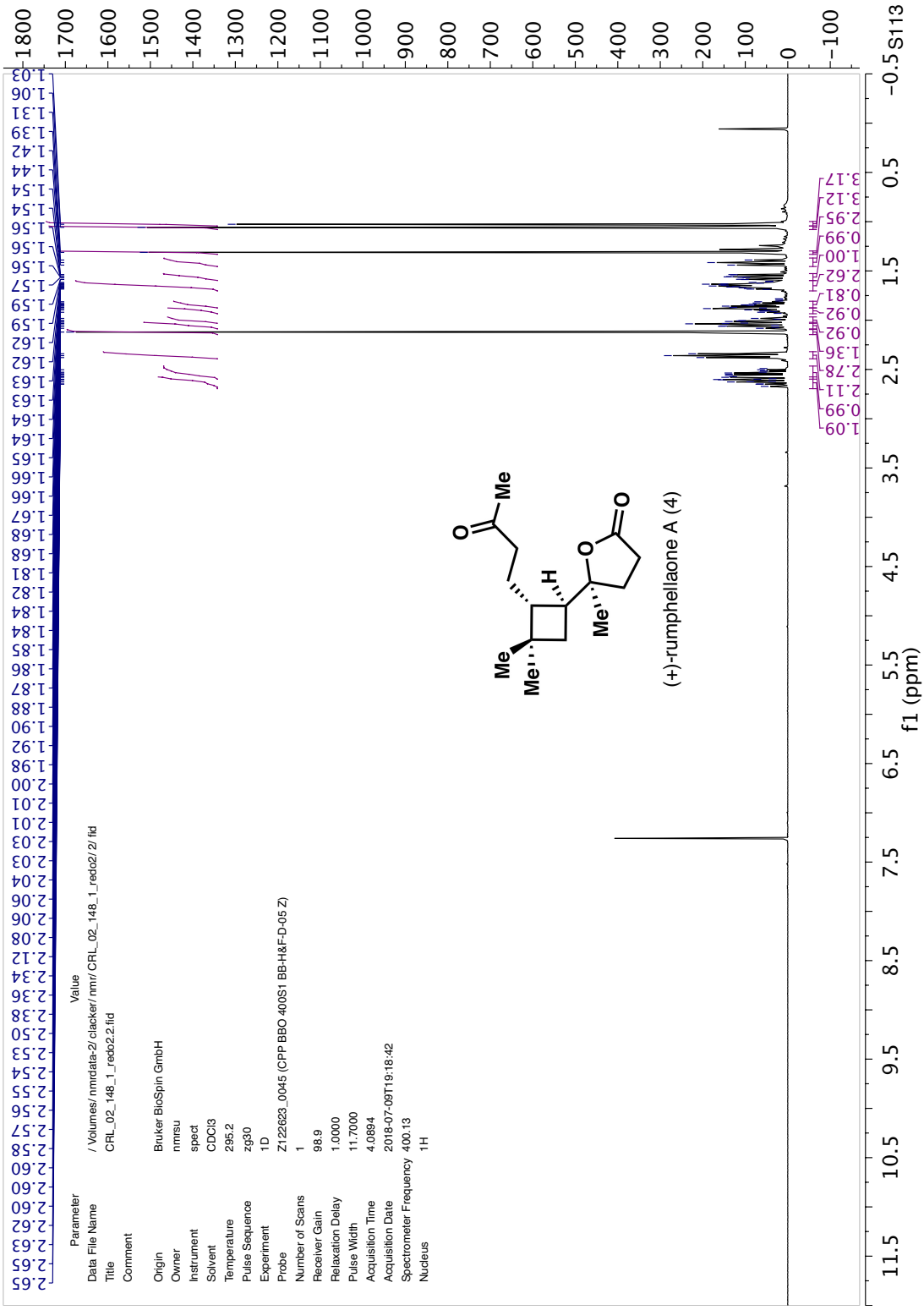
Parameter Value
Data File Name / Volumes/ nmrdata-2/ clacker/ nmr/ CRL_02_148_1_redo2/ 2/ fid
Title CRL_02_148_1_redo2.2.fid
Comment
Origin Bruker BioSpin GmbH
Owner nmrsu
Instrument spect
Solvent CDCl3
Temperature 295.2
Pulse Sequence zg30
Experiment 1D
Probe Z122623_0045 (CPP BBO 400S1 BB-H&F-D-05 Z)
Number of Scans 1
Receiver Gain 98.9
Relaxation Delay 1.0000
Pulse Width 11.7000
Acquisition Time 4.0894
Acquisition Date 2018-07-09T19:18:42
Spectrometer Frequency 400.13
Nucleus 1H
(+)-rumphellaone A (4)
f1 (ppm)
S113

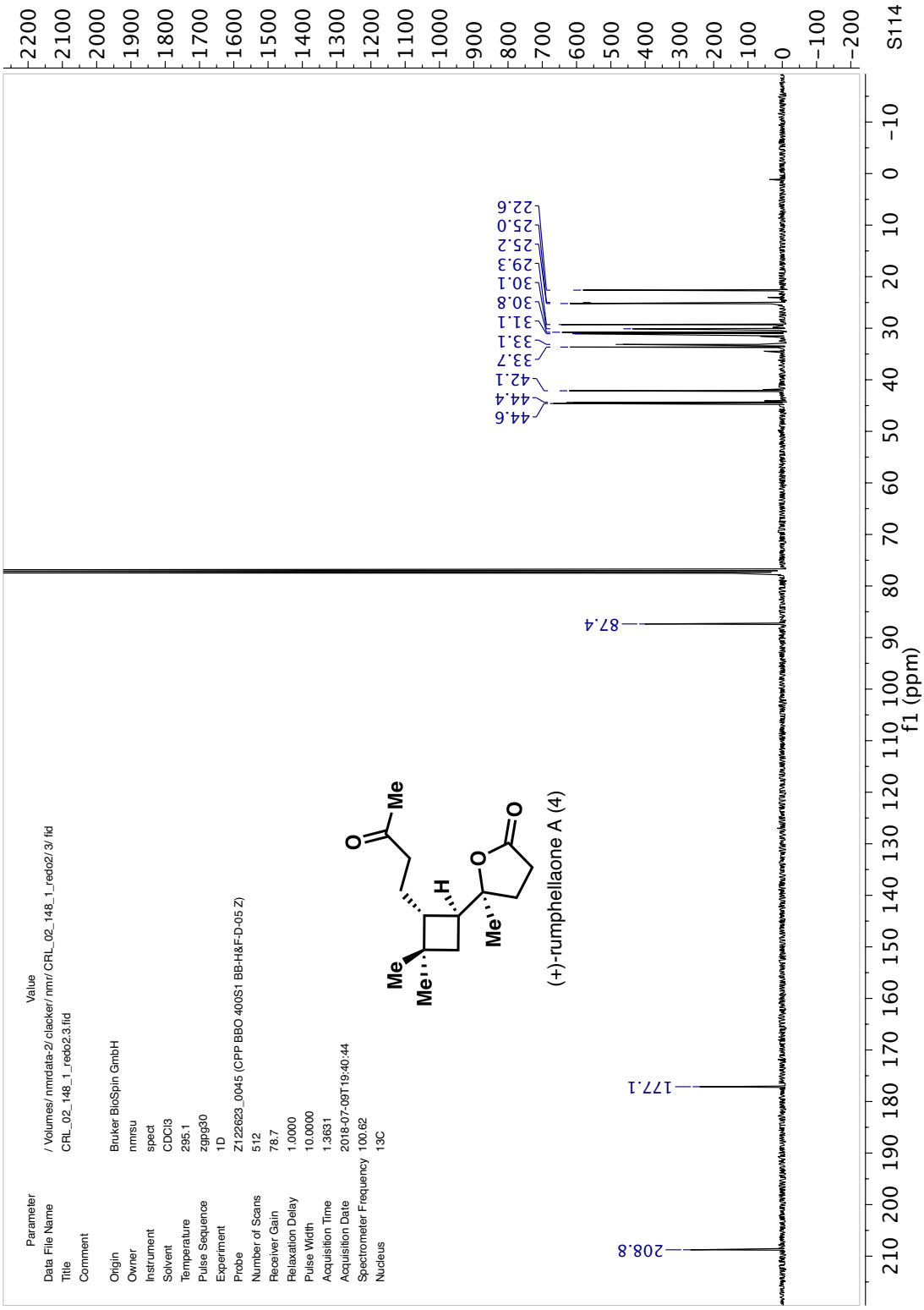
Parameter Value
Data File Name / Volumes/ nmrdata-2/ clacker/ nmr/ CRL_02_148_1_redo2/ 3/ fid
Title CRL_02_148_1_redo2.3.fid
Comment
Origin Bruker BioSpin GmbH
Owner nmrsu
Instrument spect
Solvent CDCl3
Temperature 295.1
Pulse Sequence zgpg30
Experiment 1D
Probe Z122623_0045 (CPP BBO 400S1 BB-H&F-D-05 Z)
Number of Scans 512
Receiver Gain 78.7
Relaxation Delay 1.0000
Pulse Width 10.0000
Acquisition Time 1.3631
Acquisition Date 2018-07-09T19:40:44
Spectrometer Frequency 100.62
Nucleus 13C
208.8
177.1
87.4
44.6
44.4
42.1
33.7
33.1
31.1
30.8
30.1
29.3
25.2
25.0
22.6
Me
Me
H
Me
O
O
O
(+)-rumphellaone A (4)
f1 (ppm)
S114

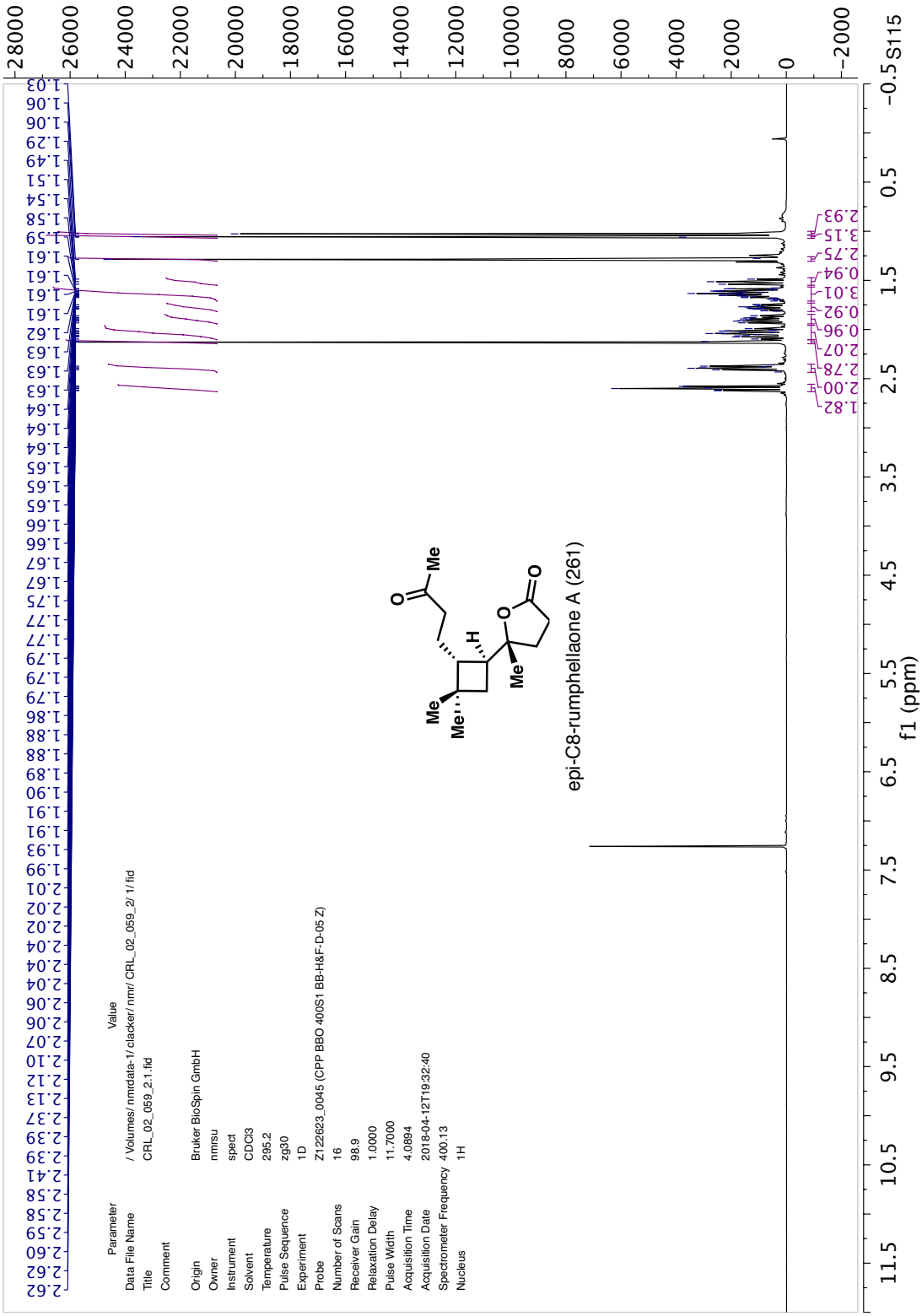
epi-C8-rumphellaone A (261)
f1 (ppm)
Parameter Value
Data File Name / Volumes/ nmrdata-1/ clacker/ nmr/ CRL_02_059_2/ 1/ fid
Title CRL_02_059_2.1.fid
Comment
Origin Bruker BioSpin GmbH
Owner nmrsu
Instrument spect
Solvent CDCl3
Temperature 295.2
Pulse Sequence zg30
Experiment 1D
Probe Z122623_0045 (CPP BBO 400S1 BB-H&F-D-05 Z)
Number of Scans 16
Receiver Gain 98.9
Relaxation Delay 1.0000
Pulse Width 11.7000
Acquisition Time 4.0894
Acquisition Date 2018-04-12T19:32:40
Spectrometer Frequency 400.13
Nucleus 1H

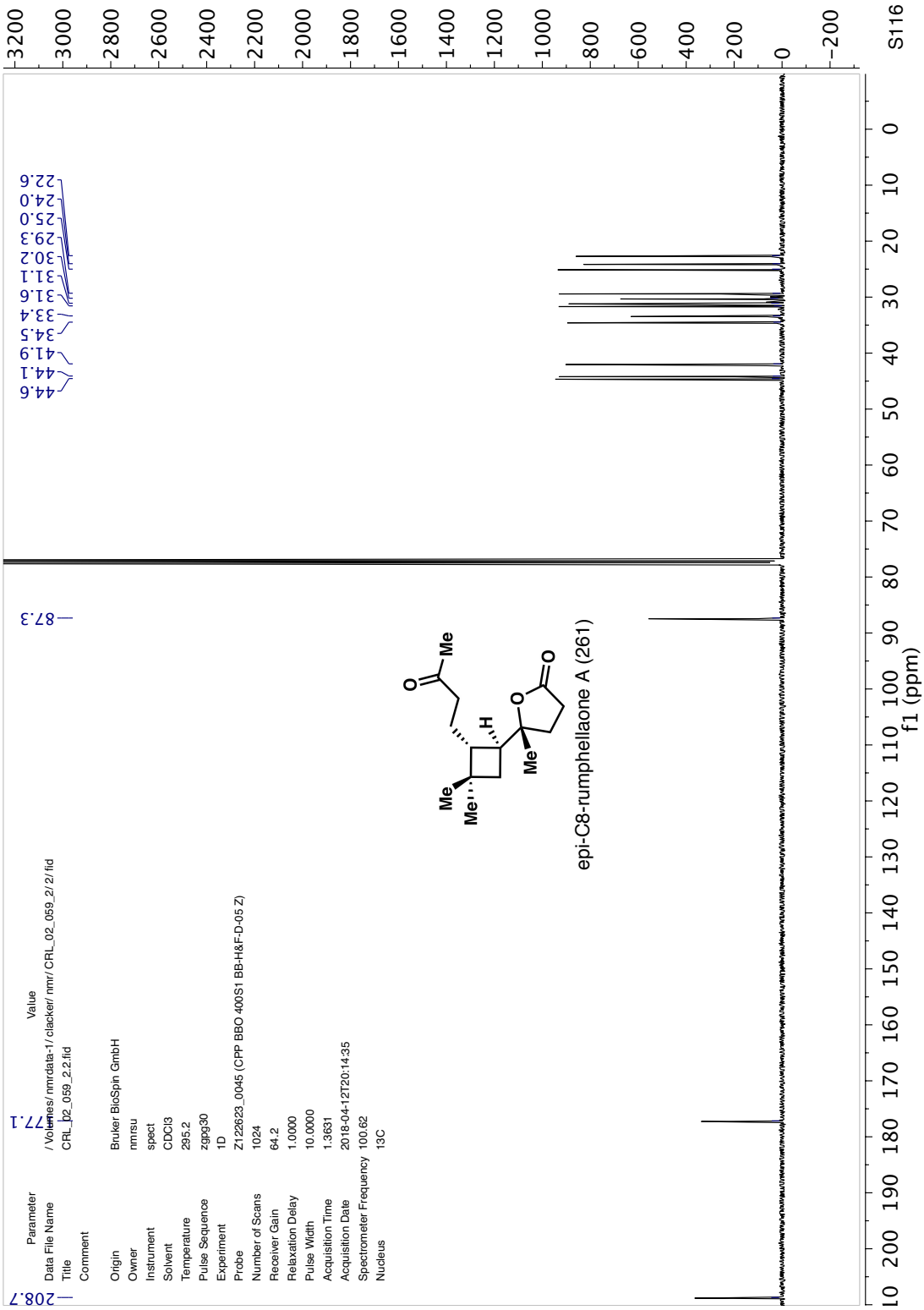
Parameter Value
Data File Name / Volumes/ nmrdata-1/ clacker/ nmr/ CRL_02_059_2/ 2/ fid
Title CRL_02_059_2.2.fid
Comment
Origin Bruker BioSpin GmbH
Owner nmrsu
Instrument spect
Solvent CDCl3
Temperature 295.2
Pulse Sequence zgpg30
Experiment 1D
Probe Z122623_0045 (CPP BBO 400S1 BB-H&F-D-05 Z)
Number of Scans 1024
Receiver Gain 64.2
Relaxation Delay 1.0000
Pulse Width 10.0000
Acquisition Time 1.3631
Acquisition Date 2018-04-12T20:14:35
Spectrometer Frequency 100.62
Nucleus 13C
208.7
87.3
77.1
44.6
44.1
41.9
34.5
33.4
31.6
31.1
30.2
29.3
25.0
24.0
22.6
Me
Me
H
O
O
O
Me
Me
epi-C8-rumphellaone A (261)
f1 (ppm)
S116

Chapter 3

Enantioselective Photoredox Catalysis for the Cross-Coupling of Azole-Containing Alkyl BF_3K Salts and Electron-Poor Aryl Bromides[1]

3.1 INTRODUCTION

Scheme 3.1 *Common disconnections for N-(hetero)benzylic azole synthesis*

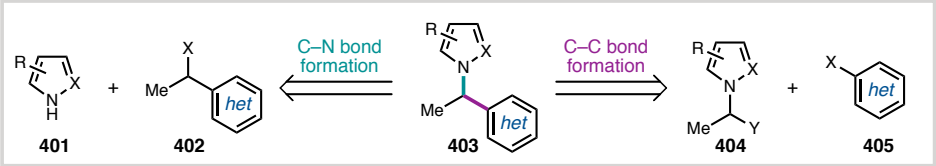

N-benzylic azoles (**403**) are an important class of compounds in the pharmaceutical industry. Azoles such as pyrroles, pyrazoles, and indoles are found in a wide variety of pharmaceuticals.[1] *N*-benzylic azoles can be synthesized several different ways. *N*-benzylic pyrroles specifically can be synthesized using modified Clauson-Kaas and Paal-Knorr protocols, though care must be taken to prevent racemization of the chiral amine starting materials.[2–10] To access a wider variety of *N*-(hetero)benzylic azoles, two common disconnections are typically used: C–N bond formation, and C–C bond formation (**Scheme 3.1**). A variety of methods have been developed using both disconnections, though few enantioselective strategies have been disclosed.

---

[1] This chapter was written concurrently with the communication manuscript to be submitted. The research discussed in this chapter was completed in collaboration with Travis J. DeLano, a graduate student in the Reisman lab, and Dr. Tiffany Piou and Kevin Belyk, researchers employed by Merck. Initial screening, HTE screens, and BF_3K substrates synthesis were performed by Kevin Belyk and Dr. Tiffany Piou, and 20 g of each enantiomer of 4-heptyl BiOX and certain aryl bromides were donated by Merck.

Scheme 3.2 *C–N coupling approaches towards N-(hetero)benzylic azoles*

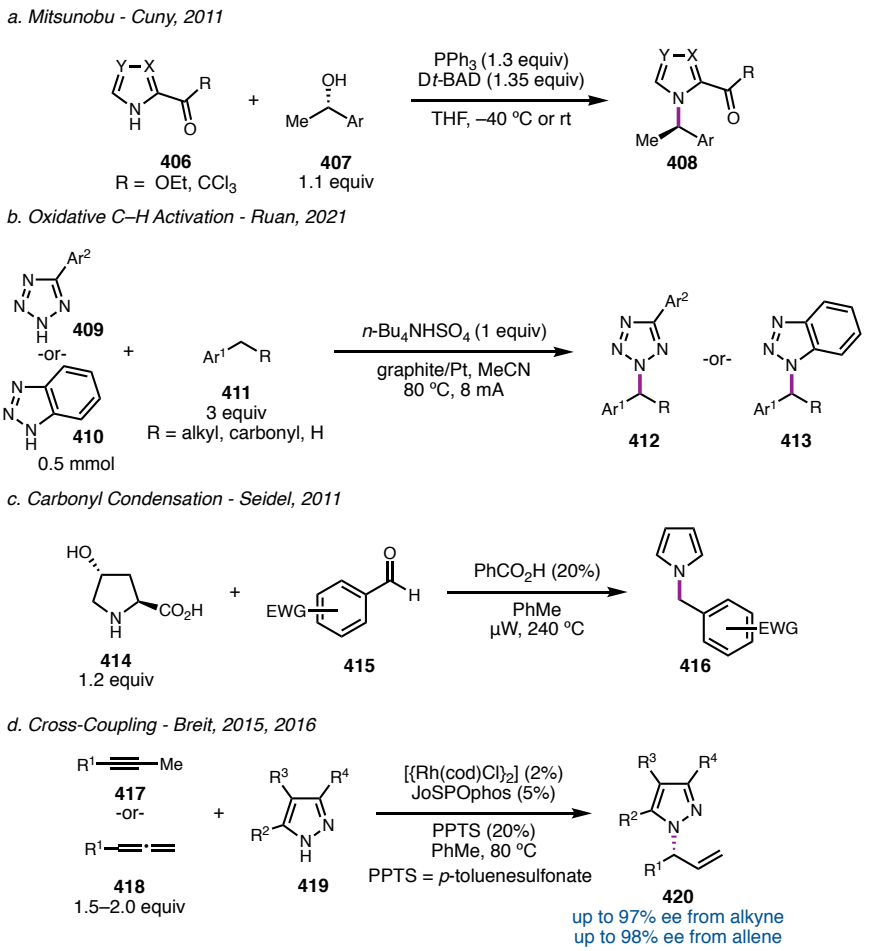

A variety of methods developed for the synthesis of *N*-(hetero)benzylic azoles utilize a C–N bond forming approach (**Scheme 3.2**). Simple Mitsunobu substitution of enantioenriched alcohols (**407**) allows for the synthesis of chiral pyrroles, pyrazoles, and indoles (**Scheme 3.2a**).[11,12] However, this approach is dependent on the use of chiral alcohol starting materials to access enantioenriched products. A variety of oxidative C–H activation approaches such as oxidative electrochemistry (**Scheme 3.2b**),[13] oxidative photoredox chemistry,[14] and other thermal strategies[15–18] have all proven effective at synthesizing *N*-(hetero)benzylic azoles containing two or more nitrogen atoms. As these methodologies are oxidative, they require a stoichiometric oxidant, which can limit the

substrate scope. Acid-catalyzed thermal condensation of pyrrolidine derivatives (**414**) and aldehydes (**415**) allows access to both primary[19,20] and secondary pyrroles (**Scheme 3.2c**).[21] Finally, Breit and coworkers have demonstrated that pyrazoles (**419**) can be cross-coupled with alkynes and allenes to form enantioenriched allylic azoles (**420**) (**Scheme 3.2d**).[22,23]

Scheme 3.3 *C–C coupling approaches towards N-(hetero)benzylic azoles*

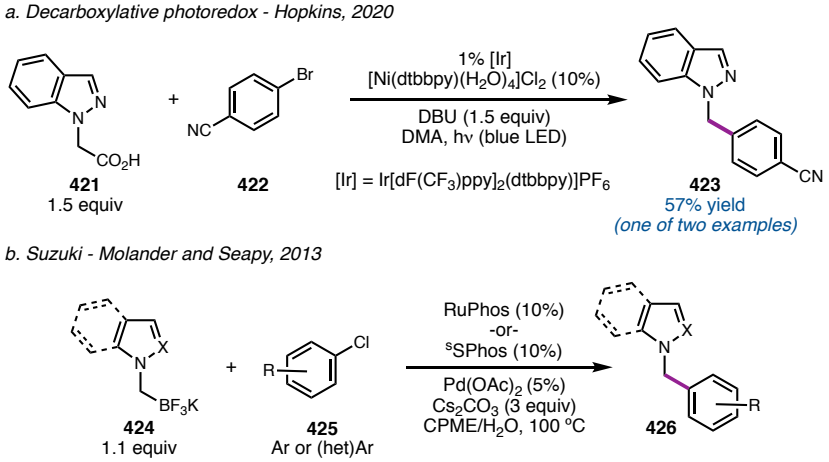

There have been comparatively few approaches towards the synthesis of *N*-(hetero)benzylic azoles that utilize a C–C bond formation approach (**Scheme 3.3**). In addition, the majority of C–C bond approaches towards *N*-(hetero)benzylic azoles are limited to primary azole nucleophiles. Hopkins and Rueping disclosed select examples of the nickel-catalyzed decarboxylative photoredox cross-couplings of α-azole carboxylic acids (**421**) with aryl bromides (**422**) and triflates, respectively (**Scheme 3.3a**).[24,25] Molander and Seapy developed palladium-catalyzed Suzuki conditions for the cross-coupling of potassium trifluoro(*N*-heteroaryl)borates (**424**) with aryl chlorides (**425**) (**Scheme 3.3b**).[26] In addition to pyrroles, pyrazoles, and indoles, similar conditions could be applied to phthalimide and isoindolen-1-one substrates.[27,28]

To the best of our knowledge, there is a single report of enantioselective C–C bond formation to form *N*-(hetero)benzylic azoles. In 2018, Bonifanzi and Davidson disclosed

Scheme 3.4 *Enantioselective cross-coupling of α-azole carboxylic acids and aryl bromides*

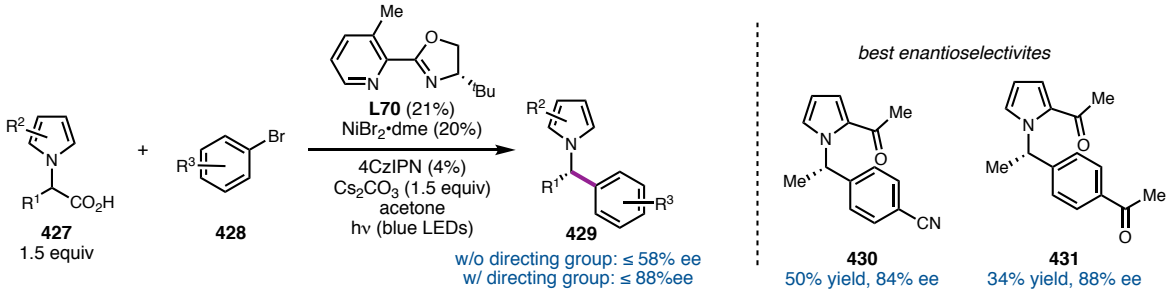

the decarboxylative enantioselective nickel-catalyzed photoredox cross-coupling of azole carboxylic acids (**427**) with aryl bromides (**428**) using pyridine oxazoline (PyOX) ligand **L70** and 4CzIPN as the photocatalyst, albeit in low to modest enantioselectivities (**Scheme 3.4**).[29] This is one of relatively few enantioselective photochemical cross-couplings published in the literature. Notably, in order to achieve greater than 58% ee, they required the incorporation of a directing group at the 2 position of the pyrrole. Methyl ketones (**430**, **431**) appeared to be the best directing group under their reaction conditions. In addition to poor enantioselectivities, they only disclose a single example of a heteroaryl bromide.

Scheme 3.5 *Initial conditions from Merck*

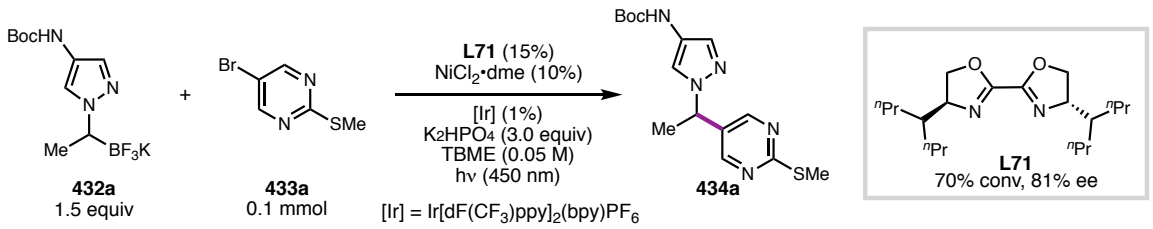

Scientists at Merck have been interested in the enantioselective cross-coupling of azole-containing nucleophiles with heteroaryl bromides to form *N*-heterobenzylic azoles using nickel photoredox catalysis. They developed conditions for cross-coupling pyrazole potassium trifluoroborate **432a** with aryl bromides to form *N*-heterobenzylic azoles such as **434a** using a ligand developed previously in our lab, **L71** (**Scheme 3.5**).[30] Excitingly, their initial results were already achieving yields and enantioselectivities surpassing

Bonifanzi and Davidson's approach for similar substrates. However, they struggled with reproducibility issues and achieving enantioselectivities greater than ~80%. Therefore, they invited us to join their efforts to further optimize the yield and ee of this reaction and address any reproducibility issues.

Scheme 3.6 *Proposed mechanism*

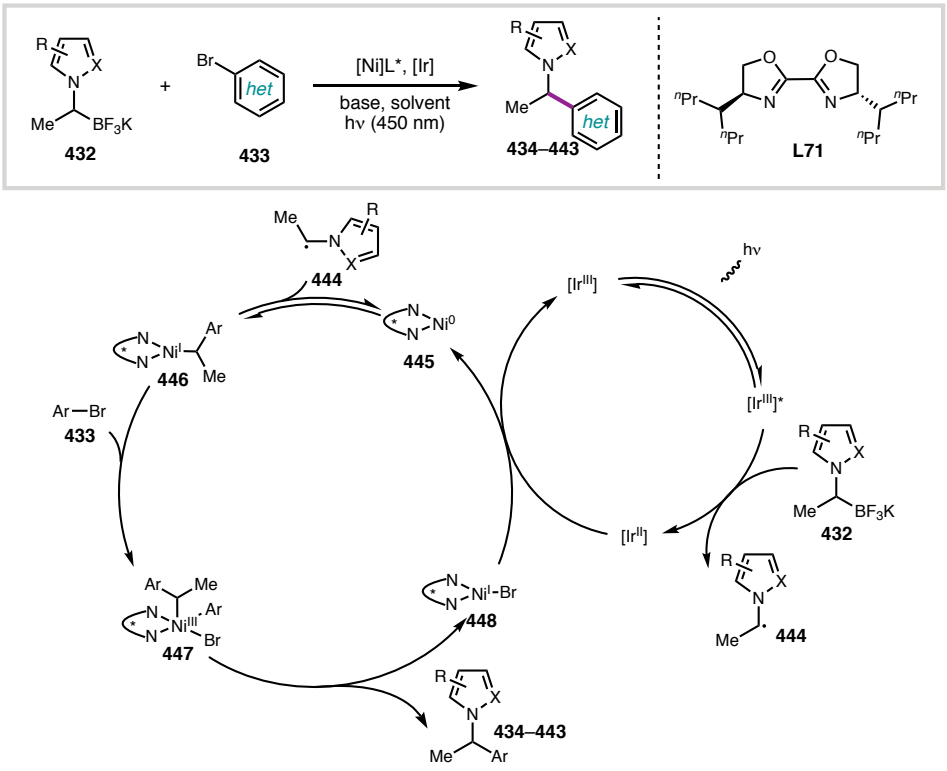

Based on previous investigations of photoredox cross-couplings of potassium trifluoroborate salts and aryl halides, a catalytic cycle can be proposed (**Scheme 3.6**).[31] First, following excitation of the photocatalyst, single-electron oxidation of the BF_3K salt (**432**) leads to oxidative cleavage and formation of stabilized radical **444**. This radical can then be trapped by the nickel catalyst to form alkyl[Ni^I] **445**. Oxidative addition of **433** forms [Ni^{III}] **447**. Reductive elimination affords the desired product (**434**–**443**) and [Ni^I]Br **448**. Reduction by the photocatalyst regenerates both the [Ni] catalyst and the

photocatalyst. Alternatively, oxidative addition of **433** to [Ni^0] could occur first, followed by radical capture of **435** by the resultant [Ni^{II}] intermediate.

3.2 OPTIMIZATION

3.2.1 Initial Conditions from Merck

Scheme 3.7 *HTE studies and ligand optimization*

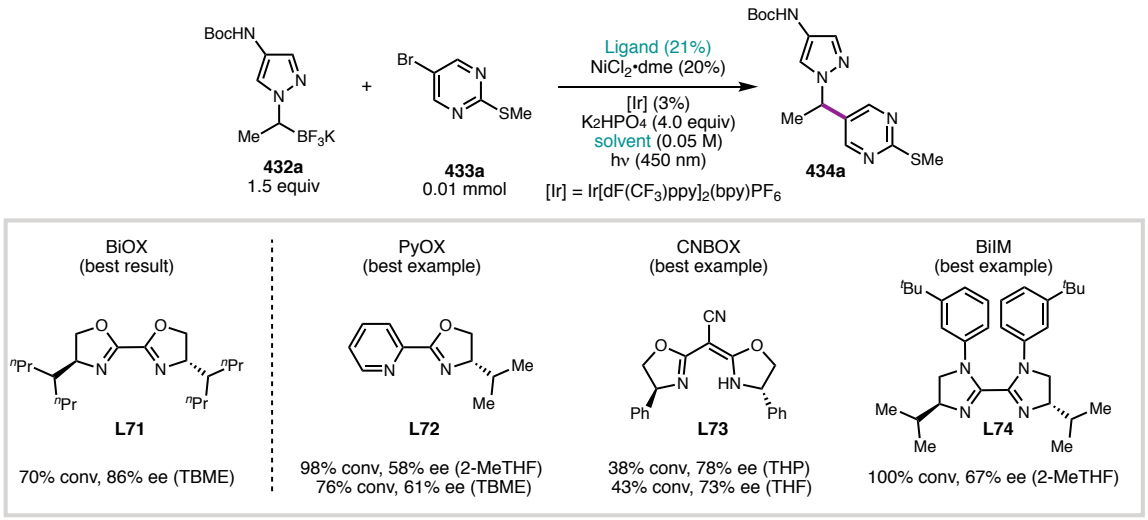

Merck approached us with initial conditions for the enantioselective cross-coupling of α-pyrazole potassium trifluoroborate salt **432a** with thiomethyl ether pyrimidine **433a** that they had developed after initial high throughput experimentation (HTE) screening (**Scheme 3.7**). At the time, they found that 4-heptyl bioxazoline (BiOX) (**L71**) afforded the desired product in the best yield and conversion on HTE scale using 20 mol % $NiCl_2$•dme as the precatalyst, 3% Ir[dF(CF_3)ppy]$_2$(bpy)PF_6 ([Ir]) as the photocatalyst, 21 mol % **L71**, and *t*-butyl methyl ether (TMBE) as the solvent. In general, PyOX ligands such as **L72** gave good conversions, but relatively low enantioselectivities. Cyano-bis(oxazoline) (CNBOX ligand) **L73** afforded the desired product in promising enantioselectivities, but in relatively low conversions. Biimidazole (BiIM) ligands such as **L74** generally gave good

conversions, but moderate enantioselectivities despite their structural similarities to BiOX ligands. Therefore, 4-heptyl BiOX was chosen for further investigation.

Scheme 3.8 *0.1 mmol scale initial conditions*

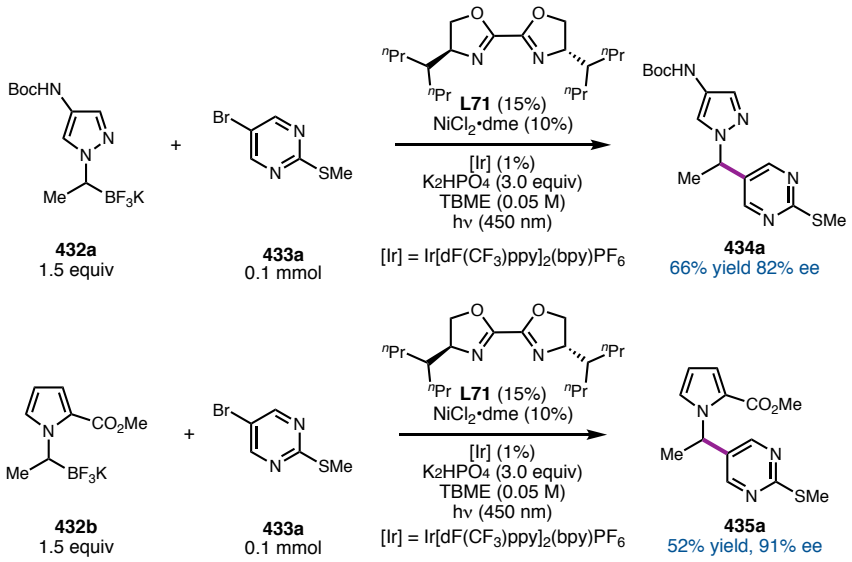

Gratifyingly, these results could be replicated on 0.1 mmol scale in a Penn PhD photoreactor on the benchtop using 10 mol % [Ni], 15 mol % **L2**, TMBE as the solvent, and 1 mol % [Ir], affording cross-coupled product **434a** in 66% yield, 82% ee (**Scheme 3.8**). Some initial issues with reproducibility on scale were addressed by changing the reaction setup to avoid adding reagents as slurries and using repurified **L71** stored in the glovebox (see Section 3.2.5). Pyrrole BF_3K (**435a**) was also successfully cross-coupled under these conditions, affording the desired product in 52% yield and 91% ee. It is thought that the ester at the 2 position can act as a better directing group than the pyrazole nitrogen, resulting in higher enantioselectivities.[29] Our goals at the outset of this project were to increase the yield and enantioselectivity of this reaction and explore the substrate scope of both cross-coupling partners.

3.2.2 Reaction Stall and Product Inhibition

Table 3.1 *Time-course studies*

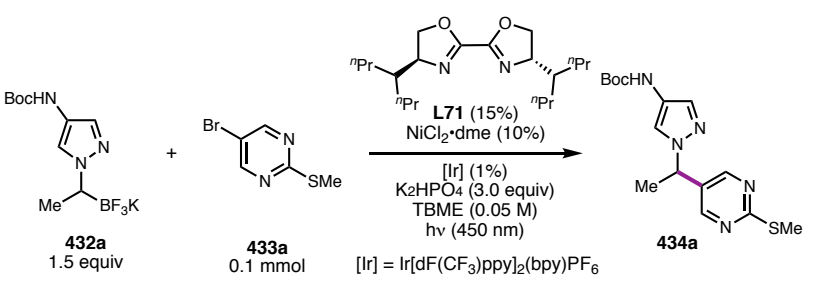

entry	time	% ArBr[a]	% pdt	% ee
1	1 h	42	**37**	**80**
2	4 h	32	**51**	**82**
3	8 h	23	**58**	**77**
4	12 h	19	**62**	**81**
5	24 h	17	**62**	**80**
6	48 h	21	**61**	**76**
7	48 h[b]	2	**59**	**80**

Note: entries 6–7 run on different days than 1–5, [a]%ArBr remaining, [b]second charge of [Ni], **L71**, [Ir] in 1.0 mL solvent

Despite the promising conversions on small scale, the reaction seemed to stall out at around 60% yield with 15-20% ArBr remaining. In order to investigate this, we performed a time course study. Five 0.1 mmol reactions were set up (the maximum capacity for the photoreactor) and were stopped and worked up at different intervals (**Table 3.1**, entries 1–5). Interestingly, the reaction appeared to be nearly complete after 8 hours (entry 3), with only a slight increase in yield at 12 hours (entry 4), and no change after 24 hours (entry 5). Even after allowing the reaction to run for 48 hours, there was no increase in yield (entry 6). Adding in fresh $NiCl_2$•**L71** complex and [Ir] only resulted in increased consumption of ArBr with no increase in product (entry 7). Therefore, it was hypothesized that as the reaction proceeded, formation of the product or other byproducts such as protodeborylation could be resulting in reaction inhibition.

Scheme 3.9 *Product inhibition studies*

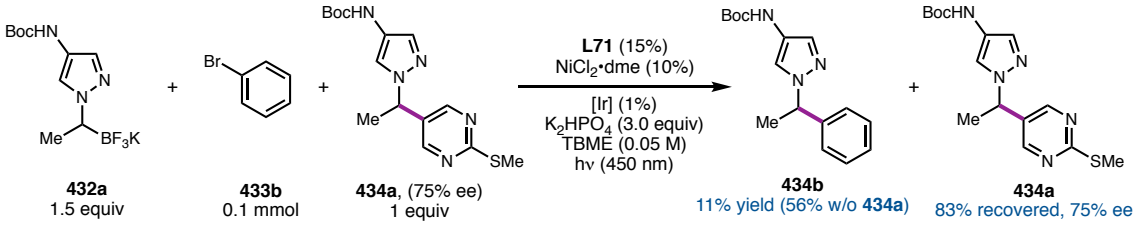

First, inhibition of the reaction by product was investigated directly. 1 equiv compound **434a** was added to the cross coupling of pyrazole **432a** with phenyl bromide (**433b**) (**Scheme 3.9**). Without any added product, the reaction proceeds to afford **434b** in 56% yield. However, upon addition of **434a**, the reaction only proceeds in 11% yield. This suggests that the product could be inhibiting the reaction. While product and protodeborylation formation could be tracked by NMR, it was difficult to monitor BF_3K consumption due to its insolubility in most deuterated solvents. In addition, **434a** was recovered with no erosion in ee, indicating that *in situ* racemization of the product was not occurring.

Figure 3.1 *Fluorescence quenching*

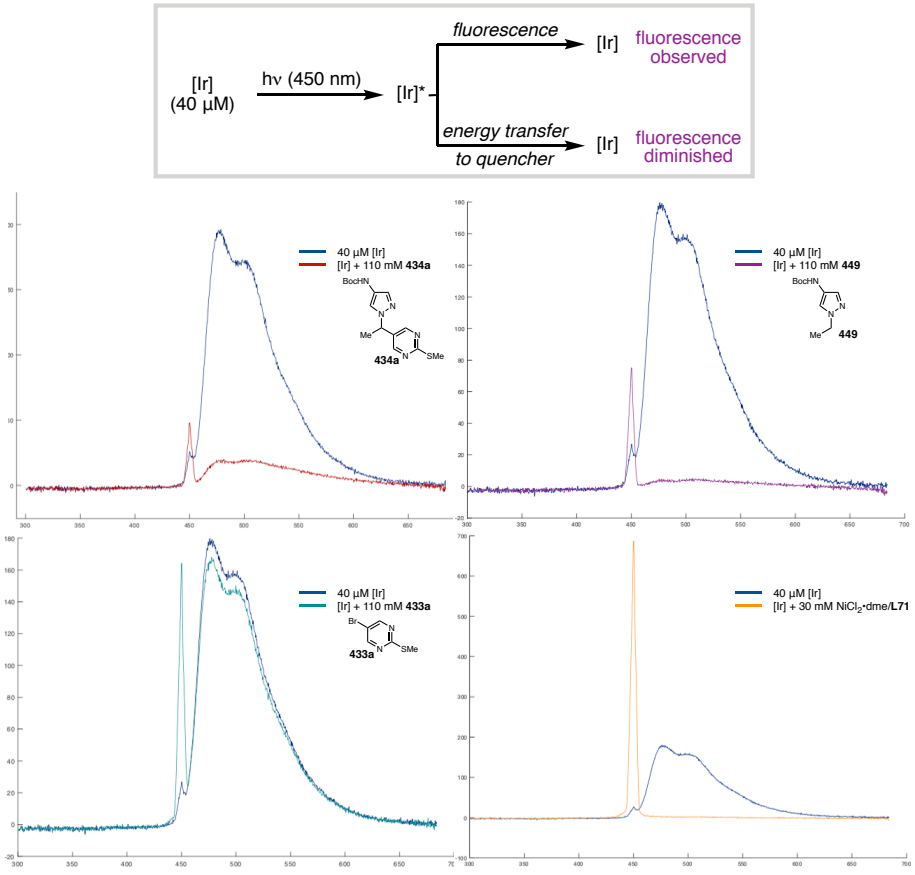

In order to probe this inhibition more directly, fluorescence studies were undertaken to determine if any of the reaction components could be quenching the photocatalyst. The fluorescence spectrum of the photocatalyst was observed and then compared to the fluorescence spectra of the photocatalyst in the presence of the cross-coupled product (**434a**), protodeborylation (**449**), ArBr (**433a**), or the [Ni]•**L71** complex (**Figure 3.1**). These studies were performed in 2-methyl tetrahydrofuran (2-MeTHF) to fully dissolve [Ir]. These initial results showed that the cross-coupled product **434a** and deborylated byproduct **440** were both capable of quenching the photocatalyst, while **433a** had little to no impact on the fluorescence of the photocatalyst. Interestingly, [Ni]•**L71** complex resulted in a new signal, suggesting it could be photoactive as well, though control studies without [Ir] indicate that the Ni catalyst complex is not a competent photocatalyst. The [Ni]•**L71** complex also appears to result in complete quenching of the photocatalyst. This could be indicative of some redox reactivity between these two complexes. These preliminary results suggest that as the reaction proceeds, the products and byproducts of the reaction could be resulting in photocatalyst quenching, causing the reaction to stall out. Therefore, we sought to attenuate these effects through investigation of [Ni]•**L71** complex loading, [Ir] loading, and additives.

3.2.3 Solvent and [Ir] Loading

One significant challenge inherent to the initial reaction conditions was the minimal solubility of most of the reagents. In particular, the solubility of the [Ni]•**L71** complex and the photocatalyst were particularly limiting. The [Ni]•**L71** complex is not readily soluble in TBME and requires long stir times at ~60 ºC to undergo complexation. Initial studies had shown that higher catalyst loadings resulted in higher yields. Therefore, finding a

solvent to fully solubilize the catalyst could result in higher yields. Similarly, Ir[dF(CF_3)ppy]$_2$(bpy)PF_6 is minimally soluble in TBME. This made it difficult to add as a stock solution and resulted in some irreproducibility. Initial studies had indicated that lowering the photocatalyst loading could be beneficial, but very low loadings were difficult to study due to the inability to make accurate stock solutions. Therefore, investigations into alternate solvent systems that solubilize the [Ni]•**L71** complex and photocatalyst were undertaken.

Table 3.2 *Solvent, [Ir], and ligand loading optimization*

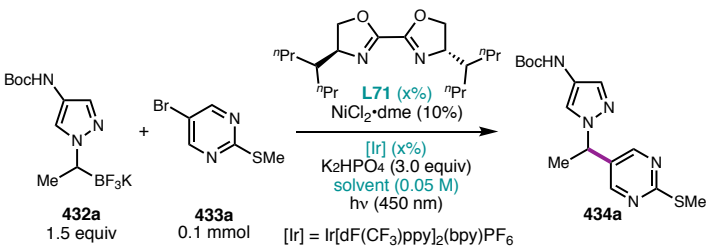

432a 1.5 equiv

433a 0.1 mmol

[Ir] = Ir[dF(CF_3)ppy]$_2$(bpy)PF_6

434a

entry	solvent	% [Ir]	% L2	% pdt	% ee
1	TBME	1.0	15	**66**	**82**
2	2-MeTHF	0.125	30	**70**	**85**
3	2-MeTHF	0.25	30	**72**	**84**
4	2-MeTHF	1.0	30	**73**	**74**
5	2-MeTHF	0.125	20	**72**	**83**
6	2-MeTHF	0.125	15	**65**	**81**
7	2-MeTHF	0	30	**6**	**85**
8[a]	TBME	0.125	30	**51**	**85**

[a]0.2 mmol scale

2-MeTHF was a potential alternative solvent due to promising observed reactivity on HTE scale and increased polarity compared to TBME. After initial HTE studies, 2-MeTHF was initially disregarded in favor of TBME as it resulted in lower enantioselectivities of the desired product. However, the [Ni]•**L71** catalyst complex is fully soluble at room temperature in 2-MeTHF after complexation at 60 ºC, and Ir[dF(CF_3)ppy]$_2$(bpy)PF_6 is fully soluble as well. Therefore, investigations into different ligand and photocatalyst loadings were undertaken in 2-MeTHF (**Table 3.2**). It was found that by decreasing the photocatalyst loading to 0.125% and increasing the ligand loading to 30% in 2-MeTHF, both the yield and the ee of the reaction increased (entry 2). As the [Ir] loading increased, the enantioselectivity decreased by about 10% (entries 3–4). Decreasing the ligand loading to 20% and 15% (entries 5 and 6, respectively) resulted in a

slight loss in enantioselectivity and a significant decrease in yield. Removing the photocatalyst from the reaction reduced the yield to 6%, though still with high ee (entry 7). When 30% **L71** and 0.125% [Ir] were used in TBME, the yield dropped significantly, likely due to the insolubility of the photocatalyst (entry 8). Lowering the light intensity from 100% only resulted in lower yields and comparable enantioselectivities. (See Section 3.5.3).

Table 3.3 *Reactivity of p-bromoanisole*

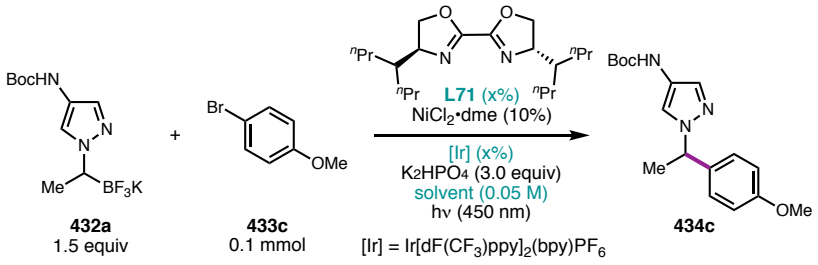

432a 1.5 equiv

433c 0.1 mmol

[Ir] = Ir[dF(CF$_3$)ppy]$_2$(bpy)PF$_6$

434c

Conditions A (entry 1a)

entry	solvent	% [Ir]	% L2	% pdt	% ee
1a	TBME	1.0	15	**44**	**81**
2a	TBME	1.0	30	**52**	**78**
3a	TBME	0.125	15	**16**	**85**
4a	TBME	0.125	30	**10**	**85**

Conditions B (entry 1b)

entry	solvent	% [Ir]	% L2	% pdt	% ee
1b	2-MeTHF	0.125	30	**11**	**80**
2b	2-MeTHF	0.125	15	**20**	**83**
3b	2-MeTHF	1.0	30	**8**	**50**
4b	2-MeTHF	1.0	15	**3**	**25**

Although the yields and ee's of our model system benefited from these changes, some aryl bromides did not perform as well under these new conditions. Notably, more electron-rich substrates such as 4-bromoanisole (**433c**) appeared to be more sensitive to changes in reaction conditions. Upon switching from conditions A (**Table 3.3a**, entry 1a), to conditions B (**Table 3.3b**, entry 1b), the yield of **434c** dropped precipitously from 44% to 11%. Increasing the loading of **L71** in TBME resulted in a slight loss in ee and an increase in yield (entry 2a), while decreasing the loading of **L71** in 2-MeTHF resulted in a slight increase in yield and ee (entry 2b). Lowering the photocatalyst loading in TBME (entry 3a) results in a significant drop in yield and a slight increase in ee. However, in 2-MeTHF increasing the photocatalyst loading to 1.0% results in a significant drop in ee

(entry 3b). This is likely due to the high solubility of [Ir] in 2-MeTHF, resulting in relatively high [Ir] loading, which has been shown to result in lower enantioselectivities in the model system. These data suggest that this reaction is highly substrate-dependent, and that different reaction conditions are optimal for different substrates.

Scheme 3.10 *Change in nucleophile reactivity*

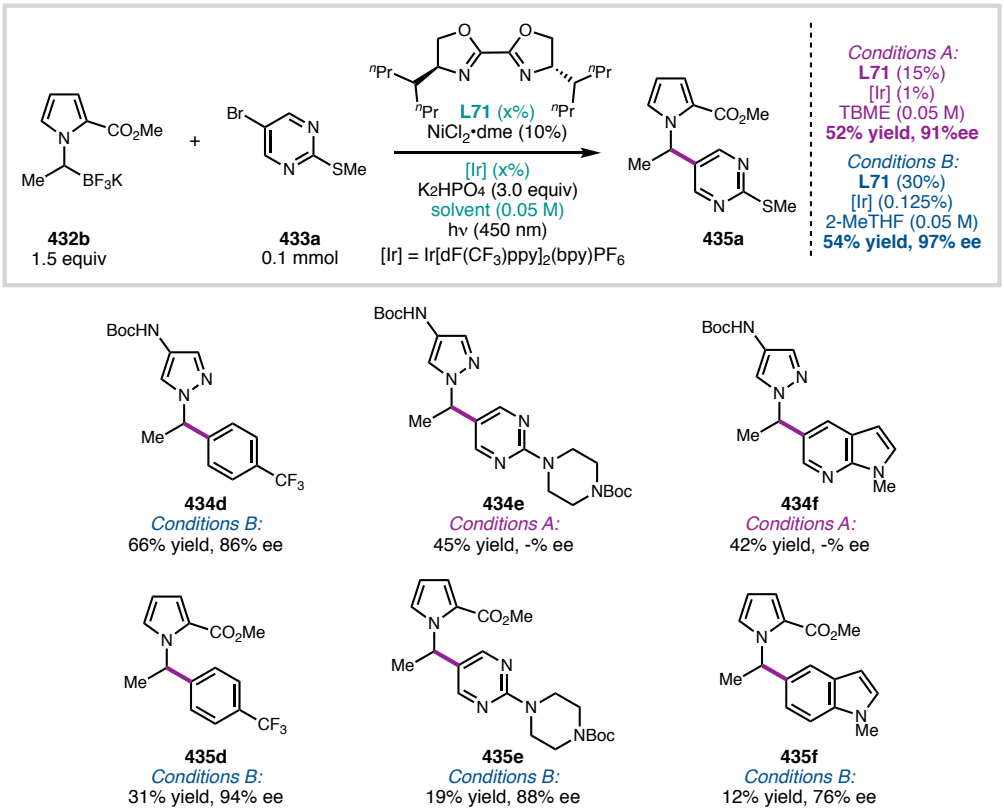

The identity of the nucleophile also appears to be a significant factor. Excitingly, when these modified conditions (Conditions B) were applied to ester pyrrole BF_3K **432b**, the ee increased from 91% to 97% with comparable yields (**Scheme 3.10**). However, the ester pyrrole product **435a** was observed in lower yields under both sets of conditions compared to pyrazole product **434a** (**Table 3.2**, entries 1–2). While the reduction in yield when using pyrrole ester **432b** compared to pyrazole **432a** is relatively minor for most pyrimidines and other very electron-poor aryl bromides, certain substrates resulted in

significantly lower yields. For example, trifluoromethyl product **434d** was observed in 66% yield, 86% ee, while the pyrrole adduct (**435d**) was observed in 31% yield, 94% ee. Other substrates also saw a significant reduction in yield upon switching conditions and nucleophiles. Despite these limitations on scope, we were encouraged by the overall increase in ee to >95% using these conditions with the pyrrole ester and electron-poor aryl bromides, and further screening efforts were undertaken with pyrrole BF_3K **432b** using 30% **L71**, 0.125% [Ir], and 2-MeTHF as the solvent.

3.2.4 Additives

Table 3.4 *Additive studies*

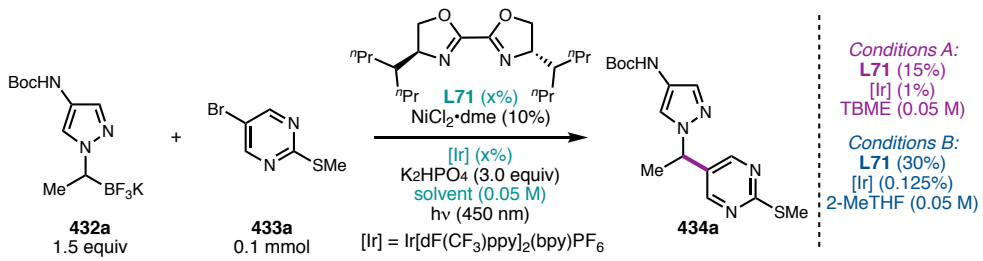

entry	conditions	additive (equiv)	% ArBr[a]	% pdt	%ee
1	A	none	15	**66**	**82**
2	A	TEMPO (0.5)	60	**12[b]**	**18**
3	A	$NaBF_4$ (0.5)	24	**59**	**80**
4	A	NaI (0.5)	19	**65**	**77**
5	A	LiBr (0.5)	9	**62**	**79**
6	A	LiCl (0.5)	17	**64**	**81**
7	A	TMSCl (0.5)	17	**52**	**73**
8	A	$ZnCl_2$ (0.5)	80	**<2**	**60**
9	A	$MnCl_2$ (0.5)	32	**53**	**81**
10	B	none	18	**70**	**85**
11	B	$MnCl_2$ (0.5)[c]	52	**38**	**84**
12	B	$Fe(OTf)_2$ (0.2)	64	**23**	**85**
13	B	$Fe(OTf)_2$ (0.2)[c]	41	**47**	**81**

[a]%ArBr remaining at the end of the reaction [b]TEMPO adduct **XX** observed by LCMS and NMR, ~18% yield [c]0.25% [Ir] instead of 0.125%

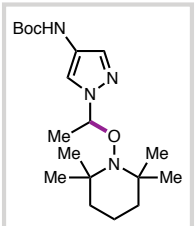

TEMPO adduct
450

A variety of additives were screened in an attempt to increase the yield of the reaction further with both sets of conditions. However, despite exploring numerous additives that have been beneficial for Ni catalysis in the past, there was no significant improvement to the yield or ee (**Table 3.4**). Excitingly, addition of 0.5 equiv of TEMPO

resulted in formation of TEMPO adduct **450**, which supports the existence of a radical intermediate generated from the BF_3K starting material (entry 2). TEMPO also resulted in significant inhibition of product formation. Most additives, such as $NaBF_4$, NaI, LiBr, and LiCl (entries 3–6) had little to no effect on the yield or ee. TMSCl (entry 7) reduced both the yield and ee slightly. Interestingly, $ZnCl_2$ (entry 8) and $MnCl_2$ (entry 9) afforded very different results, with $ZnCl_2$ completely shutting down reactivity and $MnCl_2$ only resulting in a slight attenuation in yield. Several additives were explored under the modified reaction conditions, but they only resulted in a decrease in yield (entries 11–13).

3.2.5 Final Ligand Optimization

Scheme 3.11 *Summary of HTE BiOX ligand screening*

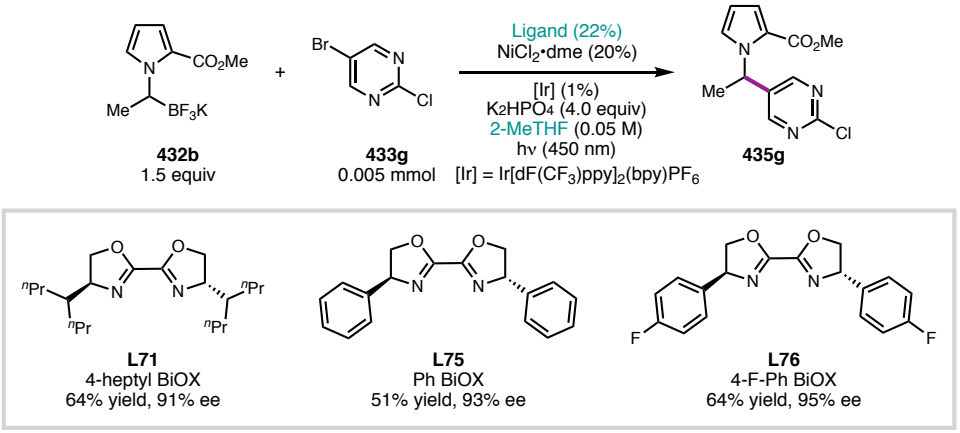

After this prior optimization was complete and the aryl bromide substrate scope was in progress, further HTE screens of 48 BiOX ligands were performed in 2-MeTHF with 20% $NiCl_2$•dme, 22% ligand, and 1% [Ir] to provide more reactivity information. Surprisingly, these studies indicated that both PhBiOX (**L75**) and 4-F-PhBiOX (**L76**) gave higher ee's and comparable yields on small scale to **L71** (**Scheme 3.11**). These two ligands had been investigated previously in TBME, however, due to the complete insolubility of the aryl BiOX [Ni] complexes in TBME, trace reactivity and little to no enantioselectivity

was observed with either ligand. In light of these results in 2-MeTHF, the reaction was investigated on scale using **L76**.

Table 3.5 *Ligand reactivity comparison for aryl bromides*

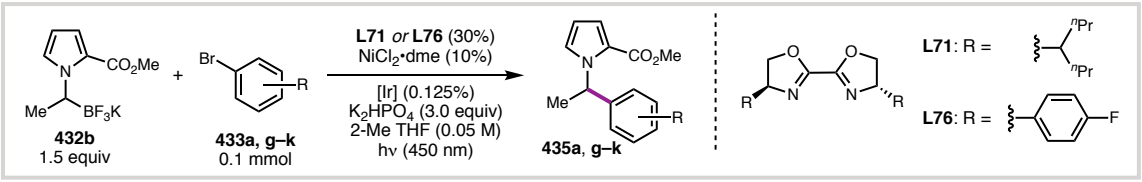

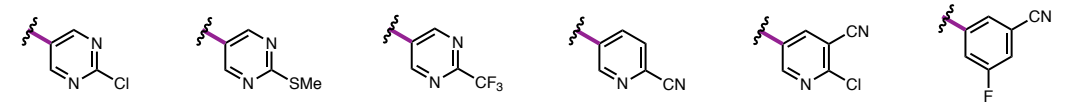

435g	**435a**	**435h**	**435i**	**435j**	**435k**
L71: 71%, 97% ee **L76**: 70%, 97% ee	**L71**: 54%, 97% ee **L76**: 71%, 97% ee	**L71**: 54%, 96% ee **L76**: 47%, 98% ee	**L71**: 56%, 90% ee **L76**: 65%, 91% ee	**L71**: 55%, 97% ee **L76**: 65%, 97% ee	**L71**: 38%, 96% ee **L76**: 68%, 97% ee

As previously mentioned, the aryl bromide substrate scope using heptyl BiOX was already underway. This allowed for quick comparison of a variety of aryl bromide coupling partners on 0.1 mmol scale using the photoreactor reaction setup (**Table 3.5**). Interestingly, unlike on small scale, both heptyl BiOX **L71** and 4-F-Ph BiOX **L76** gave nearly identical ee's for a variety of substrates. However, using 4-F-Ph BiOX resulted in increased yields for most aryl bromides. Model system **435g** was mostly unaffected on this scale, but pyrimidine **435a** and pyridines **435i** and **435j** saw increases in yield of up to 17%. Trifluoromethyl pyrimidine **435h** saw a slight decrease in yield, however. Most promising was compound **435k**, which saw an increase in yield from 38% to 68% upon exchanging ligands. These increases in yield led us to decide to redo the aryl bromide substrate scope using 4-F-Ph BiOX **L76**.

In addition, about 6 months into the project, it was found that both enantiomers of **L71** received from Merck contained ~5-6% of an undesired contaminant, hypothesized to be hydrolysis of one of the oxazolines based on the NMR and LCMS data (**Scheme 3.12**).

Scheme 3.12 *Decomposition of* ***L71***

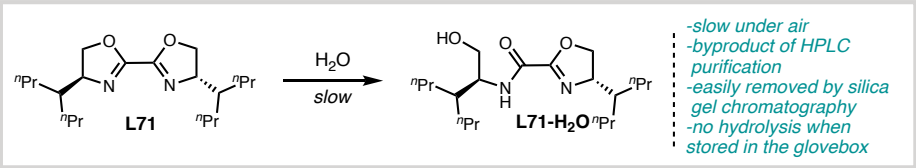

This hydrolysis product was observed by NMR in other BiOX ligands previously synthesized by our lab stored in the freezer as well. This is thought to be a relatively slow process for **L71**. However, the method of separating enantiomers of **L71** by outside contractors upon synthesis likely contributed to this hydrolysis, resulting in unusually large amounts of contaminant initially. Fortunately, this contaminant is easily separated by silica gel chromatography (see Section 3.5.2). Following this discovery, we (Caltech) would regularly purify multigram batches of this ligand and bring it into the glovebox for storage, where it was found to be stable. Minor irreproducibility issues previously observed were significantly reduced upon regular use of clean ligand. **L76** was not isolated using the same purification process and was immediately stored in the glovebox upon synthesis to prevent decomposition in normal atmosphere.

3.3 SUBSTRATE SCOPE

3.3.1 Scope of Aryl Bromides

With optimized conditions in hand, the aryl bromide substrate scope was investigated on 0.2 mmol scale using both **L71** and **L76** (**Table 3.6**). Interestingly, upon increasing the scale from 0.1 to 0.2 mmol, the yields significantly increased for almost all aryl bromides when using **L76** as the ligand. However, when using heptyl BiOX, most yields were comparable or slightly reduced upon increasing the scale. As previously mentioned, electron-poor aryl and heteroaryl bromides perform the best under these

Table 3.6 *Aryl bromide scope*

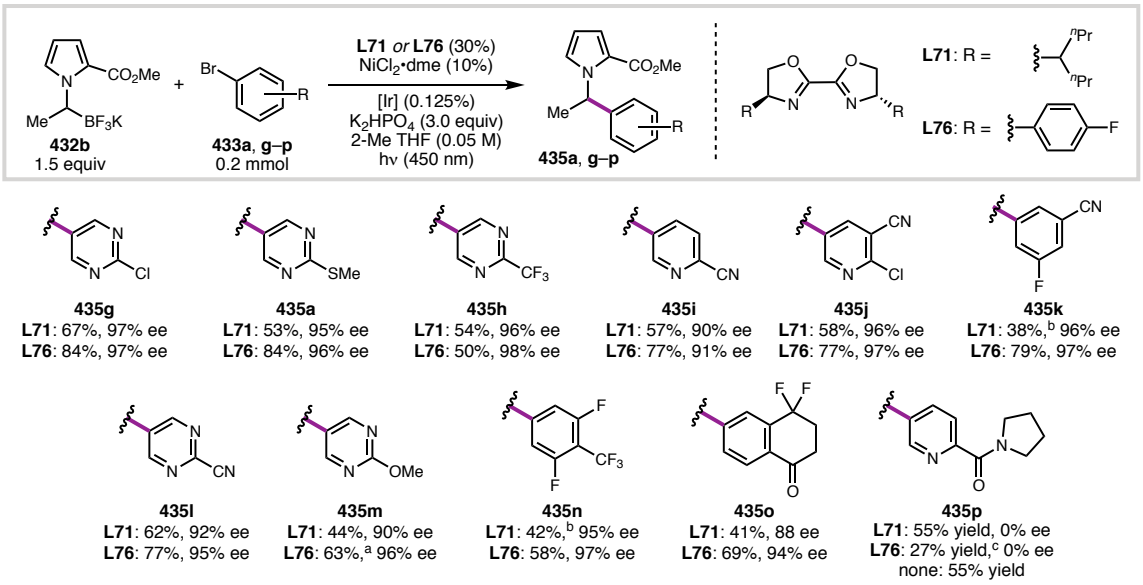

Isolated yields are reported unless otherwise indicated; ee determined by SFC using a chiral stationary phase, [Ir] = $Ir[dF(CF_3)ppy]_2(bpy)PF_6$
[a]Reaction run in THF. [b]Run on 0.1 mmol scale [c]Determined by ^1H NMR versus an internal standard

reaction conditions, with enantiomeric excesses up to 98%. Pyrimidine and pyridine substrates generally performed well (**435a**, **g**–**j**, **l**, **m**), though CF_3 pyrimidine **435h** and methoxy pyridine **435m** were both isolated in lower yields. Methoxy pyrimidine **435h** was run in THF due to insolubility of the aryl bromide in 2-MeTHF. Electron-poor aryl groups were tolerated as well, albeit in lower yields (**435n, o**). In general, more electron-poor substrates were isolated in higher ee (for example **435h**), and more electron-rich substrates were isolated with slightly lower enantioselectivity (**435o**). Overall, these conditions were generally applicable to a variety of electron-poor aryl bromides, affording the desired products in moderate to good yields and excellent enantioselectivities.

Interestingly, when (5-bromopyridin-2-yl)(pyrrolidin-1-yl)methanone (**433p**) was cross-coupled in the presence of either **L71** or **L76**, only racemic **435p** was isolated. When ligand was eliminated from the reaction mixture all together, comparable yields of the cross-coupled product were obtained (**Table 3.6**). This suggests that the pyridine amide

Scheme 3.13 *Pyridine amides as ligands*

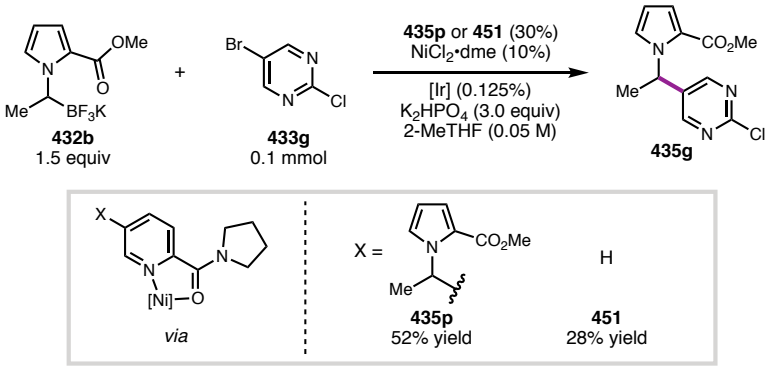

moiety itself can act as a competent ligand for this cross-coupling. Indeed, when pyridine amide product **435p** was used as the ligand for the cross-coupling of model BF_3K **432b** and pyrimidine **433g**, the desired product was observed in 52% yield (**Scheme 3.13**). Parent pyridine **451** resulted in only 28% yield, however, indicating that substitution at the 5 position of the pyridine is key to ligand efficacy.

Table 3.7 *Other aryl bromides screened*

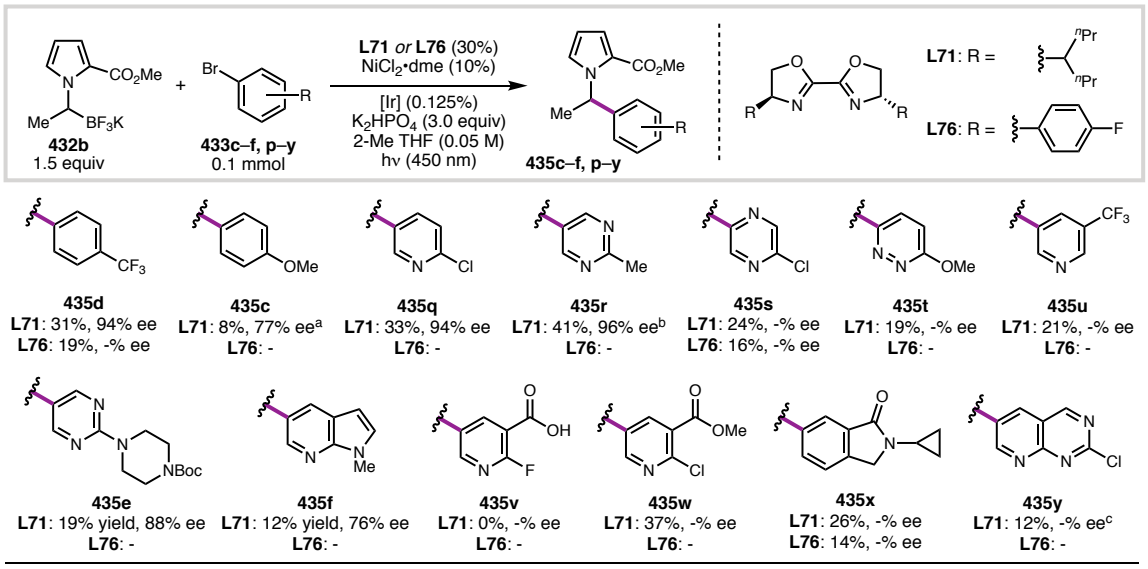

Determined by ^{1}H NMR, [a]62% recovered ArBr, [b]32% yield, 95% ee on 0.2 mmol scale with **L1**, [c]other byproducts observed, tentatively assigned as radical addition into the heterocycle

A variety of other aryl bromides were investigated as well (**Table 3.7**). Most substrates were screened with **L71** as we had over 20 g at our disposal and the increase in

yield with **L76** was discovered relatively late in the project. Interestingly substrates **433d**, **433s**, and **435x** actually underwent cross-coupling in lower yields with **L76** compared to **L71**. As previously discussed, aryl bromides without sufficiently electron-withdrawing groups were cross-coupled in relatively low yields (**435c**–**d**). Pyridine **435q** was observed in poor yield and good ee. Pyrimidine **435r** was observed in 41% yield, 96% ee on 0.1 mmol scale, but the yield dropped significantly when run on 0.2 mmol scale (see footnote). Other nitrogen-containing heterocycles cross-coupled in low yields (**435s**,**t**), and pyridine **435u** that does not have a blocking group at the 2 position was observed in 21% yield. Free carboxylic acids were not tolerated under the reaction conditions (**433v**), but methyl esters were (**433w**). Polycyclic heterocylces such as **433y** resulted in complex mixtures of products that are believed to result from direct radical addition into the heterocycle to form stabilized radical intermediates.

3.3.3 Scope of Nucleophiles

Scheme 3.14 *Different nucleophile reactivity*

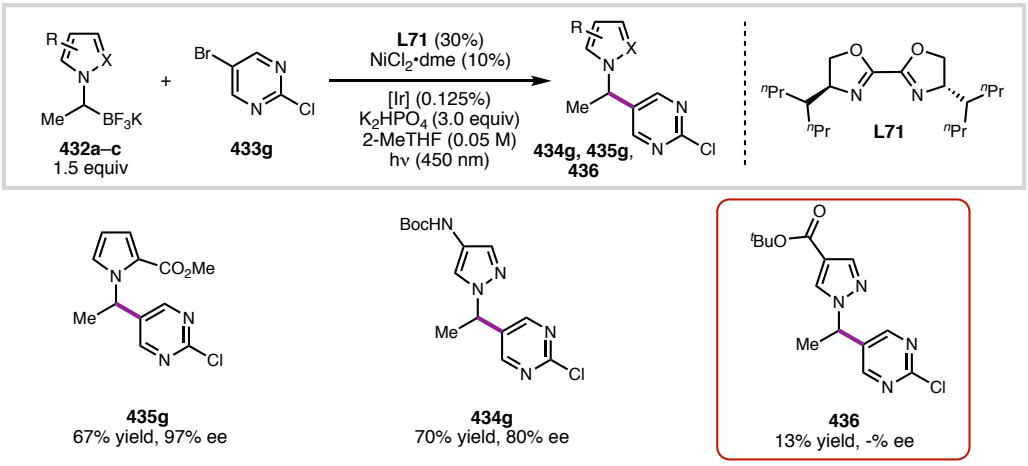

While the reaction conditions for the cross coupling of ester pyrrole **432b** with a variety of aryl bromides were fairly consistent, conditions had to be re-optimized for

certain BF_3K salts. When investigating the nucleophile substrate scope, we were surprised to find that while both pyrrole **432b** and pyrazole **432z** underwent successful cross-coupling to afford the desired products, ester pyrazole **436** was only observed in 13% yield (**Scheme 3.14**). This was especially unexpected due to the structural similarity between boc amine pyrazole **432a** and ester pyrazole **432c**. However, we noticed that while both pyrrole **432b** and pyrazole **432b** were relatively insoluble in 2-MeTHF, ester pyrazole **432c** was highly soluble. Therefore, it was hypothesized that in order for successful cross-coupling to occur, the BF_3K salt had to be relatively insoluble.

Table 3.8 *Re-optimization of reaction conditions for nucleophile* ***432c***

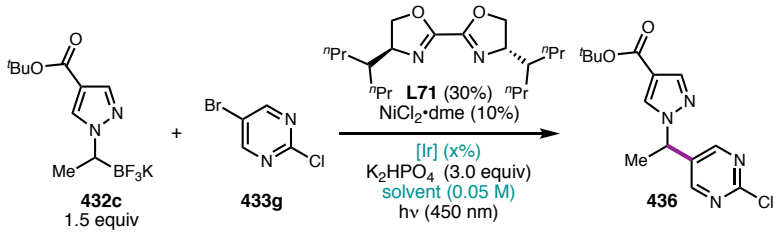

entry	solvent	%[Ir]	[Ir] soluble?	%ArBr[a]	%pdt	%ee
1	TBME	0.125	no	51	**15**	-
2	TBME	1.0	no	55	**22**	**82**
3	CPME	0.125	no	57	**13**	-
4	CPME	1.0	no	30	**47**	**86**
5	chlorobenzene	0.125	yes	43	**5**	-
6	chlorobenzene	1.0	yes	23	**37**	**83**
7	dioxane	0.125	no	65	**11**	-
8	dioxane	1.0	no	53	**5**	-

[a]%ArBr remaining

To test this hypothesis, we performed a solvent screen for the cross-coupling of ester pyrazole **432c** with **433g**. Four solvents in which **432c** is insoluble in were screened with two different [Ir] loadings (**Table 3.8**). It was found that cyclopentyl methyl ether (CPME) with 1.0% [Ir] proved to be the optimal set of conditions for the desired cross-coupling, affording the desired product in 47% yield, 86% ee (entry 4). It is thought that 1.0% [Ir] is needed due to its insolubility in CPME. Despite previous success with other substrates using TBME, it was not the optimal solvent for this substrate, though it did result

in an improvement in yield over 2-MeTHF (entry 2). Due to the insolubility of the [Ni]•**L76** complex in CPME, it could not be investigated for this cross-coupling on scale. After this discovery, our collaborators utilized HTE to identify several solvents (2-Me-THF, isopropyl acetate (^{i}PrOAc), CPME, and 1,2-dimethoxy ethane (DME)) that generally performed well across a variety of nucleophiles, simplifying the screening process. In general, it appears that in order for the reaction to afford product in synthetically useful yields, the BF_3K salt must be relatively *insoluble* in the reaction solvent. In addition, the solubility of the [Ir] photocatalyst must be taken into account. When [Ir] is fully soluble, only 0.125 % is required. When [Ir] is relatively insoluble, such as in CPME, the [Ir] loading must be increased.

Table 3.9 *Ligand reactivity comparison for nucleophiles*

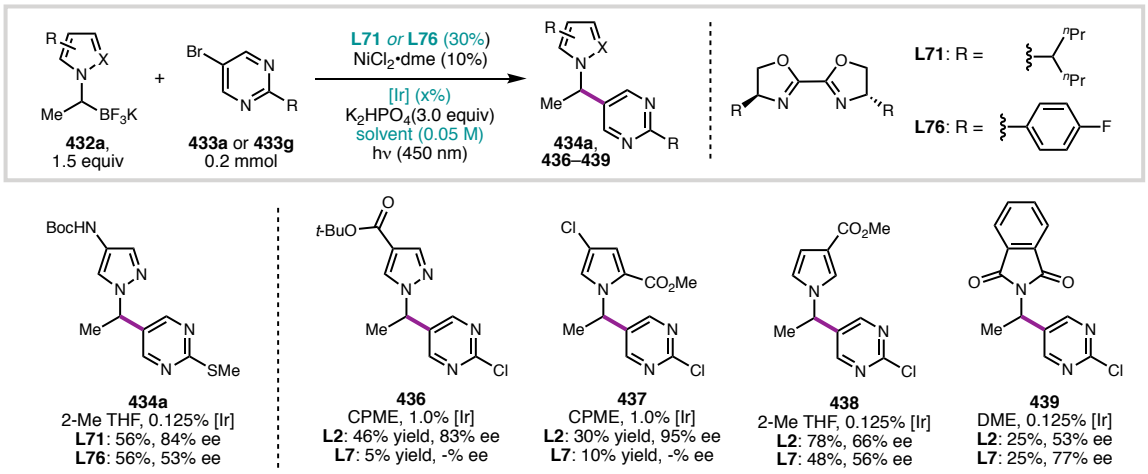

Interestingly, across a variety of nucleophiles, **L71** and **L76** perform very differently (**Table 3.9**). While **L76** proved to be optimal for the cross-coupling of pyrrole **432a** with a wide variety of aryl bromides, it yielded inferior enantioselectivities for other nucleophiles. In particular, **L71** afforded **434a** and **438** in 84% ee and 66% ee, respectively, while **L76** gave 53% ee and 56% ee. As previously stated, the [Ni]•**L76** complex is

insoluble in CPME, resulting in inferior yields for **436** and **437**. Interestingly, **L76** affords higher enantioselectivities than **L71** for phthalimide **439**.

Table 3.10 *Nucleophile scope*

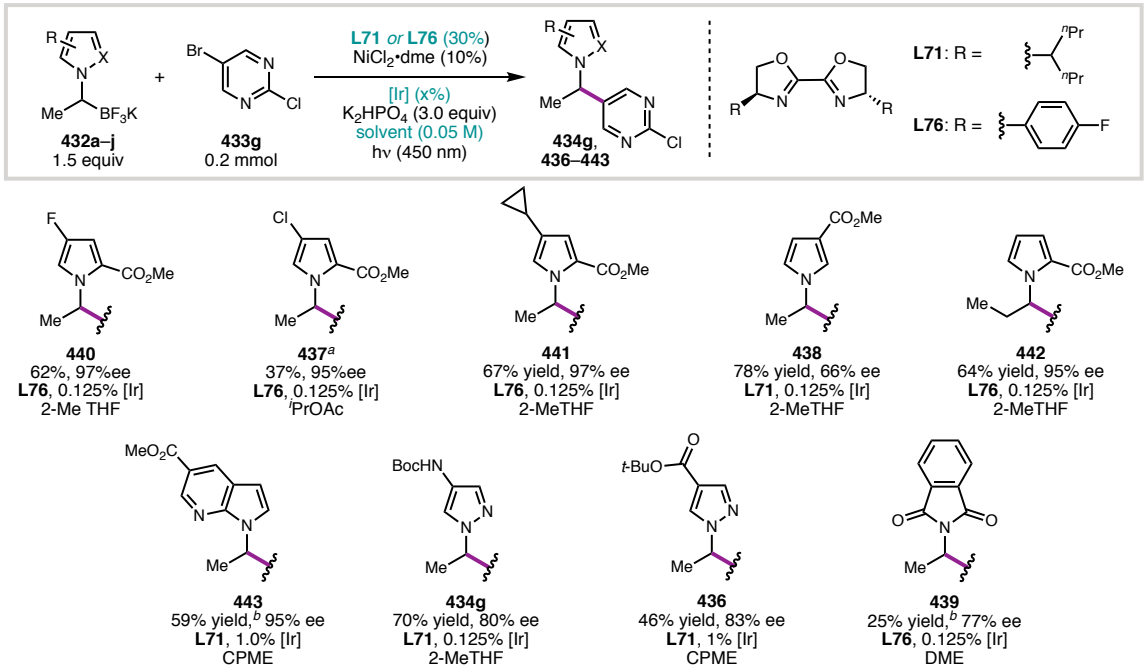

[Ir] = Ir[dF(CF$_3$)ppy]$_2$(bpy)PF$_6$. [a]0.1 mmol scale, [b]determined by ^{1}H NMR versus an internal standard

With these observations in hand, the nucleophile substrate scope was explored (**Table 3.10**). Halogen substitution at the 4 position of the pyrrole is tolerated, though chlorinated substrate **437** is observed in comparatively low yield. Fluro pyrrole **440** and cyclopropyl pyrrole **441** were isolated in good yield and ee. The hypothesis that the ester at the 2 position acts as a directing group is supported by the decrease in enantioselectivity from 97% ee to 66% ee when the ester is shifted to the 3 position (**438**). Ethyl pyrrole **442** performs comparably to model pyrrole **435**. Excitingly, azaindole **443** acts as a competent directing group for this cross-coupling, with the product observed in 56% yield and 95% ee. Pyrazoles **434g** and **436** are also competent coupling partners, albeit with lower enantioselectivity. The nitrogen at the 2 position appears to be a less effective directing

group than the ester or azaindole, though still better than no directing group. Phthalimide substrate **439** was isolated in relatively low yields. It is thought that this could be due to *in situ* decomposition through single-electron reduction of the photoexcited phthalimide product.[32]

3.4 CONCLUSION

In conclusion, we have developed an enantioselective nickel-catalyzed photoredox cross-coupling of α-*N*-heterocyclic potassium trifluoroborate salts with a variety of electron-poor aryl and heteroaryl bromides to form chiral *N*-(hetero)benzylic azoles. Cross-coupled products are afforded in up to 98% ee in good yields. This strategy is a significant improvement in yield and ee over previous approaches towards these types of products and is one of relatively few examples of enantioselective cross-coupling using photochemistry. While some nucleophiles require further reaction optimization, we have developed a simple workflow for optimizing new reaction conditions quickly.

3.5 EXPERIMENTAL SECTION

3.5.1 Materials and methods

Unless otherwise stated, reactions were performed under a nitrogen atmosphere using dried solvents. Anhydrous 2-Methyltetrahydrofuran (2-MeTHF), anhydrous *tert*-butyl methyl ether (TBME), anhydrous cyclopentyl methyl ether (CPME), anhydrous tetrahydrofuran (THF), anhydrous potassium phosphate monobasic (K_2HPO_4) were purchased from Millipore Sigma and stored in the glovebox. Nickel(II) chloride dimethoxyethane adduct ($NiCl_2$•dme) was purchased from Strem. BF_3K salts **432a**–**j** were synthesized by Merck and used as received, as were aryl bromides **433h**, **j**, **k**, and **n**–**o**. 4-heptyl BiOX (**L71**) was purchased by Merck from outside contractors. Both enantiomers were sent to us and were purified and stored in the glovebox. Unless otherwise stated, chemicals were used as received. All reactions were monitored by thin-layer chromatography (TLC) using EMD/Merck silica gel 60 F254 pre-coated plates (0.25 mm) and were visualized by ultraviolet (UV) light or with *p*-anisaldehyde or potassium permanganate staining. Flash column chromatography was performed as described by Still et al. using silica gel (230-400 mesh) purchased from Silicycle. Optical rotations were measured on a Jasco P-2000 polarimeter using a 100 mm path-length cell at 589 nm. ^1H and ^{13}C NMR spectra were recorded on a Bruker Avance III HD with Prodigy cyroprobe (at 400 MHz and 101 MHz, respectively), a Varian 400 MR (at 400 MHz and 101 MHz, respectively), or a Varian Inova 500 (at 500 MHz and 126 MHz, respectively). ^1H and ^{19}F NMR spectra were also recorded on a Varian Inova 300 (at 300 MHz and 282 MHz, respectively). NMR data is reported relative to internal $CHCl_3$ (^1H, $\delta = 7.26$), $CDCl_3$ (^{13}C, $\delta = 77.1$), C_6F_6 (^{19}F, $\delta = -164.9$), $CH_3C_6D_5$ (^1H, $\delta = 2.09$), and $CD_3C_6D_5$ (^{13}C, $\delta = 20.4$). Data for ^1H NMR spectra

are reported as follows: chemical shift (δ ppm) (multiplicity, coupling constant (Hz), integration). Multiplicity and qualifier abbreviations are as follows: s = singlet, d = doublet, t = triplet, q = quartet, m = multiplet. IR spectra were recorded on a Perkin Elmer Paragon 1000 spectrometer and are reported in frequency of absorption (cm^{-1}). Analytical chiral SFC was performed with a Mettler SFC supercritical CO_2 chromatography system with Chiralcel AD-H, OD-H, AS-H, OB-H, and OJ-H columns (4.6 mm x 25 cm). LRMS were obtained using an Aglient 1290 Infinity/6140 Quadrupole system (LC-MS) or an Agilent 7890A GC/5975C VL MSD system (GC-MS). HRMS were acquired from the Caltech Mass Spectral Facility using fast-atom bombardment (FAB), electrospray ionization (ESI-TOF), or electron impact (EI).

Commonly Used Abbreviations:

ee – enantiomeric excess; **Et_2O** – diethyl ether; **EtOAc** – ethyl acetate; **DCM** – dichloromethane; **FTIR** – Fourier transform infrared; **HRMS** – high-resolution mass spectrometry; **IPA** – isopropanol; **LRMS** – low-resolution mass spectrometry; **m.p.** – melting point; **NHP** – N-hydroxyphthalimide; **NMR** – nuclear magnetic resonance; **R_f** – retention factor; **SFC** – supercritical fluid chromatography

3.5.2 Ligand Preparation

Purification of L71

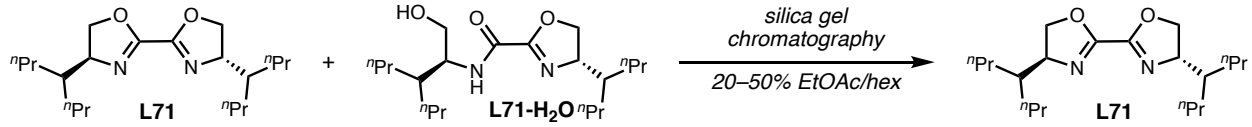

To remove undesired hydrolyzed contaminant **L71•H_2O** intermixed with **L71**, the mixture was purified by silica gel chromatography (20–50% EtOAc/hexanes, load on celite) to afford **L71.** Azeotroped with pentanes to remove excess EtOAc and scratched the side of the vial with a spatula to induce solidification of the oil. **L71** was isolated as an off-white solid and stored in a N_2-filled glovebox to prevent hydrolysis. **L71** is stable in the glovebox

^{1}H NMR (500 MHz, Chloroform-*d*) δ 4.47 – 4.32 (m, 4H), 4.15 (t, *J* = 7.9 Hz, 2H), 1.65 (h, *J* = 6.4, 6.0 Hz, 2H), 1.43 – 1.26 (m, 14H), 1.23 – 1.11 (m, 2H), 0.90 (q, *J* = 6.9 Hz, 12H).

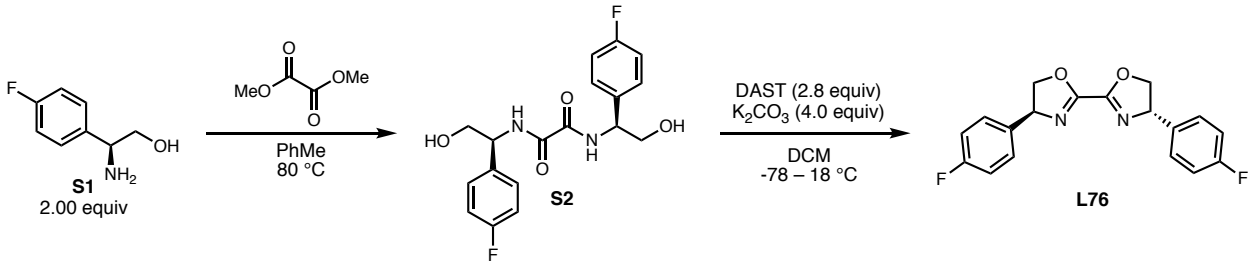

Synthesis of L76.[30,33]

Known amino alcohol **S1** was synthesized by a borane reduction of the corresponding amino acid.

To a 500 mL round bottom flask containing **S1** (4.2 g, 27.0 mmol, 2.00 equiv) was added dimethyl oxalate (1.59 g, 13.5 mmol, 1.00 equiv) and PhMe (300 mL, 0.45 M). The flask was affixed with a reflux condenser, and the reaction mixture was heated to 80 ºC under nitrogen for 20 hours. The reaction mixture was then allowed to cool and was concentrated and dried *in vacuo* to afford **S2**, which was carried forward without further purification.

To an oven-dried 250 mL rbf was added **S2** (1.82 g, 5.00 mmol, 1.00 equiv). The flask was evacuated and backfilled with N_2 x 3, and DCM (80 mL, 0.63 M) was then added. The reaction mixture was cooled to –78 ºC, and diethylaminosulfur trifluoride (DAST) (1.2 mL, 14.0 mmol, 2.8 equiv) was added dropwise over 2 minutes. The reaction was allowed to stir at –78 ºC for 1 hour, then K_2CO_3 (2.8 g, 20 mmol, 4.0 equiv) was added. The reaction was removed from the cold bath and allowed to stir for 1.5 hours. The reaction was then diluted with 40 mL DCM and 60 mL water. The layers were separated, and the organic layer was washed with sat aq. $NaHCO_3$ and brine. The organic layer was dried over Na_2SO_4, filtered, and concentrated *in vacuo*. The crude material was purified by silica gel chromatography (75% EtOAc/hexanes) to afford **L76** (329 mg, 20% yield).

^{1}H NMR (400 MHz, Chloroform-*d*) δ 7.32 – 7.24 (m, 4H), 7.11 – 7.01 (m, 4H), 5.52 – 5.36 (m, 2H), 4.86 (dd, J = 10.4, 8.8 Hz, 2H), 4.33 (t, J = 8.9 Hz, 2H).

3.5.3 Optimization of Reaction Parameters

Optimization table data gathered by Kevin Belyk at Merck

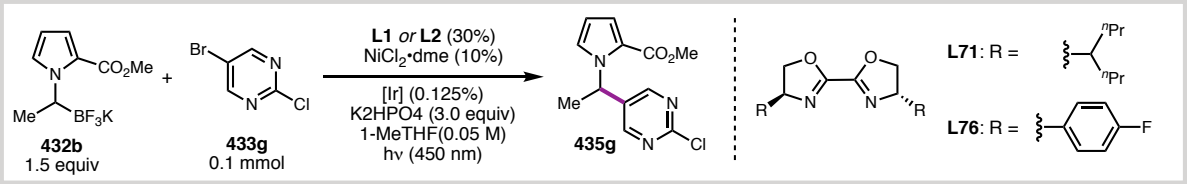

entry	deviation from Standard conditions[a]	**L71**: yield[b] (%) / ee[c] (%)	**L76**: yield[b] (%) / ee[c] (%)
1	none	81 / 97	80 / 97
2	10% [Ni], 10% **L**	53 / 94	48 / 97
3	10% [Ni], 15% **L**	81 / 96	62 / 97
4	10% [Ni], 20% **L**	81 / 97	78 / 97
5	5% [Ni], 15% **L**	73 / 97	74 / 96
6	1.0% [Ir]	74 / 93	73 / 96
7	0.5% [Ir]	71 / 95	73 / 96
8	0.25% [Ir]	81 / 97	72 / 96
9	1.0% 4 CzIPN	69 / 94	76 / 97
10	no base	32 / 97	33 / 97
11	no light	N.D. / -	<1 / -
12	no [Ir]	N.D. / -	N.D. / -
13	no [Ni] and **L**	N.D. / -	N.D. / -
14	no **L**	19 / 0	19 / 0

[a]Reaction conditions: **XX** (0.1 mmol), **XX** (0.15 mmol), $NiCl_2$•dme (10 μmol, 10 mol%), **L1** or **L2** (30 μmol, 30 mol%), [Ir] = Ir[dF(CF_3)ppy]$_2$(bpy)PF_6 (0.125 µmol, 0.125 mol%), K_2HPO_4 (0.3 mmol, 3 equiv.), 2-MeTHF (2 mL, 0.05 molar in **XX**), Pennoc M1 photoreactor, hν (450 nm), 7 cm sample holder, 500 RPM stir rate, 5200 RPM fan speed (18 h). [b]Determined by ^{1}H NMR analysis vs ethylene carbonate as an internal standard. [c]Enantiomeric excess determined by chiral RP-HPLC.

3.5.4 Enantioselective Cross-Coupling

a. General Procedure a: Reaction on 0.2 mmol scale

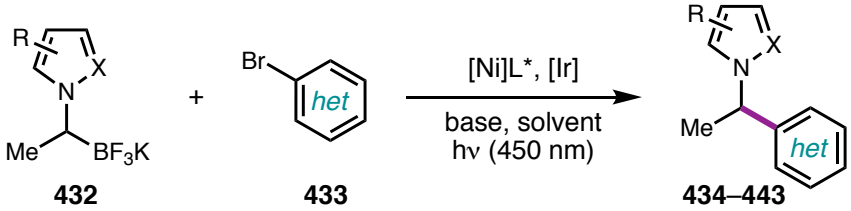

On the benchtop, to a 2-dram vial containing a 2-dram Teflon-coated stirbar was added aryl bromide **433** (if solid) (1.0 equiv, 0.2 mmol) and BF_3K salt **432** (1.5 equiv, 0.3 mmol). The reaction vial was then brought into a N_2-filled glovebox, and K_2HPO_4 (3 equiv, 0.6 mmol, 105 mg) was then added. Ir[dF(CF_3)ppy]$_2$(bpy)PF_6 (0.125 mol%, 0.25 µmol, 0.25 mg) was added as a stock solution in 2.0 mL solvent followed by aryl bromide (if liquid) (1.0 equiv, 0.2 mmol).

Meanwhile, $NiCl_2$•dme (0.1 equiv, 0.02 mmol, 4.4 mg), ligand (0.30 equiv, 0.06 mmol) and the remaining solvent (2.0 mL) (4.0 mL total, 0.05 M) were added to a 1-dram vial with a stirbar, sealed with a cap, heated to 55–60 ºC in a heating block, and stirred until complexation was complete, everything was dissolved, and a color change occurred (heptyl BiOX: clear peachy orange solution; 4-F-Ph BiOX: clear yellow solution). Once complexation was complete, the complexed catalyst solution was added to the reaction vial. The vial was sealed with a Teflon cap and tape and removed from the glovebox. The reaction vial was then placed in a vial holder in a 7 cm tall cone in a Penn PhD m2 photoreactor with a 450 nm light module. Stirring was set to 500 rpm, the fan speed was set to 5200 rpm, the LED intensity was set to 100%, and the reaction time was set to 18 hours. After 18 hours, the reaction was diluted with EtOAc and washed with sat. aq. NH_4Cl. The aqueous layer was extracted 3 times with EtOAc, and the combined organic layers were pushed through a ~8 mm by 6 cm plug of $MgSO_4$ with a layer of celite on top. The solution was concentrated *in vacuo*, and the crude material was purified by silica gel column chromatography to afford the desired product.

c. General Procedure b: Reaction on 0.1 mmol scale

Identical to General Procedure A, but using a 1-dram vial instead of a 2-dram vial.

Racemic standards were synthesized on 0.1 mmol scale using the same procedure in a 1-dram vial with ***rac*-L71**.

c. Characterization of Reaction Products – Aryl Bromide Scope

Note: At the time this section was compiled, we were in the middle of characterization of these products. Therefore, not all products that will appear in the final publication will have all of their characterization data in this document.

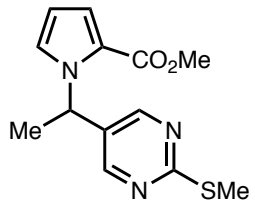

435a (TJD-6-002): Prepared from 5-bromo-2-(methylthio)pyrimidine (**433a**, 41 mg, 0.2 mmol) and BF_3K (**432b**, 81.8 mg, 0.3 mmol) according to General Procedure A in 2-MeTHF with 4-F-Ph BiOX (**L76**). The crude residue was purified by column chromatography (silica gel, 15% EtOAc/hexanes) to yield **435a** (46.5 mg, 84% yield) in 96% ee as a colorless oil.

$\mathbf{R}_f$ = 0.39 (silica gel, 20% EtOAc/hexanes, UV).

$[\alpha]_D^{22}$ = 127° (c = 1.0, $CHCl_3$).

^{1}H NMR (400 MHz, $CDCl_3$): δ 8.27 (s, 2H), 7.06 (dd, J = 2.8, 1.7 Hz, 1H), 7.01 (dd, J = 3.9, 1.7 Hz, 1H), 6.55 (q, J = 7.2 Hz, 1H), 6.23 (dd, J = 3.9, 2.7 Hz, 1H), 3.76 (s, 3H), 2.53 (s, 3H), 1.83 (d, J = 7.2 Hz, 3H).

^{13}C NMR (101 MHz, $CDCl_3$): δ 171.87, 161.63, 155.41, 131.33, 124.70, 122.15, 119.25, 109.46, 51.46, 51.31, 21.65, 14.25

FTIR (NaCl, thin film, cm^{-1}): 2948, 1699, 1584, 1537, 1438, 1400, 1338, 1227, 1111, 942, 738

HRMS (FAB, m/z): calc'd for $C_{13}H_{16}N_3O_2S$ $[M+H]^+$: 278.0963 ; found: 278.0970.

Chiral SFC: (IC, 2.5 mL/min, 25% IPA in CO_2, λ = 254 nm):

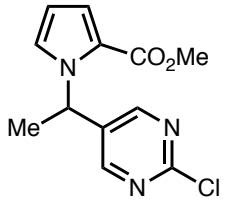

435g (TJD-5-299): Prepared from 5-bromo-2-chloropyrimidine (**433g**, 38.7 mg, 0.2 mmol) and BF_3K (**432b**, 81.8 mg, 0.3 mmol) according to General Procedure A in 2-MeTHF with 4-F-Ph BiOX (**L76**). The crude residue was purified by column chromatography (silica gel, 8.5–9% EtOAc/hexane) to yield **435g** (44.5 mg, 84% yield) in 97% ee as a colorless oil.

$\mathbf{R}_f$ = 0.36 (silica gel, 20% EtOAc/hexanes, UV).

$[\boldsymbol{\alpha}]_D^{21}$ = 79° (c = 1.1, $CHCl_3$).

^{1}H NMR (400 MHz, $CDCl_3$): δ 8.33 (d, J = 0.6 Hz, 2H), 7.10 (dd, J = 2.8, 1.7 Hz, 1H), 7.03 (dd, J = 4.0, 1.7 Hz, 1H), 6.59 (q, J = 7.3 Hz, 1H), 6.28 (dd, J = 4.0, 2.8 Hz, 1H), 3.75 (s, 3H), 1.86 (d, J = 7.3 Hz, 3H)

^{13}C NMR (101 MHz, $CDCl_3$): δ 161.6, 160.5, 157.7, 135.5, 124.6, 122.2, 119.5, 109.8, 51.4, 51.3, 21.7.

FTIR (NaCl, thin film, cm^{-1}): 3126, 2984, 2949, 1698, 1549, 1439, 1398, 1338, 1226, 1113, 1059, 940, 829, 740

HRMS (FAB, m/z): calc'd for $C_{12}H_{13}ClN_3O_2$ $[M+H]^+$: 266.0696 ; found: 266.0702.

Chiral SFC: (IC, 2.5 mL/min, 30% IPA in CO_2, λ = 254 nm):

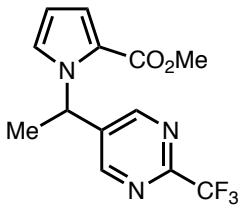

435h (CRL-6-199; TJD-5-241): Prepared from 5-bromo-2-(trifluoromethyl)pyrimidine (**433h**, 45.4 mg, 0.3 mmol) and BF_3K (**432b**, 81.8 mg, 0.2 mmol) according to General Procedure A in 2-MeTHF with 4-F-Ph BiOX (**L76**). The crude residue was purified by column chromatography (silica gel, 2.5% EtOAc/PhMe) to yield **3b** (30 mg, 50% yield) in 98% ee as a colorless oil.

$\mathbf{R}_f$ = 0.54 (silica gel, 30% EtOAc/hexanes, UV).

$[\boldsymbol{\alpha}]_{\boldsymbol{D}}^{\mathbf{21}}$ = 46° (c = 1.5, $CHCl_3$).

^{1}H NMR (400 MHz, $CDCl_3$): δ 8.55 (s, 2H), 7.15 (dd, *J* = 2.8, 1.7 Hz, 1H), 7.05 (dd, *J* = 4.0, 1.7 Hz, 1H), 6.67 (q, *J* = 7.3 Hz, 1H), 6.31 (dd, *J* = 4.0, 2.7 Hz, 1H), 3.74 (s, 3H), 1.91 (d, *J* = 7.2 Hz, 3H).

^{13}C NMR (101 MHz, $CDCl_3$): δ 161.56, 155.78, 139.11, 124.56, 122.28, 120.99, 119.66, 118.26, 109.95, 51.79, 51.42, 21.68.

^{19}F NMR (282 MHz, $CDCl_3$) δ -73.42.

FTIR (NaCl, thin film, cm^{-1}): 3124, 2991, 1956, 1704, 1698, 1714, 1568, 1441, 1353, 1118, 941

HRMS (FAB, m/z): calc'd for $C_{13}H_{13}F_3O_2N_3$ $[M+H]^+$: 300.0960 ; found: 300.0973.

Chiral SFC: (IC, 2.5 mL/min, 5% IPA in CO_2, λ = 254 nm): t_R (minor) = 3.0 min, t_R (major) = 3.7 min.

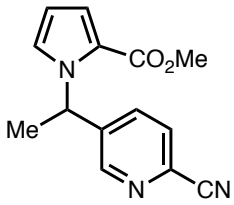

435i (CRL-6-072,197): Prepared from 5-bromo-2-pyridinecarbonitrile (**433i**, 36.6 mg, 0.2 mmol) and BF_3K (**432b**, 81.8 mg, 0.3 mmol) according to General Procedure a in 2-MeTHF with 4-F-Ph BiOX (**L76**). The crude residue was purified by column chromatography (silica gel, 10-30% EtOAc/hex) to yield **435i** (39 mg, 77% yield) in 91% ee as a colorless oil.

$\mathbf{R}_f$ = 0.39 (silica gel, 30% EtOAc/hex, UV).

$[\boldsymbol{\alpha}]_{\boldsymbol{D}}^{\mathbf{25}}$ = 71° (c = 0.7784, $CHCl_3$).

^{1}H NMR (400 MHz, $CDCl_3$): δ 8.46 (d, *J* = 2.3 Hz, 1H), 7.61 (dd, *J* = 8.1, 0.8 Hz, 1H), 7.39 (ddd, *J* = 8.1, 2.3, 0.7 Hz, 1H), 7.12 (dd, *J* = 2.8, 1.7 Hz, 1H), 7.04 (dd, *J* = 4.0, 1.8 Hz, 1H),

6.63 (q, *J* = 7.2 Hz, 1H), 6.29 (dd, *J* = 4.0, 2.7 Hz, 1H), 3.73 (d, *J* = 0.5 Hz, 3H), 1.86 (d, *J* = 7.3 Hz, 3H).

^{13}C NMR (101 MHz, $CDCl_3$): δ 161.51, 149.29, 143.21, 134.26, 132.70, 128.49, 124.82, 122.29, 119.46, 117.24, 109.59, 53.63, 51.35, 21.92.

FTIR (NaCl, thin film, cm^{-1}): 2987, 2950, 2236, 1702, 1438, 1414, 1339, 1240, 1213, 1112, 1054, 1022, 946, 848, 760, 741

HRMS (FAB, m/z): calc'd for $C_{14}H_{14}N_3O_2$ $[M+H]^+$: 256.1086 ; found: 256.1074.

Chiral SFC: (AD-H, 2.5 mL/min, 15% IPA in CO_2, λ = 254 nm): t_R (minor) = 3.3 min, t_R (major) = 3.1 min.

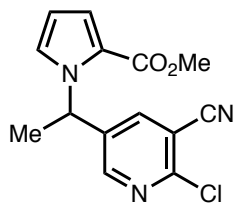

435j (TJD-6-003): Prepared from 5-bromo-2-chloronicotinonitrile (**4337**, 43.5 mg, 0.2 mmol) and BF_3K (**432b**, 81.8 mg, 0.3 mmol) according to General General Procedure A in 2-MeTHF with 4-F-Ph BiOX (**L76**). The crude residue was purified by column chromatography (silica gel, 15% EtOAc/hexanes) to yield **435j** (44.6 mg, 77% yield) in 97% ee as a colorless oil.

$\mathbf{R}_f$ = 0.39 (silica gel, 20% EtOAc/hexanes, UV).

$[\boldsymbol{a}]_D^{22}$ = 87° (c = 1.0, $CHCl_3$).

^{1}H NMR (400 MHz, $CDCl_3$): δ 8.35 (dd, J = 2.5, 0.6 Hz, 1H), 7.55 (dd, J = 2.5, 0.7 Hz, 1H), 7.12 (dd, J = 2.8, 1.7 Hz, 1H), 7.04 (dd, J = 4.0, 1.7 Hz, 1H), 6.58 (q, J = 7.2 Hz, 1H), 6.30 (dd, J = 4.0, 2.8 Hz, 1H), 3.75 (s, 3H), 1.85 (d, J = 7.3 Hz, 3H)

^{13}C NMR (101 MHz, $CDCl_3$): δ 161.5, 151.5, 150.9, 140.0, 138.9, 124.5, 122.2, 119.7, 114.7, 110.8, 109.9, 52.7, 51.4, 21.9

FTIR (NaCl, thin film, cm^{-1}): 2949, 1698, 1558, 1532, 1414, 1341, 1238, 1115, 913, 739

HMRS (ESI-TOF, m/z): $C_{14}H_{13}N_3O_2Cl$; cal'd for $[M+H]^+$: 290.0696, found: 290.0682

Chiral SFC: (IC, 2.5 mL/min, 15% MeOH in CO_2, λ = 254 nm):

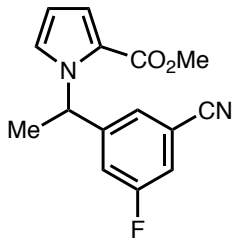

435k (TJD-5-300): Prepared from 3-bromo-5-fluorobenzonitrile (**433k**, 40.0 mg, 0.2 mmol) and BF_3K (**432b**, 81.8 mg, 0.3 mmol) according to General Procedure A in 2-MeTHF with 4-F-Ph BiOX (**L76**). The crude residue was purified by column chromatography (silica gel, 8.5% EtOAc/hexanes) to yield **435k** (43 mg, 79% yield) in 97% ee as a colorless oil.

$\mathbf{R}_f$ = 0.55 (silica gel, 20% EtOAc/hexanes, UV).

$[\boldsymbol{\alpha}]_D^{21}$ = 56° (c = 1.0, $CHCl_3$).

^{1}H NMR (400 MHz, $CDCl_3$): δ 7.24 – 7.17 (m, 1H), 7.15 – 6.94 (m, 4H), 6.58 (q, J = 7.2 Hz, 1H), 6.33 – 6.22 (m, 1H), 3.75 (d, J = 1.6 Hz, 3H), 1.87 – 1.76 (m, 3H)

^{13}C NMR (101 MHz, $CDCl_3$): δ 162.5 (d, *J* = 250.9 Hz), 161.6, 148.4 (d, *J* = 7.3 Hz), 125.6 (d, *J* = 3.3 Hz), 124.9, 122.2, 119.3, 118.3 (d, *J* = 20.2 Hz), 118.2 (d, *J* = 22.9 Hz), 114.1 (d, *J* =9.6 Hz), 109.5, 54.7, 51.3, 2.0

^{19}F NMR (282 MHz, $CDCl_3$) δ -112.41 (dd, J = 9.3, 7.9 Hz).

FTIR (NaCl, thin film, cm^{-1}): 2950, 2233, 1699, 1596, 1531, 1437, 1343, 1236, 1115, 964, 874, 743

HRMS (ESI-TOF, m/z): $C_{15}H_{14}N_2O_2F$; cal'd for $[M+H]^+$: 273.1039, found: 273.1036

Chiral SFC: (OD-H, 2.5 mL/min, 10% MeOH in CO_2, (λ = 254 nm):

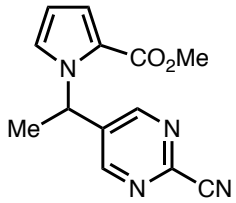

435l (CRL-6-196): Prepared from 5-bromopyrimidine-2-carbonitrile (**433l**, 36.8 mg, 0.3 mmol) and BF_3K (**432b**, 81.8 mg, 0.3 mmol) according to General Procedure A in 2-MeTHF with 4-F-Ph BiOX (**L76**). The crude residue was purified by column chromatography (silica gel, 10 to 40% EtOAc/hexanes) to yield **435l** (39 mg, 77% yield) in 95% ee as a colorless oil.

$\mathbf{R}_f$ = 0.43 (silica gel, 30% EtOAc/hexanes, UV).

$[\boldsymbol{\alpha}]_D^{22}$ = 60° (c = 1.1, $CHCl_3$).

^{1}H NMR (400 MHz, $CDCl_3$): δ 8.48 (d, *J* = 0.6 Hz, 2H), 7.15 (dd, *J* = 2.8, 1.7 Hz, 1H), 7.06 (dd, *J* = 4.0, 1.7 Hz, 1H), 6.61 (q, *J* = 7.3 Hz, 1H), 6.32 (dd, *J* = 4.0, 2.8 Hz, 1H), 3.74 (s, 3H), 1.90 (d, *J* = 7.3 Hz, 3H).

^{13}C NMR (101 MHz, $CDCl_3$): δ 161.53, 155.84, 144.01, 139.70, 124.57, 122.25, 119.79, 115.68, 110.07, 51.97, 51.46, 21.60.

FTIR (NaCl, thin film, cm^{-1}): 2950, 1699, 1555, 1438, 1416, 1339, 1242, 1214, 1114, 942, 793, 761, 743

HRMS (FAB, m/z): calc'd for $C_{13}H_{13}N_4O_2$ $[M+H]^+$: 257.1039 ; found: 257.1023.

Chiral SFC: (AD-H, 2.5 mL/min, 10% IPA in CO_2, λ = 280 nm): t_R (minor) = 4.5 min, t_R (major) = 4.2 min.

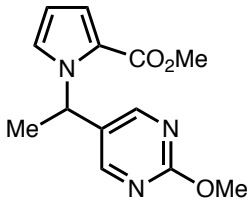

435m (CRL-6-198): Prepared from 5-bromo-2-methoxypyrimidine (**433m**, 37.8 mg, 0.2 mmol) and BF_3K (**432b**, 81.8 mg, 0.3 mmol) according to General Procedure A in 2-MeTHF with 4-F-Ph BiOX (**L76**). The crude residue was purified by column chromatography (silica gel, 30 to 40% EtOAc/hexanes) to yield **435m** (33 mg, 63% yield) in 96% ee as a colorless oil.

R_f = 0.30 (silica gel, 30% EtOAc/hexanes, UV).

$[\alpha]_D^{21}$ = 99° (c = 1.51, $CHCl_3$).

^{1}H NMR (400 MHz, $CDCl_3$): δ 8.28 (d, *J* = 0.6 Hz, 2H), 7.04 (dd, *J* = 2.8, 1.7 Hz, 1H), 6.99 (dd, *J* = 4.0, 1.8 Hz, 1H), 6.57 (q, *J* = 7.2 Hz, 1H), 6.22 (dd, *J* = 4.0, 2.8 Hz, 1H), 3.97 (s, 3H), 3.76 (s, 3H), 1.82 (d, *J* = 7.2 Hz, 3H).

^{13}C NMR (101 MHz, $CDCl_3$): δ 165.15, 161.63, 157.55, 129.74, 124.67, 122.06, 119.13, 109.38, 55.07, 51.28, 51.17, 21.74.

FTIR (NaCl, thin film, cm^{-1}): 2952, 1702, 1598, 1560, 1474, 1411, 1338, 1228, 1112, 1039, 943, 805, 738

HRMS (FAB, m/z): calc'd for $C_{13}H_{16}N_3O_3$ $[M+H]^+$: 262.1192 ; found: 262.1183.

Chiral SFC: (IC, 2.5 mL/min, 25% IPA in CO_2, λ = 254 nm): t_R (minor) = 4.1 min, t_R (major) = 4.4 min.

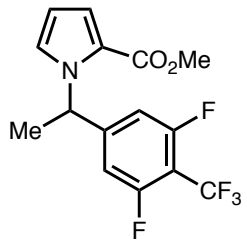

435n (CRL-6-200): Prepared from 5-bromo-1,3-difluoro-2-(trifluoromethyl)benzene (**433n**, 52.2 mg, 0.2 mmol) and BF_3K (**432b**, 81.8 mg, 0.3 mmol) according to General Procedure A in 2-MeTHF with 4-F-Ph BiOX (**L76**). The crude residue was purified by column chromatography (silica gel, 2–20% EtOAc/hexanes) to yield **435n** (38.7 mg, 58% yield) in 97% ee as a colorless oil.

R_f = 0.68 (silica gel, 30% EtOAc/hexanes, UV).

$[\alpha]_D^{25}$ = 38° (c = 0.97, $CHCl_3$).

^{1}H NMR (400 MHz, $CDCl_3$): δ 7.09 (dd, *J* = 2.8, 1.8 Hz, 1H), 7.05 (dd, *J* = 3.9, 1.7 Hz, 1H), 6.70 – 6.61 (m, 2H), 6.55 (q, *J* = 7.2 Hz, 1H), 6.28 (dd, *J* = 4.0, 2.7 Hz, 1H), 3.76 (s, 3H), 1.81 (d, *J* = 7.2 Hz, 3H).

^{13}C NMR (101 MHz, $CDCl_3$): δ 161.55 (d, *J* = 4.6 Hz), 159.20 – 158.66 (m), 151.63 (t, *J* = 9.3 Hz), 124.88, 123.04, 122.32, 120.33, 119.31, 110.14 (dd, *J* = 23.4, 3.3 Hz), 109.47, 54.86 (d, *J* = 2.0 Hz), 51.34, 21.83.

^{19}F NMR (282 MHz, $CDCl_3$) δ -59.59 (t, *J* = 21.6 Hz), -111.09 – -114.78 (m).

Chiral SFC: (OJ-H, 2.5 mL/min, 7% IPA in CO_2, λ = 254 nm): t_R (minor) = 2.9 min, t_R (major) = 2.3 min.

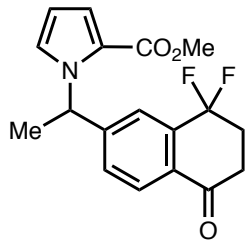

435o (TJD-6-004): Prepared from 6-bromo-4,4-difluoro-3,4-dihydronaphthalen-1(2H)-one (**433o**, 52.2 mg, 0.2 mmol) and BF_3K (**432b**, 81.8 mg, 0.3 mmol) according to General Procedure A in 2-MeTHF with 4-F-Ph BiOX (**L76**). The crude residue was purified by column chromatography (silica gel, 15% EtOAc/hexanes) to yield **435o** (45.9 mg, 69% yield) in 94% ee as a colorless oil.

R_f = 0.43 (silica gel, 20% EtOAc/hexanes, UV).

$[\boldsymbol{\alpha}]_D^{22}$ = 73° (c = 1.0, $CHCl_3$).

^{1}H NMR (400 MHz, $CDCl_3$): δ 7.97 (dt, J = 8.2, 1.3 Hz, 1H), 7.52 – 7.46 (m, 1H), 7.29 – 7.23 (m, 1H), 7.08 (dd, J = 2.8, 1.8 Hz, 1H), 7.03 (dd, J = 3.9, 1.7 Hz, 1H), 6.66 (q, J = 7.2 Hz, 1H), 6.26 (dd, J = 3.9, 2.7 Hz, 1H), 3.75 (s, 3H), 2.94 – 2.82 (m, 2H), 2.70 – 2.55 (m, 2H), 1.85 (d, J = 7.2 Hz, 3H).

^{13}C NMR (101 MHz, $CDCl_3$): δ 194.4 (t, J = 1.4 Hz), 161.6, 150.6 (t, J = 1.1 Hz), 137.3 (t, J = 25. 9 Hz), 130.5 (t, J = 5.5 Hz), 128.9 (t, J = 1.4 Hz), 127.8, 125.2, 122.3, 122.0 (t, J = 4.1 Hz), 120.6, 119.1, 118.2, 115.7, 109.2, 55.4, 51.2, 34.6 (t, J = 5.3 Hz), 32.4 (t, J = 25.7 Hz), 22.0.

^{19}F NMR (282 MHz, $CDCl_3$) δ -95.60 (t, J = 13.0 Hz)

FTIR (NaCl, thin film, cm^{-1}): 3378, 2950, 1694, 1611, 1530, 1448, 1238, 975, 849, 746

HRMS (ESI-TOF, m/z): $C_{18}H_{18}NO_3F_2$; cal'd for $[M+H]^+$: 334.1255, found: 334.1259

Chiral SFC: (OD-H, 2.5 mL/min, 30% IPA in CO_2, (λ = 254 nm)

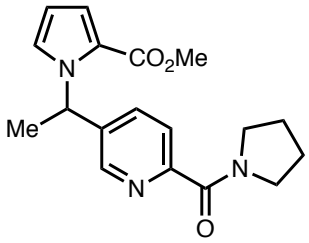

435p (CRL-6-096): Prepared from (5-bromopyridin-2-yl)(pyrrolidin-1-yl)methanone (**433p**, 51 mg, 0.2 mmol) and BF_3K (**432b**, 81.8 mg, 0.3 mmol) according to General Procedure A in 2-MeTHF with heptyl BiOX (**L71**). The crude residue was purified by column chromatography (silica gel, 60–100% EtOAc/hexanes) to yield **435p** (35.8 mg, 55% yield) in 0% ee as a colorless oil.

$\mathbf{R}_f$ = 0.3 (silica gel, 80% EtOAc/DCM, UV).

$[\boldsymbol{\alpha}]_D^{25}$ = –1.5° (c = 1.89, $CHCl_3$).

^{1}H NMR (400 MHz, $CDCl_3$): δ δ 8.36 (dt, *J* = 2.5, 0.7 Hz, 1H), 7.77 (dd, *J* = 8.1, 0.9 Hz, 1H), 7.43 (ddd, *J* = 8.2, 2.3, 0.7 Hz, 1H), 7.07 (dd, *J* = 2.7, 1.8 Hz, 1H), 7.02 (dd, *J* = 3.9, 1.8 Hz, 1H), 6.65 (q, *J* = 7.2 Hz, 1H), 6.24 (dd, *J* = 4.0, 2.7 Hz, 1H), 3.75 (s, 3H), 3.75 – 3.71 (m, 2H), 3.69 – 3.62 (m, 2H), 1.86 (s, 4H), 1.84 (d, *J* = 7.2 Hz, 3H).

^{13}C NMR (101 MHz, $CDCl_3$): δ 166.20, 161.60, 153.53, 146.10, 140.00, 134.40, 125.06, 123.99, 122.23, 119.07, 109.19, 53.47, 51.25, 49.28, 47.04, 26.76, 24.14, 22.02, 14.20.

FTIR (NaCl, thin film, cm^{-1}): 2967, 2876, 1702, 1625, 1436, 1339, 1237, 1212, 1111, 1022, 736.

HRMS (FAB, m/z): calc'd for $C_{18}H_{22}N_3O_3$ $[M+H]^+$: 328.1661 ; found: 328.1657.

c. Characterization of Reaction Products – Nucleophile Scope

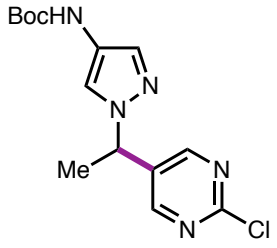

434g (TJD-6-010): Prepared from 5-bromo-2-chloropyrimidine (**433g**, 38.7 mg, 0.2 mmol) and BF_3K (**432a**, 95.1 mg, 0.3 mmol) according to General Procedure A in 2-MeTHF with 4-heptyl BiOX (**L71**). The crude residue was purified by column chromatography (silica gel, 30/20/50 EtOAc/DCM/hexanes) to yield **434g** (45.6 mg, 70% yield) in 80% ee as a white solid.

$\mathbf{R}_f$ = 0.4.6 (silica gel, 50% EtOAc/hexanes, UV).

$[\boldsymbol{\alpha}]_D^{22}$ = –7° (c = 1.0, $CHCl_3$).

^{1}H NMR (400 MHz, $CDCl_3$): δ 8.46 (s, 2H), 7.82 (s, 1H), 7.35 (s, 1H), 6.29 (s, 1H), 5.44 (q, J = 7.1 Hz, 1H), 1.92 (d, J = 7.1 Hz, 3H), 1.49 (s, 9H)

^{13}C NMR (101 MHz, $CDCl_3$): δ 161.0, 157.9, 153.0, 134.0, 130.8, 122.5, 118.7, 80.9, 56.7, 28.4, 20.8.

FTIR (NaCl, thin film, cm^{-1}): 2954, 1700, 1598, 1550, 1399, 1249, 1164, 772, 676

HRMS (ESI-TOF, m/z): $C_{14}H_{19}N_5O_2Cl$; cal'd for $[M+H]^+$: 324.1227, found: 324.1240

Chiral SFC: (AD-H, 2.5 mL/min, 35% IPA in CO_2, λ = 254 nm):

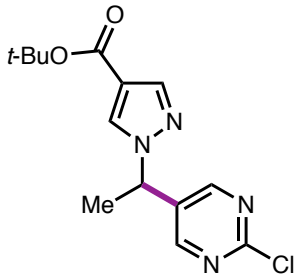

436 (CRL-6-204): Prepared from 5-bromo-2-chloropyrimidine (**433g**, 38.7 mg, 0.2 mmol) and BF_3K (**432c**, 90.6 mg, 0.3 mmol) according to General Procedure A in CPME with 4-heptyl BiOX (**L71**). The crude residue was purified by column chromatography (silica gel, 5–25% EtOAc/DCM) to yield **436** (28.3 mg, 46% yield) in 83% ee as a yellow oil.

$\mathbf{R}_f$ = 0.43 (silica gel, 20% EtOAc/DCM, UV).

$[\boldsymbol{\alpha}]_D^{21}$ = –2° (c = 1.0, $CHCl_3$).

^{1}H NMR (400 MHz, $CDCl_3$): δ 8.52 (s, 2H), 7.93 (d, J = 0.6 Hz, 1H), 7.91 – 7.86 (m, 1H), 5.52 (q, J = 7.1 Hz, 1H), 1.96 (d, J = 7.1 Hz, 3H), 1.54 (s, 9H).

^{13}C NMR (101 MHz, $CDCl_3$): δ 162.11, 161.35, 157.99, 141.98, 133.15, 131.19, 117.65, 81.15, 56.99, 29.85, 28.42, 21.04.

Chiral SFC: (IC, 2.5 mL/min, 30% IPA in CO_2, λ = 210 nm): t_R (minor) = 3.0 min, t_R (major) = 4.0 min.

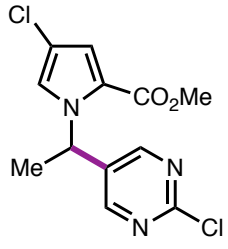

437 (CRL-6-208): Prepared from 5-bromo-2-chloropyrimidine (**433g**, 38.7 mg, 0.1 mmol) and BF_3K (**432d**, 44 mg, 0.15 mmol) according to General Procedure B in *i*-PrOAc with 4-F-Ph BiOX (**L76**). The crude residue was purified by column chromatography (silica gel, 5–30% EtOAc/hexanes) to yield **437** (11.1 mg, 36% yield) in 95% ee as a colorless oil.

$\mathbf{R}_f$ = 0.52 (silica gel, 30% EtOAc/hexanes, UV).

^{1}H NMR (400 MHz, $CDCl_3$): δ 8.38 (d, J = 0.6 Hz, 2H), 7.03 (d, J = 2.0 Hz, 1H), 6.92 (d, J = 1.9 Hz, 1H), 6.57 (q, J = 7.2 Hz, 1H), 3.76 (s, 3H), 1.84 (d, J = 7.3 Hz, 3H).

^{13}C NMR (101 MHz, $CDCl_3$): δ 160.82, 160.79, 157.67, 134.64, 121.86, 121.75, 118.41, 113.69, 51.73, 51.67, 21.56.

Chiral SFC: (AD-H, 2.5 mL/min, 7% IPA in CO_2, (λ = 254 nm): t_R (minor) = 7.5 min, t_R (major) = 9.1 min.

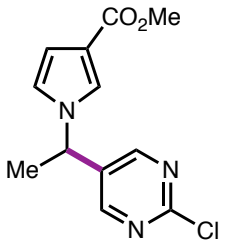

438 (TJD-6-009): Prepared from 5-bromo-2-chloropyrimidine (**433g**, 38.7 mg, 0.2 mmol) and BF_3K (**432e**, 77.7 mg, 0.3 mmol) according to General Procedure A in 2-MeTHF with 4-heptylBiOX (**L71**). The crude residue was purified by column chromatography (silica gel, 30% EtOAc/hexanes) to yield **438** (41.2 mg, 78% yield) in 66% ee as a colorless oil.

$\mathbf{R}_f$ = 0.50 (silica gel, 50% EtOAc/hexanes, UV).

$[\alpha]_D^{22}$ = –13° (c = 1.0, $CHCl_3$).

^{1}H NMR (400 MHz, $CDCl_3$): δ 8.34 (d, J = 0.6 Hz, 2H), 7.39 (t, J = 1.9 Hz, 1H), 6.70 – 6.63 (m, 2H), 5.33 (q, J = 7.1 Hz, 1H), 3.81 (s, 3H), 1.91 (d, J = 7.1 Hz, 3H).

^{13}C NMR (101 MHz, $CDCl_3$): δ 164.9, 161.3, 157.5, 134.2, 124.2, 120.4, 117.3, 111.5, 54.3, 51.4, 21.4.

FTIR (NaCl, thin film, cm^{-1}): 2950, 1698, 1538, 1398, 1158, 994, 826, 762, 67

HRMS (ESI-TOF, m/z): $C_{12}H_{13}N_3O_2Cl$; cal'd for $[M+H]^+$: 266.0696, found: 266.0703

Chiral SFC: (AD-H, 2.5 mL/min, 25% IPA in CO_2, (λ = 280 nm)

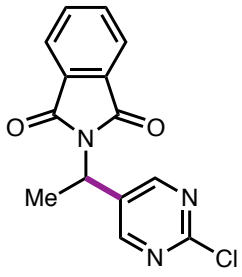

439 (CRL-6-205): Prepared from 5-bromo-2-chloropyrimidine (**433g**, 38.7 mg, 0.2 mmol) and BF_3K (**432f**, 84.3 mg, 0.3 mmol) according to General Procedure A in DME with 4-F-Ph BiOX (**L76**). 2.0 mg ethylene carbonate added, and the ^{1}H NMR was calculated (25% yield **439**). The crude residue was purified by column chromatography (silica gel, 20–40% EtOAc/hexanes).

The material was then repurified by prep TLC (5% EtOAc/DCM) to afford **429** as white solids (77% ee).

R_f = 0.4 (silica gel, 30% EtOAc/hexanes, UV).

^{1}H NMR (400 MHz, $CDCl_3$): δ 8.78 (d, J = 0.5 Hz, 2H), 7.91 – 7.79 (m, 2H), 7.79 – 7.69 (m, 2H), 5.67 – 5.49 (m, 1H), 1.94 (d, J = 7.4 Hz, 3H).

^{13}C NMR (101 MHz, $CDCl_3$): δ 167.71, 160.96, 159.27, 134.60, 132.16, 131.67, 123.74, 44.90, 17.13.

Chiral SFC: IC, 2.5 mL/min, 35% MeCN in CO_2, λ = 254 nm): t_R (minor) = 3.3 min, t_R (major) = 4.0 min.

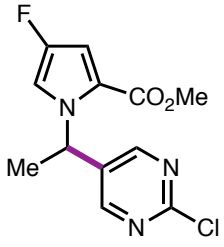

440 (CRL-6-216): Prepared from 5-bromo-2-chloropyrimidine (**433g**, 38.7 mg, 0.2 mmol) and BF_3K (**432g**, 83.1 mg, 0.3 mmol) according to General Procedure A in 2-MeTHF with 4-F-Ph BiOX (**L76**). The crude residue was purified by column chromatography (silica gel, 5–30% EtOAc/hexanes) to yield **440** (35.4 mg, 62% yield) in 97% ee as a colorless oil.

R_f = 0.47 (silica gel, 30% EtOAc/hexanes, UV).

^{1}H NMR (400 MHz, $CDCl_3$): δ 8.36 (d, J = 0.6 Hz, 2H), 6.87 (dd, J = 3.3, 2.1 Hz, 1H), 6.69 (d, J = 2.1 Hz, 1H), 6.64 – 6.52 (m, 1H), 3.75 (s, 3H), 1.82 (d, J = 7.2 Hz, 3H).

^{13}C NMR (101 MHz, $CDCl_3$): δ 161.06 (d, J = 2.9 Hz), 160.71, 157.60, 152.22, 149.80, 134.86, 118.74 (d, J = 5.7 Hz), 109.16 (d, J = 28.0 Hz), 105.73 (d, J = 15.3 Hz), 51.48 (d, J = 36.0 Hz), 21.44.

Chiral SFC: (IC, 2.5 mL/min, 15% IPA in CO_2, λ = 254 nm): t_R (minor) = 7.8 min, t_R (major) = 8.9 min.

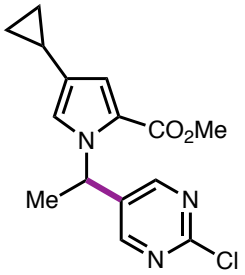

441 (TJD-6-046): Prepared from 5-bromo-2-chloropyrimidine (**433g**, 38.7 mg, 0.2 mmol) and BF_3K (**432h**, 89.7 mg, 0.3 mmol) according to General Procedure A in 2-MeTHF with 4-F-Ph BiOX (**L76**). The crude residue was purified by column chromatography (silica gel, 10% EtOAc/PhMe) to yield **441** (41.2 mg, 67% yield) in 97% ee as a colorless oil.

$[\boldsymbol{a}]_D^{22}$ = 24° (c = 1.0, $CHCl_3$).

^{1}H NMR (400 MHz, $CDCl_3$): δ 8.32 (s, 2H), 6.89 (d, J = 2.0 Hz, 1H), 6.72 (d, J = 1.9 Hz, 1H), 6.53 (q, J = 7.2 Hz, 1H), 3.73 (s, 3H), 1.83 (d, J = 7.3 Hz, 3H), 1.76 – 1.62 (m, 1H), 0.91 – 0.76 (m, 2H), 0.56 – 0.44 (m, 2H).

^{13}C NMR (101 MHz, $CDCl_3$): 161.5, 160.4, 157.7, 135.5, 128.2, 121.7, 121.7, 116.7, 51.3, 51.0, 21.5, 8.2, 8.1, 7.8.

FTIR (NaCl, thin film, cm^{-1}): 2950, 1699, 1549, 1439, 1401, 1340, 1238, 1105, 980, 830, 677

HRMS (ESI-TOF, m/z): $C_{15}H_{17}N_3O_2Cl$; cal'd for $[M+H]^+$: 306.1009, found: 306.0992

Chiral SFC: (IC, 2.5 mL/min, 30% IPA in CO_2, λ = 254 nm):

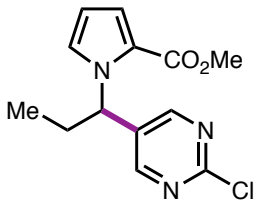

442 (TJD-6-045): Prepared from 5-bromo-2-chloropyrimidine (**433g**, 38.7 mg, 0.2 mmol) and BF_3K (**432i**, 83.9 mg, 0.3 mmol) according to General Procedure A in 2-MeTHF with 4-F-Ph BiOX (**L76**). The crude residue was purified by column chromatography (silica gel, 9% EtOAc/hexanes) to yield **442** (35.6 mg, 64% yield) in 95% ee as a colorless oil.

$[\boldsymbol{a}]_D^{22}$ = 71° (c = 1.0, $CHCl_3$).

^{1}H NMR (400 MHz, $CDCl_3$): δ 8.41 (s, 2H), 7.10 (dd, J = 2.8, 1.7 Hz, 1H), 7.00 (dd, J = 4.0, 1.7 Hz, 1H), 6.36 (dd, J = 9.0, 6.9 Hz, 1H), 6.27 (dd, J = 4.0, 2.8 Hz, 1H), 3.76 (s, 3H), 2.37 – 2.08 (m, 2H), 0.98 (t, J = 7.3 Hz, 3H).

^{13}C NMR (101 MHz, $CDCl_3$): δ 161.7, 160.6, 158.2, 134.2, 124.4, 122.5, 119.2, 110.0, 57.1, 51.4, 28.5, 11.0.

FTIR (NaCl, thin film, cm^{-1}): 2972, 1698, 1579, 1549, 1439, 1400, 1338, 1227, 1155, 1109, 1070, 851, 744

HRMS (ESI-TOF, m/z): $C_{13}H_{15}N_3O_2Cl$; cal'd for $[M+H]^+$: 280.0853, found: 280.0842

Chiral SFC: (IC, 2.5 mL/min, 20% IPA in CO_2

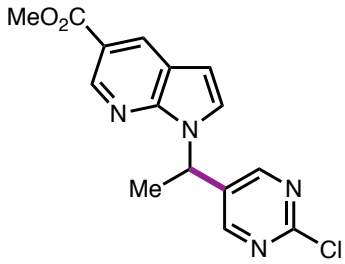

443 (TJD-6-044): Prepared from 5-bromo-2-chloropyrimidine (**433g**, 38.7 mg, 0.2 mmol) and BF_3K (**432j**, 93.0 mg, 0.3 mmol) according to General Procedure A in CPME with 4-heptyl BiOX (**L71**). Added 21.0 mg 1,1,2,2,-tetrachloroethane, and the yield was calculated by ^{1}H NMR (59% yield **443**. The crude material was purified by prep TLC (1.5% MeOH/DCM). The middle of the band was taken, and purified again by prep TLC (40% Et_2O/PhMe) to afford **443** (95% ee).

$[\boldsymbol{\alpha}]_{\boldsymbol{D}}^{\mathbf{21}}$ = 190° (c = 0.3, $CHCl_3$).

^{1}H NMR (500 MHz, $CDCl_3$): δ 8.96 (s, 1H), 8.60 (s, 1H), 8.53 (s, 2H), 7.35 (d, J = 3.5 Hz, 1H), 6.67 (d, J = 3.5 Hz, 1H), 6.38 – 6.26 (m, 1H), 3.97 (s, 3H), 2.09 – 1.96 (m, 3H).

^{13}C NMR (101 MHz, $CDCl_3$): δ 167.0, 160.9, 158.1, 149.0, 145.5, 134.0, 131.6, 125.6, 120.1, 119.6, 103.1, 52.3, 48.6, 20.0.

FTIR (NaCl, thin film, cm^{-1}): 2922, 1716, 1602, 1576, 1549, 1404, 1315, 1210 ,1162, 937, 730

HRMS (ESI-TOF, m/z): $C_{15}H_{14}N_4O_2Cl$; cal'd for $[M+H]^+$: 317.0805, found: 317.0805

Chiral SFC: (OJ-H, 2.5 mL/min, 30% IPA in CO_2

3.6 REFERENCES

(1) Baumann, M.; Baxendale, I. R.; Ley, S. V.; Nikbin, N. *Beilstein J. Org. Chem.* **2011**, *7* (1), 442–495.

(2) Josey, A. D.; Jenner, E. L. *J. Org. Chem.* **1962**, *27* (7), 2466–2470.

(3) Jefford, C. W.; de Villedon de Naide, F.; Sienkiewicz, K. *Tetrahedron Asymmetry* **1996**, *7* (4), 1069–1076.

(4) Polshettiwar, V.; Baruwati, B.; Varma, R. S. *Chem. Commun.* **2009**, No. 14, 1837–1839.

(5) Baig, R. B. N.; Varma, R. S. *Green Chem.* **2013**, *15* (2), 398–417.

(6) Aydogan, F.; Yolacan, C. *J. Chem.* **2013**, *2013*, e976724.

(7) D'Silva, C.; Walker, D. A. *J. Org. Chem.* **1998**, *63* (19), 6715–6718.

(8) Aydogan, F.; Basarir, M.; Yolacan, C.; Demir, A. S. *Tetrahedron* **2007**, *63* (39), 9746–9750.

(9) Singh, K.; Kabadwal, L. M.; Bera, S.; Alanthadka, A.; Banerjee, D. *J. Org. Chem.* **2018**, *83* (24), 15406–15414.

(10) Borghs, J. C.; Lebedev, Y.; Rueping, M.; El-Sepelgy, O. *Org. Lett.* **2019**, *21* (1), 70–74.

(11) Laha, J. K.; Cuny, G. D. *J. Org. Chem.* **2011**, *76* (20), 8477–8482.

(12) Laha, J. K.; Bhimpuria, R. A.; Hunjan, M. K. *Chem. – Eur. J.* **2017**, *23* (9), 2044–2050.

(13) Ruan, Z.; Huang, Z.; Xu, Z.; Zeng, S.; Feng, P.; Sun, P.-H. *Sci. China Chem.* **2021**, *64* (5), 800–807.

(14) Pandey, G.; Laha, R.; Singh, D. *J. Org. Chem.* **2016**, *81* (16), 7161–7171.

(15) Song, C.; Dong, X.; Yi, H.; Chiang, C.-W.; Lei, A. *ACS Catal.* **2018**, *8* (3), 2195–2199.

(16) Xue, Q.; Xie, J.; Li, H.; Cheng, Y.; Zhu, C. *Chem. Commun.* **2013**, *49* (35), 3700–3702.

(17) Liu, W.; Liu, C.; Zhang, Y.; Sun, Y.; Abdukadera, A.; Wang, B.; Li, H.; Ma, X.; Zhang, Z. *Org. Biomol. Chem.* **2015**, *13* (26), 7154–7158.

(18) Liu, X.; Yu, G.; Li, J.; Wang, D.; Chen, Y.; Shi, K.; Chen, B. *Synlett* **2013**, *24* (12), 1588–1594.

(19) Deb, I.; Coiro, D. J.; Seidel, D. *Chem. Commun.* **2011**, *47* (22), 6473–6475.

(20) Wang, J.; Shen, Q.; Zhang, J.; Song, G. *Tetrahedron Lett.* **2015**, *56* (22), 2913–2916.

(21) Pahadi, N. K.; Paley, M.; Jana, R.; Waetzig, S. R.; Tunge, J. A. *J. Am. Chem. Soc.* **2009**, *131* (46), 16626–16627.

(22) Haydl, A. M.; Hilpert, L. J.; Breit, B. *Chem. – Eur. J.* **2016**, *22* (19), 6547–6551.

(23) Haydl, A. M.; Xu, K.; Breit, B. *Angew. Chem. Int. Ed.* **2015**, *54* (24), 7149–7153.

(24) Shea, M. D.; Mansoor, U. F.; Hopkins, B. A. *Org. Lett.* **2020**, *22* (3), 1052–1055.

(25) Fan, L.; Jia, J.; Hou, H.; Lefebvre, Q.; Rueping, M. *Chem. – Eur. J.* **2016**, *22* (46), 16437–16440.

(26) Molander, G. A.; Ryu, D.; Hosseini-Sarvari, M.; Devulapally, R.; Seapy, D. G. *J. Org. Chem.* **2013**, *78* (13), 6648–6656.

(27) Devulapally, R.; Fleury-Brégeot, N.; Molander, G. A.; Seapy, D. G. *Tetrahedron Lett.* **2012**, *53* (9), 1051–1055.

(28) Nadaf, R. N.; Seapy, D. G. *Synth. Commun.* **2014**, *44* (14), 2012–2020.

(29) Pezzetta, C.; Bonifazi, D.; Davidson, R. W. M. *Org. Lett.* **2019**, *21* (22), 8957–8961.

(30) Poremba, K. E.; Kadunce, N. T.; Suzuki, N.; Cherney, A. H.; Reisman, S. E. *J. Am. Chem. Soc.* **2017**, *139* (16), 5684–5687.

(31) Lipp, A.; Badir, S. O.; Molander, G. A. *Angew. Chem. Int. Ed.* **2021**, *60* (4), 1714–1726.

(32) Cho, D. W.; Mariano, P. S.; Yoon, U. C. *Beilstein J. Org. Chem.* **2014**, *10* (1), 514–527.

(33) Bera, S.; Mao, R.; Hu, X. *Nat. Chem.* **2021**, *13* (3), 270–277.

Appendix 3

Spectra Relevant to Chapter 3:

Enantioselective Photoredox Catalysis for the Cross-Coupling of Azole-Containing Alkyl BF_3K Salts and Electron-Poor Aryl Bromides

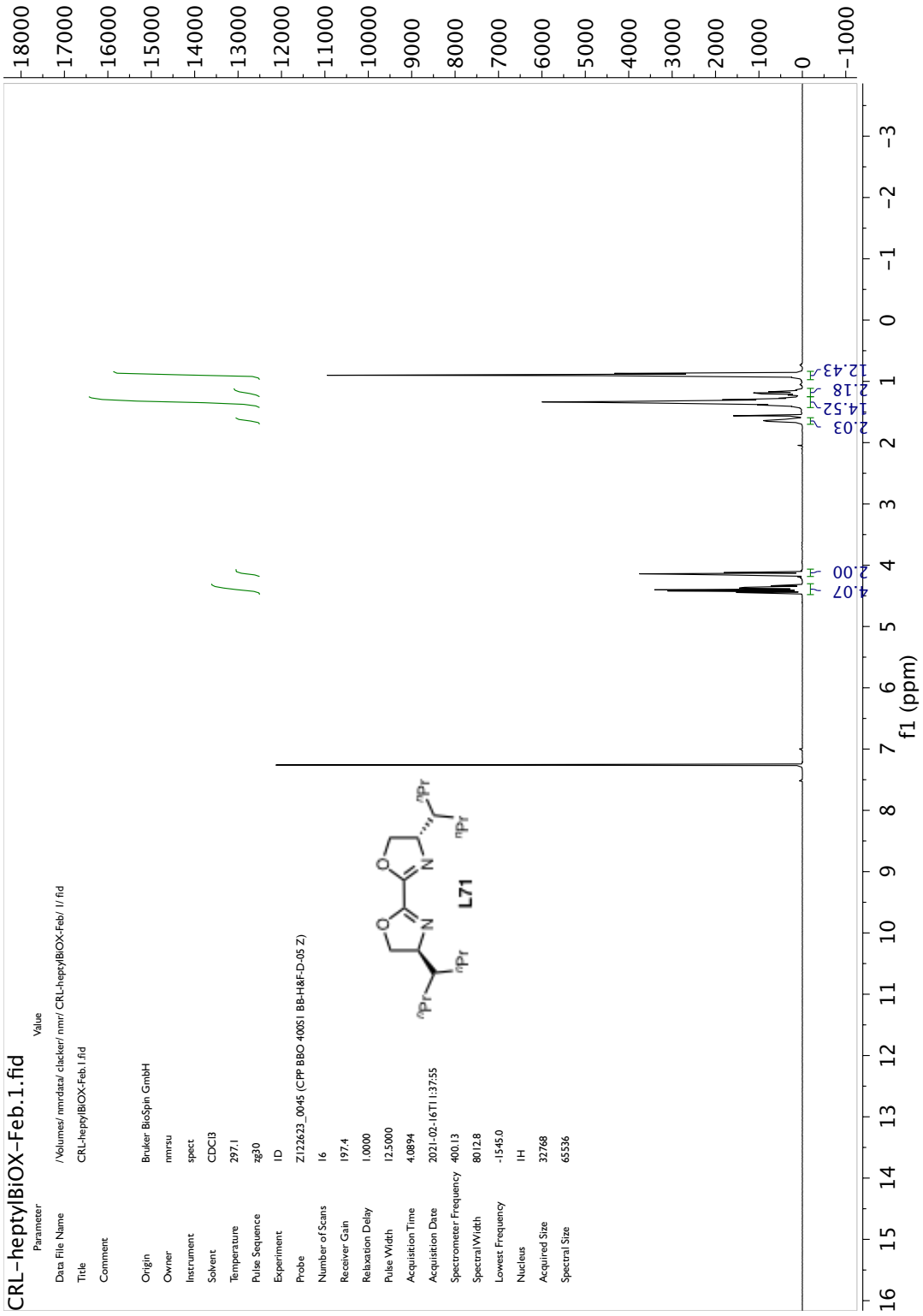
CRL-heptylBiOX-Feb.1.fid
Parameter
Value
Data File Name
/Volumes/ nmrdata/ clacker/ nmr/ CRL-heptylBiOX-Feb/ 1/ fid
Title
CRL-heptylBiOX-Feb.1.fid
Comment
Origin
Bruker BioSpin GmbH
Owner
nmrsu
Instrument
spect
Solvent
CDCl3
Temperature
297.1
Pulse Sequence
zg30
Experiment
1D
Probe
Z122623_0045 (CPP BBO 400S1 BB-H&F-D-05 Z)
Number of Scans
16
Receiver Gain
197.4
Relaxation Delay
1.0000
Pulse Width
12.5000
Acquisition Time
4.0894
Acquisition Date
2021-02-16T11:37:55
Spectrometer Frequency
400.13
Spectral Width
8012.8
Lowest Frequency
-1545.0
Nucleus
1H
Acquired Size
32768
Spectral Size
65536
L71
12.43
2.18
14.52
2.03
4.07
2.00
f1 (ppm)

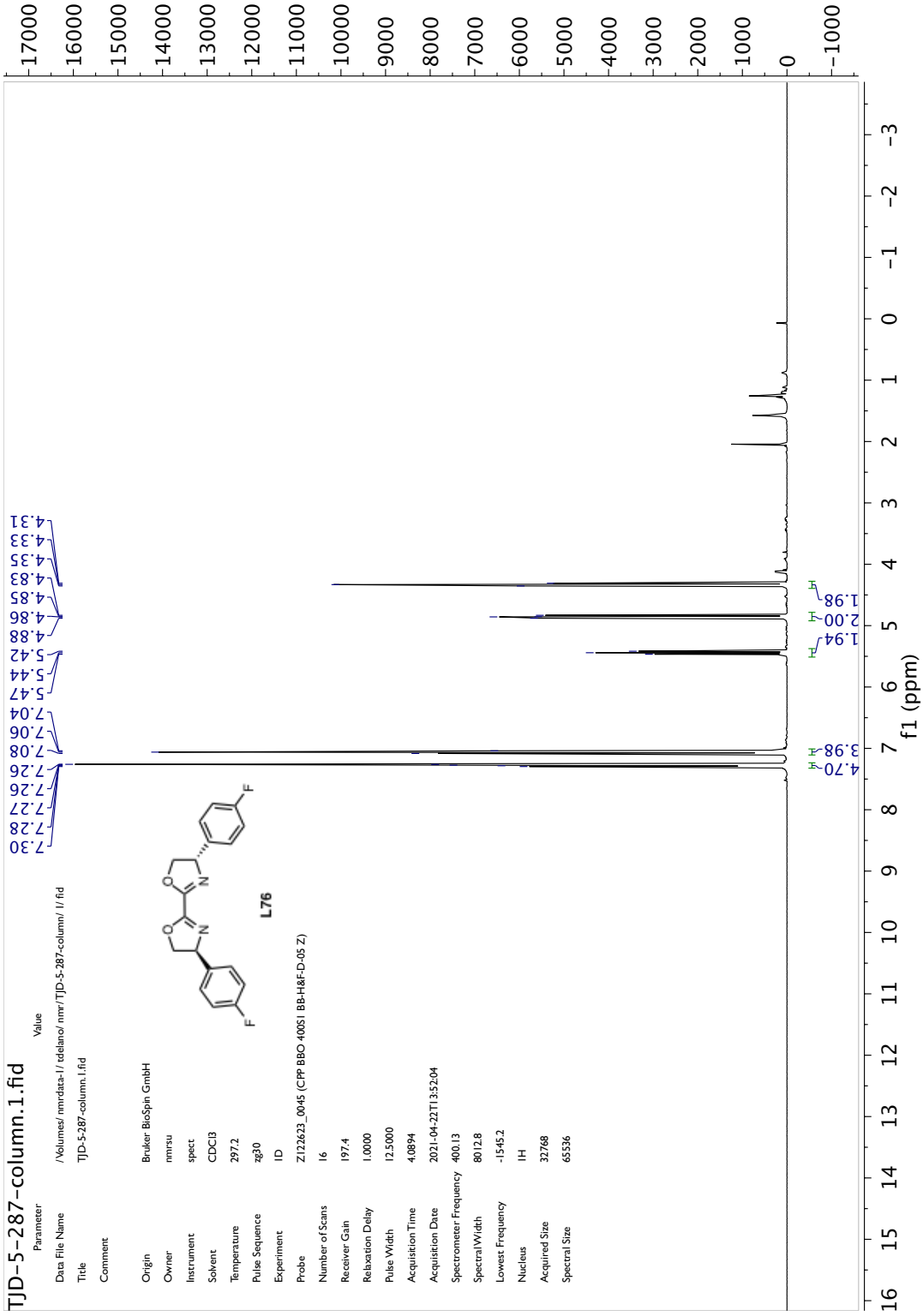
TJD-5-287-column.1.fid
Parameter
Value
Data File Name
/Volumes/ nmrdata-1/ tdelano/ nmr/TJD-5-287-column/ 1/ fid
Title
TJD-5-287-column.1.fid
Comment
Origin
Bruker BioSpin GmbH
Owner
nmrsu
Instrument
spect
Solvent
CDCl3
Temperature
297.2
Pulse Sequence
zg30
Experiment
1D
Probe
Z122623_0045 (CPP BBO 400S1 BB-H&F-D-05 Z)
Number of Scans
16
Receiver Gain
197.4
Relaxation Delay
1.0000
Pulse Width
12.5000
Acquisition Time
4.0894
Acquisition Date
2021-04-22T13:52:04
Spectrometer Frequency
400.13
Spectral Width
8012.8
Lowest Frequency
-1545.2
Nucleus
1H
Acquired Size
32768
Spectral Size
65536
L76
7.30
7.28
7.27
7.26
7.26
7.08
7.06
7.04
5.47
5.44
5.42
4.88
4.86
4.85
4.83
4.35
4.33
4.31
1.98
2.00
1.94
3.98
4.70
f1 (ppm)

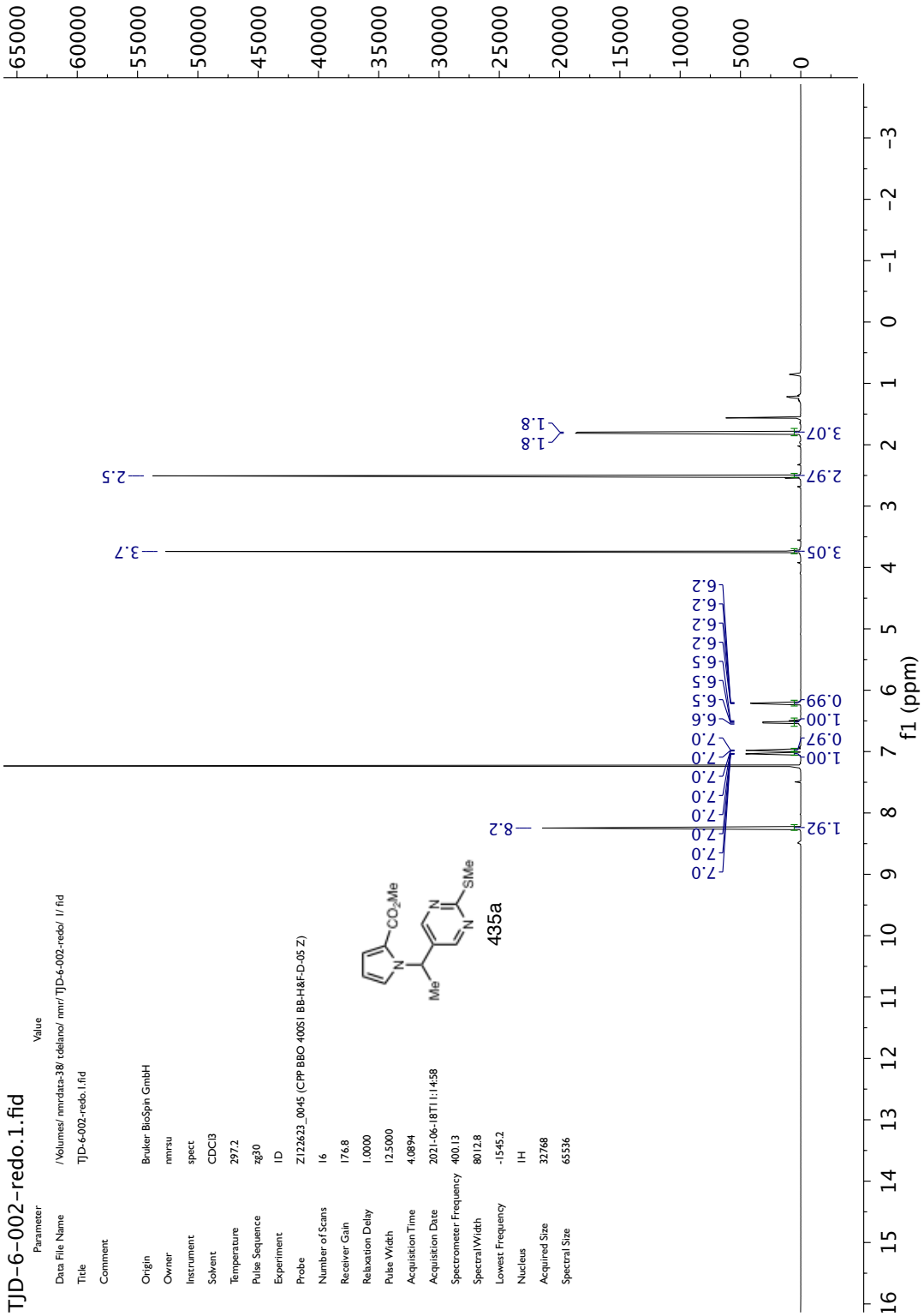
TJD-6-002-redo.1.fid
Parameter Value
Data File Name /Volumes/ nmrdata-38/ rdelano/ nmr/ TJD-6-002-redo/ 1/ fid
Title TJD-6-002-redo.1.fid
Comment
Origin Bruker BioSpin GmbH
Owner nmrsu
Instrument spect
Solvent CDCl3
Temperature 297.2
Pulse Sequence zg30
Experiment 1D
Probe Z122623_0045 (CPP BBO 400S1 BB-H&F-D-05 Z)
Number of Scans 16
Receiver Gain 176.8
Relaxation Delay 1.0000
Pulse Width 12.5000
Acquisition Time 4.0894
Acquisition Date 2021-06-18T11:14:58
Spectrometer Frequency 400.13
SpectralWidth 8012.8
Lowest Frequency -1545.2
Nucleus 1H
Acquired Size 32768
Spectral Size 65536
435a
f1 (ppm)

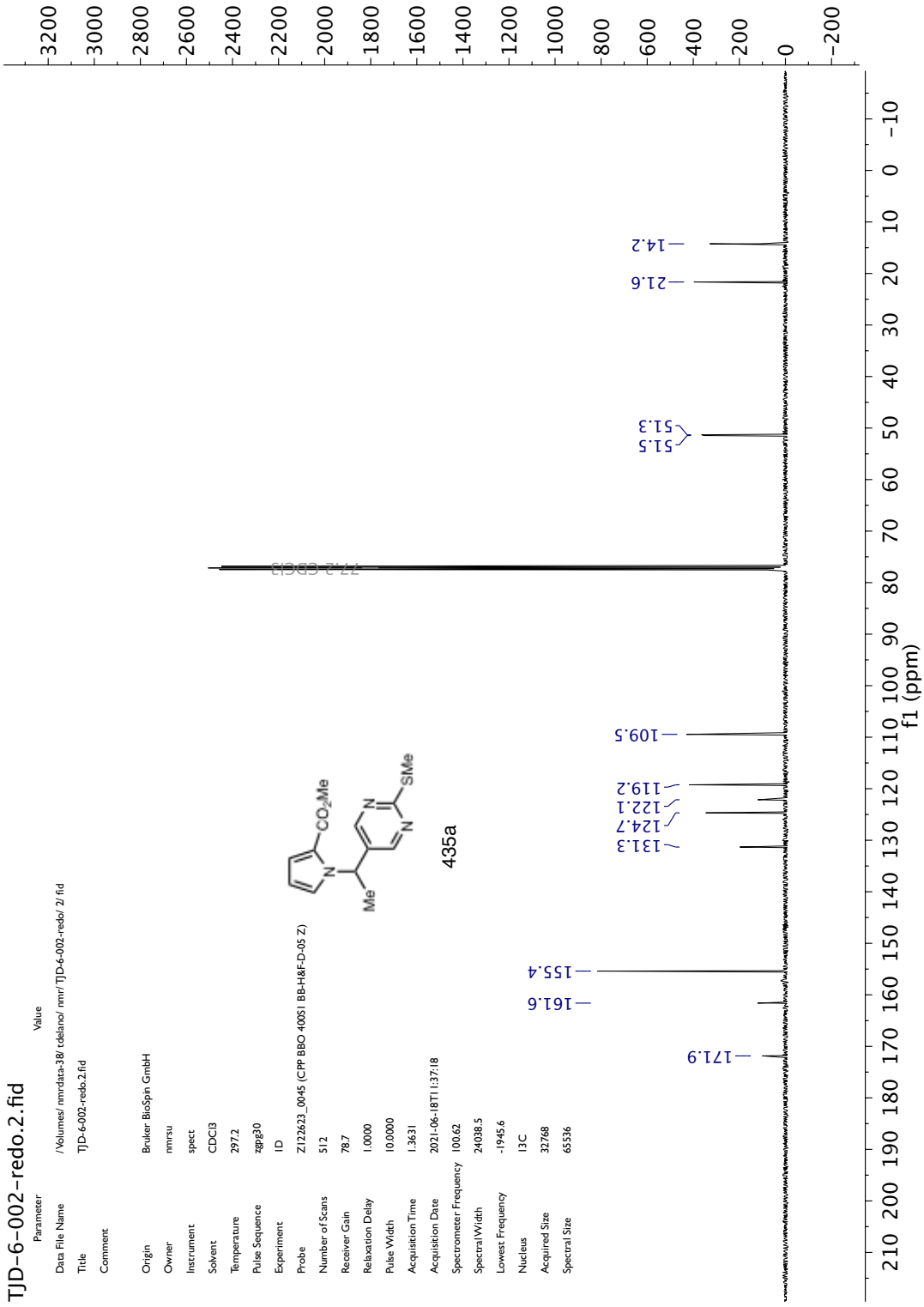
TJD-6-002-redo.2.fid
Parameter
Value
Data File Name
/Volumes/ nmrdata-38/ tdelano/ nmr/ TJD-6-002-redo/ 2/ fid
Title
TJD-6-002-redo.2.fid
Comment
Origin
Bruker BioSpin GmbH
Owner
nmrsu
Instrument
spect
Solvent
CDCl3
Temperature
297.2
Pulse Sequence
zgpg30
Experiment
1D
Probe
Z122623_0045 (CPP BBO 400S1 BB-H&F-D-05 Z)
Number of Scans
512
Receiver Gain
78.7
Relaxation Delay
1.0000
Pulse Width
10.0000
Acquisition Time
1.3631
Acquisition Date
2021-06-18T11:37:18
Spectrometer Frequency
100.62
Spectral Width
24038.5
Lowest Frequency
-1945.6
Nucleus
13C
Acquired Size
32768
Spectral Size
65536
77.2 CDCl3
51.5
51.3
21.6
14.2
109.5
119.2
122.1
124.7
131.3
155.4
161.6
171.9
CO2Me
SMe
Me
N
N
435a
f1 (ppm)

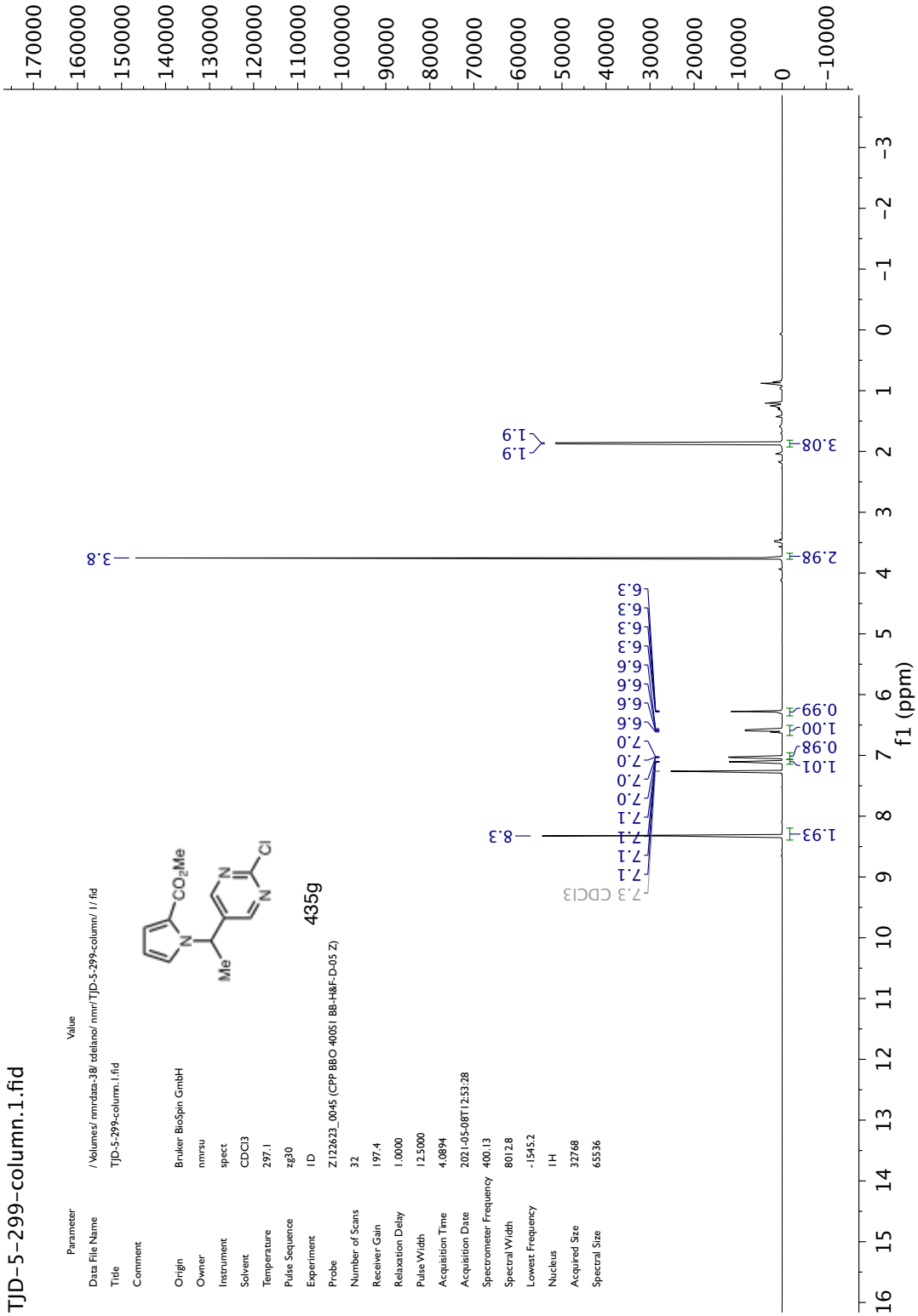
TJD-5-299-column.1.fid
Parameter
Value
Data File Name
/ Volumes/ nmrdata-38/ tdelano/ nmr/TJD-5-299-column/ 1/ fid
Title
TJD-5-299-column.1.fid
Comment
Origin
Bruker BioSpin GmbH
Owner
nmrsu
Instrument
spect
Solvent
CDCl3
Temperature
297.1
Pulse Sequence
zg30
Experiment
1D
Probe
Z122623_0045 (CPP BBO 400S1 BB-H&F-D-05 Z)
Number of Scans
32
Receiver Gain
197.4
Relaxation Delay
1.0000
Pulse Width
12.5000
Acquisition Time
4.0894
Acquisition Date
2021-05-08T12:53:28
Spectrometer Frequency
400.13
Spectral Width
8012.8
Lowest Frequency
-1545.2
Nucleus
1H
Acquired Size
32768
Spectral Size
65536
CO2Me
N
Me
N
N
Cl
435g
3.8
8.3
7.3 CDCl3
7.1
7.1
7.1
7.0
7.0
7.0
7.0
6.6
6.6
6.6
6.6
6.3
6.3
6.3
6.3
1.9
1.9
3.08
2.98
1.93
1.01
0.98
1.00
0.99
f1 (ppm)

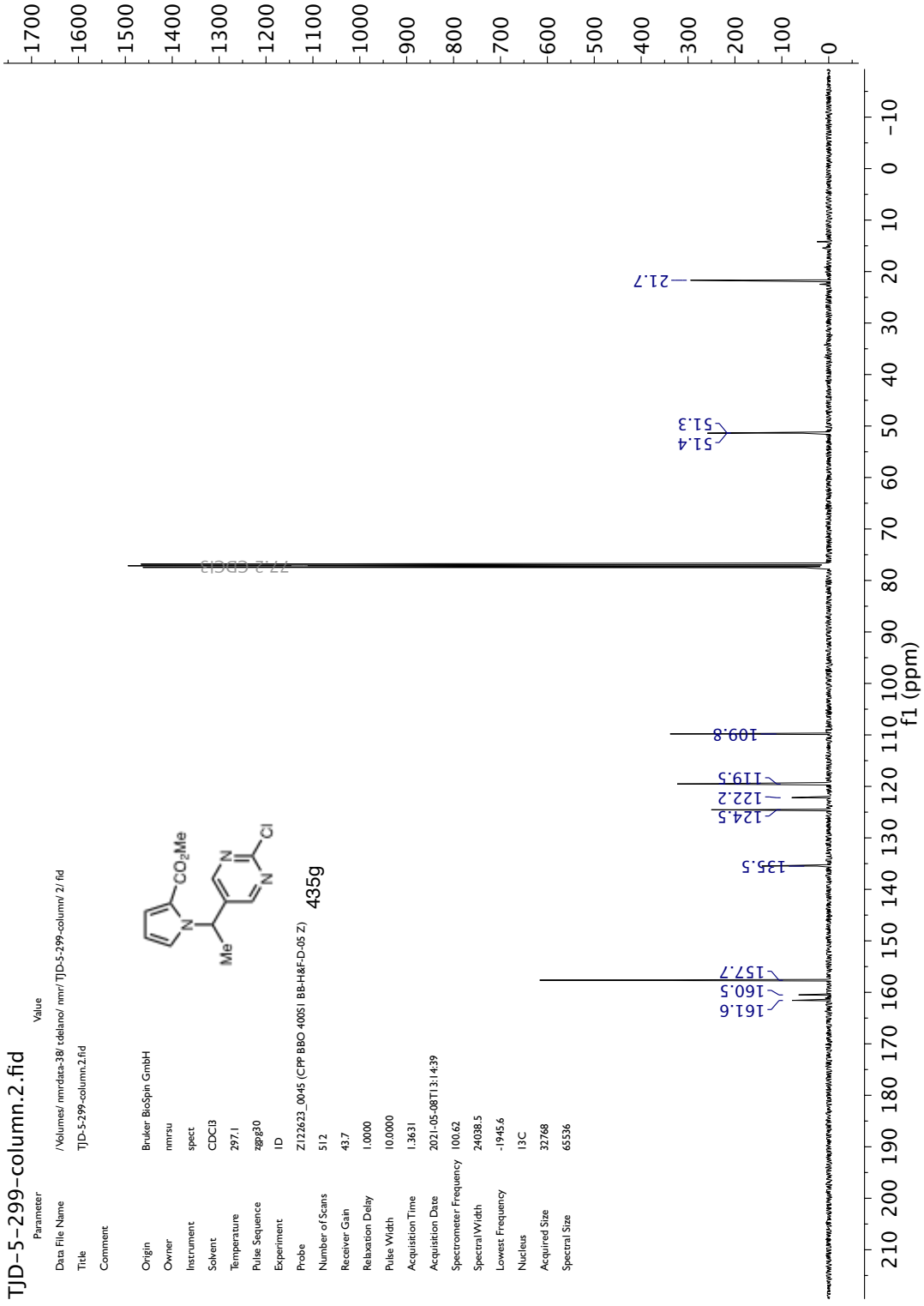
TJD-5-299-column.2.fid
Parameter
Value
Data File Name
/Volumes/ nmrdata-38/ tdelano/ nmr/ TJD-5-299-column/ 2/ fid
Title
TJD-5-299-column.2.fid
Comment
Origin
Bruker BioSpin GmbH
Owner
nmrsu
Instrument
spect
Solvent
CDCl3
Temperature
297.1
Pulse Sequence
zgpg30
Experiment
1D
Probe
Z122623_0045 (CPP BBO 400S1 BB-H&F-D-05 Z)
Number of Scans
512
Receiver Gain
43.7
Relaxation Delay
1.0000
Pulse Width
10.0000
Acquisition Time
1.3631
Acquisition Date
2021-05-08T13:14:39
Spectrometer Frequency
100.62
Spectral Width
24038.5
Lowest Frequency
-1945.6
Nucleus
13C
Acquired Size
32768
Spectral Size
65536
435g
77.2 CDCl3
21.7
51.4
51.3
109.8
119.5
122.2
124.5
135.5
157.7
160.5
161.6
f1 (ppm)

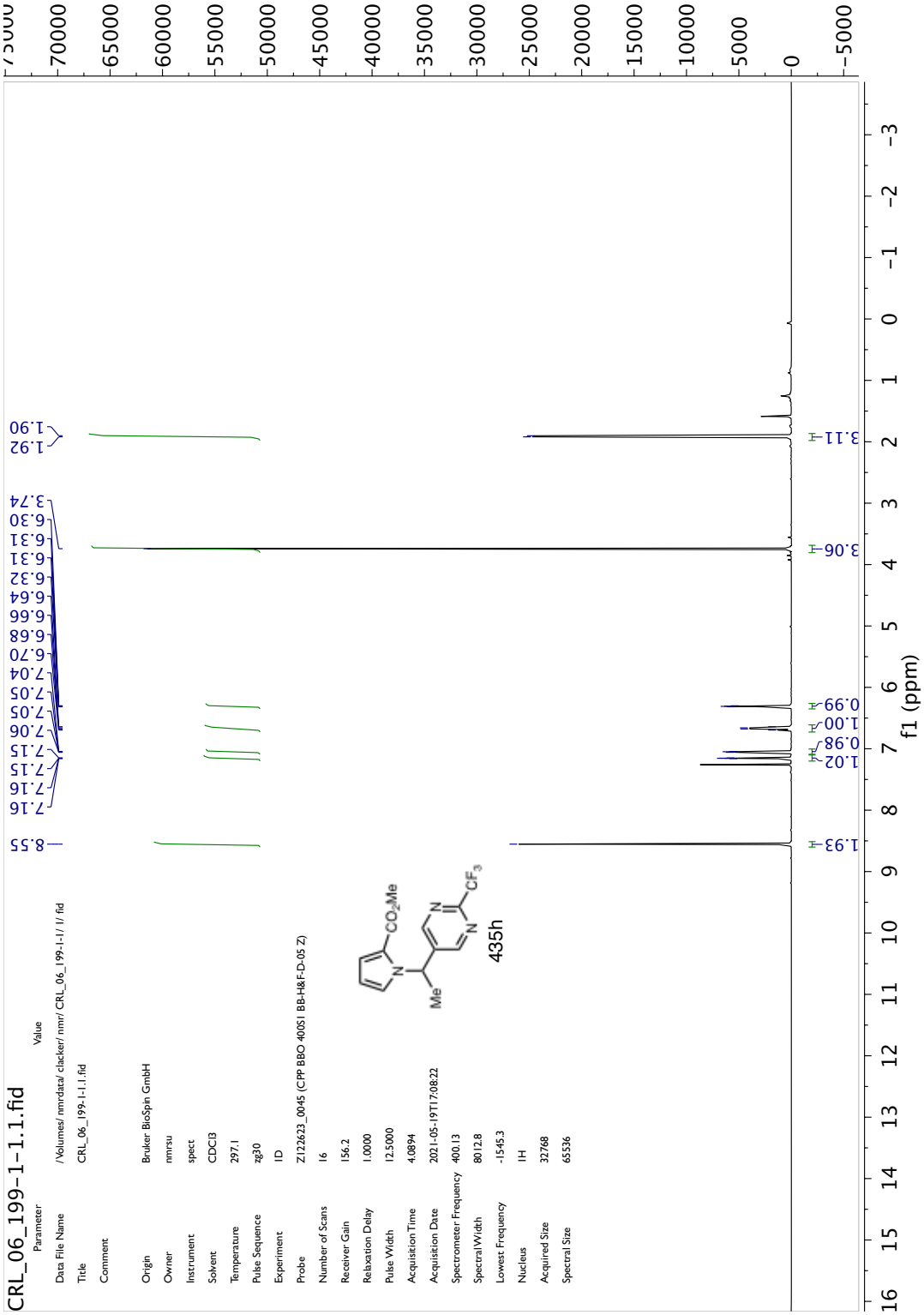
CRL_06_199-1-1.1.fid
Parameter
Value
Data File Name /Volumes/ nmrdata/ clacker/ nmr/ CRL_06_199-1-1/ 1/ fid
Title CRL_06_199-1-1.1.fid
Comment
Origin Bruker BioSpin GmbH
Owner nmrsu
Instrument spect
Solvent CDCl3
Temperature 297.1
Pulse Sequence zg30
Experiment 1D
Probe Z122623_0045 (CPP BBO 400S1 BB-H&F-D-05 Z)
Number of Scans 16
Receiver Gain 156.2
Relaxation Delay 1.0000
Pulse Width 12.5000
Acquisition Time 4.0894
Acquisition Date 2021-05-19T17:08:22
Spectrometer Frequency 400.13
SpectralWidth 8012.8
Lowest Frequency -1545.3
Nucleus 1H
Acquired Size 32768
Spectral Size 65536
435h
f1 (ppm)

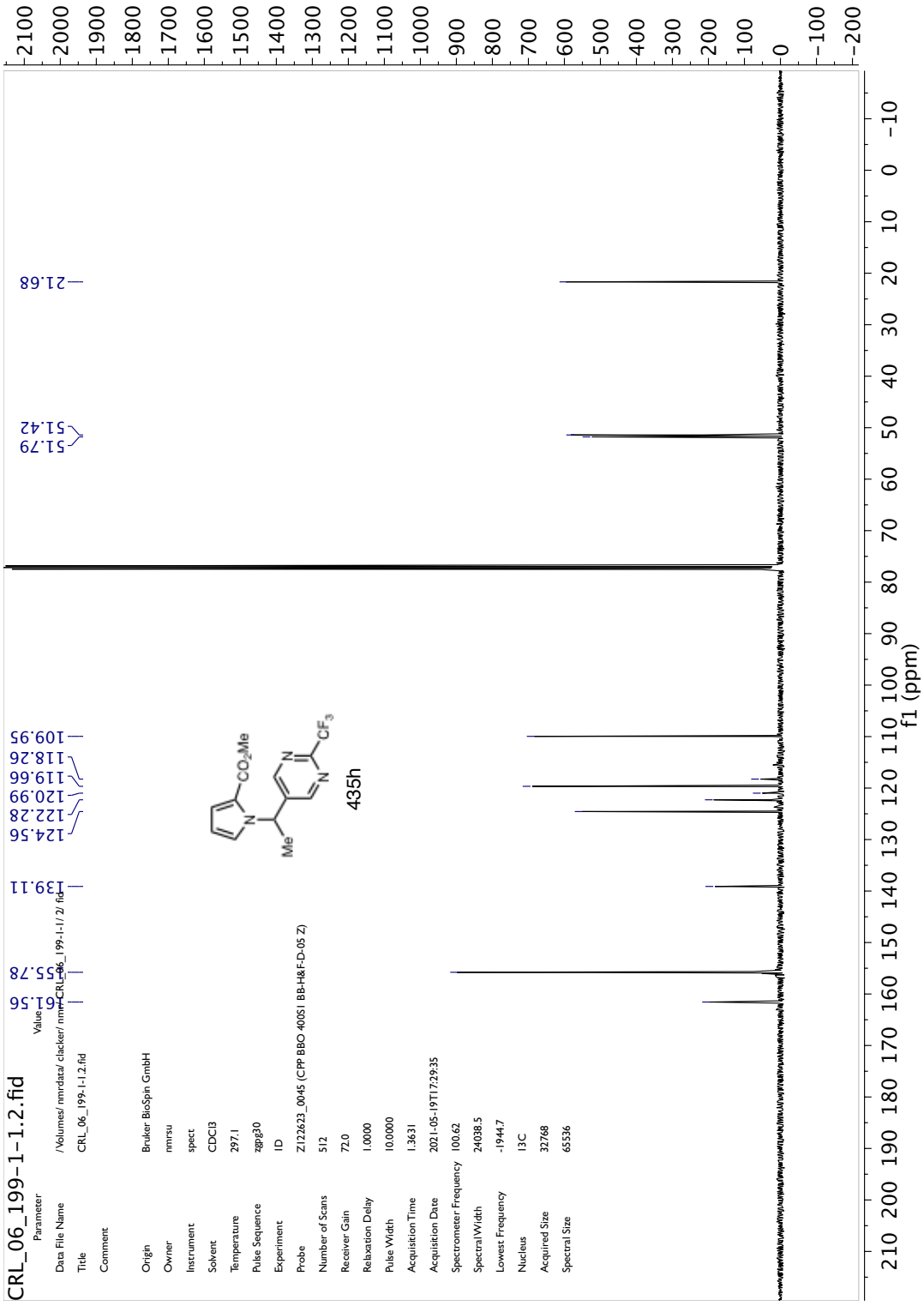
CRL_06_199-1-1.2.fid
Parameter Value
Data File Name /Volumes/ nmrdata/ clacker/ nmr-CRL_06_199-1-1/ 2/ fid
Title CRL_06_199-1-1.2.fid
Comment
Origin Bruker BioSpin GmbH
Owner nmrsu
Instrument spect
Solvent CDCl3
Temperature 297.1
Pulse Sequence zgpg30
Experiment 1D
Probe Z122623_0045 (CPP BBO 400S1 BB-H&F-D-05 Z)
Number of Scans 512
Receiver Gain 72.0
Relaxation Delay 1.0000
Pulse Width 10.0000
Acquisition Time 1.3631
Acquisition Date 2021-05-19T17:29:35
Spectrometer Frequency 100.62
Spectral Width 24038.5
Lowest Frequency -1944.7
Nucleus 13C
Acquired Size 32768
Spectral Size 65536
21.68
51.42
51.79
109.95
118.26
119.66
120.99
122.28
124.56
139.11
155.78
161.56
CO2Me
N
Me
N
N
CF3
435h
f1 (ppm)

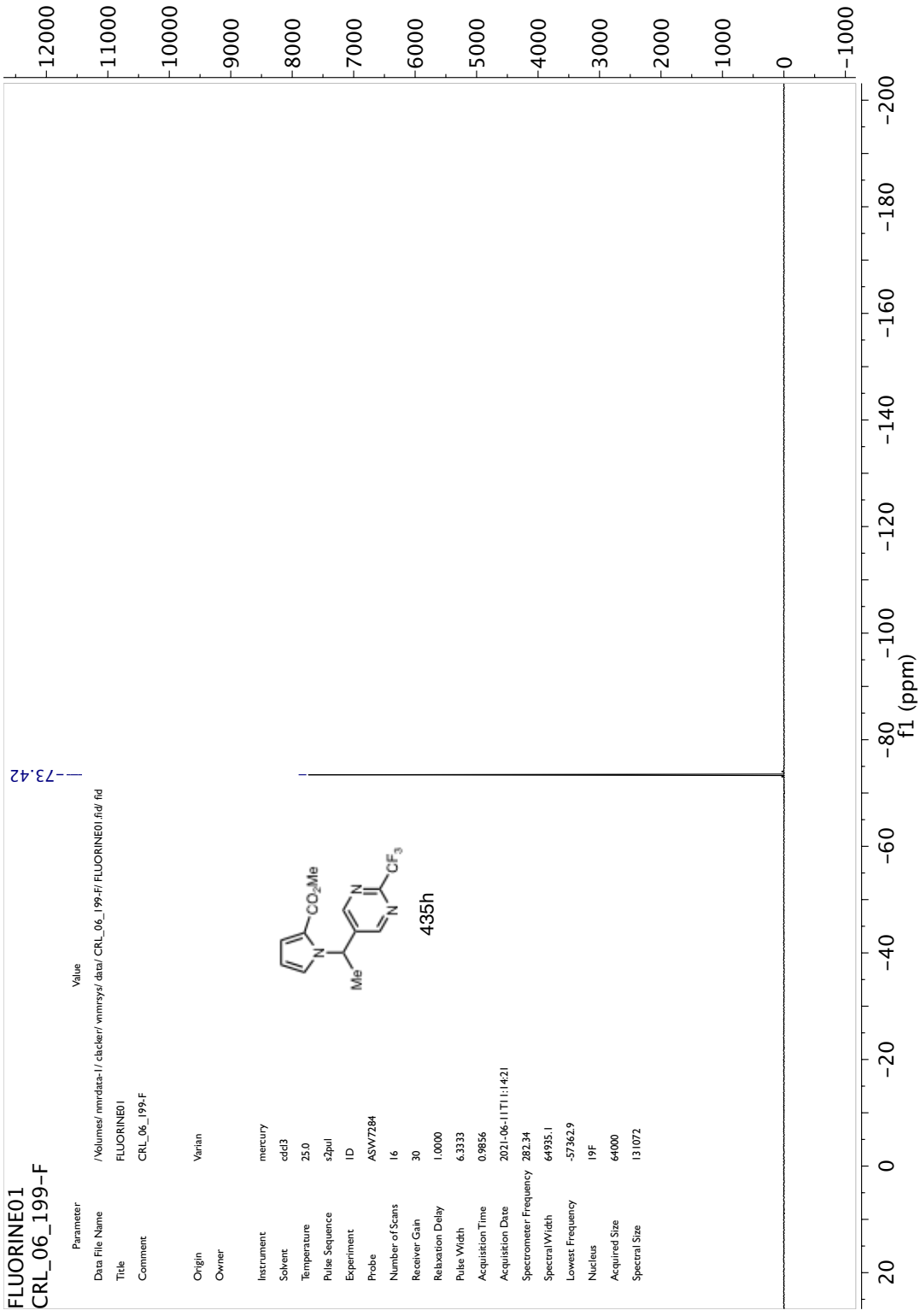

Parameter	Value
Data File Name	/Volumes/ nmrdata-1/ cbcler/ vnmrsys/ data/ CRL_06_199-F/ FLUORINE01.fid/ fid
Title	FLUORINE01
Comment	CRL_06_199-F
Origin	Varian
Owner	
Instrument	mercury
Solvent	cdcl3
Temperature	25.0
Pulse Sequence	s2pul
Experiment	1D
Probe	ASW7284
Number of Scans	16
Receiver Gain	30
Relaxation Delay	1.0000
Pulse Width	6.3333
Acquisition Time	0.9856
Acquisition Date	2021-06-11T11:14:21
Spectrometer Frequency	282.34
Spectral Width	64935.1
Lowest Frequency	-57362.9
Nucleus	19F
Acquired Size	64000
Spectral Size	131072

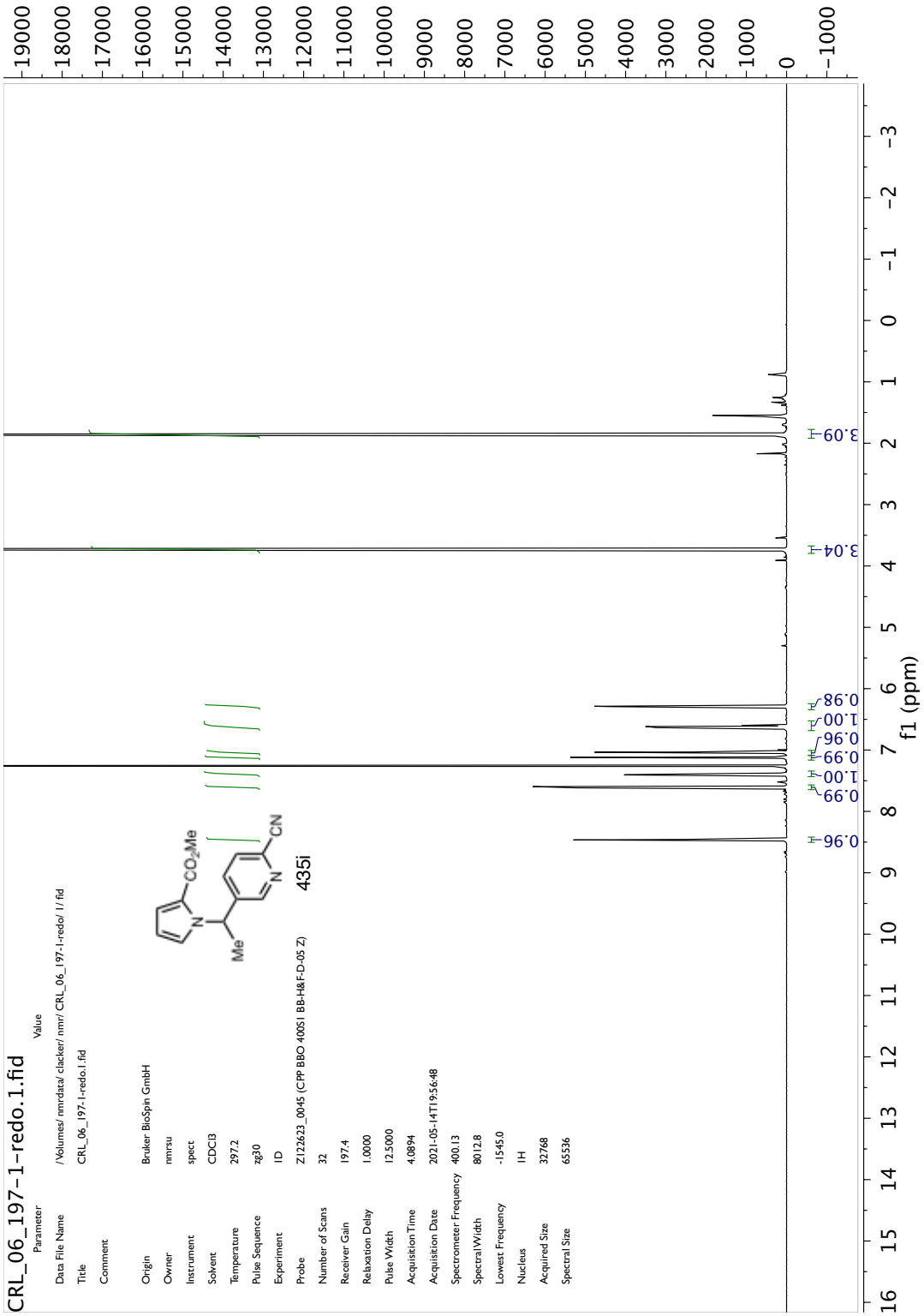
CRL_06_197-1-redo.1.fid
Parameter
Value
Data File Name
/Volumes/ nmrdata/ clacker/ nmr/ CRL_06_197-1-redo/ 1/ fid
Title
CRL_06_197-1-redo.1.fid
Comment
Origin
Bruker BioSpin GmbH
Owner
nmrsu
Instrument
spect
Solvent
CDCl3
Temperature
297.2
Pulse Sequence
zg30
Experiment
1D
Probe
Z122623_0045 (CPP BBO 400S1 BB-H&F-D-05 Z)
Number of Scans
32
Receiver Gain
197.4
Relaxation Delay
1.0000
Pulse Width
12.5000
Acquisition Time
4.0894
Acquisition Date
2021-05-14T19:56:48
Spectrometer Frequency
400.13
SpectralWidth
8012.8
Lowest Frequency
-1545.0
Nucleus
1H
Acquired Size
32768
Spectral Size
65536
CO2Me
N
Me
CN
N
435i
3.09
3.04
0.96
0.99
1.00
0.99
0.96
1.00
0.98
f1 (ppm)

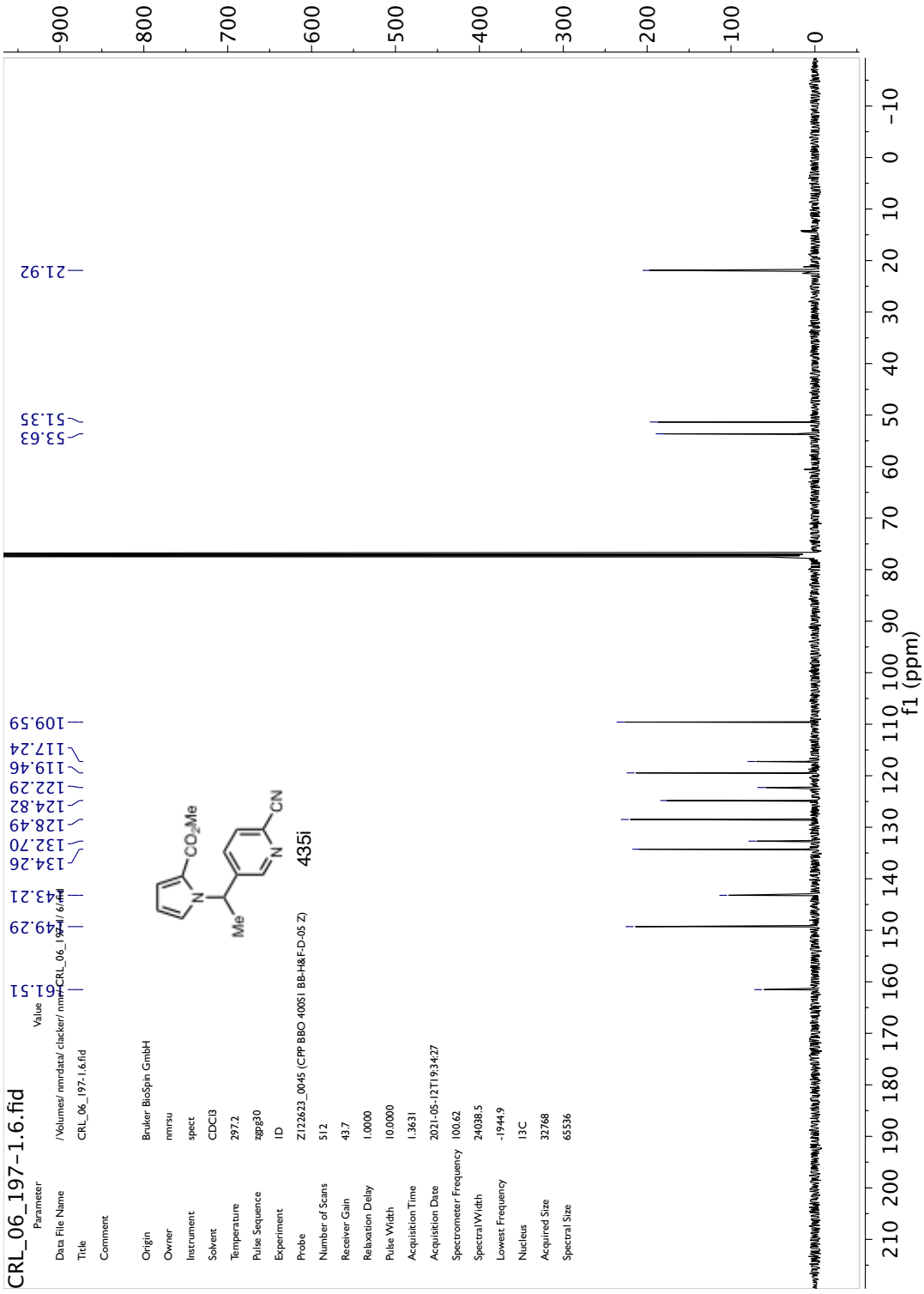
CRL_06_197-1.6.fid
Parameter
Value
Data File Name /Volumes/ nmrdata/ clacker/ nmr/CRL_06_197-1/ 6/fid
Title CRL_06_197-1.6.fid
Comment
Origin Bruker BioSpin GmbH
Owner nmrsu
Instrument spect
Solvent CDCl3
Temperature 297.2
Pulse Sequence zgpg30
Experiment 1D
Probe Z122623_0045 (CPP BBO 400S1 BB-H&F-D-05 Z)
Number of Scans 512
Receiver Gain 43.7
Relaxation Delay 1.0000
Pulse Width 10.0000
Acquisition Time 1.3631
Acquisition Date 2021-05-12T19:34:27
Spectrometer Frequency 100.62
Spectral Width 24038.5
Lowest Frequency -1944.9
Nucleus 13C
Acquired Size 32768
Spectral Size 65536
CO2Me
N
Me
CN
N
435i
21.92
51.35
53.63
109.59
117.24
119.46
122.29
124.82
128.49
132.70
134.26
143.21
149.29
161.51
f1 (ppm)

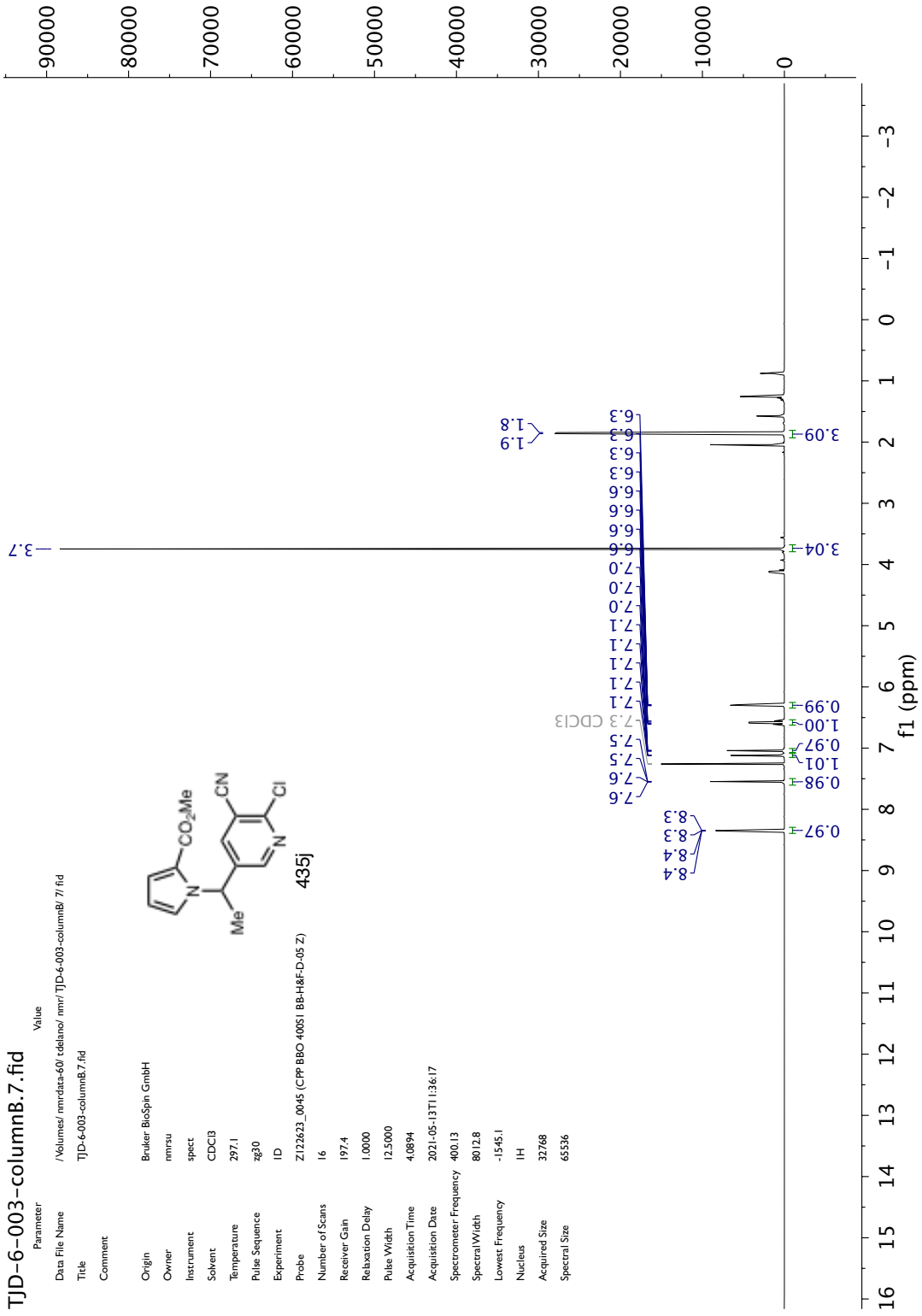
TJD-6-003-columnB.7.fid
Parameter Value
Data File Name /Volumes/ nmrdata-60/ tdelano/ nmr/ TJD-6-003-columnB/ 7/ fid
Title TJD-6-003-columnB.7.fid
Comment
Origin Bruker BioSpin GmbH
Owner nmrsu
Instrument spect
Solvent CDCl3
Temperature 297.1
Pulse Sequence zg30
Experiment 1D
Probe Z122623_0045 (CPP BBO 400S1 BB-H&F-D-05 Z)
Number of Scans 16
Receiver Gain 197.4
Relaxation Delay 1.0000
Pulse Width 12.5000
Acquisition Time 4.0894
Acquisition Date 2021-05-13T11:36:17
Spectrometer Frequency 400.13
Spectral Width 8012.8
Lowest Frequency -1545.1
Nucleus 1H
Acquired Size 32768
Spectral Size 65536
435j
CO2Me
CN
Cl
Me
N
N
3.7
3.09
3.04
1.9
1.8
0.99
1.00
0.97
1.01
0.98
0.97
7.3 CDCl3
f1 (ppm)

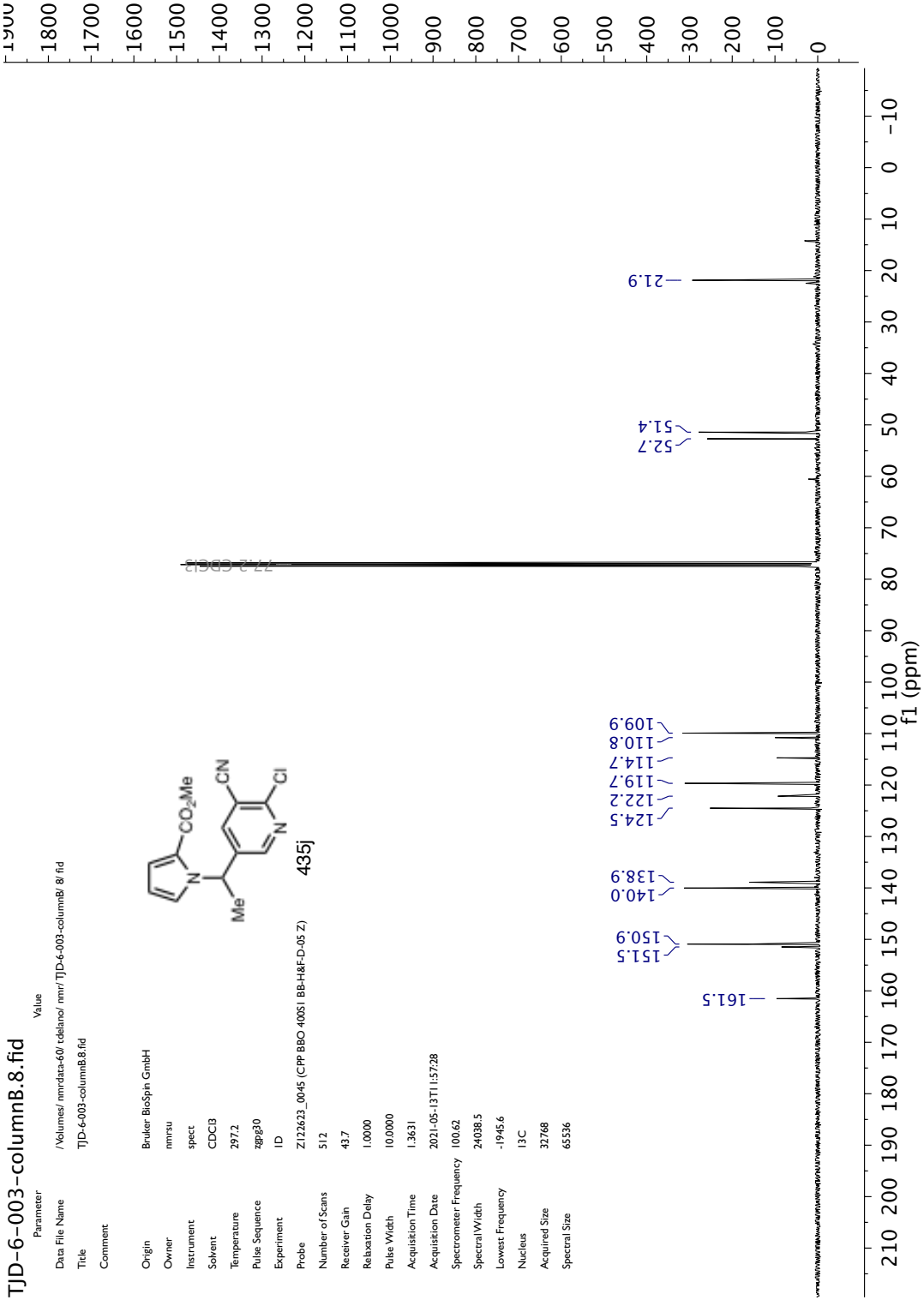
TJD-6-003-columnB.8.fid
Parameter
Value
Data File Name
/Volumes/ nmrdata-60/ tdelano/ nmr/ TJD-6-003-columnB/ 8/ fid
Title
TJD-6-003-columnB.fid
Comment
Origin
Bruker BioSpin GmbH
Owner
nmrsu
Instrument
spect
Solvent
CDCl3
Temperature
297.2
Pulse Sequence
zgpg30
Experiment
1D
Probe
Z122623_0045 (CPP BBO 400S1 BB-H&F-D-05 Z)
Number of Scans
512
Receiver Gain
43.7
Relaxation Delay
1.0000
Pulse Width
10.0000
Acquisition Time
1.3631
Acquisition Date
2021-05-13T11:57:28
Spectrometer Frequency
100.62
Spectral Width
24038.5
Lowest Frequency
-1945.6
Nucleus
13C
Acquired Size
32768
Spectral Size
65536
CO2Me
CN
Cl
N
N
Me
435j
77.2 CDCl3
21.9
51.4
52.7
109.9
110.8
114.7
119.7
122.2
124.5
138.9
140.0
150.9
151.5
161.5
f1 (ppm)

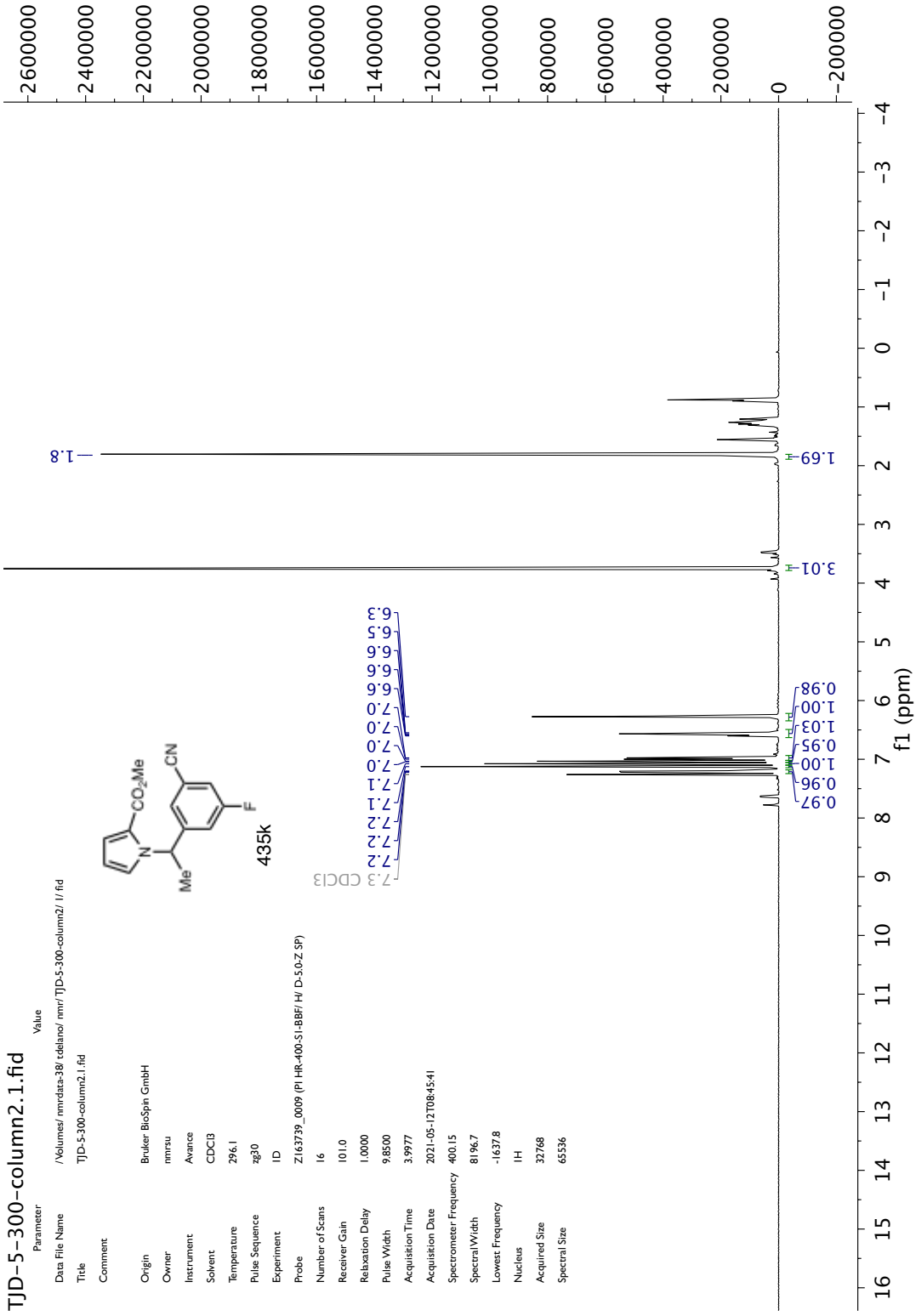
TJD-5-300-column2.1.fid
Parameter Value
Data File Name /Volumes/ nmrdata-38/ cdelano/ nmr/ TJD-5-300-column2/ 1/ fid
Title TJD-5-300-column2.1 fid
Comment
Origin Bruker BioSpin GmbH
Owner nmrsu
Instrument Avance
Solvent CDCl3
Temperature 296.1
Pulse Sequence zg30
Experiment 1D
Probe Z163739_0009 (PI HR-400-SI-BBF/ H/ D-5.0-Z SP)
Number of Scans 16
Receiver Gain 101.0
Relaxation Delay 1.0000
Pulse Width 9.8500
Acquisition Time 3.9977
Acquisition Date 2021-05-12T08:45:41
Spectrometer Frequency 400.15
Spectral Width 8196.7
Lowest Frequency -1637.8
Nucleus 1H
Acquired Size 32768
Spectral Size 65536
CO2Me
CN
F
Me
N
435k
1.8
1.69
3.01
7.3 CDCl3
0.97
0.96
1.00
0.95
1.03
1.00
0.98
f1 (ppm)

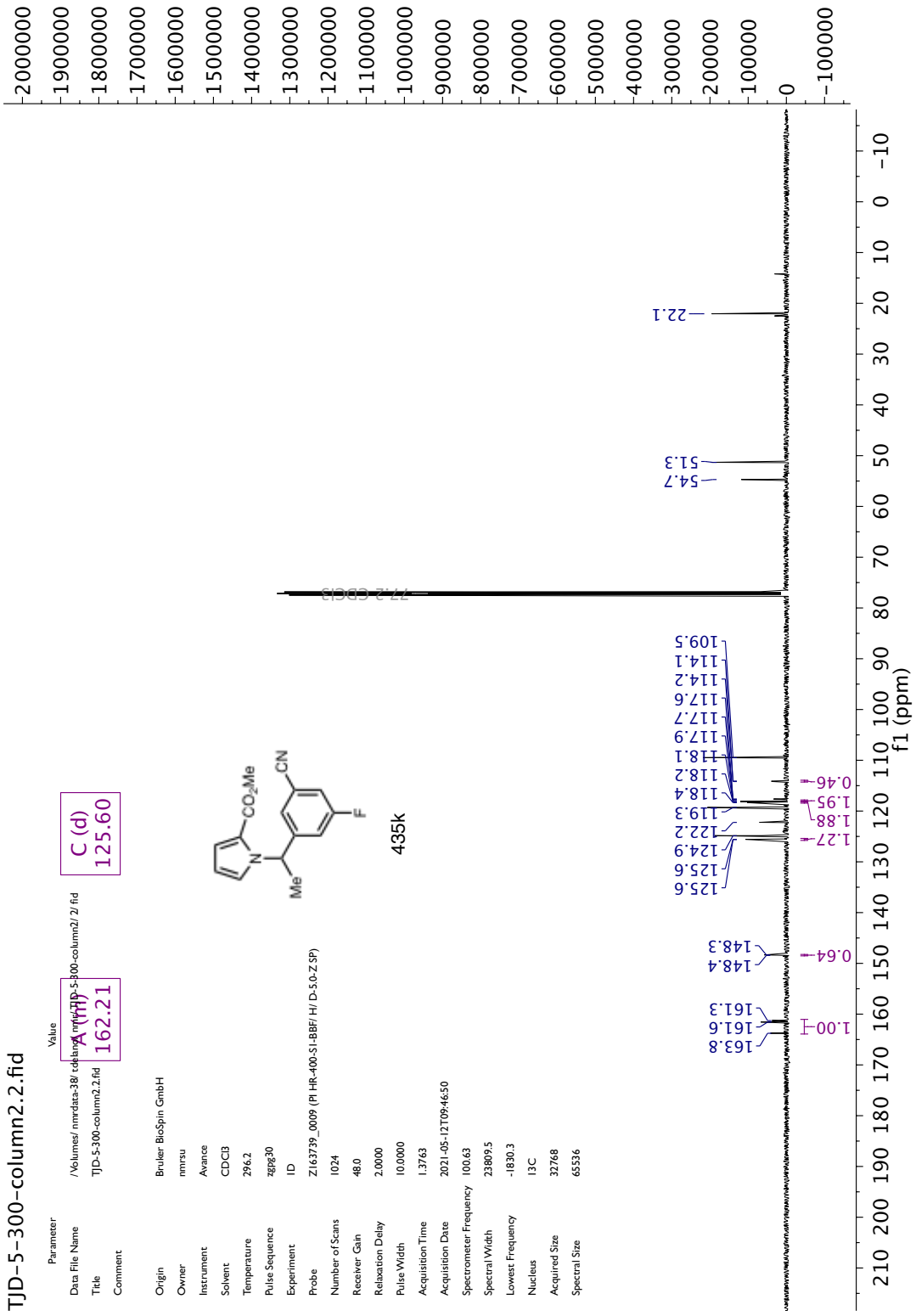
TJD-5-300-column2.2.fid
Parameter
Value
Data File Name
/Volumes/ nmrdata-38/ tdelany/ tjd/TJD-5-300-column2/ 2/ fid
Title
TJD-5-300-column2.2.fid
Comment
A (m)
162.21
C (d)
125.60
Origin
Bruker BioSpin GmbH
Owner
nmrsu
Instrument
Avance
Solvent
CDCl3
Temperature
296.2
Pulse Sequence
zgpg30
Experiment
1D
Probe
Z163739_0009 (PI HR-400-S1-BBF/ H/ D-5.0-Z SP)
Number of Scans
1024
Receiver Gain
48.0
Relaxation Delay
2.0000
Pulse Width
10.0000
Acquisition Time
1.3763
Acquisition Date
2021-05-12T09:46:50
Spectrometer Frequency
100.63
Spectral Width
23809.5
Lowest Frequency
-1830.3
Nucleus
13C
Acquired Size
32768
Spectral Size
65536
CO2Me
CN
F
N
Me
435k
77.2-CDCl3
22.1
51.3
54.7
109.5
114.1
114.2
117.6
117.7
117.9
118.1
118.2
118.4
119.3
122.2
124.9
125.6
125.6
148.3
148.4
161.3
161.6
163.8
1.00
0.64
0.46
1.95
1.88
1.27
f1 (ppm)

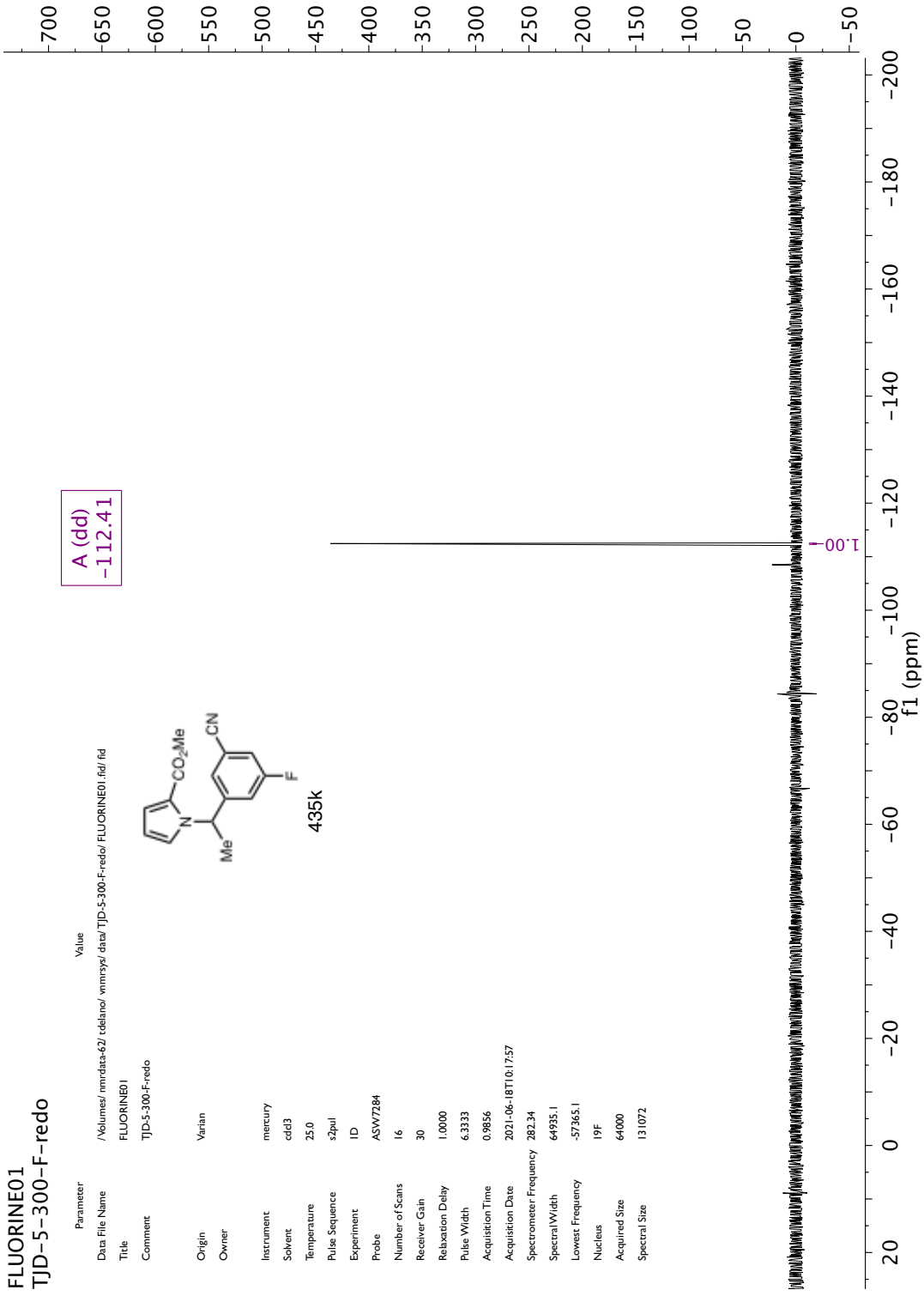
FLUORINE01
TJD-5-300-F-redo
Parameter
Value
Data File Name
/Volumes/ nmrdata-62/ tdelano/ vnmrsys/ data/ TJD-5-300-F-redo/ FLUORINE01.fid/ fid
Title
FLUORINE01
Comment
TJD-5-300-F-redo
Origin
Varian
Owner
Instrument
mercury
Solvent
cdcl3
Temperature
25.0
Pulse Sequence
s2pul
Experiment
1D
Probe
ASW7284
Number of Scans
16
Receiver Gain
30
Relaxation Delay
1.0000
Pulse Width
6.3333
Acquisition Time
0.9856
Acquisition Date
2021-06-18T10:17:57
Spectrometer Frequency
282.34
Spectral Width
64935.1
Lowest Frequency
-57365.1
Nucleus
19F
Acquired Size
64000
Spectral Size
131072
A (dd)
-112.41
435k
1.00
f1 (ppm)

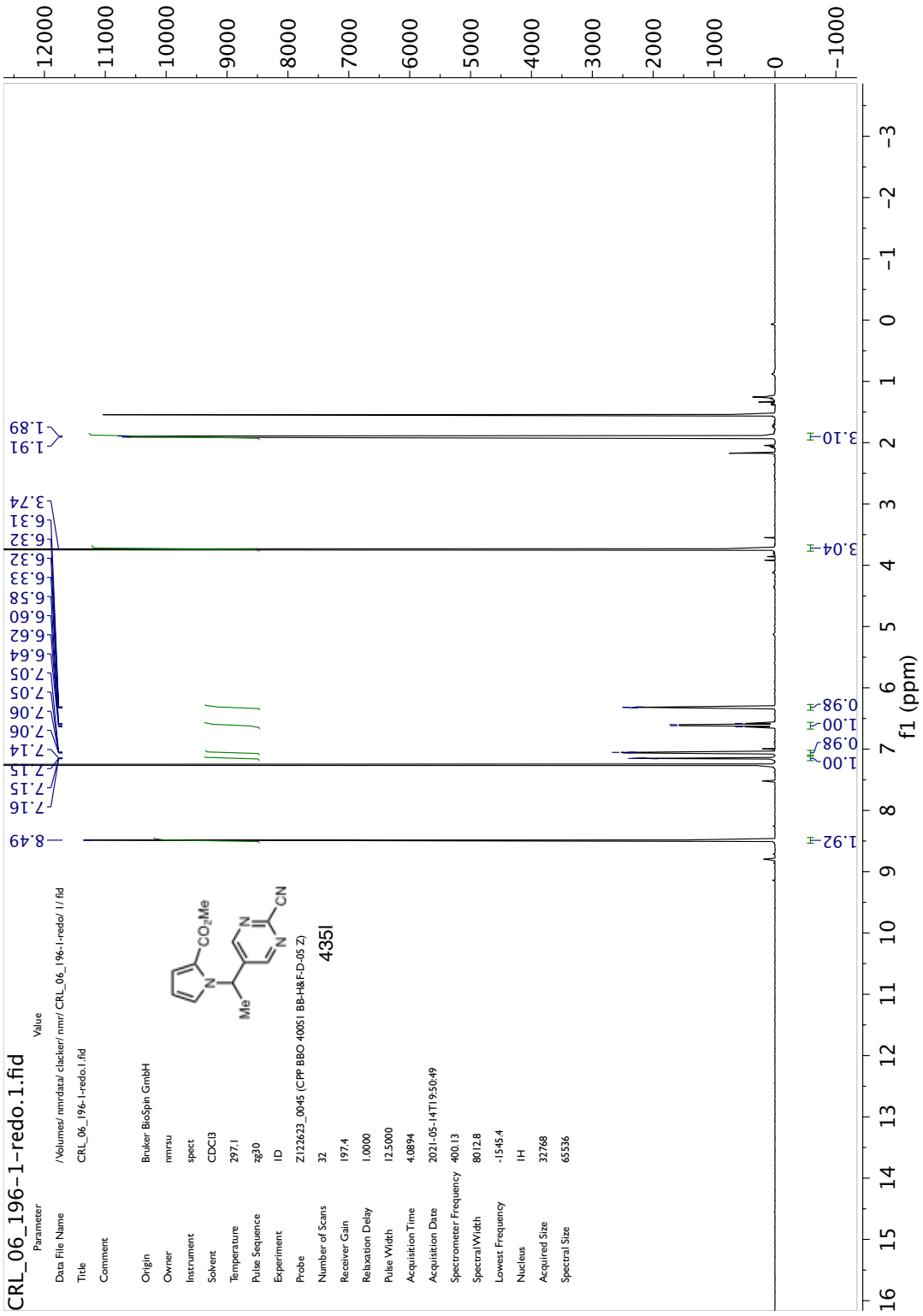
CRL_06_196-1-redo.1.fid
Parameter
Value
Data File Name
/Volumes/ nmrdata/ clacker/ nmr/ CRL_06_196-1-redo/ 1/ fid
Title
CRL_06_196-1-redo.1.fid
Comment
Origin
Bruker BioSpin GmbH
Owner
nmrsu
Instrument
spect
Solvent
CDCl3
Temperature
297.1
Pulse Sequence
zg30
Experiment
1D
Probe
Z122623_0045 (CPP BBO 400S1 BB-H&F-D-05 Z)
Number of Scans
32
Receiver Gain
197.4
Relaxation Delay
1.0000
Pulse Width
12.5000
Acquisition Time
4.0894
Acquisition Date
2021-05-14T19:50:49
Spectrometer Frequency
400.13
Spectral Width
8012.8
Lowest Frequency
-1545.4
Nucleus
1H
Acquired Size
32768
Spectral Size
65536
435l
CO2Me
Me
CN
8.49
7.16
7.15
7.15
7.14
7.06
7.06
7.05
7.05
6.64
6.62
6.60
6.58
6.33
6.32
6.32
6.31
3.74
1.91
1.89
1.92
1.00
0.98
1.00
0.98
3.04
3.10
f1 (ppm)

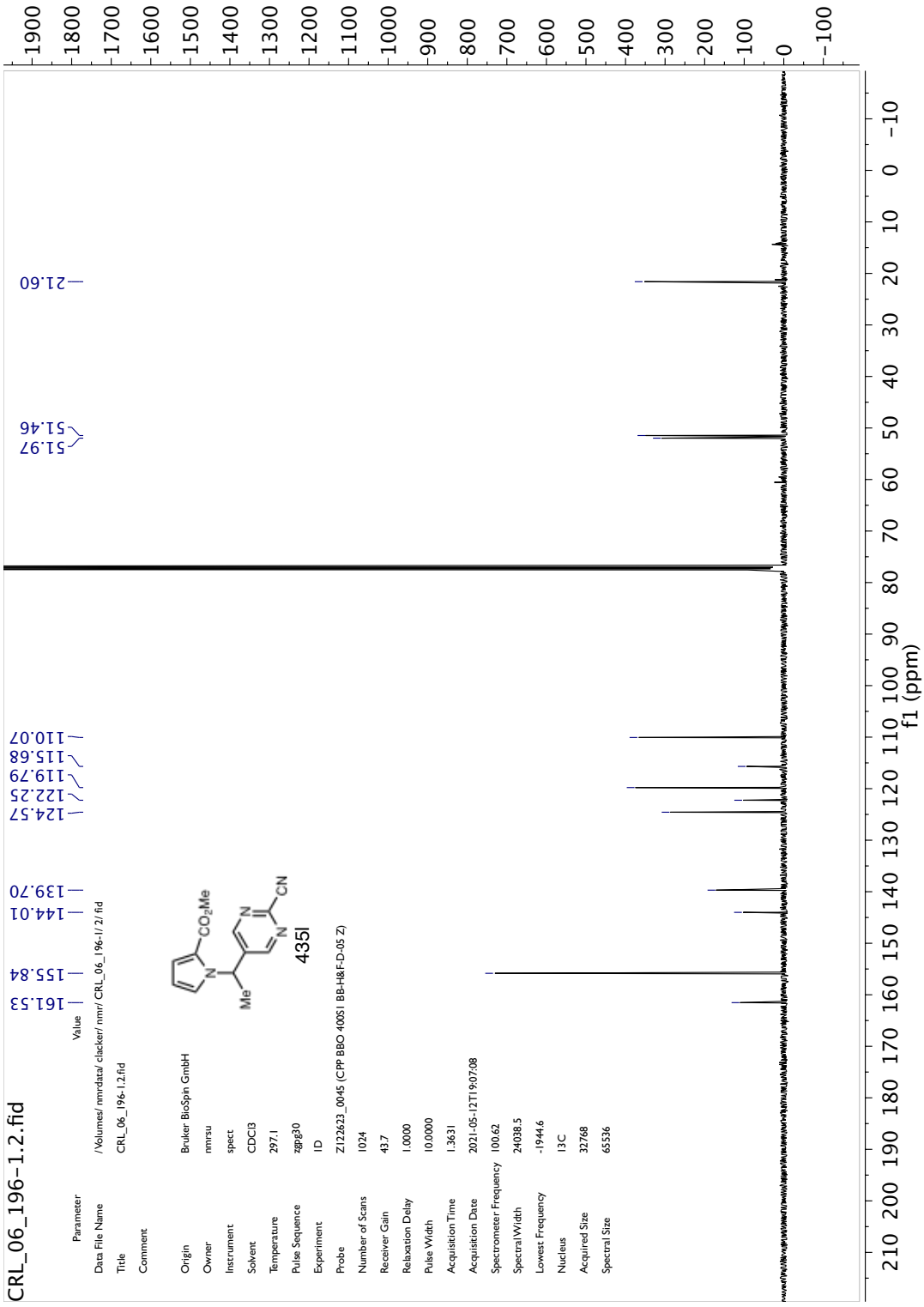
CRL_06_196-1.2.fid
Parameter Value
Data File Name /Volumes/ nmrdata/ clacker/ nmr/ CRL_06_196-1/ 2/ fid
Title CRL_06_196-1.2.fid
Comment
Origin Bruker BioSpin GmbH
Owner nmrsu
Instrument spect
Solvent CDCl3
Temperature 297.1
Pulse Sequence zgpg30
Experiment 1D
Probe Z122623_0045 (CPP BBO 400S1 BB-H&F-D-05 Z)
Number of Scans 1024
Receiver Gain 43.7
Relaxation Delay 1.0000
Pulse Width 10.0000
Acquisition Time 1.3631
Acquisition Date 2021-05-12T19:07:08
Spectrometer Frequency 100.62
Spectral Width 24038.5
Lowest Frequency -1944.6
Nucleus 13C
Acquired Size 32768
Spectral Size 65536
CO2Me
N
Me
N
N
CN
435l
161.53
155.84
144.01
139.70
124.57
122.25
119.79
115.68
110.07
51.97
51.46
21.60
f1 (ppm)

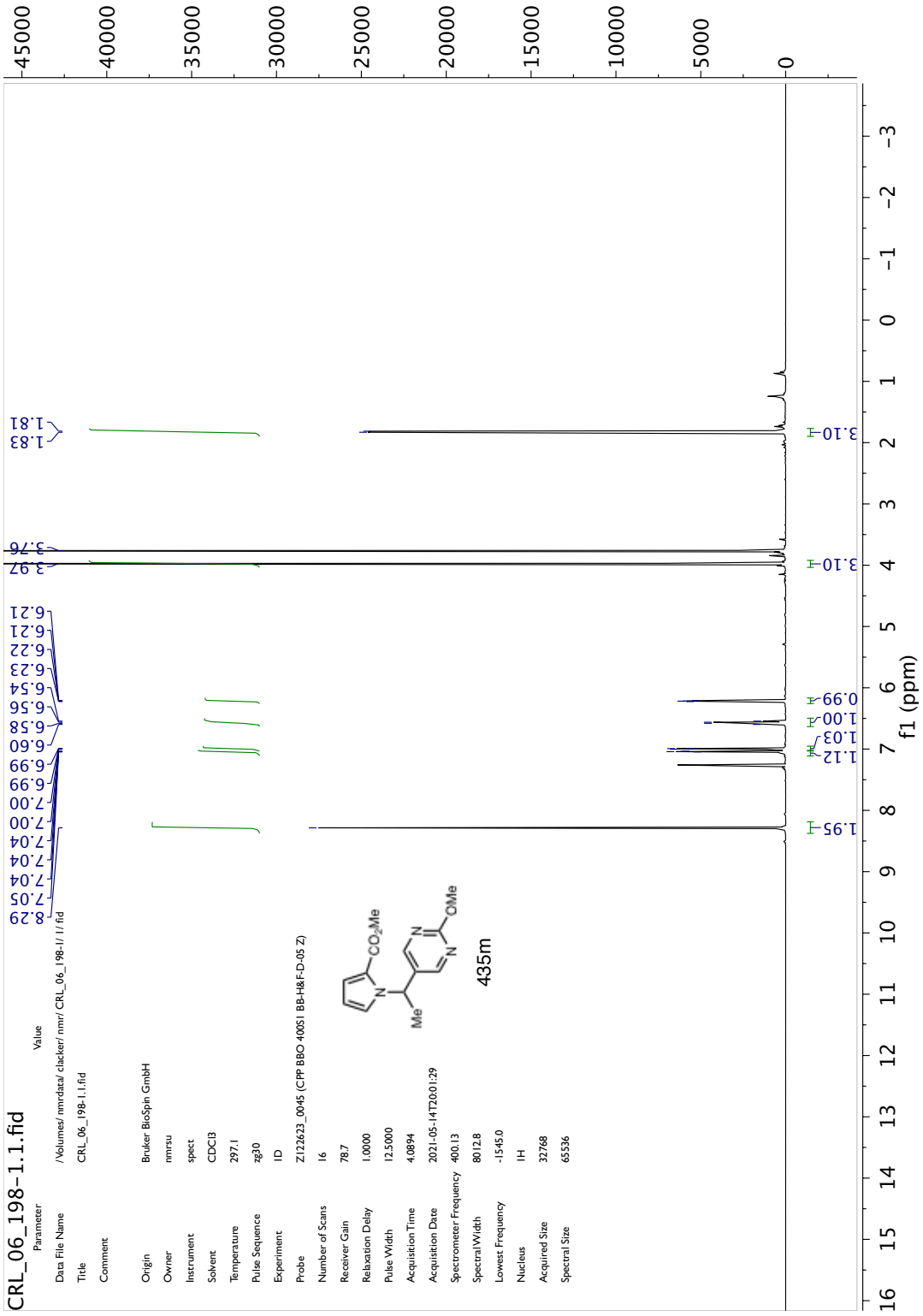
CRL_06_198-1.1.fid
Parameter Value
Data File Name /Volumes/ nmrdata/ clacker/ nmr/ CRL_06_198-1/ 1/ fid
Title CRL_06_198-1.1.fid
Comment
Origin Bruker BioSpin GmbH
Owner nmrsu
Instrument spect
Solvent CDCl3
Temperature 297.1
Pulse Sequence zg30
Experiment 1D
Probe Z122623_0045 (CPP BBO 400S1 BB-H&F-D-05 Z)
Number of Scans 16
Receiver Gain 78.7
Relaxation Delay 1.0000
Pulse Width 12.5000
Acquisition Time 4.0894
Acquisition Date 2021-05-14T20:01:29
Spectrometer Frequency 400.13
Spectral Width 8012.8
Lowest Frequency -1545.0
Nucleus 1H
Acquired Size 32768
Spectral Size 65536
435m
f1 (ppm)

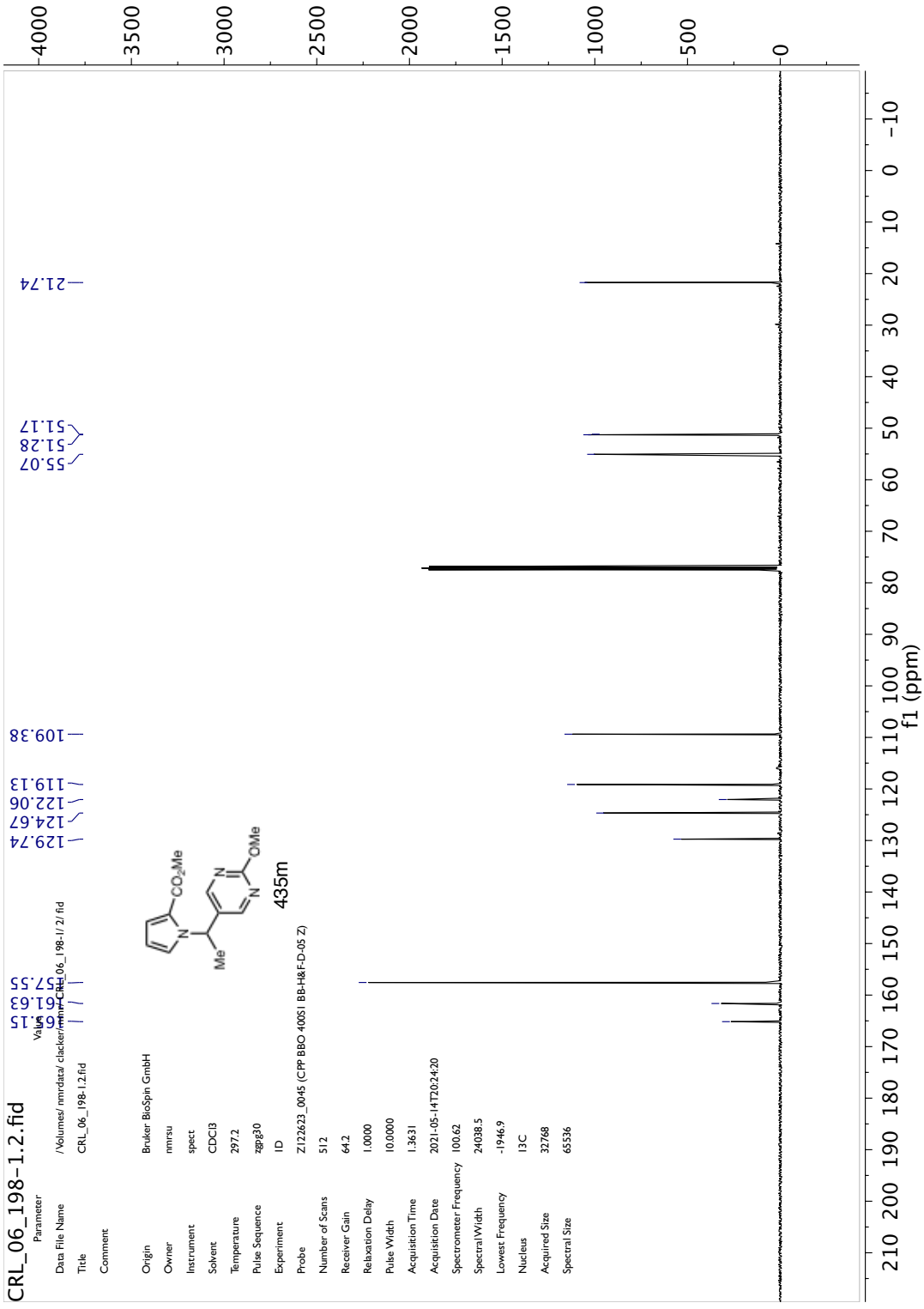
CRL_06_198-1.2.fid
Parameter
Value
Data File Name /Volumes/ nmrdata/ clacker/nmr/CRL_06_198-1/ 2/ fid
Title CRL_06_198-1.2.fid
Comment
Origin Bruker BioSpin GmbH
Owner nmrsu
Instrument spect
Solvent CDCl3
Temperature 297.2
Pulse Sequence zgpg30
Experiment 1D
Probe Z122623_0045 (CPP BBO 400S1 BB-H&F-D-05 Z)
Number of Scans 512
Receiver Gain 64.2
Relaxation Delay 1.0000
Pulse Width 10.0000
Acquisition Time 1.3631
Acquisition Date 2021-05-14T20:24:20
Spectrometer Frequency 100.62
Spectral Width 24038.5
Lowest Frequency -1946.9
Nucleus 13C
Acquired Size 32768
Spectral Size 65536
157.55
161.63
163.15
129.74
124.67
122.06
119.13
109.38
55.07
51.28
51.17
21.74
CO2Me
OMe
Me
435m
f1 (ppm)

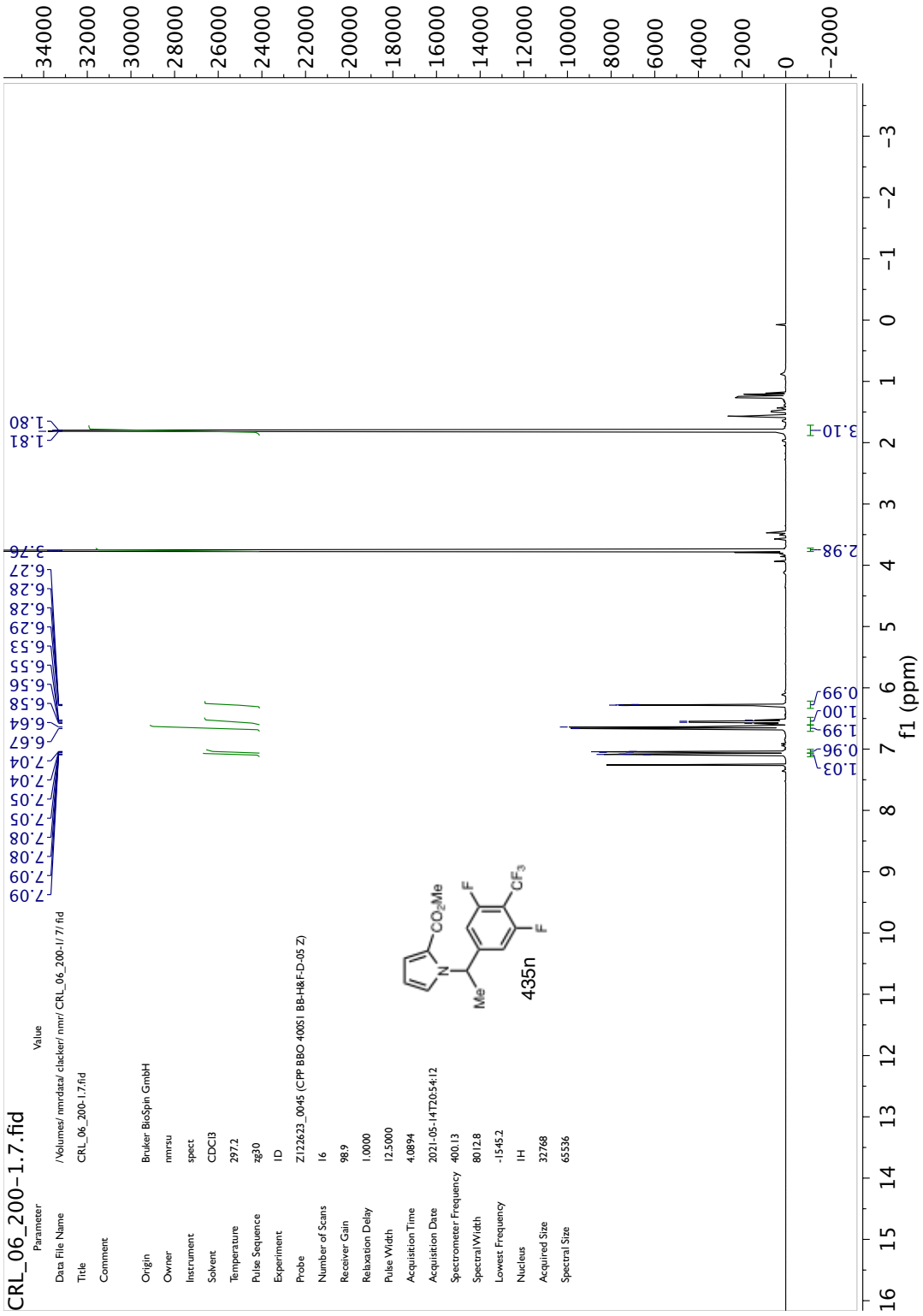
CRL_06_200-1.7.fid
Parameter
Value
Data File Name
/Volumes/ nmrdata/ clacker/ nmr/ CRL_06_200-1/ 7/ fid
Title
CRL_06_200-1.7.fid
Comment
Origin
Bruker BioSpin GmbH
Owner
nmrsu
Instrument
spect
Solvent
CDCl3
Temperature
297.2
Pulse Sequence
zg30
Experiment
1D
Probe
Z122623_0045 (CPP BBO 400S1 BB-H&F-D-05 Z)
Number of Scans
16
Receiver Gain
98.9
Relaxation Delay
1.0000
Pulse Width
12.5000
Acquisition Time
4.0894
Acquisition Date
2021-05-14T20:54:12
Spectrometer Frequency
400.13
Spectral Width
8012.8
Lowest Frequency
-1545.2
Nucleus
1H
Acquired Size
32768
Spectral Size
65536
435n
f1 (ppm)

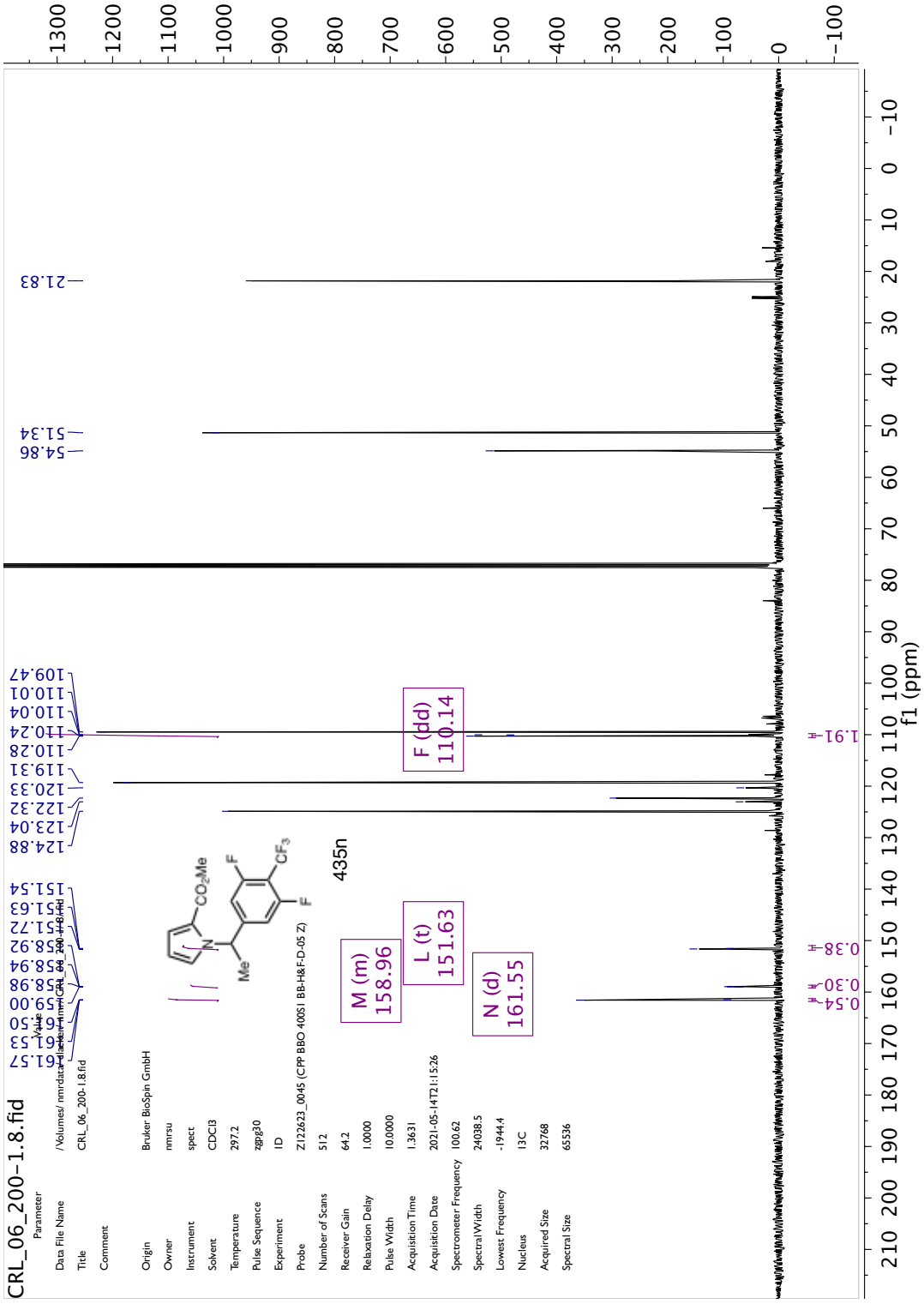
CRL_06_200-1.8.fid
Parameter
Data File Name /Volumes/ nmrdata/Hacker/nmr/CRL_06_200-1.8.fid
Title CRL_06_200-1.8.fid
Comment
Origin Bruker BioSpin GmbH
Owner nmrsu
Instrument spect
Solvent CDCl3
Temperature 297.2
Pulse Sequence zgpg30
Experiment 1D
Probe Z122623_0045 (CPP BBO 400S1 BB-H&F-D-05 Z)
Number of Scans 512
Receiver Gain 64.2
Relaxation Delay 1.0000
Pulse Width 10.0000
Acquisition Time 1.3631
Acquisition Date 2021-05-14T21:15:26
Spectrometer Frequency 100.62
Spectral Width 24038.5
Lowest Frequency -1944.4
Nucleus 13C
Acquired Size 32768
Spectral Size 65536
435n
M (m) 158.96
L (t) 151.63
N (d) 161.55
F (dd) 110.14
f1 (ppm)

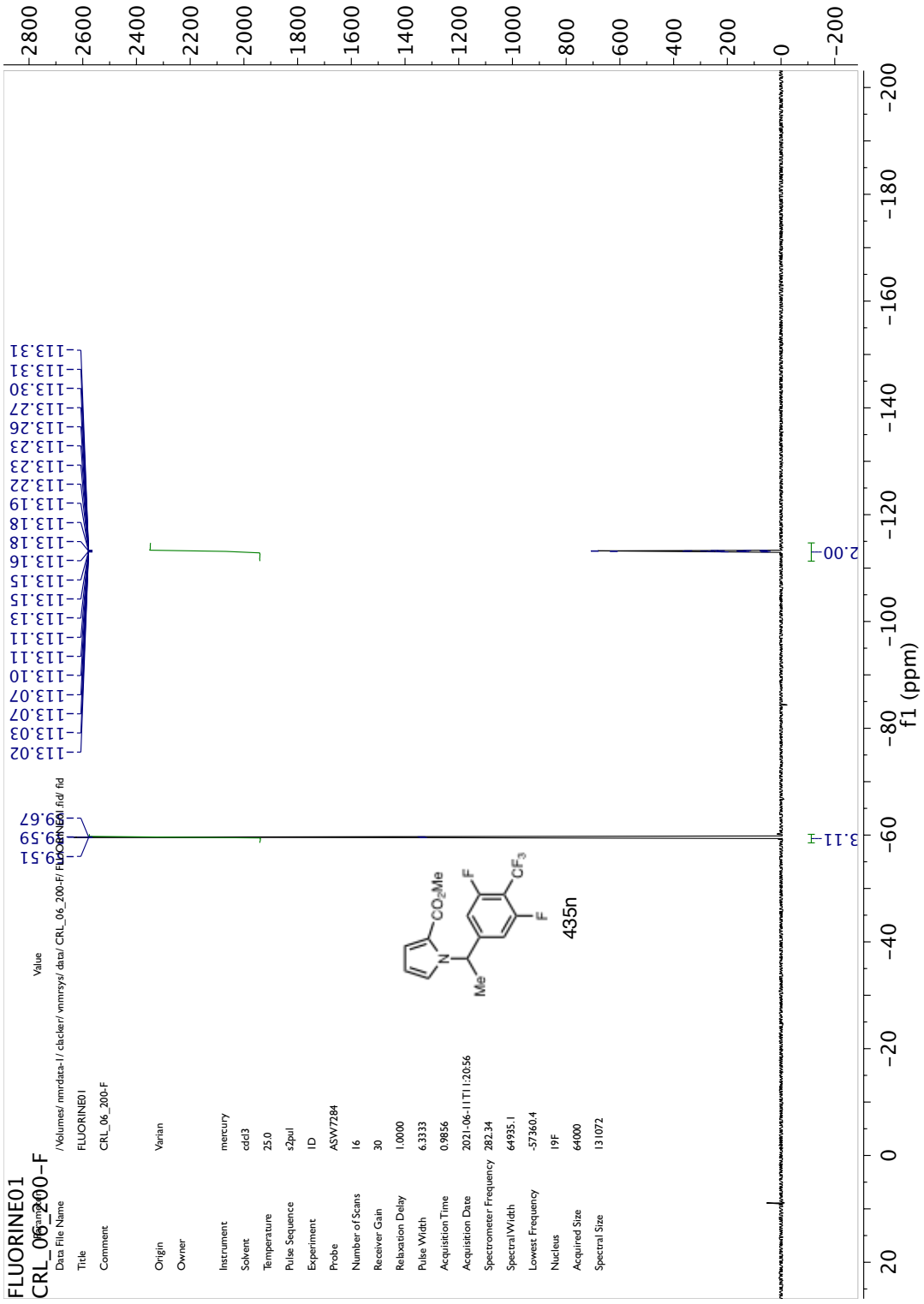
FLUORINE01
CRL_06_200-F
Name
Value
Data File Name
/Volumes/ nmrdata-1/ clacker/ vnmrsys/ data/ CRL_06_200-F/ FLUORINE01.fid/ fid
Title
FLUORINE01
Comment
CRL_06_200-F
Origin
Varian
Owner
Instrument
mercury
Solvent
cdcl3
Temperature
25.0
Pulse Sequence
s2pul
Experiment
1D
Probe
ASW7284
Number of Scans
16
Receiver Gain
30
Relaxation Delay
1.0000
Pulse Width
6.3333
Acquisition Time
0.9856
Acquisition Date
2021-06-11 11:20:56
Spectrometer Frequency
282.34
Spectral Width
64935.1
Lowest Frequency
-57360.4
Nucleus
19F
Acquired Size
64000
Spectral Size
131072
435n
2.00
3.11
f1 (ppm)

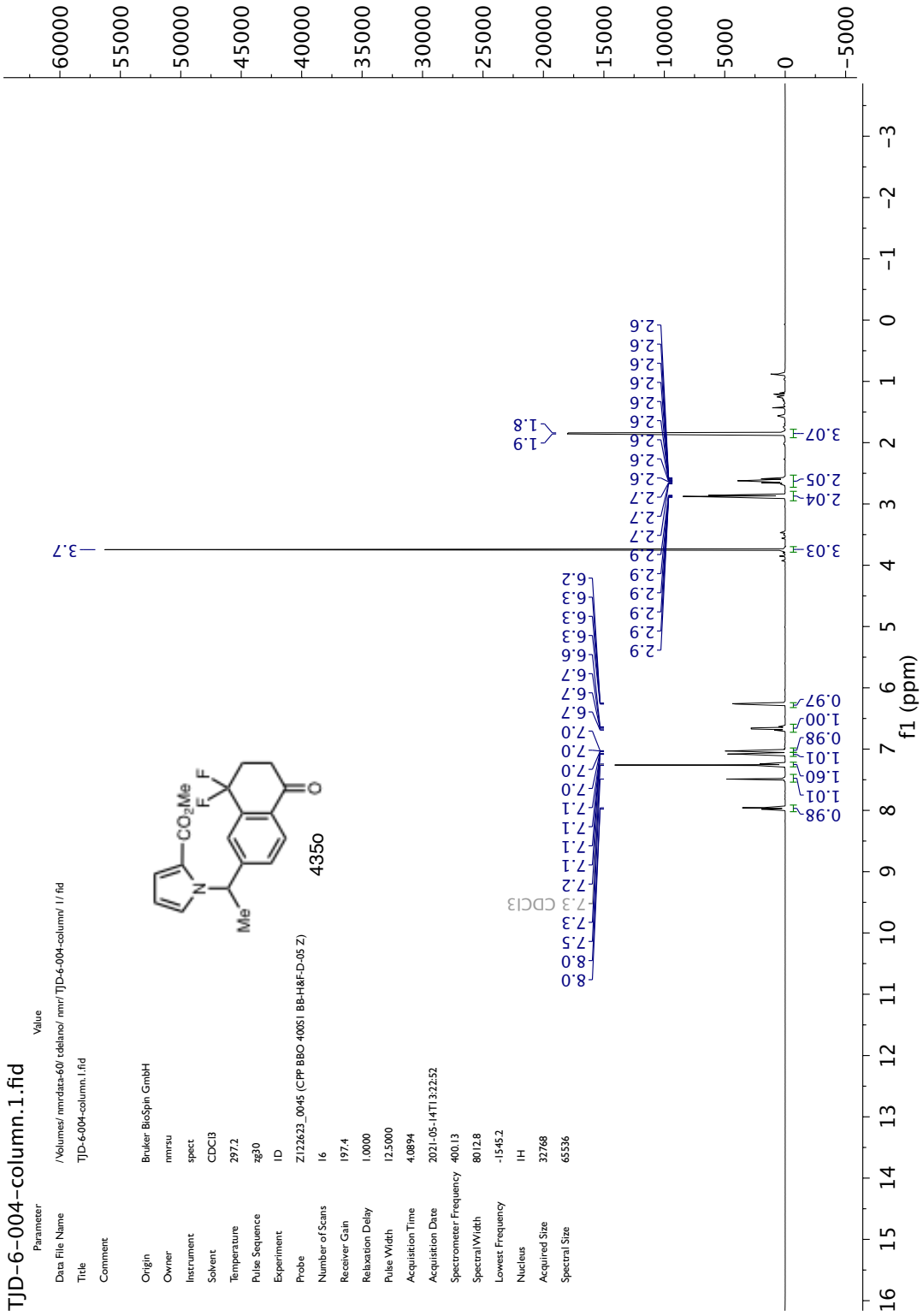
TJD-6-004-column.1.fid
Parameter
Value
Data File Name
/Volumes/ nmrdata-60/ tdelano/ nmr/ TJD-6-004-column/ 1/ fid
Title
TJD-6-004-column.1.fid
Comment
Origin
Bruker BioSpin GmbH
Owner
nmrsu
Instrument
spect
Solvent
CDCl3
Temperature
297.2
Pulse Sequence
zg30
Experiment
1D
Probe
Z122623_0045 (CPP BBO 400S1 BB-H&F-D-05 Z)
Number of Scans
16
Receiver Gain
197.4
Relaxation Delay
1.0000
Pulse Width
12.5000
Acquisition Time
4.0894
Acquisition Date
2021-05-14T13:22:52
Spectrometer Frequency
400.13
Spectral Width
8012.8
Lowest Frequency
-1545.2
Nucleus
1H
Acquired Size
32768
Spectral Size
65536
435o
CO2Me
F
F
O
N
Me
3.7
3.07
2.04
2.05
3.03
1.9
1.8
0.98
1.01
1.60
1.01
0.98
1.00
0.97
CDCl3
f1 (ppm)

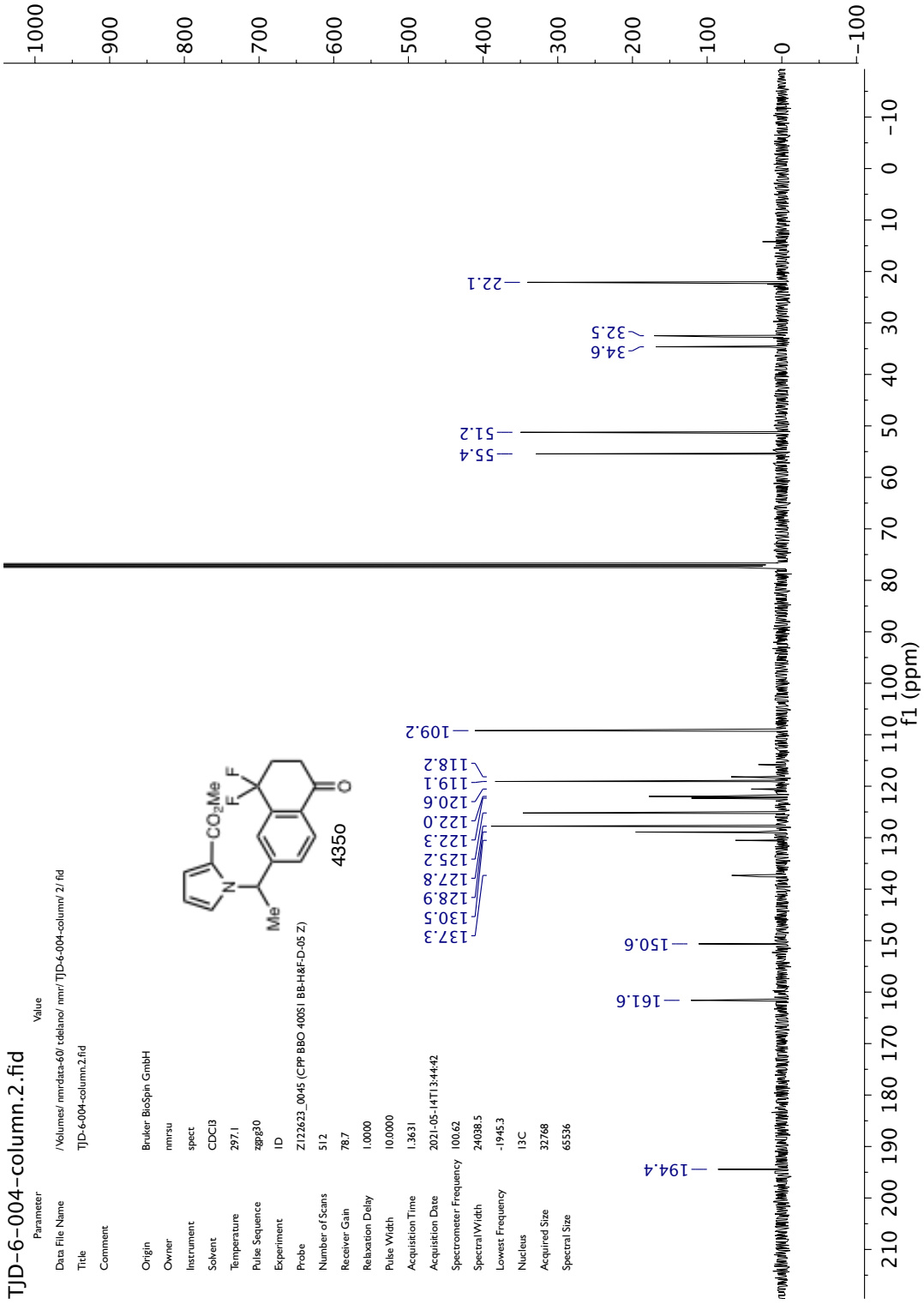
TJD–6–004–column.2.fid
Parameter
Value
Data File Name /Volumes/ nmrdata-60/ tdelano/ nmr/ TJD-6-004-column/ 2/ fid
Title TJD-6-004-column.2.fid
Comment
Origin Bruker BioSpin GmbH
Owner nmrsu
Instrument spect
Solvent CDCl3
Temperature 297.1
Pulse Sequence zgpg30
Experiment 1D
Probe Z122623_0045 (CPP BBO 400S1 BB-H&F-D-05 Z)
Number of Scans 512
Receiver Gain 78.7
Relaxation Delay 1.0000
Pulse Width 10.0000
Acquisition Time 1.3631
Acquisition Date 2021-05-14T13:44:42
Spectrometer Frequency 100.62
Spectral Width 24038.5
Lowest Frequency -1945.3
Nucleus 13C
Acquired Size 32768
Spectral Size 65536
CO2Me
F
F
O
N
Me
4350
194.4
161.6
150.6
137.3
130.5
128.9
127.8
125.2
122.3
122.0
120.6
119.1
118.2
109.2
55.4
51.2
34.6
32.5
22.1
f1 (ppm)

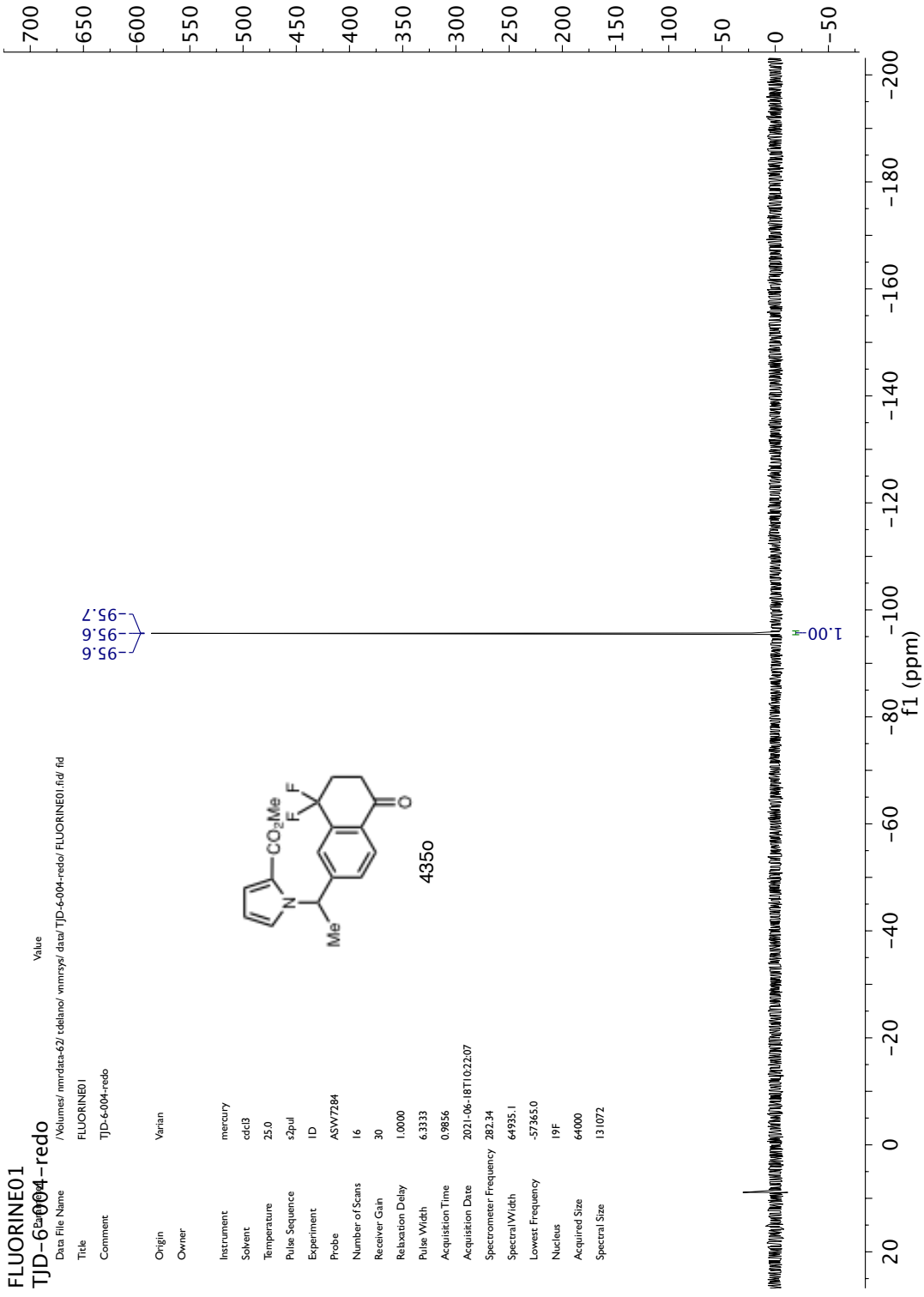
FLUORINE01
TJD-6-004-redo
Value
Data File Name /Volumes/ nmrdata-62/ rdelano/ vnmrsys/ data/ TJD-6-004-redo/ FLUORINE01.fid/ fid
Title FLUORINE01
Comment TJD-6-004-redo
Origin Varian
Owner
Instrument mercury
Solvent cdcl3
Temperature 25.0
Pulse Sequence s2pul
Experiment 1D
Probe ASW7284
Number of Scans 16
Receiver Gain 30
Relaxation Delay 1.0000
Pulse Width 6.3333
Acquisition Time 0.9856
Acquisition Date 2021-06-18T10:22:07
Spectrometer Frequency 282.34
Spectral Width 64935.1
Lowest Frequency -57365.0
Nucleus 19F
Acquired Size 64000
Spectral Size 131072
435o
-95.6
-95.6
-95.7
1.00
f1 (ppm)

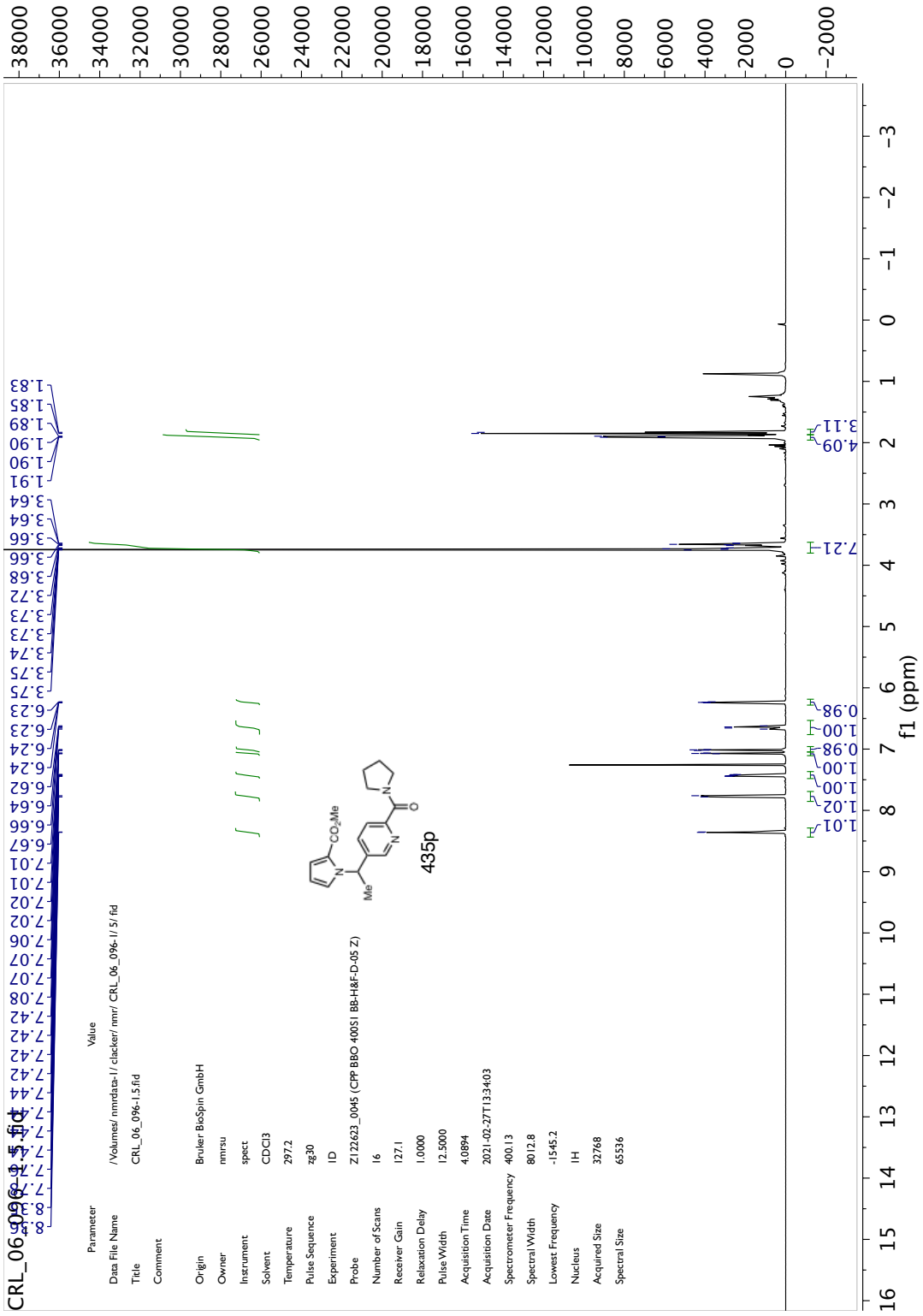
CRL_06_096-1.5.fid
Parameter Value
Data File Name /Volumes/ nmrdata-1/ clacker/ nmr/ CRL_06_096-1/ 5/ fid
Title CRL_06_096-1.5.fid
Comment
Origin Bruker BioSpin GmbH
Owner nmrsu
Instrument spect
Solvent CDCl3
Temperature 297.2
Pulse Sequence zg30
Experiment ID
Probe Z122623_0045 (CPP BBO 400SI BB-H&F-D-05 Z)
Number of Scans 16
Receiver Gain 127.1
Relaxation Delay 1.0000
Pulse Width 12.5000
Acquisition Time 4.0894
Acquisition Date 2021-02-27T13:34:03
Spectrometer Frequency 400.13
Spectral Width 8012.8
Lowest Frequency -1545.2
Nucleus 1H
Acquired Size 32768
Spectral Size 65536
435p
f1 (ppm)

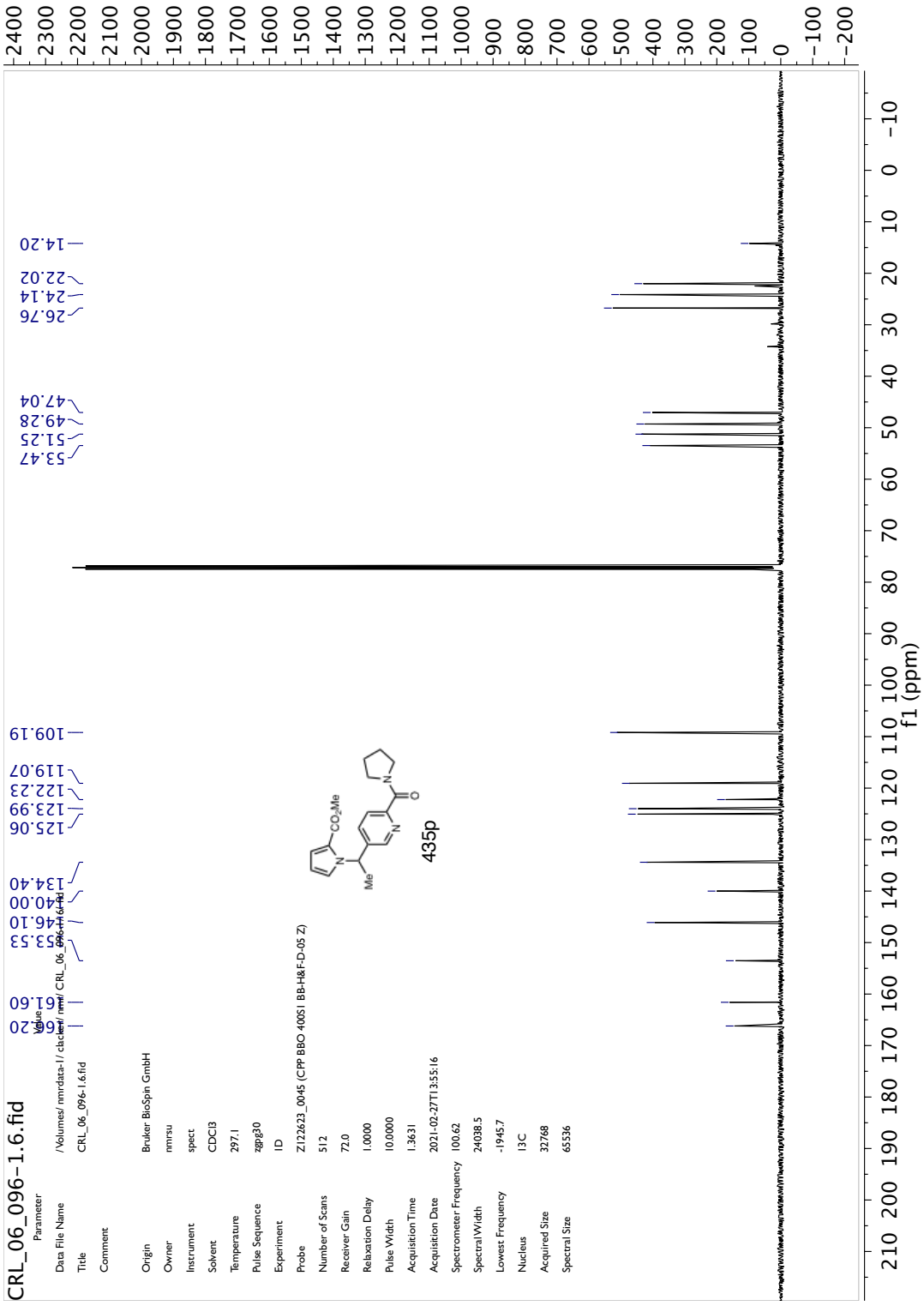
CRL_06_096-1.6.fid
Parameter
Value
Data File Name /Volumes/ nmrdata-1/ cbc1ev/ nmr/ CRL_06_096-1.6.fid
Title CRL_06_096-1.6.fid
Comment
Origin Bruker BioSpin GmbH
Owner nmrsu
Instrument spect
Solvent CDCl3
Temperature 297.1
Pulse Sequence zgpg30
Experiment 1D
Probe Z122623_0045 (CPP BBO 400S1 BB-H&F-D-05 Z)
Number of Scans 512
Receiver Gain 72.0
Relaxation Delay 1.0000
Pulse Width 10.0000
Acquisition Time 1.3631
Acquisition Date 2021-02-27T13:55:16
Spectrometer Frequency 100.62
Spectral Width 24038.5
Lowest Frequency -1945.7
Nucleus 13C
Acquired Size 32768
Spectral Size 65536
CO2Me
Me
435p
14.20
22.02
24.14
26.76
47.04
49.28
51.25
53.47
109.19
119.07
122.23
123.99
125.06
134.40
140.00
146.10
153.53
161.60
166.20
f1 (ppm)

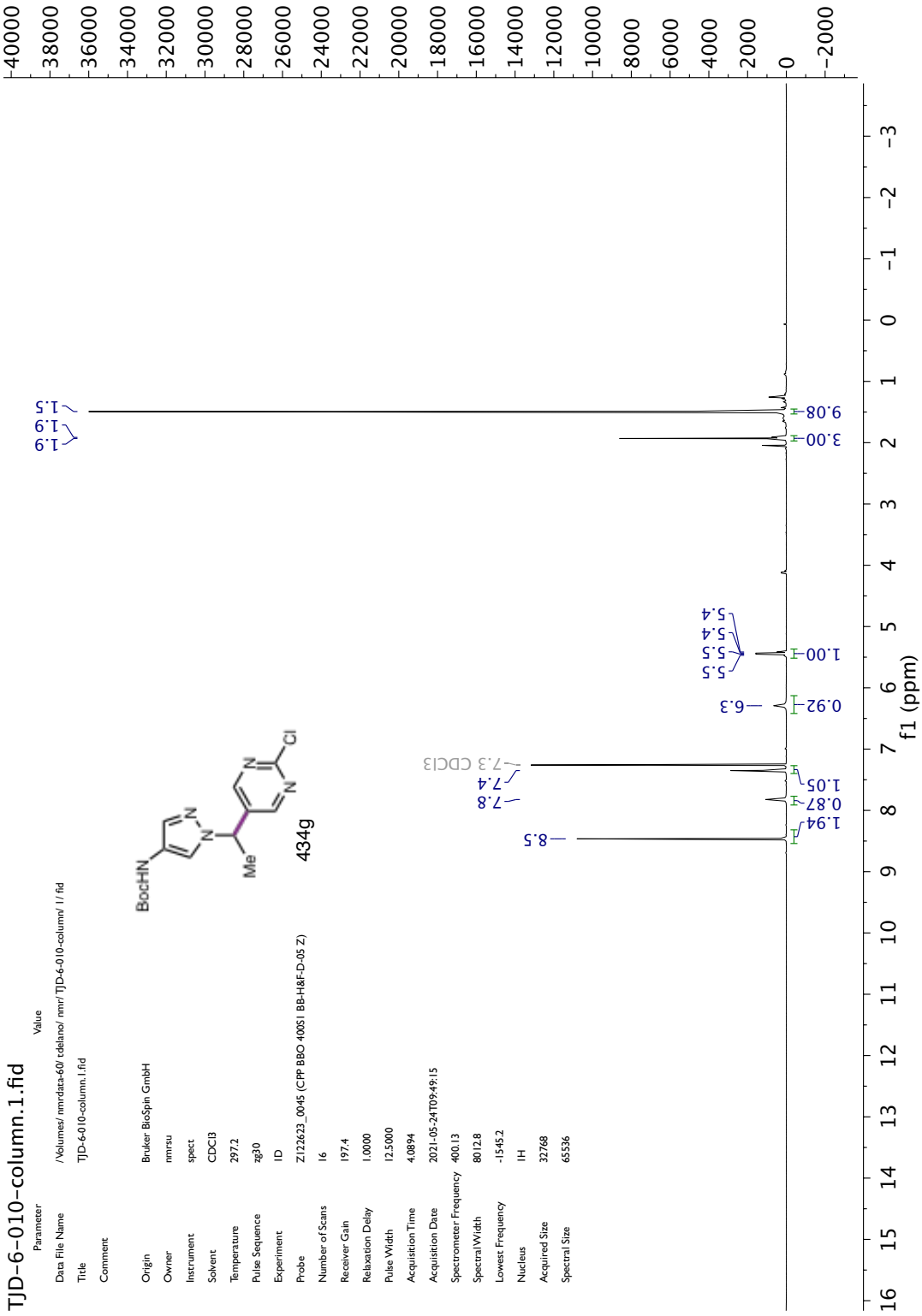
TJD-6-010-column.1.fid
Parameter
Value
Data File Name /Volumes/ nmrdata-60/ tdelano/ nmr/ TJD-6-010-column/ 1/ fid
Title TJD-6-010-column.1.fid
Comment
Origin Bruker BioSpin GmbH
Owner nmrsu
Instrument spect
Solvent CDCl3
Temperature 297.2
Pulse Sequence zg30
Experiment 1D
Probe Z122623_0045 (CPP BBO 400S1 BB-H&F-D-05 Z)
Number of Scans 16
Receiver Gain 197.4
Relaxation Delay 1.0000
Pulse Width 12.5000
Acquisition Time 4.0894
Acquisition Date 2021-05-24T09:49:15
Spectrometer Frequency 400.13
Spectral Width 8012.8
Lowest Frequency -1545.2
Nucleus 1H
Acquired Size 32768
Spectral Size 65536
BocHN
Me
Cl
434g
1.9
1.9
1.5
9.08
3.00
1.00
0.92
6.3
5.5
5.5
5.4
5.4
1.05
0.87
1.94
7.8
7.4
7.3 CDCl3
8.5
f1 (ppm)

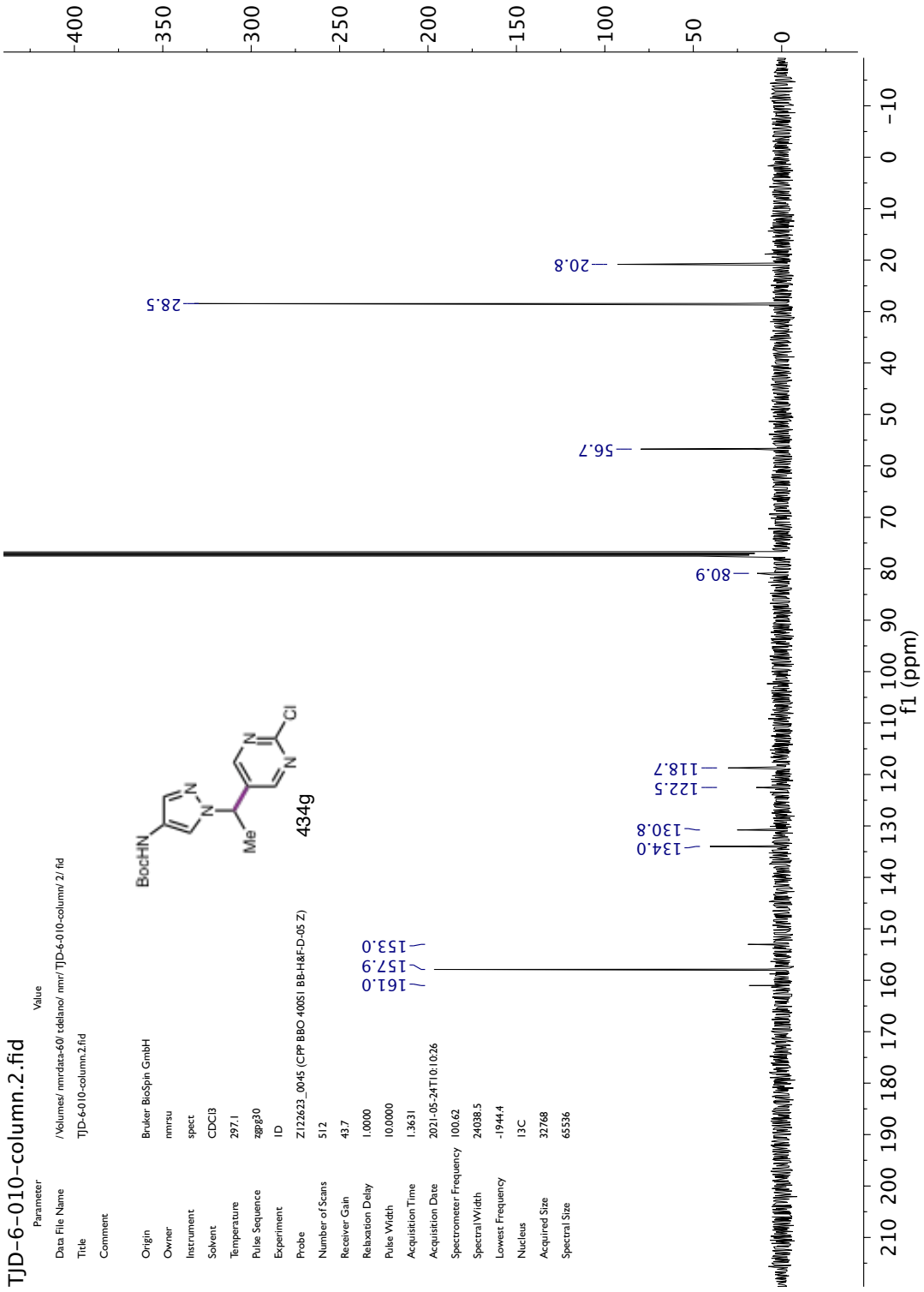
TJD-6-010-column.2.fid
Parameter
Value
Data File Name /Volumes/ nmrdata-60/ tdelano/ nmr/ TJD-6-010-column/ 2/ fid
Title TJD-6-010-column.2.fid
Comment
Origin Bruker BioSpin GmbH
Owner nmrsu
Instrument spect
Solvent CDCl3
Temperature 297.1
Pulse Sequence zgpg30
Experiment 1D
Probe Z122623_0045 (CPP BBO 400S1 BB-H&F-D-05 Z)
Number of Scans 512
Receiver Gain 43.7
Relaxation Delay 1.0000
Pulse Width 10.0000
Acquisition Time 1.3631
Acquisition Date 2021-05-24T10:10:26
Spectrometer Frequency 100.62
Spectral Width 24038.5
Lowest Frequency -1944.4
Nucleus 13C
Acquired Size 32768
Spectral Size 65536
BocHN
Me
Cl
434g
161.0
157.9
153.0
134.0
130.8
122.5
118.7
80.9
56.7
28.5
20.8
f1 (ppm)

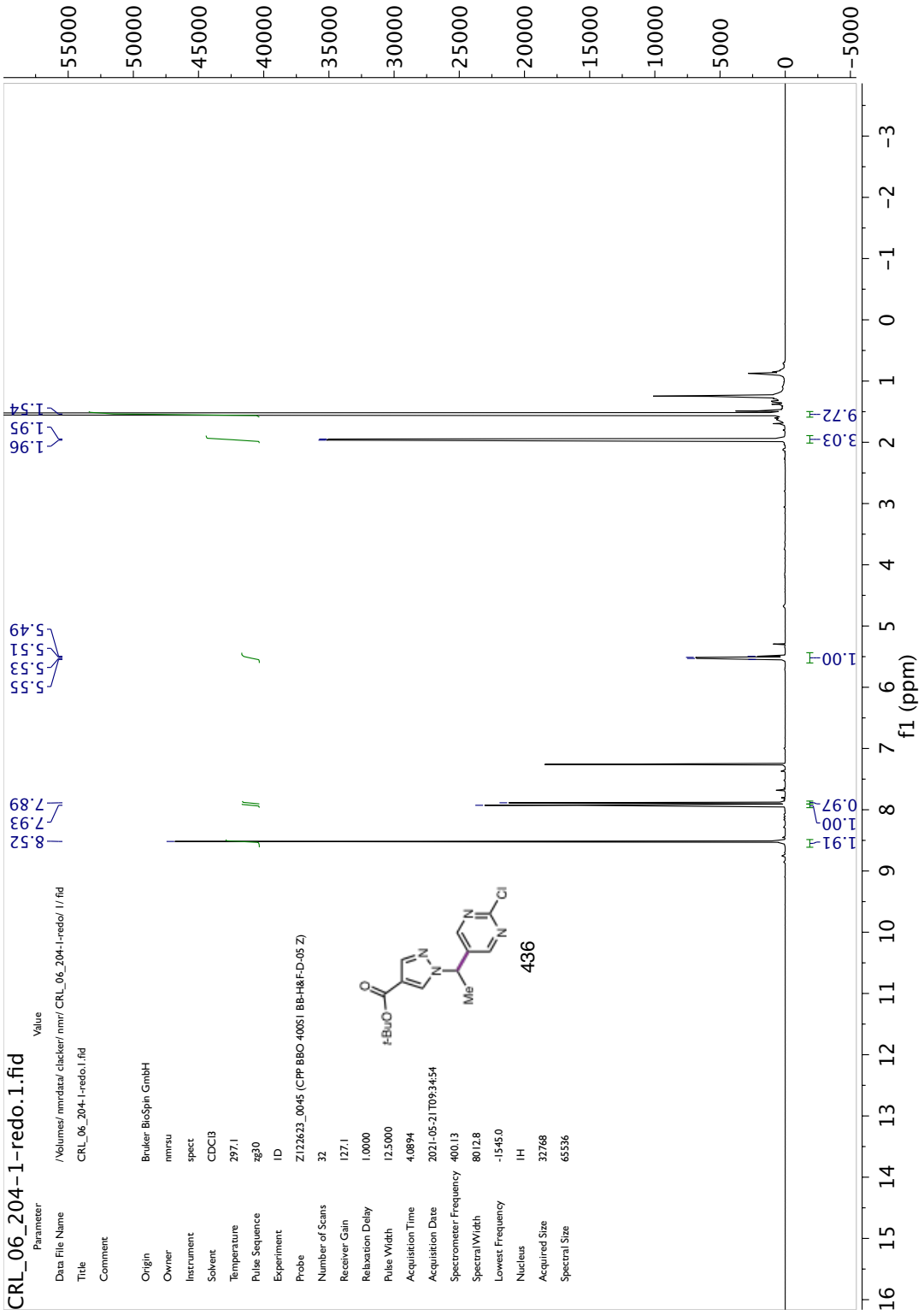
CRL_06_204-1-redo.1.fid
Parameter Value
Data File Name /Volumes/ nmrdata/ clacker/ nmr/ CRL_06_204-1-redo/ 1/ fid
Title CRL_06_204-1-redo.1.fid
Comment
Origin Bruker BioSpin GmbH
Owner nmrsu
Instrument spect
Solvent CDCl3
Temperature 297.1
Pulse Sequence zg30
Experiment 1D
Probe Z122623_0045 (CPP BBO 400S1 BB-H&F-D-05 Z)
Number of Scans 32
Receiver Gain 127.1
Relaxation Delay 1.0000
Pulse Width 12.5000
Acquisition Time 4.0894
Acquisition Date 2021-05-21T09:34:54
Spectrometer Frequency 400.13
Spectral Width 8012.8
Lowest Frequency -1545.0
Nucleus 1H
Acquired Size 32768
Spectral Size 65536
8.52
7.93
7.89
5.55
5.53
5.51
5.49
1.96
1.95
1.54
1.91
1.00
0.97
1.00
3.03
9.72
t-BuO
Me
Cl
436
f1 (ppm)

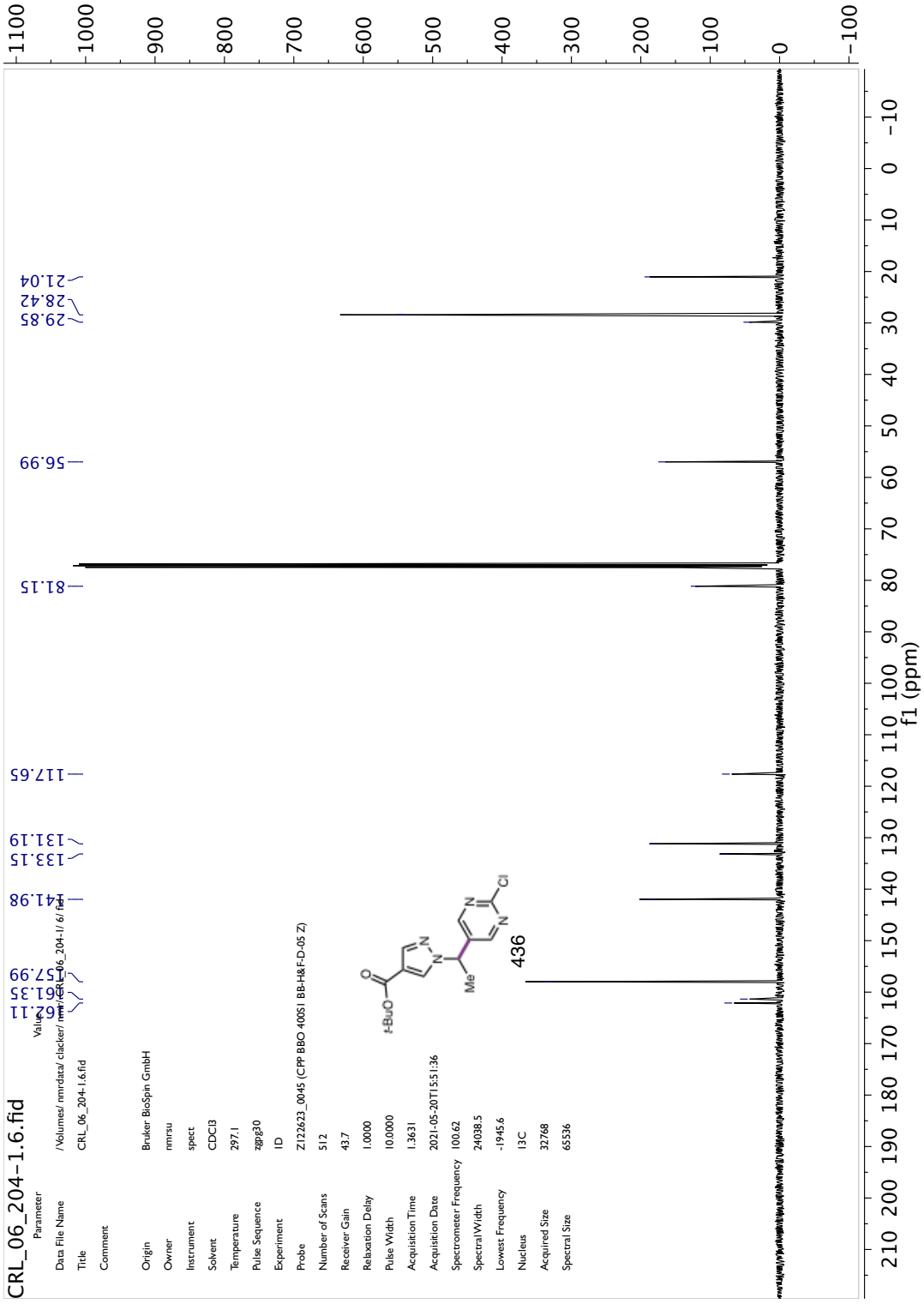
CRL_06_204-1.6.fid
Parameter Value
Data File Name /Volumes/ nmrdata/ clacker/ nmr/CRL_06_204-1/ 6/ fid
Title CRL_06_204-1.6.fid
Comment
Origin Bruker BioSpin GmbH
Owner nmrsu
Instrument spect
Solvent CDCl3
Temperature 297.1
Pulse Sequence zgpg30
Experiment 1D
Probe Z122623_0045 (CPP BBO 400S1 BB-H&F-D-05 Z)
Number of Scans 512
Receiver Gain 43.7
Relaxation Delay 1.0000
Pulse Width 10.0000
Acquisition Time 1.3631
Acquisition Date 2021-05-20T15:51:36
Spectrometer Frequency 100.62
Spectral Width 24038.5
Lowest Frequency -1945.6
Nucleus 13C
Acquired Size 32768
Spectral Size 65536
162.11
161.35
157.99
141.98
133.15
131.19
117.65
81.15
56.99
29.85
28.42
21.04
436
f1 (ppm)

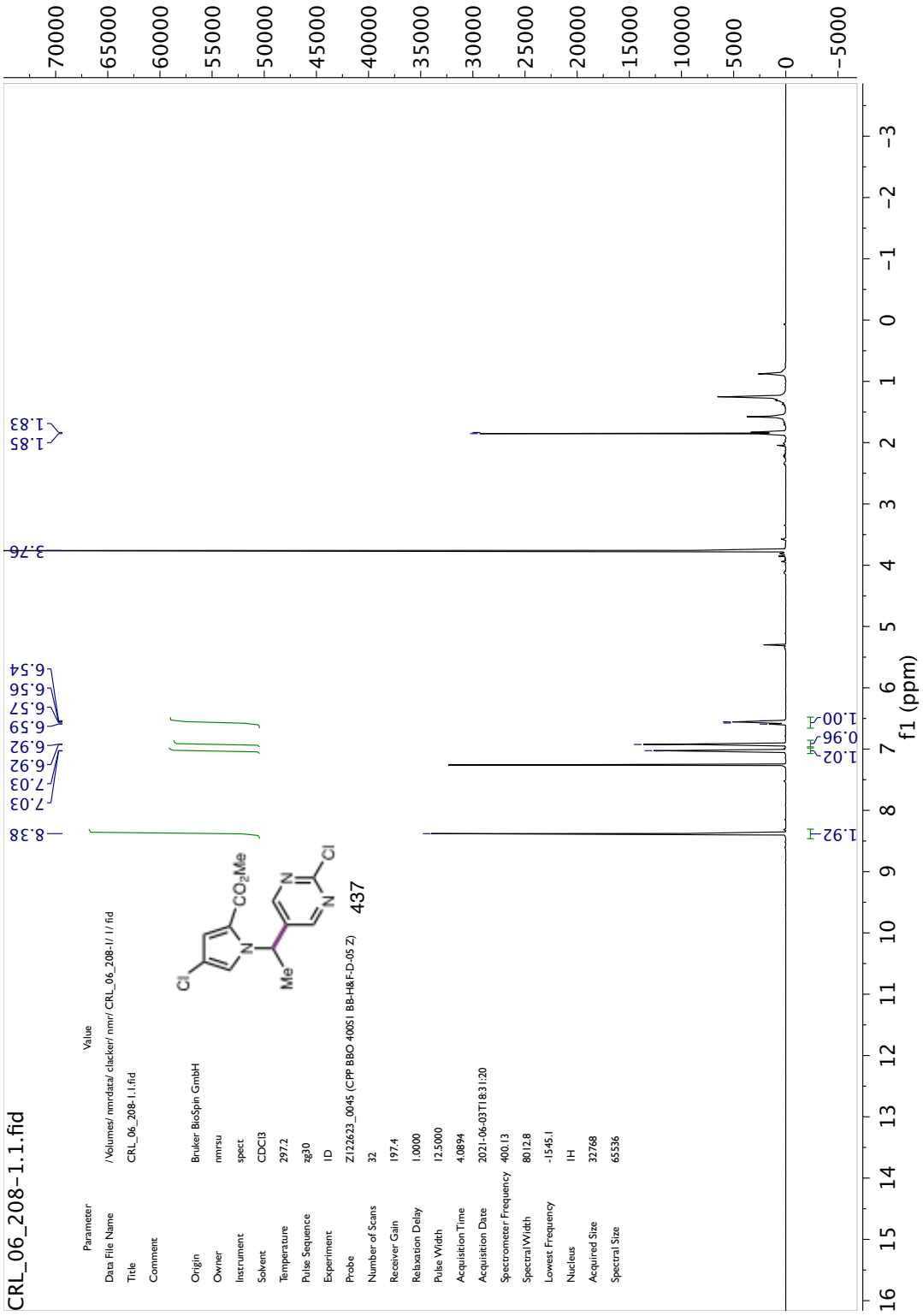
CRL_06_208-1.1.fid
Parameter
Value
Data File Name
/Volumes/ nmrdata/ clacker/ nmr/ CRL_06_208-1/ 1/ fid
Title
CRL_06_208-1.1.fid
Comment
Origin
Bruker BioSpin GmbH
Owner
nmrsu
Instrument
spect
Solvent
CDCl3
Temperature
297.2
Pulse Sequence
zg30
Experiment
1D
Probe
Z122623_0045 (CPP BBO 400S1 BB-H&F-D-05 Z)
Number of Scans
32
Receiver Gain
197.4
Relaxation Delay
1.0000
Pulse Width
12.5000
Acquisition Time
4.0894
Acquisition Date
2021-06-03T18:31:20
Spectrometer Frequency
400.13
Spectral Width
8012.8
Lowest Frequency
-1545.1
Nucleus
1H
Acquired Size
32768
Spectral Size
65536
437
8.38
7.03
7.03
6.92
6.92
6.59
6.57
6.56
6.54
3.76
1.85
1.83
1.92
1.02
0.96
1.00
f1 (ppm)

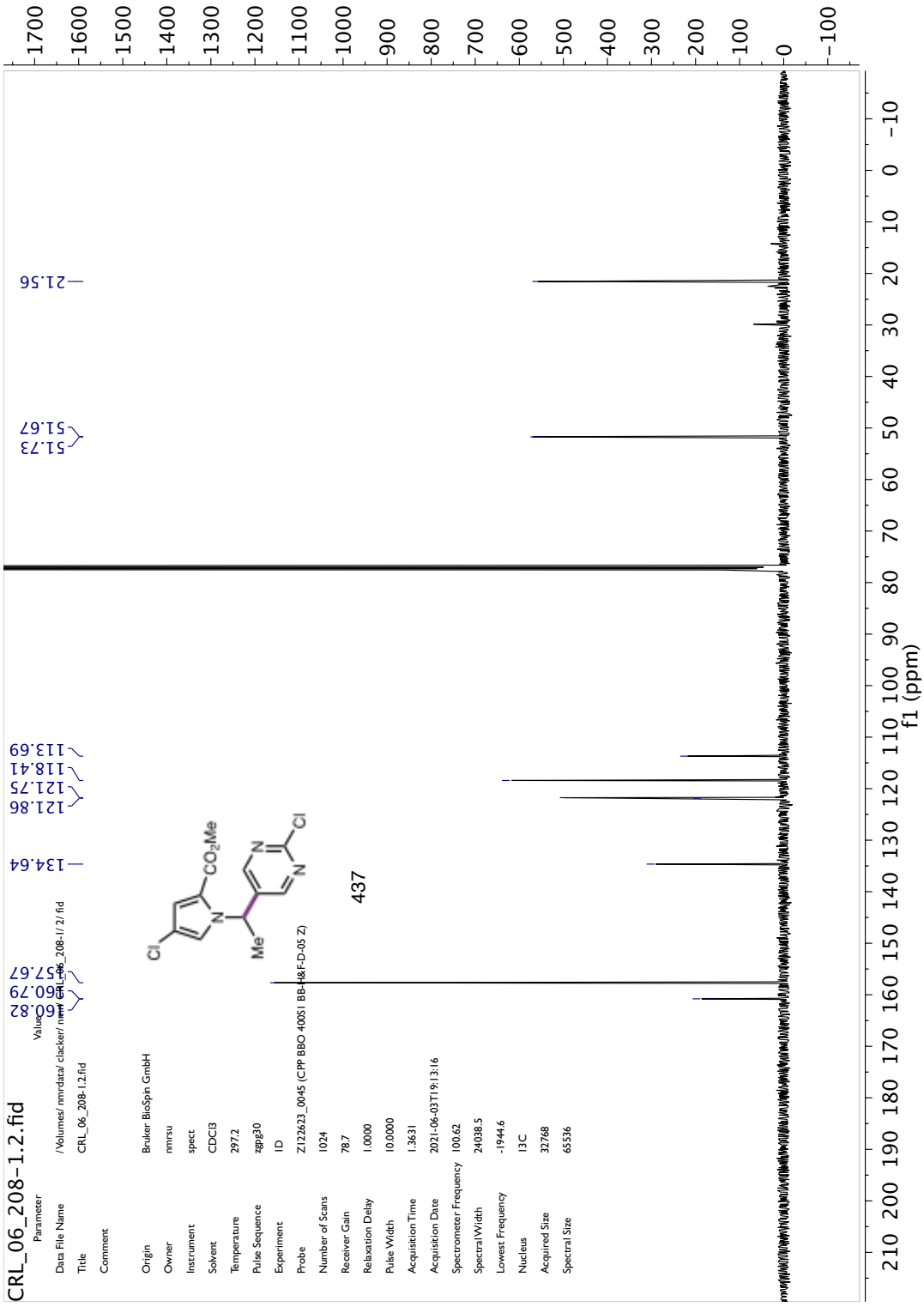
CRL_06_208-1.2.fid
Parameter
Value
Data File Name /Volumes/ nmrdata/ clacker/ nmr/ CRL_06_208-1/ 2/ fid
Title CRL_06_208-1.2.fid
Comment
Origin Bruker BioSpin GmbH
Owner nmrsu
Instrument spect
Solvent CDCl3
Temperature 297.2
Pulse Sequence zgpg30
Experiment 1D
Probe Z122623_0045 (CPP BBO 400S1 BB-H&F-D-05 Z)
Number of Scans 1024
Receiver Gain 78.7
Relaxation Delay 1.0000
Pulse Width 10.0000
Acquisition Time 1.3631
Acquisition Date 2021-06-03T19:13:16
Spectrometer Frequency 100.62
Spectral Width 24038.5
Lowest Frequency -1944.6
Nucleus 13C
Acquired Size 32768
Spectral Size 65536
160.82
160.79
157.67
134.64
121.86
121.75
118.41
113.69
51.73
51.67
21.56
437
f1 (ppm)

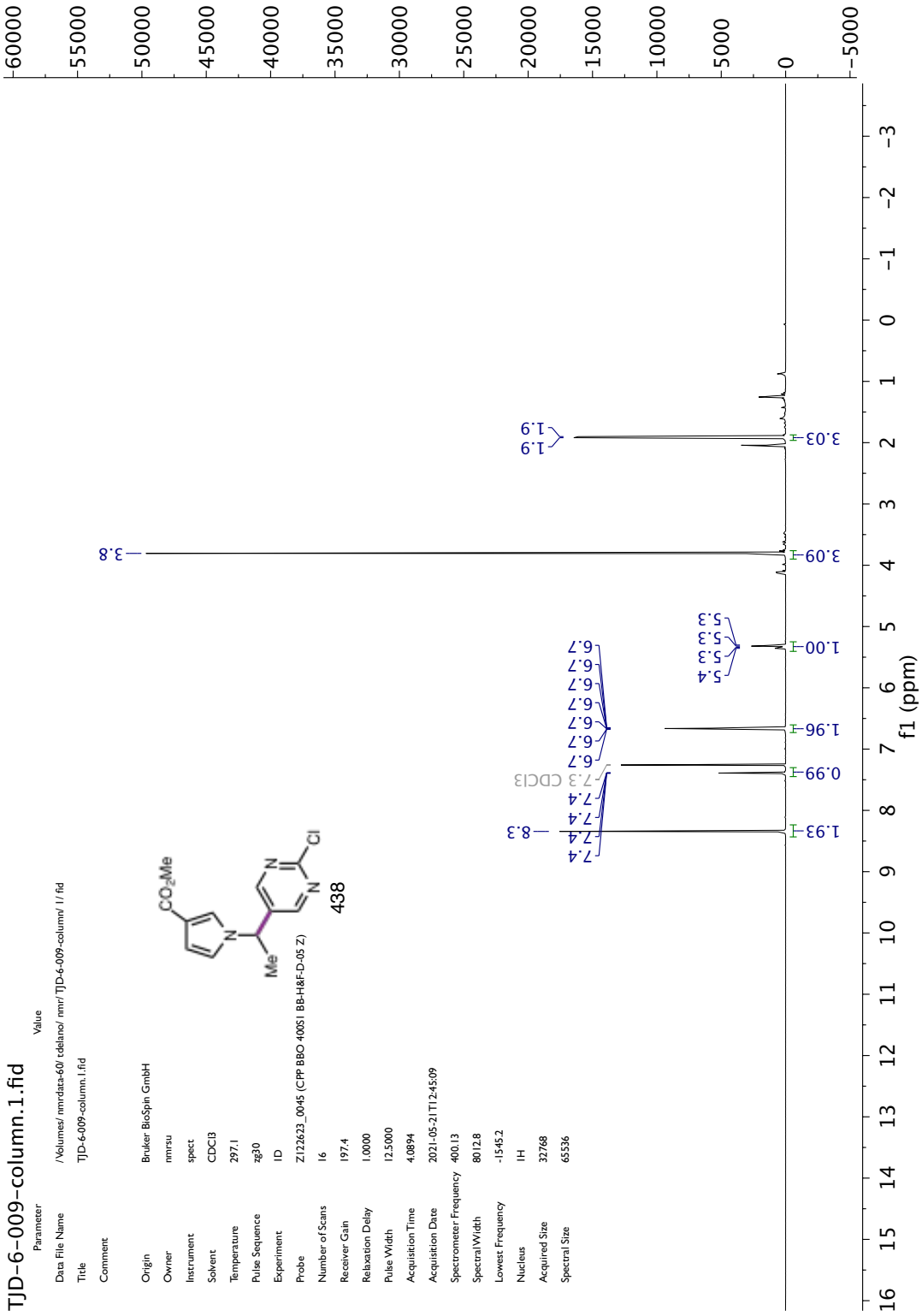
TJD-6-009-column.1.fid
Parameter
Value
Data File Name
/Volumes/ nmrdata-60/ tdelano/ nmr/ TJD-6-009-column/ 1/ fid
Title
TJD-6-009-column.1.fid
Comment
Origin
Bruker BioSpin GmbH
Owner
nmrsu
Instrument
spect
Solvent
CDCl3
Temperature
297.1
Pulse Sequence
zg30
Experiment
1D
Probe
Z122623_0045 (CPP BBO 400S1 BB-H&F-D-05 Z)
Number of Scans
16
Receiver Gain
197.4
Relaxation Delay
1.0000
Pulse Width
12.5000
Acquisition Time
4.0894
Acquisition Date
2021-05-21T12:45:09
Spectrometer Frequency
400.13
Spectral Width
8012.8
Lowest Frequency
-1545.2
Nucleus
1H
Acquired Size
32768
Spectral Size
65536
CO2Me
Me
Cl
N
N
438
3.8
8.3
7.4
7.4
7.4
7.3 CDCl3
6.7
6.7
6.7
6.7
6.7
6.7
6.7
5.4
5.3
5.3
5.3
1.9
1.9
3.03
3.09
1.00
1.96
0.99
1.93
f1 (ppm)

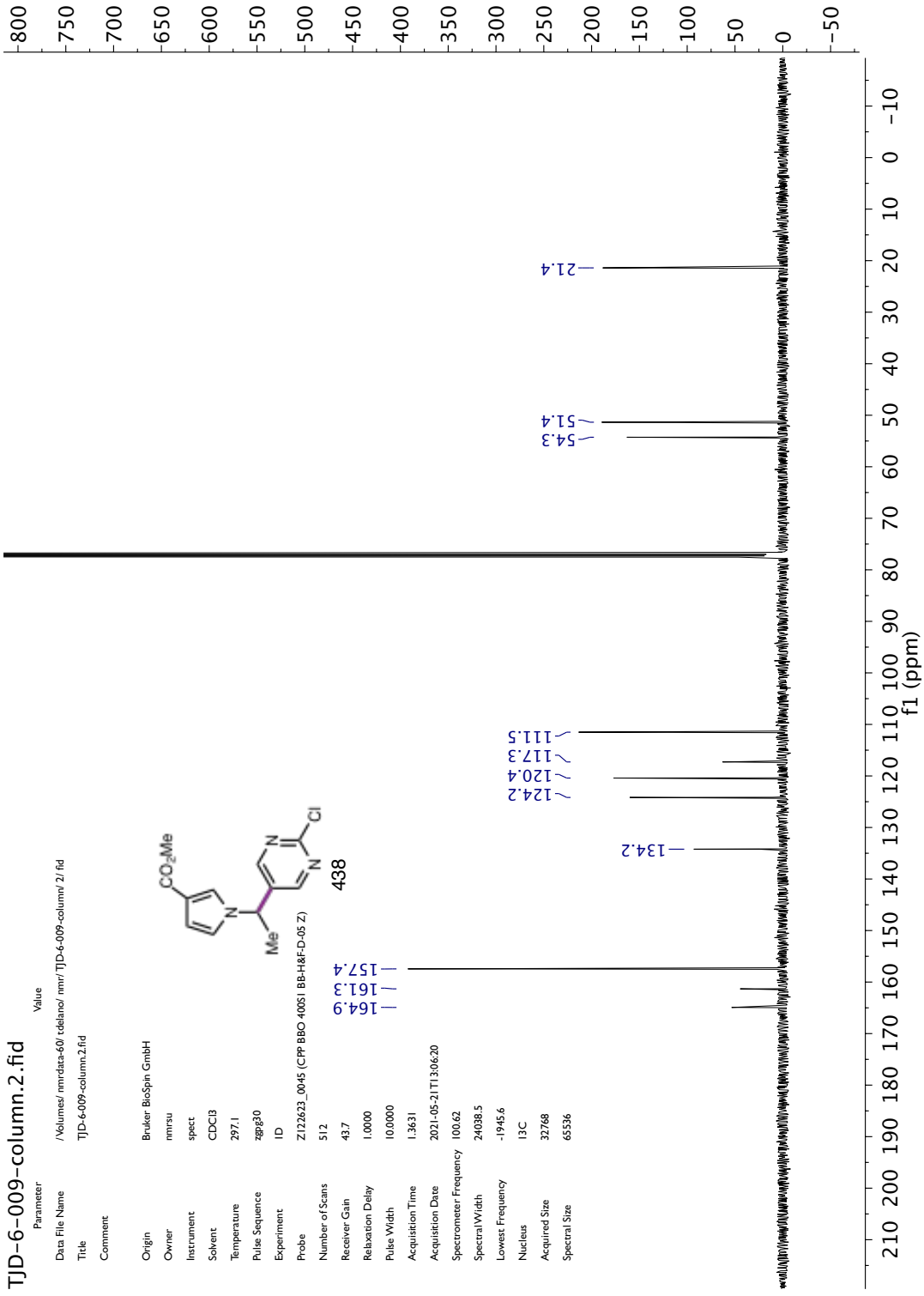
TJD-6-009-column.2.fid
Parameter
Value
Data File Name
/Volumes/ nmrdata-60/ tdelano/ nmr/ TJD-6-009-column/ 2/ fid
Title
TJD-6-009-column.2.fid
Comment
Origin
Bruker BioSpin GmbH
Owner
nmrsu
Instrument
spect
Solvent
CDCl3
Temperature
297.1
Pulse Sequence
zgpg30
Experiment
1D
Probe
Z122623_0045 (CPP BBO 400S1 BB-H&F-D-05 Z)
Number of Scans
512
Receiver Gain
43.7
Relaxation Delay
1.0000
Pulse Width
10.0000
Acquisition Time
1.3631
Acquisition Date
2021-05-21T13:06:20
Spectrometer Frequency
100.62
Spectral Width
24038.5
Lowest Frequency
-1945.6
Nucleus
13C
Acquired Size
32768
Spectral Size
65536
CO2Me
Me
Cl
N
N
438
164.9
161.3
157.4
134.2
124.2
120.4
117.3
111.5
54.3
51.4
21.4
f1 (ppm)

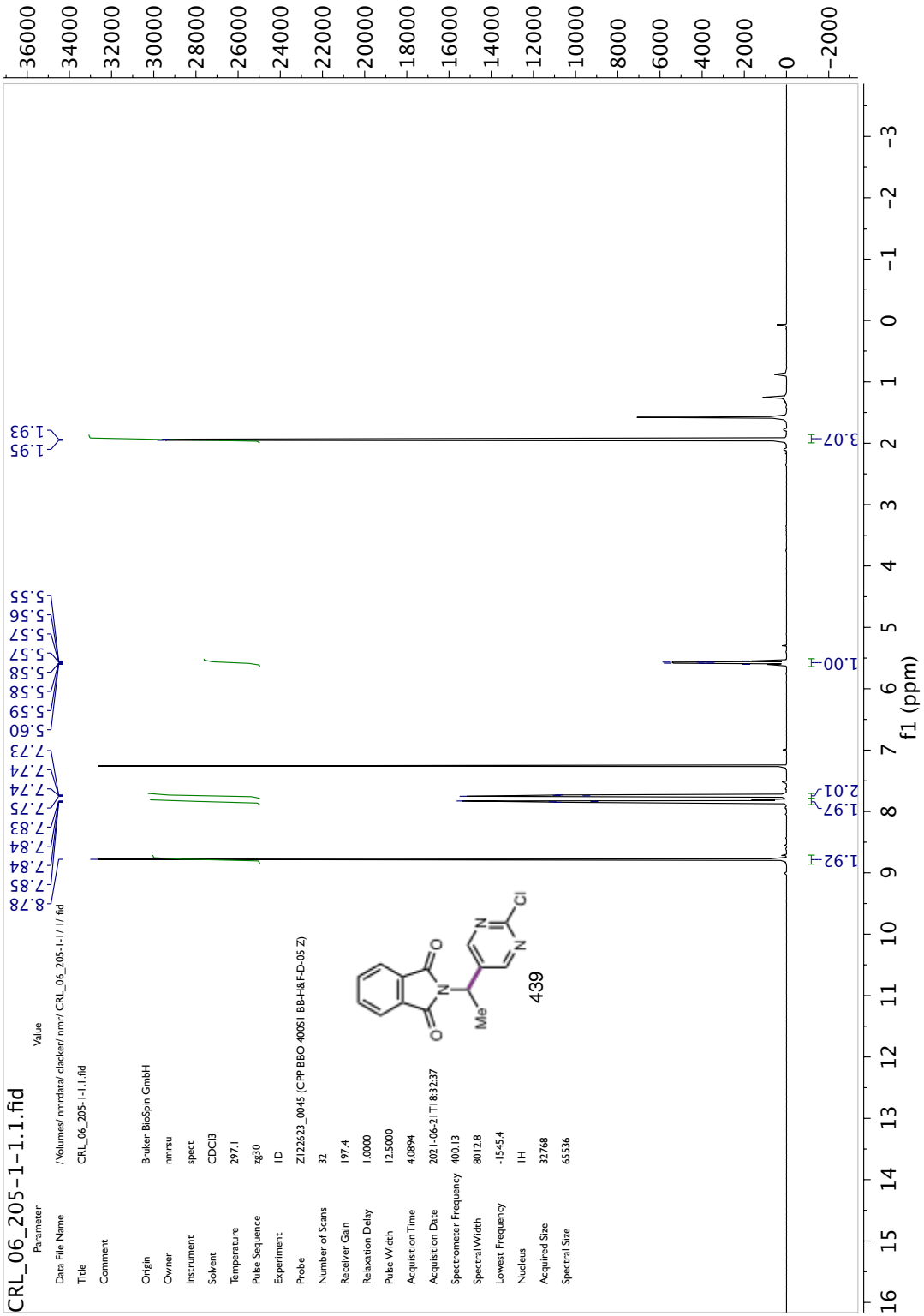
CRL_06_205-1-1.1.fid
Parameter
Value
Data File Name
/Volumes/ nmrdata/ clacker/ nmr/ CRL_06_205-1-1 / 1/ fid
Title
CRL_06_205-1-1.1.fid
Comment
Origin
Bruker BioSpin GmbH
Owner
nmrsu
Instrument
spect
Solvent
CDCl3
Temperature
297.1
Pulse Sequence
zg30
Experiment
1D
Probe
Z122623_0045 (CPP BBO 400S1 BB-H&F-D-05 Z)
Number of Scans
32
Receiver Gain
197.4
Relaxation Delay
1.0000
Pulse Width
12.5000
Acquisition Time
4.0894
Acquisition Date
2021-06-21T18:32:37
Spectrometer Frequency
400.13
SpectralWidth
8012.8
Lowest Frequency
-1545.4
Nucleus
1H
Acquired Size
32768
Spectral Size
65536
Me
Cl
439
8.78
7.85
7.84
7.84
7.83
7.75
7.74
7.74
7.73
5.60
5.59
5.58
5.58
5.57
5.57
5.56
5.55
1.95
1.93
1.92
1.97
2.01
1.00
3.07
f1 (ppm)

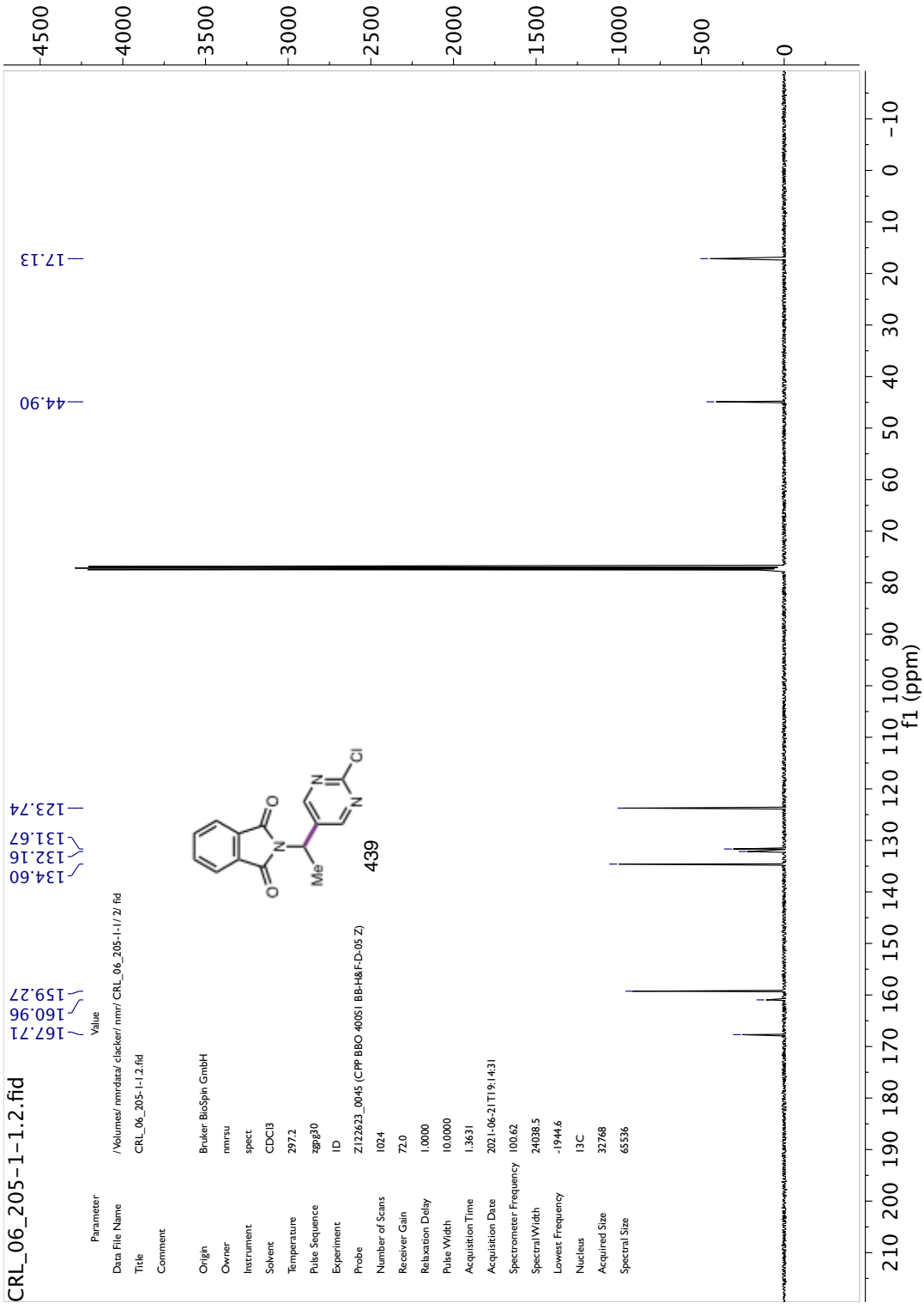
CRL_06_205-1-1.2.fid
Parameter
Value
Data File Name
/Volumes/ nmrdata/ clacker/ nmr/ CRL_06_205-1-1/ 2/ fid
Title
CRL_06_205-1-1.2.fid
Comment
Origin
Bruker BioSpin GmbH
Owner
nmrsu
Instrument
spect
Solvent
CDCl3
Temperature
297.2
Pulse Sequence
zgpg30
Experiment
1D
Probe
Z122623_0045 (CPP BBO 400SI BB-H&F-D-05 Z)
Number of Scans
1024
Receiver Gain
72.0
Relaxation Delay
1.0000
Pulse Width
10.0000
Acquisition Time
1.3631
Acquisition Date
2021-06-21T19:14:31
Spectrometer Frequency
100.62
Spectral Width
24038.5
Lowest Frequency
-1944.6
Nucleus
13C
Acquired Size
32768
Spectral Size
65536
167.71
160.96
159.27
134.60
132.16
131.67
123.74
44.90
17.13
439
Me
f1 (ppm)

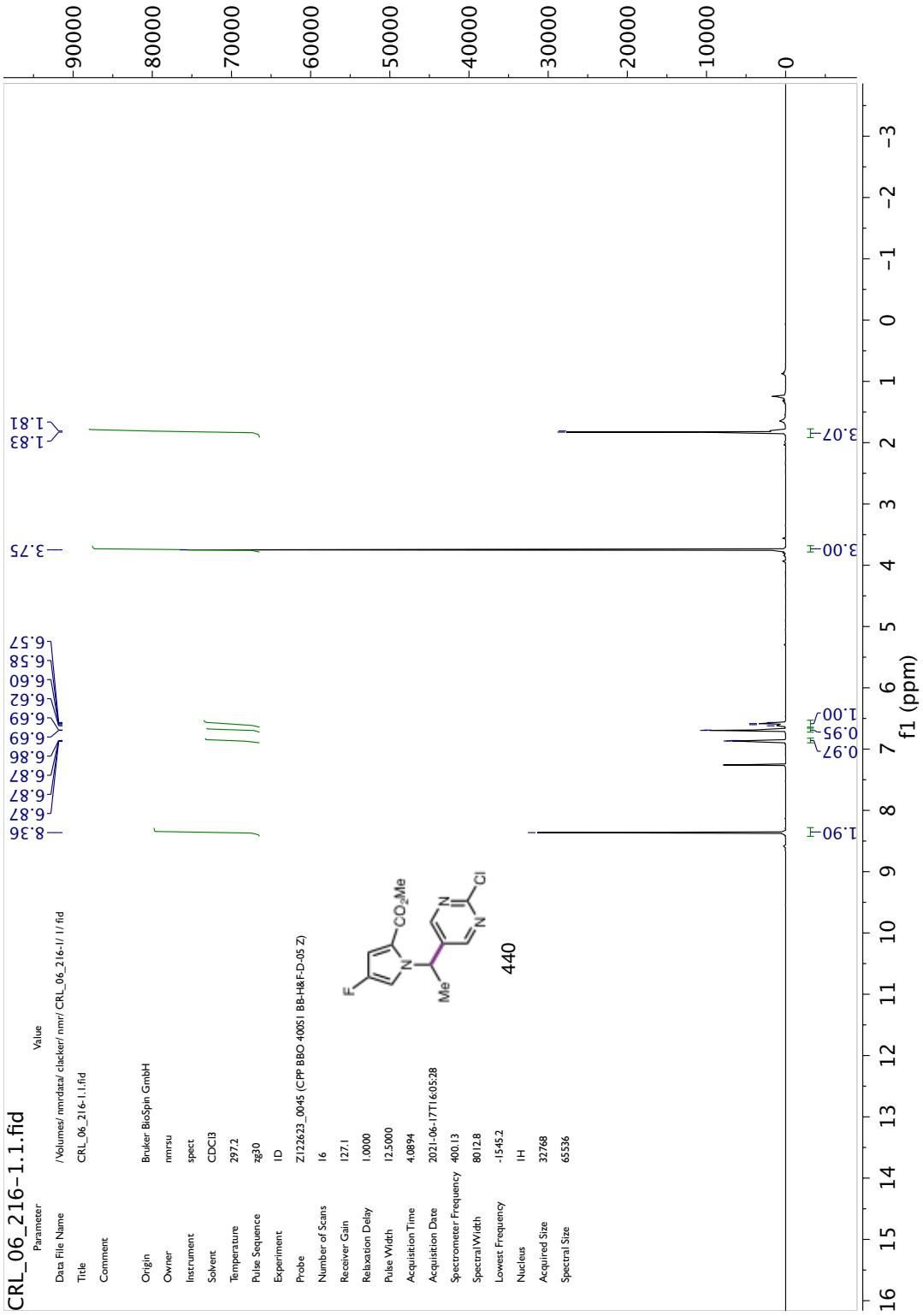
CRL_06_216-1.1.fid
Parameter
Value
Data File Name
/Volumes/ nmrdata/ clacker/ nmr/ CRL_06_216-1/ 1/ fid
Title
CRL_06_216-1.1.fid
Comment
Origin
Bruker BioSpin GmbH
Owner
nmrsu
Instrument
spect
Solvent
CDCl3
Temperature
297.2
Pulse Sequence
zg30
Experiment
1D
Probe
Z122623_0045 (CPP BBO 400S1 BB-H&F-D-05 Z)
Number of Scans
16
Receiver Gain
127.1
Relaxation Delay
1.0000
Pulse Width
12.5000
Acquisition Time
4.0894
Acquisition Date
2021-06-17T16:05:28
Spectrometer Frequency
400.13
SpectralWidth
8012.8
Lowest Frequency
-1545.2
Nucleus
1H
Acquired Size
32768
Spectral Size
65536
440
8.36
6.87
6.87
6.87
6.86
6.69
6.69
6.62
6.60
6.58
6.57
3.75
1.83
1.81
1.90
0.97
0.95
1.00
3.00
3.07
f1 (ppm)

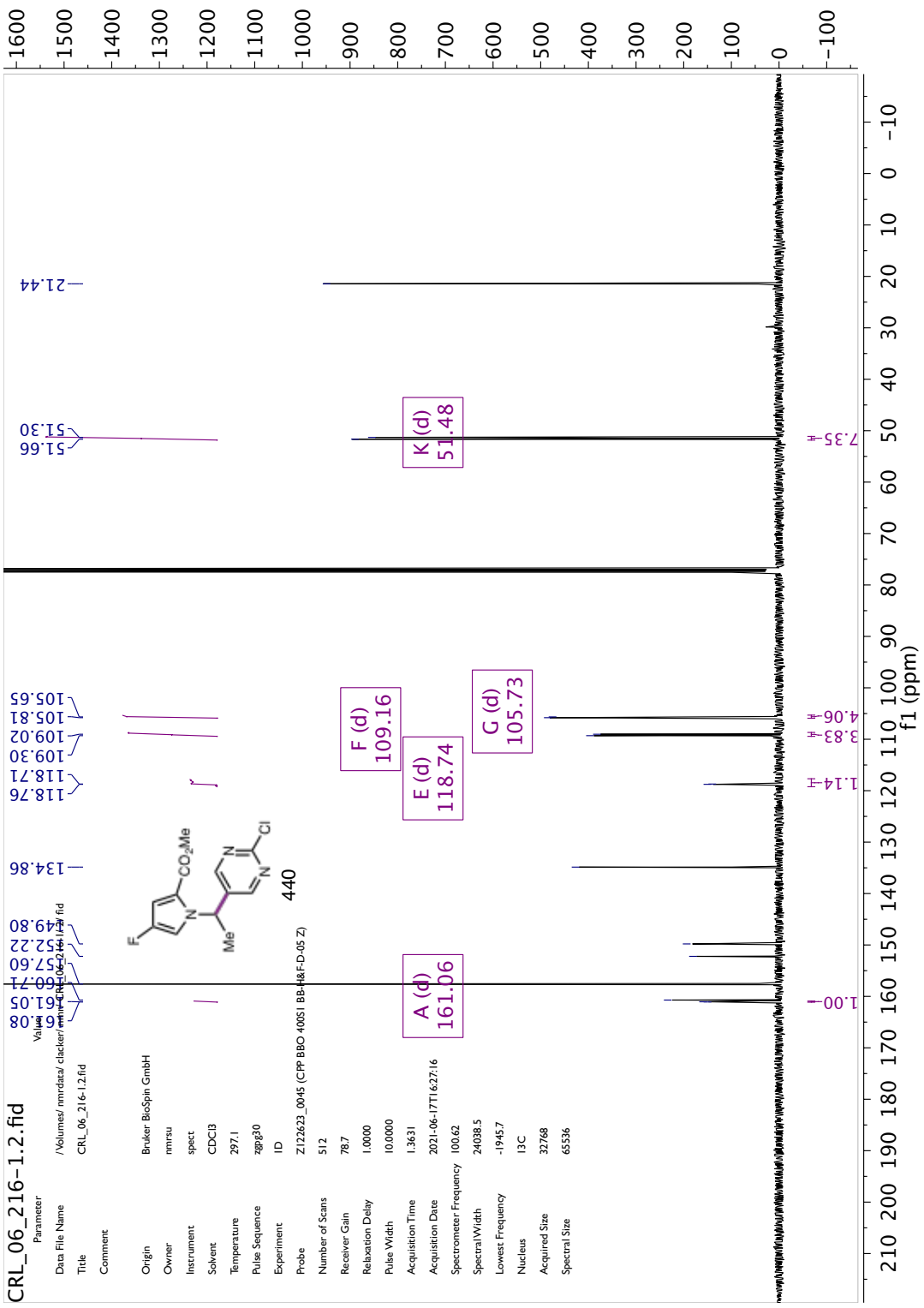
CRL_06_216-1.2.fid
Parameter Value
Data File Name /Volumes/ nmrdata/ clacker/ nmr/ CRL_06_216-1.2.fid
Title CRL_06_216-1.2.fid
Comment
Origin Bruker BioSpin GmbH
Owner nmrsu
Instrument spect
Solvent CDCl3
Temperature 297.1
Pulse Sequence zgpg30
Experiment 1D
Probe Z122623_0045 (CPP BBO 400S1 BB-H&F-D-05 Z)
Number of Scans 512
Receiver Gain 78.7
Relaxation Delay 1.0000
Pulse Width 10.0000
Acquisition Time 1.3631
Acquisition Date 2021-06-17T16:27:16
Spectrometer Frequency 100.62
Spectral Width 24038.5
Lowest Frequency -1945.7
Nucleus 13C
Acquired Size 32768
Spectral Size 65536
440
A (d) 161.06
E (d) 118.74
F (d) 109.16
G (d) 105.73
K (d) 51.48
161.08
161.05
160.71
157.60
152.22
149.80
134.86
118.76
118.71
109.30
109.02
105.81
105.65
51.66
51.30
21.44
1.00
1.14
3.83
4.06
7.35
f1 (ppm)

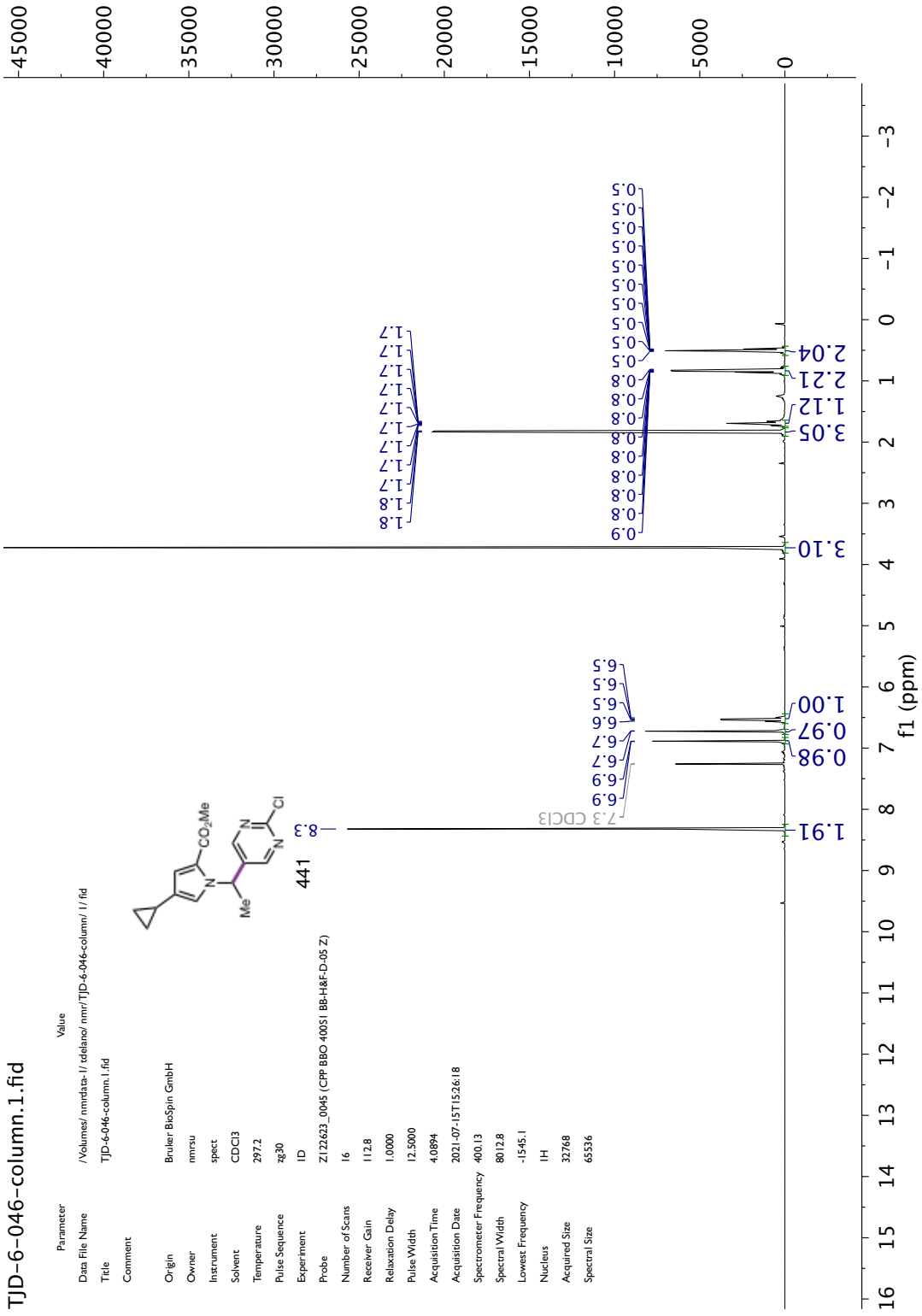
TJD-6-046-column.1.fid
Parameter Value
Data File Name /Volumes/ nmrdata-1/ tdelano/ nmr/TJD-6-046-column/ 1/ fid
Title TJD-6-046-column.1.fid
Comment
Origin Bruker BioSpin GmbH
Owner nmrsu
Instrument spect
Solvent CDCl3
Temperature 297.2
Pulse Sequence zg30
Experiment ID
Probe Z122623_0045 (CPP BBO 400S1 BB-H&F-D-05 Z)
Number of Scans 16
Receiver Gain 112.8
Relaxation Delay 1.0000
Pulse Width 12.5000
Acquisition Time 4.0894
Acquisition Date 2021-07-15T15:26:18
Spectrometer Frequency 400.13
Spectral Width 8012.8
Lowest Frequency -1545.1
Nucleus 1H
Acquired Size 32768
Spectral Size 65536
441
8.3
7.3 CDCl3
6.9
6.7
6.6
6.5
1.8
1.7
0.9
0.8
0.5
1.91
0.98
0.97
1.00
3.10
3.05
1.12
2.21
2.04
f1 (ppm)

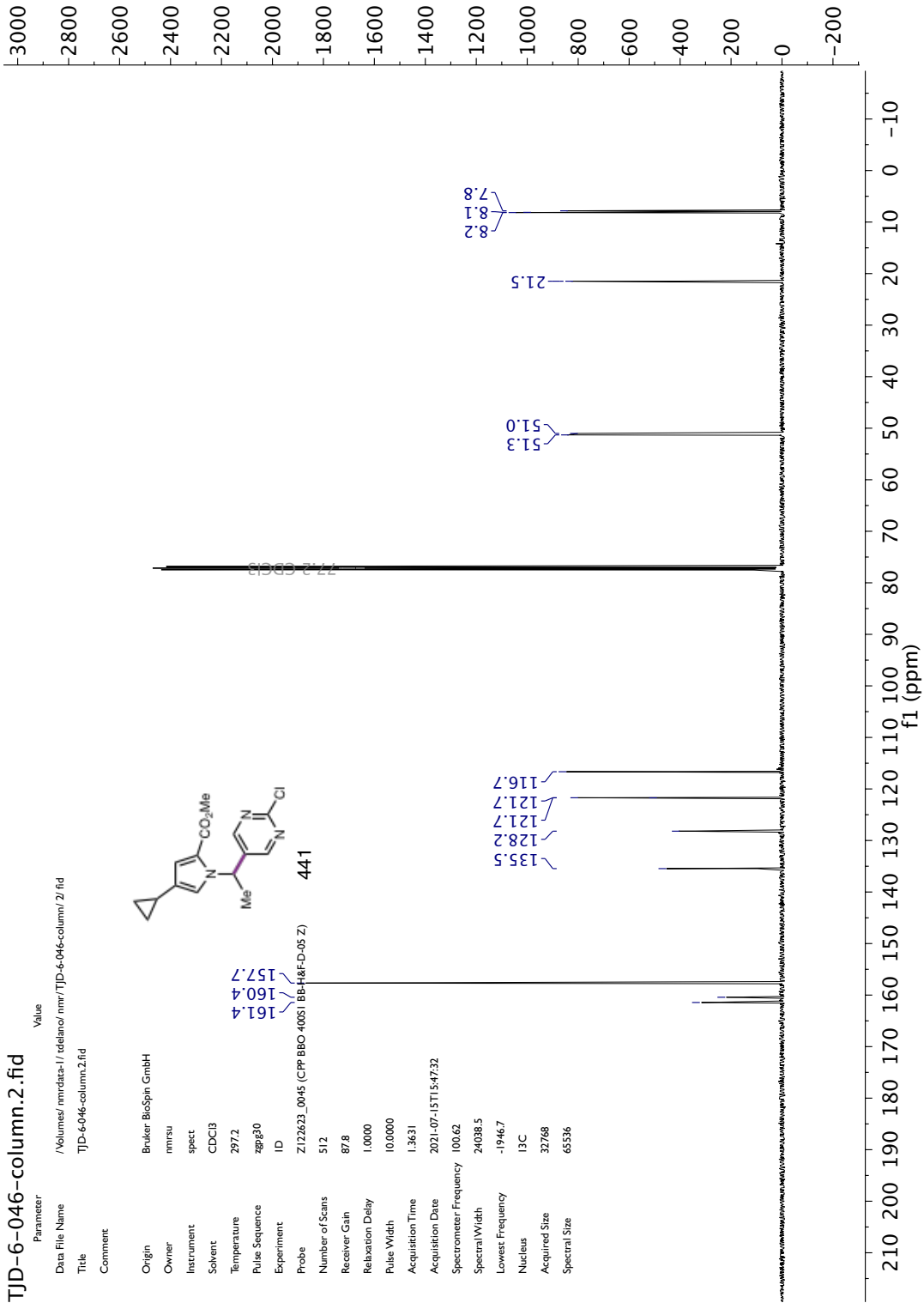
TJD-6-046-column.2.fid
Parameter
Value
Data File Name /Volumes/ nmrdata-1/ tdelano/ nmr/TJD-6-046-column/ 2/ fid
Title TJD-6-046-column.2.fid
Comment
Origin Bruker BioSpin GmbH
Owner nmrsu
Instrument spect
Solvent CDCl3
Temperature 297.2
Pulse Sequence zgpg30
Experiment 1D
Probe Z122623_0045 (CPP BBO 400S1 BB-H&F-D-05 Z)
Number of Scans 512
Receiver Gain 87.8
Relaxation Delay 1.0000
Pulse Width 10.0000
Acquisition Time 1.3631
Acquisition Date 2021-07-15T15:47:32
Spectrometer Frequency 100.62
Spectral Width 24038.5
Lowest Frequency -1946.7
Nucleus 13C
Acquired Size 32768
Spectral Size 65536
441
CO2Me
Me
Cl
157.7
160.4
161.4
77.2 CDCl3
51.0
51.3
21.5
7.8
8.1
8.2
116.7
121.7
121.7
128.2
135.5
f1 (ppm)

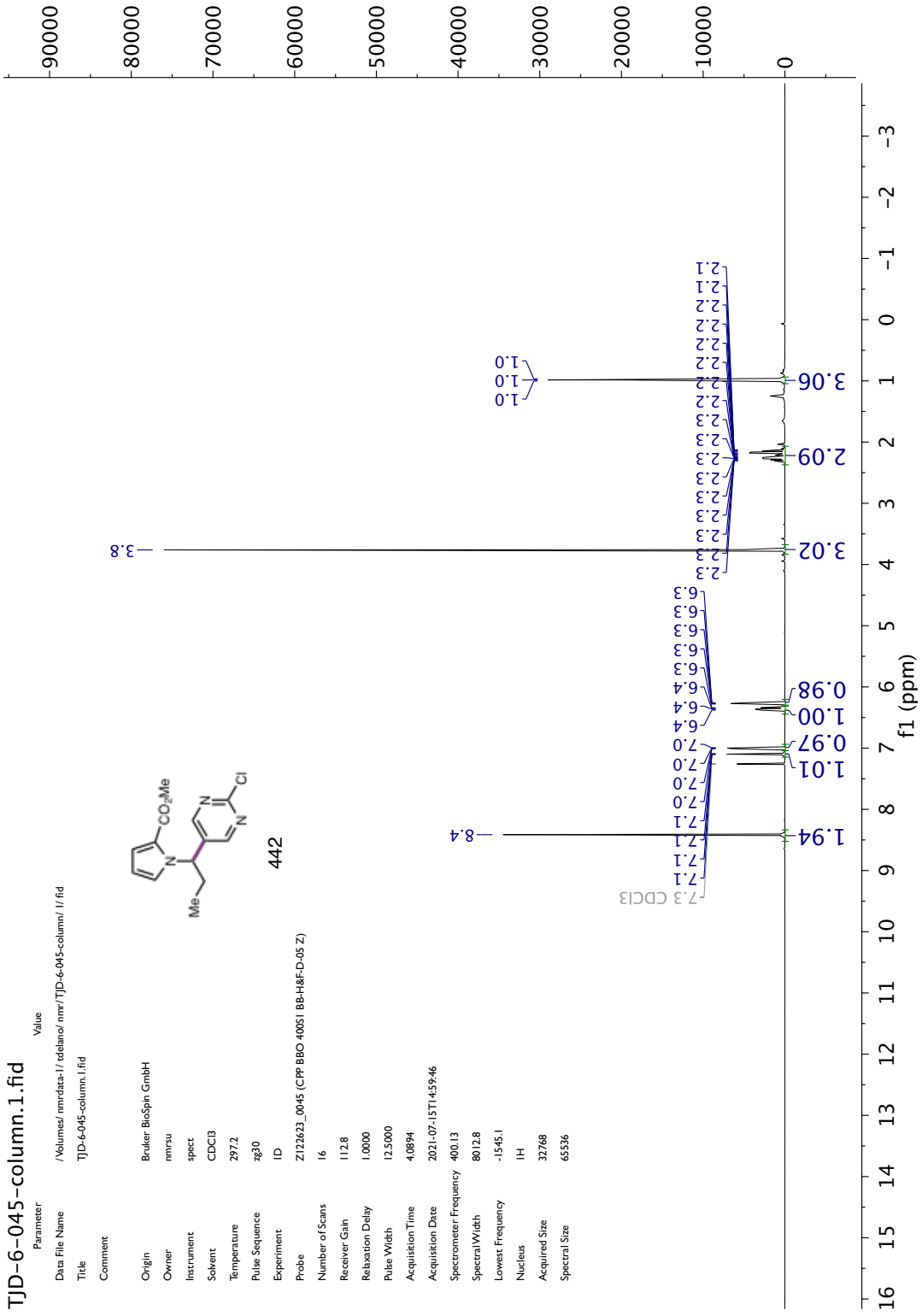
TJD-6-045-column.1.fid
Parameter
Value
Data File Name /Volumes/ nmrdata-1/ tdelano/ nmr/TJD-6-045-column/ 1/ fid
Title TJD-6-045-column.1.fid
Comment
Origin Bruker BioSpin GmbH
Owner nmrsu
Instrument spect
Solvent CDCl3
Temperature 297.2
Pulse Sequence zg30
Experiment 1D
Probe Z122623_0045 (CPP BBO 400S1 BB-H&F-D-05 Z)
Number of Scans 16
Receiver Gain 112.8
Relaxation Delay 1.0000
Pulse Width 12.5000
Acquisition Time 4.0894
Acquisition Date 2021-07-15T14:59:46
Spectrometer Frequency 400.13
Spectral Width 8012.8
Lowest Frequency -1545.1
Nucleus 1H
Acquired Size 32768
Spectral Size 65536
442
CO2Me
Me
Cl
N
N
8.4
3.8
7.3 CDCl3
1.94
1.01
0.97
1.00
0.98
3.02
2.09
3.06
f1 (ppm)

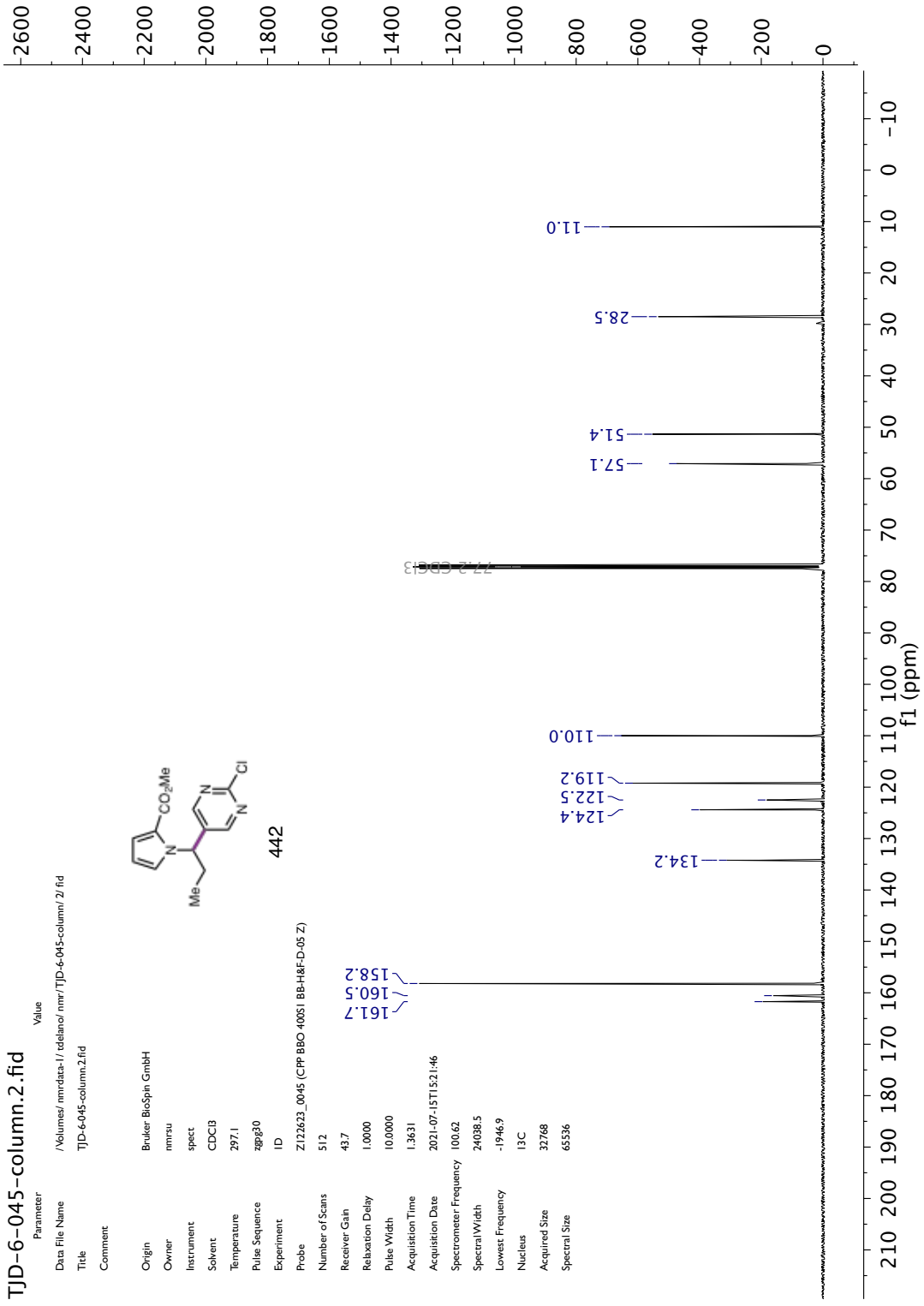
TJD-6-045-column.2.fid
Parameter
Value
Data File Name
/Volumes/ nmrdata-1/ tdelano/ nmr/TJD-6-045-column/ 2/ fid
Title
TJD-6-045-column.2.fid
Comment
Origin
Bruker BioSpin GmbH
Owner
nmrsu
Instrument
spect
Solvent
CDCl3
Temperature
297.1
Pulse Sequence
zgpg30
Experiment
1D
Probe
Z122623_0045 (CPP BBO 400S1 BB-H&F-D-05 Z)
Number of Scans
512
Receiver Gain
43.7
Relaxation Delay
1.0000
Pulse Width
10.0000
Acquisition Time
1.3631
Acquisition Date
2021-07-15T15:21:46
Spectrometer Frequency
100.62
Spectral Width
24038.5
Lowest Frequency
-1946.9
Nucleus
13C
Acquired Size
32768
Spectral Size
65536
CO2Me
N
Me
N
Cl
442
161.7
160.5
158.2
134.2
124.4
122.5
119.2
110.0
77.2 CDCl3
57.1
51.4
28.5
11.0
f1 (ppm)

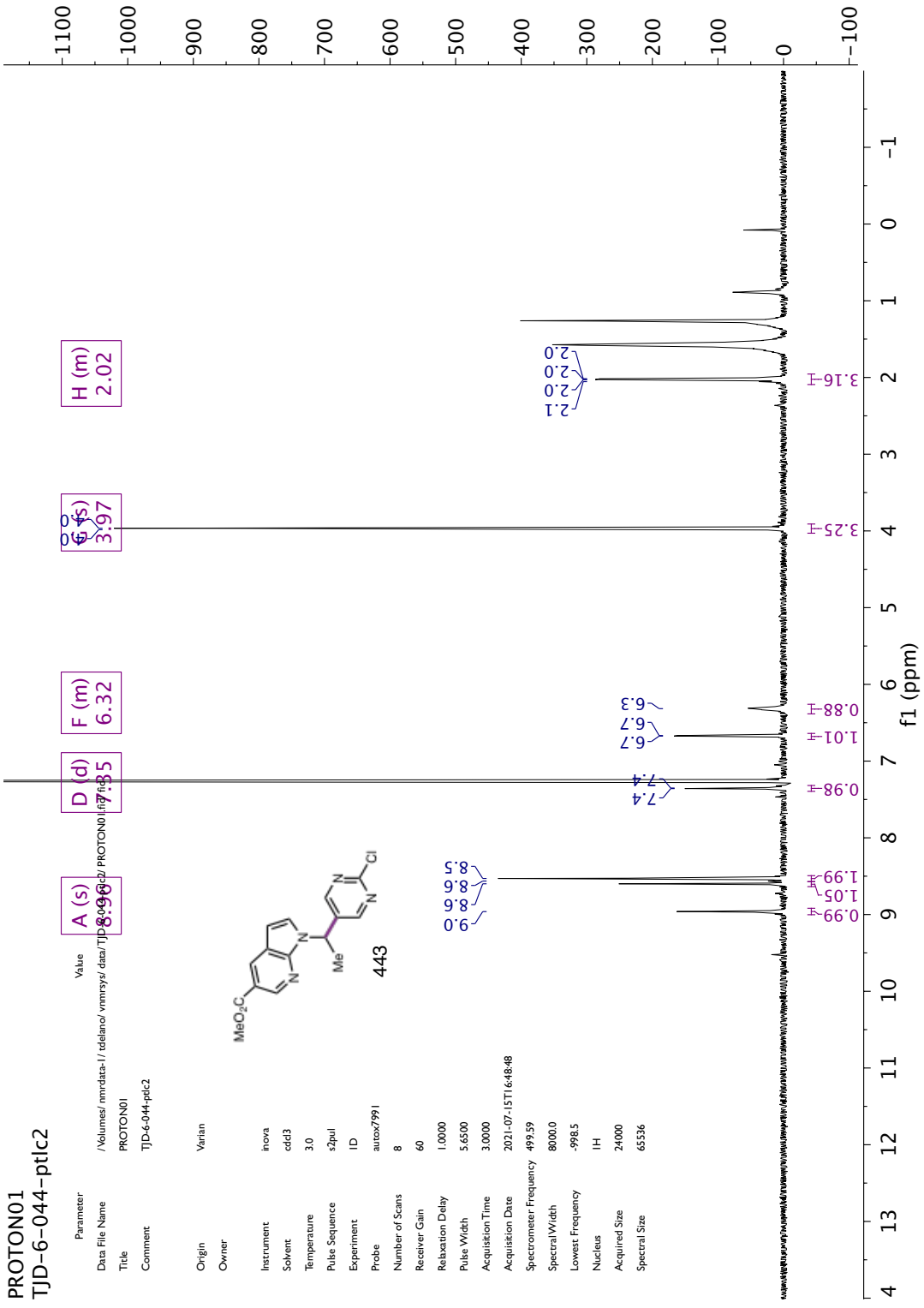
PROTON01
TJD-6-044-ptlc2
Parameter Value
Data File Name /Volumes/ nmrdata-1/ tdelano/ vnmrsys/ data/ TJD-6-044-ptlc2/ PROTON01.fid
Title PROTON01
Comment TJD-6-044-ptlc2
Origin Varian
Owner
Instrument inova
Solvent cdcl3
Temperature 30
Pulse Sequence s2pul
Experiment ID
Probe autox7991
Number of Scans 8
Receiver Gain 60
Relaxation Delay 1.0000
Pulse Width 5.6500
Acquisition Time 3.0000
Acquisition Date 2021-07-15T16:48:48
Spectrometer Frequency 499.59
Spectral Width 8000.0
Lowest Frequency -998.5
Nucleus 1H
Acquired Size 24000
Spectral Size 65536
A (s) 0.990
D (d) 7.35
F (m) 6.32
H (m) 2.02
3.97
MeO2C
Me
Cl
443
f1 (ppm)

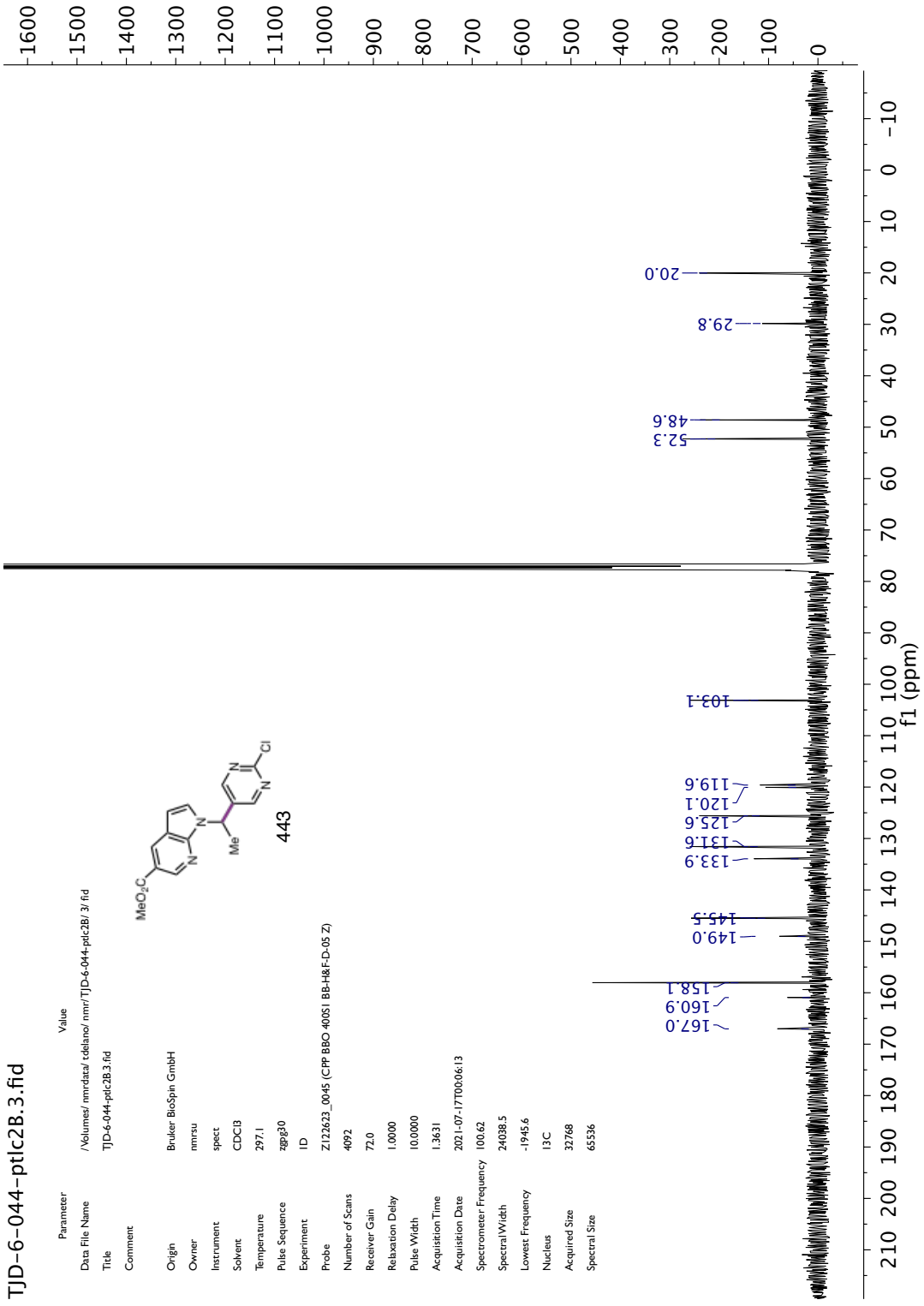
TJD-6-044-ptlc2B.3.fid
Parameter
Value
Data File Name
/Volumes/ nmrdata/ tdelano/ nmr/TJD-6-044-ptlc2B/ 3/ fid
Title
TJD-6-044-ptlc2B.3.fid
Comment
Origin
Bruker BioSpin GmbH
Owner
nmrsu
Instrument
spect
Solvent
CDCl3
Temperature
297.1
Pulse Sequence
zgpg30
Experiment
1D
Probe
Z122622_0045 (CPP BBO 400S1 BB-H&F-D-05 Z)
Number of Scans
4092
Receiver Gain
72.0
Relaxation Delay
1.0000
Pulse Width
10.0000
Acquisition Time
1.3631
Acquisition Date
2021-07-17T00:06:13
Spectrometer Frequency
100.62
Spectral Width
24038.5
Lowest Frequency
-1945.6
Nucleus
13C
Acquired Size
32768
Spectral Size
65536
443
MeO2C
Me
Cl
N
N
N
N
20.0
29.8
48.6
52.3
103.1
119.6
120.1
125.6
131.6
133.9
145.5
149.0
158.1
160.9
167.0
f1 (ppm)

ABOUT THE AUTHOR

Caitlin Rebecca Lacker was born on September 1, 1993 to Stephen G. Lacker and Ann C. Lacker in Austin, Texas. She grew up in Austin and the surrounding country, frequently visiting interesting and underrated locales all over Texas with her parents. Her family encouraged her curiosity and love of learning through nature walks, library books, and fossil hunts at the local creek.

In 2012, Caitlin began her undergraduate education at Southwestern University, not knowing if she wanted to pursue chemistry or engineering. However, she very quickly became fascinated with organic chemistry upon studying it for the first time during her sophomore year. She immediately became interested in summer research and had the privilege of working in the laboratory of Professor Michael Gesinski, who was also her organic chemistry professor. It was with his support and encouragement that she applied for graduate school to pursue her doctorate.

Following her graduation from Southwestern, Caitlin moved halfway across the country to pursue her graduate studies under the direction of Professor Sarah E. Reisman at the California Institute of Technology. Her graduate work had allowed her to study a variety of topics, with a focus on modular, stereoselective approaches towards diverse libraries of compounds, most notably cyclobutanes. Following the completion of her Ph.D, Caitlin will move to Madison, Wisconsin to conduct postdoctoral studies under the direction of Professor Tehshik P. Yoon at the University of Wisconsin, Madison.